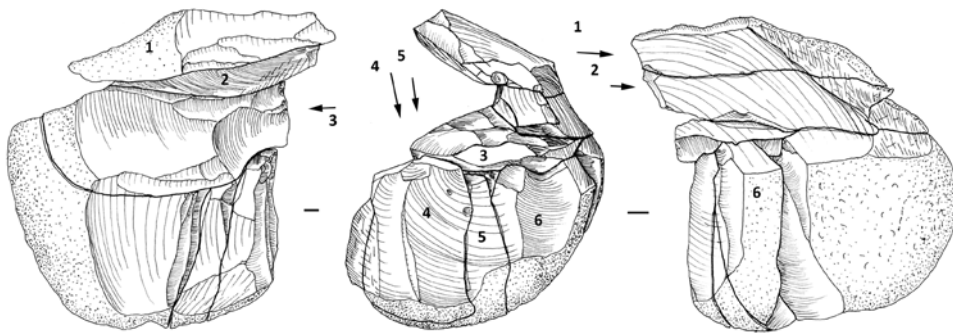


AN INVESTIGATION OF LATE PALAEOLITHIC STONE TOOL ASSEMBLAGES FROM THE NEJD PLATEAU, SOUTHERN OMAN

by
Yamandú Hieronymus Hilbert



A thesis submitted to the
University of Birmingham
for the degree of
DOCTOR OF PHILOSOPHY

Institute of Archaeology and Antiquity
University of Birmingham
September 2012

UNIVERSITY OF
BIRMINGHAM

University of Birmingham Research Archive

e-theses repository

This unpublished thesis/dissertation is copyright of the author and/or third parties. The intellectual property rights of the author or third parties in respect of this work are as defined by The Copyright Designs and Patents Act 1988 or as modified by any successor legislation.

Any use made of information contained in this thesis/dissertation must be in accordance with that legislation and must be properly acknowledged. Further distribution or reproduction in any format is prohibited without the permission of the copyright holder.

to Eva Hilbert

An Investigation of Late Palaeolithic Stone Tool
Assemblages from the Nejd Plateau, Southern Oman

Yamandú Hieronymus Hilbert

Abstract

Technological and typological analysis of lithic assemblages from southern Oman have been undertaken for this study. These assemblages are characterized by the production of elongated end products (i.e., blades/leptoliths) using varied core reduction modalities exemplified here. These modalities have been identified based on technological analysis of production waste and core reconstructions using artefact refittings. Such blade technologies are accompanied by formal tool such as tanged projectile called Fasad point, burins, endscrapers and pseude-backed knives. This technological and typological package has been identified on both systematic surface collections and stratified sites, making it possible to place these assemblages chronologically between 10.000 and 7.000 before present (BP). The chronological and techno-typological characterization of these blade assemblages warrants its status as a lithic industry of the Late Palaeolithic technocomplex. At present, blade assemblages from stratified sites in Yemen (Shi'bat Dihya) and Oman (al Hatab) which dated to 55.000 and 11.000 BP, represent the possible source of the techno/typological package found across Southern Oman at the beginning of the Holocene. No technological or typological resemblance with any other industry from outside of Arabia has been noted, enforcing the local , Arabian, origin of the Early Holocene Populations of the South Arabian Highlands.

Acknowledgments

The process of writing this dissertation would not have been possible without the undying support of a few people and a legion of friends; first and foremost I am in debt to my advisor Dr. Jeffrey Rose who has been like a brother to me since I started the Ph.D program in 2009. From letting me live in his house in England for over 6 month (without paying any rent), helping me financially and feeding me across these past three years and so many other things, thanks Jeff ; I will never be able to pay you back. I also owe a great deal to Prof. Anthony Marks, for supporting me from the start when all seemed lost and I was almost ready to look for a real job (a cook or something like that), thanks Tony. For all the help with the bureaucratic jungle nightmare that are English academic institutions I am in debt to Dr. Paul Garwood, my second supervisor. For nearly maddening discussions about technological processes and intentionality outside the Levallois technological mantle I am grateful to Dr. Vitaly Usik. Thanks also goes to the remaining DAP team members, Amir Beshkani, Chris Galletti, Ash Parton, Dr. Mike Morley. I am also grateful for the Australian dating specialists Prof. Bert Roberts and Lauren Linnenlucke; thanks and keep the dates coming.

For very insightful discussions and memorable hang over I am grateful to Dr. Rémy Crassard, Ash Parton, Viola Schmidt, Christoph Wissing, Björn Bitterlich, Dominik Koscielny, Dr. Hannes Napirala, Bernd Trautmann, Krischan Hoyer and Dr. Paul Preston. Which comes to show that it has not all been rocks and sand for the past three years, to all those with whom I have spent my spare time and kept me away from work cheers and rock on. In Germany thanks goes out especially to Andreas Taller for all the mountain biking, BBQs, drinks and discussions about technology ; and Markus Schumacher for all the Call of Duty hours in front of the XBOX and for always having a spare beer in his refrigerator. In Oman a big thanks goes to Mags Kleszczewska Rose for letting me spread the rock across the house in Qantab (and all the other cools stuff, rock on Mags), Assad al Hassni, Luca Belfioretti, Valentina Àzzara and many more.

Thanks also goes out to my family, my mother Liliana Mendiburu and brother Lautaro in Brazil; my uncle Hannes, aunt Iola and my cousins Pati and Martin in Marburg; my cousin Joschka Scherer in Munich. Last but not least I thank my fiancé J. Marie Geiling for every moment we spent together.

I also thank the AHRC for partial funding. I also acknowledge the support from the Ministry of Heritage and Culture of Oman.

TABLE OF CONTENTS

1 Introduction	1
2 Archaeological evidence from South Arabia dating between 50 to 10 ka BP	9
2.1 Assemblages A from Faya NE-1	11
2.2 Shi'bat Dihya	14
2.3 Al Hatab	19
2.4 Summary	28
3 Climate frame and data for South Arabia	31
3.1 The Marine record	32
3.2 The Indian Ocean Monsoon	35
3.3 The terrestrial records	39
3.4 Summary	47
4 Dhofar and the Nejd Plateau: Geomorphology and geography	55
4.1 The Sultanate of Oman	57
4.1.1 The Hajar Mountains and central Omani plain: Geography and geomorphology	58
4.2 Dhofar: Geography and geomorphology	63
4.2.1 The costal plain and the Dhofar Mountain Chain	64
4.2.2 The Nejd Plateau and the Rub al Khali desert	70
4.3 Summary	86

5 Towards understanding lithics: Theory and method	88
5.1 Reconstruction of reduction sequences	89
5.1.1 Refittings	90
5.1.2 Replication studies in lithic technology	93
5.1.3 Chaîne opératoire	94
5.2 Débitage Analysis	96
5.2.1 Blank orientation and measurements	99
5.2.2 Blank Type	101
5.2.2.1 Flake	101
5.2.2.2 Blade	101
5.2.2.3 Technologically diagnostic débitage	102
5.2.3 Blank Condition	103
5.2.4 Patina	104
5.2.5 Edge damage	106
5.2.6 Raw Material	107
5.2.7 Platform Morphology	109
5.2.7.1 Débitage platform types	109
5.2.7.2 Lipping	111
5.2.7.3 Platform abrasion	112
5.2.8 Blank Shape	113
5.2.9 Blank midpoint cross-section	115
5.2.10 Blank distal portion	117
5.2.11 Blank Longitudinal profile	119
5.2.12 Axis	119
5.2.13 Cortical percentage on blanks dorsal surface	120
5.2.14 Scar pattern on dorsal surface	120
5.3 Core Analysis	122

5.3.1 Core orientation, metrics and other numerical attributes	124
5.3.2 Core Typologies	126
5.3.3 Core Striking Platform	129
5.3.4 Cortex	130
5.3.5 Core flaking surface (vertical convexity)	130
5.2.6 Position of Flaking surface (horizontal convexity)	132
5.4 Tool Analysis	135
5.4.1 Tool Type	136
5.4.2 Position of retouch	140
5.4.3 Type of Retouch	140
5.4.4 Characterization of the blank	142
5.5 Summary	142
 6 ALPHA Transect	 144
6.1 ALPHA Transect Sites	147
6.2 Jebel Eva (TH.67)	153
6.2.1 Site Location	153
6.2.2 Sampling strategies and documentation	154
6.2.3 Spatial distribution	155
6.3 The assemblage	157
6.3.1 Débitage	159
6.3.2 Cores	166
6.3.3 Tools	169
6.3.4 Refittings	170
6.4 ALPHA Transect comments	174
6.4.1 TH.59	174
6.4.2 Jebel Eva (TH.67)	175

7 BRAVO transect	177
7.1 Khumseen Rockshelter (TH.50)	178
7.1.1 Site location	178
7.1.2 Sampling Strategy	183
7.1.3 Spatial Distribution	190
7.1.4 The assemblage	192
7.1.5 Débitage	195
7.1.6 Cores	203
7.1.7 Tools	207
7.1.8 Refittings	208
7.2 Ghazal Rockshelter (TH.47)	216
7.2.1 Site location	216
7.2.2 Sampling Strategy	220
7.2.3 Spatial Distribution	224
7.2.4 The assemblage	227
7.2.5 Level 2	227
7.2.5.1 Débitage	228
7.2.5.2 Cores	235
7.2.5.3 Tools	238
7.2.5.4 Level 2 refittings	240
7.2.6 Level 1	251
7.2.6.1 Débitage	252
7.2.6.2 Cores	255
7.2.6.3 Level 1 refittings	257
7.3 BRAVO Transect Comments	267
7.3.1 Khumseen Rockshelter	267
7.3.2 Ghazal Rockshelter	267

8 GOLF Transect	270
8.1 Gulf Transect Sites	271
8.1.1 TH.125	271
8.1.2 TH.128	275
8.1.3 TH.133	280
8.2 Wadi Haluf 1 (TH.124b)	283
8.2.1 Site Location	283
8.2.2 Sampling strategy and documentation	285
8.2.3 Spatial distribution	286
8.2.4 The assemblage	288
8.2.5 Débitage	289
8.2.6 Cores	295
8.2.7 Tools	297
8.2.8 Refits	299
8.3 GOLF transect comments	304
8.3.1 TH.125, TH.128 and TH.133 refits	304
8.3.2 Wadi Haluf 1 comments	305
 9 Conclusions	 307
9.1 The Late Palaeolithic of Dhofar	308
9.1.1 Reduction modalities	309
9.1.2 Débitage and cores	317
9.1.3 Tools	325
9.1.4 Raw material economy	328
9.1.5 The Khashabian: a new south Arabian lithic industry	329
9.2 The Khashabian: landscape and climate	332
9.3 The Khashabian in Arabia	333

9.4 The Khashabian: local or exogenous?	337
9.4.1 Exogenous	337
9.4.2 A local source	341
9.3.3 Palaeodemographics and genetics	343
9.5 Transition to the Neolithic	345
9.6 Summary	347
Appendix A	349
Appendix B	361
Bibliography	369

Figures

Figure 2.1 Map showing the location of MIS 3 and 2 sites.	10
Figure 2.2 Photograph of the site.	12
Figure 2.3 Profile of the main section from Faya NE-1.	12
Figure 2.4 Artefacts from assemblage A.	13
Figure 2.5 Plan showing the concentration at SD1.	16
Figure 2.6 Artefacts from SD1.	17
Figure 2.7 Tools from SD1.	19
Figure 2.8 Topographic map of al Hatab.	20
Figure 2.9 Excavation areas at al Hatab.	21
Figure 2.10 Section 2 from al Hatab area 3.	23
Figure 2.11 Section 1 from al Hatab area 1.	23
Figure 2.12 Artefact patination at al Hatab.	25
Figure 2.13. Artefacts from al Hatab.	26
Figure 2.14 al Hatab Tools.	28
Figure 3.1 Migration of Indian Ocean Monsoon.	34
Figure 3.2 Monsoon intensity.	38
Figure 3.3 Linear dunes at the Wahiba Sands, Oman.	42
Figure 3.4 Northward migration of the ITCZ.	47
Figure 3.5 Sum probability curve for the Late Pleistocene of Arabia.	48
Figure 4.1 Map showing the Location of the South Arabian Highlands.	56
Figure 4.2 Map of the Sultanate of Oman and its regions.	57
Figure 4.3 Photographs of distinct environments within the Hajar Mountains and northern Oman.	59
Figure 4.4 Photographs of the Wahiba and Rub al khali deserts.	60
Figure 4.5 Sand dune morphology.	61
Figure 4.6 Schematic of windborne transport.	62
Figure 4.7 Panoramic image of the Salalah coastal plain.	66
Figure 4.8 Sketch of the main geological formations and schematic profile across the tertiary sediment sequence.	67
Figure 4.9 Wadi Darbat waterfall.	68
Figure 4.10 Photograph of southern Dhofar during the monsoon.	69
Figure 4.11 Transition between the Dhofar escarpment and the Nejd Plateau.	71
Figure 4.12 Flint artefact carved.	71
Figure 4.13 Photographs of Wadis Aybut.	74
Figure 4.14 Photograph of the Mudayy Member near Habarut.	75
Figure 4.15 Rockshelter schematic.	76
Figure 4.16 Rockshelters and karstic features in South Arabia.	78
Figure 4.17 Map of Dhofar showing different ecozones.	78
Figure 4.18 Panoramic images of the Southern Nejd.	80
Figure 4.19 central Nejd Plateau.	82
Figure 4.20 Springs by Mudayy.	83

Figure 4.21 Northern Nejd and Rub al Khali desert.	85
Figure 5.1 Diverse situations in the field susceptible to production refits.	91
Figure 5.2 Example of illustrated refit from SJ. 51.	93
Figure 5.3 Blank orientation and measurements.	99
Figure 5.4 Edge damage on artefacts for archaeological context.	107
Figure 5.5 Raw material nodules in situ at Wadi Haluf .	108
Figure 5.6 Blank platform types.	111
Figure 5.7 Blank Shape.	115
Figure 5.8 Blank midpoint cross-section schematics.	116
Figure 5.9 Blank termination.	118
Figure 5.10 Blank dorsal scare pattern.	122
Figure 5.11 Arabian Middle Palaeolithic core and Late Palaeolithic Core.	123
Figure 5.12 core measurements and orientation.	125
Figure 5.13 Core convexity schemata.	131
Figure 5.14 Core work surface position.	134
Figure 6.1 ALPHA transect and sites mentioned in text.	145
Figure 6.2 Panoramic view over large lithic scatter.	146
Figure 6.3 Blade scatter at TH.123c.	147
Figure 6.4 Photograph of refit #2.	149
Figure 6.5 Refit #3 débitage.	150
Figure 6.6 Refit #3 stages A and B.	152
Figure 6.7 Refit #3 stages C and D.	152
Figure 6.8 Photograph of the site prior to collection.	153
Figure 6.9 Topographic map of Jebel Eva.	155
Figure 6.10 Artefact density at Jebel Eva.	156
Figure 6.11 Artefacts patina and photo of refit.	159
Figure 6.12 Jebel Eva débitage.	163
Figure 6.13 Jebel Eva cores.	167
Figure 6.14 Jebel Eva tools.	170
Figure 6.15 Jebel Eva refit #4.	172
Figure 6.16 Jebel Eva Refit #13.	173
Figure 7.1 BRAVO transect and sites mentioned in text.	176
Figure 7.2 Photographs of the sites surrounding area.	179
Figure 7.3 Panorama photograph of the Khumseen Rockshelter.	180
Figure 7.4 Chert outcropping directly at the site.	181
Figure 7.5 Topographic map of Khumseen Rockshelter.	182
Figure 7.6 Fireplaces at Khumseen Rockshelter.	184
Figure 7.7 East profile of area 1.	186
Figure 7.8 South and east sections of area 2.	188
Figure 7.9 Area 1 and 2 vertical density.	191
Figure 7.10 Photograph of refit # 11.	195
Figure 7.11 Khumseen bladelets.	200
Figure 7.12 Khumseen blades.	201
Figure 7.13 Khumseen cores.	204

Figure 7.14 Khumseen tools.	207
Figure 7.15 Khumseen refit #10 débitage.	209
Figure 7.16 Khumseen refit #10.	210
Figure 7.17 Khumseen refit #11 débitage.	211
Figure 7.18 Khumseen refit #11.	212
Figure 7.19 Khumseen refit #16 débitage.	213
Figure 7.20 Khumseen refit #16.	214
Figure 7.21 Khumseen refit #13.	215
Figure 7.22 Khumseen refit #14.	215
Figure 7.23 Photograph of the Ghazal prior to excavation and during excavations.	218
Figure 7.24 Topographic map of Ghazal.	219
Figure 7.25 Surface plot of Ghazal.	221
Figure 7.26 Profile EAST 1 from Ghazal.	221
Figure 7.27 Profile EAST 2 from Ghazal.	222
Figure 7.28 Profile SOUTH 1 from Ghazal.	222
Figure 7.29 Photograph of the roof collapse and eolian sediments below.	223
Figure 7.30 Artefacts from Ghazal.	225
Figure 7.31 Distribution of artefacts per square meter.	226
Figure 7.32 Ghazal débordant débitage Level 2.	230
Figure 7.33 Ghazal débitage from Level 2.	233
Figure 7.34 Ghazal convergent core from Level 2.	236
Figure 7.35 Ghazal cores from Level 2.	238
Figure 7.36 Ghazal tools from Level 2.	239
Figure 7.37 Hammerstone from Ghazal Level 2.	239
Figure 7.38 Ghazal level 2 refit #2 débitage.	241
Figure 7.39 Ghazal level 2 refit #2.	242
Figure 7.40 Ghazal level 2 refit #5 débitage.	243
Figure 7.41 Ghazal level 2 refit #5.	244
Figure 7.42 Ghazal level 2 refit #20 débitage.	245
Figure 7.43 Ghazal level 2 refit #20.	246
Figure 7.44 Ghazal level 2 refit #25 débitage.	247
Figure 7.45 Ghazal level 2 refit #25.	248
Figure 7.45 Ghazal level 2 refit #19 débitage.	249
Figure 7.47 Ghazal level 2 refit #19.	250
Figure 7.48. Ghazal Level 1 cores.	255
Figure 7.49 Ghazal level 1 refit #28 débitage.	258
Figure 7.50 Ghazal level 1 refit #28.	259
Figure 7.51 Ghazal level 1 refit #29.	260
Figure 7.52 Ghazal level 1 refit #30 débitage.	261
Figure 7.53 Ghazal level 1 refit #30.	262
Figure 7.54 Ghazal level 1 refit #31 débitage.	263
Figure 7.55 Ghazal level 1 refit #31.	264
Figure 7.56 Ghazal level 1 refit #31.	265
Figure 7.57 Ghazal level 1 refit #31.	265
Figure 7.58 Ghazal level 1 refit #31.	266
Figure 7.59 Ghazal level 1 refit #31.	266

Figure 8.1 GULF transect and sites mentioned in text.	270
Figure 8.2 Photograph of TH.125 locality.	271
Figure 8.3 TH.125 refitting débitage.	272
Figure 8.4 TH.125 refitting.	274
Figure 8.5 Photograph of TH.128 locality.	275
Figure 8.6 Photograph of TH.128 biface.	276
Figure 8.7 TH.128 refitting débitage.	277
Figure 8.8 TH.128 refitting .	278
Figure 8.9 TH.133 refitting débitage.	281
Figure 8.10 TH.133 refitting.	282
Figure 8.11 Wadi Haluf 1 photographs.	284
Figure 8.12 Wadi Haluf 1 artefact density.	286
Figure 8.13 Wadi Haluf 1 spatial distribution.	287
Figure 8.14 Wadi Haluf 1 débitage.	293
Figure 8.15 Wadi Haluf 1 BTF's .	294
Figure 8.16 Wadi Haluf 1 cores.	296
Figure 8.17 Wadi Haluf 1 two unopposed platform core	297
Figure 8.18 Wadi Haluf 1 tools.	298
Figure 8.19 Wadi Haluf 1 trifaces.	299
Figure 8.20 Wadi Haluf 1 refit #14 débitage.	300
Figure 8.21 Wadi Haluf 1 refit #14.	301
Figure 8.22 Wadi Haluf 1 refit #1.	302
Figure 8.23 Wadi Haluf 1 refit #5 débitage.	303
Figure 8.24 Wadi Haluf 1 refit #5.	303
Figure 9.1 Reduction modality 1 schematic.	311
Figure 9.2 Technologically diagnostic débitage produced by Modality 1.	312
Figure 9.3 Reduction modality 2 schematic.	313
Figure 9.4 Reduction modality 3 schematic.	314
Figure 9.5 Technologically diagnostic débitage produced by Modality 3.	315
Figure 9.6 Artefact count per site.	318
Figure 9.7 Artefact platform type.	319
Figure 9.8 Artefact cortical cover.	319
Figure 9.9 Artefact longitudinal profile.	319
Figure 9.10 Artefact termination.	320
Figure 9.11 Artefact midpoint cross section.	320
Figure 9.12 Artefact shape.	320
Figure 9.13 Artefact scar pattern.	321
Figure 9.14 Blade index of elongation.	321
Figure 9.15 Blade relative platform size.	322
Figure 9.16 Blade index of platform flattening.	322
Figure 9.17 Débordant blade index of elongation.	323
Figure 9.18 Débordant blade index if relative platform size.	323
Figure 9.19 Débordant blade index of platform flattening.	325
Figure 9.20 Pseudo-backed knives.	327
Figure 9.21 Selected Artefacts typical for the Khashabian.	331
Figure 9.22 Selected Artefacts typical for the PPNB.	339

Figure 9.23 Selected Artefacts typical for the Proto-Neolithic.	340
Figure 9.24 Main branches of the complete R0a mtDNA tree.	344
Figure 9.25 Trihedral projectile points from diverse sites across the Nejd.	346

Tables

Table 6.1 Jebel Eva assemblage.	158
Table 7.1 Dates for Khumseen Rockshelter.	190
Table 7.2 Late Paleolithic artefacts from Khumseen.	193
Table 7.3 Artefacts from Ghazal Level 2.	229
Table 7.4 Artefacts from Ghazal Level 1.	252
Table 7.5 Refittings from Ghazal level 1.	258
Table 8. 1 Wadi Haluf 1 artefact count.	289
Table 9.1 Distribution of the reduction modalities across the analysed samples.	317
Table 9.2 Absolute dates for sediments holding Khashabian assemblages.	331

INTRODUCTION

There is much to be done in South Arabia: a variety of undefined lithic industries carpet the landscape. It is only a matter of time until stratified Palaeolithic sites, which have eluded Arabian archaeologists for over half a century, will be unearthed.

– Jeffrey I. Rose, *Among Arabian Sands: Defining the Palaeolithic of Southern Arabia* (2006, 333)

When I was an undergraduate student starting work in the Arabian Peninsula, the “*tabula rasa*” scenario proposed by Rose (2006) was the default model for Palaeolithic habitation in Arabia. *Tabula rasa* is based on the assumption that Arabia was only able to support human populations during pluvial phases - periods of increased rainfall and, consequently, elevated landscape carrying capacity. Conversely, during glacial phases, the Arabian climate was characterized by extreme aridity, at which times human populations were not present. In the words of Thesiger (1959: 1) “a cloud gathers, the rain falls, men live; the cloud disperses without rain, and men and animals die.” When rainfall increased, the desiccated Arabian landscapes were transformed into more fertile ecosystems, drawing in populations from outside the peninsula to colonize these uninhabited territories. Since each new population would have brought with them the lithic technology from whence they came, it follows that the *tabula rasa* model should be verifiable from the material culture at Stone Age sites in Arabia.

Marks (2008) explores the implications of this point: Palaeolithic sites found across Arabia will either bear the technological and typological features of their origin, or show a unique set of characteristics indicating their indigenous development. Either Palaeolithic sites are the product of local populations that survived at least one climatic cycle, or were created by foreign groups that moved into Arabia during pluvial phases. Given that most of the territories surrounding Arabia (i.e. Southwest Asia and

Northeast Africa) have enjoyed a long and comprehensive history of archaeological and paleoanthropological research (e.g. Bar-Yosef, 1980; Hublin, Valladas *et al.*, 1988; 1993; Schwarcz, 1994; McBrearty & Brookes, 2000; Monigal, 2002; Van Peer & Vermeersch, 2007; Barham & Mitchell, 2008; Van Peer *et al.*, 2010), we should be able to determine if the various prehistoric populations in Arabia came from the Levant, Africa, or across the Arabo-Persian Gulf.

Lower Palaeolithic sites are reasonably well known throughout Arabia (e.g. Amirkhanov, 1994; 2006; Biagi, 1994; Whalen & Schatte, 1997; Zarins, 1998; Whalen *et al.*, 2002, Petraglia, 2003; Jagher, 2009; Petraglia *et al.*, 2009). Attribution of these sites to a specific source area outside of Arabia is difficult, because of the homogeneity of the lower Palaeolithic record across Arabia and its neighbouring regions (Marks, 2008; 2009; Chauhan, 2009). The archaeological situation is much clearer in the Middle Palaeolithic; sites discovered in Arabia bear distinct African features and indicate multiple population expansions into Arabia between 128-75 ka before present (BP) (Petraglia, 2011; Armitage *et al.*, 2011; Rose *et al.*, 2011a; Usik *et al.*, 2012). Regardless of the route they took entering Arabia (i.e. Sinai or Bab Al Mandeb), these Middle Palaeolithic/Middle Stone Age (MP/MSA) sites indicate that hunter-gatherer groups occupied the peninsula during MIS 5, at least one of which can be confidently ascribed to anatomically modern humans (Rose *et al.*, 2011a). These expansions out of Africa and into Arabia occurred along the posited southern dispersal route (e.g. Quintana-Murci, 1999; Stringer, 2000; 2003; Field & Lahr, 2006; Field *et al.*, 2007; Oppenheimer, 2008).

What happened next remains a mystery. Did these MIS 5 populations die out during the MIS 4 climatic downturn, as the *tabula rasa* scenario predicts? This question cannot yet be unanswered, given that there is still too little information on MIS 4 and MIS 3 occupation(s) of Arabian. It is noteworthy that the few dated assemblages from this time period bear no resemblance to either Levantine or African industries after MIS 5 (<74 ka BP). The geographic distribution of modern mitochondrial DNA (mtDNA) haplogroups

(e.g. Černý *et al.*, 2011; Fernandes *et al.* 2012; Al-Abri *et al.*, 2012), evidence from Late Pleistocene archaeological sites (e.g. Armitage *et al.*, 2011; Rose *et al.*, 2011a; Delagnes *et al.*, 2012; Usik *et al.*, 2012;), and climatic record (e.g. Fleitmann & Matter, 2009; Rosenberg *et al.*, 2012) hint at some degree of population continuity in the Late Pleistocene of Arabia.

Archaeological evidence from Arabia is even more rare from MIS 2 and early MIS 1. The possibility of population continuity versus discontinuity across this oscillating hyperarid-pluvial cycle has considerable implications for the demographic source of “Neolithic” populations in southern Arabia. In the past few years, the Holocene peopling of Arabia has increasingly become a subject of debate. Uerpmann *et al.* (2009) propose that a specific *tabula rasa* event took place in Arabia between 34 and 12 ka BP. During this interval, the prehistoric populations that inhabited southern Arabia are thought to have died out and been replaced by groups emigrating from the Levant in the Early Holocene. In support of this hypothesis, researchers point to a sterile sand lens found at Jebel Faya NE-1, which is interpreted as an archaeological hiatus between the Holocene occupation and Palaeolithic assemblage A. This localized sand layer has been dated by OSL between 40.2 ± 3 ka and 38.6 ± 3.1 ka BP (Uerpmann *et al.*, 2009; Armitage *et al.*, 2011). The archaeological layer attributed to the Early Holocene at Jebel Faya NE-1 contain what Uerpmann *et al.* (2009) refer to as the “post Palaeolithic occupation of Arabia”; a designation that implies fundamental cultural differences between these two periods. Blade production and tanged arrowheads characterize the Jebel Faya NE-1 and many other early Holocene assemblage from southern and eastern Arabia, which has led Uerpmann *et al.* (2009, 211) to draw a connection between the Arabian Neolithic and Levantine PPNB:

Putting the observations of blade arrowheads and domestic herds together, many scholars working in eastern Arabia have long supported the tacit assumption that the earliest occupation of the region, which to this day has not demonstrated relationship with earlier Paleolithic populations in the Arabian peninsula, may have had its roots in the stockbreeding, blade arrowhead-using, PPNB cultures of the southern Levant (Uerpmann *et al.*, 2009, 211).

This posited connection between South Arabia and the Levant (dubbed by

Uerpmann *et al.* 2009 the “Levantine Hypothesis”) is based on the results of the Danish Archaeological Expedition to Qatar in the 1960s. A distinct constellation of sites was reported by the expedition, containing an elaborate blade production technique¹ associated with the manufacture of pressure and flaked tanged arrowheads, which they termed “Qatar B-type.” These were dated by a single radiocarbon date to the end of the 6th millennium BC, and were speculatively attributed to a southward migration of Levantine pastoralists into Arabia (Kapel, 1967).

This dissertation explores an alternate scenario to *tabula rasa*: did early humans persist in southern Arabia across one or more climatic downturns? Specifically, this study examines whether there was population continuity across the Late Glacial Maximum (LGM), which took place between 20 and 15 ka BP, or whether hyperarid conditions led to an extinction of the Late Pleistocene indigenous inhabitants of the peninsula. Archaeological research undertaken throughout Arabia has unearthed some stone tool assemblages that bear distinct local characteristics that may signal the persistence of human populations during climatic downturns (e.g. Marks, 2009; Rose & Usik, 2009; Rose, 2010; Armitage *et al.*, 2011; Delagnes *et al.*, 2012; Usik *et al.*, 2012). The emergence of such local cultural evolutionary trajectories are possible through the persistence of human populations within environmental refugia such as the Arabo-Persian Gulf (Rose, 2010) and the Red Sea basin (Bailey, 2009). An additional refugium within southern Arabia may have been the landscape spanning the Hadhramaut Plateau, the Yemeni Highlands, the Dhofar escarpment, and the Nejd Plateau in Oman, which McCorriston *et al.* (2002, 63) designate the “South Arabian Highlands.” Providing relatively stable and predictable cycles of annual precipitation, this region may have provided habitable conditions, in which South Arabian populations might have survived during hyperarid phases. Such environmental refugia are posited to have played a significant role in the survival of plant and animal species throughout the world during Pleistocene glacial cycles (Steward & Stringer, 2012).

1 A bidirectional blade technology that makes use of naviform cores (Inizan, 1978; 1980a; 1980b).

It is posited that within these refugia, given time and demographic isolation, human groups unique cultural features will be formed. In prehistory, where stone tool technology is the most durable relic of cultural transmission, such distinct cultural features can be defined through the analysis of technological traditions. This, however, is complicated by the possibility that the *tabula rasa* and refugia hypotheses are not mutually exclusive, particularly given the varied landscapes found across Arabia. It is necessary to consider that some technological features were erased by population bottlenecks² linked to climatic downturns, while others may have survived in more favourable areas, where they were able to adapt to challenging, albeit still habitable conditions. In any discussion of prehistoric demographics in Arabia, it must be emphasized that the region is not simply one homogenous landmass; rather, the peninsula is composed of a mosaic of diverse environments, as will be seen throughout chapters Three and Four. Therefore, a thorough understanding of the landscape and a rigorous use of designations concerning stone tool industries are necessary for a broader understanding of Arabian prehistory.

To address the possibility of demographic continuity in Arabia, this dissertation explores an indeterminate Late Pleistocene/Early Holocene archaeological tradition in southern Arabia referred to as the Nejd Leptolithic. This designation, which describes the morphology of a particular group of assemblages that are ubiquitous across the Nejd Plateau, derives from the Greek word *lepto* meaning “slender”, “fine”, and “slight”. The term was reintroduced into the literature by Monigal (2002) in her monumental dissertation “The Levantine Leptolithic” (Monigal, 2002). In order to fully define and describe this lithic technocomplex in southern Arabia, the research presented here uses lithic attribute analysis, quantitative analysis, and refitting data from fieldwork conducted in the Dhofar Governorate between 2010 and 2012. For the purposes of this dissertation, the Nejd Leptolithic tradition falls within the “Late Palaeolithic” of Arabia, a term that shall be used

² Population bottlenecks are a reduction in size of a population. Such events may be triggered by catastrophic events such as volcanic eruptions, glacial conditions, or severe drought. The major effect of such a population bottleneck is the reduction in genetic variability within a given population (Ambrose, 1998; 2003).

to refer to assemblages presenting none MP/MSA features and preceding the emergence of pastoral communities across southern Arabia.

The definition of various techno/typological packages within the Late Palaeolithic is achieved by synthesizing these new data collected by the Dhofar Archaeological Project (DAP) to organize the diverse assemblages into a temporal and geographic framework. I will explore techno/typological parallels elsewhere within Arabia and outside the peninsula. In doing so, this dissertation seeks to clarify whether the Late Palaeolithic assemblages of Dhofar are derived from a northern migration (i.e. Levantine PPNB populations), a migration from either the Gulf or Yemeni highlands refugia, a population movement from Africa, the product of endemic development, or a combination of these possibilities.

This thesis is divided into four sections: background information is described in Chapters Two and Three; analytical methods and research design are presented in Chapters Four and Five; data and analyses appear in Chapters Six to Eight; and summary, synthesis, and conclusions are discussed in Chapter Nine.

Chapter Two summarizes the archaeological record of the Late to Terminal Pleistocene (50 to 10 ka BP), focusing specifically on the stratified and dated sites found across southern Arabia. Although the record from this period is meagre, the three known stratified sites provide some insight into this previously unknown archaeological phase. The sites al Hatab, Shi'bat Dihya and Jebel Faya NE-1 are considered in terms of local and regional settings, chronology, and lithic assemblage characteristics. The chapter concludes with a comparison of technological and typological features among the assemblages.

Chapter Three summarizes the available palaeoclimatic data for southern Arabia, reviewing the substantial climatic and environmental fluctuations that have affected this region. The terrestrial and marine archives used to reconstruct environmental oscillations that affected Arabia over the course of the Late Pleistocene and Holocene are presented. Different climatic regimes influencing southern Arabia, such as the Indian Ocean winter and summer monsoons, Shamal winds, and Northwesterlies are described. The chapter

concludes with a summary of the palaeoenvironmental chronology and implications for prehistoric demographics.

Chapter Four provides the reader with an overview of arid/semi-arid geomorphology and the different environments of the study area in the Governorate of Dhofar. Within Dhofar, the Nejd Plateau deserves special emphasis given its rich archaeological heritage. Understanding of the dynamics that produced the geomorphological features found across Dhofar is essential for working in and describing the immediate surroundings of the prehistoric sites presented in the data chapters. Following the discussion of landscape geomorphology, Chapter Four reviews the wider ecological and geographic context of the study area and describes the site sampling strategies.

Chapter Five addresses the methodology to carry out the lithic analysis that is the core of this dissertation. The reproduction of specific technological sequences and their use as descriptive and classificatory aids are explained. The *chaîne opératoire* concept is elucidated. The attribute analysis designed specifically for this study is presented and the qualitative and quantitative attributes that have been recorded on blanks, cores and tools are defined. Additionally, the various techniques used by archaeologists to reconstruct the diverse blank production strategies employed by prehistoric flintknappers are explained. Central to this analysis are the stages of core reduction that are reconstructed by lithic refitting studies. The methodology section concludes by summarizing the different lines of evidence used to categorize the samples collected during DAP's 2010-2012 fieldwork campaigns.

Chapters Six through Eight present the sites and data that were mapped and analysed over the course of this study. Comments on the sites' general location, geological setting, raw material availability and disposition will be given, providing a comprehensive description of the localities based on the methodology described in Chapters Four and Five. The three chapters are organized by survey transect: ALPHA, BRAVO and GULF transects.

In the case of buried sites, stratigraphy and dating methods are also provided. The context of each surface site is considered in regards to horizontal distribution of artefacts and post-depositional displacement.

The lithic samples from selected, relevant sites found along each transect are then described. The results of the qualitative and quantitative analyses carried out on the assemblages are presented. Observations regarding artefact class counts, raw material type, artefact size, condition, morphology, etc. are provided. Together, these descriptions serve as the building blocks used to articulate the technological and typological features of the Late Palaeolithic in Dhofar. Particular effort has been placed on the reconstructions of the core reduction sequences through refittings, which are described and illustrated.

Chapter Nine synthesizes the archaeological data presented in Chapters Six to Eight. From this, it is possible to define a specific industry associated with the Late Palaeolithic of Dhofar. This technocomplex is then considered within an intra- and inter-regional framework. The Late Palaeolithic of Dhofar is compared to contemporaneous assemblages within and around the Arabian Peninsula. In particular, its relationship to the Levantine PPNB is evaluated to assess archaeological affinities. Coeval archaeological records in the Horn of Africa and the Zagros in Iran are also considered to explore the possibility that these regions were the source of human populations that moved into the South Arabian Highlands around the Pleistocene-Holocene transition.

ARCHAEOLOGICAL EVIDENCE FROM SOUTH ARABIA DATING BETWEEN 50 TO 10 KA BP

As the newly found assemblages presented here show, there is much more to the prehistory of southern Arabia than its use by early modern people as a pathway to Australia. What little we know points to a long and complex local prehistory that needs explanation within a local framework.

–Anthony E. Marks, *Into Arabia, perhaps, but if so, from where?* (2008, 16)

Publications on the Pleistocene archaeology of Arabia typically start with this sentiment: “Very little is known about the Palaeolithic of Arabia”(Marks, 2009, 295); “...the middle Palaeolithic record of the Arabia Peninsula has been sidelined in Paleoanthropological synthesis...” (Petraglia & Alsharekh, 2003, 671); “Unlike Palaeolithic studies in other parts of the world, ..., Arabian prehistory has remained (pardon the pun) in the Stone Age” (Rose & Bailey, 2008, 65); “Over the past 20 years a virtual moribundity has descended on Palaeolithic research in the region of the Persian Gulf” (Scott-Jackson *et al.*, 2009, 125). Despite the dearth of physical evidence, for decades, scholars have puzzled as to the role the peninsula played in hominid dispersals over the course of the Pleistocene (e.g. Caton-Thompson, 1954; Tchernov, 1992; Lahr & Foley, 1994; Stringer, 2000; 2003; Derricourt, 2005; Mellars 2006; Field & Lahr, 2006; Field *et al.*, 2007; Rose 2007; Parker & Rose 2008; Marks 2008, 2009, 2011; Petraglia, 2011).

The situation has changed and Arabia is no longer *terra incognita*. As this chapter’s epigraph suggests, we find that prehistoric Arabia was more than just a highway for population dispersal. On going research continues to produce unexpected data, requiring a reconsideration of fundamental assumptions. This chapter presents a synthesis of dated and published assemblages that are beginning to clarify Palaeolithic occupation in Arabia during the later half of the Late Pleistocene (Rose & Usik, 2009; Armitage *et*

al., 2011; Delagnes *et al.*, 2012; Hilbert *et al.*, 2012). A period that has received copious amounts of speculation in the literature, specifically in regards to the dispersal of modern humans out of Africa after 70 ka BP, but has not yet been tested against the archaeological record (e.g., Mellars, 2006; Field *et al.*, 2007; Oppenheimer, 2009). As the first chapter of the background section the published data on the Palaeolithic archaeological record of Southern Arabia will be explored here.

Rather than providing the reader with a detailed overview on the history of research starting from the first archaeological prospections and survey activities undertaken in Arabia, a task that has already been carried out by several authors (Zarins, 1998; Rose, 2000; Petraglia & Alsharekh, 2003; Rose, 2006; Crassard, 2007), this chapter will focus on recently dated archaeological evidence pertaining to the later half of the Late Pleistocene (MIS 3 and MIS 2 respectively).

Archaeological evidence signalling a human presence in Arabia during MIS 3 (60-20 ka BP) and MIS 2 (20 – 10 ka BP) comes from Jebel Faya assemblages A in the United Arab Emirates (Armitage *et al.* 2011), Shi'bat Dihya 1 and 2 in Yemen (Delagnes *et al.*, 2012) and a series of collapsed rockshelters in southern Oman (Rose & Usik 2009, Hilbert *et al.*, 2012) (Figure 2.1).



Figure 2.1 Map showing the location of MIS 3 and 2 sites.
1, Shi'bat Dihya; 2, al Hatab; 3 Jebel Faya NE-1. (Map Google Earth®)

2.1 Assemblages A from Faya NE-1

Between 2003 and 2010, a joint German (Institute of Early Prehistory of the University of Tübingen) and Emirati (Directorate of Antiquities of the Department of Culture and Information) expedition has conducted archaeological investigations at the Jebel Faya NE-1 site in the central region of the Emirate of Sharjah (UAE). The site is characterized by a prominent rockshelter positioned on the northeastern flanks of the Jebel Faya limestone anticline. To the east of the site, a wide plain dissected by short-lived erosional gullies transporting water away from the escarpment may be described. To the south, a well-developed palaeolake sequence has been mapped and studied (Parton *et al.*, 2010; 2012). Debouching from the site itself, a small drainage channel meanders towards the plain. It was this particular geomorphological feature that ensured a constant supply of water for occupants of the site throughout prehistory, also acting at times as a highly destructive erosional force. During periods of increased precipitation, sediment and clastic debris was transported down from the limestone escarpment and deposited in front of the rockshelter, causing considerable sedimentation over time.

Over the course of eight seasons of excavation, researchers working at Faya have exposed a five metre deep, multilayer site containing a lithic assemblage bracketed between MIS 5e (130 – 115 ka BP) and the present. Jebel Faya NE-1 is currently the most extensive Pleistocene site excavated in Southern Arabia; by the end of the 2008 field campaign, a total of 150 m² had been excavated (Figure 2.2 – 2.3). Although detailed publication of the site is still in preparation (Marks, personal communication), some aspects of the sites stratigraphy, dating and general observations on the lithic material have been made available (Marks, 2008; 2009; Uerpmann *et al.*, 2009; Armitage *et al.* 2011).

According to these publications, four main phases of occupation may be identified at Jebel Faya NE-1 rockshelter: (1) assemblage C, composed of stone tools tentatively attributed to an early movement of AMH out of Africa at the onset of the last interglacial ~130 ka BP; (2) assemblage B, which is bracketed between assemblage C and A attesting

for a relatively continuous occupation of the area across the Late Pleistocene; (3) assemblage A, in which the associated geological unit was dated by OSL to 40.2 ± 3 ka and 38.6 ± 3.1 ka BP; (4) the overlying Holocene assemblage, for which little has been written other than that it contains tanged arrowheads (simple arrowheads that present minimalistic retouch to the hafting element at its base which form a short protruding “foot,” also called a tang or peduncle), dating to 8,454 – 7,761 Cal. BC (Uerpmann *et al.*, 2009).

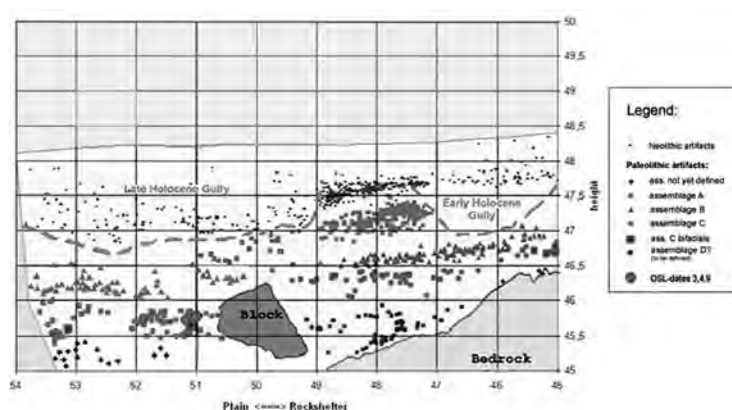


Figure 2.2 Photograph of the site. (Left) Excavations at Faya NE-1 during the 2008 field campaign (Photograph by Y. Hilbert).

Figure 2.3 Profile of the main section from Faya NE-1. (Above)(Armitage *et al.*, 2011, fig. S4).

Given the MIS 3 date for assemblage A, this industry falls within the period of consideration in this dissertation, and so will here be summarized. Assemblage A is separate from the underlying assemblages B by sterile sediment and may be stratigraphically distinguished from the overlying Holocene industries by a localized sand layer; dated to 38.6 ± 3.2 and 34.1 ± 2.8 ka.

Artefacts are manufactured on local raw material, primary chert that outcrops on the flanks of the Jebel Faya limestone *cuesta* (from Spanish: a ridge formed by gently tilted sedimentary rock strata in a homoclinal structure); nodules vary greatly in size and knapping properties. The technological repertoire of the MIS 3 occupants includes parallel, kombewa and radial cores (Figure 2.4). Most frequent are multiple platform cores

for the production of flakes. Among these types, the reduction sequence is characterized by alternating platforms where the former plane of removal is used as a new platform from which further removal on a new plane of the core takes place. No striking platform preparation, nor preparation of the respective work surfaces was observed on either blanks or cores. Percussion was administered with the use of the direct hard hammer technique (Armitage *et al.*, 2011).

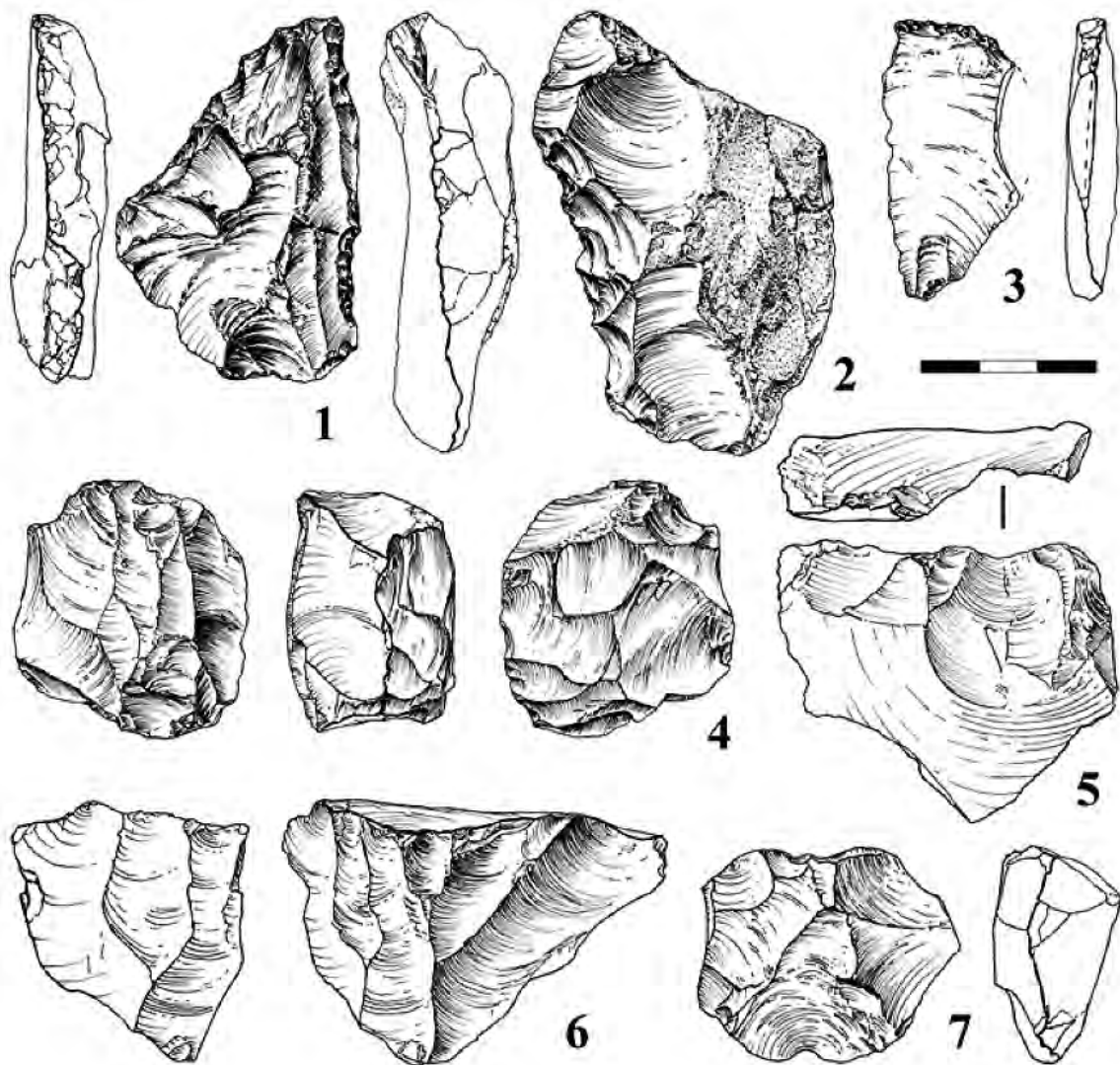


Figure 2.4 Artefacts from assemblage A.

1, Converging straight side scraper; 2, Denticulate; 3, inversely retouched endscraper; 4, Multiple platform core; 5, Kombewa core; 6 single platform core; 7, radial core.

(After Armitage *et al.*, 2011, fig. S7)

Cores and blanks are of small dimensions. Owing to the successive change in blank removal directionality, *débordant* elements occur relatively often within assemblage A. Although blades (Leptoliths) occur within this assemblage, there is no indication of deliberate blade or bladelet production. Armitage *et al.* (2011, Supporting online material) note that “the paucity of retouched tools and the relatively large number of cores indicates that the Assemblage A represents a primary workshop area.” Tools are of generic character, consisting of denticulates, endscrapers, a single burin, and informally retouched flakes. There are no indications of bifacial production, backing, bipolar cores, carinated pieces, retouched points, or any other such diagnostic UP/LSA techno-typological features found in surrounding regions.

So far, no comparable assemblages have been found anywhere in or outside the Arabian Peninsula. As noted by the researchers, the workshop character and generic tool forms found within assemblage A make the affiliation of this industry challenging. In southeastern Arabia, the use of multiple platform cores has been documented in several assemblages of the mid to late Holocene (Usai, 2005; Charpentier, 2008; Rose *et al.*, 2011b; Hilbert & Azzarra, 2012), making the identification and affiliation of surface sites with a comparable suit of technologies to Faya assemblage A problematic.

2.2 Shi’bat Dihya

The Shi’bat Dihya site complex, situated at the base of the Yemeni Highlands and bordering the Tihama coastal plain, has revealed several localities indicating human occupation during an arid phase in mid-MIS 3 (Delagnes *et al.*, 2012). At the confluence of Wadi Surdud and two of its tributaries, Shi’bat Dihya and Shi’bat al Sharj, a basin has formed, where a series of archaeological sites have been found preserved within a sedimentary sequence composed of interstratified sands and silts (*ibid.*). At Shi’bat Dihya 1 (SD1), artefacts were found eroding from a natural section cut by recent fluvial activity. Archaeological excavation undertaken by the Paleo-Y project between 2006 and

2008 (Delagnes et al, 2008; Macchiarelli, 2009), have revealed a rich buried find scatter composed primarily of flint-knapping debris and a small sample of faunal remains.

All artefacts have been found within the *Shi'bat Dihya member*, a truncated alluvial sediment body. Geomorphological and geochemical analysis of this sediment log indicated that the deposition of the strata containing the archaeological finds prevailed during a dry climatic phase. Additional sites have been found by the Paleo-Y project at two other localities in the area; namely Shi'bat Dihya 2 (SD2) and al-Sharj 1 (AS1). SD2 is situated approximately 100 metres south of SD1 on the opposite side of the riverbank. Stratigraphically, the SD2 material has been found seven metres above the stratum containing the SD1 assemblage. Approximately 400 metres further to the west and stratigraphically six metres above SD2, researchers have found the AS1 material. The two sites, SD2 and AS1, were found in different stratigraphic positions, although both within the *Shi'bat Dihya member*. Thus, SD1 is stratigraphically the oldest occupation of the three identified sites, while AS1 belongs to the latest phase.

Nineteen OSL samples were taken in order to place these distinct industries into an absolute chronological framework by dating the deposition of the sediments. From these samples, an average of 55 ka BP was established for the SD1 sediments. Samples retrieved from SD2 and AS1 have presented slightly younger mean ages, suggesting that the deposition of the upper portion of the *Shi'bat Dihya member* took place between 55 and 45 ka BP. Notably, this 10 thousand year time frame also encompasses the error margin of the dates provided by the OSL analysis.

All artefacts found were manufactured using local raw material, a large portion of which (over 93%) was manufactured on fine-grained rhyolite. Within the lithic assemblage of SD1, a smaller numbers of quartz, basalt, sandstone and phonolite artefacts were found. These raw materials have been found cropping out from primary deposits on the northern banks of the Wadi Surdud and in secondary context within the 150 to 200 meter wide wadi bed.

Technological and typological comparisons were made between the samples from SD2 (n=1.336) and the robust samples from SD1 (n=30.488). Concerning sample sizes, the authors state that “...archaeological investigations run so far at both SD2 and AS1 have only provided an initial sample of their lithic industries, given the small size of the excavated areas (for SD2, cleaning of the section)”(Delagnes *et al.*, 2012, 4).

A total of 21 m² have been excavated at the SD1 locality (Figure 2.5). Excavations were undertaken in square meter units following the previously identified layers (*décapage* method). All artefacts larger than 2 cm have been piece plotted and the excavated sediments have been sieved. Spatial distribution of the artefacts indicates some degree of post depositional disturbances caused primarily by the flooding and deflooding of the overbanked deposits, which buried the site in the first place. Within the find scatter, the researchers were able to identify clear concentrations within the scatter that represent discrete knapping events. Artefacts found within these concentrations are derived from a specific raw material nodule or raw material type (such as rhyolite, basalt etc...), further attesting the pristine condition of the site.

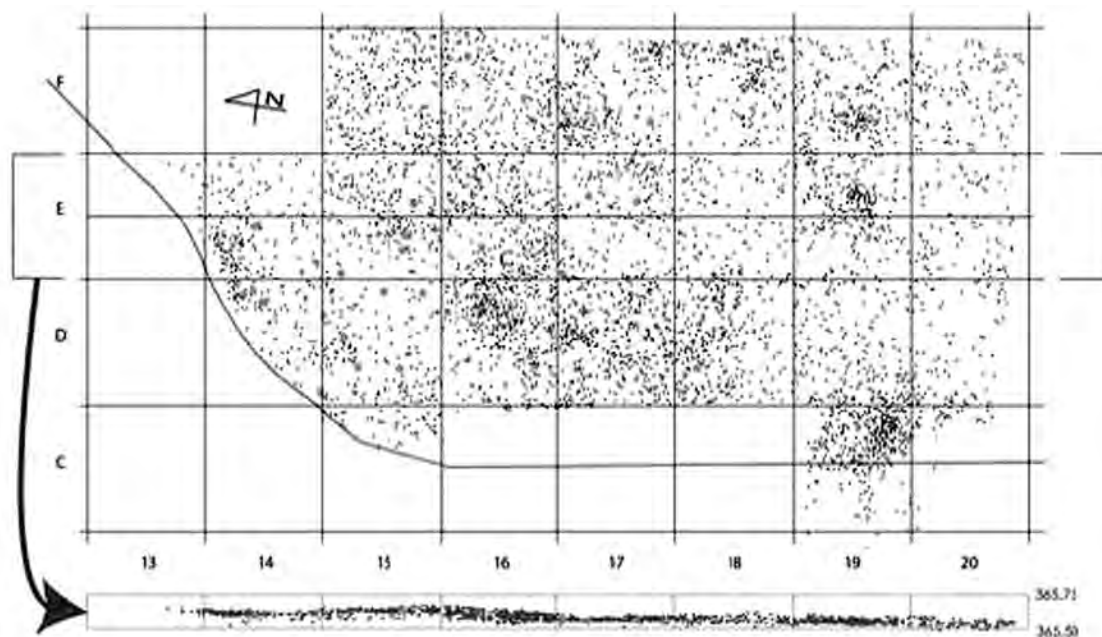


Figure 2.5 Plan showing the concentration at SD1.
(After Delagnes *et al.*, 2012, fig. 4)

The lithic samples from SD1 and SD2 were studied using attribute (qualitative), metric (quantitative), and refitting analyses. Based on these studies, the researchers were able to identify techno-typological patterns enabling them to thoroughly describe the Shi'bat Dihya assemblage. Both samples are chiefly composed of blank production by-products; including cores, chips and blanks (Figure 2.6). Few tools have been found and they have not been regarded as particularly indicative of any specific industry.

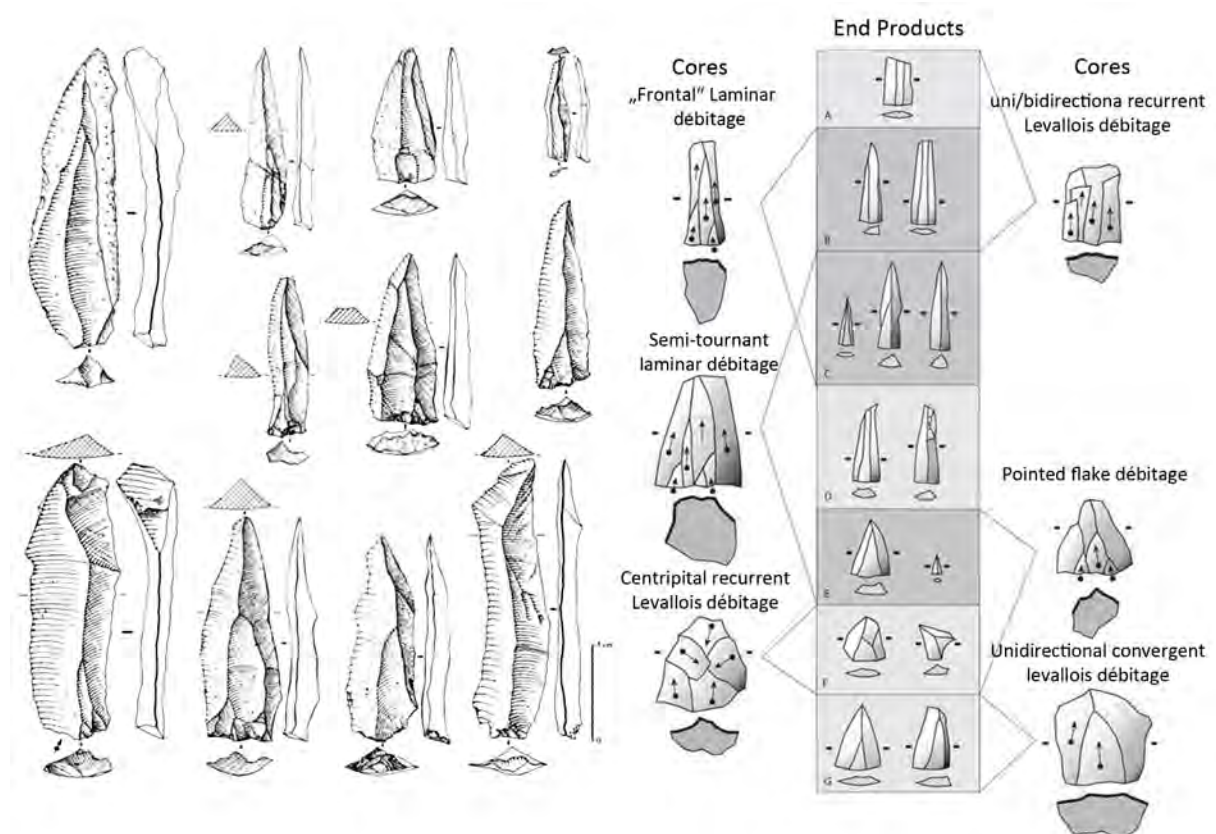


Figure 2.6 Artefacts from SD1.

(Right) elongated débitage form SD1; (Left) principal reductions strategies employed at SD1 and their related end products. (After Delagnes *et al.*, 2012, fig. 9 and 10)

Three distinct volume management strategies have been observed, based on the refittings of blank production sequence: *semi-tournant*, frontal (*sensu* Delagnes, 2000) and an atypical variation of the Levallois technique. According to the diagram presented by the authors, it is possible to discern the variability within the reduction modalities and

blank shapes produced. It is also evident that the production of Leptoliths was favoured over the production of flakes. While the semi-tournant and frontal reduction strategies have preferentially produced elongated blanks, it may also be said that a fair amount of the flake-proportioned *débitage* was produced using these strategies. The blade *chaîne opératoire* (chain of reduction), aside from the occasional removal of a partial crested element, or the preparation of the striking platform by a maximum of three removals, is marked by its simplicity. The raw material volumes are exploited using direct hard hammer percussion; used hammerstones have been found associated with the lithic scatters at SD1. Flintknappers took advantage of the raw materials morphology during the reduction process; in many cases blade production was initiated by the removal of a naturally crested element (*lame d'entame*) (Delagnes et al 2012). The Levallois-like reduction method however, has produced clear distinguishable blanks; mostly short with rectangular to convergent edges.

It was possible to recognize an association between the reduction method and the raw material used. The majority of lithics artefacts found at the site have been manufactured on rhyolite using the two blade and pointed flake-blade reduction strategy and to a lesser extent the Levallois-like reduction of flat pebbles on their widest dorsal or ventral surface. Two basalt chopping tool/cores were found at the site, while the remaining artefacts made on the other raw materials consist of undiagnostic primary flakes or unmodified pebbles.

Tools, purposefully modified volumes of raw material, are rare and consist of undifferentiated retouched pieces. Among these, notched and denticulated blanks are most common (Figure 2.7).

Sample sizes for the SD1 and SD2 samples are of different sizes (SD1 n= 30.488 and SD2 n= 1.336), making the direct comparison between the two sites problematic. While the SD1 assemblage is dominated by blade and point-producing strategies, the SD2 assemblage contains primarily unifacial centripetal cores. The difference between the two assemblages may be related to the small sample and the scattered disposition of the site

showing artefacts concentrations separated by areas of low artefact density. Possibly the sample from SD2 represents one isolated knapping event within a larger site.

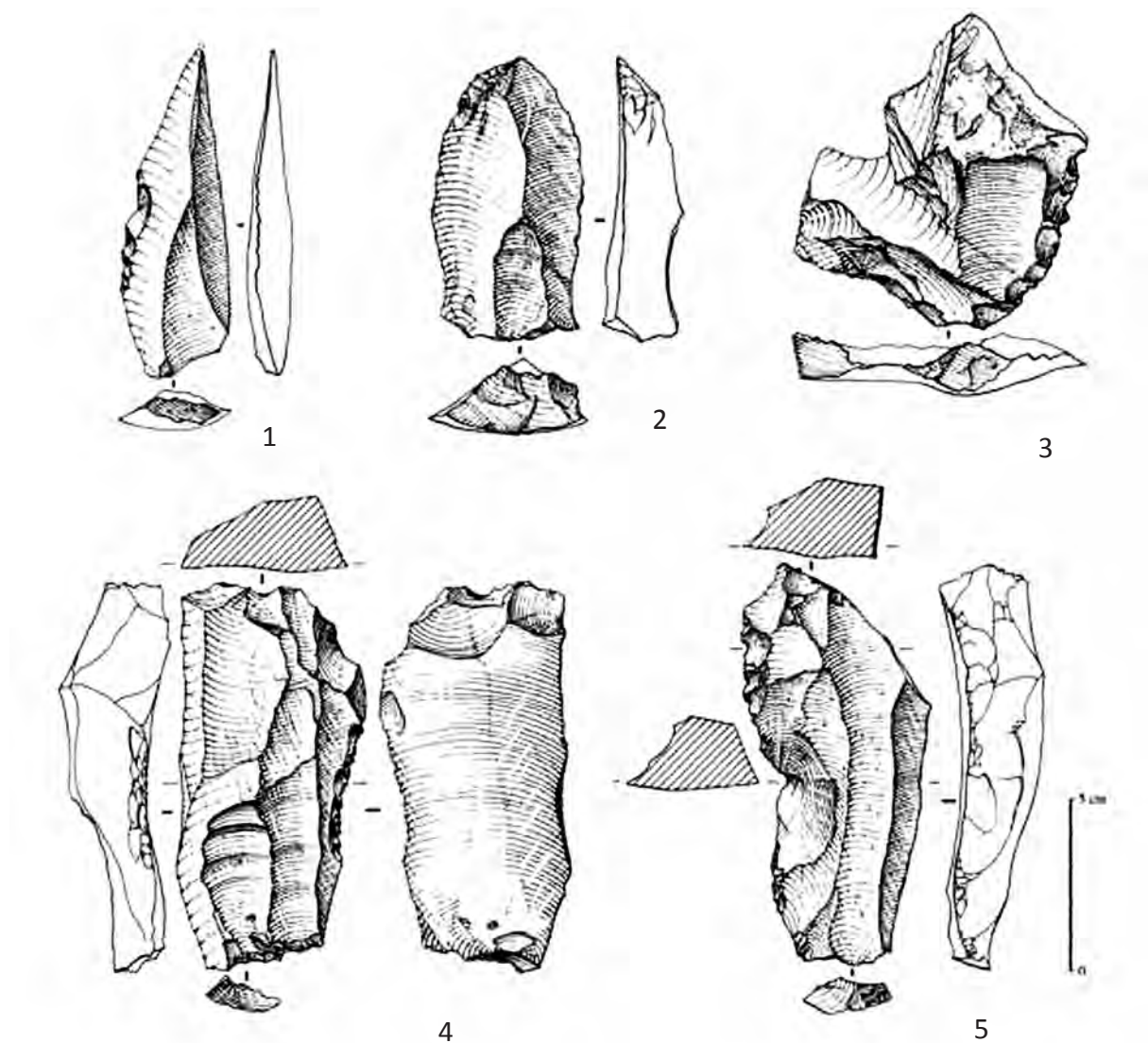


Figure 2.7 Tools from SD1. 1, 2 and 5 retouched blanks; 3, denticulate; 4, atypical endscraper (After Delagnes et al., 2012, fig. 15).

2.3 Al Hatab

Evidence for a MIS 2 occupation of southern Arabia comes from Dhofar, in the far south of Oman. In 2004, the Dhofar Archaeological Project (DAP) research team discovered the site of Al Hatab (TH.29). The small collapsed rockshelter is situated on the southern

Nejd plateau, just north of the Dhofar Mountains. A preliminary description of the lithic assemblages, C14 and OSL dating, and stratigraphy are described in Rose & Usik (2009), while detailed aspects of the lithic technology, namely the blank production sequences, have recently been published in Hilbert *et al.* (2012). Two archaeological levels have been excavated and both are attributed to the Nejd Leptolithic Tradition (*Ibid.*).

As noted above, Al Hatab is a small collapsed rockshelter on the northern fringe of Jebel Ardif. South of al Hatab, the Dhofar mountain chain towers nearly 200 metres over the Nejd Plateau and over 800 metres above sea level (Platel *et al.*, 1992). To the east of the site there is a tributary of Wadi Dawkah, while to the west and north the plateau is dotted by occasional limestone inselbergs.

Al Hatab is characterized by a semicircular depression upon which erosion has carved out a low (max. 120 cm in height) limestone overhang. Two rockshelters situated on the facing flanks of the depression have been identified; both were scoured of sediments by erosional action. Two gently grading talus slopes, one on each side, are cut by a small gully that runs parallel to the longitudinal axis of the site and disembogues into a flat wadi terrace to the east (Figure 2.8).

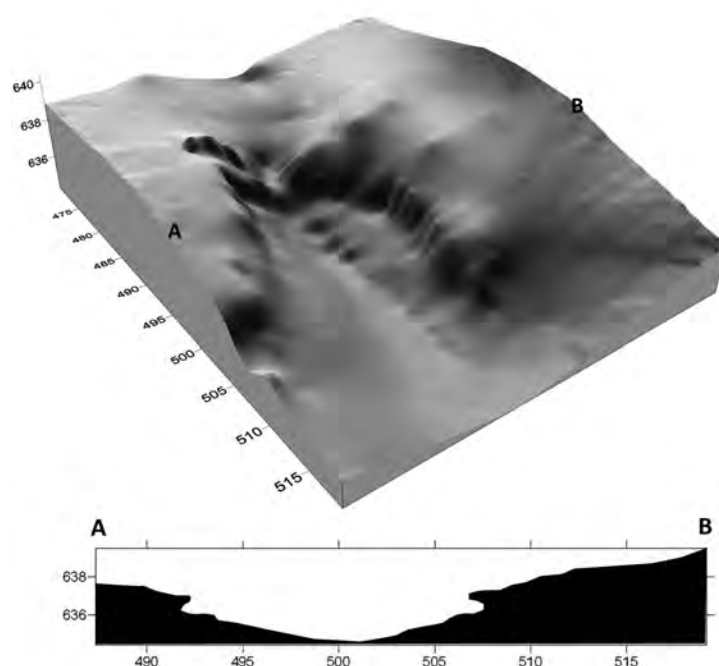


Figure 2.8 Topographic map of al Hatab. The image is vertically exaggerated in order to provide better topographic understanding of the site. Cross section showing the talus and rockshelter situation. (Image by Y. Hilbert).

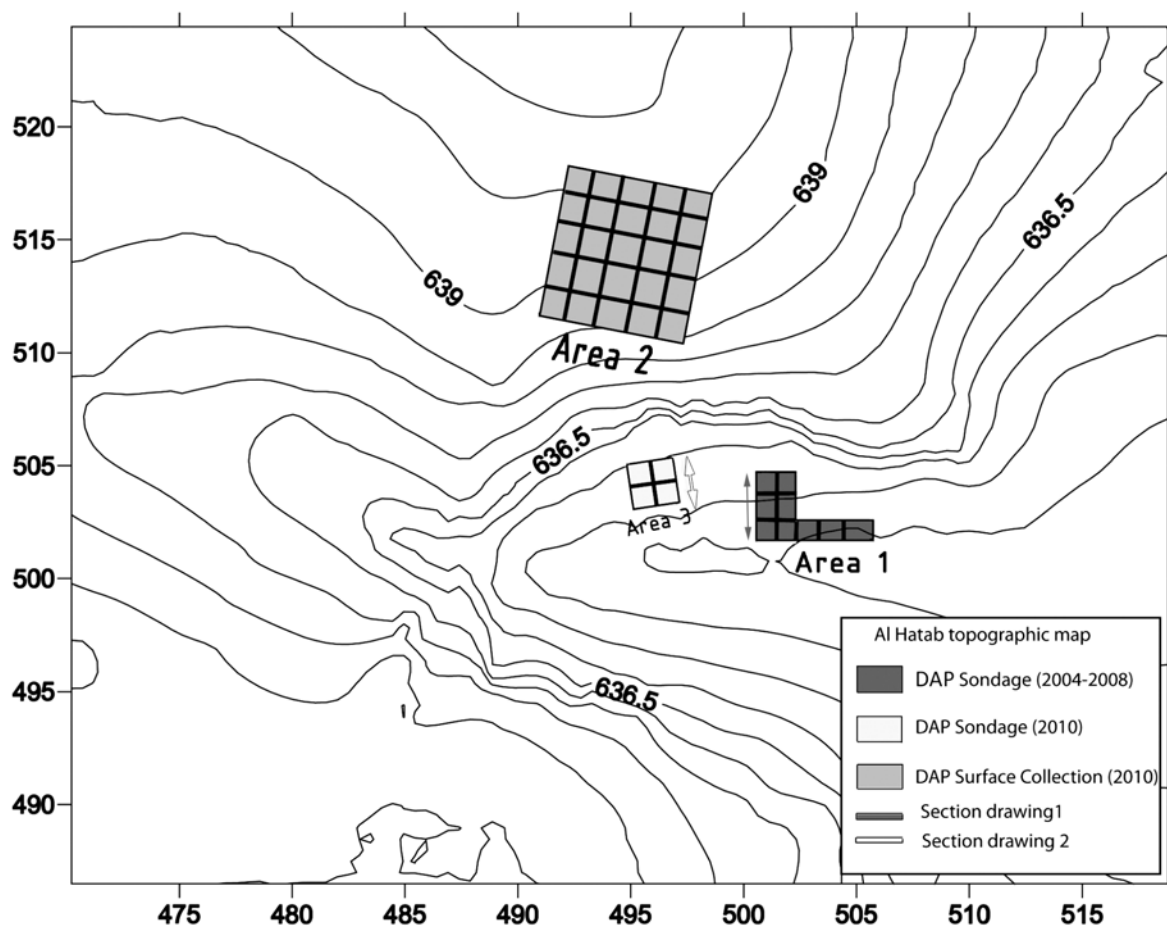


Figure 2.9 Excavation areas at al Hatab.

Topographic map showing the position of the test pits and systematic surface collection undertaken at Al Hatab. (Image by Y. Hilbert).

Al Hatab was excavated intermittently between 2004 and 2010. By the end of the 2010 field season, a total of thirteen square metres had been excavated, yielding 3556 artefacts; including tools, cores, blanks and chips¹. During the 2010 field season, the DAP team conducted additional surface collections above the rockshelter to test for differences between the surface and buried assemblages (Figure 2.9).

Geoarchaeological investigation have revealed two archaeological levels and articulated eight geological horizons (GH). The sequence exposed in the eastern section of area 3 (Figure 2.10) is composed of a minerogenic suite of gravel- and silt-dominated

¹ Artefacts smaller than one centimetre.

sediments with both natural and chipped chert debris inclusions. Of the eight GH that have been detected, GH 1 and 2 most likely relate to deposition during the mid to late Holocene, the GH 2b was cut by an intrusive Iron Age hearth. GH3 is a poorly sorted diamict (a sediment that consists of a wide range of non-sorted to poorly sorted sands or larger size particles including a wide range of fine and coarse components), which in this context suggests a colluvial deposit probably deriving from the mechanical and chemical breakdown of both the walls and roof of the rockshelter. The thickness of this GH towards the northwest suggests that the sediments originated from the back of rockshelter and not from the small tributary wadi in which al Hatab is formed. GH 4 is composed of moderately compacted sands and silt ordered in a homogenous manner. This depositional sequence may relate to a brief phase of increased eolian activity. GH 5 and 7 are primarily characterised by coarse sediments, comprised of fine gravels that do not appear elsewhere in the exposed profile. While the coarse inclusions found within GH 3 indicate a downslope movement, the inclusions in GH 5 and 7 suggest that the wadi deposited these sediments, possibly during ephemeral flooding events. GH 6 is found sandwiched between the fluvial/colluvial episodes represented by GH 5 and 7, perhaps due to an intermittent phase of aridity. At the base of the sequence is GH 8, which is a thick (~40 cm) accumulation of silt and fine sand that contains occasional coarse components.

Anthropogenic chert debris has been found interstratified throughout most of the sequence and is attributed to two archaeological horizons (or levels). Archaeological level 1 artefacts have been identified in GH 3 and 4 while artefacts attributed to level 2 have been excavated from GH 5 and 7.

The two OSL samples (Tube 1 and 2 in Figure 2.11) provide an approximate age for the al Hatab level 1 and 2 assemblage between 14.1 and 11.7 ka BP. An additional C14 sample from a non-burrowing terrestrial snail (*Euryptyxis latirefl exa*) from the top of level 1 produced a date of $10,430 \pm 140$ cal. BP (Beta-237899) (Rose & Usik, 2009). Thus placing the al Hatab assemblage at the end of MIS 2 and the beginning of the Holocene.

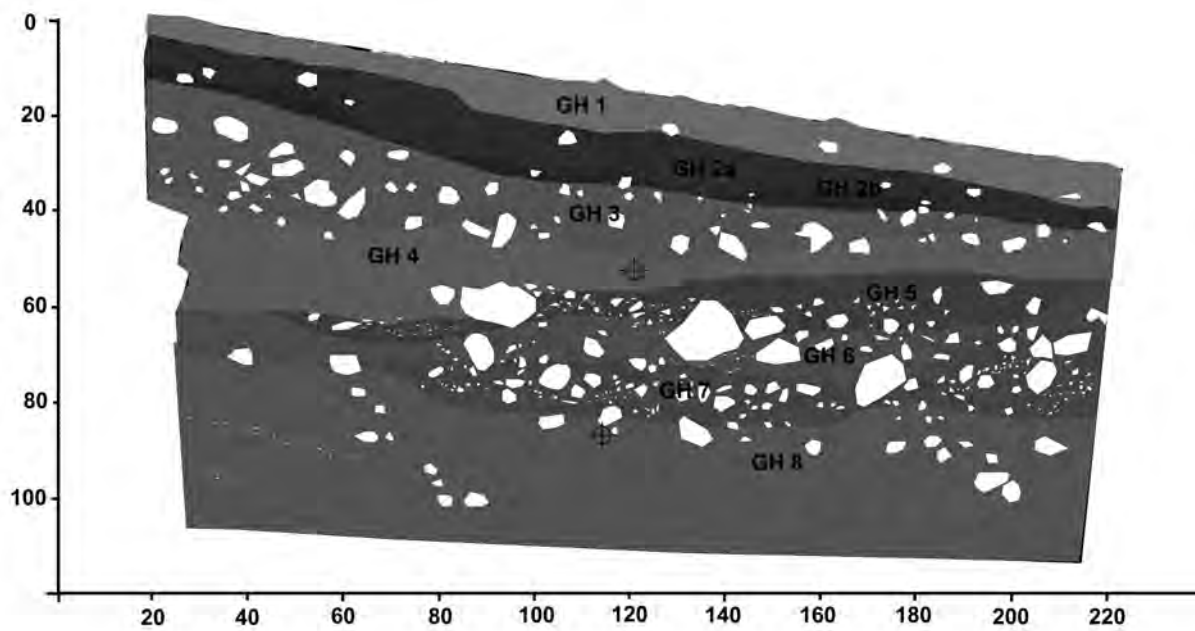


Figure 2.10 Section 2 from al Hatab area 3. The figure depicts geological horizons (GH). (Image by Dr. M. Morley and Y. Hilbert).

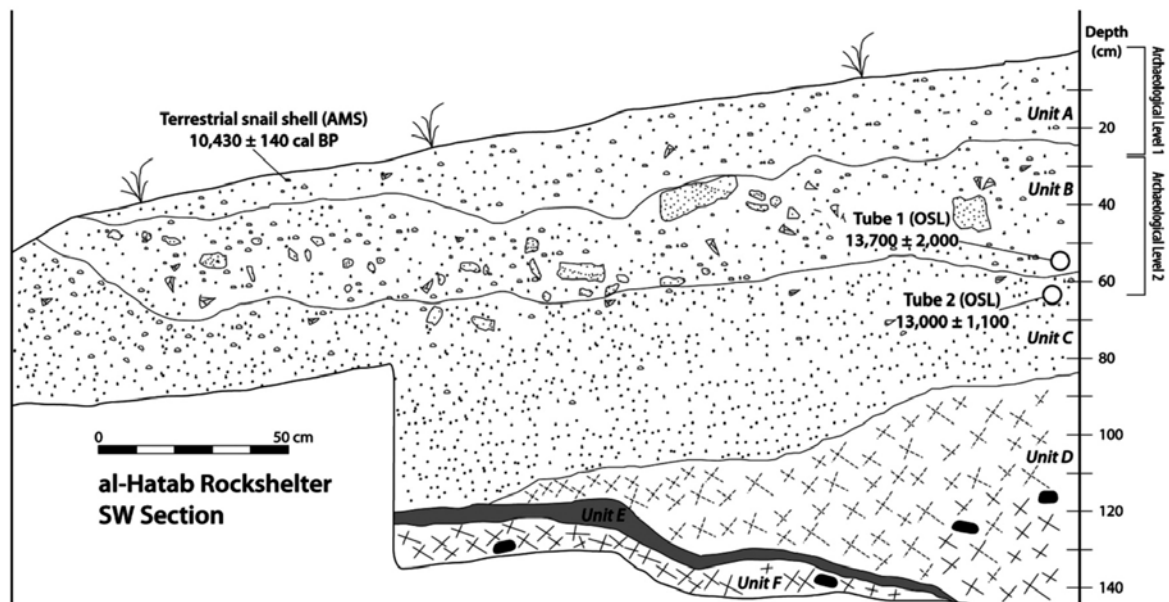


Figure 2.11 Section 1 from al Hatab area 1. The figure depicts the position of the OSL samples and their respective dates (After Rose & Usik., 2009, fig. 5).

Artefacts have been manufactured exclusively on chert nodules and blocks that crop out from the Rus Formation. Two distinct raw material types are found within the Rus Formation, Gahit and the Aybut chert-bearing members. Both geological members have high to moderate quality chert nodular inclusions that vary greatly in size and disposition. At al Hatab, three chert varieties have been identified: (a) Gahit 1 is characterized by a thick chalky cortex, nodules are of medium size (max. 25 cm in diameter) and are of light grey coloration when freshly knapped; (b) Gahit 2 has a thin dark cortex, when freshly knapped the raw material presents itself in grey to bluish hues with distinct dark banding; and (c) the Aybut chert characterized by a thin, yellowish and coarse cortex, with a yellow patina; when freshly knapped, the chert is grey and slightly translucent.

Artefacts recovered from both levels have varying gradients of patination, ranging from white to dark brown. As the geoarchaeological investigation of the site suggests, both the sediments and the artefacts found there have undergone some degree of post depositional displacement. Aside from the extreme white to dark brown patination range, additional taphonomic alteration is exhibited on the artefacts. A small portion of the sample excavated in 2010 (n=32 from total n=758) has a light red iron oxide film, while four have a black manganese film. Both features have been found in combination with minimally weathered, whitish patinated artefacts (Figure 2.12). This divergence in patination indicates that some amount of redeposition occurred and hints at the different conservations states within the sediments. Organic materials, however, could not be detected.

Blank production and tool types are fairly similar in both archaeological levels (Rose & Usik 2009). Blank production systems are strictly laminar; most commonly, cores are exploited in unidirectional parallel fashion from either a narrow edge of a raw material block or the frontal face of a rounded nodule. The use of additional working surfaces has been attested; these new planes of removal are commonly placed adjacent to the main work surface (*Semi- tournant sensu* Delagnes, 2000) (Hilbert et al., 2012). This

particular blank reduction modality is linked with the production of blades and bladelets; nonetheless flake proportionate blanks are also by-products of this reduction modality. Blank production is dictated by the continuous production of blades. Little preparation to either the striking platform or the work surface is evident, interconnected core convexity maintenance measures, called débordant elements, are used to ensure a recurrent (continuous) blank production. Reduction directionality is strictly unidirectional; the few examples of bidirectionality are due to the abandonment of a former striking platform in exchange for the opposed platform, allowing the flintknapper to reduce an untapped volume on the same nodule (*Ibid.*). In addition to this particular reduction modality, which has been reconstructed through refits from Level 1 (Figure 2.13), a strictly volumetric reduction has been observed (Rose & Usik, 2009). To a lesser extent, the production of kombewa elements was carried out as well (Rose, 2006; Rose & Usik, 2009). The kombewa method is used to produce small circular flakes with flat cross sections, always struck from other flakes (e.g. Tixier & Turq, 1999; Usik, 2004).



Figure 2.12 Artefact patination at al Hatab. 1 Patina with red oxide film; 2 two patination phases; 3 dark surface patina; 4 light/whitish patina (Photograph by Y. Hilbert).

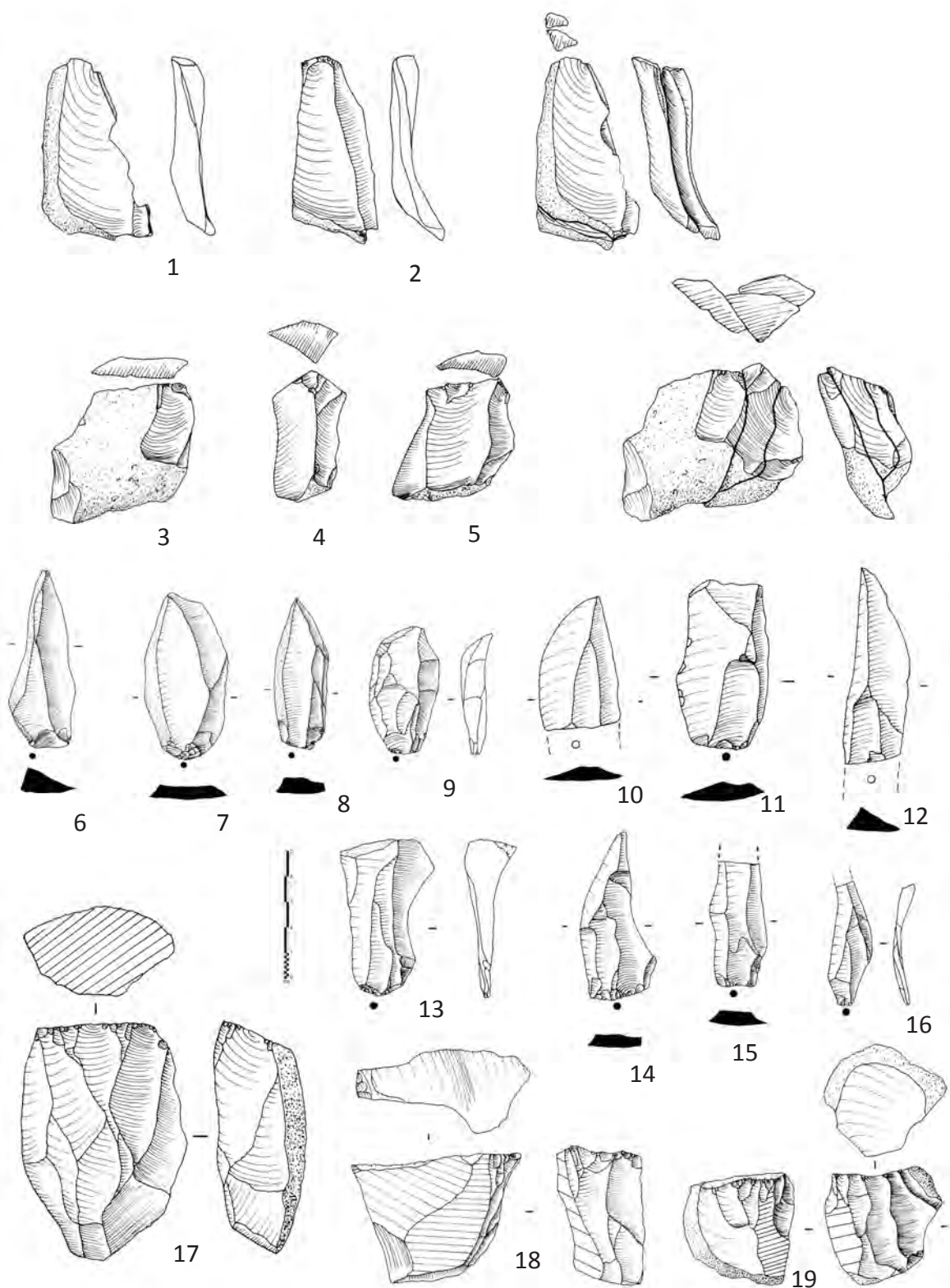


Figure 2.13. Artefacts from al Hatab. 1 to 2 , refitted débordant blades; 3 to 5, refitted débitage; 6 to 16 diverse blades and débordant blades; 17 single platform unidirectional core; 18 single platform core with work surface on narrow portion of raw material block; 19 single platform core with lateral work surface. (Illustrations by Y. Hilbert)

Flakes, blades and chert nodules have been modified into both formal and informal tools. Formal tools are recognized by a repetitive pattern of shape and/or retouch including burins, endscrapers, heavy sidescrapers, perforators, and bifacial foliates (Figure 2.14). While burins show some degree of variability, the majority of these tools were manufactured on blades. Most often at al Hatab, the characteristic “burin blow” was administered along the long-axis of the blank, struck from a specially prepared truncation. Also found within the assemblage are two tanged projectile point, one in each level. These points show no intentional modification other than the peduncle (tanged) hafting element at its base, a form resembling the “Fasad point,” which is thought to characterise the Early Holocene in southern Arabia (Charpentier 2008). A variety of bifacial implements have also been excavated from both levels at al Hatab (total n=10). These are made by hard hammer percussion and display a variety of shapes and cross sections. Commonly, these are biconvex in cross section and of oval to elongated in shape. Notably, they are cruder in manufacture and do not share the thin, lenticular cross-section that characterise the “Khasfian” bifacial foliates described in Rose (2006).

The similarities between these two levels cannot be explained by post depositional mixing. Given the clear differentiation within the sediments in which these two archaeological horizons were excavated, level 1 being related to the mechanical break down of the roof and back of the shelter, while level 2 is found within overbank fluvial deposits. It is unlikely that these artefact were produced elsewhere and brought to the site by fluvial activity and/or slope waste. Thus, we interpret the OSL and AMS dates to indicate that the site was visited intermittently between 14 and 10 ka BP, suggesting a more or less continuous occupation across the Pleistocene-Holocene boundary in Dhofar.



Figure 2.14 al Hatab Tools. 1 to 5, diverse burins on truncation; 6 retouched blank; 7 partially retouched point; 8 Fasad point ; 9 and 10, biface. (Illustrations by Dr. V. Usik and W. Spring).

2.4 Summary

From this review, three basic observations can be made: (a) evidence for occupation of southern Arabia during MIS 3 and 2 is scarce but present; (b) the technological and typological packages found across southern Arabia are unlike that of its adjacent regions (a.i. Levant, Africa and Asia); (c) there is a techno-typological discrepancy between Faya NE-1 assemblage A site and the sites situated in the South Arabian Highlands.

While the lithic industry uncovered at Jebel Faya assemblage A has no parallels anywhere inside or outside Arabia, the SD1/SD2 and al Hatab assemblages share a specific blade technology. The archaeological finds from Dhofar and western Yemen are not individual cases and may be related to a pan-southern Arabian leptolithic tradition. Blade assemblages have been found across the Hadhramaut and Dhofar (e.g. Amirkhanov, 1994; Rose, 2006; Crassard, 2007; Hilbert *et al.*, 2012), while further extensive scatters have been recorded in central Oman and the Rub al Khaly desert (e.g. Biagi, 1994; Jagher *et al.*, 2011). To which extent these blade assemblages were coeval still remains to be determined. Given that the majority of these sites are surface scatters chronological attribution has to be done in relation to climatic events visible on the landscape and the findscatters themselves. The next chapter will explore the climate record of southern Arabia in order to establish a succession of dry and wet phases in order to determine a relative chronology for the archaeological record.

Although al Hatab, Shi'bat Dihya 1, and Faya NE-1 assemblage A have been found in different regions of South Arabia and most likely represent different technocultural units, they all share one thing in common: their deposition did not occur during a wet phase. In considering the temporal ranges of these assemblages, it should be stressed that they were all dated using OSL, which does not provide a direct age of the archaeological occupation, and rather gives a minimum age for the deposition of the sediments in which the artefacts were buried. This limits our ability to draw conclusions regarding the significance of these sites, other than their technological description and rough timeframe during different phases of MIS 3 and MIS 2.

As aforementioned these sites and their assemblages provide a valuable frame of reference for the many surface sites found in Arabia. Despite the wide differences in age, the persistence of a laminar technological component throughout the South Arabian Highlands indicates some degree of technological continuity between the human occupation found at Shi'bat Dihya, and later occupation excavated al Hatab. The sites presented in this chapter

have almost nothing in common with any other techno/typological complex outside of Arabia, suggesting the development of autochthonous lithic industries regardless of the climatic conditions governing the peninsula.

The perusal of a possible continues human occupation across Southern Arabia calls for certain questions and estimations. Namely how variable is the Late Palaeolithic record across Arabia? Does the Late Palaeolithic of Arabia have a local or exogenous source? And ultimately what happened to it? Did the local Early Holocene communities of Dhofar independently developed “Neolithic” subsistence strategies or did populations carrying these new technologies replace them? The majority of these questions are based on the premise that population continuity is possible within climatic refugia and that population continuity causes some degree of material cultural stability, which is detectable through lithic analysis. Stability within the material cultural record means that decedents of a given population, archaeologically represented by a lithic industry, will show a techno/typological package comparable to the package of their ancestors. While this discussion may be further explored by analysing new assemblages, the issue involving the climatic oscillations can be elucidated by a review of the South Arabian paleoclimate.

CLIMATE FRAME AND DATA FOR SOUTH ARABIA

Evans and O'Connor defined climate as the interplay of cool and warm air masses, variation in pressure and humidity, local topography, latitude and global hydrosphere, whether in the form of oceanic water or polar ice (Evans & O'Connor, 1999, 12-13). The following background chapter will explore the interplay between the diverse features named above and synthesise the available climate data of Southern Arabia. From the review of the archaeological record presented in chapter Two, it is obvious that the Arabian paleo-climate was subjected to oscillations during the Pleistocene. These oscillations had some effect on the indigenous populations, possibly constraining their habitat during climatic downturns. During periods of amelioration the Arabian landscape carrying capacity increases, allowing expansion from within and possibly outside of the Peninsula to spread across its landscapes. The perusal of the paleo-climatic record of Arabia may help to establish how intense these climatic oscillations have been and whether climatic downturns were inevitably responsible for population discontinuity across the Late Pleistocene.

The published record of Arabia's paleo-climatic history is rich and manifold (e.g. McClure 1976; 1978; 1984; 1988; Burns *et al.*, 1998, 2001; Neff, 2001; Preusser *et al.*, 2002; Parker *et al.*, 2006b; Parker, 2009; Rose, 2006; Rose & Parker, 2008; Fleitmann *et al.*, 2004, 2007; Hoorn & Cremaschi 2004, Cremaschi & Negrino 2005; Beineke, 2006; Lézine *et al.*, 2007; Fleitmann & Matter, 2009; Preusser, 2009; Parton *et al.*, 2010; Rosenberg *et al.*, 2012). It has been pointed out that the emphasis in Arabian climate research has favoured the reconstruction of the terminal Pleistocene and Holocene environments (Fleitmann *et al.*, 2003; Parker, 2009). Over the past decade mid- to late Pleistocene environmental

reconstruction based on terrestrial records have contributed to an increasingly complex account of Arabia's environmental history. The inaccessibility of some key areas in the Arabian Peninsula and the destructive depositional character of its sediments, however, still hamper the advance of climate research in the peninsula.

Over the next pages diverse data sets, the deep-sea-cores and ice-cores, terrestrial records, lacustrine deposits, pollen diagrams and alluvial features, will be presented and discussed as to their implications on the reconstruction of past climatic events. The Indian Ocean Monsoon, South Arabia's main weather system will be discussed regarding its periodicity and intensity. Special attention will be given to the impact this major force has on Southern Arabia. A short synthesis of Arabian paleoclimate based on the available literature will follow. In this chapter's summary the relations between climatic deterioration, population demographics and environmental deterministic models, such as the *tabula rasa*, will be discussed.

3.1 The Marine record

Global climate is dictated, among other elements, by the disposition and amount of water available in the earth's weather system. A major role in this equation is played by the expansion and retreat of glaciers in the northern and southern hemispheres during cooler climatic phases. These glacial phases had great influence on the global climate given that they trapped large quantities of water within the glaciers across the planet. Indirect evidence for climate changes is provided by continuous deep-sea cores and their O^{18} and O^{16} isotopic values. During glacial periods, evaporated water containing the lighter O^{16} isotope becomes trapped within glaciers, leaving the oceans with a higher concentration of the heavier O^{18} Isotope. The O^{16} and O^{18} isotope ratios become incorporated in the carbonated skeleton of deep-sea foraminifers that build up the ocean floor sediments. By analysing the O^{16} and O^{18} ratios of deep-sea cores, the intensity and periodicity of glacial and interglacial periods can be estimated. The global Marine Isotope Stage (MIS)

sequence consists of even number, representing glacial periods, and uneven number, representing interglacial or warm phases. The MIS may also been detected on the basis of ice cores retrieved from the North and South Poles (Webb & Bartlein, 1992; Petit *et al.*, 1999; Waerlbroeck *et al.*, 2008).

Deep-sea cores relevant for the review at hand were retrieved from the coasts of Oman, Yemen, the Strait of Hormuz, the north west and east of the Indian Ocean (Schulz *et al.*, 1998; van Rad *et al.*, 1999; Leuschner & Sirocko, 2000; 2003). The marine cores provide data that helps understand greater global climatic phenomena. Additionally the driving forces behind the major weather system acting on the area in focus, the IOM, are elucidated (Clemens *et al.*, 1991).

Marine sedimentation dynamics in the Arabian Sea are dictated by the seasonality of the south western and north eastern monsoons. The south western monsoon-induced upwelling on the South Arabian coast influences the bio-productivity of the Arabian Sea (Ivanochko, 2004; Schulz *et al.*, 2002a; 2002b; Saher *et al.*, 2007). Indices of bio-productivity may be used to measure monsoonal intensity over the time span of the last decades and beyond. Data on sedimentation rates under present conditions provide scientists with valuable information when analysing older deep sea sediment cores.

The inversion of the atmospheric pressure zone over the Arabian Peninsula across the summer and winter months additionally affects marine productivity and terrestrial climate conditions. During summer months the temperature over the Arabian Peninsula is higher than the temperature over the sea surface, causing the activation of south westerly winds bringing in moisture from the sea into South Arabia. The inverse condition is observed during winter months, when seawater surface temperatures are higher than over the Arabian land mass, causing dry north-eastern winds to blow toward the ocean (Zarins, 2001: 22). Past changes in the Earth's orbit and solar radiation have greatly influenced the dynamics over the Arabian Peninsula causing a drastic increase in monsoonal intensity (Clemens *et al.*, 1991; Lézine *et al.*, 1998; Lauchner & Sirocko, 2003).

This increase results in higher precipitation levels, which influence the landscape carrying capacity across the area.

The Intertropical Convergent Zone (ITCZ), which may be described as a narrow convergent wind and precipitation zone that dictates the onset, periodicity and strength of the rainfall in tropical zones, additionally played a role in the weather dynamics over South Arabia (Fleitmann *et al.*, 2007; 2011). Under present conditions, the ITCZ and its associated precipitation belt rests south of the equator during winter months. This condition and the high pressure cells over the Eurasian continent result in moderate north eastern winds over the Indian Ocean. Due to the heating of the northern tropical and subtropical continental landmasses during spring, the ITCZ migrates northward resulting in a pressure inversion, causing a shift in the wind regimes over the Indian Ocean (Figure 3.1). The south westerly winds bring in considerable amount of moisture from the equatorial zone, which is released over the northern Indian Ocean and subsequently South Arabia.

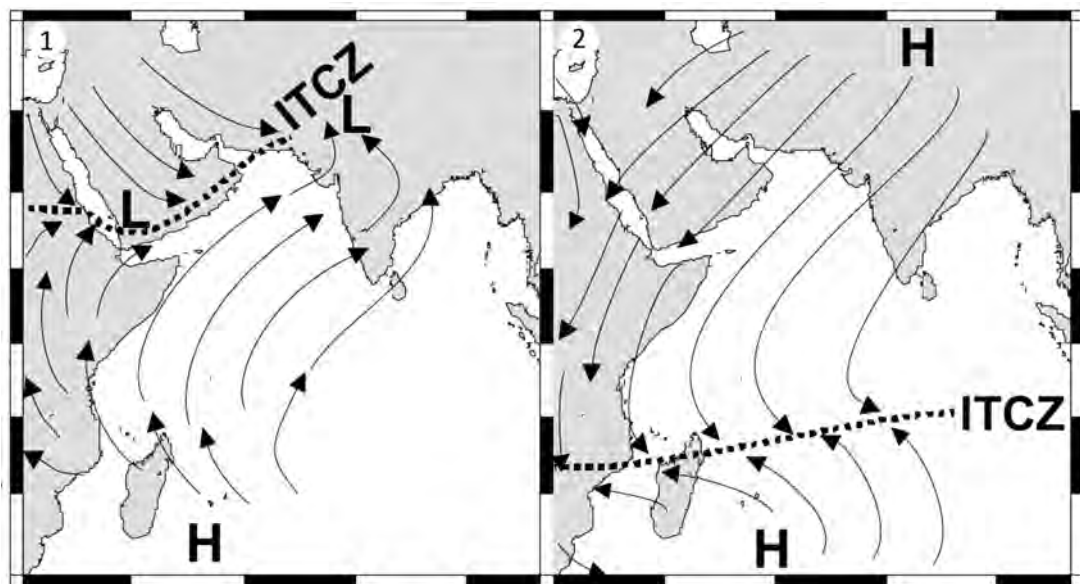


Figure 3.1 Migration of Indian Ocean Monsoon.

In part 1 of the image the position of the IOM during the summer months is depicted while in part 2 the position during the winter months is shown. The dotted line represents the Inter Tropical Convergence Zone. Arrows in the image indicate the directionality of the prevailing wind regimes. (After Fleitmann *et al.*, 2004, fig. 1)

Further implications of the northward migration of the ITCZ during the onset of the Holocene may be seen in speleothems from three different sites in Yemen (Socotra) and Oman (Dhofar and Hajar Mountains). Based on four sampled localities researchers were able to track the migration of this weather-forcing agent by means of dating cave speleothem growth (using Th-U dating methods¹). Speleothem growth provides a reliable indicator for both constant and periodic rainfalls. According to this study the mean latitudinal position of the ITCZ and its associated rain belt rapidly migrated northwards during the early Holocene. Over the course of the mid Holocene, however the ITCZ gradually migrated back southward as a response to solar insolation; causing decrease in precipitation and shortening of the summer monsoon phases (Fleitmann *et al.*, 2007).

The ice cores, deep sea cores and other marine data sets are key elements, helping scientists to understand fluctuations and periodicities of the earth's climate. Ice cores allow scientists the measure the content of green house gases in the atmosphere and the detection of rapid climate fluctuations (Orembelli *et al.*, 2010). Deep sea cores give information's regarding climatic fluctuations in the northern hemisphere and their effect on low-latitude monsoonal climate variability. Both data sets help shed light on global forcing agents such as green house gasses and atmospheric moisture (Schulz *et al* 1998). These agents have great affect on global climate; however, in order to understand the imprint they have on a more regional scale the investigation of local dynamics are needed. The climate fluctuations over southern Arabia are a response to diverse factors, as has been see a major role in this equation is played by the IOM and the migration of the ITCZ. These elements will therefore be further discussed over the next pages.

3.2 The Indian Ocean Monsoon

The Indian Ocean Monsoon (IOM) is the principal weather agent acting over

¹ The Uranium Thorium dating method is a radiometric dating method used to date calcium carbonates, such as cave speleothems and flowstones. Based on the detection by mass spectrometry of the Uranium (²³⁴U) and Thorium (²³⁰Th) products of decay and calculating the initial amount of both elements in the sample an absolute age for the carbonates can be obtained (Neff, 2001).

the Indian Ocean and the Arabian Sea. Its impact over South-West Asia, Arabia and the Horn of Africa is great under present conditions and was presumably also fundamental for prehistoric populations living in those regions during the Pleistocene. Understanding the elements governing the IOM under present conditions is of vital importance for comprehension of its past dynamics.

Forcing factors of the IOM intensity and periodicity are, after Clemens *et al.*, (1991) mainly related to insolation and heating of the continental and oceanic masses. Variations in the earth's obliquity and precessional orbit, the availability of latent heat and the amount of continental albedo, which is linked to the intensity and duration in continental glaciations, are further agents impelling monsoonal strength. According to Clemens and his team a strong relation between global insolation and the inclination of the Earth's axis during its orbit around the sun can be inferred. An equally fundamental part is played by the transport and availability of latent heat over the equatorial belt. In the case of the IOM this part is played by the accumulation and release of heat over the Asian Plateau (Clemens *et al.*, 1991, 725).

IOM peaks are related to solar radiation and its associated body of traits named earlier, the interplay of the atmospheric, topographic and climatic traits may be read from diverse lines of evidence. Deep sea cores bearing laminated layers have been collected along the Arabian coast. The laminations within these cores are related to silica based skeletons of planctonites foraminifera, mainly *Globigerinoides ruber*, *Globigerina falconensis* and *Globigerina bulloides* (Schulz *et al.*, 2002b). The presence and abundance of these planctonites relates to different oceanic conditions. Productivity levels, post-depositional and sedimentary factors dictate the presence of planctonites in marine sediment records.

In order to fully comprehend and draw conclusive data out of the marine cores retrieved from the Arabian Sea, the sedimentation, suspension and transport factors involved during monsoonal activity must be understood. The north eastern IOM creates a low pressure zone over Pakistan and north India that draws the equatorial trade winds

and subsequently generates a strong low-pressure wind jet, called the Findlater Jet stream, which blows parallel to the Arabian Peninsula (Rixen *et al.*, 2000). This stream is responsible for the disturbance of marine sediments along the Southern Arabian coast.

Schulz *et al.* (2002b) conducted investigations in the northern Arabian Sea off the Pakistani coast. There the weather regime is dictated by the north eastern monsoon, which is active during the winter months. Particle flux and plankton foraminifera samples collected from sediment traps retrieved by Schulz and colleagues helped to reconstruct the seasonal intensity of both, south western and north eastern monsoons for the past 25 ka BP. The researchers conclude that *Globigerina bulloides*, a foraminifera related to the south western summer upwelling showed little precipitation in the north eastern Arabian Sea. Whereas *Globigerina falconensis*, which is a marker for winter like conditions, was abundant in the north eastern Arabian Sea. Using the occurrences of these foraminifera, the settings in which these two specimens occur and the factors that lead to their dispersal across the Arabian Sea, Schulz *et al.* concludes that during MIS 2 the south western and the north eastern monsoons acted independently from each other. During the Heinrich Meltwater² and the Younger Dryas event the north eastern monsoon was active while the south western remained dormant. During the onset of the Holocene both systems become activated and show levels of intensity above the ones presently observed (Figure 3.2).

In concordance with the data presented by Schulz and colleagues, Ivanova *et al.* (2003) demonstrates a similar pattern for earlier monsoonal activity discordances. Based on foraminifera productivity ratios she and her team conclude that during MIS 1, 3 and 5 monsoonal related productivity peaks occurred induced by deep water upwelling. During the transition between MIS 5 and 4 a high foraminifera productivity event in the northern Arabian Sea may be marked, whereas the south western monsoon seems to show a low activity phase (Ivanova *et al.*, 2003, fig. 9).

² Heinrich events are typical for the North Atlantic Ocean marine cores and are characterized by coarse grained materials found in oceanic sediments these sediments were caused by ice rafted debris related to massive iceberg discharges into the Atlantic Ocean. These events, which took place every 10 ka years, had a cooling effect over the global climate (Claussen *et al.*, 2003).

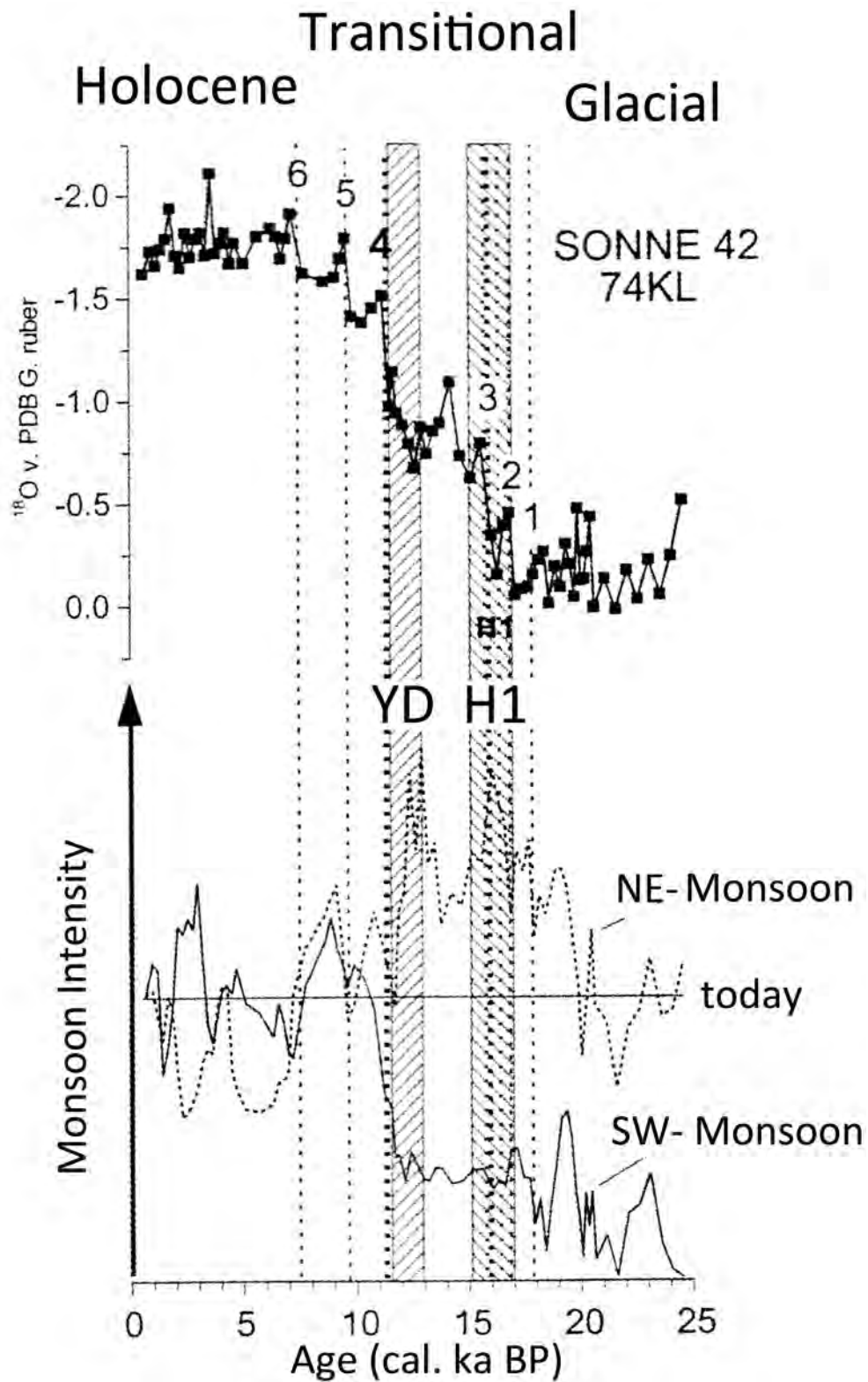


Figure 3.2 Monsoon intensity.

The graph presents the intensity of the NE-Monsoon and SW- Monsoon in relation to each other. (After Schulz *et al.*, 2002b, fig. 9)

The variability and periodicity of the IOM is linked to climatic oscillations that take place in the northern hemisphere, such processes are known under the term teleconnections. Glacial periods in the northern hemisphere and the IOM may relate to higher ratios of global insolation (Clemens *et al.*, 1991; Leuchner & Sirocko, 2003; Neff, 2001; Neff *et al.*, 2001). IOM intensity peaks coincides with northern hemisphere insolation and decreases in glacial ice volumes, therefore this climate agent is of great importance when analysing changes and variability in the Earth climatic history. In a millennial scale, monsoonal variations seem to be related to insolation forced pressure gradients over the central Asian plateau and the Indian Ocean (Leuschner & Sirocko, 2003).

The data and research presented here marks the Earth's climate as one interconnected system. The tendencies observed in the Arabian and Indian Ocean marine records indicate a strong relation between pressure zones, wind regimes, ice sheet extends and global insolation (Clemens *et al.*, 1991; Schultz *et al.*, 2002; Ivanova *et al.*, 2003; Leuschner & Sirocko, 2003). The data discusses here indicates that there are subtle differences in the south western and north eastern IOM regimes. This difference in monsoonal intensity over the Late Pleistocene probably influenced the archaeological record. The dissimilar archaeological pattern expressed by the Shi'bat Dihya and Jebel Faya NE-1 assemblages may be related to two different populations inhabiting two different areas affected by diverging weather systems. In order to measure the impact of the different Monsoonal regimes on the Southern Arabian landscape, and test the demographic implications indicated above, one has to turn his attention to the terrestrial record of this region.

3.3 The terrestrial records

The terrestrial climate record for Arabia is manifold; (a) ancient lake profiles that aside from giving information on wet phases may provide important pollen data (e.g. McCollure, 1976; 1978; Parker *et al.*, 2004; 2006a; 2006b; Lézine *et al.*, 2007; McLaren *et*

al., 2009; Parton *et al.*, 2010); (b) speleothem calcites, giving additional data on wet spells, variations between winter and summer precipitation rates and average temperatures (e.g. Burns *et al.*, 1998; Fleitmann *et al.*, 2003, 2004 and 2007; Fleitmann & Matter, 2009); (c) eolian sediments that may be dated using Optical Stimulated Luminescence³ (OSL), providing information about changes in wind regimes and sediment availability (e.g. Stokes & Bray, 2005; Glennie & Singhvi, 2002); (d) cave deposits (e.g. Cremaschi & Negrino, 2005; Immenhauser *et al.*, 2007); (e) inland alluvial fans (e.g. Blechschmidt *et al.*, 2009); and (f) coastal sediment deposits (e.g. Hoorn & Cremaschi, 2004).

Eolian environments make up most of the desert landscape in South Arabia. According to Holms (1960), approximately one third of the Arabian Peninsula is covered with sand; the Rub al Khali alone covers approximately 600.000 square kilometres of the 1.7 mil square kilometres of the Arabian Peninsula. Sand dune movements are chiefly dictated by local wind regimes. Arabia's eolian environments are dictated by two diachronic wind systems sweeping over the landscape in the past and under present conditions. The *Shamal* winds, mainly a winter phenomenon, blow down the Arabian Gulf and reaching the Emirates turn clockwise towards the Rub al Khali desert and the peninsulas interior. The south western monsoon winds blow from the African continent towards the Indian sub-continent and on their way sweep past the South Arabian coast line, passing over the Wahiba Sand and reaching the Omani Mountains. Those winds blow during the summer months and are responsible for sporadic torrential thunderstorms in the north of Oman (Glennie & Singhvi, 2002).

The origin of eolian sediments provides critical data on the variability of the wind systems over the Arabian Peninsula through time and the disposition of the landscape itself. During the Late Glacial Maximum (LGM) the global sea levels dropped due to the

³ This dating method makes use of the electrons trapped within the crystalline structure of quartz, feldspate or aluminum oxide grains in sediments or archaeological materials such as pottery and burnt flint. These electrons become excited by solar radiation or heat. Under controlled laboratory conditions, the electrons in a given sample become stimulated again causing them to emanate light. The photons are then detected using a photomultiplier tube. This device calculates the dose the sample had observed. It is then possible to infer the samples last exposure to sunlight or intense heat (Aitken, 1998).

amount of water trapped within the Earth's glaciers. Given the shallow depth of the Arabian Gulf, a great portion of this area became emerged. This area was dissected by the paleo-Tigris and Euphrates river basins (Lambeck, 1996). The dry sea bed would have been a prolific source of eolian sediments (Glennie & Singhvi, 2002).

In contrast to the notion of the dry Gulf being the source of unconsolidated sediment during the LGM, Stockes and Bray (2005) argue in favour of a divergence between sea level change and sediment supply. Based on OSL dates from paleo-dunes, test pits and exposed paleo-dune profiles, the researchers concluded that eolian sediment accumulation in the Liwa and Al Qafa regions of the Emirate of Abu Dhabi took place during MIS 5 (ca. 75-130ka) and MIS 1 (ca. 2-6 ka). Little evidence for eolian activity during MIS 2-4 could be found. This could be due to an extensive organic cover over the emerged Gulf-Oasis, which hampered sediment transport by eolian means. Combined with the north eastern monsoonal evidence, the eolian terrestrial record provides support for the Gulf-Oasis Hypothesis (Rose, 2010). Likely this region served as a refugia for human populations living in the area during MIS 4 and 2.

Using dune size indices, Warren and Alison (1998) reconstruct the paleo-wind regimes that shaped the Wahiba Sands in the north east of Oman. This sand desert, approximately 10,000 km² in size, is characterized by linear dunes with up to 60 metres in height oriented at a south to north axis (Figure 3.3). The researchers suggest that dune size is not related to wind intensity and sediment supply only. The periodicity of the weather regime that gave rise to the winds acting on central coastal Oman also played a considerable role in the emergence of the Wahiba Sands. Wind cycles trigger diurnal phases of eolian activity, these cycles coupled with sufficient sediments appropriate for wind transport lead to dunal displacement, growth or destruction. Past three metres of height, dunes become susceptible to destruction or redeposition. In order to remain developing in size a constant weather system are needed. Changes in global climate caused by oscillations in the Earth's obliquity, eccentricity and precession deeply influence the consistency of

regional wind regimes. Mega-dunes, as observed in the Wahiba Sands, occur because of long constant phases presenting the same climate or a series of successive, similarly manifested, phases with the same climate. Mega dunes accumulated in the Wahiba during the LGM, according to this theory.



Figure 3.3 Linear dunes at the Wahiba Sands, Oman.
(Photograph by Y. Hilbert)

Seashell fragments detected in the lithology of the Wahiba Sands sediments indicates a marine origin, the now submerged Omani continental shelf being the most probable source of the eolian sediments (Radies *et al.*, 2004). Eolian sediment aggregation appears to coincide with global low sea level periods. Given the marine environment and the northward migration of the ITCZ during favourable phases, sediment preservation as opposed to further transportation was hampered by punctuated wet spells during MIS 6 and 5. These events were responsible for dune stabilization and soil formation processes in the central Oman. OSL dating on eolian deposits in the area show four phases of deposition, MIS 1 ($10 \text{ ka} \pm 4$, $10 \text{ ka} \pm 1$), MIS 2 ($18 \text{ ka} \pm$, $23 \text{ ka} \pm 3$), early MIS 5 ($110 \text{ ka} \pm 11$, $117 \text{ ka} \pm 12$,

112 ka \pm 12) and MIS 7 (229 ka \pm 19) (Juyal *et al.*, 2006). Additional OSL dating provided by Preusser (2009) indicates further eolian accumulation during MIS 6, 5b, 5d, 4 and increased activity between 3-1, with a peak during the LGM. Apparently eolian sediment deposition in the Rub al Khali desert and the Wahiba sands were synchronous during dryer phases of both MIS 6 (186-130ka) and MIS 5d (115-106ka). The lack of eolian deposition in the Rub al Khali dating to that period may be related to absence of unconsolidated sediment and their constant redeposition. Probably sediment stabilization related to an extensive grass cover in the Arabian Gulf Oasis, or cementation of the sediments during this period would have hampered eolian sediment transport making up for the lack of deposits dating to the MIS 4 and 2 in central Arabia (Lambeck, 1996; Teller *et al.*, 2000). The accumulation of eolian sediment in central Oman and the Rub al Khali formed a desert that may have acted as a barrier hampering human movements between the Gulf Oasis and the South Arabian Highlands.

Fresh water lake deposits provide indirect evidence for wet phases across Arabia. McClure published some of the early radiometric dates on lake deposits in Arabia (McClure, 1976). The set of dates acquired from the fossil lakes in the Mundafa area in southern Saudi Arabia suggests two main phases of lacustrine deposits. The relatively recent deflation of the surface uncovered approximately twenty-eight metres of lake deposits consisting of calcareous and fossiliferous marl layers interstratified with eolian deposits. The two major depositional events were identified based on geomorphological aspects and radiometric dating methods. The lowest lacustrine deposit rest on top of alluvial deposits and date roughly to MIS 3, with a peak in deposition between 30 and 21 ka BP. These lake sediments are covered by eolian sands, which in turn are covered by a second lacustrine deposit dating to the early Holocene, 9 and 6 ka BP. Additional lake sediments have been recorded by Schulz and Whitney (1986) in the An Nafud region in northern Arabia. The sediment sequence is similar to the sequence described by McClure. The early lake phase consists of calcareous marl interbedded with eolian sediments dating between 8.4 and 5.4

ka BP. The lower lake sequences are Late Pleistocene in age and dates between 34.000 and 24.000 BP based on radiocarbon dates. Additional dates on lake sediments from Arabia come from a site called Al-Quwaiyah in central Saudi Arabia. McLaren and her research team (McLaren *et al.*, 2009) have produced OSL dated on fluvial deposits associated with lacustrine accumulations. The lake deposits have formed during more humid phases of the late Pleistocene, around 54 ka (MIS 3). The aggregation of lacustrine deposits in central Saudi is indicative of improved climatic conditions occurring across Arabia during MIS 3. Parallel to these discoveries in Parton *et al.* (2010) have uncovered a lake sequence close to Jebel Akhaba in the Emirate of Sharjah. The lake sequence uncovered at Akhaba presents successive aggregation and desiccation events going back to the MIS 6. Parton *et al.* identified a fluvial episode marked by gravels at 56 ka BP, MIS 3, roughly coinciding with the result from Saudi Arabia.

The geomorphology of South Arabia, with the Red Sea basin and the Arabian Shield to the west and the Hadhramaut and Dhofar Plateau to the south, may explain why during wet periods the IOM seldom reached the inland zones (Lézine *et al.*, 2007). The topography may have functioned as a moisture trap, causing the discharge of rainfall over these regions. Late Pleistocene and early Holocene lakes in Yemen (Davies, 2006; Lézine *et al.*, 2007), central Saudi Arabia (McClure, 1976, 1978; Schulz & Whitney, 1986) Oman (Urban & Buerkert 2009) and the UEA (Parker *et al.*, 2004, 2006a; 2006b; Parton *et al.*, 2010) support this assumption. In most of the sites the waters feeding the lacustrine environments during the early Holocene (12-7 ka) derived from run-offs coming from torrential seasonal precipitation in the mountains. Little evidence supports the notion that constant inflow from persistent flowing riparian settings have fed the lacustrine environments of Arabia. The lacustrine sediments are interlaced with eolian sediments, as seen in the samples from Liwa in the Emirates, the Maqta site in the north of Oman and the al-Hawa sediment series from Yemen. Such laminated sediments indicate that although these lakes have been formed rapidly, they persisted and where slow to dry out.

Botanical data from South Arabia strengthens the notion of soil formation processes during the early wet spells of the Holocene. A shift from C4 type vegetation generally associated with a warm and dry climate, to a C3 vegetation that is related to a savannah like humid and warm climate may be observed in localities across the Emirates and Oman (Urban & Buerkert, 2009; Parker *et al.*, 2004). This transition would have stabilized the large bodies of eolian sediments that accumulated during the dry phases and the short but rather strong sedimentation phase postdating the late Pleistocene to Holocene transition, particularly the Younger Dryas⁴.

While most terrestrial climate records in Arabia are from paleolakes, which are highly susceptible to C¹⁴ dating errors, cave speleothems may be accurately dated and therefore provide high-resolution climate data (e.g Fleitmann *et al.*, 2003; Preusser, 2009). South Arabia provides a variety of cave and travertine environments from where such information might be gathered. Karstic cave sequences from Dhofar, the north of Oman, Yemen and Saudi Arabia have yielded valuable Speleothem climatic data (Burns *et al.*, 1998, 2002; Neff, 2001; Fleitmann *et al.*, 2003; 2004; 2011; Fleitmann & Matter, 2009).

By measuring the oxygen ($\delta^{18}\text{O}$) and the hydrogen (δD) ratios of calcite speleothems, and analysis of the fluid inclusions trapped within the stalactites, the source of moisture and the respective intensity of wet spells over Arabia may be detected. Given the dating advantage of cave speleothems over lake deposits⁵, tracking wet spells by means of identifying speleothem growth periods as opposed to growth stagnation may provide continuous climatic data for South Arabia (Neff, 2001; Fleitmann & Matter, 2009).

A series of eleven stalactites from Dhofar and Northern Oman were analysed in order to create a reliable data set used to determine the dynamics of the IOM and the

4 The Younger Dryas, or „Big Freeze“, comprises a relatively short phase of approximately 1.300 years of cold climatic conditions in the temperate zones and severe drought across Africa and Arabia. This period of Rapid global climate change took place between 12.900 and 10.000 Bp.

5 Speleothems may be dated using Th-U method, by which samples older than 500ka may be dated, whereas lake deposits are traditionally dated using the C¹⁴ method which becomes highly incurred when the samples surpass the 40ka age barrier.

subsequent migration of the ITCZ. Speleothem growth phases and the isotopic signature of these samples provide further information on the periodicities and paucities of wet spells in South Arabia. Given that speleothems growth phases require moisture that seeps through cave systems, displacing and redepositing calcite on its way, Fleitmann and Matter identified five wet phases over the past 330 ka. These were interrupted by long periods of growth stagnation, phases where little to no moisture was present in the regions hydrology. Speleothem deposition coincided with interglacial periods related to the (Holocene, MIS 5a, 5e, MSI 7a and MIS 9. Speleothem growth seemed to follow phases of deglaciations in the northern hemisphere, pointing to maximum solar insolation and minimum glacial extent leading to subsequent albedo, forcing the IOM to discharge high amounts of moisture over southern Arabia.

Analysis of the speleothems from Hoti Cave (northern Oman) dating to the last interglacial (5e) revealed relatively low ^{18}O values, as opposed to the $\delta^{18}\text{O}$ water values recorded under present conditions further inland. The current sources of moisture in northern Oman are mainly the Northwesterly winds that blow down the Arabian Gulf bringing in moisture from the Mediterranean. The negative isotopic values identified in the Hoti Cave speleothems during the period between from 130 to 120 ka suggest a different source of moisture for this period. Negative isotopic values are recorded in regions where the main source of water derives from monsoonal rains, like the tropical parts of India and south East Asia. It is therefore feasible that the recorded values in north Oman are related to a northward migration of the mean latitudinal position of the ITCZ as it was suggested for the early Holocene wet phase (Figure 3.4) (Burns *et al* 1998; Fleitmann *et al* 2007; Fleitmann & Matter 2009).

Climatic data presented here consists of a fraction of what is available. The increasing interest in Arabia's paleoenvironments and archaeology generates a fair amount of information every year. The data presented above represents a compromise of older and newer proxy data available for Arabia.

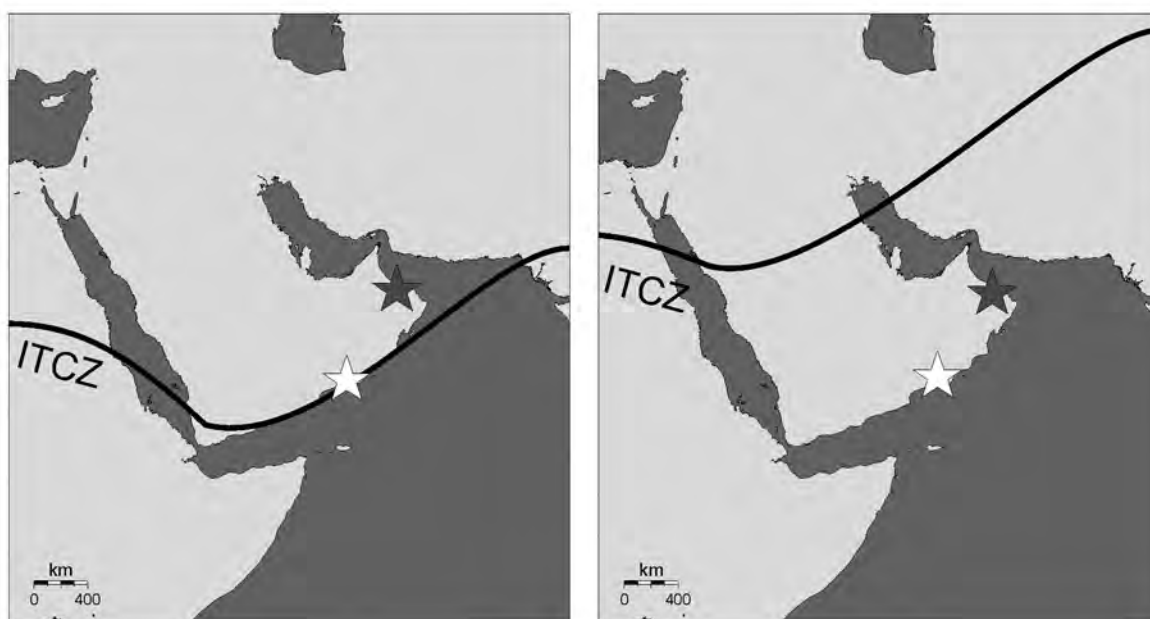


Figure 3.4 Northward migration of the ITCZ. In the maps above depict the position of the ITCZ during its northernmost reach within a year cycle for dry phases (left) and wet phases (right). (After Neff, 2001, fig. 4.5)

3.4 Summary

Intensity and paucity of wet and dry spells have affected the landscape in very distinct ways. During periods of environmental deterioration, depending on local wind regimes, the overall availability and disposition of eolian sediments, the accumulation of sand seas like the Nafud, Wahiba and Rub al Khali desert took place. During phases of environmental restoration, induced by both global and solar agents, the northward migration of the mean latitudinal position of the ITCZ would bring in considerable amounts of moisture to South Arabia. Coupled with the rise of global ocean water level and subsequent rise of the ground water level in South Arabia during pluvial phases increase in precipitation would have triggered a landscape reactivation event visible in the diverse terrestrial climate records (Figure 3.5). These landscape activation phases had great affect on human populations and subsequently, the archaeological record. The focus of the following discussion is the integration of the climatic data presented here with the review of the archaeological record presented in chapter Two.

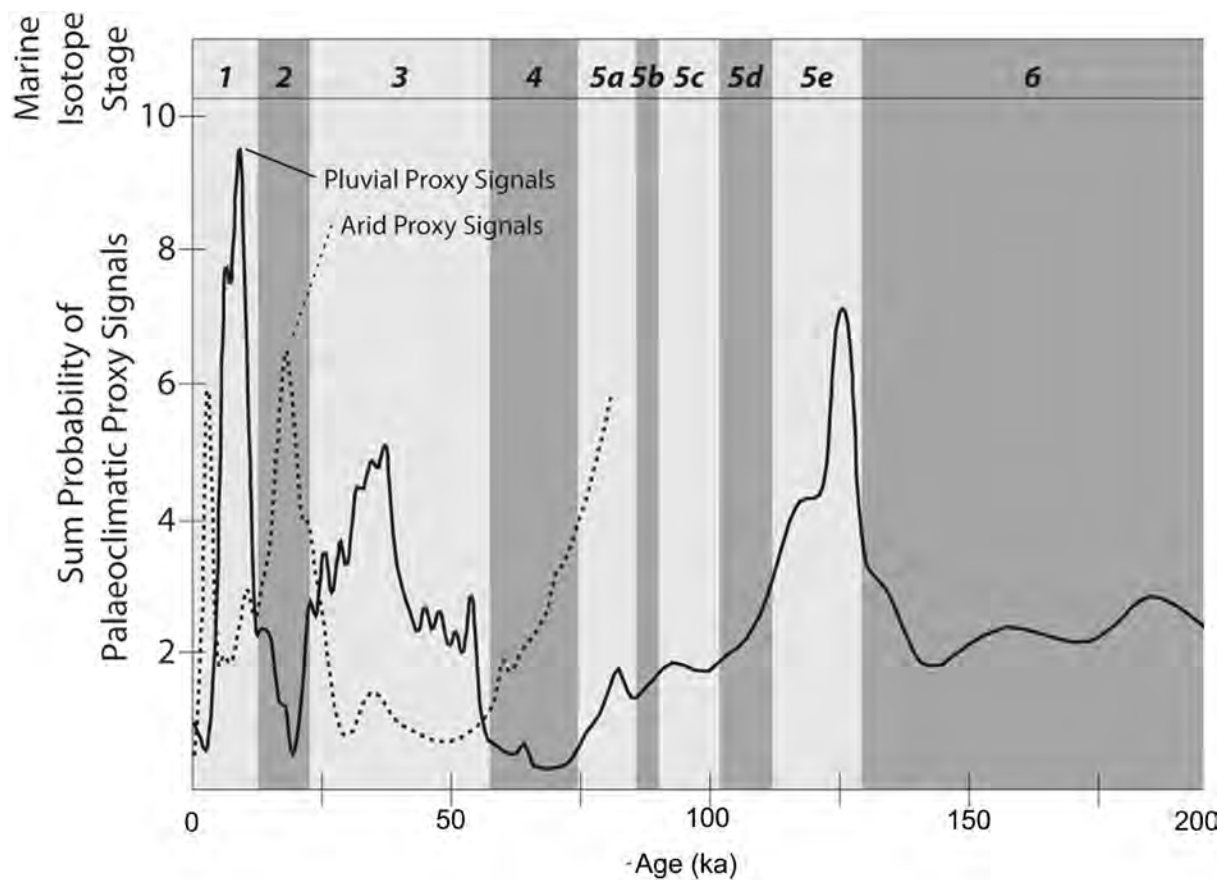


Figure 3.5 Sum probability curve for the Late Pleistocene of Arabia.
(Parker & Rose, 2008, fig. 4)

During periods of climate amelioration, South Arabia was considerably wetter than under present conditions. The reactivation of dormant springs would feed the once seasonally active wadis. These would run year round given the rise of the ground water level. The consequences of this would be a shift from a deserted rocky landscape to a Highland savannah across southern Arabia. The increase in moisture would serve as a temperature regulation agent and further increase precipitation. Following the advance of this savannah-like flora, medium to large herbivore populations would procreate and expand, attracting top predators like *Panthera pardus* (Leopard), *Acinonyx jubatus* (Cheetah) and *Homo sapiens*.

While environmental amelioration was relatively fast-paced in South Arabia, southward migration of the ITCZ and subsequent climatic deterioration of inhabitable landscapes occurred over longer periods (e.g. Beineke, 2006; Fleitmann *et al.*, 2007; Fleitmann & Matter 2009). Gradually, as the Monsoonal belt drifts southward, desertification advances. The ground water levels sink and the rare seasonal storms cause the erosional depletion of the available soils and the transport of piedmont debris creating large alluvial fans in the inland of South Arabia. Those factors had great influence on the character of the archaeological record of Arabia, which is marked by artefact surface scatters that have once been buried.

With the erosion of the fertile soil cover the savannah grassland gives way to arid adapted scrubs. The biomass, including human groups, contract into refugia, like the Dhofar Mountains in the south, the Red Sea Basin to the west or the Arabian Gulf (Parker & Rose, 2008; Bailey, 2009; Fedele, 2009; Rose & Petraglia, 2009; Rose, 2010). The expansion and contraction of this semiarid belt and the conjectured movements of the human groups expanding within those regions is of relevance to understanding the archaeological material present in the diverse ecological zones of Southern Arabia. The archaeological background presented in chapter Two focused on sites dating to the MIS 3. Based on the investigation of the lithic technology and stone tool spectrum researchers postulated local origins for the industries uncovered at Jebel Faya NE-1 and Shi'bat Dihya (Armitage *et al.*, 2011; Delagnes *et al.*, 2012). This implies that these populations are descendent of human groups that expanded into Arabia during or before MIS 4.

Climate proxies for MIS 6 consist of eolian accumulation dated by OSL method in the Liwa region of the Rub al Khali and the Wahiba sands, indicating that this period was marked by dry and inhospitable conditions (Preusser *et al.*, 2002; Radies *et al.*, 2004). Population movements into the Peninsula recorded for the MIS 6 are non-existent, nor are any archaeological sites dating to this period known in Arabia. Following the climatic pattern of global amelioration triggered by the retreat of the northern hemisphere glaciers,

the increase in solar insolation and the rise of global sea level, the last interglacial in South Arabia is marked by phases of increased precipitation. The northward migration of the IOM precipitation belt may be held responsible for an expansion of the savannah belt across South Arabia. The speleothem record of northern Oman signals a major wet phase at the onsets of the last interglacial that appears to have been stronger than the post-dating pluvial events in the course of the quaternary (Burns *et al.*, 1998; 2001; Fleitmann & Matter 2009). Between 130 and 120 ka BP (MIS 5e) the ITCZ migrated northward bringing in substantial amount of rain to the Arabian Peninsula, causing a stabilization of the eolian bodies and ceasing dune accumulations.

Archaeologists working across Southern Arabia believe that Anatomical Modern Humans (AMH) left Africa and expanded into Arabia during the onset of the MIS 5 pluvial phase. Although human remains attesting this hypothesis have not been found yet, the archaeological evidence uncovered at Faya NE-1 presents general African traits (Armitage *et al.*, 2011, 455) hinting at possible connections between assemblage C and East Africa. A stronger case is provided by the presence of Nubian technology found in Dhofar dating to the MIS 5c (Rose *et al.*, 2011; Usik *et al.*, 2012). Both discoveries point to Africa as the source of human populations living in Arabia during MIS 5.

It has been argued that the transition between MIS 5 to 4 was triggered by the mega eruption of the Toba Volcano. This catastrophic event is thought to have plunged global climate into a volcanic winter that lasted several years, possibly decimated human populations living outside of isolated refugia (e.g. Ambrose, 1998; Steward & Stringer, 2012). Contrary opinions have been uttered by many scholars regarding the impact of this event on both climate and human evolution (Schulz *et al.*, 2002a; Oppenheimer, 2002; Gathorne-Hardy & Harcourt-Smith, 2003; Petraglia *et al.*, 2007). One of the main arguments brought by Schulz *et al.* (1998, 2002b) is that the onset of glacial conditions and their further development showed little susceptibility to the Toba “super eruption”. Global climate was shifting towards glacial condition before the Toba eruption happened. Arabia

climate during MIS 4 was marked by dry condition, the ceasing of speleothem growth and eolian accumulation in the Wahiba Sands represented by four IRSL dates clustering between 79.9 ± 7.6 ka and 63 ± 4 ka BP (Radies *et al.*, 2004) support this notion. Also, the onset of a super dry phase recorded in Africa by 74 ka, visible in the maximum extension of the Sahara and the Kalahari Desert (Bahrman & Mitchels, 2008) may be noted here. In general the overall lack of data from MIS 4 (Parker, 2009) hampers interpretations regarding the extent of this phase throughout Arabia. While archaeological sites dating to the MIS 4 are unknown in southern Arabia, Usik *et al.* (2012) explore the possibility of a persistence of the Dhofar Nubian Complex across the MIS 5 and MIS 4. This persistence is visible on the basis of technological continuity of the Nubian reduction method and its use during the Mudayyan industry. Additional data supporting the persistence of human occupation across southern Arabia comes from Jebel Faya NE-1 assemblage B, which possibly represents the source for assemblage A (Armitage *et al.*, 2011).

The MIS 3 wet phase is signalized by a diverse set of paleoenvironmental data. While there seems to be little resonance of this phase in the speleothem and marine records of Arabia, researchers have reported a large number of lacustrine deposits throughout the interior of the Peninsula. Whereas most of those lakes, which have been dated using fervently disputed C^{14} samples from fresh water molluscs (Preusser, 2009; Parker, 2009; Wilkinson, 2009), cluster around 30-21 ka and 34-24 ka BP, newly acquired dates from Saudi Arabia obtained using the OSL method yielded a lacustrine phase dating to the early MIS 3 (53-39 ka). Marine records support the notion that MIS 3 fluctuated between periods of aridity and increased precipitation (Schulz *et al.*, 1998; Beineke, 2006). The actual imprints of those fluctuations during MIS 3 on the South Arabian climate record seem to be manifested by the reactivation of the older Pliocene and Pleistocene riparian systems culminating in the accumulation of large bodies of water in depressions within the landscape. Given the sedimentary scope of the lakes identified in the Rub al Khali, Beineke (2006) concludes that these would have formed relatively fast and were slow

to dry out. Varying greatly in size, these lakes would have offered both flora and fauna sufficient moisture to transform the immediate surroundings of those environments into semiarid savannahs. Dating of fossil groundwater from Saudi Arabia and central Oman have the accumulation of rain waters between $24,630 \pm 500$ BP and $20,400 \pm 500$ BP for the western Rub al Khali and 30 KA BP to 20 Ka BP for the Nejd Plateau (*Ibid.* 54). Landscape revival around these lakes would have been short lived, as stated above. Nonetheless, archaeological evidence for MIS 3 in Arabia is consistent and shows, as has been stated in chapter Two, some variability. This variability may relate to two different populations living in separate refugia; one in the Gulf and one in western Yemen.

The last glacial period in Arabia is marked by a drastic sea level drop and intense eolian reactivation. Signs of this arid phase are visible in the marine record, showing a decrease in the south western monsoonal activity (Schulz *et al.*, 1998; Leuschner & Sirocko, 2000, 2003), and increase in north eastern winter Monsoonal conditions (Schulz *et al.*, 2002b). Eolian reactivation is principally observed in the Wahiba Sands and in the marine sediment cores. Here the changes in wind pattern induced by the southward migration of the ITCZ are visible in the linear deposition of mega dunes in this region (Warren & Alison, 1998; Glennie & Singhvi, 2002; Preusser *et al.*, 2002). Evidence for a short-lived wet phase during MIS 2 has been summarized by Parker (2009). Marine records from the northern Indian Ocean, off the coast of Pakistan show an oscillating regional record for the glacial/interglacial transition in concordance with the H1 event (Heinrich) in the northern latitudes (Schulz *et al.*, 1998 fig. 3). Speleothem growths dating back to $15,78 \pm 0.15$ KA BP from the Summan-Plateau in Saudi Arabia and travertine deposits from the Nizwa region, Oman, dated between 16.3 and 13 ka BP, indicate the presence of some regionally specific wet phenomena around the Later LGM (Fleitmann *et al.*, 2004; Clark & Fontes, 1990). This period was then again interrupted by the onset of the Pleistocene/Holocene dry phase, a phase related to the YD event in the northern hemisphere. In Arabia this period is visible in the dune displacements in the Wahiba sands and the Awadi region dating between 13-

9ka (Warren & Alison 1998; Goudi *et al.*, 2000).

The dry conditions during the MIS 2 and the lack of archaeological horizons dating to this period at Jebel Faya NE-1 led Uerpmann *et al.* (2009) to flag a *tabula rasa* event for this period. An alternate model explaining the lack of archaeological material from the MIS 2 at Jebel Faya envisions the abandonment of the area in favour of refugia within the Gulf Oasis. At al Hatab, Rose and Usik (2009) uncovered two archaeological horizons dating to the later half of the MIS 2, indicating that no population extinction had occurred in this region. As stated in chapter Two the al Hatab material shared technological features with the Shi'bat Dihya industry, this similarity may be interpreted as a link between the two industries, which would imply some degree of occupation continuity across the MIS 3 and 2.

According to speleothem data, the early Holocene wet phase has set in with the northward migration of the mean latitudinal position of the ITCZ (Fleitmann *et al.*, 2007). Dates from Socotra Island in the Gulf of Adam, Dhofar and Northern Oman suggest that this was a phenomenon that stretched over a period of one thousand years (10.5-9.5 ka). Speleothem dates acquired by Cremaschi and Negrino (Cremaschi & Negrino, 2005), from a series of rockshelters and caves from both northern and southern faces of the Jebel Qara escarpment in Dhofar suggest a slightly younger age for the onset of the early Holocene wet phase. Due to problems encountered by the two researchers with the Th-U dating of speleothem deposited, age of these sequences has to rely on the stratigraphic affiliation of these deposits in the overall sequence recorded in the southward facing rockshelters and caves of the Jebel Qara escarpment. Cremaschi and Negrino positioned the onset of this wet phase at 8.7 ka BP, based on dates acquired on the so called "Mollusc unit" which underlay the calcite speleothems. According to their data the Nejd Plateau remained arid during the onset of the Holocene given that the Monsoonal rains did not pass the barrier of the Dhofar escarpment.

Lakes occurred throughout the Arabian Peninsula during the onset of the early

Holocene wet phase. These are to some extent accompanied by landscape reactivation and dune stabilization by a consistent C3 vegetation cover (Parker *et al.*, 2004; Urban & Buerkert, 2009). Lézine and her research group has argued in favour of an earlier onset of the Pleistocene/Holocene wet phase (Lézine *et al.*, 2007), according to her studies lake formation began at 12 ka BP and lasted till 7.5 ka BP. During this period the lake at al-Hawa experienced periods of regression and expansion, however lake salinity remained stable. Pollen analysis suggests that those lakes have formed in semiarid environments, and that the presence of large bodies of water had little influence on the overall dry and deserted appearance of the Arabian Inland during the Holocene. Similar to the Lakes described by McClure (1976) in the Mundafan region of the Rub al Khali, the lakes at al-Hawa formed due to the flat morphology of the surrounding landscape. The runoff streams from the summer monsoonal rains falling in the Red Sea mountain coast and the Yemeni Highlands would have gathered in its flat basin forming the lakes. According to speleothem data, the ITCZ slowly migrated southward, causing the decrease in rainfall observed in South Arabia after 7.8 ka BP (Fleitmann *et al.*, 2007; 2011). From this point onward the Arabian climate becomes more and more like what it is today. The lakes in the Rub al Khali, Yemen and Emirates dry out and the hot and dry adapted C4 grasses replace the former C3 vegetation cover. Subsequently dune emplacement is reactivated.

The Early Holocene archaeological record is highly variable across the Arabian Peninsula. During the last interglacial, increased precipitation caused the South Arabian landscape to change into a green savannah attracting human groups from Africa. What happened during the early Holocene? Did foreign groups venture into this landscape? The different industries recorded across the Nejd may help answer at least some of these questions. In the following section the methodology used to investigate the Early Holocene archaeological record will be described. Also a brief description of the studied area and the sampling methodology applied to it will be given.

DHOFAR AND THE NEJD PLATEAU: GEOMORPHOLOGY AND GEOGRAPHY

In a land as little known as South-west Arabia there is danger to the scientific traveler of getting lost. Not lost in the geographical sense, though at times that might be easy in the unending monotony of its valley floors and desert plateaux, but lost in the intricacies of a myriad detailed observations concerning them and the parts they played thousands of years ago in the lives of their inhabitants. –Gertrude Caton-Thompson & Elinor W. Gardner, *Climate, Irrigation, and Early Man in the Hadhramaut* (1939, 18)

The preceding chapters discussed aspects of the archaeological and paleo-climatic records available for southern Arabia. It is clear from these discussions that during phases of increased precipitation Arabia was inhabited by prehistoric populations. During phases of intensified aridity, however, inhabitable environments shrunk and were restricted to environmental refugia. Climate data suggest that environmental deterioration happened more gradually, and took longer than environmental recovery, allowing human and animal populations to adapt and contract into posited refugia. Dhofar, in southern Oman, with its constant climate, is theoretically one such environmental refugium that may have harboured human populations during the LGM.

In order to make the most out of archaeological sites located in arid and semiarid environments, like those encountered across southern Oman, researchers rely on the description of these sites' immediate surroundings under present conditions. The motive behind such descriptions is to reconstruct the sites' local setting during the time it was occupied (Evans & O'Connor, 1999). Dhofar, the region with which this dissertation deals, is characterized by a variety of geomorphic features that bear the marks of repeated climatic oscillations. This chapter will describe the geomorphic and geographic features found across Oman. The Sultanate of Oman is unique in its geographical disposition in

that it presents very diverging ecosystems fuelled by diverse weather regimes. Oman can be broadly divided into three regions: (a) the Hajar mountains; (b) the central plain; and (c) Dhofar (Platel *et al.*, 1992). As was discussed in chapter Three, the Hajar Mountains receive moisture brought in by the Northwesterly winds, while the Dhofar Mountains chain receives moisture in form of seasonal rains and fog brought by the Summer Monsoon (Neff, 2001; Burns *et al.*, 2001). While precipitations over the Hajar Mountains are sporadic, the IOM visits the coast of Dhofar every year for the duration of the summer, utterly changing the landscape and deeply influencing this region's environments.

A comprehensive description of Oman's geography, demographics and biosphere will be provided here. Emphasis will be placed on the description of the Nejd Plateau, located in the Governorate of Dhofar. As mentioned in the introduction and chapter Two, the Nejd Plateau is part of a greater, continuous geographical landscape called the South Arabian Highlands (McCorriston *et al.*, 2002), which encompasses the governorate of Dhofar, the Mahra province and the Jol in Yemen (Figure 4.1).

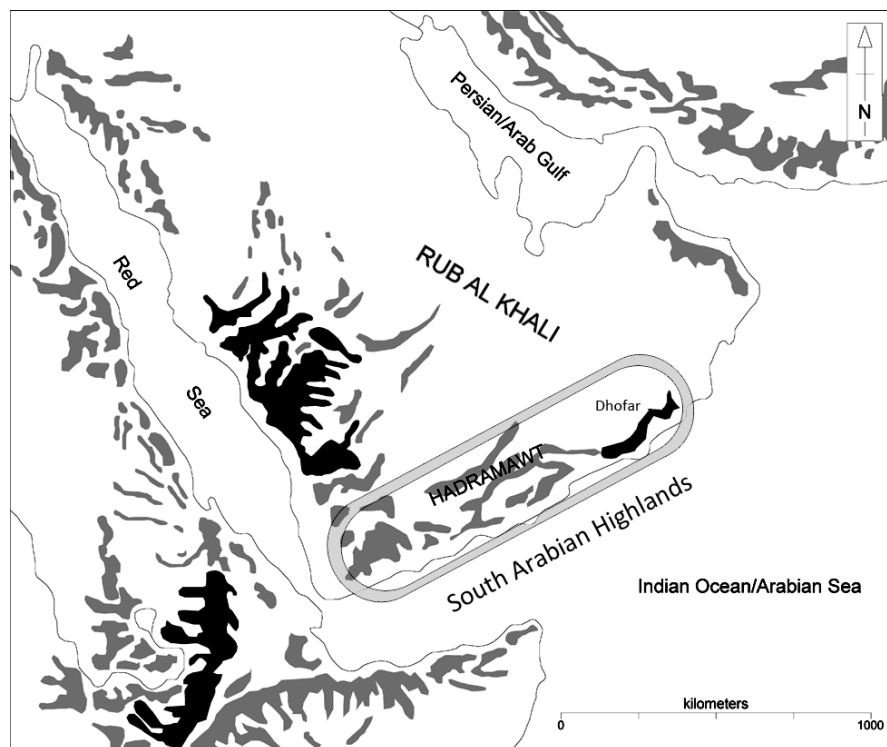


Figure 4.1 Map showing the Location of the South Arabian Highlands. (Modified after Martin *et al.*, 2009, fig. 1).

4.1 The Sultanate of Oman

The Sultanate of Oman, with an approximate area of 309,500 square kilometres, is situated in the south of the Arabia Peninsula between latitudes 16° and 28° N, and longitudes 52° and 60° E. The country shares political borders with the United Arab Emirates (UAE), The Kingdom of Saudi Arabia and Yemen. Geographically it is delimited by the Rub al Khali desert to the west, the Arabian Sea to the east, the Yemeni Highlands to the southwest and the Strait of Hormuz to the Northeast (Figure 4.2).

The demographics of the country follow the disposition of these aforementioned zones. That is to say, modern day populations concentrate in the more hospitable mountainous and coastal environments, while the central plains are sparsely populated. Some of Oman most densely populated urban centres are situated in the northern areas of the country (e.g. Muscat, Sohar, Suwaiq, Nizwa). The regions and governorates situated along the Hajar Mountains are inhabited by over 50% of the country's population, corresponding to the administrative and economic centres of the Sultanate. A second urban centre is situated in Dhofar along the coastal plain around the International port of Salalah.



Figure 4.2 Map of the Sultanate of Oman and its regions. (Image by Y. Hilbert).

With the exception of Dhofar, which receives considerable amounts of moisture given the annual incursions of the IOM, Oman's climate is marked by hot and dry conditions all year round. During the summer months, between mid-April to October, temperatures in the country's interior may rise up to 50° Celsius while along the coastal plain, east of the Hajar Mountains temperatures are lower seldom surpassing 45° Celsius. Along the coast and especially the capital region of Muscat high levels of humidity (up to 90%) are registered during this time of the year. During winter months temperatures are relatively homogenous across the country and oscillate between 18 and 26° Celsius. The low humidity levels and at times intense winds may drop the perceived temperature considerably during the winter months.

Precipitation in the inland and northern areas of the Sultanate ranges between 20 – 100 mm per year and commonly fall during the winter months. Annual rainfall is higher across the Hajar reaching 200mm around Jebel Akhdar. Torrential precipitations in form of winter cyclones moving in from the Northern Indian Ocean have been known to reach the Omani coast during the Pleistocene and Holocene pluvial phases. More recent cyclonic incursions occurred in 2007, when Cyclone Gonu brought intense precipitation and causes massive landslides in the eastern portion of the Omani coast.

4.1.1 The Hajar Mountains and central Omani plain: Geography and geomorphology

The Hajar Mountains stretch across the eastern territories of the UAE and the northern territories of Oman. On Omani territory, the Hajar Mountains reach from the Musandam peninsula in the north to the town of Sur in the south east of the Sultanate. This mountain chain composed of ophiolite, an oceanic crystalline rock, stretches over 700 km and rises up to 3000 meters above sea level, reaching its highest point around Jebel Shams and Jebel Akhdar; making this area the highest habitat in south eastern Arabia. The Hajar Mountains are the earth's largest ophiolite outcrops; a second outcrop is located in the south of Oman on Masirah Island (Garzanti et al 2002). This chain is

further divided into the Al Hajar al Gharbi Mountains and the Al Hajar ash Sharqi (Eastern Al Hajar) Mountains. Separating these two mountain ranges are a series of intricate wadi systems that transport the detritus coming from the slopes towards the inlands or the coastal plain (Blechsmidt *et al.*, 2009); the largest of these being Wadi Samail.

A sparse dryland type of vegetation and climate characterizes the mountain desert environment (Figure 4.3), which is the most commonly observed type of environment across the Hajar Mountains. Ephemeral streams, activated by sparse precipitation, are responsible for sediments transport within the mountainous environments of the Hajar (Fuch & Buerkert, 2008). Local fauna is composed of birds, including both endemic and migratory species from Africa, Arabian Leopard (*Panthera pardus nimr*) and Arabian Tahr (*Arabitragus jayakari*) (Ghazanfar, 2004).



Figure 4.3 Photographs of distinct environments within the Hajar Mountains and northern Oman. 1, Qantab village, close to Muscat; 2, Oasis at Wadi Beni Khalid; Village in the Hajar; 4, plains around Nizwa. (Photographs by Y. Hilbert)

A 150 km wide coastal plain composed of alluvial and eolian deposits intermingled with *sabkha* deposits delimits the Hajar Mountains to the east. Costal *sabkhas* start off as bays (*Khors*) that become filled with nutrient rich sediments and evolved into mangrove swamps. These coastal mangrove swamps are eventually filled by the build-up of clay, detritus from the decomposition of algae and other biomass living in such nutrient rich environments, and finely sealed by laminated eolian sediments (Holm, 1960, Warren & Kendall, 1985; Macumber, 2011). Once the sediment aggregation ceases the *sabkha* is cut off from oceanic water inflow. The *sabkha* is only flooded by terrestrial runoff and becomes susceptible to ground water levels. The costal plain is dotted with farms and groves that were planted on top of the fertile *sabkha* deposits. The local vegetation consists of spatially delimited coastal mangrove (e.g. *Avicennia marina*) and inland savannah species include *Ziziphus spina-christi*, *Prosopis cineraria* and the *Acacia tortilis* (Cleuzeu & Tosi, 2000).

The central plain that extends from the Arabian Sea to the Rub al Khali in the east-west axis, and from the Hajar mountains to Dhofar in the north-south axis is part of the Governorate of al Wusta. A large portion of this area is composed of eolian environments: dune fields. The Ramlat al Wahaybah (Wahiba Sand) in the north east, characterized by parallel linear dunes running from south to north and the Rub al Khali desert to the west are the most prominent examples (Figure 4.4).

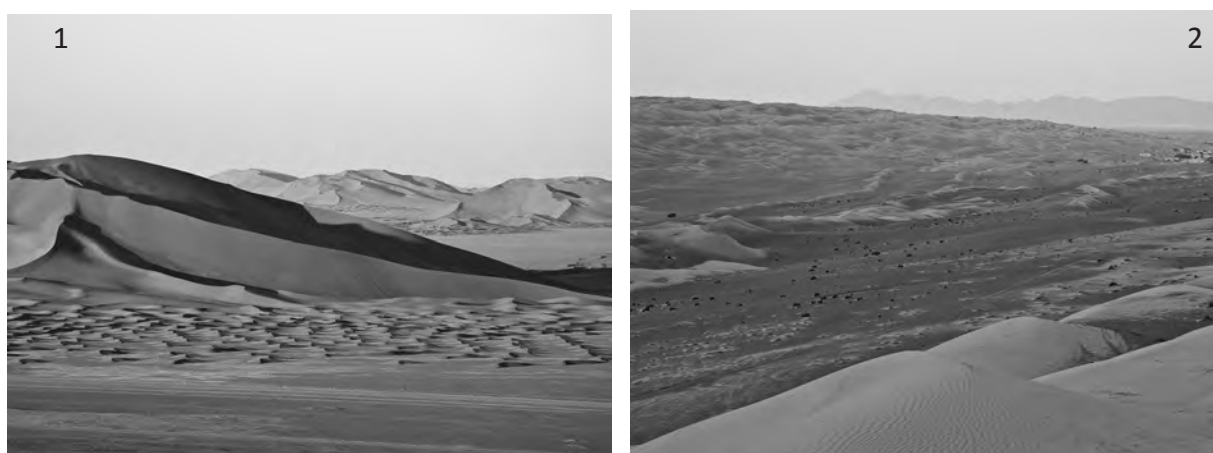


Figure 4.4 Photographs of the Wahiba and Rub al khali deserts. 1, Rub al Khali dunes; 2, Wahiba linear dunes. (Photograph by Y. Hilbert).

Chiefly dictated by erosional windborne processes such as deflation and deposition of sediments, eolian environments occur wherever the following conditions are met: an ample source of unconsolidated sediment, wind that is strong enough to mobilize the sediments particles, and the absence of vegetation or other obstacles hampering the transport of these sediments (e.g Butzer, 1971; Waters 1996; Glennie, 2005). As noted throughout chapter Three sand dunes are the most common aspect of arid to semiarid eolian environments; i.e. deserts. Sand dune morphology is dictated by the various processes named above, the following features are universal to all eolian structures: (a) a slowly rising slope called backslope, (b) a crest, (c) a steep falling slipface, and (d) an interdune area, in which ponds sometimes form (Figure 4.5).

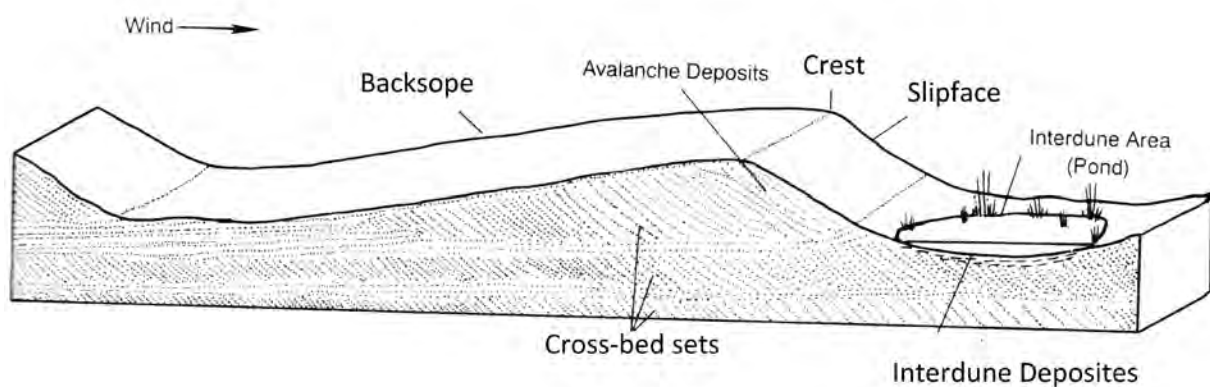


Figure 4.5 Sand dune morphology.

In the figure are shown the specifics for the elements described in the text above plus additional nomenclature. (after Waters, 1996, fig. 4.3)

Three kinds of particle transportation contribute to dune formation: suspension, saltation and surface creep (Figure 4.6). Most of the sediments transported by eolian action in arid and semi-arid environments take place by saltation. Saltation occurs when particles are launched for short intervals in a parabolic trajectory; upon impact, further particles are then mobilized. These newly mobilized particles are carried further in the form of a “near-surface cloud” called surface creep (Glennie, 2005, 118). Also referred to as reputation, surface creep results from the transfer of kinetic energy generated by sand particle saltation, thus moving clasts too large to be transported by eolian action.

The accumulation of eolian sediments into sand dunes is the result of a decrease in wind velocity. Consequently, as wind velocity decreases and the energy keeping eolian sediments suspended dissipates, suspended particles are deposited on the ground.

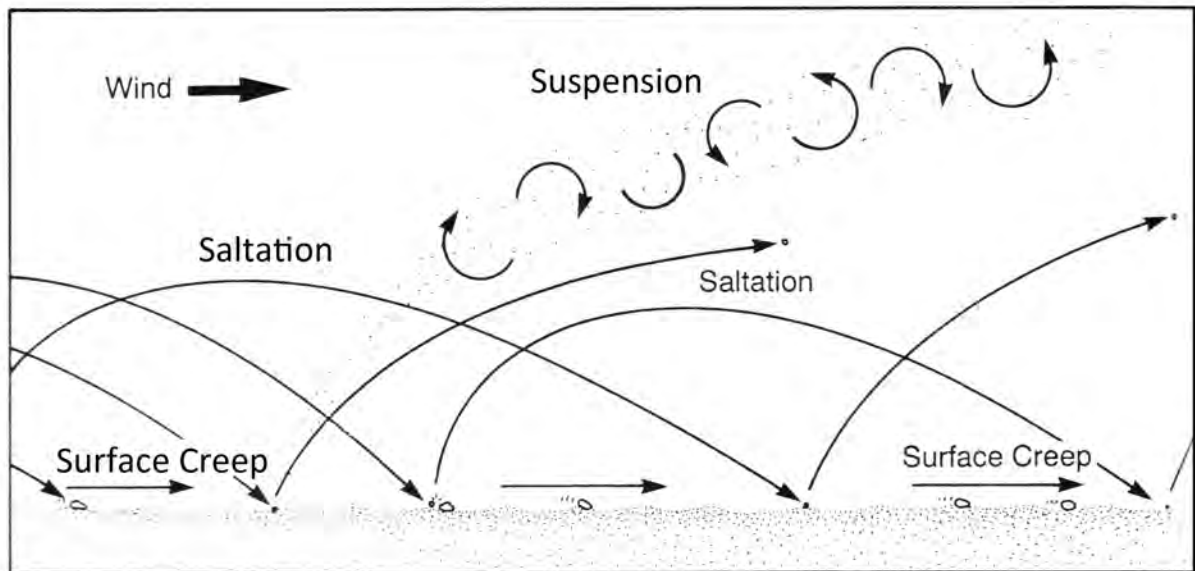


Figure 4.6 Schematic of windborne transport.
Particle sized sediments are transported by means of saltation, suspension and surface creep. (After Waters, 1996, fig. 4.2)

Dune shape is dictated by the wind regimes acting upon the landscape where these features form. The great diversity of dune shapes observed in the Rub al Khali is used to calculate variation in wind intensity and direction in the central portion of the Arabian Peninsula (Holm, 1960, 1373). Dune shapes are a function of the topographic layout, wind intensity, and directionality. While barchan dunes form under steady wind conditions (i.e. constant and unchanged across a considerable amount of time), linear dunes, such as in the Wahiba Sands, form under strong and discontinuous wind conditions (Radis *et al.*, 2004; Beineke, 2006). As was discussed in chapter Three, the Wahiba sands were continuously formed over several dry phases and experienced periods of sediment stagnation.

South of the Wahiba lies the Haushi-Huqf depression, this landscape is marked by table hills, dry riverbeds, inland *sabkhas* and Pleistocene river terraces. *Sabkhas* are depressions in arid to semiarid landscapes that occasionally hold water. Across southern

Arabia, *Sabkhas* are divided into different types according to their geographical position, the sediments they contain and amount of inflowing water brought by seasonal rains. In the interior of Oman and in the Rub al Khali desert, *sabkhas* form within basins with no outflow, fed by seasonal runoff and rising of ground water levels. Due to the disposition of the sediments in these regions, the water gathered in these *sabkhas* is highly saline. Most *sabkhas* are now dry and only the laminated evaporites and eolian silt filled depressions remain. These are of variable size, the biggest in southern Arabia being the 5000 km² *Umm As Samim* located in central Oman. As result of these harsh eolian and saline conditions, vegetation is sparse and composed of desert scrubs. Further to the south west a extensive gravel plain, the *Jiddat al Harassis*, stretches towards Dhofar.

4.2 Dhofar: Geography and geomorphology

The governorate of Dhofar encompasses almost one third of the country's total area. Dhofar borders the Saudi Arabian province of asch-Scharqiyya to the north, to the west with the Mahara Province of Yemen and to the east with the al Wusta governorate. While Dhofar's borders to the north and east are political as well as geomorphological, and marked by deserts and desiccated plains, the mountainous landscape composing the Dhofar Escarpment extends well beyond Oman, reaching across the Mahara province in Yemen. Dhofar represents the eastern extend of the South Arabian Highlands.

Dhofar can be partitioned into four major ecological zones: (a) the coastal plain around the capital city of Salalah; (b) the Dhofar escarpment; (c) the Nejd Plateau; and (d) the Rub al Khali desert (Zarins, 2001). The formation and configuration of these four very distinctive ecosystems are to a greater part the result of the interplay between the local lithology, the tectonic uplift of the South Arabian Highlands and the effects of the locally prevailing weather system upon the regional morphology. Dhofar and particularly the Dhofar Mountains are marked by the influence of the most powerful weather system along the coast of the Indian Ocean; namely the IOM, which hits the coast of Dhofar during

the summer months.

Survey activities conducted by the DAP encompassed the investigation of specific areas within the four distinct zones of Dhofar. In order to cover as much terrain and record as many sites as possible, transects have been laid across areas of potential interest. The criteria for selecting the location of these transects were: a complex morphology (encompassing as many geomorphic features as possible), raw material availability and assessable conditions. Once transects were laid, the groundtruthing took place. DAP team members would drive to the chosen transect, and using GPS navigation proceeded on foot, mapping and cataloguing each site along the transects course. Sites with potential for preserving Pleistocene or Early Holocene sediments were also mapped during the survey activities; mostly rockshelters were mapped and subsequently excavated.

The observations made on the landscape throughout the groundtruthing activities were used to further differentiate specific areas of archaeological interest within the greater ecological zones of Dhofar. Although the majority of sites have been recorded across the Nejd Plateau, the description of the Dhofar escarpment and the costal plain is equally relevant given this area's status as posited environmental refugia.

4.2.1 The costal plain and the Dhofar Mountain Chain

The costal setting of Dhofar is unique to Arabia due to the amount of fresh water brought by the IOM during the *Khareef*¹ season. The effects of the annual monsoon have greatly influenced Dhofar and molded its current configuration across the millennia. The coastal plain is a crescent shaped landmass some 90 kilometres long and approximately ten to fifteen km wide, which stretches from Ras Raysut to Taqa. The coastal plain is mainly composed of Quaternary conglomerates, mostly alluvial fans. These are formed by the redeposition of slope detritus from the Dhofar escarpment by fluvial agents. Alluvial fans

¹ Khareef is the Omani name for the south western Monsoon that reaches the Salalah coast in Dhofar between mid- June until mid- September. The word monsoon has its roots in the Arabian language and means "season". During this period ship navigation becomes favorable given the constant strong winds. From the 16th century AD onward the Portuguese adopted this term and used it to describe a specific kind of wind "Monção" (Neff, 2001, 26).

faound along the costal plain rise approximately 30 meters above the current sea level and are cut by short wadis all draining southwards towards the Arabian Sea. The coastal plain and especially the area around the capital of the Governorate, Salalah, is intensely used agriculturally; date groves, coconut palms, bananas and other tropical fruits prosper in this prolific environment.

The plain itself gently and steadily dips toward the ocean where eolian sands and low limestone cliffs mark the beaches. A series of interdunal and coastal estuaries have formed form here. These are protected by sand barriers and, consequently, have no connection to the ocean. Those estuaries are locally known as *khors* (Hoorn & Cremaschi 2004), and exist in this manner only in Dhofar. Given that these receive a great amount of fresh water from spring settings along the southward facing scarps waters within these *Khors* are brackish.

The highest point on Salalah plain, some 100 meters above sea level, is located on the very foot of the Jebel Qara escarpment, which is part of the Greater Dhofar mountain chain (Platel *et al.*, 1992) (Figure 4.7). These elevated areas consist of the piedmont detritus that accumulate at the base of the escarpment. Along the seaward facing side of the escarpment springs and sinkholes have formed (Hoorn & Cremaschi 2004). Springs and their associated ground water dynamics are key elements in the Dhofar environment. Springs are either gravitational or artesian, gravity springs form where the surface topography intersects or is cut below the level of the water table, allowing water to drain from the water table through fissures in the bedrock by the force of gravity. Artesian springs are activated when water saturated sediments become confined and then, under pressure, the water forces its way via the bedrock, thereby forming a pond. Artesian spring ponds usually form in the proximity of weak points in the bedrock, such as faults or fractures (Waters, 1996). Both types of spring settings have been recorded along the southern face of the Dhofar escarpment.



Figure 4.7 Panoramic image of the Salalah coastal plain.
(Photograph by Y. Hilbert).

Between Taqa and Mirbat, the Dhofar escarpment extends into the Arabian Sea. Here, a series of major faults within locally outcropping Tertiary limestone formations are responsible for this regions irregular relief. The majority of the local lithology is marked by the Hadhramaut Group, a 300 metre thick sedimentary package of tertiary and later sedimentary rock (figure 4.8) (Platel *et al.*, 1992; Thompson, 2000). The crystalline basement found east of Mirbat represents an exception to that rule. This crystalline basement is composed of metamorphic and plutonic rocks, occasionally cut by dolerite dykes.

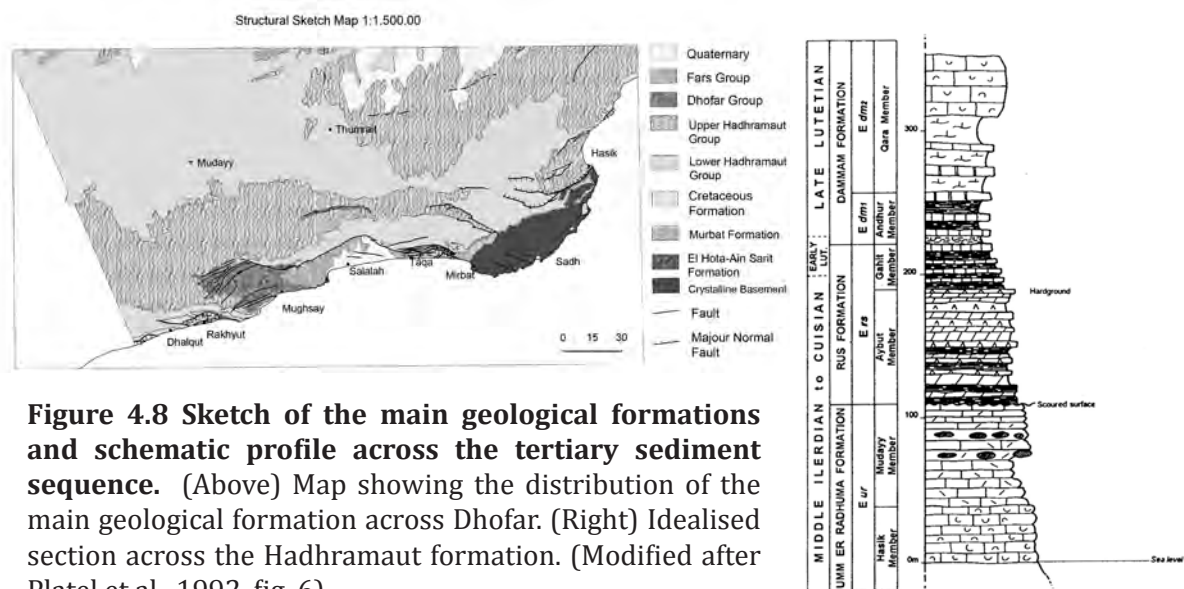


Figure 4.8 Sketch of the main geological formations and schematic profile across the tertiary sediment sequence. (Above) Map showing the distribution of the main geological formation across Dhofar. (Right) Idealised section across the Hadhramaut formation. (Modified after Platel *et al.*, 1992, fig. 6)

Among the limestone deposits encountered in this area, the *Rus formation* is of considerable importance. This re-crystallized collapsed breccia contains chert nodules of relative homogeneity, well suited for the production of stone tools. An outcrop of this facies lies just east of Taqa. The tectonic uplift that formed the Dhofar escarpment also caused the chert nodules at the base of the *Rus formation* in this zone to shatter, making the chert nodules brittle and rife with fracture planes, making them unsuited for the production of stone tools.

North of the coastal plain, towering to a maximum height of 850 meters, the Jebel Qara and Jebel Samhan ranges form the Dhofar escarpment. This escarpment operates

as a trap for the moisture brought by the IOM (Neff, 2001; Cremaschi & Negrino, 2005; Fleitmann *et al.*, 2007). The Dhofar escarpment is made up of shallow maritime sediments of the Tethys Sea that overlay the crystalline basement of the Arabian shield. The southern face of the escarpment is incised by a series of southward draining wadis. The major catchment systems in this area include Wadis Jarzis, Arbat, Arzat, Haskeem, Darbat and Hinna (Platel *et al.* 1992).

A massive amount of recent to sub-recent travertine has been deposited within these wadi valleys; most distinctive of which is the Darbat waterfall (Figure 4.9), a towering wall of travertine over 100 meters height. Alongside the wadi valleys are numerous rockshelters, karstic features and sinkholes. Although the karstic cavities encountered in Jebel Qara-Jebel Samhan are counted among the deepest in the world and have yielded valuable paleo-climatic speleothem records (Fleitmann & Matter 2009), they are typically sinkholes and not conducive to human habitation. No Pleistocene or Early Holocene archaeological finds have been made by the DAP within the caves and rockshelters found along the southward facing scarps.



Figure 4.9 Wadi Darbat waterfall. (Photograph by J. Geiling)

The high amount of moisture brought in by the IOM every year is responsible for a dark brown clay soils that covers the Dhofar escarpment, the high plateau close to the watershed and parts of the coastal plain. The native vegetation, attributed to the Somalia-Masai centre of endemism, consists of acacia, ficus, dense scrubs and grasses (Figure 4.10). Cattle, camels, goats and sheep are the most common domestic animals found across the coastal plain and escarpment. The ecosystems of Dhofar support a fair diversity of medium sized carnivores; including mongoose, desert fox, honey badger, caracal, jungle cat, and golden jackal. Most of these species, however, are currently limited in their geographic extension to the Nejd (Ghazafar, 1999).



Figure 4.10 Photograph of southern Dhofar during the monsoon.
(Photograph by Dr. J. Rose)

The costal plain and the Dhofar escarpment present aspects that warrant the attributions of these areas as environmental refugia: a constant supply of moisture, fertile soils, abundant vegetation etc. Late Pleistocene populations would likely survive phases of climatic downturn within this stable environment. Transects surveyed along the costal plain, however, have failed to produce any evidence of Late Palaeolithic occupation.

As a matter of fact the DAP survey failed to produce any evidence for the Pleistocene occupation along the costal apart from surface sites attributed to the Lower Palaeolithic. The identification of a lower Palaeolithic site in the proximities of Taqa, is indicative that some surfaces have remained stable for greater parts of the late Pleistocene. Theoretically, sites pertaining to younger lithic industries should, if present within the costal plain, be easily spotted. The fact that none were found indicates that the costal plains was either not inhabited or human groups favoured different areas along the costal plain that are now buried.

Survey of the Dhofar escarpment also failed to produce convincing archaeological evidence supporting this areas status of refugium. The thick soil covering this area greatly constrains archaeological visibility, while the relative densely populated and agriculturally used terrain makes the survey of continuous transects difficult. Northwards past the orographic barrier and the high plateau, the vegetation thins out and gives way to the bare rocky desert of the Nejd plateau (Chaudhary & Houérou 2006).

4.2.2 The Nejd Plateau and the Rub al Khali desert

The transition from the Dhofar escarpment to the Nejd Plateau is a drastic one (Figure 4.11), mainly because of the sudden drop in elevation and the ceasing of the monsoonal affect beyond the orographic barrier. These factors cause the soil cover that blankets most of the escarpment to disappear beyond this point; additionally, strong winds blowing across the Nejd Plateau caused the deflation of this landscape. As a result of these environmental conditions, lag surfaces and desert pavements are ubiquitous across the Nejd. This specific feature, coupled with a seemingly unending supply of chert, makes the Nejd Plateau so interesting for archaeologists. In Arabia, archaeological surface sites are either incorporated into such stone pavements or stone pavements consist chiefly of archaeological material. Crassard (2008a) observed the presence of “tapis de silex taillés,” (flint artefact carpets) during his survey of the Hadhramaut drainage system in Yemen. As

such, stone pavements composed of stone tools are encountered across the entire Nejd Plateau (Figure 4.12).



Figure 4.11 Transition between the Dhofar escarpment and the Nejd Plateau. Beyond the green escarpment where cows may be described grazing the Nejd plateau stretches for over 250 km towards the north before changing into the Rub al Khali desert. (Photograph by Y. Hilbert)



Figure 4.12 Flint artefact carped. Recorded near the Yemeni border during 2012. (Photograph by Y. Hilbert)

The Nejd Plateau is primarily characterized by northward draining wadi systems, Pleistocene terraces, inselbergs and lag surfaces. The Nejd is rich in archaeological sites and the source of the lithic samples analysed throughout this dissertation, and will be described in more detail. Currently, the Nejd is not particularly densely populated if compared to the costal plain in the south. The small town of Thumrayt, situated at the main road that connects Dhofar to the rest of the Sultanate, was the base of operations for the survey activities during the DAP field campaigns. Thirty kilometres south of Thumrayt lays the village of Haluf, while approximately 80 kilometres west of Thumrayt lays the village of Mudayy. Both have been built around active springs and are worth mentioning here given the rich archaeological imprint of their immediate and nearer surroundings.

As the main characteristic of the Nejd Plateau the remnants of fluvial systems, named wadis, and their associated body of traits will find a brief illustration here. As was demonstrated in chapter Three, remnants of alluvial features found across the Nejd Plateau are indicative of climatic oscillations that took place across pluvial episodes. Common features observed across the entire Nejd include alluvial fans, river terraces and seasonally active wadis. All alluvial features obey the mechanism of gravity imposed by the landscape topography, in the case of the Nejd, a slight south-to-north dip. The water flowing within streams comes from drainage basin/watershed, which consists of the total catchment area that collects and directs the water into channels upslope. Governed by the position of hill slopes and outcropping bedrock, each drainage basin is made up of channels that connect and debouch from the basin, joining up with additional drainages downstream. Natural topographic barriers, like hills and ridges, delimit these channels from one another (Waters, 1996; Brown, 1997; Glennie, 2005). Across the Nejd, and especially along the contacts zone between the northern face of the Dhofar escarpment and the southern portion of the Plateau, countless small drainage basins are described.

The fluvial systems found dissecting the Nejd plateau are ephemeral, braided riverbeds. A network of channels that split and conjoin around bars forms the braided

pattern seen in wadi beds. These are accumulations of coarse sediments, gravels and cobbles intermingled with sands and silts. Braided patterns are formed by highly energetic and irregular stream flow associated with ephemeral streams; as a consequence of these characteristics, the meandering channel becomes obstructed by alluvial sediments. As such these features are held indicative for the last fluvial event that activated the riparian systems across the Nejd, which was likely a flash flood caused by a winter storm. The full activation of these river systems would require a constant baseflow².

For obvious reasons, riparian settings were undoubtedly crucial to prehistoric populations living in arid to semiarid environments. These settings provide water during wet phases that attracts local game, and also serve as important land/territory markers, and as conduits for human groups traveling across the landscape (e.g Kelley, 2003; Parker & Rose, 2008). As the climatic data presented in chapter Three suggests, the presently ephemeral wadis of the Nejd may have been intermittent over certain phases of the Quaternary (Fleitmann & Matter, 2009; Preuser, 2009). During wet spells, both fauna and human populations are posited to have expanded along these fluvial settings (Rose, 2006, 2007; Parker & Rose, 2008; Petraglia *et al.*, 2009; Rose & Petraglia, 2009; Armitage *et al.*, 2011; Rose *et al.*, 2011; Petraglia, 2011; Petraglia *et al.*, 2011; Rosenberg *et al.*, 2012).

Given the abundance of wadi networks dissecting the Nejd Plateau, archaeological sites are bound to be found on some of the wadi terraces, these were specially targeted by the survey transects. Alluvial terraces are created by alluvial deposition (erosion). Characteristic of alluvial terraces are a relatively flat surface, called a tread, which is situated above the stream channel and enclosed on one side by a steep slope called a riser, and on the other end by the next valley wall or the next higher tread. Alluvial terraces may formed by the downcutting of a stream channel into pre-existing alluvial deposits; in such cases, these terraces are referred to as depositional terraces. Terraces may also be formed

² Water originating from the water table is called baseflow. Baseflow provides a stable influx of water into a stream, as this source is released slowly when sediments are sufficiently saturated with moisture. Baseflow supplies rivers year round, for as long as the water table remains constant (Waters, 1996).

by the downcutting of bedrock, called erosional terraces. The majority of the larger wadis found across the Nejd Plateau have been cut into the bedrock and likely represent ancient riparian systems (Zarins, 2001) (Figure 4.13).



Figure 4.13 Photographs of Wadis Aybut. (Photograph by Y. Hilbert)

Two main lithological groups compose the exposed bedrock observed across the Nejd: the Lower Hadhramaut group consisting of the *Umm er Radhuma* and *Rus formation*, and the Upper Hadhramaut group made of the *Dammam* and *Aydim formations*. The *Umm er Radhuma formation* is a thick, shallow marine unit that forms the main Tertiary carbonate sequence. Jebel Qara and the high plateau around Medinat al Haq are mainly made of this geological unit.

Within the *Umm er Radhuma formation*, the *Mudayy member* is noteworthy for its chert bearing qualities. This thin bedded whitish dolomite chalk and bioclastic limestone member is dotted with large chert nodules characterized by a homogenous crystalline matrix. Also found within this member are calcite druses, which aid the identification of this member in the field (Figure 4.14). Most of the Mudayy chert nodules, blocks and plaquettes found during the DAP survey were well crystalized and showed no severe natural fractures, which would have hampered stone tool production. Raw material colour

has proven to be considerably varied; in some cases, colour variability within the same nodule surpassed the expected range. Colours varying from beige, grey and grey-pinkish were observed. Commonly the exterior fraction, close to the cortex, had translucent properties and showed the highly of variable properties.



Figure 4.14 Photograph of the Mudayy Member near Habarut.
(Photograph by Y. Hilbert)

As previously mentioned, the *Rus formation* is significant for this study due to its chert bearing qualities and distinct features found within the raw material's matrix. Chert from the *Rus formation* is easily recognizable when found in archaeological assemblages. The *Rus formation* is divided into two members; the lower Chalky *Aybut member* and the upper marly-carbonate *Gahit member* (Platel et al 1992). A three to five metre thick brecciated dolomite limestone characterizes the *Aybut member*, with brown chert debris at its bottom. The breccia has been afflicted by re-crystallization caused by the dissolution of evaporates that culminated in the collapse of this member some time after its formation. The quality and size of this raw material is highly variable due to its displacement; most of

the chert encountered is highly fractured and ranges greatly in size and quality. The *Gahit member* consists of thinly bedded, post-evaporitic clay and marl. Signs of bioturbation are seen in this bioclastic layer. Chert nodules were found within the *Gahit member*. The Gahit chert is grey to light grey in colour and often banded. It is well crystalized and exhibits fair knapping qualities. Small darker crystalline impurities, visible within the matrix of the chert nodules, have not influenced its knapping properties. Cortex characteristics and nodule size vary greatly. Specimens have been observed presenting a thick white and chalky cortex, while other pieces had a thin, dark and porcelain like cortex. Nodule size varies between marble-sized specimens and watermelon-sized nodules.

Within the *Mudayy member*, at the contact zone between the soft dolomitic chalk and the carbonated limestone and similar compositions found within the *Rus formation* rockshelters have formed. As such, rockshelters might be described as “shallow niches or ledges under overhanging bedrock” (Waters 1992, 240). Sediments accumulating inside rockshelters (Figure 4.15) may be divided into endogenous and exogenous types. Endogenous sediments form by chemical and mechanical processes, including the physical deterioration of the walls, ceiling and bedrock floor of rockshelters. Sediment particles vary greatly in size, from silt-to-sand-size grains, coarse angular rubble (also known as *éboulis*) to large slabs and boulders. Chemically formed sediments are divided into dripstones and flowstones; these occur when carbonate infused water percolates through the bedrock and on its way precipitates deposits of calcium carbonate (*travertine*). Drip stones, commonly known as stalagmites and stalactites, typically form in karstic caves systems, while flow stones are commonly found in the back wall of rockshelters. Exogenous sediments are brought into rockshelters and caves through the entrance or any other fissure in the back or ceiling of the shelter. Depending on the shape, size, position, orientation and the immediate surroundings of the rockshelter, exogenous sediments may be derived from eolian, alluvial, lacustrine, marine, biological or anthropogenic processes.

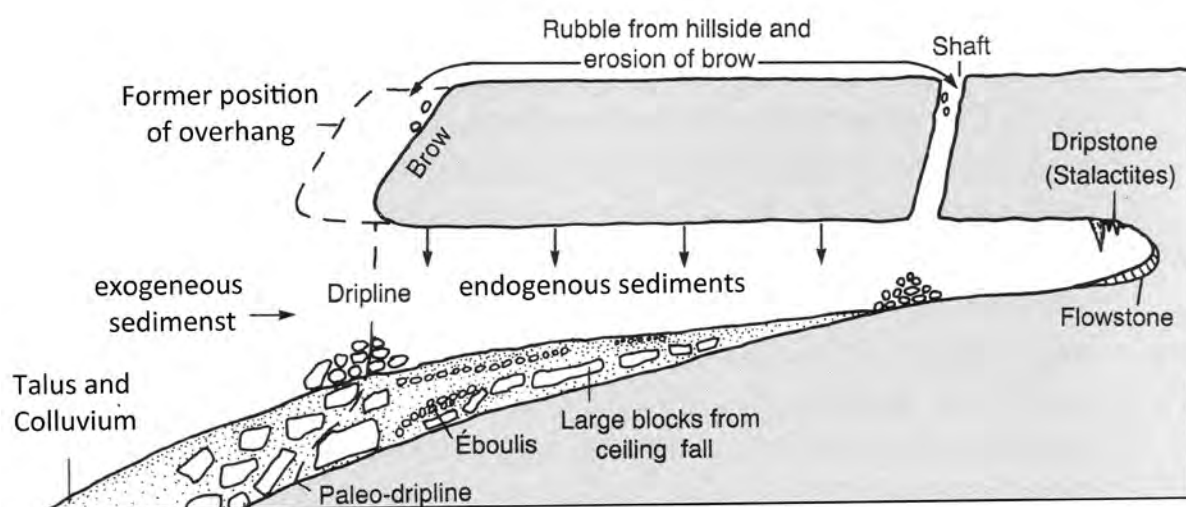


Figure 4.15 Rockshelter schematic. Cross-section across a idealised rockshelter situation depicting the diverse sediment sources. (After Waters, 1996, 5.13)

The disposition of sediments found within caves and rockshelters is highly dependent on the lithology, weathering processes, hydrologic conditions and the local surroundings of these features. Those aspects contribute to the uniqueness of every rockshelter and cave in its structure and stratigraphy (Waters, 1996; Goldberg & Macphail, 2006; Heydary, 2007). Rockshelters and caves offer favourable conditions for the preservation of archaeological material. Still, the post-depositional factors acting in caves and rockshelters and the continuous development of these features may disarticulate the archaeological horizons or lead to their total erosion and subsequent destruction. Most of the rockshelters visited by the DAP team in Dhofar were completely stripped of sediments (Figures 4.16).

For the purposes of this study the Nejd Plateau is partitioned into an eastern portion and a western portion, the gravel plain around Thumrayt being the frontier between the two. Each side is further divided into southern, central and northern portions. The division of the Nejd into these sections is based on geomorphic observations such as elevation, terrain roughness and the presence of large wadi systems in each area (Figure 4.17).



Figure 4.16 Rockshelters and karstic features in South Arabia. Photographs of diverse rockshelter environments and karstic features across southern Arabia (photographs by M. Morley and Y. Hilbert)

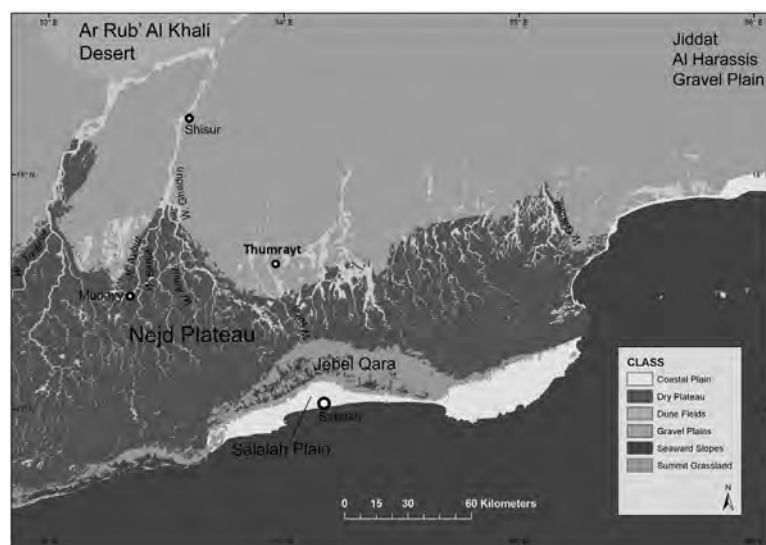


Figure 4.17 Map of Dhofar showing different ecozones. (After Rose et al., 2011a, fig. 3)

The southern Nejd is characterized by the interplay of a series of smaller wadis dissecting a barren and steep tableland. This particular feature is related to the proximity of the southern Nejd to the orographic barrier, which triggered intense erosional sedimentary activities. These countless small catchment systems would have fed the higher streams with considerable amounts of limestone detritus and gravels. At its southern border, table mountains and inselbergs consisting of Tertiary limestone characterize provide further complexity to this landscape serving as sediment supply, which becomes incorporated into gravel plains situated between these elevations. These intra hill basins would have been optimal spots for faunal and human activities. Additionally, low terraces occasionally displaying more than one activation phase, have formed along the larger wadis in the area (Figure 4.18).

The interplay between these ephemeral erosional fluvial systems and the soft bedrock, which across the southern Nejd is constrained primarily to the *Rus formation*, has created an abundance of complex rockshelter situations. These have shown a high level of variability concerning their size and both, supply and conservation of native sediments. It has been observed throughout the DAP field seasons that rockshelters tended to form along previously eroded aquifers. Within these rockshelters, native sediment accumulation resulting from the mechanical breakdown of the back and the sealing of the shelter have been found to be susceptible to further erosion in case of the subsequent reactivation of the stream. Therefore the majority of rockshelters excavated in this area have been scoured of sediments. Two of the transects that will be discussed further on in the data section of the dissertation were placed along site-rich areas across the southern portion of the Nejd Plateau. Of these the BRAVO transect had the greatest density of rockshelters with preserved terminal Pleistocene/Early Holocene sediments. This density of preserved sediments is due to the configuration of this landscapes hydrology and morphological complexity, which protects the sediments from torrential storms and erosion.



Figure 4.18 Panoramic images of the Southern Nejd.
(Photography by Y. Hilbert).

When torrential storms hit the Dhofar escarpment the water gatherers within the myriad small catchment basins of the southern Nejd. Further downstream these systems gathered large masses of water that sum up a considerable erosional force. Therefore, erosion and re-deposition of sediments is more intense within the central portions of the Plateau as opposed to the southern Nejd.

The southern Nejd region and the northern fringes of the Jebel Qara are known for the occurrence of the Frankincense tree (*Boswellia sacra*). The dried sap of this tree remains Dhofar's greatest export across prehistoric and historic times (Van Beek, 1958; Zarins 2001). Aside from the Frankincense tree the flora and fauna found across the Nejd is considerably homogenous; mostly desert scrub and occasional acacia tree groups. During the month of November in 2011 a considerable amount of precipitation had fallen over the Nejd, the results of which were observed by the DAP team during the 2012 season; the Nejd had partially turned green. Carnivore species inhabiting the Nejd are the same as found on the escarpment and the plains; large mammals include, among other species, hyena and diverse species of gazelle.

Past the village of Haluf, situated within the Haluf valley, where the wadis become considerably larger in comparison to the riparian systems identified in the south, the central Nejd commences. Here the wadis that progressed across the southern Nejd conjoin, forming larger drainage systems while the landscape becomes more homogeneous in term of its relief (Figure 4.19). The wadis are filled with large heavily rounded cobbles while extremely high terraces flank the wadi valleys. These wadis show "at least three recognizable terrace systems spanning 2.0 million years" (Zarins, 2001, 24). The major wadis systems running west of Thumrayt are Wadis Haluf, Dawkah, Ribkhut, Aydim, Aybut, Banut, Amut and Ghadun. East of Thumrayt Wadis Dahabun, Afuf and Halit dissect a low limestone plateau. According to Zarins (2001), Dahabun, Dawkah, Ribkhut, Aydim and Ghadun began as major Pleistocene river systems draining towards the Rub al Khali.



Figure 4.19 central Nejd Plateau.

right) C. Galletti, Dr. V. Usik and Dr. J. Rose during survey at wadi Aydim; 3, panoramic view over Wadi Aybut. (Photographs by J. Geiling and Y. Hilbert)

Tectonic displacement of the tertiary sedimentary rocks has caused the recurrent activation of countless fresh water springs across the central Nejd Plateau, particularly around the village of Mudayy (Figure 4.20). Springs are not constant features in the landscape; in particular, artesian springs may become inactive over the course of time and then reactivated in a completely different setting, creating a new spring pond and travertine spring mound. Deactivation of springs occurs due to climatic variations, triggered by a change in the water table or by tectonics. Due to the highly active sediments in spring environments, artefacts and archaeological sites encountered in such settings are often not in their primary depositional context, in addition, artefacts may show considerable damage and rounding due to water wear. On the surfaces adjacent to springs, the likelihood of encountering archaeological sites in less reworked conditions

increases. The majority of springs identified by the DAP across the Nejd were categorized as gravitational springs, which are highly dependent on the ground water levels that *per se* is considerably susceptible to climatic oscillation. The use of modern day boreholes and pumps has considerably lowered the inland ground water level (Johnson, 1998; Beineke, 2006) causing springs across the Nejd to dry out.



Figure 4.20 Springs by Mudayy.
both remnant of springs and active springs like the one shown above. (Photograph by Y. Hilbert and J. Geiling).

Rockshelters and vertical sinkhole features found across the central Nejd are unlike those found across the southern Nejd. This is mostly due to the diverging lithology observed across these two regions, while in the south the *Rus formation* predominates the central Nejd is marked by the presence of the *Umm er Radhuma* formation. Rockshelters in the central area are close to the main wadi systems across the central Nejd; being of considerably greater dimensions and commonly presenting native sediments allocated in front of the shelter situation.

To the east and west of Thumrayt a flat alluvial gravel plain partially covered by eolian sediments marks the area. The occasional inselberg and other remnants of the Lower or Upper Hadhramaut Formations may be spotted across the plain. This plain is dissected by numerous flat erosional gullies and ephemeral streams that carve one meter deep longitudinal trenches across these flood plains. These gullies do not form large wadi systems as seen on either side of the gravel plain surrounding Thumrayt.

Past the central Nejd the plateau dips northward and gives way to a gently undulating plain. The northern Nejd is a flat and homogenous plain that borders the Rub al Khali desert. On the north western side of the northern Nejd the wadi Aydim flows through the low gravel hills while to the north wadis Ghadun, Banut, Amut and Aybut conjoin into the al Burj al Sallyah that also empties into the Rub al Khali. Flat gravel plains covered with reworked fluvial sands and recent to sub-recent and even ancient alluvial fans give the northern Nejd some variability. Additional travertine deposits of diverse age and calcareous paleosols intermingle with Miocene limestone lacustrine deposits are also attested across the northern Nejd. Based on remote sensing images, Zarins (2001, 24) proposes that a minor folding event occurred in the Late Pleistocene, which opened up springs throughout this region. The area around Shisr was particularly affected by this event, which was responsible for the diversion of stream flow in some of the wadis in the area (Figure 4.21).



Figure 4.21 Northern Nejd and Rub al Khali desert.
(Photographs by Y. Hilbert)

Further to the north, past the Nejd, the vast Rub al Khali desert stretches over most of the central Arabian Peninsula. Barchan sand dunes reaching over 200 meters in height seem to sail across the gravel plains. Late Pleistocene wadi systems running toward the Arabian Gulf and interdunal fossil lake deposits have been attested throughout the central Arabian Desert (e.g. Holms, 1960; McClure, 1976, 1978). Alluvial fan remnants have been found within the Rub al Khali portion surveyed by the DAP demonstrating the continuation of the Nejd riparian systems into the desert.

4.3 Summary

In this chapter a description of the geology and geomorphological settings encountered by the DAP team during the field campaigns across Dhofar was given. A brief description of the Sultanate of Oman was also provided, giving the reader a sense of the myriad ecosystems and niches found across this part of southern Arabia. Emphasis has been placed on the description of the lithology, geomorphology and ecology of the Nejd plateau. Based on Zarin's partitioning of the Dhofar region into four zones, the coast, the escarpment, the Nejd and the Rub al Khali desert, further segregation of the Nejd Plateau into southern, central and northern areas was proposed. These areas have been described and the relevant geological formations, namely the chert bearing layers that served the local prehistoric populations as raw material sources for the manufacture of stone tools, outlined. The three chert types, Mudayy, Aybut and Gahit described as to their appearance and knapping properties.

The fact that no Late Palaeolithic sites have been found across the Dhofar escarpment and the costal plain is likely due to the low archaeological visibility and poor accessibility of the divers landscapes within these environments. Alternatively, it may be argued that enough moisture reached the southern Nejd enabling Late Paleolithic populations to remain in this region. The three transects have been chosen for analysis, ALPHA, BRAVO and GULF are located within the southern and central territories of the

Nejd. These have produced *in situ* assemblages and surface samples located on stable and deflated surfaces. The following chapter will present the theoretical and methodological background for the lithic analysis undertaken on the samples retrieved from the Nejd Plateau.

TOWARDS UNDERSTANDING LITHICS: THEORY AND METHOD

The activities of living creatures, not just the anatomical structures which facilitate their activities, are vital factors in the struggle for existence. Since the time when culture first began to develop, it has influenced the activities of our ancestors. Culture is not only our creation but our creator.

–Frederick S. Hulse, *The Human Species* (1971, 489)

As Hulse observed in “The Human species” (1971) culture and its expressions have enabled our survival across climatic oscillations, natural catastrophes and culturally induced calamities (e.g. wars, epidemic outbreaks etc.). Any attempt to archaeologically grasp a given cultural entity is therefore limited to the analysis of its products and by-products. As has been noted throughout chapters Three and Four, archaeologists working in Southern Arabia are forced to focus on the most resilient of cultural expressions; lithics.

Any deliberate technological process is part of the cultural system of a population and therefore part of a collective cognitive repertoire (e.g. Jelinek, 1976; Sackett, 1982; Davidson & Nobel, 1993; Ingold, 1993). Through cultural transmission technological processes are passed on through generations, making this most basic aspect of stone tool technology more resilient to change (Tixier, 1984; Hahn & Owen, 1985; Bar-Yosef & Meignen, 1992; Monigal, 2002). In order to best categorize and define the samples pertaining to the Nejd Leptolithic technocomplex, lithic analysis was undertaken. The analysis of the diverse Late Palaeolithic stone tools found across Dhofar should ultimately lead to the identification of a local industry. Once its defined comparisons between the Late Palaeolithic of Dhofar and industries found in adjacent regions may be made. Such comparisons relay on technological processes used to produce stone tools and the morphology and taxonomic variability of these stone tools.

Among the goals of this dissertation are the categorization of these technical

processes and the placement of these cultural traits into a regional and chronological framework. This technological framework is accompanied by a specific set of formal and informal tools, which once recognized can be used as markers of a specific industry.

This chapter will focus on the clarification of the taxonomic nomenclature and definitions used throughout the analysis. The methodology used to identify the aforementioned reduction modalities will be explained and exemplified. Stone tools typology, used to define the Nejd Leptolithic tradition tool kit will be elucidated.

5.1 Reconstruction of reduction sequences

The products of a deliberate knapping event may be divided into cores and blanks, the earlier being the source of the later. During the production process, the objective piece, in this theoretical case a flint nodule, is hit in a controlled manner in order to create a blank, the detached piece (Inizan *et al.*, 1992; Whittaker, 1994; Kooyman, 2000; Andrefsky, 2005). It is important to keep in mind that the core and blank concept is by no means a static construct; any blank may serve as a source for further blanks, thus being assigned a core status (Inizan *et al.*, 1992; Hahn, 1993; Usik, 2004).

Further complicating matters, intentionality plays a considerable roll in lithic technology. By using core reconstructions, diverse phases within knapping events may be differentiated (e.g. Volkman, 1983; 1989; Demidenko & Usik, 2003). The analysis of core reconstructions and products of knapping events are here used to recreate the reduction sequence used by the Late Palaeolithic populations of Dhofar. Refittings and conjoins will play a major role in the reconstruction of the reduction sequences used across the aforementioned period.

The term reduction sequence used above is to a certain degree akin to the *chaîne opératoire* concept that will be explained later on. Of interest for this study is the intentional production of standardized blanks anchored within a culturally set array of reduction modalities. The use of a given reduction modality over another is related to

intentionality and choice, making the reconstruction of these modalities a useful marker for identifying culturally specific traits within the Nejd Leptolithic technocomplex and any other given cultural unit.

5.1.1 Refittings

The act of piecing together diverse flakes, blades, cores and tools is termed refitting. This method has been applied to archaeological samples for over a century and is not restricted to the study of lithic assemblages (Leroi-Gourhan & Brézillon, 1966; Hofman, 1992). Refitting studies shed light on site formation processes, taphonomic processes, and organization of living space, raw material economy and the reconstruction of technological processes (e.g. Bosinski & Hahn, 1972; Cahen, 1976; Hiatala, 1983; Usik, 1989; Adler & Conard, 1997).

The reconstruction of cores using the refitting method not only enables the identification of specific stages within a technological continuum (Volkman, 1983, 1989; Bleed, 2002a; Schimelmitz *et al.*, 2011; Hilbert *et al.* 2012), it also provides verification for more general lithic analysis (Monigal, 2002). Additionally, this technological component coupled with spatial analysis provides insights into raw material economy and site function. Drawbacks of this method are¹ the inability to grasp short discontinuous knapping events undertaken on a given core, and the difficulties of using refittings in an empirical way.

The use of refitting analysis in Arabia is rare, aside from a few exceptions (Rose, 2006; Rose *et al.*, 2011a; Usik *et al.*, 2012; Hilbert *et al.*, 2012; Delagnes *et al.*, 2012). Possible reasons for this are the dearth of well sampled sites coupled with the overall lack of technologically oriented studies. This scenario is likely to change given the growing interest in the area.

Three types of refit-producing sites have been identified and sampled: immediate, surface and buried (Figure 5.1). Immediate sites are spatially delimited small-scale scatters

¹ Not to mention that the process of refitting may at times be painstaking, frustrating, time consuming, frustrating, time consuming and requires considerable amount of lab space; nonetheless, all these troubles are forgotten in the very same moment when artifacts start to fit on to one another.

pertaining to a single knapping event. Such sites have shown great potential for refittings and, as will be seen in following data chapters, often yield complete core reconstructions. These isolated scatters present the possibility of identifying desired products. Artefacts removed from the sites have obviously been transported away from the workshops for further processing.



Figure 5.1 Diverse situations in the field susceptible to production refits.

1, photograph of Ghazal Level 2 surface and artefacts; 2, isolated knapping event near Wadi Haluf; 3, large surface site at Wadi Haluf. (Photographs by Dr. Rose and Y. Hilbert)

The majority of the surface sites identified by the DAP across Dhofar are extensive workshop scatters located adjacent to raw material sources. Given the wealth of artefacts observed on such scatters, selective sampling of smaller unites within such sites was undertaken. In these cases, refittings help establish the zonation of artefacts within these immense scatters. Refitting studies were also applied on samples excavated from buried sites. In these cases refitting studies helped establish stratigraphic integrity and technological diachronic change (Marks, 1983b).

The methodology applied followed the suggestions made by Demidenko and Usik (2003). Artefacts have been organized according to category, square units, raw material and dorsal cortex cover. Three reconstruction types have been identified: conjoins, phase refits and major core reconstructions. The term conjoin is used to address fragments from a single blank or core that have been refitted into a complete object. Phase refits are composed of a series of artefacts refitted to a constellation representing a specific phase within a continuous reduction sequence. Major core reconstructions are refits that depict a complete reduction sequence encompassing decortication, core preparation and blank production.

Based on these criteria, core reconstructions, conjoins and phase refits were either illustrated or photographed, and described as to the method of reduction used. In the case of illustrations, the blanks are numbered according to the succession of reduction, commencing with the first attached piece and ending with the last. These are illustrated in separate phases in order to make the reconstruction of the cores comprehensible (Figure 5.2). Aside from the identification of reduction modality used, variations within the diverse methods are described. Based on these observations and the results of the lithic analysis, reduction patterns can be established. These are used to draw intra site comparisons, helping to establish the range of technological plasticity within the Late Palaeolithic of Dhofar.

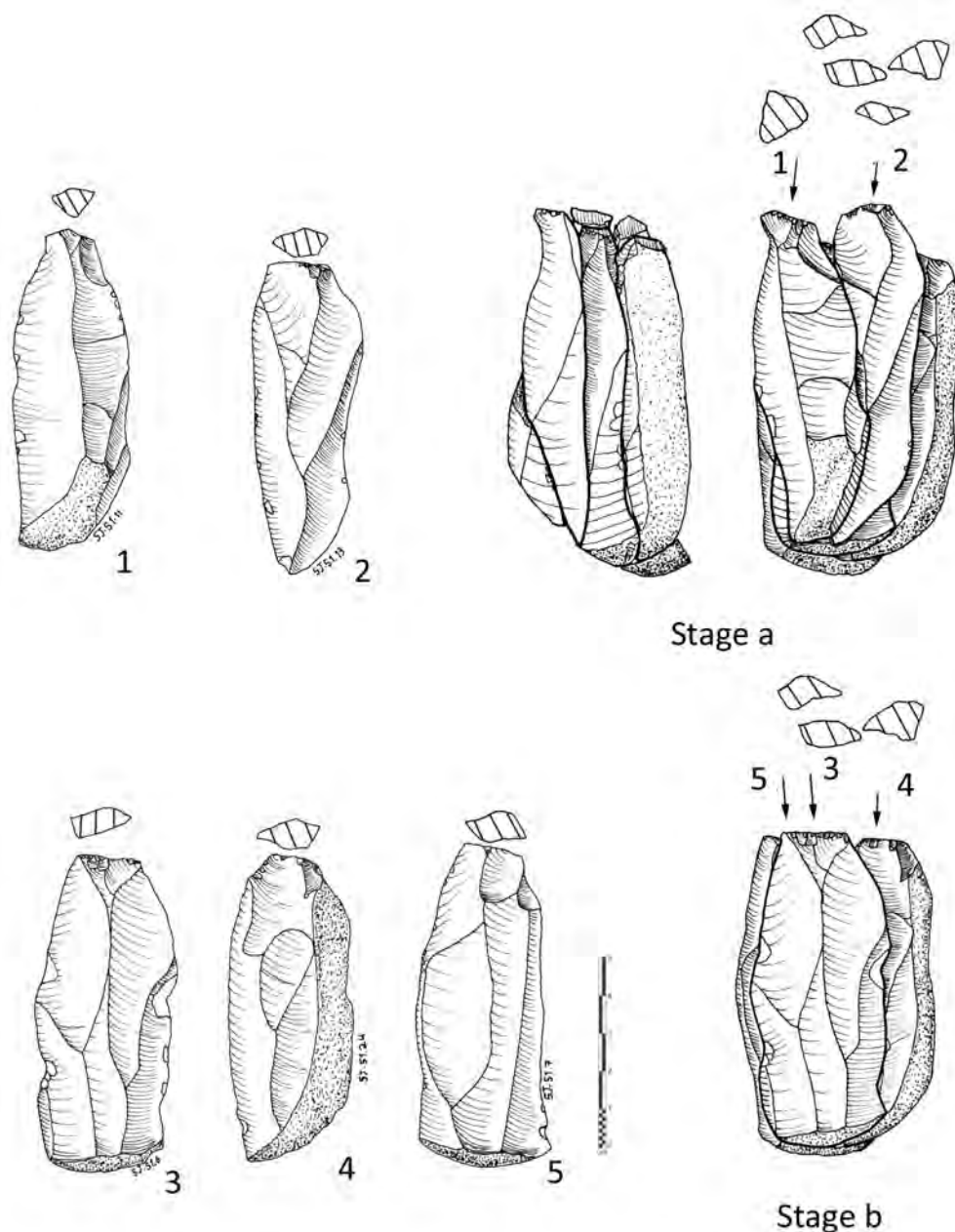


Figure 5.2 Example of illustrated refit from SJ. 51.(Illustration by Y. Hilbert).

5.1.2 Replication studies in lithic technology

The technologies and procedures involved in the production of a stone tool are myriad. Reconstruction of these work steps may be achieved through replications done by modern day flintknappers or by drawing analogies from ethnographic contexts. Given that modern day populations that still depend on and use lithic technology have become rare,

replications experiments offer a fair alternative to the reconstruction of past technological dynamics. Either way, by analysing projectile technology use by Bushmen or replications done by experienced contemporary flintknappers, information gathered on variability, and the lack of it, are extremely valuable.

Three distinct approaches to understanding lithic technology through replications are given: laboratory experiments, modern flintknappers and fracture mechanics theory (Kooyman, 2000). Laboratory experiments are used to isolate particular elements within lithic technology (e.g. Dibble & Whittaker, 1981; de Wilde & De Bie, 2011; Dibble & Rezek, 2009; Rezek *et al.*, 2011). These controlled experiments are used to assess variability within this one isolated feature. This category also includes experiments conducted outside of laboratory conditions that assess specific questions; for example impact fractures on projectile points shot at dead animals (e.g. Odell & Cowan, 1986), striation patterns on ground stone tools (e.g. Adams, 2002; Dubreuil, 2004) or blade pressure flaking (e.g. Pelegrin, 2006). Moreover modern day replications of lithic technological procedures help develop possible trajectories used to achieve one specific goal.

In general replications provide important insights into stone tool manufacturing processes. Given the myriad variables these replications are subjected to, result should be viewed as theoretical constructs. These theoretical constructs can then be used to explain the pattern we seen on the archaeological material, offering insightful information regarding flintknapping dynamics.

5.1.3 Chaîne opératoire

The *chaîne opératoire* is a technological approach that aims at the reconstruction of the technical procedures used by prehistoric populations. In other words, through it the archaeologists seek to elucidate the succession of mental operations and technical gestures used by cultural actors to accomplish a given task (Perlès, 1987; Sellet, 1993; Shott, 2003). Consequently, this analytical principle aims at the description of the transformations

processes applied to a given raw material starting with its acquisition and ending with the abandonment of the exhausted tool (Binford, 1977, 1979; Tixier *et al.* 1980). Through it a chronological segmentation within this aforementioned continuum is achieved. Each of these chronologically divided phases encompasses distinct mental processes required to accomplish all stages of tool manufacture and maintenance.

Through the reconstruction of the raw material procurement systems exerted by past populations, statements concerning basic constraints on stone tool technology may be made. The availability of high, or low, quality raw material at a given site has been known to affect the organization of technology; namely the production of formal vs. informal tools (e.g Inizan *et al.*, 1992; Andrefsky, 1994). Raw material size constrains the dimensions of the artefacts found at a given site, making the localization and description of the raw material outcrops central when dealing with stone tool size variability. In regards to organization of blank production systems and the configuration of site assemblages, site distance to source may bring forth diverging solutions to raw material curation prior to transport. In other words rocks are heavy and to carry them around costs energy. Early stage maintenance, as in decortication of nodules and core preparations, is more intense at the quarry sites if the distance to the living site is greater (e.g Newman, 1994; Beck *et al.*, 2002). If the raw material source is close to the site, entire nodules will be transported and reduced directly at the site. In general the analysis of raw material economics should serve to determine the type of raw material, its quality and how it got to the site (Ericson, 1984; Sellet, 1993).

The analysis of lithic production, based on refittings, perusal of cores and metrical/morphological analysis of the blanks are undertaken in order to establish pattern of lithic reduction. Within the *chaîne opératoire* analysis of the blanks, each piece is appointed a specific place within the reduction. The objective of this step is to identify the goal or preferential end products of a deliberate blank producing system (e.g Van Peer, 1992; Boëda, 1994; 1995; Usik, 2006). The categorization of lithic production technology into

stages is based on what is done within each of these stages, thus blanks will bear features that may be associated with one of these phases (Kooyman, 2000; Bar-Yosef & Van Peer, 2009).

Once a blank is modified by retouch it is here considered a tool. The study of tool use, maintenance and discard complete the scope of the *chaîne opératoire* approche. The goal of this phase is not the reconstruction of the tools function (this aspect is better enlightened by use wear and trace analysis), but rather to refine the data provided by the typological analysis. By analysing the processes that created the tool, thus applying a technological perspective, better taxonomic control over tool variability may be made.

5.2 Débitage Analysis

Any archaeologist that has worked or enjoys the fortune to be working with a lithic assemblage will confirm that the amount of work invested in sorting through countless bags of flakes, blades, chips, bladelets and other blanks is enormous. The amount of information gathered is immense, raising the question of what to do with all this data and most importantly what does it mean? Entire volumes and countless articles have been dedicated to inferring meaning and order onto *débitage* (e.g Dibble & Whittaker, 1981; Sullivan, A. & Rozen, C. 1985; Ahler, 1989; Shelley, 1990; Bradbury & Carr, 1995; 1999; Ballin, 2000; Andrefsky, 2001).

The term *débitage* is derived from the French school of lithic analysis (e.g. Bordes, 1961; Inizan *et al.*, 1992; Boëda, 1994) and stands for all products a deliberate knapping event, including cores. A narrower definition of this term is used here, synonymous with the term blank. Following Munday (1976) and Fish (1976) *débitage* encompasses all product and by-products of any deliberate knapping event (either blank production or tool manufacture) excluding only cores and tools.

Within the Anglophone school of lithic technology blanks have also been viewed as products of deliberate knapping events; these desired products were chosen for further

modification into tool (Bradley, 1975; Sullivan & Rozen, 1985). The waste of a deliberate knapping event, primary, secondary and tertiary flakes (cortical elements) were not considered to be blanks. Based on the *chaîne opératoire* approach it has been shown that cortical elements, regardless of the amount of cortex they possess, have some potential of becoming a blank for tool manufacture (David, 1993; Roth *et al.*, 1998; Stout, 2002). Thus the segmentation of knapping products into blanks and waste will not be used throughout this study.

Using theoretical constructs, experimental replications and refits, researchers infer meaning and order upon *débitage*. Based on these, some basic assumptions may be made: *débitage* are volumes of raw material produced from other volumes by percussion or pressure. These can be further divided into sub categories based on metrical proportions (flakes, blades, bladelets and chips) and the amount of cortex on their dorsal surface (cortical pieces). Other objects may be identified as part of specific technological reduction modalities (bifacial thinning flakes, *débordant* elements, crested blades, Levallois preferential products etc.). These classificatory terms are used to infer when within the *chaîne opératoire* the artefact was produced. *Débitage* showing a considerable cortical dorsal percentage are held to be part of the early decortication stage, but identifying the transitions between each stage is difficult. Artefacts produced at the end of a reduction stage and artefacts produced in the initial phase of the subsequent stage will share very similar morphologies, making classification problematic. The categorization of these theoretical stages of reduction is a useful analytical tool, but it has to be kept in mind that core reduction is a continuous process subject to many variables (e.g. Marks, 1983b; Boëda, 1994; Whittaker, 1994; Bradbury & Carr, 1999; Tostevin, 2007; Bar-Yosef & Van Peer, 2009; Van Peer *et al.*, 2010).

The taxonomic attribution of *débitage* alone is of little use considering the static characterization of *débitage* typology. By analysing set features observed on blanks and the interplay between these features the technological processes that generated the

débitage may be laid bare making such analysis valid (Hahn, 1993). The identification of purpose within the *débitage* production system is one of the central dilemmas within lithic analysis. Whether a flake was produced using a blade reduction system or the shaping of a bifacial tool may be answered based on the analysis of separate lines of evidence (Hahn, 1993; Odell, 2004; Andrefsky, 2005; 2009). Identifying intentionality implies looking into the mind of the maker. Through refitting studies, variability within technological processes and behavioural aspects of raw material economy may be inferred (Demidenko & Usik, 2003), thus allowing for the reconstruction of the processes that produced the object in the first place. On the other hand, over-formalization and the lack of an empirical basis in technological studies have clouded our ability to explaining patterns identified by the *chaîne opératoire* approach (Bar-Yosef & Van Peer, 2009). So why go through all the trouble? If typology is not the answer and the tools used by prehistorians to reconstruct past processes are not entirely based on empirical data how do we proceed? Technological reconstruction of past processes can provide vivid insights into activities undertaken by past population, thus making it feasible to sort through tons of *débitage*. The principle limitation of archaeology lays in our incapability of fully reconstructing the cultural systems that created the artefacts we study.

Keeping these thoughts in mind this study addresses the classification and definition of material culture pertaining to Late Palaeolithic of Dhofar. Neglecting the *débitage* would be like cooking without a fire; it can be done but the result will not satisfy every palate². By looking at scar patterns, striking platform morphology, vertical and horizontal cross-section, blank terminations and metrical parameters a profile for each artefact is created. Thanks to core reconstruction and replication experiments the parameters responsible for the configuration of the established blank profile may be inferred.

2 Like Japanese food (sushi) for example.

5.2.1 Blank orientation and measurements

Blank dimensions are sensitive to a series of factors, mostly related to raw material dimensions and knapping qualities, and reduction modalities used (Dibble & Whittaker, 1981; Newman, 1994; Shott, 1994; Kooyman, 2000; Dibble & Rezek, 2009). At illustrations and during analysis *débitage* are oriented with their striking platforms pointing down and the terminal portion pointing away from the viewer. Blank length, width, thickness, weight, platform width, platform thickness and platform angle were measured for this study (Figure 5.3). The three main measurements taken directly on the artefacts, length, width and thickness, reflect the blanks approximate volume. Blank and blank striking platform dimensions were taken using an electronic calliper, with an output directly into the database used (given in millimetres: mm). Blank length was determined starting from the striking platform to the furthest point following the blanks' technological axis. Blank widths were taken at the central portion of the artefacts oriented horizontally to the technological axis and blank thickness was determined perpendicular to where the artefacts' widths were determined.

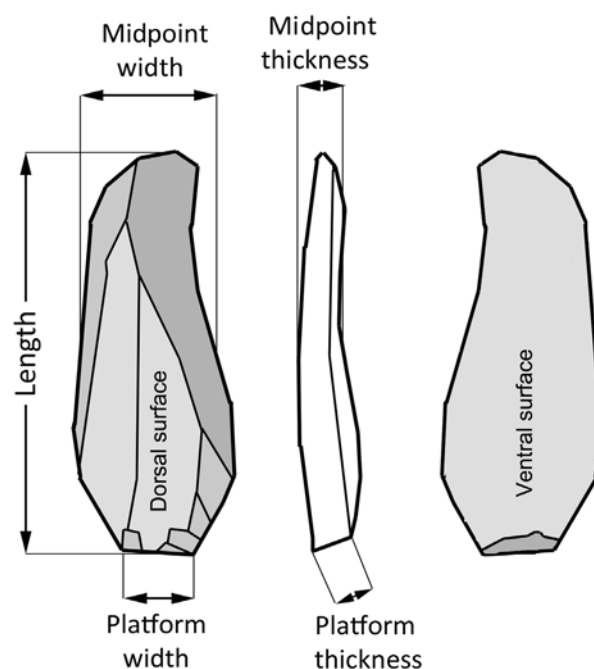


Figure 5.3 Blank orientation and measurements. As noted in the text, artefacts are oriented with their striking platforms down, except when incorporated into refittings. In these cases, for clarity sake artefacts are depicted with the striking platforms pointing up, matching the illustrated core and reduction orientation. (Image by Y. Hilbert)

Striking platform dimensions were taken (width and thickness) following the method applied to determine overall blank dimensions. Platform width was measured as the distance between the edges of the plane following blank midpoint width. Platform thickness was determined as the distance between the point of percussion and the intersection of the striking platform and the dorsal surface of the blank. Platform size, width and thickness, were found to have great influence on overall blank volume (e.g Dibble, 1997; Kooyman, 2000)

In order to determine the metrical variability among the *débitage* for a given assemblage, indices have been calculated based on the above described metrical parameters. Average values (arithmetical mean) and standard deviation (calculated on the basis that the samples dealt with are but a part of the population rather than representing the complete population) are used to represent both variability and lack thereof within the analysed assemblages. Index of platform flattening (IPF), is found by dividing platform width by platform thickness. Values around 2 indicated that the blank is rectangular in shape and twice as wide as it is thick. Values approaching 1 indicate that the platform is square. The higher the values the thinner and wider the platform is. The index of blank relative platform size (RPS), estimated by dividing the blank's area (length multiplied by width) by its platform area (platform width multiplied by platform thickness), has been estimated for all complete blanks within each of the samples. This index indicates the relative size of the platform in respect to the blank's size. The higher this value the smaller the blank's platform is in regard to the blank's size. Index of elongation was equally determined to grasp the extent of general elongation; this value is determined by dividing the blank's length by its width. By definition, blades and bladelets will have values equal or above an index value of 2. The higher the value the longer the blank, and if the value of a blank is lower than 1, the piece is wider than it is long.

5.2.2 Blank Type

Although little information *per se* is given by this taxonomic attribution, the percentage of specific types of *débitage* within a given assemblage (blades, bladelets and *débordants*) may represent a useful indicator for identifying specific production modalities. Furthermore these rough markers may be used for drawing comparisons between assemblages on a lower analytical scale.

5.2.2.1 Flake

The word flake refers to any piece of *débitage* detached from a core or tool. No specific morphology, use or dimensions are inferred by this terminology. If a flake was smaller than a thumbnail (10 mm in maximum diameter) it was termed a chip. Flakes have been further segregated into cortical, *débordant* or bifacial thinning flakes depending on morphological characteristics. Cortical flakes have more than half their dorsal side covered by cortex (over 50%). If the flake was detached from the lateral portion of the core, removing either a former lateral striking platform or simply having a cortical back the termed *débordant* flake is used. These are mostly lateral and steep in horizontal cross-section, and reduced off-axis in relation to the dorsal scar pattern.

Bifacial thinning flakes (BTF) are produced as a result of a *façonnage* oriented reduction of specific tool forms, mostly bifacial implements. The *façonnage* reduction method aspires to shape a desired tool form by means of progressive retouch of a given block of raw material (Inizan *et al* 1992; Hahn, 1993; Debénath & Dibble, 1994). BTF's are identified based on metrical parameters and morphological characteristics. These present an intensely faceted striking platform and are curved to twisted in their horizontal cross-section.

5.2.2.2 Blade.

The term blade is used here in a strict Bordian sense of a given flake that is at

least twice as long as it is wide (Bordes, 1961). Interpretative segregations between “true blades” (Bordes & Crabtree, 1969) and “flake-blades” (e.g. Singer & Wymer, 1982) have been discussed elsewhere (Monigal, 2002), and are not considered further here. The purely metrical definition serves the purpose of this study just fine.

Within this cadre of elongated *débitage* the following variations were found relevant and have been differentiated: cortical blades, *débordant* blades and bladelets. Having more than half their dorsal surface covered by cortex marks cortical blades. *Débordant* blades are *débitage* elements reduced from the lateral edges of a core’s working surface that are at least twice as long as they are wide. Commonly, *débordant* blades are struck off-axis and present a lateral steep medial cross-section. The lateral portion of these artefacts is cortical, and given their appearance these artefacts have been named “naturally backed knives” (NBK) (Shimelmitz *et al.*, 2011). Attribution of *débordant* blades as NBK is regarded as inappropriate for the samples from Dhofar given that no signs of use, or retouch have been observed on any of the *débordant* elements analysed for this study. Moreover, the technological aspect of these removals, in many cases with overshoot terminations, appears to be related to horizontal and vertical convexity creation and maintenances (e.g Meignen, 1995; Hays & Lucas, 2001; Le Brun-Ricalens, 2005;).

Bladelets are diminutive blades, created by diverse reduction strategies (e.g. Owen, 1988; Blades, 2001; 2005; Kuhn, 2002; Bleed, 2002b; Le Brun-Ricalens, 2005; Taller & Floss, 2011). The definition adopted here is a pure metrical one and follows Tixier (1963), which states that elongated, twice as long as broad artefacts not wider than 12 mm are regarded as bladelets.

5.2.2.3 Technologically diagnostic *débitage*.

This term assembles the remaining *débitage* that are found to be characteristic of specific technological processes and therefore associated with specific types of stone tools and reduction modalities. These are: crested blades, core tablets and burin spalls.

Crested blades are associated with true volumetric blade technology as described for diverse Palaeolithic assemblages in the old world (see Demidenko & Usik, 1993b). The purpose of this particular step in blade production is the creation of a triangular central guiding ridge on a core's working surface. This is achieved by transverse bifacial removals along the narrow edge of a raw material nodule; once direct percussion removes the guiding ridge, recurrent blade reduction on this face takes place.

Core tablets are part of blade production sequences, these are flakes struck perpendicular to the core's working surface, serving the purpose of renewing faulty and/or exhausted striking platforms.

Burin spalls are by-products of burin production. These tools are characterized by the removal of narrow, bladelet-dimensioned blank from the edges of a flake, blade or any other given *débitage*. Burin spalls are triangular or trapezoidal in cross-section and present dorsal scars that are perpendicular or highly oblique to the plane of the blank itself (Marks, 1976; Inizan *et al.*, 1992).

5.2.3 Blank Condition

Blanks were found either in complete, proximal, medial or distal states. Occasionally false burin fractures were observed. Only complete *débitage* were fully measured, blanks that were missing a small part of their proximal or distal portions have been regarded as incomplete. These pieces have been measured as well, given that such small fractures would have had little influence on the overall dimensions of the blank. Proximal, medial and distal fragments have been partially measured; only width and thickness were taken. False burin blows, also termed *siret fractures* (Inizan *et al.*, 1992) occur when the force created by the hammerstone hits the striking platform and travels unexpectedly along raw material faults, causing the blank to splitter into two pieces on a vertical axis. The term used by Anglophone researchers hints at the similarities between this rupture and the purposefully administered burin blow.

Further notes on the condition of *débitage* found at a site include whether artefacts have been burned, indicating the use of fire at the site. It has been observed that some artefacts from surface scatters were covered with podlits fractures. These are naturally occurring fractures induced by temperature oscillations; small circular flakes are detached from a parent block. In cases observed across Dhofar, fracture was so intense that only rough scar patterns could be identified on the affected *débitage*.

5.2.4 Patina

Patination is a process that affects all kinds of archaeological vestiges (Rottländer, 1975; Schiffer, 1983); it forms on the surface of artefacts and is triggered by chemical processes. Patination occurs when artefacts are logged within stable sediments or resting on stable surfaces. In lithic studies the term patination has been used to describe a series of macro-chemical and physical effects on stone tools. Experiments and formation-process oriented studies have shown that several specific elements related to environmental, mineralogical and anthropic factors have considerable effect on surface modification (Goodwin, 1960; Ackerman, 1964; Rottländer, 1975; 1978; Purdy & Clark, 1979; 1987).

Studies of both surface and buried materials are dependent on the quality and integrity of the archaeological finds (Hodder & Hutson, 2003). Artefact patination may be used as an indicator that pieces resting on stable surfaces have gone through similar post-depositional trajectories (Hunt, 1954). That is to say are likely to be coeval. Patination processes are related to a series of factors as was stated above, crucial to its formation and further development is the matrix in that the artefacts are bedded or have been bedded in (Schiffer, 1983). During the DAP field campaigns it has been repeatedly observed that at prominent raw material outcrops clusters of diversely patinated artefact presented diverging technological reduction strategies. Especially at Umm Mudayy, this pattern has been found accompanied by a special element related to the general landscape evolution prevailing across the Nejd. The site is marked by a limestone remnant that continuously

suffered erosion across the Late Pleistocene. As further back this limestone remnant eroded, high quality Mudayy chert become exposed, which has then been exploited by diverse human groups across time. It may be inferred from this evidence that, while patination cannot be used as proof of antiquity, the identification of diverse patterns on surface scatters may possibly indicate a certain time depth between the creations of the diversely patinated objects and the availability of raw material at their primary sources.

Advances in microscopy have revealed the additional potential in patination studies (Burroni *et al.*, 2002; Fernandes *et al.*, 2007). By using data from knapping experiments and naturally occurring flint comparative examples have been gathered. It is clear that the abovementioned factors had a greater effect on patination of lithics than time has.

Give the above mentioned specifics the patination observed at each of the analysed sites were dealt individually. Among both surface and buried sites the repeated occurrence of artefacts presenting two patination phases were observed. This phenomenon relates to the re-utilization of flint artefacts that have been lying on the surface and were collected intentionally for further modifications. At the Jebel Eva (TH.67) site, described in full later, artefacts presenting two distinct patination patterns have been refitted to one another. The artefacts were collected from restricted areas and yet have shown great variability in patination, the refits and technological analysis revealed they belong to the same technological tradition. Further occurrences similar to the one described above have been mentioned for other sites in Southern Arabian (Crassard, 2008a). The cause of this phenomenon may be seen in the possible effect of past climatic oscillation in the area and the impact of these oscillations on vegetation dynamics. A possible scenario for the development of such patination discrepancies may be related to punctuate vegetation occurrences; these would have increased soil moisture. This increase in moisture would have had local effects on artefacts in a small range leaving artefacts located further away unaffected. Post-depositional deflation and site disarticulation would then shape the sites

into their present condition.

5.2.5 Edge damage

Of interest to the reconstruction of the post-depositional trajectory of surface and buried assemblages is the influence of physical force on the artefacts themselves. Post-depositional deflation and/or erosion by fluvial and eolian factors are known to have specific effects on all sorts of archaeological artefacts (Dunnell, 1990; Gregg *et al.*, 1991; Lyman, 1994; McBrearty *et al.*, 1998; Eren *et al.*, 2011). One of the effects of physical displacement may be read directly on the artefacts' edges. Hahn summarizes these appearances as *GSM-Retusche* (*Gebrauchs- Sediments – Museums- Retusche*; use, sediment and museum retouch), and defines these as being edge damages that have no intentional origin (Hahn, 1993, 167).

For the purpose of estimating how intense post-depositional displacement influenced both surface and buried assemblages, edge damage analyses on artefacts have been conducted. Artefacts have been placed into one of four categories depending on how intense edge damage appeared (Figure 5.4).

No edge damage. Artefacts presenting pristine edges have been placed in this category, indicating no post-depositional displacement or very gradual and low energy displacement that left no visible signs on the artefacts edges.

Slight edge damage. Artefacts showing minimal and infrequent damage across one or more edges have been placed in this category. Small negative scars not following any pattering across one or more edges, sometimes alternately between ventral and dorsal surface have been attributed to sedimentary motion and minimal post-depositional displacement of the artefacts.

Moderate edge damage. This rubric characterizes artefacts showing continuous, unsystematic abrupt to semi-abrupt breakage across one or more edges. Similar to the damage described above, the alternation of negative directionality between ventral and dorsal is regarded as typical for so called sediment retouch. The appearance of this damage pattern is indicative of some degree of displacement suffered by the site and the artefact.

Heavy edge damage. Characterized by intense rounding and abrupt truncation like damage on the artefacts' edges. This type of heavy damage is related to intense redeposition. Not necessarily long distance transport from its original source is implied here, rather intense as in highly energetic over a short distance.

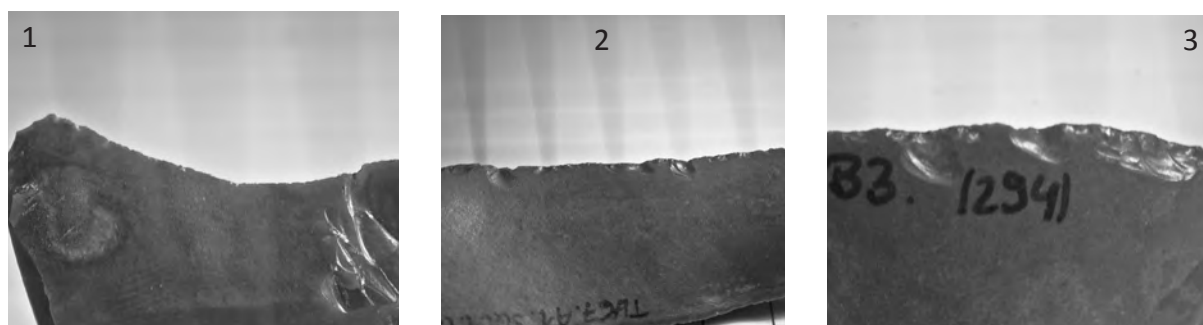


Figure 5.4 Edge damage on artefacts for archaeological context.
1, blank with no edge damage; 2, slight edge damage; 3, moderate edge damage. (Photograph by Y. Hilbert)

5.2.6 Raw Material

Raw material specifics have been found to be highly site specific and will therefore be discussed separately for each presented assemblage within the data chapters. The following general remarks concerning variability, or the lack of it, may be made. The presence of raw material across the Nejd Plateau is ubiquitous, and both nodules and plaquettes are of superb knapping quality (Figure 5.5). As it has been pointed out in chapter Five, the Southern Nejd is marked by two chert bearing members within the *Rus formation*. This geological formation is mostly absent from central and northern portions of the Nejd; there, different chert bearing formations have been identified as noted in

chapter Five. Chert outcropping from the *Mudayy member* has been found in the proximity of the Jebel Eva site (TH.67) located in the central portion of the Nejd.



Figure 5.5 Raw material nodules *in situ* at Wadi Haluf . (Photograph by Dr. J. Rose)

5.2.7 Platform Morphology

By looking at the striking platform the original core striking platform may be reconstructed. Additionally specific treatment of each individually detached blank may be analysed (Dibble, 1997; Monigal, 2002). Information related to the percussion tool the prehistoric craftsman used to produce the archaeological evidence may be read from breakage patterns on the blank's striking platform. The following striking platform characteristics have been recorded in order to assess blank production variability within the Nejd Leptolithic: platform type, the presence or absence of lipping and the presence or absence of abrasion.

5.2.7.1 *Débitage platform types*

Striking platforms prepared by direct flaking will be visible on the blanks reduced from the core. These removals, intended to eliminate any irregularities on the striking platform and enhance blank detachment control are elements of technological action passed on within a cultural frame and therefore specific to a given lithic industry. Platforms have been divided into eight categories defined below (Figure 5.6).

Cortex. The striking platform on the blank is either cortical or made up of any other given naturally weathered surface. No preparation prior to blank removal has been undertaken, indicating that the core's striking platform presented a natural suitable angle for blank production.

Unfaceted. Blank removal was done on a flat core striking platform, prepared by a single blow; leaving the striking platform of the blank plane and straight.

Punctiform. The striking platform on the blank was heavily reduced by abrasion and small removals. Punctiform striking platforms are characterized by their diminutive

size and show a great deal of percussion control by the prehistoric craftsman.

Dihedral. The blank was struck on or in the proximity of the intersection of two former removals on the core's striking platform.

Faceted. The blank striking platform shows three or more removals undertaken by the precursor in order to enhance blank removal control. Preparation of a faceted striking platform must take place from the intersection of the core's plane of removal and the striking platform. Given the absence of the Levallois method within the Nejd Leptolithic core reduction spectrum, blanks presenting faceted striking platforms are attributed to reorganization of removal directionality within core reduction.

Transverse. This type of striking platform, although similar to the above described dihedral and faceted striking platforms differ from the two later in that removals on the core's striking platform were administered transversely to the orientation of the core's plane of removal. These transverse striking platforms occur due to the rearrangement of the directionality of blank reduction, and are not considered part of intentional striking platform preparation.

Crushed. The removing blow was undertaken too close to the core striking platform edge thus damaging the striking platform on the blank. Crushed striking platforms could not be measured, however, considering the limited effect to the blank overall dimensions, artefacts with this particular damage have been considered complete.

Absent/ unidentifiable. This category was applied when the striking platform has been found missing due to breakage or attribution to any of the above mentioned categories has failed.

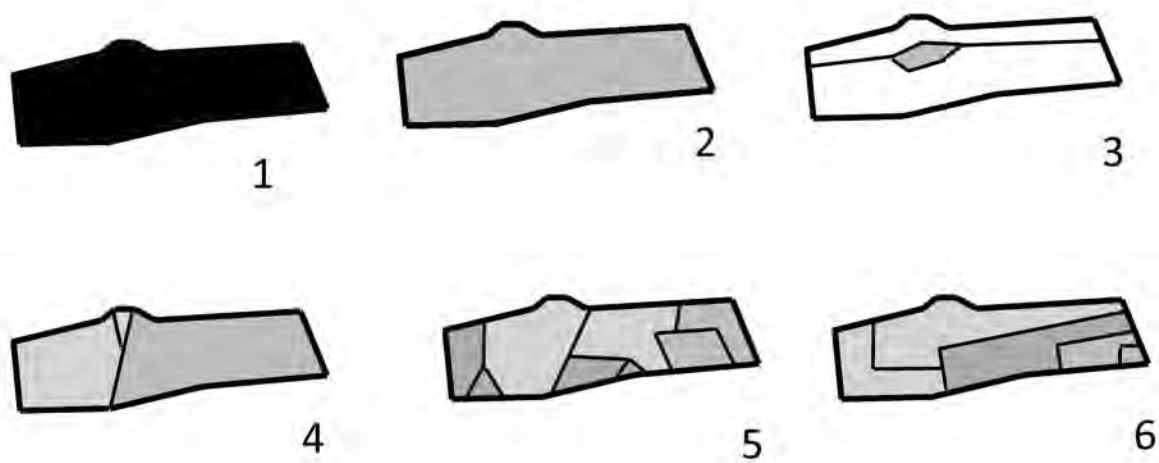


Figure 5.6 Blank platform types.

1, cortical; 2, straight; 3, punctiform; 4, dihedral; 5, faceted; 6, transverse. (Image by Y. Hilbert).

5.2.7.2 Lipping

The term lip refers to a slightly projecting overhang at the interface between the blanks striking platform and its ventral surface (Bordes, 1961; Marks 1976; Inizan *et al.* 1992). The presence or absence of this particular aspect of striking platform morphology has been attributed to the usage of a soft percussion instrument vs. the hard hammer technique (Inizan *et al.* 1992; Hahn, 1993). Hard hammer percussion is associated with the formation of a herzian cone and a prominent bulb of percussion, which involves immediate fracture directly at the striking point. Soft hammer percussion, however, is associated with bending fracture mechanisms that cause the fracturing and subsequent detachment of the blank to occur at some distance from the point of percussion (Kerkhof & Müller-Beck, 1969). While diverse features are related to the formation of such a bending fractures (Crabtree, 1970; Whittaker, 1994; Kooyman, 2000), mostly related to raw material properties and platform angles, both hard and soft fabricators may cause the formation of a lip.

For the purpose of identifying variability among percussion tools used by Late

Palaeolithic flintknappers of Dhofar a distinction between lipped, “semi-lipped” and not lipped was made. Semi-lipped artefacts present a blend of both aforementioned categories: (a) a lip, although not as prominent as in the lipped category; (b) a diminished and flat bulb of percussion.

5.2.7.3 Platform abrasion

The mechanical act of wearing away the intersection between the striking platform and the blanks’ dorsal surface is termed platform abrasion. This procedure would have been performed prior to blank removal in order to smooth any overhangs from the cores striking platform, thus stabilizing it. Given the preparatory character of this act, platform abrasion will be visible only on the dorsally facing portion of the blanks’ striking platform. This procedure is held to be conducive to blade production (Crabtree 1970; Inizan *et al.*, 1992; Delagnes 2000; Monigal, 2002). Given that the Late Palaeolithic is characterised by blade production, the occurrence of this feature should help establish variability within the reduction methods used. Four distinctive variations of preparatory platform treatments have been distinguished: no preparation, partial preparation, preparation and inverse preparation.

Artefacts presenting platform abrasion covering part of the intersection between the striking platform and the dorsal surface of the blank have been classified as partially prepared. The reason for such a partial treatment of the striking platform may have had two possible causes; (a) platform abrasion was administered once for every reduction cycle, thus only a few blanks with completely abraded platforms would have been produced leaving the subsequent blanks with either partially or unprepared striking platforms; (b) selective abrasion intended to reduce only disturbing factors on the core striking platform resulted in a partial abraded pattern.

Additional variability within this particular platform treatment is related to the disposition of the striking platform itself. Some cores have received more attention

than others, meaning that specific technical curation measures, such as striking platform renewal, were not undertaken on all cores. In those cases where renewal has been undertaken, additional inverse platform edge grinding has been observed. This means that instead of moving the hammerstone along the striking platform towards the flaking plane on the core, directionality followed the inverse motion from the flaking surface towards the striking platform. The identification of such curation methods helps the identification of cycles within recurrent, seemingly linear, blank production systems.

5.2.8 Blank Shape

This specific aspect of blank morphology is dictated by an interconnected set of morphological traits. It is thought that a deliberately prepared core should deliver a certain number of pre-set shaped blanks (Van Peer, 1992; Demidenko & Usik, 1993a; Monigal, 2002; Schimelmitz *et al.*, 2011). Major factors determining blank shape are the technological procedures of core preparation, the core's striking platform layout and the preceding removals on the core's working surface. The latter are of great significance for a recurrent blank production system given that the *arêtes* (negative edges) left on the cores working surface by preceding blank negatives serve as guiding elements for the following blanks detached.

Given the Leptolithic character of the blank production systems used during the Late Palaeolithic in Dhofar, overall blank shape of both blades and flakes are highly related to the technological organization of the core working surfaces used (Hilbert *et al.*, 2012). Blanks have been divided into eight morphological categories based on the disposition of their lateral edges (Figure 5.7)

Parallel. The blank is rectangular in shape presenting two parallel sides. Within a recurrent unidirectional reduction system this particular blank form will be most common.

Expanding. The blank's width increases toward its distal part. The edges of the blank expand forming an upside down triangle, resembling a fan.

Convergent. The sides of the blank converge towards the distal portion, creating a blank with pointed end. The blank is triangular in shape.

Débordant/lateralized. These blanks present one incurved and one linear or semi-linear edge. For a greater part this blank shape is associated with *débordant* elements removed from a lateral edge of the core's working surface. These removals are intended to recreate the cores working surface convexity (Meignen, 1995; Barkai *et al.*, 2005; Shimelmitz *et al.*, 2011; Hilbert *et al.* 2012).

Ovoid. This blank form is characterized by edges that extend proximally and converge distally gradually, without angular changes along its silhouette. thus forming a circular outline.

Curved. These are blanks presenting two parallel converging edges that do not proceed in a straight line. The blank's edges stray towards one of its two sides.

Diamond. This shape has been repeatedly observed within the late Nejd Leptolithic and has been found associated with the *Wa'shah* reduction method (Crassard & Bodu, 2004; Crassard, 2008a; 2008b). The diamond shaped blanks are characterized by a bilateral divergence in the proximal medial portion of the blank, followed by convergent edges culmination in a point at the distal portion.

Irregular. When the silhouette of the blank does not match any of the above mentioned classificatory types.

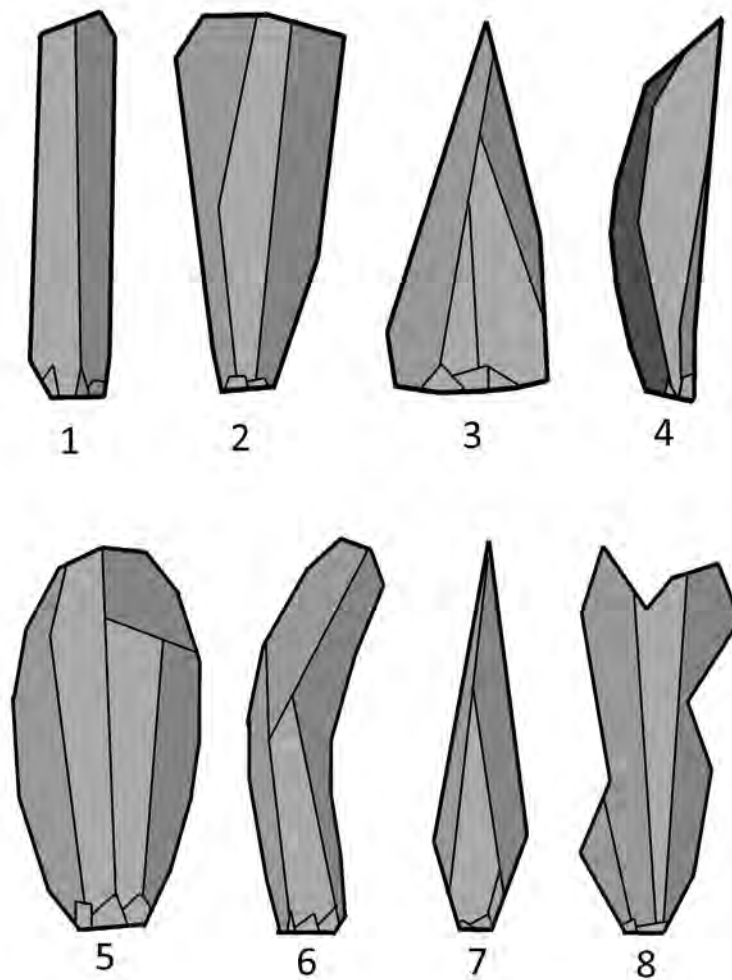


Figure 5.7 Blank Shape.

1, parallel; 2, expanding; 3, converging; 4, lateralized; 5, ovoid; 6, incurvated; 7, diamond shaped; 8, irregular. (Image by Y. Hilbert)

5.2.9 Blank midpoint cross-section

This particular feature of blank morphology is related to the core's working surface layout and where the removing blow was administered at the core's striking platform. These factors influence the metrical morphologies of the blank, which in turn influences the shape of blanks midpoint cross-section. Especially within a blade reduction system, where each successfully removed blade creates additional *arêtes* that serve as guiding ridges for subsequent blade removals, blank cross-section may give valuable information regarding the use of such recurrent reduction system. For the purpose of this study eight distinct cross-section types have been identified (Figure 5.8).

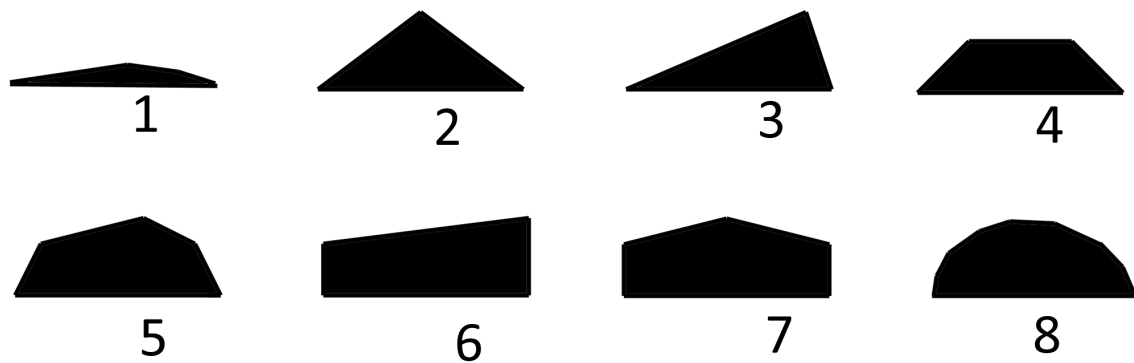


Figure 5.8 Blank midpoint cross-section schematics.

1, flat; 2, triangular; 3, lateral steep; 4, trapezoidal; 5, more than three vectors; 6, rectangular; 7, pitched; 8, convex. (Image by Y. Hilbert).

Flat. No *arêtes* are present on dorsal surface, indicating that the dorsal surfaces was either formed by a single negative on the core's dorsal surface or a flat natural fracture. *Débitage* exhibiting such cross-sections are usually very thin.

Triangular. One central ridge visible is on the blanks dorsal surface and was caused by two removals on core's working surface. The position of this central *arêtes* varies in respect to its position across the midpoint section of the blank.

Lateral Steep. Also triangular in cross-section, this pattern has been found typical on *débordant* elements. Characteristic for this cross-section is the one lateralized ridge forming a right-angled triangle.

Trapezoidal. Three parallel plains, with two central ridges, form the dorsal surface of the blank. Trapezoid cross-sections have been observed repeatedly on elongated blanks; indicating a specific exploitation patterns for these blanks.

More than 3 vectors. This cross-section type shares certain aspects with the previously described trapezoid cross-section. The main difference lies in the greater amount of parallel to sub parallel planes and ridges, giving the blank a more complex cross-section.

Rectangular. Similar to trapezoidal this cross-section presents three parallel plains, yet the two ridges separating these planes are localized on the very edges of the blank and arranged in a right-angle to each other. Blanks removed from the narrow edge of a core often display such a cross-section. On some occasions, when a chert plaquette is used as a core and reduction starts at one of the narrow ends, the produced blanks will show a rectangular cross-section where the two edges will be cortical.

Pitched. Like the rectangular type this particular type of cross-section presents two perpendicular sides parallel to each other with the addition of one dihedral plane on its dorsal surface.

Convex. The blanks presenting this cross-section have no planes associated with preceding removals. The convex shape is due to the cortical surface.

5.2.10 Blank distal portion

The condition of the blank's terminal portion describes the distal end of the detached piece; thus giving information about the cores horizontal convexity. Additionally the state of the distal termination yields evidence as to the amount of force, how this force was applied to the core and possible mishaps involving any of the two aforementioned variables. Experimental data based on fracturing mechanism pinpoint the exterior flaking angle as being one of the main guiding mechanisms governing blank termination (Bonnichsen, 1977; Cotterell & Kamminga, 1979). This data refers to the angle formed

between the core's striking platform and its working surface. Dibble and Whittaker (1981, 287-288) were able to demonstrate that mean exterior platform angles resulted in diverse blank terminations.

Blank termination was certainly an important feature for prehistoric flintknappers; depending on the termination, feathered, hinged/step or overpassed, blank and core volumes would have suffered different treatments. Five diverse terminations have been identified and will be discussed here (Figure 5.9).

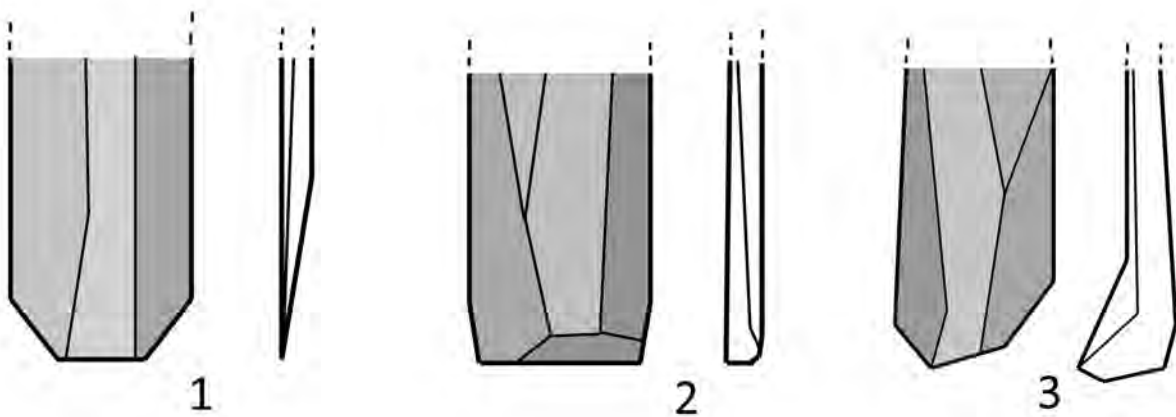


Figure 5.9 Blank termination. 1, feathered; 2, hinged; 3, overpassed. (Image by Y. Hilbert).

Feathered. A thin, tapering, distal termination; this is considered a desired termination conducive to further recurrent removals on a core's flaking surface. The impact force travels evenly through the core and detaches a blank of pre-set dimensions.

Hinged/ step fracture. This occurs when the impact force dissipates towards the lateral portion of the core's flaking surface, reducing the downward (distal) trend causing a sharp drop in velocity. The blank removed has a rounded termination (*Angelbruch*, see Hahn, 1993). This particular breakage has been associated with exterior platform angles averaging close to 90° (Dibble & Whittaker, 1981; Whittaker, 1994). Unlike feathered terminations, hinge/ step fractures impend the continuous reduction of the core's working surface by disturbing its convexity.

Overpassed. Whereas hinged fractures occurred when core convexity and impact force are insufficient, overpassed or overshoot terminations occur when the force that was intended to detach the blank travelled through the core removing its distal portion. Blanks with overpassed terminations may be purposefully removed in order to create and retain flaking surface convexity. Additionally, valuable metrical data may be gathered given that the length of overshoot blanks is related to core overall working surface length.

Absent. The distal termination cannot be recorded due to breakage after detachment from the core. In cases where the distal termination was removed due to retouch a note was added to the database.

5.2.11 Blank Longitudinal profile

This particular feature of blank morphology describes the silhouette of the blank when viewed in vertical profile (Andrefsky, 1986). Three diverse stages of blank longitudinal profile have been observed on the blanks: flat, incurvate and twisted. The longitudinal layout of the blanks is thought to reflect architectural features on the core's working surface and the position from where these blanks have been reduced.

A blank presenting a flat profile is characterized by a plain ventral surface with no bends or rotations to either side. If the blank presents an arched ventral surface, it is attributed an incurvate profile. Laterally-curved blanks have been attributed to the twisted category. These are associated with the removals from peripheral portions of a core's working surface.

5.2.12 Axis

This rubric describes whether the technological axis, the axial directionality of the removals visible on the dorsal surface of the blank, coincides or not with the directionality observed on the blank's ventral surface. Whether a blank is on or off-axis has been found

to relate to the intentionality of the flintknapper and core platform disposition. *Débordant* elements have often been found struck off-axis (Monigal, 2002). If the coincidence of the dorsal end ventral disposition of the technological axis is unclear on a given blank no attribution was made.

5.2.13 Cortical percentage on blanks dorsal surface

The amount of cortex on a blank has been estimated by eye only and therefore represents an approximate value. Estimates of all cortex observed on a blank's dorsal surface, excluding the striking platform, is given. If present, the amount of cortex on a blank was attributed to one of these numerical estimates; 1-25 % and 26-50 % for non-cortical blanks, and 51-75 % and 76-100% for cortical blanks.

The amount of cortex on a given blank coupled with blank size and distal morphology gives information about nodule size. Also, the analysed *débitage* may be ranked within the blank production phase of the *chaîne opératoire* depending on the amount of cortex they possess (Shott, 1994; Andrefsky, 2005).

5.2.14 Scar pattern on dorsal surface

Given that core reduction is understood as a continuous process and each blank bears the negatives of the preceding blank removals on its dorsal face, dorsal scar pattern analyses may expose information as to the configuration of the core's working surface. Based on the directionality and patterning of the negatives it is possible to discern the number of platforms a core possesses, and orientation of removals. Eight scar patterns have been identified (Figure 5.10).

Unidirectional. Indicates that the negatives visible on the dorsal surface of the blank follow the same direction as the removal of the blank itself.

Unidirectional Crossed. These blanks possess some scars originating from the same platform as the actual removal, plus negatives resulting from removals administered from an additional platform oriented nearly perpendicular to the main platform.

Unidirectional Parallel. Blanks showing a series of unidirectional removals oriented parallel to each other.

Unidirectional Convergent. Following the unidirectional tendency, the dorsal *arêtes* originate from the lateral portions of the striking platform and are oriented towards a central point in the distal portion of the blank.

Unidirectional Crested. Characterized by scars originating on a central ridge along the longitudinal axis of the dorsal face of the blank. These removals were undertaken perpendicular to the technological axis and the remaining unidirectional removals on the dorsal surface of the blank.

Bidirectional. The negatives are oriented parallel to each other and coming from two platforms placed opposite of each other. These scars intersect either in the center or one of the longitudinal extremities of the blank.

Radial. Removals have been administered from platforms placed around the circumference of the core's periphery. Directionality of removals is centripetal.

Opposed. Removals are unidirectional originating from two platforms placed opposite to each other. This scar pattern is associated with alternation in removal directionality and the use of a new distal platform.

Transverse. The blank bears the negatives from removals coming from a platform arranged perpendicularly to the technological orientation from the blank's ventral surface.

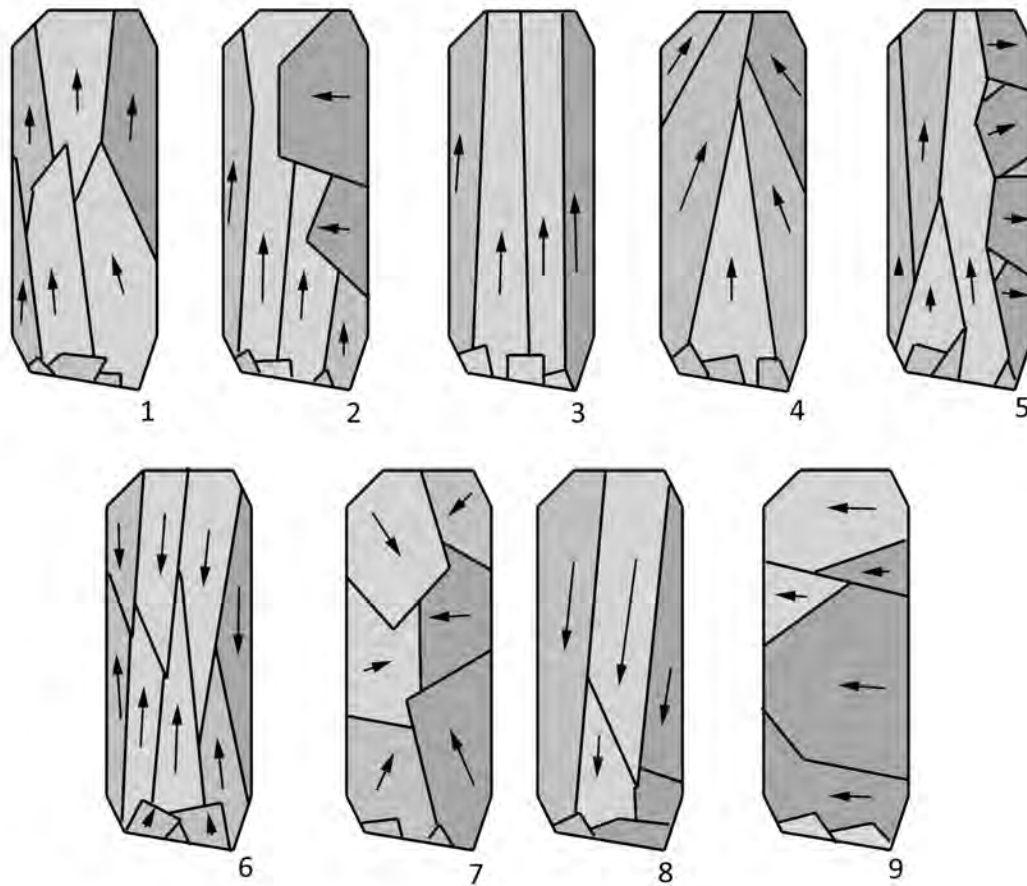


Figure 5.10 Blank dorsal scar pattern.

1, unidirectional; 2, unidirectional crossed; 3, unidirectional parallel; 4, unidirectional convergent; 5, unidirectional crested; 6, Bidirectional; 7, radial; 8, opposed; 9, transverse. (Image by Y. Hilbert)

5.3 Core Analysis

Given that cores are the source of blanks produced by diverse reduction modalities (Inizan *et al*, 1992; Hahn, 1993; Andrefsky, 2005), the study of these objects should provide data helping the reconstruction of the reduction modality used by a given prehistoric population. The analysis of cores is subject to diverse taxonomic systems (e.g. Bordes,

1961; Tixier, 1978; Boëda *et al.*, 1990; Van Peer, 1992; Hahn, 1993; Conard *et al.*, 2004), and choosing an adequate one for the purpose of this study hinged on the absence of a taxonomic system fit for southern Arabia. Late Palaeolithic cores possess a striking platform and a working surface. The striking platform is where the flintknapper hits in order to detach a blank from the core's working surface. During the DAP campaign a simple in-the-field categorization of cores was undertaken. This categorization rested on technological parallels from better known areas around Arabia. Later during the laboratory work each object has received a more specific categorization. In general, early field attributions were used to separate Arabian Middle Palaeolithic sites from Arabian Late Palaeolithic ones (Figure 5.11); aiding the selection of sites and assemblages incorporated in this study.

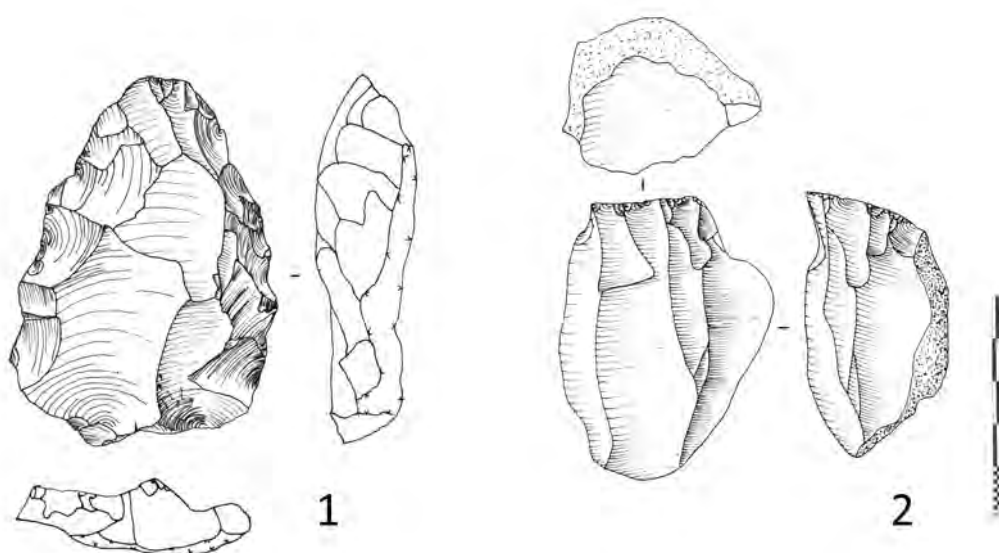


Figure 5.11 Arabian Middle Palaeolithic core and Late Palaeolithic Core.
1, levallois point producing core from TH.260; 2, unidirectional parallel core from TH.34. (Illustration by Y. Hilbert)

It must be kept in mind, however, that the information provided by a single core extracted from an assemblage reflects only the last stage of the reduction process. Only by analysing the assemblage (incorporation cores and *débitage*) the identification of patterns is possible (Inizan *et al.*, 1992; Whittaker, 1994; Kuhn, 1995). Based on these patterns, the reconstruction of the reduction modalities used becomes possible.

Cores attributed to the Nejd Leptolithic technocomplex have been reduced from a single platform in a unidirectional manner (Rose, 2006; Rose & Usik, 2009; Hilbert *et al.*, 2012). Preliminary studies of Nejd Leptolithic core technology revealed a uniform reduction pattern:

...typified by unidirectional-parallel blades removed from the flat working surface of lineal cores. There are also bidirectional cores with supplementary distal platforms (Levallois *sensu latu*), as well as simple, volumetric flake-blade cores. (Rose, 2006, 283)

The examination of buried and dated Nejd Leptolithic assemblages made it possible to identify additional variability within the unidirectional parallel blade producing technologies. The use of different convexity and volume exploitation modalities across the Pleistocene/Holocene divide by the cultural bearers of the Nejd Leptolithic tradition has been attested (Hilbert *et al.* 2012).

In order to further define technological plasticity within the Late Palaeolithic, detailed analysis of cores from both surface and buried assemblages were undertaken. The following qualitative observations were made on the cores: core type, core metrics, disposition and number of striking platforms, core flaking surface, position of flaking surface, and vertical disposition of flaking surface.

5.3.1 Core orientation, metrics and other numerical attributes

Platform cores have been oriented with their platforms up. Core length, widths, thickness and weight have been recorded for the purpose of this study (values are given in mm). Core lengths were measured starting from the striking platform and going to the furthest opposite point on a vertical axis. Core widths were taken across the horizontal axis perpendicular to the cores plane of removal. Core thickness was ascertained by measuring the maximum distance between the cores plane of removal and its back, perpendicular to the core's striking platform (Figure 5.12). Core weight was determined using a scale and

is given in grams (g).

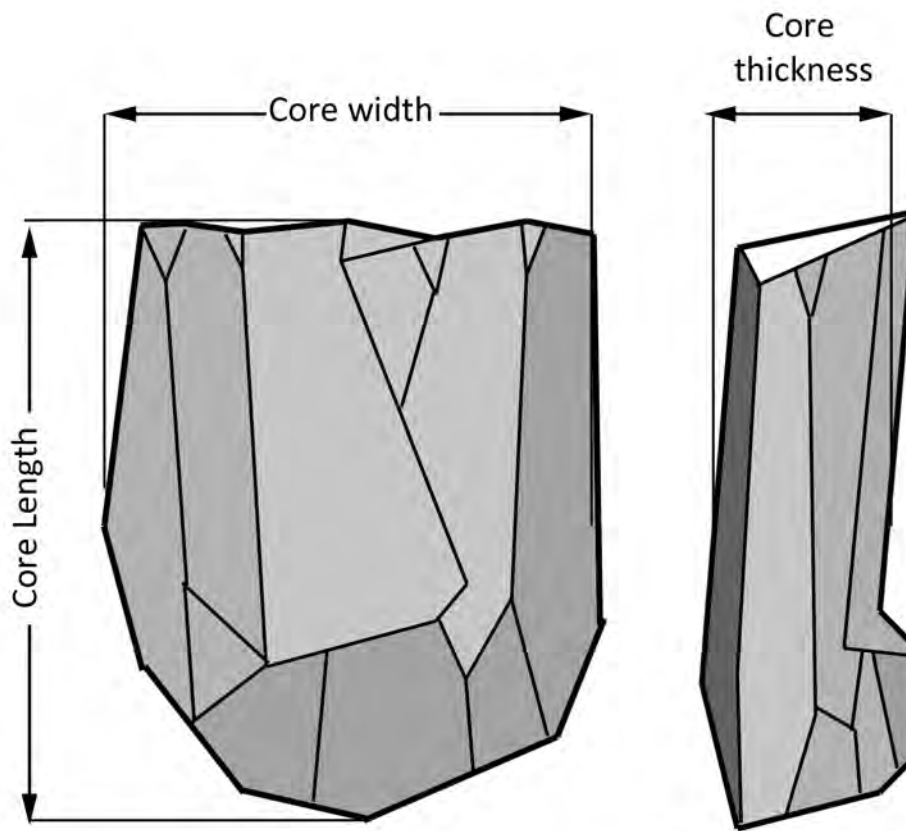


Figure 5.12 core measurements and orientation.
(Image by Y. Hilbert)

Additionally, in order to assess the intensity of exploitation the cores have been subjected to, the number of scars on the working surfaces have been counted and the last complete scar measured. Avowedly, only relative intensity of reduction could be measured using the above described parameter. Given that within a recurrent volumetric reduction system, as it has been encountered within the Nejd Leptolithic, each subsequent removal erases the previous removals, obscuring the actual number of removals taken from the core. Thus the number of scars on a given platform must be used in conjunction with additional information regarding core's working surface morphology in order to address reduction intensity. A descriptive approached will be use here, combining metric and morphological parameters: core vertical and horizontal convexity, the number of scars

and the core's mass, should give an approximate value of reduction intensity.

5.3.2 Core Typologies

Based on the number of striking platforms and the orientation of the removals a given core displayed, attribution to one of the following core types was administered. Central to the analysis undertaken in this study was the identification of variation within the otherwise uniform appearance of the Nejd Leptolithic core exploitation.

Single platform parallel core. This core presents one striking platform used to remove recurrent blanks. Striking platform preparation is absent or minimal (encompassing few removals in order to create a plain striking platform at an approximate 90° angle to the working surface). Scars on the core's working surface are parallel. Reduction may take place on additional working surfaces on the lateral edges of the core. These are supplementary to the main working surface and are administered from the same striking platform.

Single platform convergent core. These cores have a large convex prepared or naturally convex striking platform from which blanks are detached. The prepared striking platform is the main technological feature of the recurrent unidirectional convergent reduction method (e.g. Crew, 1975; 1976; Meignen & Bar-Yosef, 1988; Demidenko & Usik 1993a; 1995; Meignen, 1995). The blanks must be removed aiming towards a central/distal point on the core's working surface. Scars intersect on the core's working surface and form a triangular pattern. Preliminary analysis of the material indicated that striking platform preparation was minimal across the Nejd Leptolithic tradition making an attribution of the cores with distally converging scars into a true technological unidirectional convergent system (*sensu* Tabun D in Monigal, 2002) unwarranted. Artefacts here classified as unidirectional convergent cores show specific morphologies. Characteristic

for unidirectional convergent cores of the Nejd Leptolithic are the intersecting scars along the central longitudinal technological axis of the core's working surface, which is wider than that of the unidirectional parallel ones, giving these cores a sub-triangular to fan-like silhouette.

Opposed platform core. This core type is relatively common within the Arabian Middle Palaeolithic (Crassard & Hilbert, 2011; Rose *et al.*, 2011a; Usik *et al.*, 2012). It presents two opposed striking platforms used alternatively free of hierarchy, this means that both striking platforms are used to produce blanks. Removals from each striking platform intersect on the core's main working surface. In the case of the Nejd Leptolithic opposed platform cores, hierarchy is visible and platforms were used sequentially. First a main striking platform was set up and the frontal working surface exploited. Once the convexity of the working surface was exhausted an additional distal striking platform was set up and the same working surface exploited from this supplementary platform. This alternation is not analogous to convexity maintenance procedures achieved by additional distal platforms, as is the case in the middle Upper Palaeolithic of Central and Western Europe (e.g. Oven, 1988; Moreau, 2009)

Two unopposed platform core. This core type presents two platforms that do not intersect. The surfaces of removal do not implicitly have to be on the same core face; usually the frontal and posterior sides of the core are used. Given that the working surfaces do not intersect hierarchy may only be inferred by measuring the intensity of removals on each working surface (measured by counting the number of removals). For the two unopposed platform cores, as was the case for the opposed platform cores found associated with Nejd Leptolithic inventories, a sequential exploitation of the platforms is observed.

Multiple platform core. When the core presents more than two striking platforms

that use more than one working surface in a random and alternating fashion. Studies of assemblages presenting multiple platform cores in Arabia (from both Palaeolithic and Neolithic periods) have revealed that these cores are reduced opportunistically using old working surfaces as striking platforms, subsequently turned in a 90° angle and again reduced from a old working surface (Armitage *et al.*, 2011; Rose *et al.*, 2011b; Hilbert & Azzarà, 2012). This intense and seemingly random alternation between platforms gives these cores a distinctive globular morphology.

Perpendicular core. Following the reduction pattern of the Nejd Leptolithic tradition, this type of core has two striking platforms placed perpendicular to each other. The removals from these striking platforms exploit the main core working surface and blank negatives may intersect. The uses of these striking platforms to obtain blanks from a single plane of removals are sequential or alternating, depending on the disposition of the working surface. If the removals administered from the main striking platform show severe hinge fractures the additional, lateral striking platform was set up in order to continue reduction on the same face. Blanks from such cores should present the accompanying unidirectional crossed dorsal scar pattern.

Core on flake. As stated above the concept of a core being the source for additional volumes is universal and not restricted to nodules or amorphous raw material blocks. Prehistoric craftsmen have used flakes, blades and other *débitage* to produce additional blanks (Iniza *et al.*, 1992). It has been stated in previous studies (Rose, 2006; Rose & Usik, 2009; Hilbert *et al.*, 2012) that Nejd Leptolithic populations used the kombewa method to produce thin and round flakes.

Preform core. This type was identified based on the following criterion: the removal of few (maximum three) flakes possibly to test the raw material nodules knapping

properties or the setting up of a striking platform and subsequent abandonment of the nodule. In most cases no particular pattern could be discerned from these preforms had occasionally rough features that could be attributed to one of the above described core types were present allowing a rudimentary categorization of the object. In these cases the attribution of the preform to one of the above described reduction patterns occurred in the note section of the database.

Broken/ unidentifiable. These are objects that suffered severe fracture and no longer present the required characteristics needed to assign these pieces to any of the aforementioned types. In some cases, however, traits allowing the rough categorization of these pieces to a core remain. Common fractures are severe patination, heat and other fractures of mechanical origin.

5.3.3 Core Striking Platform

This attribute describes the disposition of the core's surfaces that served the production of blanks. Measured on the intensity of curation this feature of core architecture has received, intentionality in blank production may be read. Core striking platform maintenance plays a central role in reduction systems involving the use of prepared cores, such as the Levallois method (e.g. Bordes, 1961, 1980; Bosinski, 1967; van Peer, 1992; Boëda, 1993; Demidenko & Usik, 1995) and the Grand-Pressigny blade technique (e.g. Riquet & Cordier, 1957; Cordier, 1961; Hahn, 1993).

The number of striking platforms a core possesses was also recorded and each platform was described on its own. Core platforms were divided into three categories:

Unfaceted natural. Blank reduction took place from a suitable (straight) natural platform. This platform may have been either a natural fracture (neocortex) or a straight cortical surface.

Faceted. The term faceted implies the intentional shaping and maintaining of the cores striking platform through purposeful removals. These removals, depending on the core reduction technique used, serve the purpose of exerting additional control over the point of percussion. Faceted or prepared striking platforms may be straight or convex in their disposition.

Straight. A direct blow created this type of striking platform. Unlike the faceted striking platform the straight platforms received less attention and shows fewer removals (maximum three). In some cases the core is turned and a former reduction plane is use as a striking platform, thus resulting in corresponding patterns on the *débitage* butts (dihedral and to a lesser extend faceted).

5.3.4 Cortex

The term cortex refers to the “skin” of the unworked raw material (flint, chert, rhyolite, etc...). It encompasses the primary cortex, which is formed coevally with the actual raw material and is characterised by a rough peripheral mineral texture, and the neocortex. Which relates to post-depositional, pedogenic processes that naturally alter fractured surfaces on the raw material nodules. Depending on the grade and disposition of the surface modification it is possible to retrace the diverse processes a given raw material nodule has been subjected to (Hurst & Kelly, 1961; Burroni *et al*, 2002; Fernandes *et al*, 2007). The amounts of cortex visible on the cores given here are approximate values and by no means absolute, these values are given in percentages and follow the same norm as for *débitage*.

5.3.5 Core flaking surface (vertical convexity)

This feature of core architecture describes the disposition of the cores flaking surface. By it, information related to the cores vertical outlook in cross-section is given.

The core's flaking surface is the portion of the core from where blanks were produced. This feature, together with the disposition of the core's striking platform and angle of reduction, are responsible for blanks morphology (Whittaker, 1994; Kooyman, 2000; Rezek *et al*, 2011). Should more than one flaking surface be visible on one core, each of the surfaces is described separately as to its morphological disposition (Figure 5.13). The observations taken from the core's flaking surface reflect the last stage prior to abandonment, making it possible to infer the reason for the cores abandonment (Monigal, 2002).

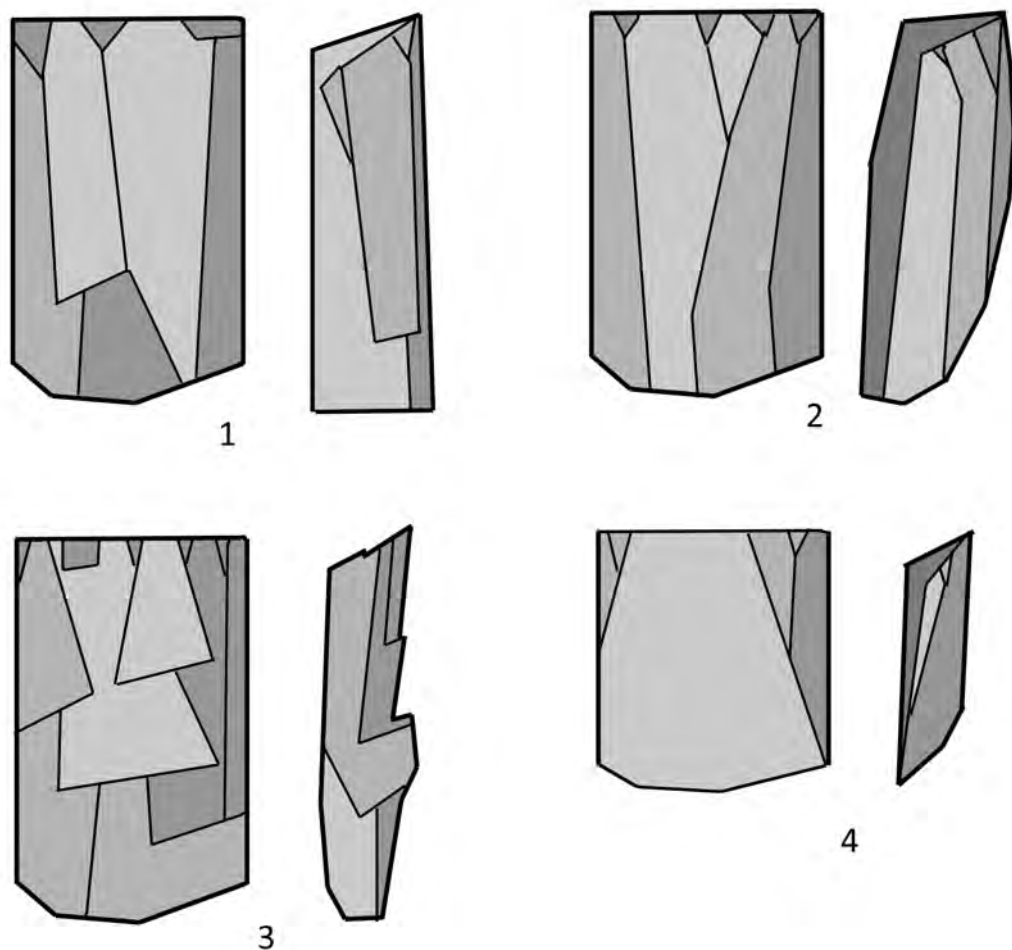


Figure 5.13 Core convexity schemata. 1, straight; 2, convex; 3, botched; 4, overpassed. (Image by Y. Hilbert).

Flat. This term means that the core's working surface is straight. Vertical convexity has been exhausted due to recurrent removals and was not restored.

Convex. This means that the vertical axis from where blanks were removed is convex and is suitable for continues reduction.

Botched. This type occurs when the main face of removals is covered with hinge fractures. This hampers the reduction of determined *débitage* by stopping the dissipation of the knapping energy through the length of the flaking surface. If corrected by a blow that detaches most of the cores flaking surface, convexity is re-established and reduction may restart.

Overpassed. This occurs when one of the later stage removals overpasses and removes a large portion of the distal end of the core, spoiling its distal horizontal convexity. This feature occurs relatively often within the analysed assemblages and hints towards the use of too much force while striking the cores platform.

5.2.6 Position of Flaking surface (horizontal convexity)

The reduction of recurrent volumetric blanks occurs on one or more planes on the core. The use of distinct flaking surfaces on a single raw material nodule has been observed on single platform unidirectional, two unopposed platform cores and multiple platform cores. When a core presents more than one flaking surface each surface is dealt with separately in order to give a detailed description of the object. The position of the flaking surface indicates where on the nodule these platforms have been set up (Figure 5.14). Together, the disposition (vertical) and position (horizontal) of the cores flaking surface provide insights to core curation and abandonment.

Front. When the cores working surface is situated on the frontal face of the nodule. Commonly, south Arabian blade cores display such a working surface exploitation pattern, where convexity maintenance is undertaken by removing cortical *débordant* elements from the lateral peripheries of the working surface.

Lateral. This term applies when only one of the core's narrow edges is exploited. This occurs repeatedly in Late Palaeolithic core reduction and is not seen as a raw material constraint. The narrow edge limits the reduction of cortex-free blades to a recurrent short cycle. In order to maintain and create convexity, laterally detached cortical *débordant* elements must be reduced prior to volumetric exploitation. The deliberate use of the narrow portion of a raw material block by means of the above described reduction modalities was been observed in the Yemeni Hadhramaut valley by Crassard (2008b).

Front and Lateral. This occurs when in addition to the frontal face of the core one of its lateral sides is exploited as well. The use of two separate working surfaces occurs subsequently, first one surface and later the other. The second, lateral work face is set up after reduction on the main face has halted. Thus, the supplementary work face, which shares the striking platform with the frontal working surface, is set up on a narrower edge of the core. This narrower working surface is considered to be supplementary given the restricted potential for yielding symmetric elongated blanks free of cortex.

Front and bilateral. This type is evident when both sides plus the frontal face of the core are exploited. Such cores are generally cuboid in form. This specific core format may be associated with the use of additional platforms and does not have to be unidirectional. Multiple platform and unidirectional crossed cores tend to display such a setup of working surfaces.

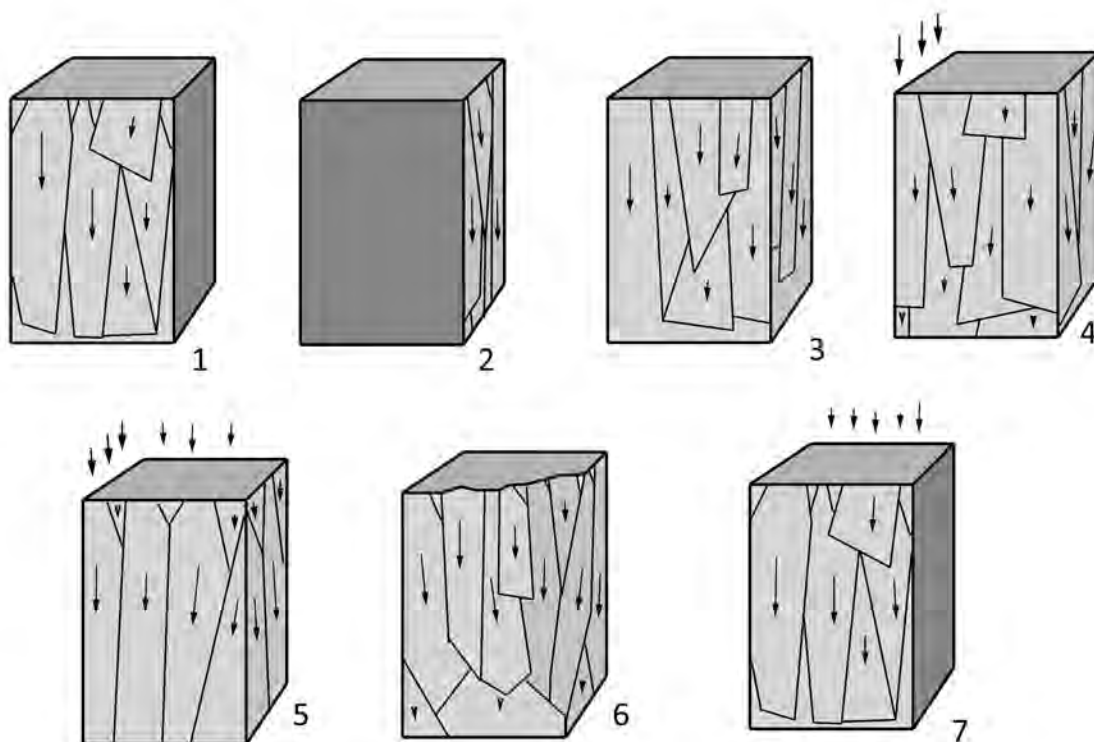


Figure 5.14 Core work surface position.

1, front; 2, on narrow edge; 3, front and lateral; 4, front and bilateral; 5 all around; convex over two workings surfaces; front and back. (Image by Y. Hilbert)

All round. Single platform cores exhibiting no hierarchical working face and no back. The working surface extends along the complete circumference of the core. Cores presenting this particular set-up may be considered prismatic in their typological attribution (e.g Bordes, 1988; Monigal, 2002; Teyssandier, 2003). These are extremely rare among the Nejd Leptolithic assemblages.

Convex over two working faces. A horizontally convex exploitation surface extending from the cores frontal to one of the lateral portion of the raw material block marks these cores. Cores presenting such a configuration may be classified as partially prismatic following Monigal (2002).

Front and back. The arrangement of two working surfaces reduced from either one or two unopposed striking platforms has been observed among Nejd Leptolithic platform core technology. Mostly two unopposed platform cores with parallel, opposed or transverse removals exhibit such a working surface arrangement.

5.4 Tool Analysis

All blanks that have undergone intentional modification by percussion, pressure or abrasion are here considered tools. By analysing stone tools morphology, some insight into the function of the artefact is given, whether the analysed object is a projectile point, a hammerstone or a cooking pot. Given that no use-wear study has been performed on the blanks, the question whether some of the *débitage* analysed may in fact have been used without any modification must remain unanswered. Stone tools function is linked to a set of variables that are not evident on the artefacts themselves. Stone tools sharing a large number of morphological characteristics may have been used to accomplish very different goals; likewise artefacts having little in common morphologically, may be used to complete the same task. These are just some limitations to “the form follows function” statement (Dunnell, 1978; Sackett, 1982).

Tools sharing similar constellations of morphological characteristics are considered analytical types. The archaeologist imposes this typological segregation within an otherwise continuous morphological line (Ford, 1952). Identification of such emic categories, as recognized by the informant or culture under study, versus etic categories, such as recognized by the archaeologist is problematic. The notion of tools being desired end products is an additional problem given the continuous mutation of a given tool after each cycle or retouch (see. Dibble, 1984; 1987; Shott & Weedman, 2007). Considering these limitations of taxonomy, a full restoration of stone tool economy that mirrors the cultural systems that created these object is impossible. Archaeologists, however, need taxonomy in order to classify and organize myriad sets of distinct samples (Brew, 1946; Orton, 2000;

Marks & Conard, 2006). A compromise may be found in understanding the limitations of the taxonomic system used. A consequent use, rather than abuse, of taxonomy enables the repeated identification of specific types within a given assemblage.

Microscopic use-wear analysis supported by experimental replication and blind tests have increased our knowledge concerning tool use (Semenov, 1964; Keeley, 1974; 1980; Odell, 1981; Stafford & Stafford, 1983; Rots, 2005). Use-wear traces and hafting traces are important sources of information. By differentiating the hafting element from the working edge or surface on a given tool, morphological and functional aspects may be laid bare (Rots, 2004; 2010; Rots & Williamson, 2004)

The majority of samples collected for the purpose of this dissertation were retrieved from surface work shops sites and it is not surprising therefore, that only few tools have been found at all. The recovered modified and supposedly used volumes have been divided accordingly into diverse tool types, and described in terms of the position and disposition of their modifications. Additionally, further modified blanks have been described using a selection of the analytical parameters described for the *débitage* (metrics, blank type, blank condition, amount of cortex on dorsal surface, blank shape and type of platform).

5.4.1 Tool Type

Tools have been classified based on the blanks used the type and position of secondary modifications. A large number of tools have been found to be of rather simple design. Identification of variation and possible patterning of implements produced and used was achieved through descriptions of retouch modalities and orientation on the blanks. Retouched and partially retouched objects identified as tools have been dealt with accordingly.

End Scrapers. A flake, blade or bladelet retouched systematically to create a

scraper plane located on an extremity of the blank is here termed an end scraper. Further categorization of this tool type followed the disposition of the tools working edge. The outline of the scraper plane determined whether an end scraper has been termed nosed/shouldered, simple or ogival (Marks, 1976).

Side scrapers. These are unifacial to bifacially modified tools presenting continuous and systematic retouch along at least one of its peripheral edges. Type and position of retouch have been recorded in order to grasp typological variability within this type.

Retouched Pieces. These are blanks exhibiting, discontinuous retouch along a portion of either the blank's ventral or dorsal surface. Retouch type was recorded following the retouch type variation explained below. Retouched pieces are considered part of an *ad hoc* technological process and have, presumably, been used to accomplished myriad tasks.

Bifaces. Manufactured on nodules, blocks, tabular chert, blanks, cores or chunks, bifaces are by far the most prominent. Characteristic for these forms are the symmetrically retouched edges and the surface modifications on dorsal and ventral faces. Bifacial technology has been observed in Arabia and is assign a great time and morphological depth. Setting up a classificatory system for these bifacial implements would require a dissertation on its own, and a descriptive approach has therefore been adopted for the purpose of this study. Aside from metrics, bifacial cross-sections and shape have been recorded.

The identification of preforms, artefacts showing bifacial reduction that have been abandoned, was possible based on the configuration of the surface modification. Bifacial preforms have been divided into four stages of reduction. *Stage 1* is characterized by the few removals organized bifacially on either a nodule or blank. During *Stage 2*, the artefact is further shaped and bifacial reduction is clear although no specific morphology

aside from its rough categorization as a biface may be detected. The intensification of surface modification and sculpting of the tools specific and desired morphological characteristics mark the *stage 3* bifaces. During *stage 4*, bifaces are considered nearly finished end products, if such a thing exists, and are marked by well worked out bifacial features; symmetric cutting edge, symmetrically prepared distal and proximal portions and intensive bifacial retouch (e.g. Petterson, 1990; Andrefsky, 2005).

Trifacials. These tools are not to be mistaken for Mid- Holocene Trihedrals, so often found associated with fully developed pastoral economic structures (e.g. Crassard, 2006; Charpentier, 2008; Martin *et al.*, 2009; McCorriston & Martin, 2009). Trifaces are medium to large (8-20 cm), elongated, bifacially worked implements found in association with Nejd Leptolithic surface scatters. Rose describes these tools as “naviform in plane view with a plano-keeled cross-section” (Rose, 2002, 11). Trifaces have triangular cross-sections and three fully retouched faces; two lateral and one ventral face. Occasionally the ventral face has less retouch than the lateral faces.

Projectiles. Two types of projectiles have been identified within the Nejd Leptolithic, Fasad point and partially retouched points. Fasad points are characterized by their simple configuration and extensive morphological variability. The main feature of this projectile type is the peduncle hafting element created by direct and abrupt retouch to the distal portion of either flakes or blades. Partially retouched points are made on slender blades and exhibit little modification. The main characteristics are convergent to diamond-shaped blank outlines and nibbling retouch across one or both edges of the blade’s distal portion. The projectile character of these implements is based on simple morphological characterization; the pointy end. These implements, although few within the studied inventories and of questionable function, have been observed repeatedly across the Nejd Plateau associated with blade industries.

Denticulates. These are tools presenting continuous denticulated retouch along one of its edges. Denticulate retouch is marked by convex negatives adjacent to one another. The working edge of these tools may be formed by either single blows to the blank or a series of removals, either way the result is a teeth like serrations along the tool working edges.

Notches. These differ from denticulates in that the removals are not aligned against one another. Moreover the modifications on the tools edges are either isolated or pairwise (Thiébout, 2007; Picin *et al.*, 2011). One steep removal or several smaller and successive blows to the same area may form the notch.

Burins. These are tools created using a specific production method, namely the burin blow. The term, coined by Breuil (1909) and later defined by Bourlon (1911) describes the reduction of a burin spalls by means of pressure or percussion from a blank in order to create a faceted *biseau* (slanting edge). The work end of these tools resembles a chisel; these are formed by the intersection of two edges, one of them formed by the negative of the burin blow (Sonneville-Bordes & Perrot, 1956; Stafford, 1977; Marks, 1976; Sackett, 1989; Inizan *et al.*, 1992; Hahn, 1993; Marks *et al.*, 2001).

Burins have been further classified according to the number of burin spalls removed from a single edge and the number of burin work edges. The disposition of the “streaking platform” for the burin spall has also been recorded. Burins made on truncations, a narrow 90° edge formed by continuous and abrupt retouch, have been found to dominate the tools spectrum of the Nejd Leptolithic (Rose & Usik, 2009; Hilbert *et al.*, 2012). Truncation of burins was straight, convex or heavy convex. Dihedral burins are formed by subsequent detachment of burin spalls from either side of the blank forming a pointed working edge, the facets of earlier removed burin spalls serve as striking platform for the following removals. Burins on natural surfaces, break or snaps have also been observed.

Truncated pieces. These are tools exhibiting one or more retouched edges creating a 90°. Unlike end scrapers, truncated pieces are made using abrupt retouch.

Hammerstones. These are percussion tools used to fabricate stone tools. Classification was based on the type of blank, the number of battered edges and the disposition of these edges.

5.4.2 Position of retouch

This indicates where on the blank, following its technological axis, the modification was placed. Positions identified include: lateral, distal, proximal, distal and proximal, bilateral, distal and lateral and along the blank's circumference.

5.4.3 Type of Retouch

Retouch type identified here follow the definitions of Hahn (1993) and Inizan, Roche and Tixier (1992). The negatives of the removals on the volume characterize the retouch, depending on morphological differences between these negatives diverse retouch types may be identified. Retouch and tool morphology have been viewed as continuous and variable, making it difficult to place within one or more set categories. Gradual transitions between types of retouch are expected when working with large sample sizes. Categorization of retouch must therefore be viewed as an attempt to grasp variability and serves the identification of patterns.

Following both morphological and technological criteria, retouch has been divided into nibbling, normal, inverse, bifacial, steep, semi-steep, abrupt, invasive, scaled, stepped and pressure. Given that there are cases where more than one of these types fit the description of the tools retouch the aforementioned types can be combined to give a better description of the tool.

When the retouch does not extend more than a few millimetres into the surface of

the volume it is termed fine or nibbling. Such a modifications, identified by Hahn as *GSM Retouche* (1993) described earlier, are relates to the use of the tool, or in some cases, post-depositional events. Normal retouch is characterized by parallel to sub-parallel removals on the edges of a volume. These do not advance far into the surface of the volume and served the renewal of the volumes edges. Invasive retouch is characterized by its flat angle and intrusive distribution across one of the volumes faces. This type of retouch may be related to biface manufacture and requires a special treatment of the striking platform (Tixier, 1980; Hahn, 1993;). Further classification of retouch is based on the angle of the modified edges, these may be semi-steep, steep or abrupt.

When retouch was applied to the ventral side of the blank, the term inverse was used. *Façonnage*, bifacial retouch is applied equally to both dorsal and ventral sides of a given blank. This specific retouch is found in combination with invasive, scaled or stepped retouch. Scaled retouch is characterized by flat and invasive removals with feathered terminations. Negative morphology resembles fish scales: these present narrow points of percussion and extending edges towards the termination of the negative. Stepped retouch is similar to scaled retouch in the sense of presenting comparable negative morphologies except for the distal termination with is stepped to hinged.

Pressure retouch has been found throughout the Arabian Peninsula usually in association with both Middle and Late Holocene inventories (e.g. Uerpmann, 1992; Edens & Wilkinson, 1998; Charpentier; 2008). Retouch by pressure is administered using a tool with a protuberance. This point is placed on the edges of the blank, by applying controlled force to that edge a blank of varying sizes may be won. Pressure retouch is easily identified thanks to the configuration of the negatives fracture and the often deep bulbar scar. Pressure retouch negatives have been found to be very symmetric, parallel and elongated, and metrically these seldom surpass 10-15 mm in length (Plisson & Geneste, 1989).

5.4.4 Characterization of the blank

Completing the typological description of the tools recovered from the Nejd Leptolithic sites across Dhofar, the blanks selected to be modified into tools were described. Five morphological characteristics have been recorded: blank type, blank condition, amount of cortex on dorsal surface, blank shape and type of platform. These aspects of blank morphology have been explained above and have been equally allied to the blanks modified by retouch. The blank types have been enhanced in order to best describe the raw volume used by the Late Palaeolithic hunter-gatherers of Dhofar to produce their tools; natural, tabular chert, nodular chert and cores were added. Blank measurements have also been taken.

5.5 Summary

This chapter concludes the methodology section, it dealt with some of the background knowledge used to infer meaning to stone tools and the methods here used to categorize and describe the samples from Dhofar. The measurements and morphological characteristic recorded here have been chosen based on the theoretical framework elucidated and should best serve the purpose of characterizing both lithic technology and stone tool typology of the Late Palaeolithic of Dhofar. The *débitage*, cores and tools collected from the sites chosen for this study have all been analysed based on the parameters described above.

Description of the *chaîne opératoire* that led to the manufacture of the stone tools used by the Nejd Leptolithic populations will be the focal point of this dissertation. Therefore, analysis of all *débitage* has been undertaken in addition to core reconstructions based on refittings. These serve the incorporation of the analysed *débitage* into one of the specific phase within the reduction modalities observed.

Compared to the *débitage*, core analysis has been kept simpler and restricted to describing both platform and working surface morphologies, though categorization into

diverse variations within a unidirectional platform core system has been undertaken. The tool typology discussed has here been applied to the archaeological sample and is used to classify the assemblage and allow for auxiliary comparisons with assemblages in adjacent regions of the same period.

Although the results of the analysis presented further on are divided respectively into each of the described categories, none of these should be valued over the other. As the only material culture available to archaeologists dating back to the Late Palaeolithic of Dhofar, the stone tools samples will be dealt with as one unit and shall be here presented as a package of technological and typological features.

Chapter 6

ALPHA TRANSECT

The data section is organized into three chapters, each chapter deals with one survey transect. Along these transects, surface and buried sites have been identified. Based on where across the Nejd Plateau transects were placed, different landscapes and archaeological sites were observed. As discussed in chapter Four, the Nejd was divided into a southern, central and northern portion. Depending on the climatic parameters discussion in chapter Three each of these zones was influenced differently over the past climatic oscillations, and therefore presents different types of archaeological sites.

This chapter deals with the ALPHA transect, which was placed parallel to Wadi Aybut between two of its tributaries (Figure 6.1). The position of this transect, within the central portion of the Nejd Plateau, was chosen given the geomorphological features encountered along the wadi terraces. Chert of supreme quality outcrops along the banded beige limestone of the *Mudayy member* that composes the terraces of Wadi Aybut. The transect starts approximately 500 meters north of the road leading to Qafa in the north-western part of the Nejd. From this point, a low terrace landscape stretches for many kilometres; these flat terraces are dissected by a series of small gullies and wadis, some of which had been active during the last interglacial. The transect ends at the convergence of two larger secondary tributaries of wadi Aybut. The wadi beds are filled with limestone detritus, while a thin eolian blanket covers the terraces; in some cases, deflation has completely exposed the geological substrate. Sediment aggregation is rare and related to flash flood events possibly connected to the onset of the Holocene or an earlier wet phase. The 3,7 km transect was surveyed on foot. A total of nineteen sites were discovered, most of which had occupational phases belonging to diverse lithic industries, possibly

separated in time. Few sites discovered along the ALPHA transect could be assigned to a single lithic industry. Of these nineteen sites, six possessed either Nejd Leptolithic components or could be entirely attributed to this tradition. Sites exhibiting uniform and spatially constrained artefact scatters were collected and analysed. The results of these analyses will be presented in the following sections of this chapter. Informal collections of so-called “diagnostic” pieces were conducted at large surface sites.



Figure 6.1 ALPHA transect and sites mentioned in text.

TH. 59, N 17.507583° and E 53.318067°; Jebel Eva, N 17.510233° and E 53.317750°;
TH.123c, N 17.511720° and E 53.328270°. (Satellite image courtesy of Google© Earth)

The sites found along the ALPHA transect were low to moderate density scatters stretching for hundreds of square metres. Within these large scatters, smaller concentrations pertaining to individual knapping events could be identified (Figure 6.2).



Figure 6.2 Panoramic view over large lithic scatter.
Large scale surface site at Aybut al Auwal, photograph taken during 2010 field campaign. (Photograph by Y. Hilbert)

6.1 ALPHA Transect Sites

Given the lack of sediment aggregation, which would have preserved archaeological horizons, mostly surface sites have been identified along the ALPHA transect. Three surface scatters found along this transect were chosen for analysis given the pristine appearance of their samples. These are: the surface scatter TH.123c, TH.59 and Jebel Eva (TH.67).

At the find spot TH.123c a carpet of blades was identified directly on a high quality Mudayy chert outcrop (Figure 6.3). Blades were found associated with single platform unidirectional cores, no bidirectional or other cores types have been identified. The prominent bulbs of percussion on the blades indicated the use of hard hammer percussion. No tool have been identified at the site, nonetheless, the TH.123c assemblage presents clearly affinities with other known Late Palaeolithic assemblages from across Dhofar. A systematic collection was not undertaken because of the similarities between the TH.123c scatter to the previously collected sample from Jebel Eva (TH.67).



Figure 6.3 Blade scatter at TH.123c.

Flint carpet composed of blade production debris and blades, scatter was well delimited and not larger than six meters in diameter. (Photograph by Y. Hilbert)

The TH.59 site has yielded a small sample of Nejd Leptolithic artefacts. The site was repeatedly surveyed over the course of the DAP seasons of 2010 and 2011, making it possible to identify concentrations of Nejd Leptolithic flaking debris. Two refittings from this concentration are of considerable interest to the identification of Nejd Leptolithic reduction strategy and the identification of this tradition *per se*. Attribution of artefact found at the site to specific industries is difficult given the limited direct chronological control over the scatter, however, based on the variability observed within dated Leptolithic assemblages the comparisons made here are valid.

Refit # 2 was found on the western edge of the TH.59 scatter. Several blades, flakes and a biface pre-form were collected and attributed to the Nejd Leptolithic tradition. Given that the artefacts were spatially constrained the scatter was collected *in toto*. The refitting of the artefacts took place in the lab and revealed a reduction strategy antonymic with Nejd Leptolithic blade reduction. Rather than depicting blade production sequences, the constellation revealed the shaping of a bifacial preform. After initial bifacial reduction the thin Mudayy chert plaquette was reduced in size by a series of subsequent blade removal, starting from the narrow portion of the raw material blank. The end product, an unfinished biface pre-form, was abandoned and is incorporated in the refit. The blades produced resemble those removed during early core maintenance practices observed at other Nejd Leptolithic sites across Dhofar. The artefacts from TH.59 Refit #2 are characterized by a high number of cortical blanks and blades with unidirectional to unidirectional crossed scar patterns. Large cortical flakes and biface thinning flakes were also refitted to the biface blank (Figure 6.4). The production of bifaces and trifaces has been attested for the Nejd Leptolithic at Al Hatab (Rose & Usik 2009; Hilbert *et al.* 2012). Given that the specimen dealt with here is unfinished and was found isolated from any other technological or typological *fossile directeur*, the cultural and chronological attribution of this refit must remain unsettled.



Figure 6.4 Photograph of refit #2.
(Photograph by Y. Hilbert)

Refit #3 was found whiting the TH.59 site, the patination differences between the artefacts pertaining to the Late Palaeolithic occupation and the Nubian artefacts facilitated the collection and refitting of blades at the site. While the MSA artefacts exhibited varying shades of black and dark brown, accompanied by a manganese shine, Late Palaeolithic artefacts lacked the mineral coating and exhibited lighter patination. Additionally, the technological divergences observed on the blanks. Resulting from the antonymic reduction methods used, allowed for a secure identification of artefacts from both periods.

Refit #3 is composed of eight *débordant* blades and one blade (Figure 6.5). Although the area was intensively searched, the core could not be found and was likely removed from the site. Reduction took place from a simple striking platform created by a single blow. The striking platform was a suitable point of origin for the following removals; no additional striking platform treatment was needed. The *débordant* blades exhibit similar

morphologies; blank cross-sections are mostly trapezoidal with a steep cortical back. No intense edge grinding or platform maintenance was observed, bulbs of percussion are visible and lipping was not identified on any of the *débitage* indicting the use of a hard hammer. Aside from the blade, all blanks exhibit slightly twisted or incurved longitudinal profiles.

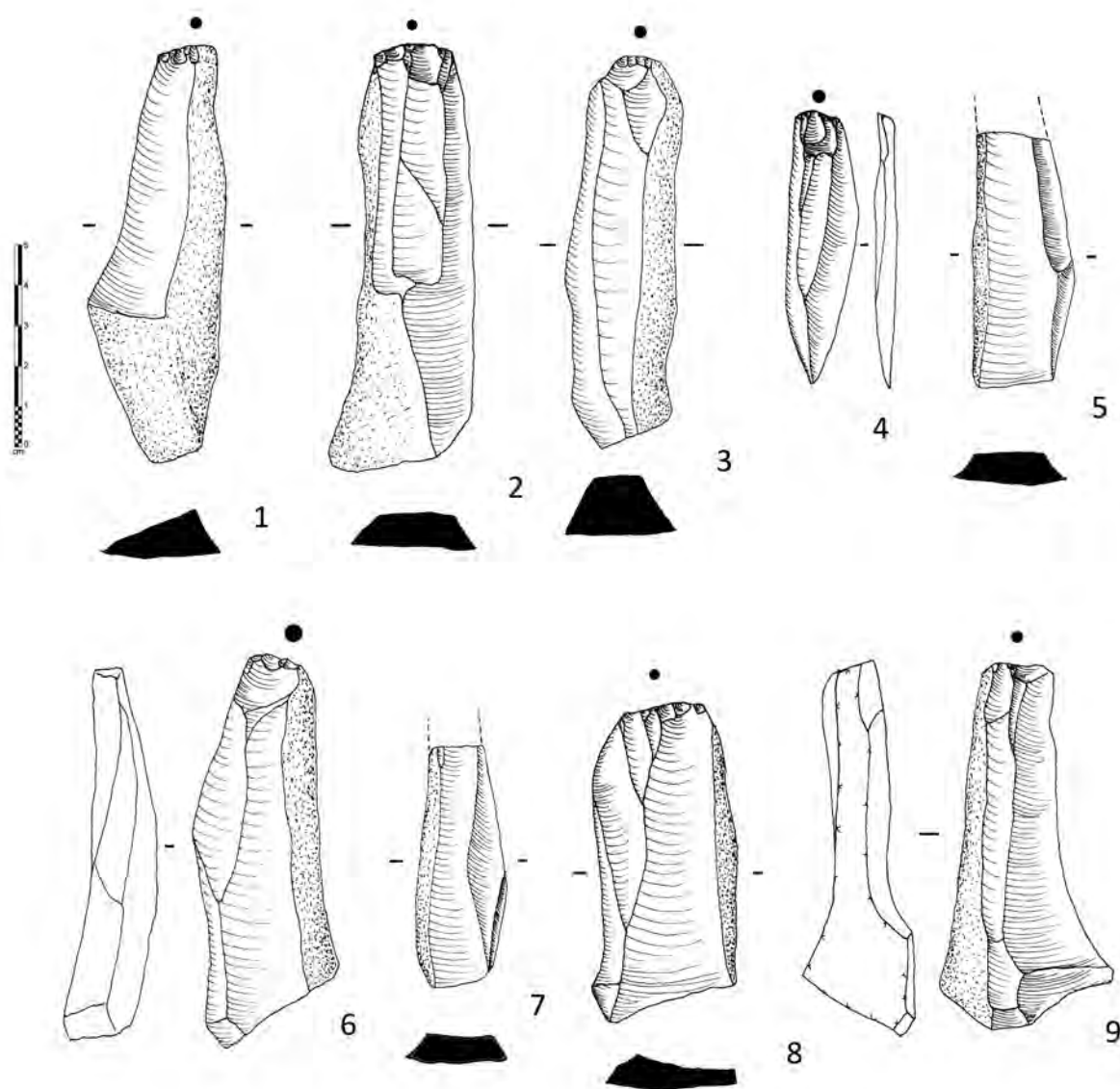


Figure 6.5 Refit #3 débitage.
Débordant blades from TH.59. (Illustration Y. Hilbert)

The reduction sequence depicted by the refit is simple but highly productive; maintenance and reduction cycles are extremely short and interconnected. Reduction started with the decortication of the narrow edge of a max 5 cm thick *Mudayy* chert plaquette, the cortical flakes were not found and suggest that the cores was transported away from the source where it received initial preparation (Figure 6.6). Given that raw material is ubiquitous in the area, transport was probably minimal (some 50-100 metres). After the first, mainly cortical *débordant* was removed, the flintknapper attempted to use the convexity created. A series of short blades with hinged terminations were produced, indicating failed convexity exploitation or lacking enough force while hitting the striking platform. A subsequent large overpassed *débordant* element was struck creating a flat working surface. A third *débordant* blade was removed creating a dihedral working surface with fair symmetry and convexity from where a pointed blade was removed. Another *débordant* element removal followed.

In figure 6.7 the remaining stages of refit #3 are illustrated. Stage B ended with the reestablishment of the core's working surface convexity, which in turn was exploited during stage C. After the removal of a second triangular blade¹, a *débordant* blade was struck from the right edge of the core. A third triangular blade was removed using the previously produced guiding *arêtes*; this piece was also removed from the site and is not depicted in the illustrations. Reduction continued by removing a *débordant* blade from the left side of the core, making the working surface ready for the removal of a forth diamond shaped elongated blank.

The last cycle depicted above is marked by the subsequent removal of two *débordant* blades, one from each of the lateral core portions; this step restored the core's working surface convexity.

1 Not shown in the illustration but visible on the dorsal negatives of the blanks.

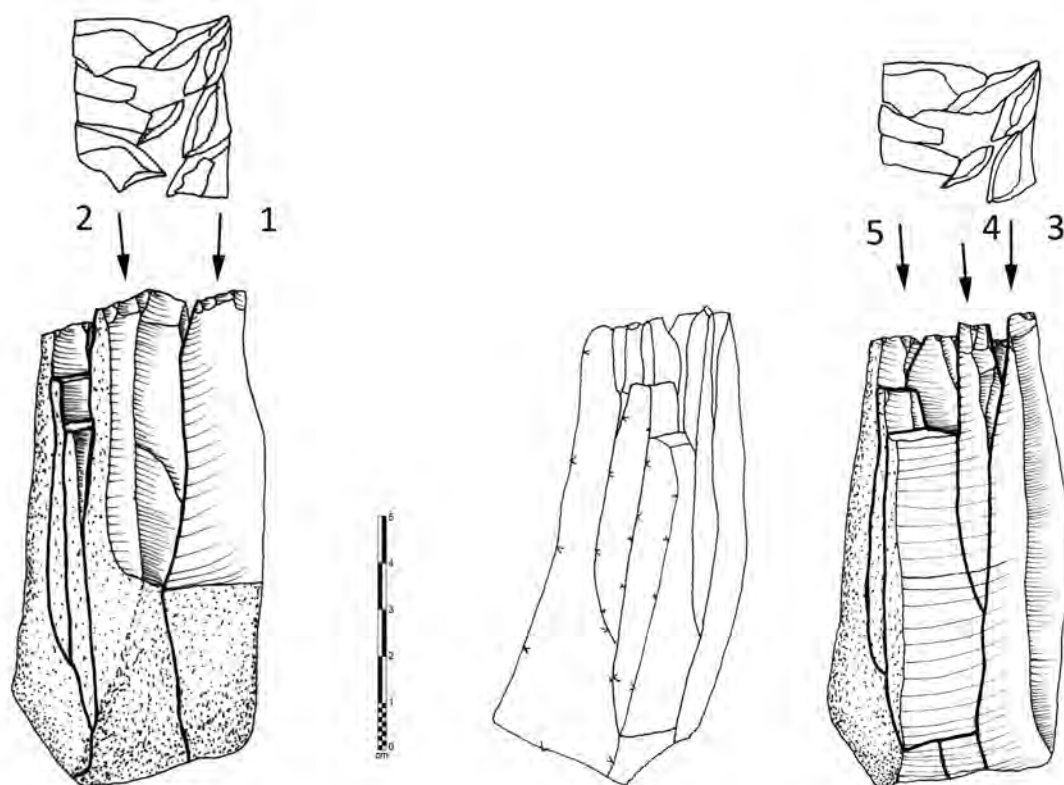


Figure 6.6 Refit #3 stages A and B.
(Illustration by Y. Hilbert)

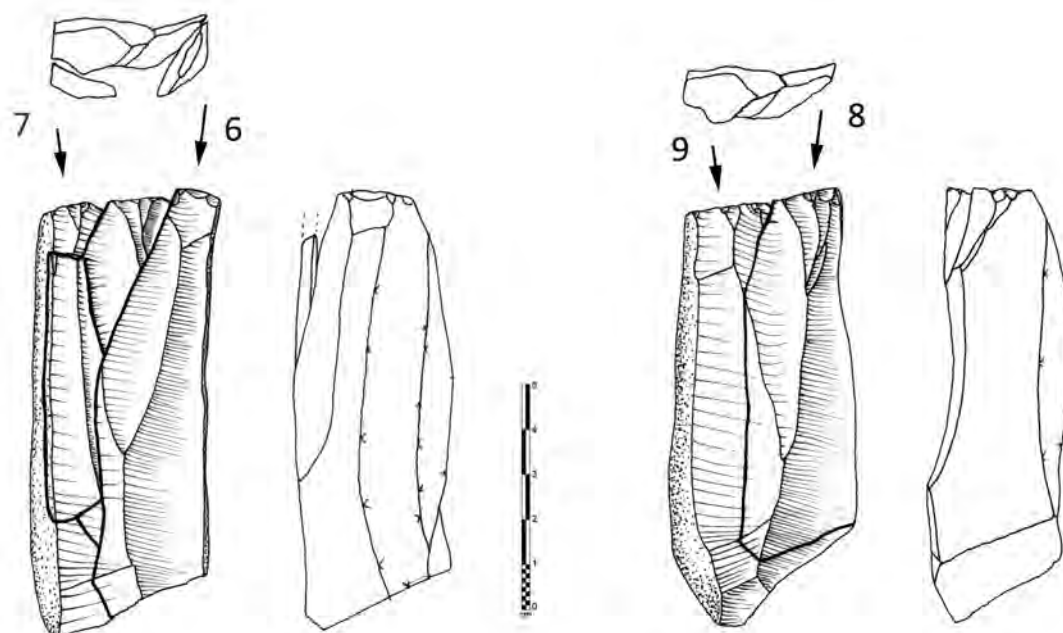


Figure 6.7 Refit #3 stages C and D.
(Illustration by Y. Hilbert)

6.2 Jebel Eva (TH.67)

The Jebel Eva site (TH.67) was discovered and sampled during the 2010 DAP field season; the surface scatter is located east of TH.59. A three by three metre collection was made; the assemblage is marked by the production of elongated *débitage*. Similar *in situ* assemblages have been reported at Al Hatab, Khumseen and Ghazal Rockshelter (Hilbert *et al.*, 2012). The description of the sites immediate surroundings, spatial distribution and the presentation of the attribute and refit analysis are the subject of the following pages.

6.2.1 Site Location

The Jebel Eva site is located approximately five kilometres to the north east of the village Mudayy, directly below a five metre high terrace. Situated within the network of small tributary wadis feeding Wadi Aybut, the site is characterized by two more or less concentric, high density scatters laying on a flat surface. This surface is composed of a thin eolian desert carpet, containing unworked chert plaquettes, bioclastic limestone shatter and larger dolomitic chalk slabs. Bellow this carpet an evaporite layer of varying thickness has been observed resting on top of the limestone bedrock. Several small gullies have been found cutting through the desert carpet and debouching onto the plain to the east of the scatter. One of these erosional gullies has partially disturbed the site (Figure 6.8).

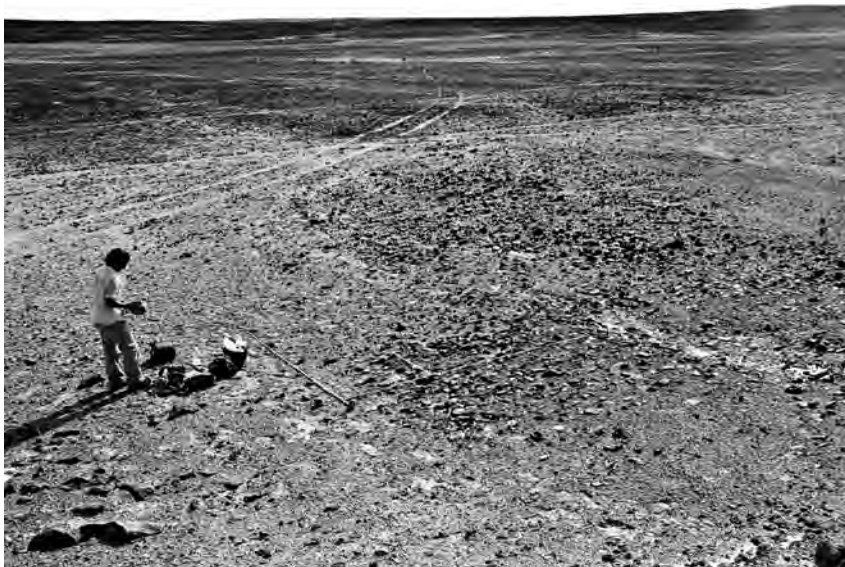


Figure 6.8 Photograph of the site prior to collection. J. Geiling preparing the collection grid at Jebel Eva. (Photograph by Y. Hilbert)

6.2.2 Sampling strategies and documentation

Preliminary investigation indicated that the two concentrations exhibited similar configurations (the larger being ca. eight meter in diameter while the second one was ca. six meters in diameter). Most of the artefacts were of blade dimension and all core seemed to be single platform specimens. Considering the size and density of the scatter, at its most prolific areas the desert carpet was composed solely of artefacts, a complete collection of the site would have produced enough material for a second (very boring) dissertation. Also, the erosional gully that cut the contact zone between the two concentrations would have disturbed the sample, making refitting analysis more difficult than they already are. Therefore, a collection grid was placed over part of the smaller artefact concentration, away from the erosional feature. All artefacts collected were labelled and analysed; in addition to the standard attribute analysis refittings were undertaken.

In order to best document the spatial distribution and layout of the site, a three dimensional topographic map with vertically exaggerated proportions and a two dimensional plot showing the position of the collection area in regard to the surface scatter were made (Figure 6.9). The outline of the concentrations and the position of the sampled area were also mapped.

Given the time constraints piece plotting of every artefact within the collection area was regarded as ineffective, considering the amount of information obtained by this method. Artefacts were, however, labelled conforming to the square meter unit; these allow for rudimentary spatial understanding of the collected area.

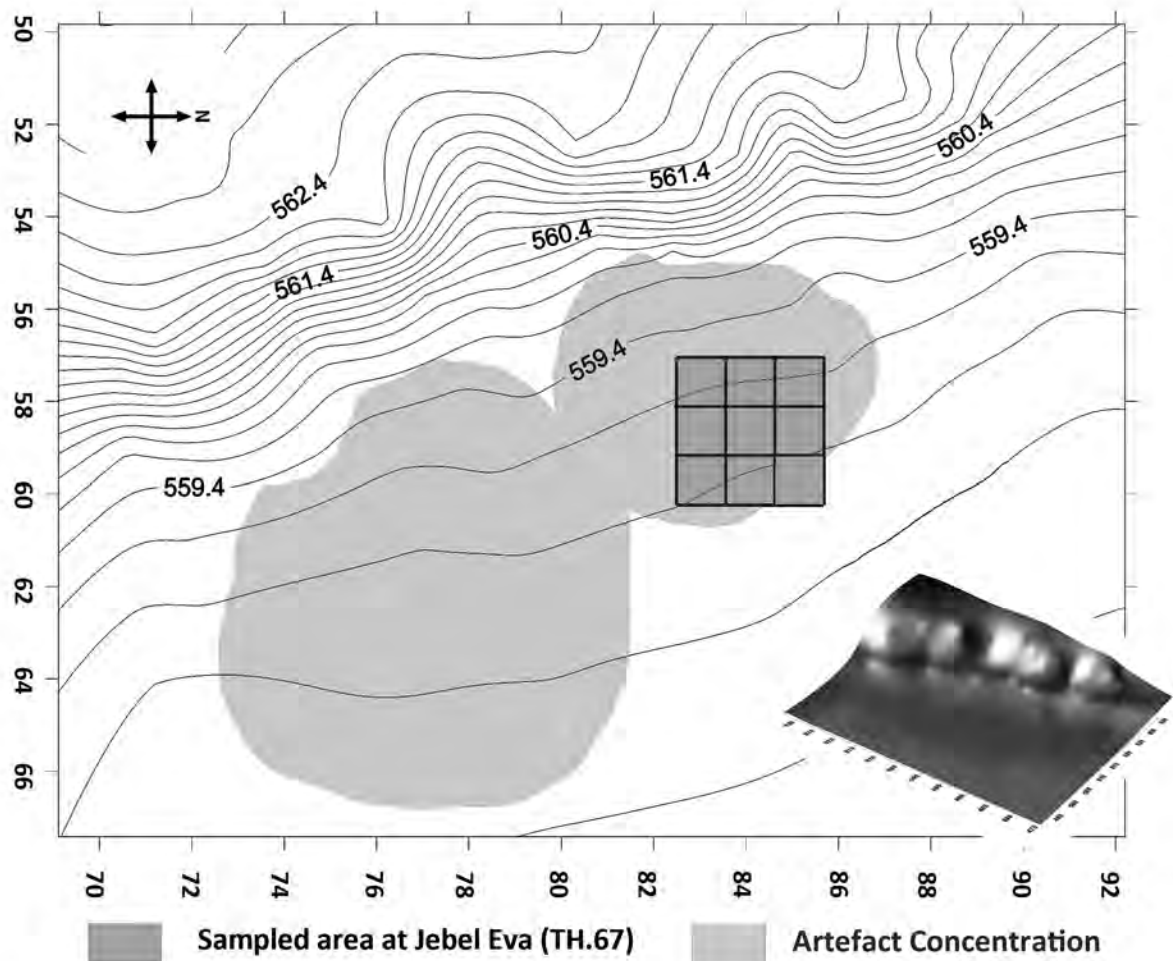


Figure 6.9 Topographic map of Jebel Eva.
(Image by Y. Hilbert)

6.2.3 Spatial distribution

The collection area was so placed that a reasonable sample size could be obtained and the artefact density within the distribution could be defined. Squares A1 and A2 were placed into the centre of the concentration and yielded the highest number of artefacts per square meter. Units located further away from the core area of the concentration contained smaller numbers of artefacts (Figure 6.10).

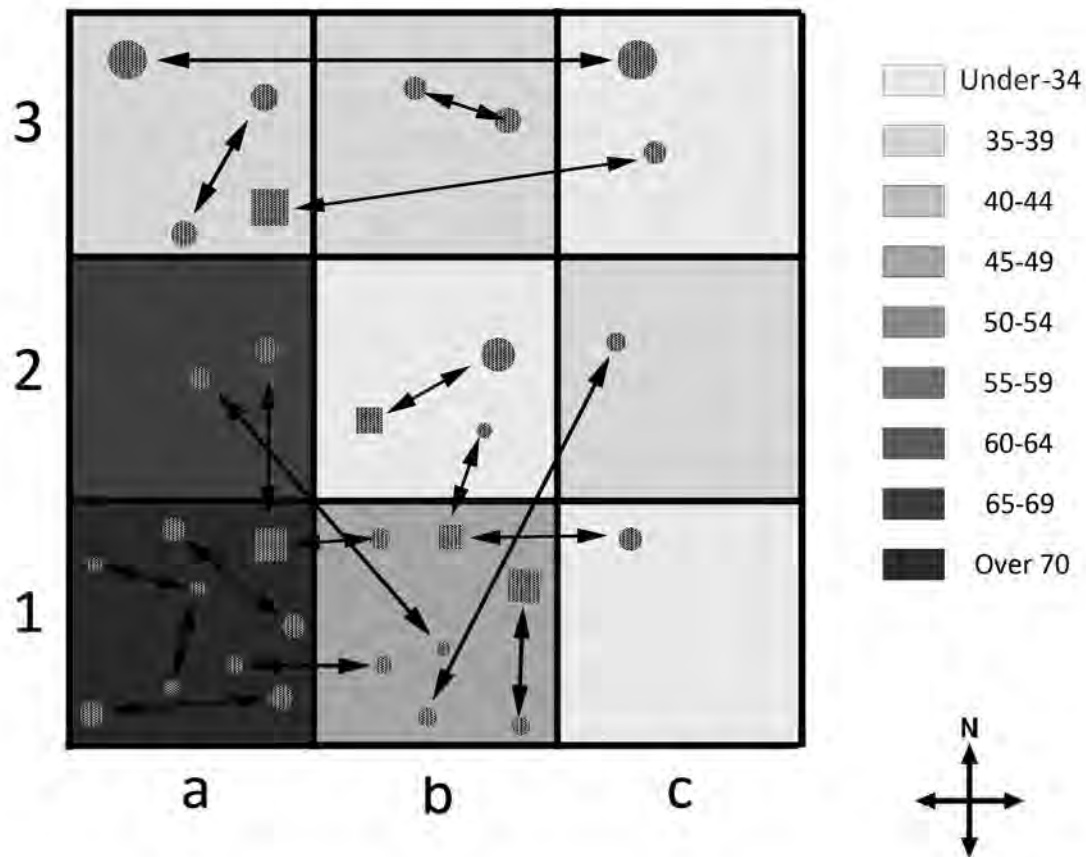


Figure 6.10 Artefact density at Jebel Eva.

Shapes and arrows in the image indicated the approximate position of the fourteen refits; circles represent débitage and rectangles represent cores. (Image by Y. Hilbert)

A total of fourteen refits have been made and indicate a north west down slope movement of the artefact concentration. Whether the arrangement of the concentration mirrors the configuration of an undisturbed knapping event or the product of repeated visits by the same flintknapper or cultural group is impossible to say. Considering the size of the sample, inferences on spatial distribution of artefacts must remain on a basic level. Aside from the gully running in an east to west axis across the central portion of the site (to the south of the collection area), little appears to have disturbed the configuration of the scatter.

6.3 The assemblage

Prior to analysis the sample contained 666 pieces, of these 421 objects were classified as artefacts and the remaining 245 were geofacts. Obviously, this study will deal with the part of the sample related to the expression of cultural knowledge. The assemblage analysed here contained, 392 pieces of *débitage*, twenty two cores and seven tools. Among the *débitage*, three chips were found; bladelets were completely absent. Although the effect of post-depositional factors were deemed minimal, it is likely that the absence of both chips and bladelets is related to some taphonomic process.

Considering the limited size of the total collected area, the sample size is significant. Giving the composition of the sample (Table 6.1) the description of the results will concentrate on the three main artefact types: flakes, blades and *débordant* blades.

Table 6.1 Jebel Eva assemblage.

	TOTAL	%
<i>Flake</i>	51	12
<i>Blade</i>	89	21
<i>Cortical Flake</i>	38	9
<i>Cortical Blade</i>	80	19
<i>Débordant Flake</i>	5	1
<i>Débordant Blade</i>	110	26
<i>Natural crests</i>	16	4
<i>Chips</i>	3	1
<i>Cores</i>	22	5
<i>Tools</i>	7	2
Total	421	100

The leptolithic character of the sample is obvious from the high percentage of elongated *débitage* and the prevalence of the unidirectional parallel and convergent reduction methods observed on the cores. There is relatively more *débitage* than there are cores (ratio of 1:18). The ratio between non-cortical and cortical *débitage* is 1:2. *Débordant* blades are by far the most numerous blank type found, followed by blades, cortical elements and flakes.

Slender chert nodules and plaquettes with thin cortex were used at the site. Raw material is found to be extremely homogenous throughout the assemblage. Chert outcropping from the *Mudayy member* is found in the immediate proximity of the site and was the only type of lithic raw material used. These are, as aforementioned, of supreme knapping properties. Freshly struck flakes are of bluish grey to cream colour, the outer portion of the chert, closer to the cortex, is translucent, displaying lighter hues of red.

The patination observed on the artefacts gives insights to the post-depositional history of the Jebel Eva scatter and aids the reconstruction of the immediate environment. Three diverse patination types have been observed (Figure 6.11). Type 1 is characterized by dark brown, smooth and glossy patina: type 2 patination is considerably lighter than type 1, additionally artefacts present a coarse texture and partially to completely chemically desilicified on the artefact's surface. Type 3 is a mixture of both the above observed patination gradients. At first, considering the severe difference in patination, a palimpsest scenario for the Jebel Eva site was favoured. Attribute analysis and refit studies, however, have proven that this is not the case. It was possible to refit artefacts presenting diverging patination types (Figure 6.11), while attribute analysis confirmed the leptolithic character of the whole assemblage. If diverging chronological depth of deposition is not to blame for the patination discrepancies observed, what caused this pattern to emerge? A probable scenario envisions extremely localized diverging soil conditions. In arid environments where deposition and erosion of sedimentary bodies is separated by short and cryptic soil formation processes one tends to see the landscape in deposition and subsequent erosional terms. In this particular case, erosion and possibly deflation have erased any direct evidence of a pedogenic events, however, the patination seen on 18% (n=73) of the artefact sample can only develop in organic milieu. The fact that not all artefacts within the scatter exhibit this patination is likely due to the character of the soil cover. Rather than covering the entire site patches of vegetation across the landscape created highly localized organic milieus. Artefacts located in the proximity of these patches were affected

by deselicification, while artefacts slightly further away were not.

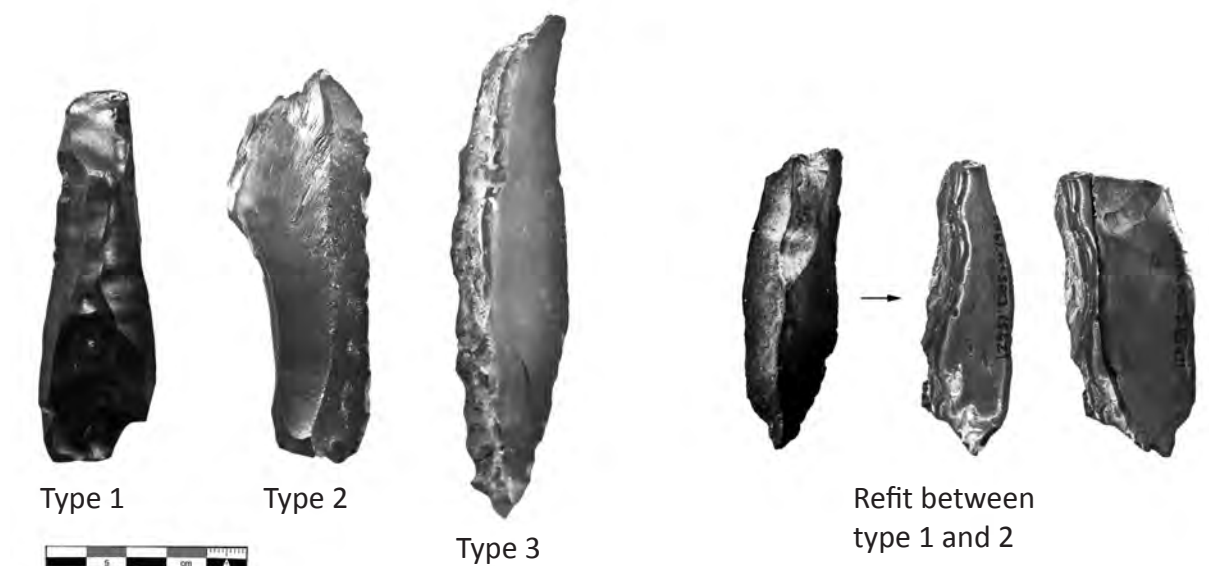


Figure 6.11 Artefacts patina and photo of refit.
(Photograph by Y. Hilbert)

6.3.1 Débitage

The distribution of blank types and the low number of perceived tools observed in the scatter indicate that the production of elongated blanks was the most common activity undertaken at the site. Based on blank fracturing level and edge damage observed on the specimens, assessment of the sites integrity will be made. Considering the three main blank types (cortical pieces will be dealt with separately) flakes, blades and *débordant* blades it may be said that blank fracturing, although present was not indicative for severe trampling. Blades and flakes are less fragmented than *débordant* blades, 77% (n=44) of all flakes and 81 % (n=70) of the blades were complete, while 66% (n= 72) of the *débordant* blades were complete. Aside form regular brakeage of the *débitage* into proximal, medial and distal fragments, fifteen pieces exhibited severe damage by podlids. Artefact edge damage was found to be limited, considering that 69 % (n=268) of the total *débitage* presented either no or only slight edge damage. Only two specimens exhibited severe

edge damage possibly related to movements or trampling. Considering the disposition of the scatter, it is likely that the edge damage observed related to the deflation and erosion of the original soil cover. As seen by the spatial analysis and refits a southeast to northwest axis may be observed, consistent with the slightly inclined surface of the site.

The cortex observed on the artefacts resembled that found on the Mudayy chert plaquettes outcropping in the proximity of the site. The chert plaquettes and artefacts exhibit a dark and thin cortex; occasionally small pits and irregularities can be observed on its surface. A fair number of chert plaquettes collected for flintknapping experiments exhibited natural fractures, usually along its longitudinal axis, providing a 90° platform from where reduction could commence.

Blades and flakes exhibit a moderate cortical cover; blades presenting 11% to 25% of cortical cover are more numerous than blades with 0% to 10% of cortical cover, respectively 19% (n=16) and 43% (n=37). Pieces with 0% to 10% and 11% to 25 % of cortical cover make up 37,5% (both n=21) of the flakes from the assemblage. The number of both flakes and blades with 26% to 50% of cortex have been found relatively often within the assemblage, respectively 25% (n= 14) and 38% (n=32). *Débordant* blades exhibit mostly 26% to 50 % of cortical cover, 67%(n=69). Natural crests (n=16) have been found to have complete cortical cover.

Striking platform morphology visible on the *débitage* presents little variation. Most blanks have plain striking platforms, 55% (n=26) for the flakes, 77% (n=54) for the blades, and 89% (n=65) for the *débordant* blades. Flakes also have 30% (n=14) of cortical striking platforms, 2% with dihedral (n=1), 4% with punctiform (n=2) and 9% with a crushed sticking platform (n=4). Crushed platforms have also been observed on 14% of blades and 4% *débordant* blades (n=10 and n=3). Cortical elements exhibit similar striking platforms with the exception of five pieces with dihedral and two with faceted platforms. Given that only four flakes and six blades exhibit intentionally abraded striking platforms and no sign of lipping was observed, it is safe to say that core preparation was minimal and blank

removal was undertaken using the hard hammer technique. The few punctiform platforms observed appear to represent outliers, considering the low percentage of blades and flakes exhibiting this feature. The faceted and dihedral characters observed are not considered preparation for reasons related to the core configuration, which will be elucidated in the section on the cores.

Débitage midpoint cross-sections show some variability; flakes have homogeneously distributed cross-section types, while leptoliths predominantly have trapezoidal cross-sections; 56% blades (n=48) and 56% *débordant* blades (n=59). Flat midpoint cross-sections were observed on 21% of the flake (n=12); the remaining pieces were to 20% triangular (n=11), 12 % lateralized (n= 7) and 25% trapezoidal (n=14). To a lesser extent rectangular, three vector or pitched midpoint cross-section were observed. Blades exhibit some variability, although in different proportions when compared to the flakes; 13% are triangular (n=12) and 13% rectangular (n=11) in cross-sections. To a lesser extent blades with triangular lateralized, three vector and pitched cross-sections were found. The most numerous cross-section observed on the *débordant* blades after trapezoidal, which in these cases usually presents a cortical back at a 90° orientation to the ventral surface of the blank, is triangular lateralized with 21% (n=21), which also present the steep cortical back described above. Otherwise, *débordant* blades exhibit similar cross-sections to the blades: rectangular, triangular, three vector and pitched cross-sections have been observed in smaller amounts. In total 59% (n=47) of the cortical blades present dorsal cortical values between 51% to 75%. Due to this fact, and the plaquettes shape, triangular and rectangular cross-sections prevail over convex ones. This particular pattern is indicative of an interposed decortication of the nodules; rather than decorticating the entire plaquette, only the immediate plane of removal was freed of cortex. If additional planes were created on the core, decortication started anew. The objects termed natural crests are considered the result of these initial plane decortication/ preparations and have exhibit mostly convex cross-sections. In some cases, depending of the raw material

configuration, specimens with rectangular cross-section have been observed.

Longitudinal cross-sections and blank distal terminations recorded at Jebel Eva show little variability. While 40% of the flakes (n=21) and 42% of the blades (n=32) exhibit straight longitudinal profiles, respectively 50% (n=30) and 58% (n=34) within the assemblage present feathered terminations. *Débordant* elements exhibit different features; 52%(n=52) of the *débordant* blades have twisted longitudinal profiles and 51 % (n=49) have overshoot terminations. The combination of these features indicates that these convexity maintenance elements were struck with a lot of force from the lateral portion of the core's plane of removal.

Supporting the aforementioned notion, *débordant* blades were regularly struck off axis. In 50% (n=52) of the cases the *débordant* dorsal technological axis and the technological axis of the blank removal did not coincide. This feature indicates a change in core orientation and striking position. Although not observed on all elements, *débordant* blades were used to retain and create convexity on narrow chert plaquettes. Flakes and blades, however, were frequently struck following the same technological axis as seen on their dorsal faces.

Overall blank shape has revealed some variability between the three main blank types recorded at Jebel Eva (Figure 6.12). Flakes were 19% ovoid or converging in shape (n=10), the majority of 36 % however, exhibited expanding lateral edges (n=20). The majority of blades have parallel edges making for 38% (n=32); 26% presented expanding lateral edges (n=22), which is the second most common blade silhouette observed. *Débitage* with converging edges is also present and makes up for 18% of the flakes, 25% of the blades and 23% of the *débordant* blades (respectively n=10, n=21 and n=25). The *débordant* blades exhibit a relatively balanced distribution of shapes, although the majority of 29% of them are parallel (n=31). *Débordant* blades with expanding lateral edges make up 20% of this blank type, while 24% exhibit a lateralized silhouette (n=21 and n=25). Cortical elements and natural crests are usually ovoid or rectangular in shape,

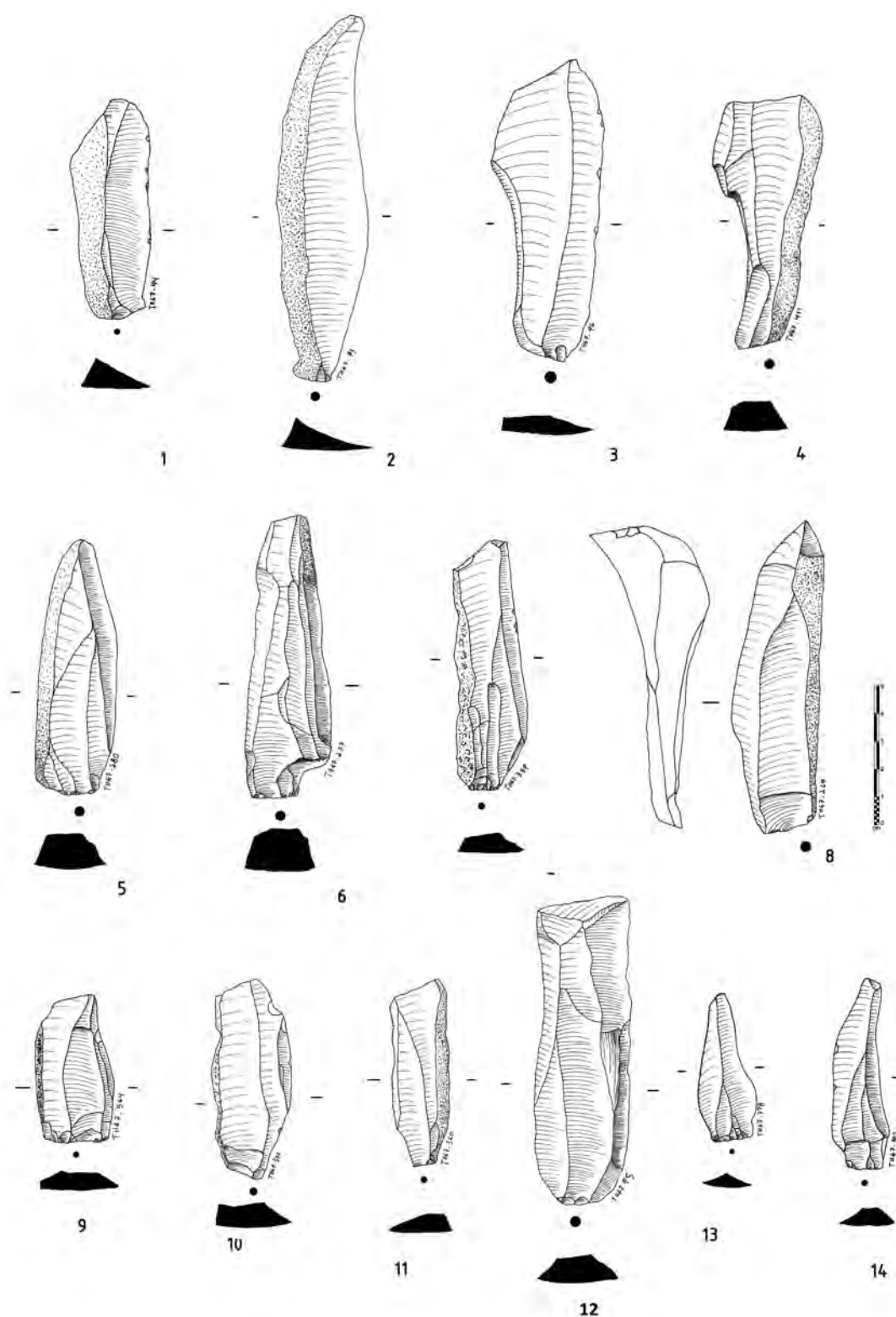


Figure 6.12 Jebel Eva débitage.

1 to 4, débordant lades with unidirectional scar pattern; 5 to 8, débordant blades with unidirectional convergent scar pattern; 9 to 11 short débordant elements with unidirectional and unidirectional convergent scar pattern; 12 blade with unidirectional crossed scar pattern; 13 and 14 short convergent blades. (Illustration by Y. Hilbert)

depending on the configuration of the raw material. The divergence between the flakes and blades is noteworthy at this point, considering the differences in shape. While blades show a tendency towards both parallel and converging edges, flakes are for the greater part either expanding or ovoid.

Blank dorsal scar patterns support the divergence between flakes and blades in that these blank types display somewhat different dorsal ridge configurations. Obviously, however, 67% (n=36) of the flakes, 66% (n=57) of all blades and 77% (n=81) of the blade *débordant* elements exhibit simple unidirectional scar patterns, accounting for the greater part of the entire *débitage*. The divergence lays in the second most common dorsal configuration; 17% (n=9) of flakes exhibit unidirectional crossed scar patterns, indicating the use of an additional striking platform on the lateral side of a core. Blades exhibit 16% of unidirectional convergent scar pattern. Flake dorsal scar pattern variability encompasses the following configurations: 5% with parallel (n=3), 2% convergent, 2% radial, 2% opposed (each n=1) and 5% transverse (n=3). The flakes with transverse scar pattern are of interest, given that these have been removed from orthogonally placed striking platforms on the core. Two blades with unidirectional crossed scar patterns have been found (3%) and while blades with transverse scars do not occur in this sample. Blades with parallel dorsal scars, however, are relatively more common and occur at 9% of the identified cases (n=8). Only 4,5% of the blades have shown bidirectional (n=4) whereas a single specimen has opposed (1%) scar pattern. In this case scar patterns are not indicative of bidirectional reduction.

The technical processes behind this pattern are the same as for the unidirectional ones; rather, the raw material shape and the core configuration are responsible for this set up. Conforming to the blades, the *débordant* blades exhibit matching scar patterns, converging dorsal ridges have been observed on 19% (n=20) and bidirectional on 5% (n=3). Of interest for the reconstruction of the reduction sequence used at the site is the presence of a *débordant* blade with a unidirectional crest scar pattern. Rather than

implying the use of any elaborate core preparation technique, this piece indicates a rotation of the core at 90° clock- or counter-clockwise. Subsequently, perpendicular to the original technological axis of the core, additional reduction takes place. This alternation and the production of such *débordant* elements have been repeatedly observed among Nejd Leptolithic assemblages (Hilbert *et al.*, 2012).

Following the high percentage of cortical elements with triangular cross-sections, converging, parallel and crossed variations of the unidirectional, and to a smaller extent opposed, patterns have been observed on 43 specimens. Three of the sixteen natural crests recorded have negatives on their dorsal face; these are unidirectional and to a smaller extent opposed.

A rough pattern emerges based on *débitage* average length, *débordant* blades being longer than non-cortical blades (respectively avg. 81,21 mm and 73,5 mm). Cortical blades however, show the highest average value (avg. 88,06 mm). The use of the narrow sides of chert plaquettes as the plane of removal constrained both average and maximum width of the blanks; the widest leptolithic blank is a cortical blade measuring 45,82 mm. As the attribute analysis indicates, flakes have not only been struck from the narrow portion of single platform parallel cores and show a maximum width of 82,2 mm. This metrical divergence indicates that a portion of the produced flakes at the site have been reduced from the frontal face of flat cores.

Blank thickness remains homogenous across the blank types, cortical blades being the thickest with an average of 19,03 mm and blades being slightly thicker than flakes, averaging 11.02 mm over 9,85 mm. If *débitage* weights are considered, on a total of 13,711 kg, 85% of the produced *débitage* is of Leptolithic character.

Based on the index of elongation (IOE) average for the blades (avg. 3,01), it is safe to argue that the production of slender blanks dominates over the production of flake-dimensioned *débitage*. Likewise, *débordant* blades present high values of average elongation (avg. 3,44). Blade and flakes have been found to present wide platforms, based on the index of platform

flattening (IPF); striking platforms on the flakes being in average wider than the striking platforms on the blades (respectively avg. 2,64 and 1,97). *Débordant* blades, however, have narrow striking platforms (avg. 1,67); this may possibly relate to the elongated and narrow dimension of this *débitage* category.

The indexes of relative platform size indicate an unbalanced proportion towards blades and *débordant* blades. While cortical elements have relatively similar proportions of platform size in relation to the surface of the blank (avg. 12,66 for the cortical flakes and avg. 12,64 for the cortical blades), leptoliths shows average values of 23,01 for the blades and 15,36 for the *débordant* blades. This denotes that elongated blanks posses relatively small platforms in relation to the dorsal surface of the blank.

6.3.2 Cores

A total of twenty two cores were collected and analysed; six single platform convergent, eight single platform parallel, four two unopposed platform and two multiple platform cores were found. Two pieces were removed from the sample, one intrusive Levallois core (Nubian type 1) and one core fractured beyond recognition. Two diverging uses of the available raw material were identified during the core analysis. While the greater portion of the plaquettes was reduced from a narrow side, some cores were reduced using either the frontal or back faces of the raw volume (Figure 6.13).

Single platform convergent cores were strictly used to produce elongated *débitage*. Metrical variability is minimal, cores averaging 96,19 mm in length, 34,4 mm in width, 71,7 mm in thickness. They average weighing 356 g in weight. Decortication was also minimal; most single platform convergent cores have 51 to 75% of cortical cover. Reduction took place from unprepared flat natural striking platforms, using the narrow edges of the plaquette as the core working surface. All cores exhibit faulty plains of removal, either ruined due to repeated hinging or overshoot removals that caped a great portion of the core, in some cases even both errors were observed on the same specimen.

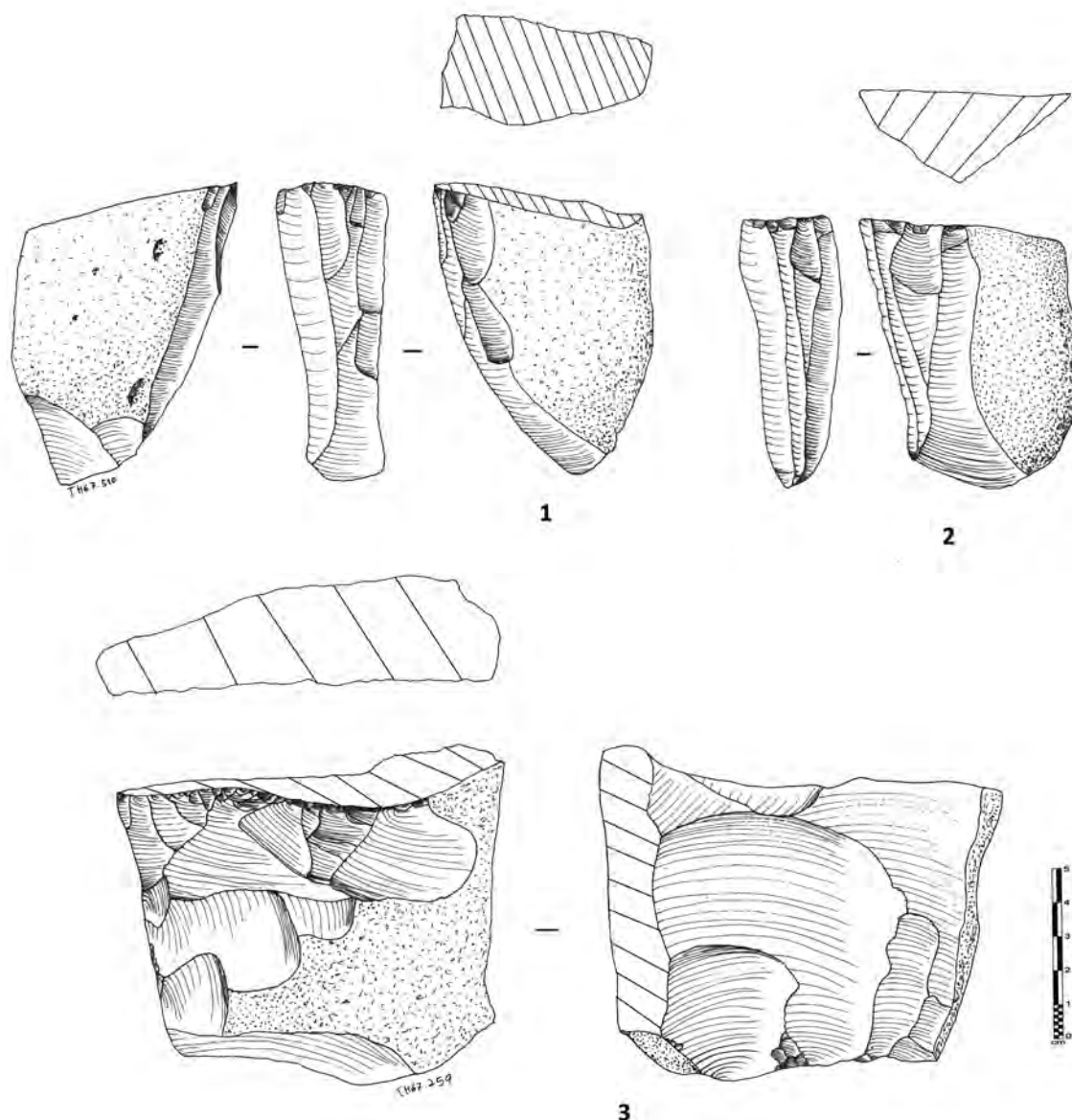


Figure 6.13 Jebel Eva cores.

1 and 2, unidirectional blade cores on narrow work surface; 3 multiple platform flake core on flat surface. (Illustration by Y. Hilbert)

Single platform parallel cores have one of two diverging reduction and exploitation sequences, one dedicated to the production of flakes and one to the production of blades. Rectangular, trapezoidal and ovoid flat flakes were produced from unidirectional parallel cores with one large working surface placed on the frontal face of chert slabs and

plaquettes. Two cores were reduced in that fashion; one of them had a crudely prepared sticking platform formed by two removals, while the other had a plain natural fracture as a striking platform. The flake producing cores are also larger in comparison to the blade cores, weighing 1,299 kg and 665 kg. Unidirectional parallel blade cores are smaller than convergent ones, being on average 82,17 mm in length, 36,31 mm in width and 59,17 mm in thickness. Flaking surfaces were either ruined by hinge fractures or lack of longitudinal convexity due to flat working surfaces.

Four unopposed striking platform cores were within the Jebel Eva assemblage. Negatives on the cores suggest that these were purely blade producing and both have core working surfaces placed at the narrow portions of slender chert plaquettes. Metrical divergence between these cores and the single platform ones is minimal, varying average values are attributed to sample size disparities (avg. length 100,42 mm, width 36,64 mm, thickness 83,79 mm and weight 400 g). Striking platforms shows few signs of preparation; they were set up on natural fractures oriented in a nearly 90° angle to the areas used as flaking surfaces. On one of these cores the striking platform of the main working surface functioned as a plain of removal for a supplementary platform. Rather than representing an additional blank producing system used as the site, this variation of blade production is analogous to that visible on both single platform convergent and parallel cores. The main difference lies in the use of additional volume on the chert plaquettes to produce elongated blanks; the technological organization is the same.

Two multiple platform cores complete the studied assemblage. While one of the collected specimens displays clear blade negatives and blade, flake scars and a distinct volumetric use mark the second core. The blade-producing core fits the description of the two unopposed platform cores. This specimen displays three platforms all arranged on the narrow portion of a triangular chert plaquette. Each working surface also functioned as a striking platform for the following blank producing component on the plaquette. Flaking surfaces display faulty longitudinal and horizontal convexities, due to either

hinge fracture or simply were wasted due to lacking convexity maintenance. The flake producing cores exhibit some similarities with the earlier described flake producing method employed at the site. This specimen was, as were the two aforementioned flake cores, exploited using the frontal and dorsal faces of the plaquette shaped raw material. Striking platform maintenance was kept minimal, all three used platform were plain and made up of fracture plains on the raw material. The frontal face the plaquette, which represented the main plain of removal, was exploited from two perpendicularly arranged platforms. Flakes produced from this surface would have presented unidirectional crossed negatives on their respective dorsal surfaces. The dorsal face of the core was exploited from a plain striking platform in unidirectional parallel manner. Both plains of removal exhibit exhausted surface convexities, due to repeated hinge fractures.

6.3.3 Tools

A total of eight tools were recorded; these fit well with the typological spectrum of the Nejd Leptolithic tradition (Rose & Usik, 2009). The tool sample is composed of one Fasad point, one pseudo-backed knife, one endscraper, one notch and three retouched blades (Figure 6.14). A hammerstone was also found within the assemblage; the specimen was made on an ovoid chert nodule and was most likely brought to the site, given the absence of such raw material in the immediate surroundings of Jebel Eva.

The retouched blades received nibbling retouch along one edge; one of these pieces exhibits lateral inverse retouch, as well. The peduncle on the Fasad point was made by direct and abrupt retouch to the proximal portion of a narrow, triangular blade. Unfortunately, the piece was incomplete; its distal portion broke off (possibly the reason for its discard). The single notched *débordant* blade exhibited little retouch; its working surface is on the opposite side to the cortical back. The pseudo-backed knife displays clear signs of modification to the blank's formally cortical back. The retouch is semi abrupt and likely served as hafting modification. The cutting edge suffered little modification aside

from some modifications to the point of the knife. The use of nibbling retouch on the edge opposed to the hafting element indicates that a cutting/pulling motion was exerted with this tool.

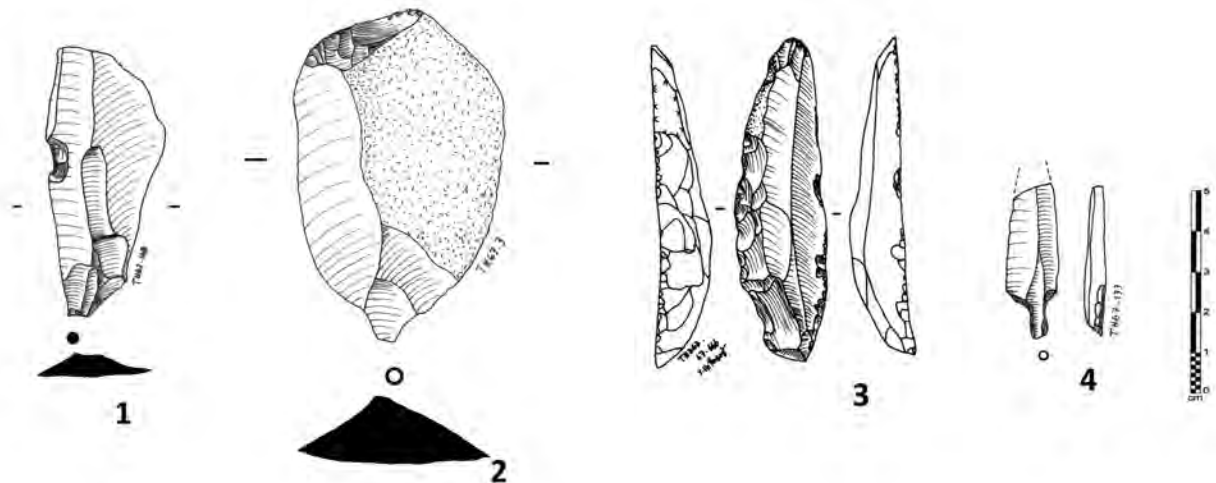


Figure 6.14 Jebel Eva tools.

1 notch; 2 endscraper; 3 pseudo-backed knife; 4 Fasad point.
(Illustration by Y. Hilbert)

6.3.4 Refittings

Fourteen refits reinforce the technological patterns observed based on the core and *débitage* attribute analysis from the Jebel Eva. It was possible to reconstruct reduction sequences depicting exploitation and maintenance of the core's working surface. As stated earlier, two distinct reduction modalities have been identified; one flake producing and one blade producing strategy; no bifacial component was observed. Both modalities were partially reconstructed based on the few refits, which will be presented shortly. Additionally, some apparent disconformities regarding blank morphology were also clarified. As stated earlier, no Levallois concept was observed within the sample. How, in that case, can the presence of few flakes and blades with faceted and dihedral striking platform be explained? As the results and interpretations of the attribute analysis indicate

and the Refit #1 confirms, no striking platform preparation took place. Refit #1 depicts two blades; one cortical and one non-cortical blanks removed subsequently displaying dihedral and faceted striking platforms. This constellation signals the shift from one blank producing component on a raw material block onto a new surface of the raw material volume. The apparently prepared striking platforms are but the remnant of a former working surface.

Most of the refits however, depict the most common reduction method used at the site. Refits #4 and #13 (Figure 6.15 and 6.16) depict how the reduction of blades from the cores narrow edges took place. Commencing from one of the core's working surface, an elongated *débordant* element was struck off. In the cases presented here a second additional removal created a central guiding ridge along the technological axis of the core. If convexity is lost after the removal of a non-cortical blank this step is repeated. Refit #12 depicts the same convexity maintenance scheme on the lateral side of a core.

Refits #2, #5, #7, #8, #11 and 14, depict isolated stages of this type of reduction. Most of these show early decortication measures, which in these cases, given the raw material configuration, are held analogous to core convexity measures. Refits #6 and #9 show fragmented blades reconstructed to their original dimension.

Refits #3 and #10 are of particular interest, given that these show the flake producing method. As indicated by the core and flake attribute analysis, wide ovoid to rectangular flakes were produced from the frontal face of plaquettes. It was possible to reattach one large flake to each of the cores frontal working surface. These large flakes were removed early in re reduction of these cores and are to a large extent covered by cortex.

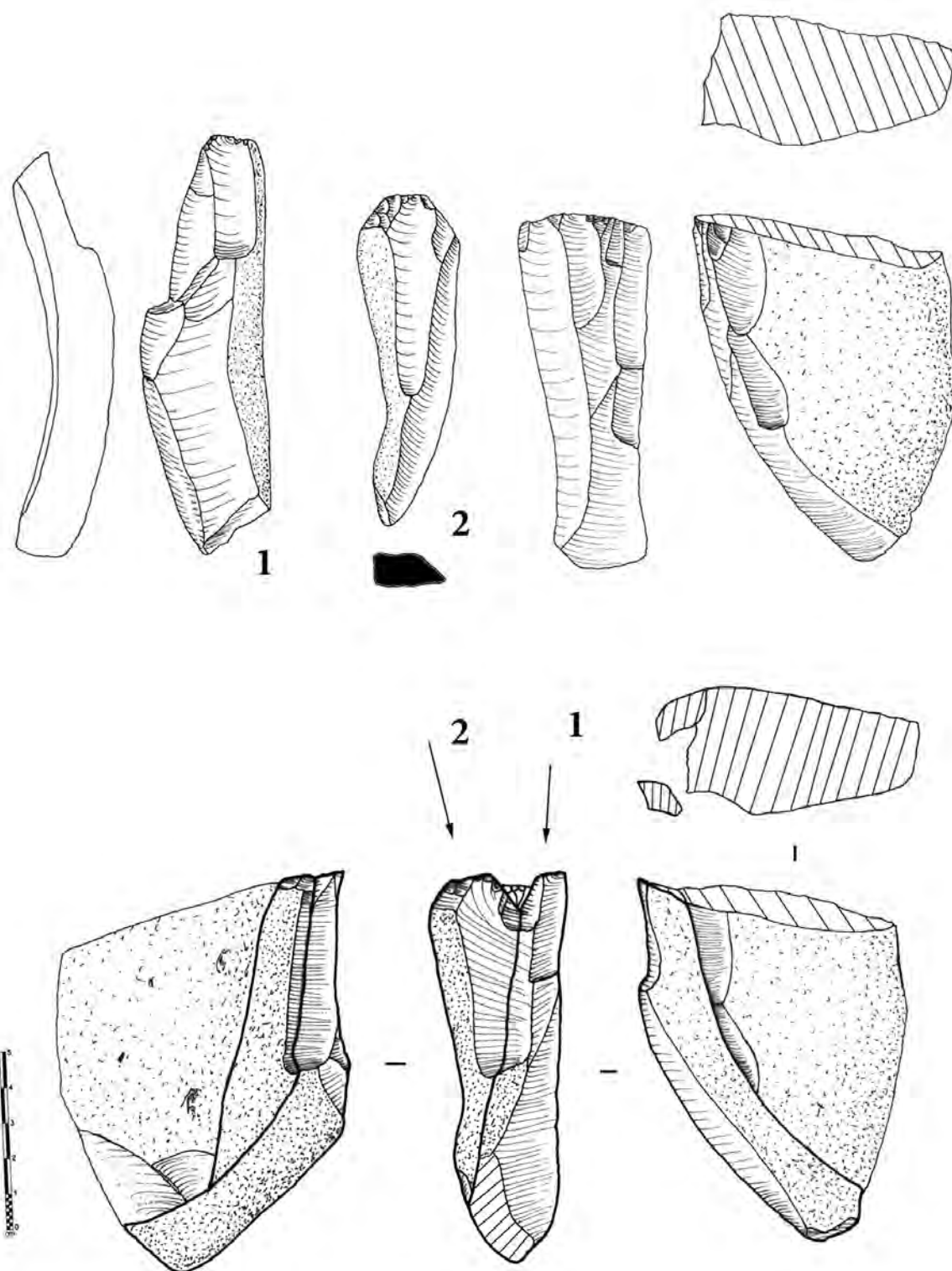


Figure 6.15 Jebel Eva refit #4.
(Illustration by Y. Hilbert)

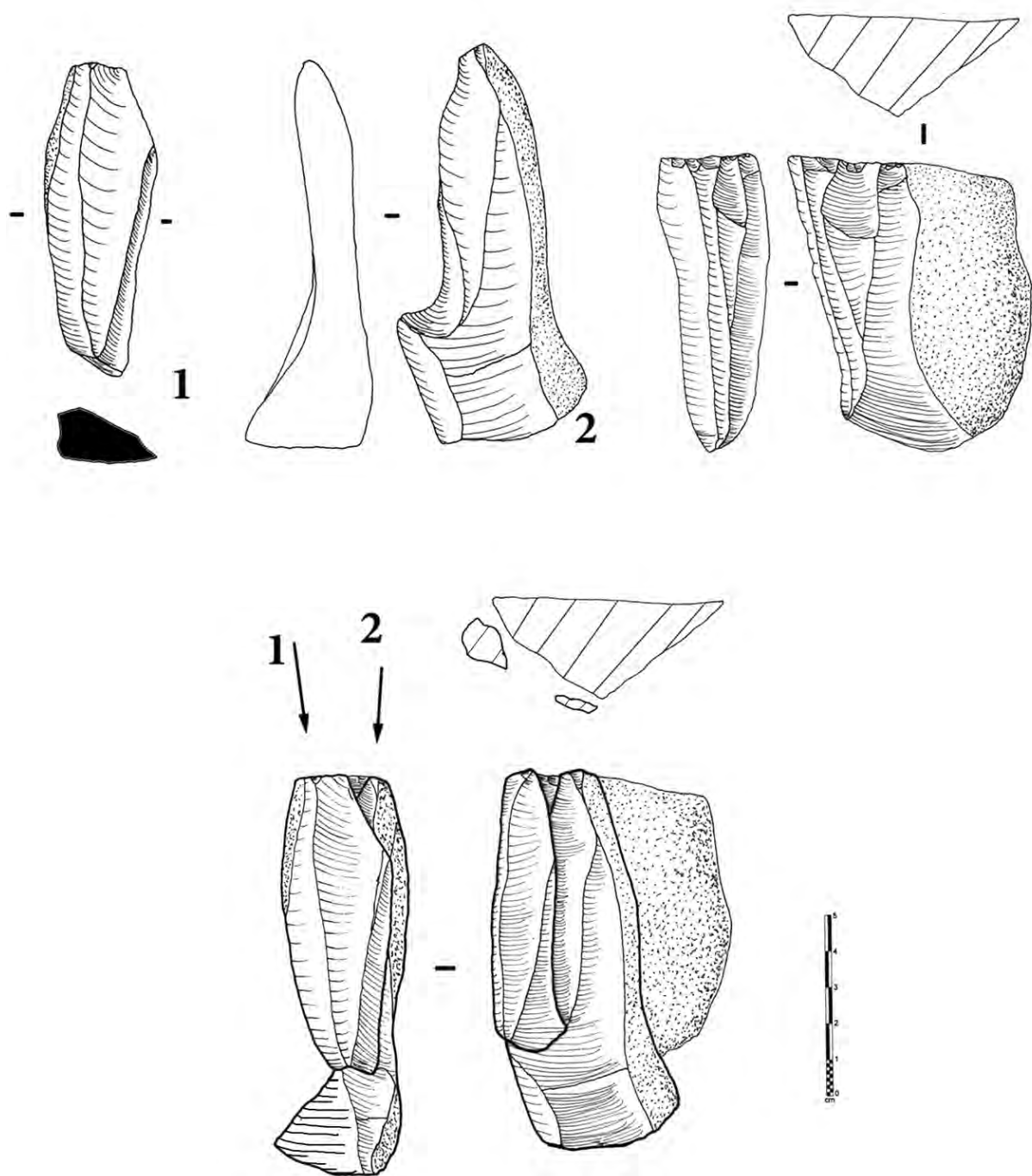


Figure 6.16 Jebel Eva Refit #13.
(Illustration by Y. Hilbert).

6.4 ALPHA Transect comments

6.4.1 TH.59

The leptolithic refits from TH.59 (Refit #2 and #3) have produced similar archaeological vestiges, although reduction sequences depict diverging desired end products. While Refit #2 is associated with the manufacture of bifacial implements, the reduction sequence that produced the artefacts involved in Refit #3 is guided by the deliberate production of standardised blanks; thus, diverging intentions can be read from the technological aspects of these constellations. Whether these two sequences are akin and derive from the same tradition, although unlikely, must remain unanswered. Refit #3 is a classical example of Leptolithic reduction, where four elongated and triangular desired end products were created; three of these were removed from the site.

Refit #3 also depicts some economic behaviour of the Nejd Leptolithic tradition bearers. Given that not all elements involved in the reduction of the core were present at the site, it is possible to argue that: (a) the core received some treatment directly at the raw material point of extraction; (b) the core was transported from the point of extraction to the site and reduced; (c) elongated diamond shaped preferential blanks and the prepared core itself were transported away from the site for further transformation and exploitation.

While Refit #3 shows a single sequence of reduction, surface scatters like Jebel Eva and TH.123c are the results of several reduction events and may be associated with longer stays or repeated visits by diverse groups across time. The sporadic character of the Late Palaeolithic occupation of TH.59 is no individual case, along the GULF transect several similar single episodic occurrences have been recorded. The reconstruction of the knapping events at TH.59 provides information as to how raw material was transported and exploited by Nejd Leptolithic populations.

6.4.2 Jebel Eva (TH.67)

The lithic assemblage of Jebel Eva (TH.67) was analysed and the fundamental results of the analysis were presented. The patterns observed are used to enforce the categorization and definition of the technological and typological variability observed with the Late Palaeolithic material culture.

The raw material used at the site was retrieved directly from its source within the perimeters of the site. Two reduction modalities have been observed and their reduction sequence reconstructed. Flakes and blade were both produced using single platform unidirectional cores. The main difference between the two may be seen in the discrepancies concerning how the core's working surfaces were used. While flakes were produced on the frontal or ventral faces of flat plaquettes, blades were reduced from the narrow edges.

Blade reduction followed the creation of a guiding ridge by convexity maintenance detachments, mostly struck of axis. Flakes, however, are reduced unsystematically from the frontal working surface. Reduction proceeds until the convexity is exhausted. From this point on two options were available to the prehistoric flintknapper: either convexity was restored using débordant elements struck from the core's working surface peripheries, or reduction continued on a newly arranged working surface on the same core. Such behaviour could be identified based on the presence of cores with more than one working surface within the Jebel Eva assemblage. Given the abundance of raw material directly at the site, often cores with faulty convexity were simply abandoned and new nodules prepared into cores.

The tool spectrum is simple, informally retouched blanks and standardized tool forms are found within the sample. The tool kit found at Jebel Eva possibly represents the tool kit of a small hunting party, which visited the raw material outcrop to retool their

arrows with new heads, leaving broken specimens behind. The blade production, thus, may be related to the creation of favoured standardised shapes to serve as arrowhead blanks.

BRAVO TRANSECT

The BRAVO transect, placed on a east to west axis, parallel to the orographic barrier that marks the southern Nejd plateau, yielded ten Nejd Leptolithic sites along its 4,2 km length (Figure 7.1); most of this distance was covered on foot. Four sites yielded archaeological material *in situ*; of these three have been dated for the purpose of placing the Late Palaeolithic into a chronological framework. Khumseen Rockshelter (TH.50) and Ghazal Rockshelter (TH47) are two buried sites, which will be dealt with in this dissertation.



Figure 7.1 BRAVO transect and sites mentioned in text.

Khumseen Rockshelter, N 17.313517° and E 54.042111°; Ghazal Rockshelter, N 17.314483° and E 54.056617° (Satellite image courtesy of Google© Earth).

The southern Nejd Plateau is marked geomorphological and hydrological features that make this region interesting for archaeologists. As noted in chapter Four, the small catchment basins that would gather rain falling over the northern face of the Dhofar escarpment would produce enough energy to bury archaeological sites without dismantling them. The diverse rockshelter excavated by the DAP across the southern Nejd provide valuable archaeological and geomorphological data helping to reconstruct the Late Palaeolithic occupation of this region.

7.1 Khumseen Rockshelter (TH.50)

The presentation of Khumseen Rockshelter's stratigraphic succession, absolute dates and archaeological record are the main topics of this section. The site is situated at the southern edge of the Nejd Plateau. The site's proximity to the region's major hydrographical barrier has attracted human groups living in the area from the Early Holocene until the present. Excavations revealed a succession of occupation layers, each showing a distinct set of lithic technologies and specific tool types. The lowest level has been attributed to the Nejd Leptolithic tradition, the subject of this dissertation.

7.1.1 Site location

The site was discovered during the 2010 field campaign. The landscape surrounding the site is characterized by the shift from the Jebel Qara high plateau to the northward dipping plateau of the Nejd. As noted in chapter Four the transition between these two environments is a drastic one. Less than 500 metres from the site the northern *cuesta* of the Dhofar mountain chain rises to 790 metres above sea level; over 100 metre higher than the elevation of the rockshelter. A plain dissected by several gullies and covered by chert nodules and limestone shatter stretches between the site and the mountain chain to the south (Figure 7.2). To the north, northeast and northwest of the site, limestone hills and inselberg chains are seen. West of Khumseen a prominent drainage system, fed by the

many primary fluvial branches coming in from the Dhofar Maintains, meanders towards the northeast.

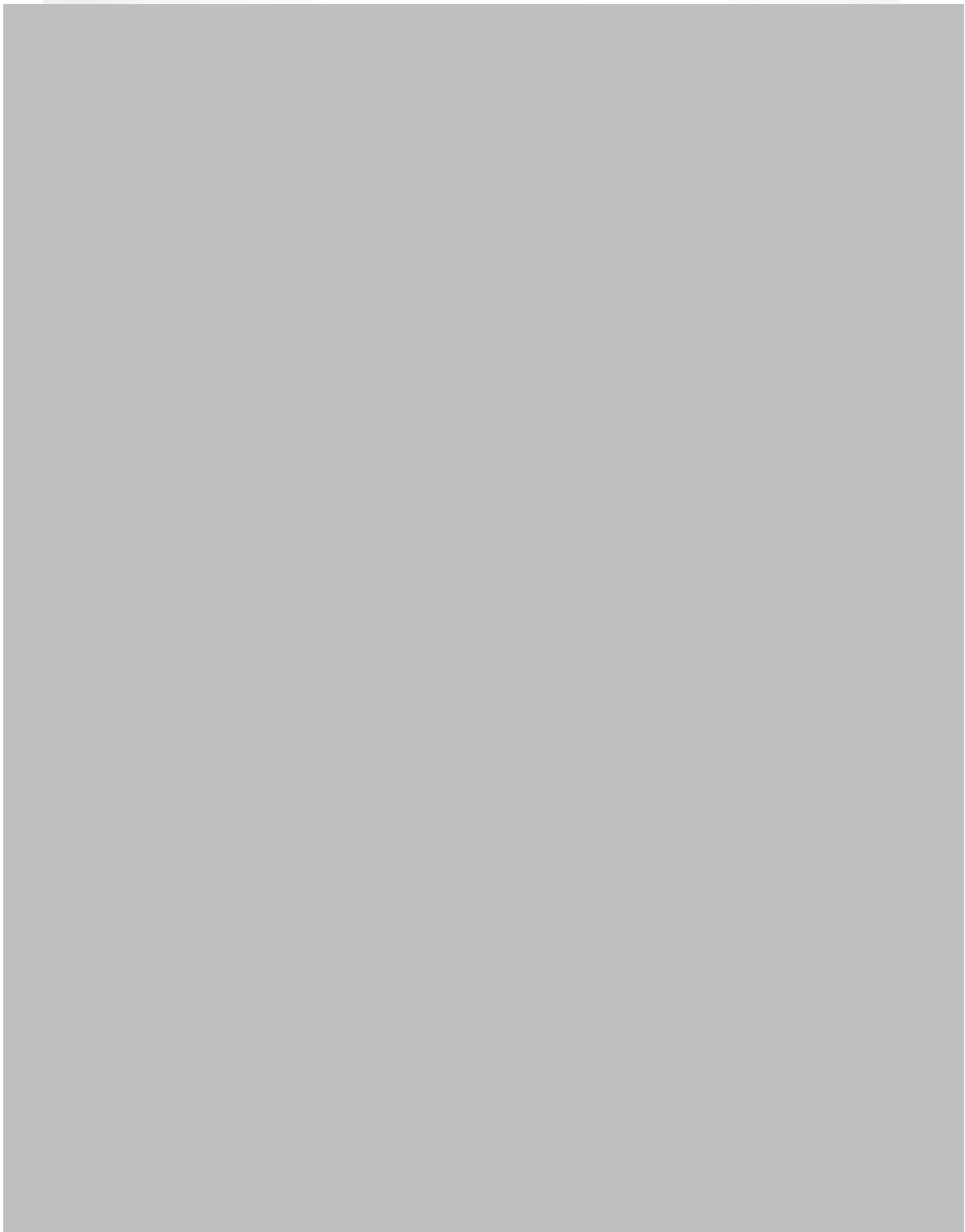


Figure 7.2 Photographs of the sites surrounding area.

Beshkani during survey of the southern area of Khumseen; 2, photo of the southern plain next to the site (Photographs by Dr. V. Usik).

Khumseen Rockshelter is a semi-circular depression some five metres deep and approximately 47 metres south to north and 43 metres west to east axis (Figure 7.3). The depression opens toward the northeast where a wadi system feeding a tributary of Wadi Dawkah plunges from the plain to the southeast. Sediments have accumulated on the peripheries of the depression close to the rockshelters overhang, forming a talus slope of varying steepness. Near the rockshelter several tomb and possible stable structures pertaining to more recent occupations by local Bedouin can be observed. The site has been reoccupied by Bedouin tribes between 2010 and 2011 and can no longer be excavated.



Figure 7.3 Panorama photograph of the Khumseen Rockshelter.

For size comparison note the 4x4 parked inside of the rockshelter. (Photograph by Y. Hilbert).

The Upper Hadrhamaut Group marks the local geology. While the *Qara* and *Andhur* members compose the Dhofar escarpment, the Southern Nejd is composed by the *Rus Formation*. As has been described in previous chapters, the *Rus Formation* is formed by a lower chalky fraction termed *Aybut member* and an upper laminated calcarenite portion termed the *Gahit member*; both geological formations are known to include chert nodules of varying size and knapping properties. At Khumseen Rockshelter these two geological members are found in their respective stratigraphic position. Similar to other rockshelter situations in the area (Al Hatab and Ghazal Rockshelter), the roof of the shelter is formed

by the lower bioturbated calcarinit horizon containing dark chert nodules, the *Gahit member*, while the back wall and the exposed (bedrock) parts of the talus are formed by dolomitic chalk and gypsum, also containing chert debris and nodules, the *Aybut member* (Figure 7.4). Considering the geological situation and raw material availability, it is safe to argue that little effort was placed in the acquisition of chert nodules of acceptable quality at the site.

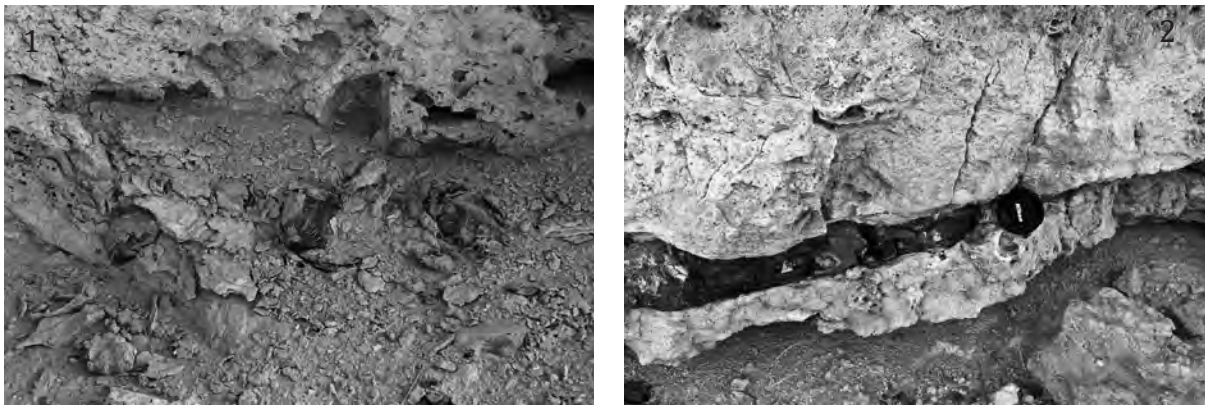


Figure 7.4 Chert outcropping directly at the site.

1, Aybut chert cropping out at the back of the shelter; 2, Gahit chert seam above the shelter (Photograph by Y. Hilbert).

In order to assess the archaeological potential of the site two test trenches were excavated, these have been termed *area 1* and *area 2*. The archaeological samples pertaining to the Nejd Leptolithic strata will be the subject of this section. The two four square metre trenches were so placed within the rockshelter that a maximum amount of find bearing strata could be excavated. *Area 1* was placed in the northwestern part of the site, a few metres above a boulder that collapsed from the roof of the shelter and aided the accumulation of sediments. *Area 2* was situated opposite to *area 1* in the southeastern portion of the shelter. The trench was placed on top of a sediment body lodged against the back of the shelter, some 10 metre away from a small waterfall feature at the base of the wadi running to the east of the site (Figure 7.5).

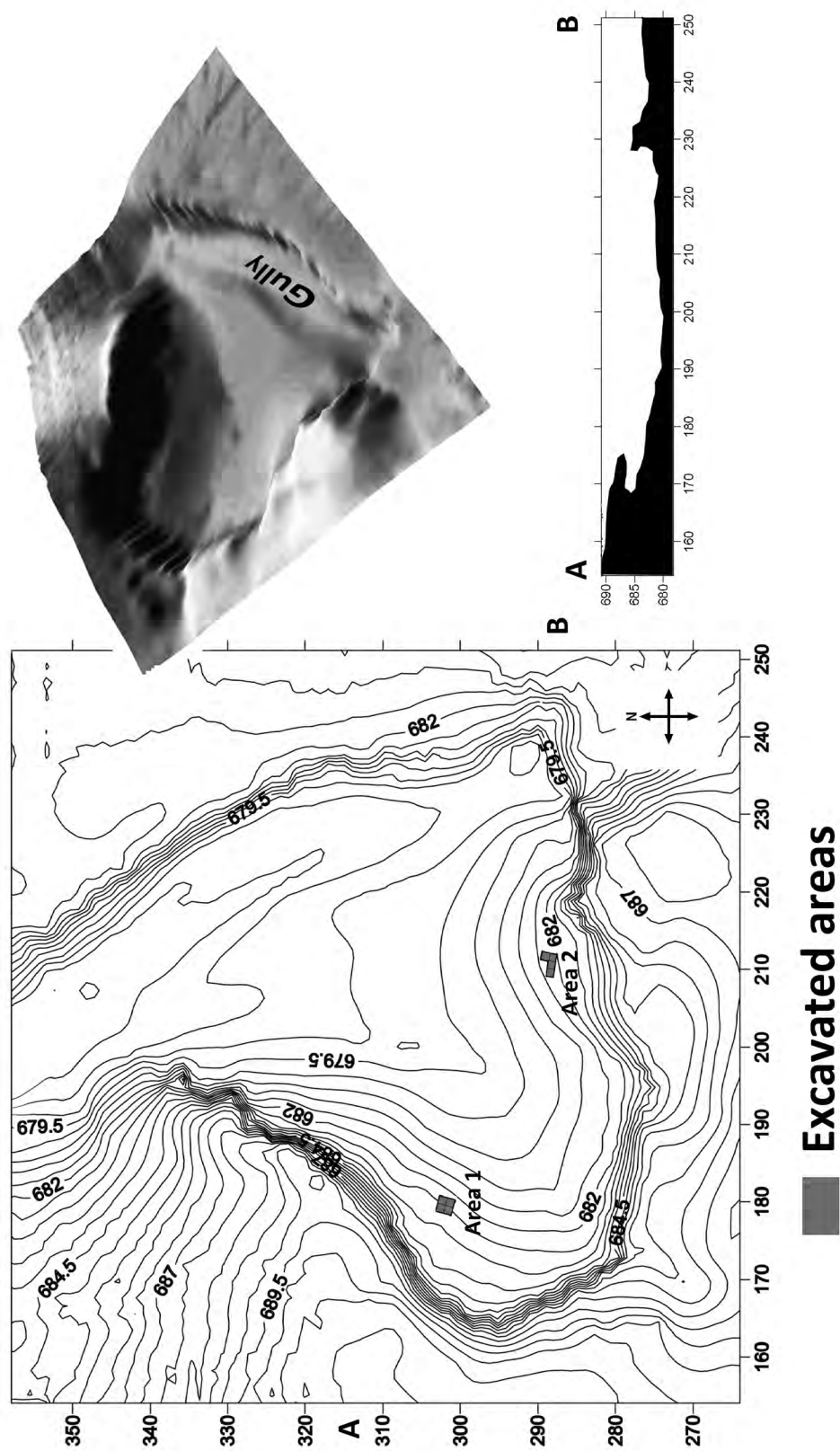


Figure 7.5 Topographic map of Khumseen Rockshelter.
(Image by Y. Hilbert).

7.1.2 Sampling Strategy

The sampling strategy adopted at Khumseen was dictated by the simple principle of excavating as much as possible without the loss of potential information, in order to acquire an adequate lithic sample. Considering the magnitude of the rockshelter, the excavation of at least two trenches in two distinct areas within the site seemed prudent; fortunately, both test pits yielded comparable samples in regards to artefact numbers, configuration of the artefacts classes and stratigraphic succession of archaeological cultures. The stratigraphic configuration and post-depositional history of the sediments, however, presented some divergence.

The excavations at *areas 1* and *2* were conducted following the identified geological horizons (GH); artefacts found within these horizons were subscribed to their respective layer. Sediments retrieved from the excavated areas were carefully sieved through a five-millimetre mesh and finds ascribed to their respective GH. The presence of features within the strata was also observed in both excavation areas and dealt with adequately. No architectural feature was observed aside from the tombs in the back of the rockshelter; nonetheless, it was possible to identify several combustion features through the stratigraphic succession in both test pits. These features were neither encircled by a stone ring nor were they embedded in pits (Figure 7.6). Samples were retrieved from the fireplaces, in order to obtain chronometric dates and enable the study of organic remains. Granulometry samples were also taken from the profile in *area 1* and are currently awaiting analysis.

Aside from the identification of GH's and the documentation of profiles and sedimentary succession, the site was mapped using a total station, in order to produce both two- and three-dimensional maps of the rockshelter. Artefacts retrieved from the sediments were, as mentioned earlier, labelled and catalogued accordingly to their original GH.



Figure 7.6 Fireplaces at Khumseen Rockshelter. 1 fireplace as seen on the excavation surface; 2 fireplace depths (Photographs courtesy of Dr. J. Rose).

Nine GH's were identified in *area 1* and are documented in the eastern profile of the test pit (Figure 7.7). The surface cover, GH1, is composed of loose sand with a high organic component (sheep or goat dung), which is responsible for the dark brown colour of the layer. Also within this unit, limestone shatter of uniform size (5-15mm) was found uniformly sorted within the sediment. Below the 5-8 centimetre thick surface cover the organic component drastically drops and the matrix (mostly eolian material) is comparably uniform throughout the lower GH's. GH2 is divided into two sub units termed *a* and *b*, the sediment matrix is composed of fine eolian dust with a higher amount of larger unsorted clasts of varying dimensions; the layers texture is slightly more compact than that of the surface cover. Two fireplaces were found within this unit. These had not been dug into the sediment, causing any perturbation or admixture of younger material into the lower strata. GH3 is comparable in its composition to GH2, aside from a reduction in clast size, this 20 to 23 centimetre horizon shows no particular orientation of its inclusions. GH3 was equally divided into two sub- units; at the contact zone of the upper and lower units, a fireplace was identified and sampled for C¹⁴ dating.

GH4 is divided into an upper part, with similar matrix to GH3 and containing higher amounts of large limestone blocks, and a lower portion characterized by the decrease in number and size of the limestone fraction. This 36 – 48 centimetre thick sediment unit was dated using both OSL and C¹⁴. The organic fraction of a combustion feature situated at the interface of the GH4*b* and the upper portion of the GH5*a* provided an age for this feature, while the OLS sample taken below the rocky fraction of GH4 yielded additional numerical dates for this layer.

The archaeological samples described here come from the upper GH5*a* (which has been further divided into two phases, termed 1 and 2) and the lower GH5*b*. This 78 – 90 centimetre unit is composed of a fine wind blown matrix and a coarse fraction, consisting of decaying limestone from the back wall of the rockshelter. The lower part of GH5 is resting directly above the bedrock, which in turn consists of dolomitic chalk. GH5*b* is also

marked by large 30 to 50 kg limestone boulders, which appear to be decaying within the sediment and are considered to be an additional source of the small to medium size clasts found within the sediment.

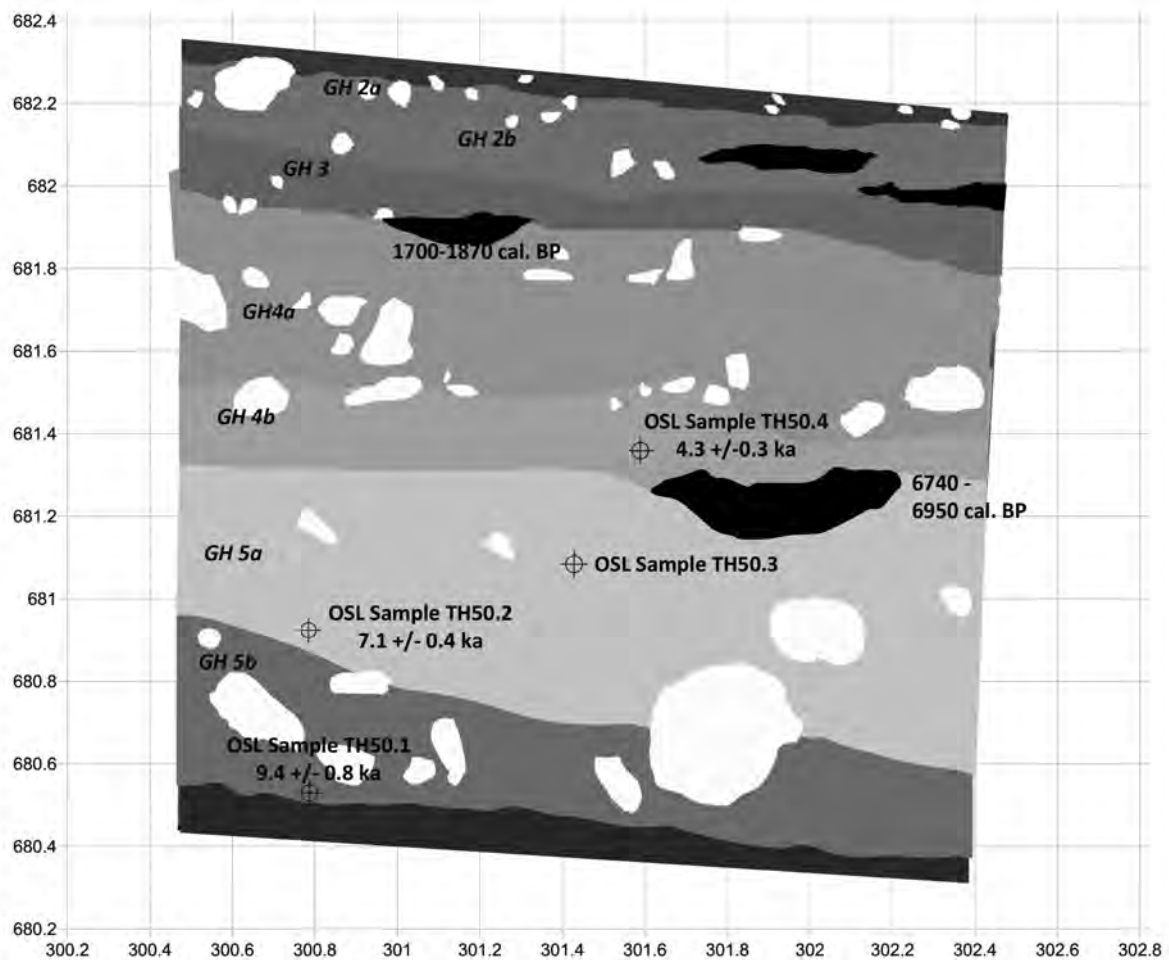


Figure 7.7 East profile of area 1.

Position of the OSL samples are marked in the images as are the samples fireplaces and respective dates summarized in table 8.1 (Image by Y. Hilbert).

The stratigraphic succession from *area 2* was documented on the eastern and southern sections (Figure 7.8). In squares A1 and B1 bedrock was reached after 41.8 cm, while in square A3 the bedrock was reached after 134.5 cm. The GH's mirror the inclination of the bedrock observed in *area 2*. Below 3-5 cm of loose surface sediments, a light brown loose sand/dust matrix with small sharp edged limestone debris and fist sized

limestone rubbles were observed. This layer (GH1) was divided into two sub units were the upper *a* horizon is marked by a darker colour in comparison to the lower *b* horizon. Within the lower GH1*b* a combustion feature was identified in square B1, the fireplace's outline is clear towards the sides of the pit. The feature was embedded into the sediment; a connection to the surface was not visible. No charcoal could be found in the pit, which was filled with ashy sand.

The interface between GH1 and 2 is marked by a clear erosional surface; the sediments below abruptly change configuration and are marked by a more consolidated texture. GH2 is divided into three horizons, termed *a*, *b* and *c*. The horizon GH2*a* is composed of light yellowish sandy/dusty sediment, with moderately to badly sorted limestone inclusions. The sediment was fairly concreted and contained small to medium sized limestone debris. The layer below (GH2*b*) is marked by a similar matrix, with occasional lenses of slightly weathered, and well-sorted limestone debris. The lowest level, GH2*c*, is characterized by light yellow eolian sediment with moderately to badly sorted small limestone shatter and larger 10-20 kg boulders.

The two lower strata of GH2 are only visible in squares A2 and A3. Possible explanations for this configuration involve the orientation of the underlying chalky bedrock and a large decomposing limestone bolder in square A1. A central part in the arrangement of the strata in *area 2* was determined by the erosional event that capped the upper sediments. The catalyst for this erosional event was clearly fluvial and gravitational in character. To the west of the trench a large roof collapse is seen, above the shelter a gully runs towards the overhang and plunges into the site. The gully is also seen in the 3D topographic map.

Considering the stratigraphic disconformity presented by the erosional event documented in *area 2* and the apparent lack of such an incident in the stratigraphy of *area 1*, absolute dating methods were applied to the southern profile of the later. As mentioned in the description of the GH's, the fireplaces in GH's 3*a* and at the intersection between 4*b*

and 5a were sampled. Based on the archaeological remains it was clear that GH5 belonged to a Nejd Leptolithic occupation; therefore, three OSL dates were taken from different elevations within this unit (dates are summarized in table 7.1).

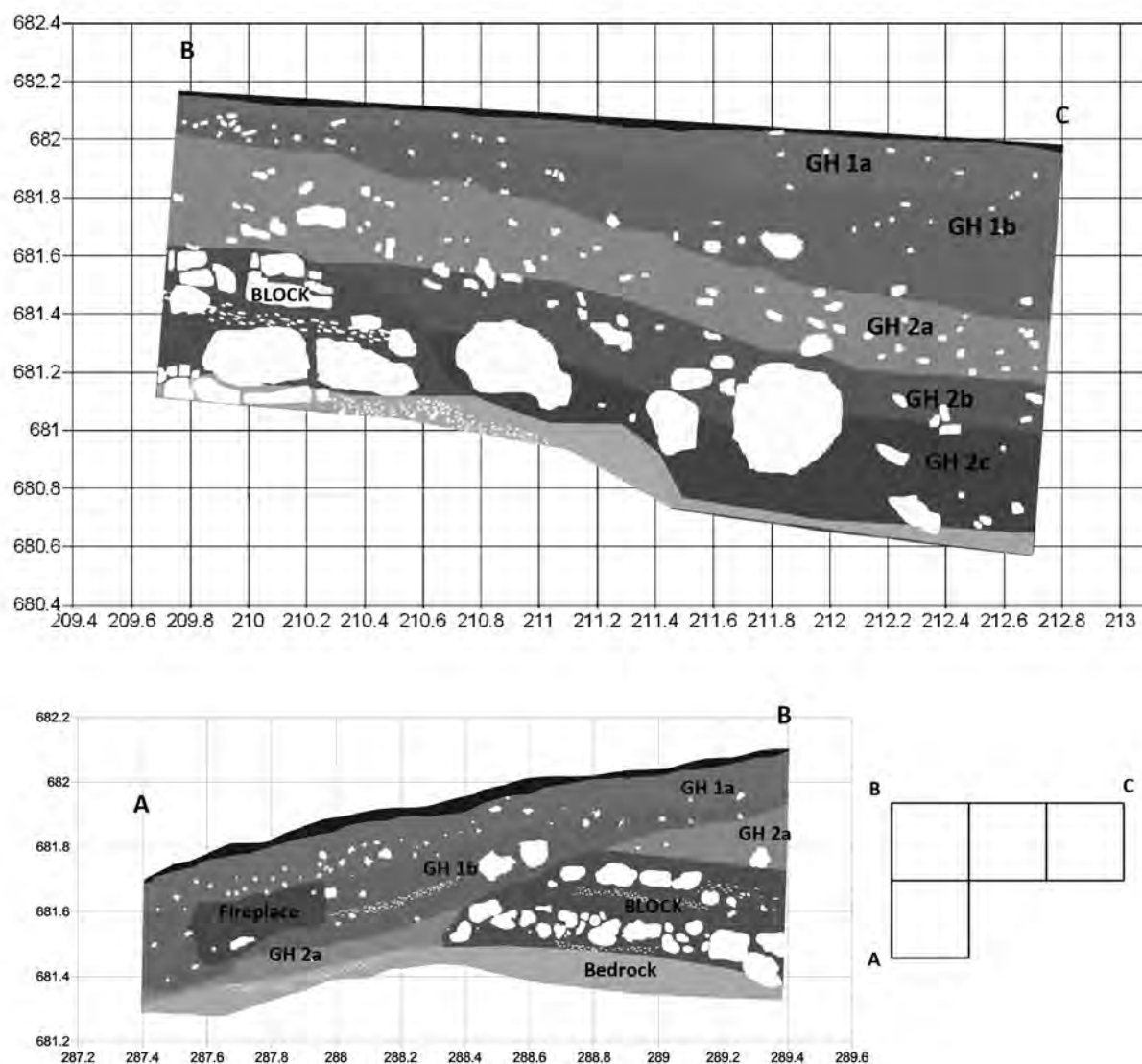


Figure 7.8 South and east sections of area 2.
(Image by Y. Hilbert).

Table 7.1 Dates for Khumseen Rockshelter.

Layer	Depth	Method	Material	Date	Laboratory Nr.
GH3a	40.1 cm	AMS Standard	Ash	1870 to 1700 Cal BP	BETA-281553
GH4b	89.4 cm	OSL	Quartz grains	4.3 ± 0.3 ka BP*	TH50.4
GH4b	103.2 cm	AMS Standard	Ash	6950 to 6740 Cal BP	BETA-281554
GH5a	140.8 cm	OSL	Quartz grains	7.1 ± 0.4 ka BP*	TH50.2
GH5b	179.9 cm	OSL	Quartz grains	9.4 ± 0.8 ka BP*	TH50.1

*Uncalibrated before present.

Although different dating methods were applied, the numerical ages are in perfect stratigraphic succession and, therefore, provide a reliable temporal anchor for the GH5 and GH4.

Summarizing the data on the site's stratigraphy and post-depositional events, it's plausible to state that these factors have had a great influence on the excavated archaeological samples. As will be seen later in this section, patination and edge damage suggest some degree of disturbance across all levels and areas. Granted, post-depositional disturbance was less intensive in the lower levels as opposed to the upper levels. The main symptom indicating this disturbance is the high variability between patination gradients within the sample, the root for this divergence may be related to sedimentary accumulation factors at the site itself. Considering that the raw material used at Khumseen remains the same across all GH's, uniform stages of patination within a sequential gradient was expected. The lack of visible pedogenic horizons within the stratigraphic succession, which would have caused chemical weathering of the chert inclusions within the sediment, indicates a stable and constant redeposition of the sediments body at the site. The fact that whitish patinated artefacts have been found more abundant within the lower units (GH5

in *area 1* and GH 2c in *area 2*) suggest that such pedogenic events developed at the onset of the Holocene wet phase and were subsequently destroyed by erosion after these climatic conditions changed. The artefacts from these lower levels have become incorporated into the sedimentary matrix of the site, any further accumulated and redeposited sediments containing cultural inclusions become contaminated by the already existing artefacts within the sediment's matrix. These sedimentary factors also erased the traces of Early to Mid Holocene soils. Gravity is deemed to be the great force behind the redeposition of the sites sediments; eolian agents have transported additional matrix to the site.

These factors and the above-described scenario are best seen in the cultural inclusions of the upper horizons of *area 2*. These erosional events are not directly visible in the sedimentary succession of *area 1*; however, patination and artefact class configurations support this scenario.

7.1.3 Spatial Distribution

Artefacts were, as stated above, assigned to the identified GH's within each of the test pits. Given the small size of the sampled areas within the rockshelter, piece plotting was not undertaken making the documentation of the artefacts horizontal and vertical distribution difficult. Vertical density within the sediment bulk excavated in *areas 1* and *2* is used to identify the sites main phases of occupation. Coupled with the results from the absolute dating methods it was possible to identify two major phases of occupation in the sedimentary succession of *area 1*. *Area 2* has revealed a truncated stratigraphy, given the erosional event observed at the interface between GH's 1b and 2a; nonetheless, artefact density and configuration of artefact groups are tentatively used to combine the Leptolithic samples from *area 1* and *2*.

In *area 1* two clear peaks of artefact density may be read, presumably indicating intense stone tool production at the site within the GH's. These may be chronologically and stratigraphically placed at: (a) GH3 between approximately 4000 and 1800 B.P; (b) GH5

between approximately 7100 and 9800 BP. Although no absolute dates are available for *area 2*, the roughly comparable artefact density and similar techno/typological patterns indicate that the samples from GH2a and 2c are possibly related to the GH3a and 5 from *area 1* (Figure 7.9).

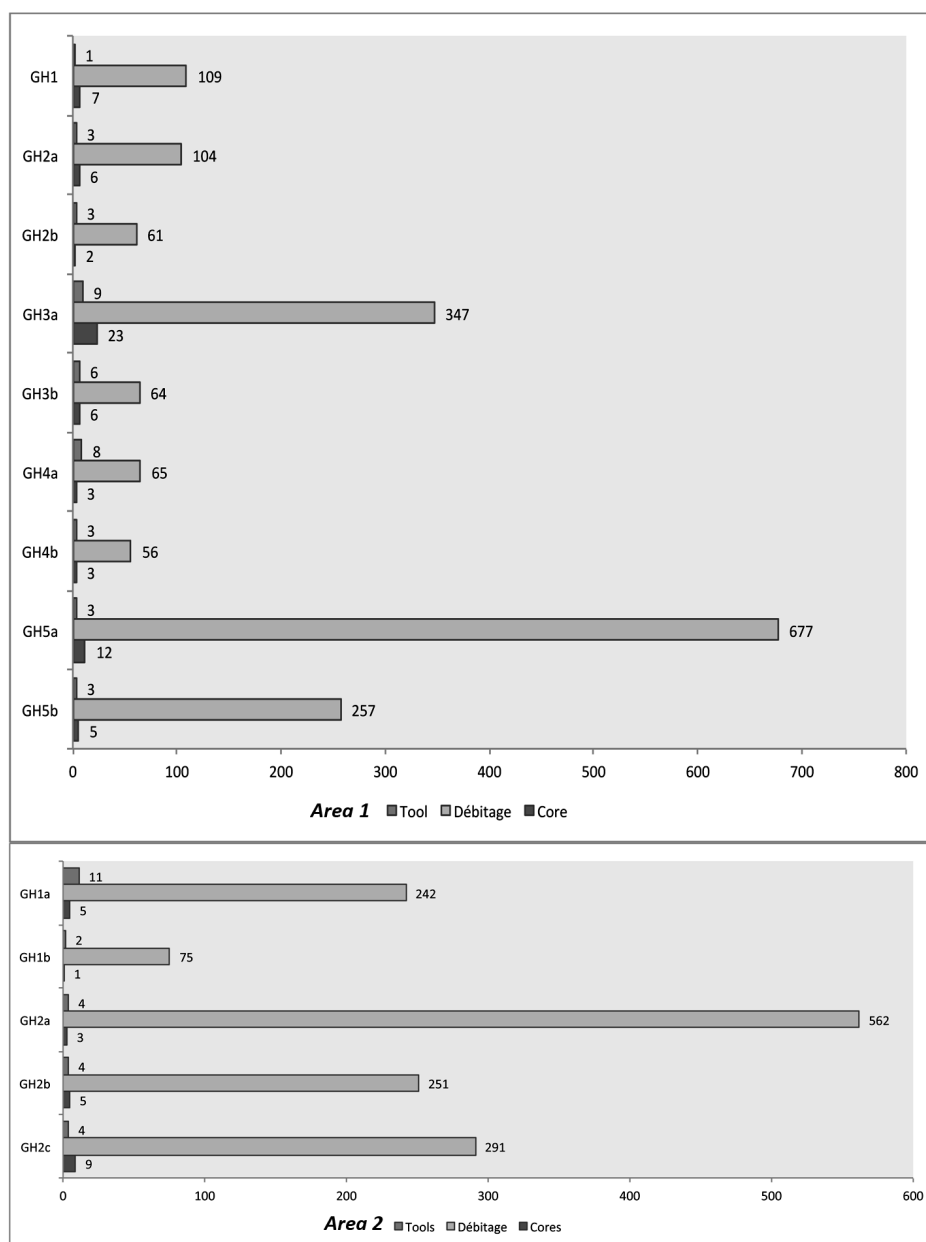


Figure 7.9 Area 1 and 2 vertical density.
(Image by Y. Hilbert).

Additional factors supporting the assumption of a broader unity between the samples from *area 1* GH 5, aside from the technological similarities, are the refits made between artefacts pertaining to GH's 5a1 and 5a2 and GH's 5a2 and 5b. The combined samples of archaeological levels GH5 from *area 1* and GH2c from *area 2* pertain to the Nejd Leptolithic tradition constitutes the here analysed sample.

7.1.4 The assemblage

In total 767 artefacts pertaining to the Nejd Leptolithic tradition were excavated from Khumseen Rockshelter and have been analysed for the purpose of this study (Table 7.2). Of these, 357 have been identified as chips and will be excluded from the formal analysis. Considering the technological and typological similarities between the excavated GH's 5a1, 5a2 and 5b from *area 1*, and GH 2c from *area 2* these will be presented as a single assemblage, attributable to the Nejd Leptolithic tradition.

Table 7.2 Late Paleolithic artefacts from Khumseen.

Blank Type	GH 2c	GH 5a1	GH 5a2	GH 5b	Total
Flake	48	19	23	39	129
Blade	43	11	21	10	85
Bladelets	53	7	9	5	74
Cortical Flakes	15	6	4	13	38
Cortical Blades	5	2	1	4	12
Débordant Flakes	1	1	5	6	13
Débordant Blades	7	2	8	3	20
BTF	2	0	0	0	2
Chips	57	222	50	28	357
Core Type					
Single platform convergent	2			1	3
Single platform parallel	5	5	3	2	15
Opposed platform			1		1
Two unopposed platform	2		1		3
Multiple platform		1	1	2	4
Tool Type					
Informally retouched blank	2	2		2	6
Piercer	1			1	2
Fasad Point	1		1		2
End Scraper		1			1
Total	244	278	129	116	767

Table 7.2 presents the configuration of each single GH and the combined sample that has been analysed. The pattern observed across the samples varies little in its overall composition of tools, *débitage* and cores. The tool sample is minuscule in comparison to the *débitage*; nonetheless, the identification of two Fasad points in both *areas 1* and *2* makes a strong case arguing in favour of a shared cultural set of typological forms within the samples. Striking within the combined sample is the low percentage of *débordant* elements; possible causes for this pattern may be related to the taphonomic and post-depositional character of the site itself. GH 5a2, which yielded two complete core reconstructions (one of them, refit # 10, included 4 *débordant* elements), exhibits a slightly higher number of *débordant* elements when compared to the other GH's. Equally attributed to post-depositional displacement is the presence of two bifacial thinning flakes (BTF) within *area 2*. No other *façonnage* elements has been found within the Nejd Leptolithic levels of Khumseen, making the attribution of this technology to the blade industries of the Early Holocene problematic.

The large number of bladelet proportioned *débitage* in *area 2*, GH 2c, is regarded as the result of a localized activity workshop zone. Bladelets were observed sporadically throughout the sequence in *area 1* and were not found to be any different from the blades found in *area 2*.

Edge damage visible on the artefacts is used to argue in favour of episodic displacement and redeposition of the sediment matrix bearing the artefacts. The amount of edge damage is consistent across both areas. In general, the amount of edge damage was minimal across the sample: 226 artefacts were in pristine condition; 101 artefacts suffered slight edge damage, while twenty nine showed medium edge damage and three pieces heavy edge damage (respectively 63%, 28%, 8% and 1%). The edge damage observed on the artefacts is regarded as indicative for “downslope creep”, gravitationally induced downslope movement of loosely consolidated sediments, rather than aggressive

erosion caused by fluvial agents. Thus, attribution of artefacts to any former surface must be regarded as highly speculative and the inferences involving relative amounts of artefacts in relation to each other must be viewed with some caution.

The core to *débitage* ratio of 1:14 is thought to reflect the economic strategy applied regarding raw material exploitation at the site. In cases where the ratio is higher (at Jebel Eva or at Wadi Haluf 1), decorticated and prepared cores were transported away from the site. The low percentage of cortical elements found at the site, n=50 (12%) indicates that decortication took place in some other area in the site or, possibly, directly at the raw material outcrop.

Two raw material types were used at the site; these have been identified as coming from the *Gahit member* and the *Aybut member* of the *Rus formation*. Both geological members outcrop directly at the site and its surroundings. Artefacts made on the Aybut chert are more numerous than artefacts made on the high quality Gahit chert: 211 (55%) and 107 (28%) respectively. In addition to these two identified raw material units, a third source has been identified; at Khumseen Rockshelter, older previously worked pieces of chert were collected and further reduced at the site. Unfortunately, the age of these artefacts cannot be determined. Refit # 11 incorporates one such example; an older unopposed platform core was reduced, using the original platforms as starting points for further blade reduction (Figure 7.10).

Artefact patination was found to be homogeneous across the assemblage; most artefacts exhibit a light chemical weathering, which gives the pieces a whitish coating: 305 pieces or 84% of the sample. Two percent of artefacts (n=7) exhibit a dark patina, as seen on artefacts that have been lying on the surface. A slightly higher number of artefacts (n=49), representing 14%, exhibit two patination phases and are attributed here to the use of older artefacts as raw material source.



Figure 7.10 Photograph of refit # 11.
(Photograph by Y. Hilbert)

7.1.5 Débitage

Blank production is central in the configuration of the lithic samples, as may be seen in table 7.2: the larger portion of the assemblage is composed of *débitage* and to a lesser degree cores. This section will deal with the categorization and description of the blank attribute analysis undertaken in order to classify and describe the Khumseen Late Palaeolithic lithic sample. Additionally, the assemblage's internal variability in regard to the blank producing sequences is addressed. More detailed description will be given for the following blank categories: flakes, blades and bladelets.

Blank fragmentation in the leptolithic levels of Khumseen occurs in moderate percentages. In total 61% (n=81) of the flakes were complete, fragmentation of flakes into proximal and distal fragments was found to be the most common type of breakage: 15% (n=19) of flakes were broken proximally, while 11% (n=14) were distal fragments. The

remaining 10% are flake medial fragments, false burin blows or burnt pieces (respectively 4, 4 and 5). Blades show similar breakage patterns to flakes, 57% (n= 46) were complete while proximal and distal fragments are represented by 18% and 19% of the pieces (n=14 and n=15). Medial fragments, false burin blows and burnt pieces are present in low percentages; 3% (n=3) are medial fragments, while false burins and burnt pieces are represented by 1% (n=1) each. Bladelets were less fragmented than blades; 60% (n=44) were complete. A higher percentage of distal fragments mark the broken bladelets with 22% (n=16). Proximal, medial, and burnt pieces with 3% (n=3) are found in low numbers within the sample and are represented by respectively 10% (n=7), 5% (n=4) and 3% (n=2) of the bladelets.

The number of cortical pieces in the assemblage is relatively low, so is the overall percentage of cortical cover on the dorsal face of the blanks. Cortical flakes with percentages between 76% to 100% of cortical cover occur in 58%(n=22) of the observed cases and are slightly more common than cortical flakes with 51% to 75% of cortical cover. In comparison to this pattern, cortical blades show a higher number of pieces with 51% to 75% of cortical cover, in total 67% of all cortical blades (n=8). Granted, the number of pieces classified as cortical (primary) at Khumseen is low; however, it is unclear whether this pattern is a result of this low percentage or simply represents divergent strategies of reduction. If the latter is the case, arguments favouring an incorporation of the primary blades as part of the actual blade reduction sequence, rather than merely decortication of raw material volumes must be considered. Non-cortical *débitage* are marked by low percentages of cortical cover; of these, flakes have a higher amount of pieces with 11% to 25 %, 17% (n=21), and 26% to 50% of cortical cover, 10% of all flakes (n=13). Blades and bladelets, to a large extent, are free of cortex; 89% (n=73) of all blades and 91% (n=67) of all bladelets were free of cortex. Artefacts with values between 11% and 25% occur on 10% (n=8) of the blades and 8% (n=6) of the bladelets. Values between 26% to 50% of cortical cover are rare and encompass the remaining 1% of the blades and 2% of the bladelets.

This distribution is indicative off largely decorticated core's working surface.

Blank striking platform morphologies are characterized by their simple configuration. Striking platform lipping and platform abrasion have been found on only a few specimens. Flakes have partial platform abrasion in 18% (n=16) of the cases; only in two cases (2%) platform abrasion was observed across the full intersection of the striking platform and the flakes dorsal surface. One case of inverse abrasion was identified. Blades and bladelets show similar patterns, indicating the sporadic use of this technical element. Partial abrasion was observed on 23% of the blades and 17% of the bladelets (n=12 and n=6); one blade had intentional inverse abrasion, while normal abrasion was observed on 11% of the blades and 8% of the bladelets (n=6 and n=3). Lipped and semi lipped striking platforms were rarely seen; only 11% of all blades and bladelets have lipped or semi lipped platforms (lipping n= 2 and n=2 semi lipped n=4 n=2). A total of 8% of the flakes exhibit lipped or semi lipped platforms (lipping n=2, semi lipping n=5). According to this pattern, hard hammer percussion technique was used to produce the *débitage* at the site.

Flake, blade and bladelet platform morphology is dominated by plain, unfaceted striking platforms, mostly created by a single blow that set up the striking platform on the core. In total, 73% of the flakes, 71% of all blades and 64% of the bladelets have plain striking platforms (respectively, n=79, 45 and 34). Crushed striking platforms were observed on 14% (n=19) of the flakes, 17% (n=9) of the blades and 32% (=17) of the bladelets. Cortical striking platforms occur in low percentages in the Late Palaeolithic levels; 7% (n=8) of the flakes, 5% (n=3) of the blades and 4% (n=2) of the bladelets presented this type of platform. Blades showed some minimal variability in respect to the striking platform preparation: 5% of the blades showed punctiform (n=3), 3% dihedral (n=2 3%) and to an even 2% of simple faceted (n=1) striking platforms.

Flake midpoint cross-sections show greater variability than that of the blades and bladelets. Blades and bladelets are to 36% and 47% triangular (respectively n= 20

and n=34) or trapezoidal in cross-section, with respectively 46% (n=36) and 30% (n=22). Additionally, 20% (n=17) of all flakes have triangular lateralized cross-sections, while 14% (n=24) have flat cross-sections. Flake midpoint cross-sections, aside from the previously described types, also include 26% (n=32) of triangular and 34% (n=41) trapezoid cross-sections. Cortical elements are to a greater part, with 50% (n=25), flat in cross-sections; 26% (n=13) present triangular and 12% (n=6) had convex cross-sections.

Analysis of the *débitage* longitudinal cross-section revealed a slightly divergent pattern for flakes and leptolithic blanks (blades and bladelets). The three main blank types have mostly flat longitudinal cross-sections; 49% (n= 53) of the flakes, 52% (n=38) of the blades and 56% (n=40) of the bladelets have this pattern. Flakes have a relatively high percentage of curved profiles, 25% of all flakes (n=27). If compared to the low percentages of this feature among blades and bladelets, respectively 5% (n=6) and 7% (n=5), it suggests the use of diverging core's working surface configurations for the production of these blanks. There after, flakes have been removed from the cores frontal working surfaces, which showed convex architecture. Blades and bladelets have been additionally reduced from the narrow edges of the core's working surfaces, as is indicated by the high percentages of blades and bladelets with twisted profiles, respectively 40% (n=29) and 37% (n=26).

Most of the *débitage* has feathered terminations, indicating the right amount of force used to detach the blanks from the cores and well established core convexities. In total, 63% (n=63) of the recorded flakes, 64% (n=40) of the blades and 81% (n=50) of all bladelets have this pattern. The most common error observed on detached flakes, blades and bladelets was the unsuccessful use of the complete core working surface characterized by hinged terminations; respectively, observed on 20%(n=20) of all flakes, on 26% (n=16) of all blades and on 18% (n=11) of the bladelets. Flakes have a higher percentage, 17% (n=17), of specimens with overpassed distal terminations when compared to the total of 10% (n=6) for the blades. Only one bladelet measuring 22,76 mm presented this feature.

In this case, the length of the bladelets mirrors the length of the core's working surface, indicating that this bladelet was produced on a diminutive single platform parallel core.

The determination of the technological axis of the detached blanks posed ambiguous results. A great number of the *débitage* analysed yielded undetermined result, due to fragmentation of the blanks or obscured technological patterns. Nonetheless, a course pattern emerged, suggesting a more frequent reduction of the blade and bladelet proportioned *débitage* following the technological axis of the core. Altogether, 43% (n=35) of the analysed blades have been struck on axis, while 47% (35) of the bladelets show this feature. *Débordant* elements were reduced off the core's technological axis in 56 % (n=20) of the analysed cases. Flakes seemed to have been reduced perpendicular to and along the technological axis of the core in 32% (n=41) of the analysed cases, while in 25% (n=25) of the cases the analysed pieces have been struck off axis.

Overall, blank shape from Khumseen mirrors the configuration and exploitation of the cores. Flakes show the greatest variability; 25% (n=31) were parallel, 27% (n=33) were expanding and 21 % (n=26) have converging sides. To a lesser extent lateralized, ovoid or irregular shapes have been recorded; respectively, 9% (n=11), 10% (n=13) and 8% (n=11). Blade and bladelet shapes are dominated by roughly similar patterns, mirroring the pattern observed on the flakes. Blades and bladelets have 39% and 41% of the observed cases parallel edges (n=32 and n=30), expanding sides occurred on 20% of the blades and on 11% of the bladelets (n=16 and n=8) while converging sides occurred on 30% and 38%, respectively (n=25 and n=28). To a lesser extent lateralized (n=5 6% and n=6 8%) and irregular forms occurred; while lateralized blades occurred on 6% of the observed cases, 8% of the bladelets have this pattern. Irregular shaped blades and bladelets occur on 5% and 2% of the analysed cases (n=4 and n=1). The predominant occurrence of parallel and convergent forms among blades and bladelets, as opposed to flakes, indicates a controlled use of the core's working surface in the production of these blanks (Figures 7.11 to 7.12)

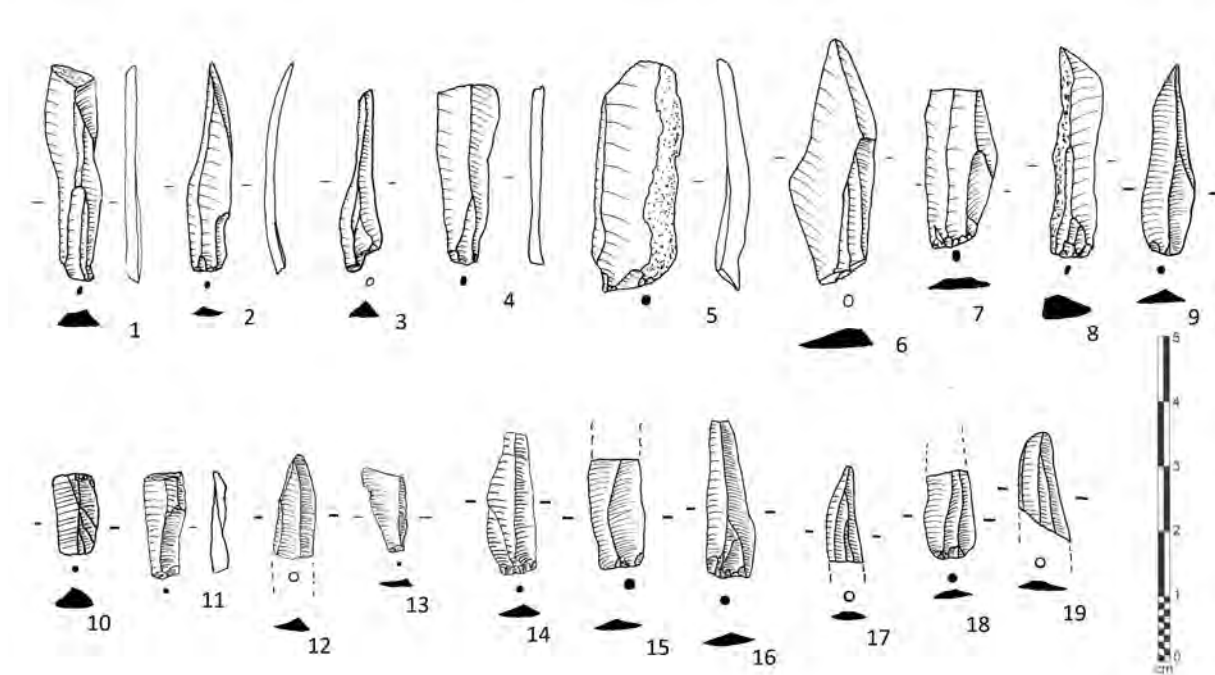


Figure 7.11 Khumseen bladelets.

1, 4, 7, 10, 11, 13 bladelets with parallel edges and unidirectional scar patterns; 5, and 8 bladelet dimensioned débordant elements; 2, 3, 6, 9, 14 and 16 bladelets with convergent edges; 12, 15, 17, to 19 bladelet fragments with parallel scar pattern. (Illustrations by Y. Hilbert).

Blank dorsal scar pattern is dominated by simple unidirectional configuration of the dorsal scars; 77%, of the flakes ($n=90$), 67% ($n=52$) of the blades and 80% of the bladelets ($n=58$) exhibit this pattern. Blades and bladelets show little variability in respect to the remaining scar patterns. The remaining blades and bladelets exhibit 15% and 3% of unidirectional convergent ($n=12$ and $n=2$) and 17% of parallel scars for both blank types ($n=13$ and $n=12$). One blade fragment illustrated in the *débitage* table has a bidirectional dorsal scar pattern. Also presenting this particular pattern, three *débordant* blades have been identified and attributed to change of orientation of the core, rather than true bidirectional volumetric blank production. Enforcing this hypotheses, only 4% of the flakes have opposed ($n=1$), unidirectional crested ($n=1$) or transverse scars ($n=2$). The impending discussion of the core analysis should help to shed some light on the reduction sequences used at the site.

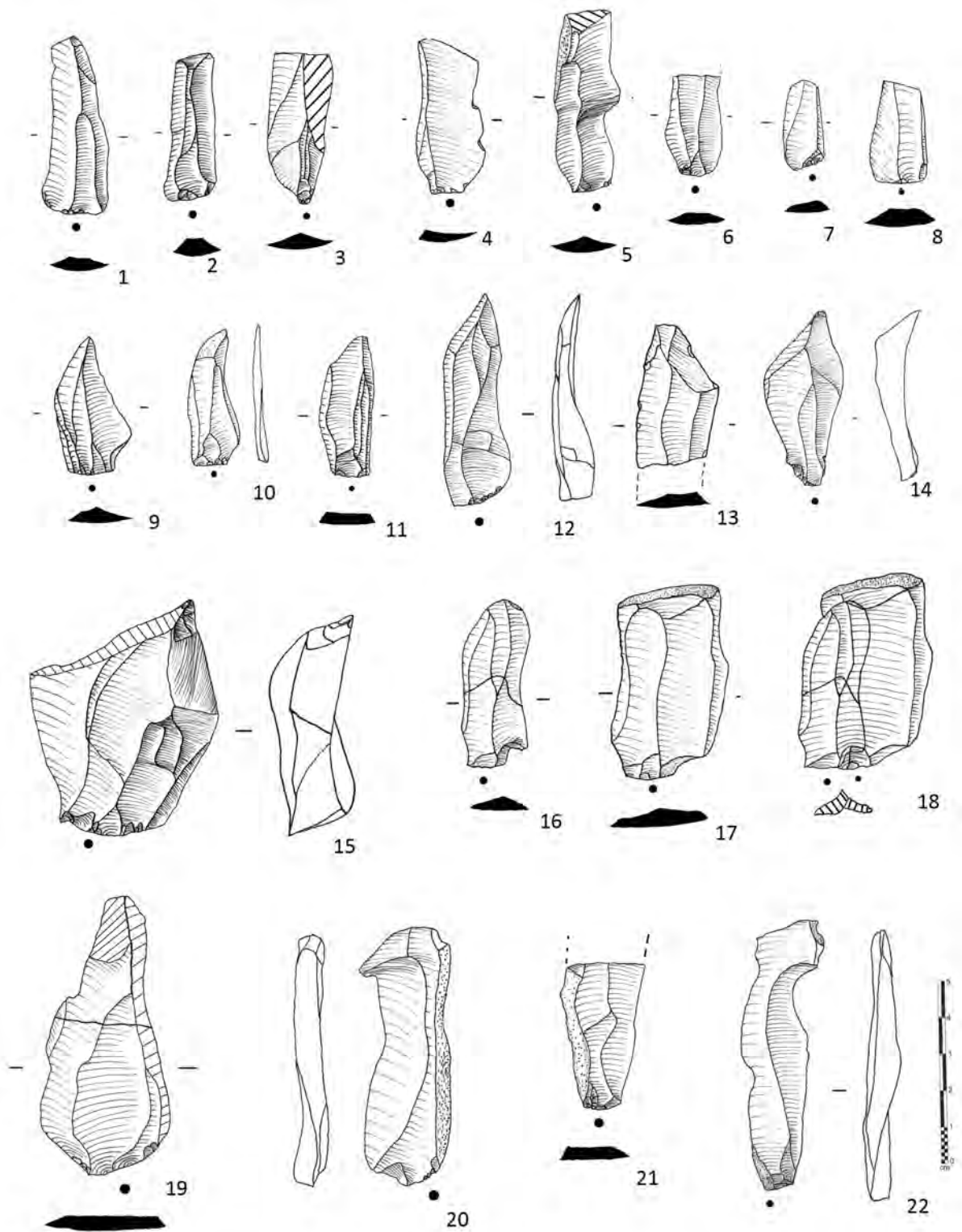


Figure 7.12 Khumseen blades.

1, 9, 10, 11, 12 and 14 blades with convergent sides; 2 to 8 blades and blade fragments with parallel edges; 13, blade fragment with bidirectional scar pattern; 15 flake with unidirectional crested scar pattern; 16 to 18 refitted blanks; 19 to 22 débordant blades. (Illustrations by Y. Hilbert).

Metrical analysis of the *débitage* was used to further classify the reduction modalities used and determine variability within and between blank types. Based on the IOE (index of elongation), blades and bladelets exhibit diverging average values (2,53 and 3,18). The few *débordant* blades are on average longer and more slender than the actual intended products (2,91). Flakes are only slightly longer than they are wide (avg. of 1,39), indicating that, although part of the unidirectional parallel production system, these blanks followed diverging production designs.

Blades, bladelets and *débordant* blades have relatively short proportions; blades are on average 44,69 mm in length, rather small if compared to other Late Palaeolithic assemblages. As in other assemblages, *débordant* blades are longer (avg. 57,74 mm) than blades and show high values of standard deviation (s.d. 19,48). Average blade widths (17,33mm) show little variability (s.d. 5,01), as does the average bladelet width (8,35 mm, s.d. 2,05). The flakes from Khumseen Rockshelter were equally diminutive; in average these were 23,57mm in width and show higher standard deviations of 10,06 in comparison to those of the leptolithic *débitage*. *Débordant* blade width shows higher average (avg. 22,32 mm) values than that of the blades; the standard deviation of 8,47, however, is considerably higher.

Based on the index of elongation (IOE), blades are shorter and wider in comparison to blades from other assemblages (avg. 2,43). On average, blades were 4,79 mm, while bladelets were 2,73 mm thick; little variability was identified (respectively std. 1,72 and 1,08). *Débordant* blades were thick on average (11,72) and showed the highest variability among the leptolithic *débitage* (std. 6,87). Flakes showed values in between that of the blades and *débordant* blades, averaging 6,71 mm in thickness and varying little (std. 3,99).

If the total weight of the *débitage* is considered, 5657g, a total of 1198g are of Leptolithic proportions. The metrical analysis presented above supports the intentional production of blades and bladelets.

Débitage striking platform measurements were used to produce the IPF (index of platform flattening). Flakes and blades show similar average values of 2,5 and 2,58 respectively, blade standard variation being slightly higher than that of the flakes (1,03 and 0,84). Striking platforms were mainly twice as wide as they were deep. Combined with the measurements of the blanks volumes, the index of relative platform size (RPS) was determined. Blades showed the highest RPS value (19,84), indicating that this blank type had the largest surface in relation to their platforms. Blades have also shown the largest variability in respect to that specific aspect of their dimensions (s.d. 19,39). Oddly, bladelets produced the lowest value, indicative of large platforms in comparison to their dorsal surfaces. Standard deviation values (s.d. 6,58), however, were relatively low if compared to that of the blades. Flake RPS values show average (12,85) and standard deviations (s.d. 13,83) located between those values provided by the blades and the bladelets.

7.1.6 Cores

In total twenty six pieces have been identified as cores: three single platform convergent cores, sixteen single platform parallel cores, one opposed platform core, three unopposed platform cores and four multiple platform cores (Figure 7.13).

The metrical analysis of the cores presented no surprises, although pieces ranged greatly in weight (8g to 185g), morphologically little variability could be determined. Considering the limited number of cores, the significance of the pure metrical dimensions of these artefacts for the analytical purpose of this dissertation should not be over estimated.

The unidirectional parallel reduction of raw material nodules and blocks was the most common used blank production system. A total of sixteen specimens have been recorded, more than half of the cores. The *Aybut member* chert was the most common type of raw material used (n=8), followed by Gahit chert and the use of older artefacts as raw material the source (n=3 and n=5). Most cores (n=10) were only partially freed from

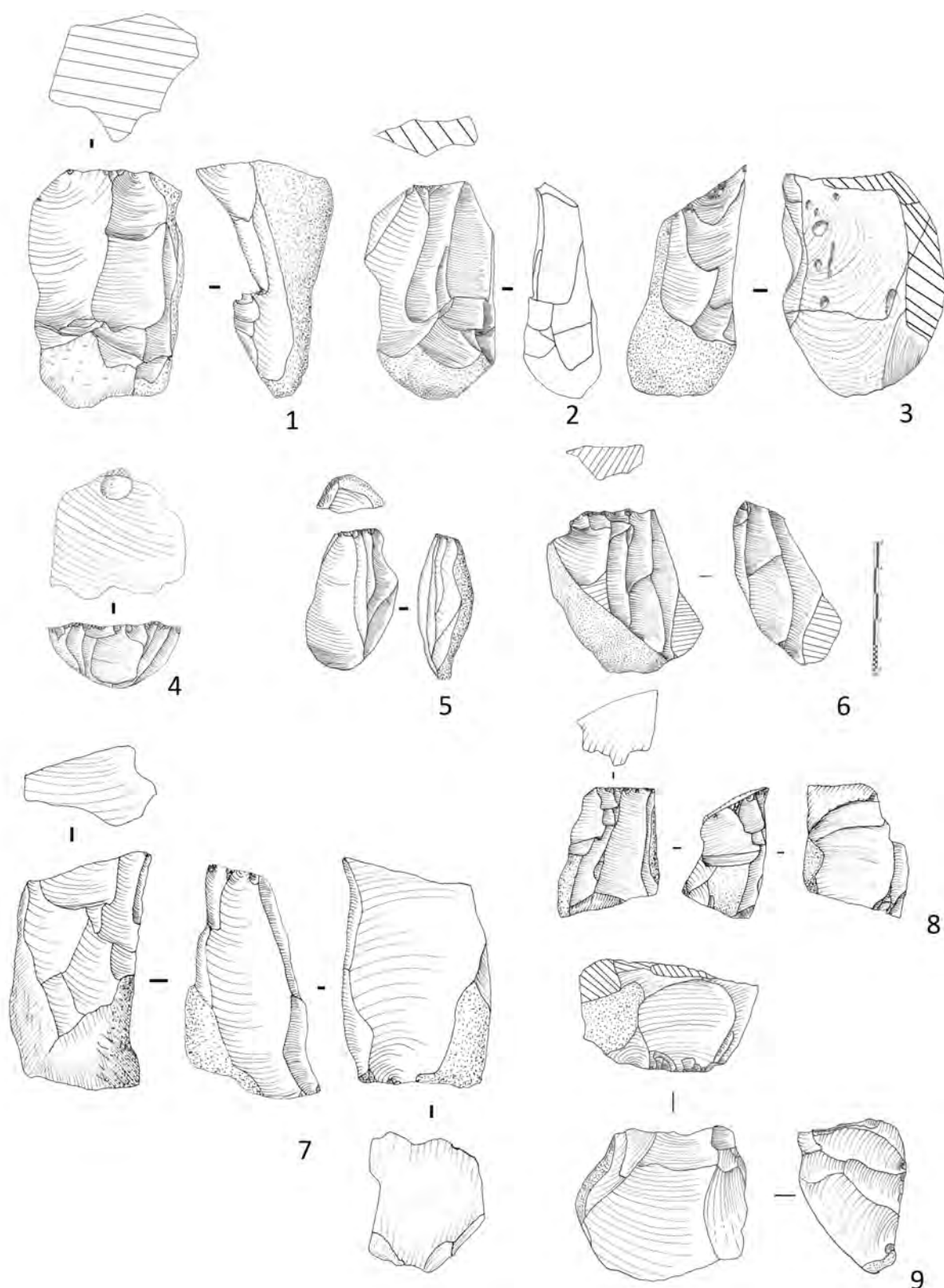


Figure 7.13 Khumseen cores.

1 and 2, unidirectional parallel blade cores; 3, unidirectional blade core with narrow working surface; 4, convergent bladelet core; 5 bladelet core; 6 bidirectional core; 7 and 8 two unopposed platform cores; 9, multiple platform flake core. (Illustrations by Y. Hilbert)

cortex or neo cortex (having between 26% to 50% of cortical cover), only two cores have undergone more intensified decortication (11% to 25%).

Core striking platforms, with one exception, are plain and crated by a single blow perpendicular to the core's technological axis. One piece exhibited what seemed to be a faceted striking platform; after closer inspection it was possible to determine that the platform was not faceted but merely had been used as a former plane of removal on the same volume. The change in orientation of the reduction of a volume, plus the use of the former plane of removal as a striking platform is common at other Nejd leptolithic (see Ghazal Rockshelter section). The core's working surfaces had, to a greater part (n=7), been placed on the longer and broader face of the raw volume. In three cases, expansion toward the raw volumes supplementary lateral face was observed; two specimens were exploited using the frontal and both lateral narrower faces, indicating the intentional exploitation of previously untapped zones on the core, resulting in a semipiramidal morphology. In four other cases, reduction started directly using the narrow portion of the core, in order to obtain narrow and elongated blanks.

The truncated dimension of the main exploitation face of the cores (average length 57,27 mm) suggests that most of the parallel unidirectional cores reached the end of their productive cycles. The greater number of the cores (n=7) exhibited flat plane of removals, indicating that, although the surfaces were not ruined due to excessive hinging, these were abandoned due to their small size. Cores with ruined convexities, either botched by hinge fractures or the detachment of overpassed blanks that removed a relatively large portion of the core, have also been observed (respectively n=5 and n=1).

Unidirectional convergent cores follow a similar technological parameter as the cores described above, the difference between the two lays rather in their morphology. The main characteristic of the two identified specimens is the relatively wide working surface in respect to the cores lengths. No specific treatment was given to the striking platform, making the attribution of these specimens to a technological convergent pattern

unwarranted. Given the convex and wide core's working surface, blanks removed from the cores edges have converged to the centre of the technological axis on the distal portion of the core. That is to say, reduction of these cores follow a unidirectional parallel technology but the morphological criteria warrants their categorization as convergent cores.

A single opposed platform core was found within the leptolithic core assemblage of Khumseen Rockshelter. The core's opposed striking platforms are unprepared. The core's working surface is placed on a narrow portion of the raw material block and exhibits good horizontal and longitudinal convexities. The succession of scars on the core's working surface indicates that rather than being used alternatively, the striking platforms were used in sequence.

Three unopposed platform cores have been identified. As was the case for the single platform cores, striking platforms were simple and created by a single blow to the top of the raw material volume. Core working surfaces were either on two opposite narrow portions of the raw material, on a frontal and back surface of a raw material block or on the raw materials frontal and lateral portions. As the definition of this core type demands, planes of removal and scars do not intersect. The cores were heavily exploited and presented botched planes of removal.

Four multiple platform cores have been identified, all heavily exploited and abandoned due to their small size or ruined convexities (or complete lack there of). Morphologically these are cuboid and seldom show intersecting planes of removal. A strong alternation tendency dictated the reduction of these raw material volumes, indicates the conversion of these cores from a simple unidirectional reduction on a single plane to multiple planes, in order to maximize the volume reduction. Although refits supporting this shift were not achieved, the morphology of these specimens surely favours this scenario.

7.1.7 Tools

Few tools have been identified within the assemblage. The few tools present, however, conform to the spectrum identified on surface collections presenting identical technological patterns of blank production and volume exploitation. Six informally retouched pieces, two piercers one endscraper and two projectile point fragments were found (Figure 7.14).

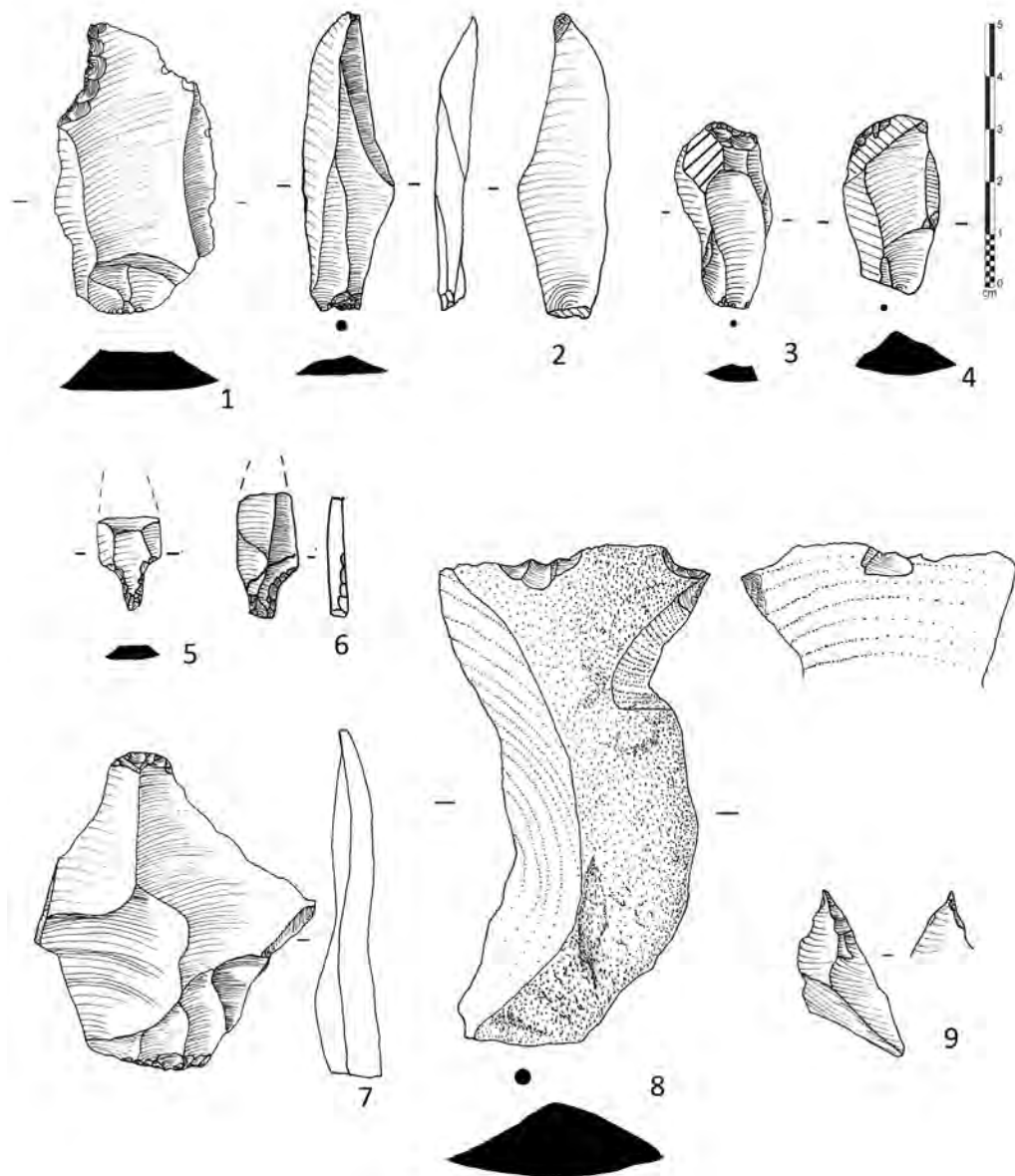


Figure 7.14 Khumseen tools.

1 to 4, retouched blanks; 5 and 6, Fasad point fragments; 7 endscraper on flake with unidirectional scar pattern; 8 and 9, piercers. (Illustrations by Y. Hilbert).

The projectile points have been identified as Fasad points based on the steep to semi steep direct retouch on the proximal portion of elongated slender blanks. The retouch that created the hafting element of these armatures, the peduncle, was administered from the ventral surface and no inverse retouch or pressure retouch was used to further modify this element. Unfortunately, both artefacts were fragmented; the pointy ends had broken off. Attribution of these artefacts to the Fasad point category is warranted by the choice of the blanks and the characteristics of the retouch on the proximal end; both have semi abrupt direct retouch.

The two piercers are of very distinct proportions, one of them made on a small flake with minimal alternating retouch to the distal portion, while the second piece was fabricated on a older, large *débordant* blade showing older patination. Retouch on the second specimen is identical to that of the first with minimal alternating retouch to the dorsal and ventral faces of the blank. The endscraper has received enough retouch to be identified as such. A flake with convergent distal termination was chosen to serve as a blank for this tool.

Blades, bladelets and flakes have undergone some degree of transformation; a total of six retouched pieces have been identified. Retouch is to a large extent obverse; one distally inverse retouched blade was identified. Retouch is nibbling and seldom extends across the complete edge of the blanks. Mostly lateral or distal retouch has been observed.

7.1.8 Refittings

In total, seventeen refits were made using the leptolithic assemblage of Khumseen Rockshelter; of these Refits # 10, #11, #13, #14 and #16 will be presented and discussed regarding the patterns these constellations reveal.

Refit #10 shows a successive volumetric reduction of fourteen blades from a single platform core (Figure 7.15). The constellation shows all stages of reduction, decortication, and convexity maintenance by *débordant* removals, as well as continued blade production

from the core's plane of removal (Figure 7.16). Ideal convexity, however, was not achieved, since all the reattached blanks had hinged terminations. The produced *débitage* was considered unsuitable for use or modification. Decortication was to a certain extent incorporated into the flat reduction running parallel from the core's striking platform. No striking platform preparation was undertaken; a natural fracture on the raw material volume served the purpose of reduction just fine. After most of the cortex on the main plane of removal had been reduced, two successive *débordant* removals were detached from the core's right edge. After the created convexity had been exploited, reduction shifted towards the central left portion of the volume. Two *débordant* blades were removed from each of the core's lateral peripheries. Exploitation of the nodule proceeded until the core's working surface convexity was exhausted.

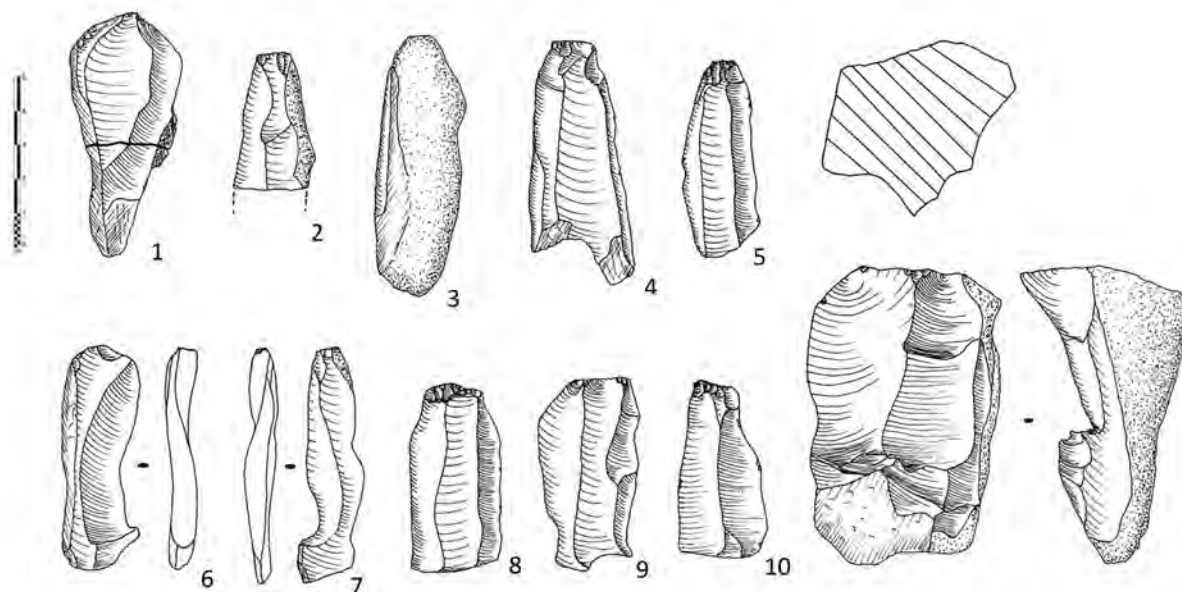


Figure 7.15 Khumseen refit #10 débitage.
(Illustrations by Y. Hilbert)

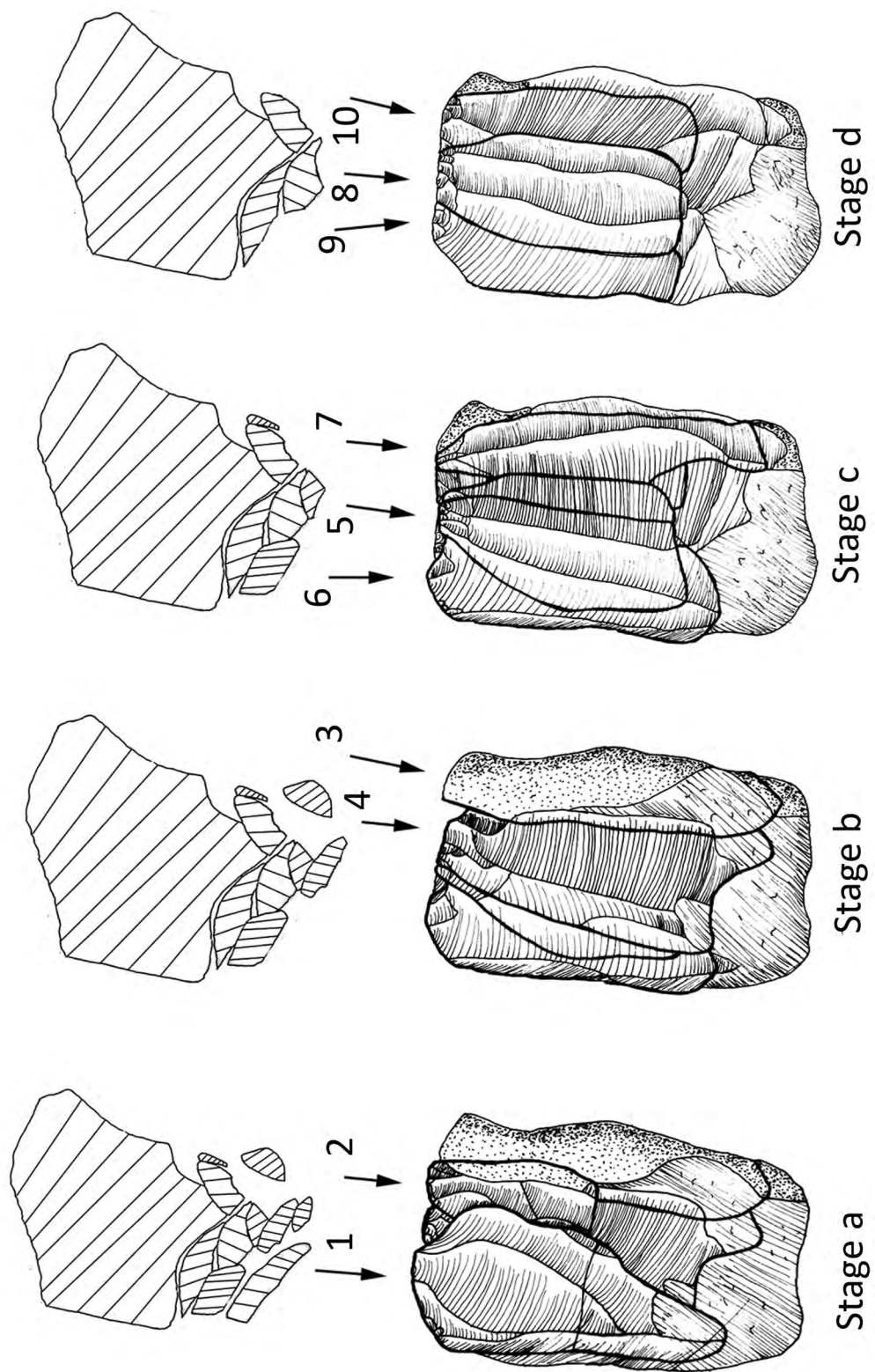


Figure 7.16 Khumseen refit #10. (Illustrations by Y. Hilbert).

Refit #11 exhibits a specific aspect of the raw material used at the site; namely, the use of older, previously knapped raw material volume as additional source for blank production. The chronological depth between the two knapping events cannot be estimated, given the lack of any preserved levels below the Late Palaeolithic horizons. A two unopposed platform core was used and reduced, using the already existing platforms (Figures 7.17 and 7.18). First, one plane of removal was exploited then the second. The reduction of a large overshoot blade capped the striking platform on the opposite inverse side of the core. The nearly perpendicular negative on the distal portion of the first plane of removal was used to produce three blades on the opposite plane of removal. Considering that required convexity was not achieved on either of the core's working surface the *débitage* was irregular in shape and was not further transformed.

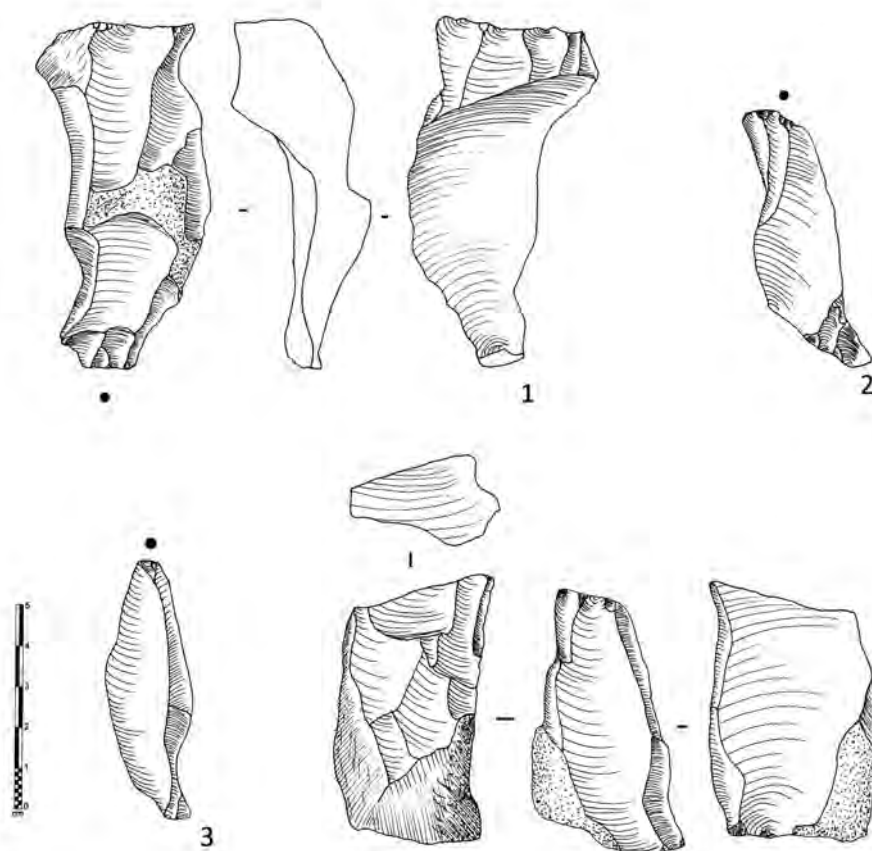


Figure 7.17 Khumseen refit #11 débitage.
(Illustrations by Y. Hilbert).

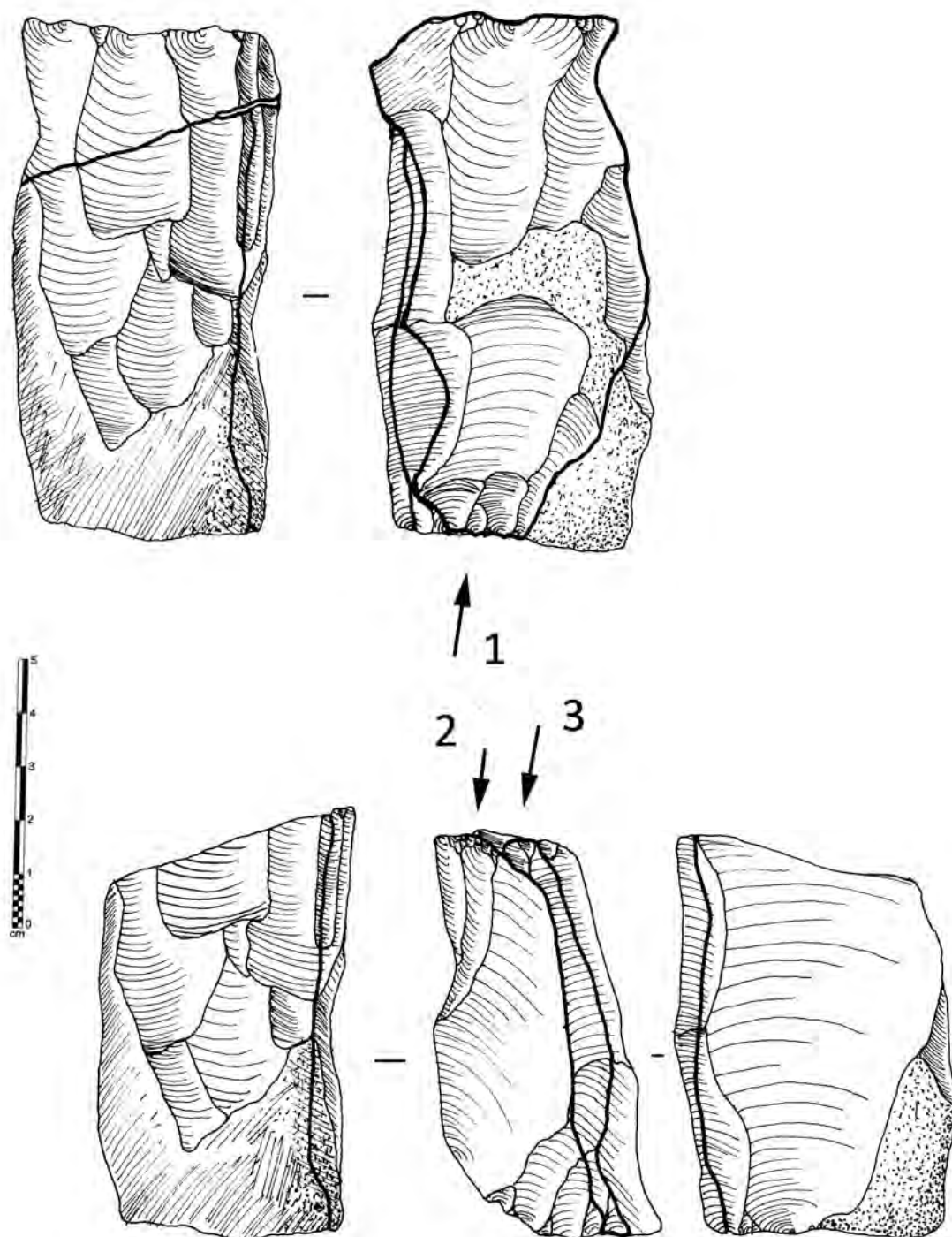


Figure 7.18 Khumseen refit #11.
(Illustrations by Y. Hilbert).

Refit # 16 mirrors that of refit # 11. The difference between them lays in the fact that refit #16 shows but one patination phase and, therefore, indicates that identical reduction strategies have been used (Figures 7.19 and 7.20). A two unopposed platform core of slightly truncated dimensions if compared to that of refit # 11 was first reduced from its back plane of removal. A large overpassed removal created the striking platform that would later be used to reduce the frontal plane of the core. Reduction continued on the backside only to produce a hinged and botched core working surface. Subsequently, reduction shifted to the frontal plane of reduction; a total of three blanks could be reattached to the core, two blades and one flake.

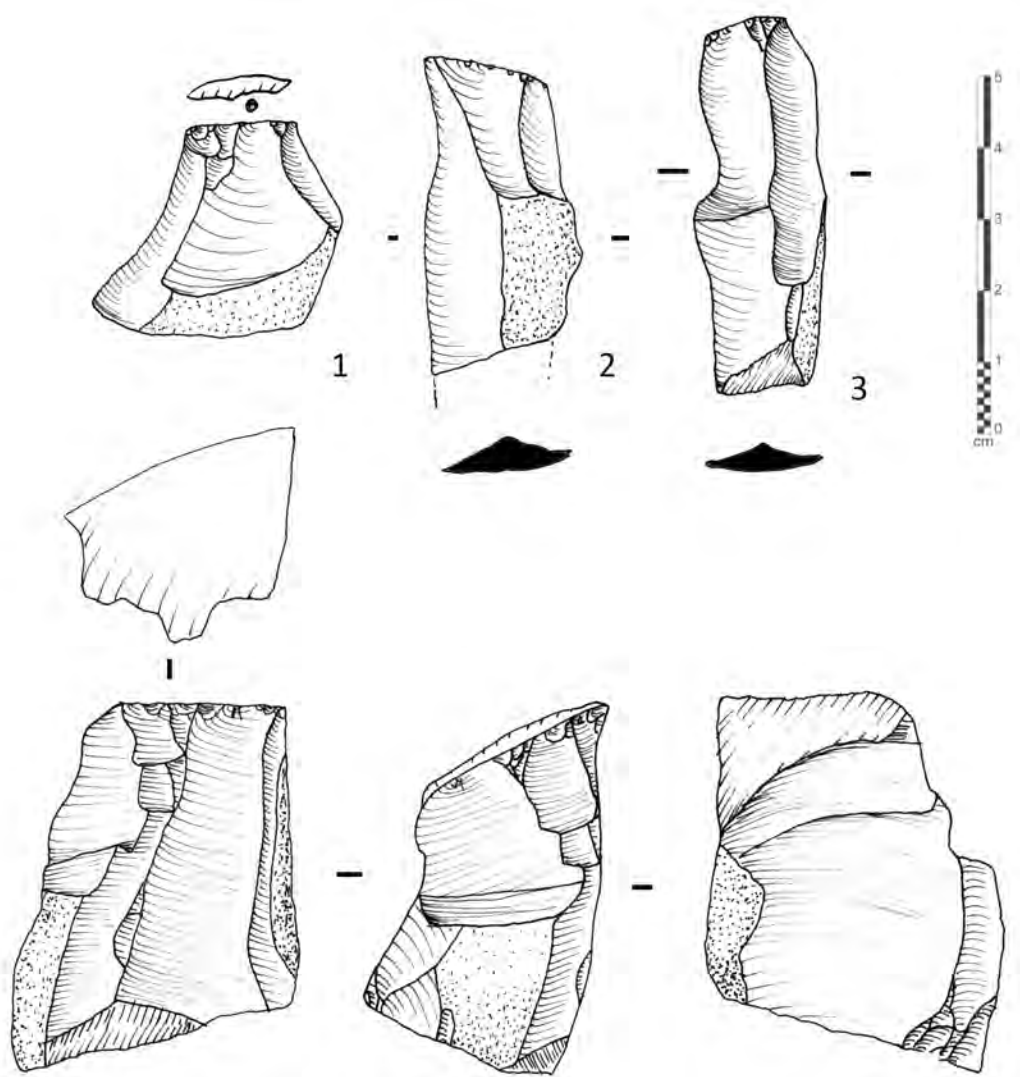


Figure 7.19 Khumseen refit #16 débitage.
(Illustrations by Y. Hilbert).

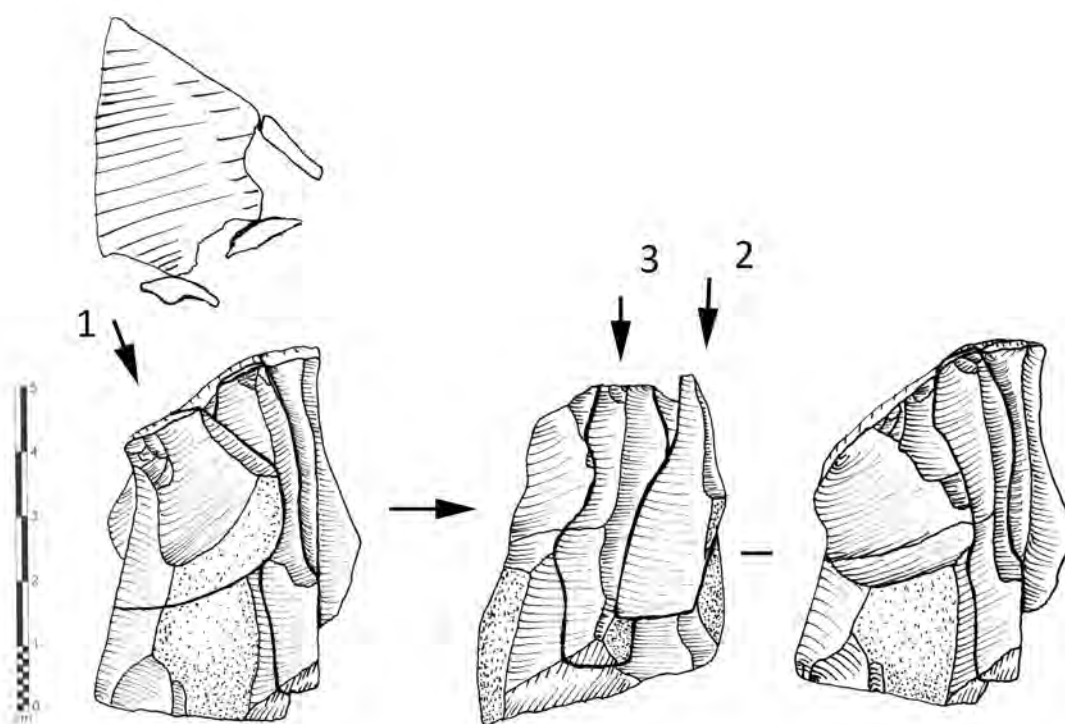


Figure 7.20 Khumseen refit #16.
(Illustrations by Y. Hilbert).

The constellations #13 and #14 depict specific aspects within the reduction systems used at the site. Refit # 13 incorporated two *débordant* elements struck to correct the convexity of the core's plane of removal (Figure 7.21); these were removed alternatively from opposite core peripheries. Between the removals of these two elements, core exploitation along the created dihedral face on the plane of removal took place. Refit #14 is composed of four blanks, although the core pertaining to the constellation could not be found this reconstruction gives some insights as to how the core might have looked during its reduction. Early within the reduction, a large *débordant* flake was removed from the left side of the core; reduction followed exploiting the convexity created. Reduction then shifted to the right side and moved towards the centre (Figure 7.22). The converging flakes removed last indicate that the emphasis was placed on the maintenance of a dihedral plane of removal exploited by more than one subsequent removal. The core was possibly of similar proportions to most unidirectional parallel cores depicted above.

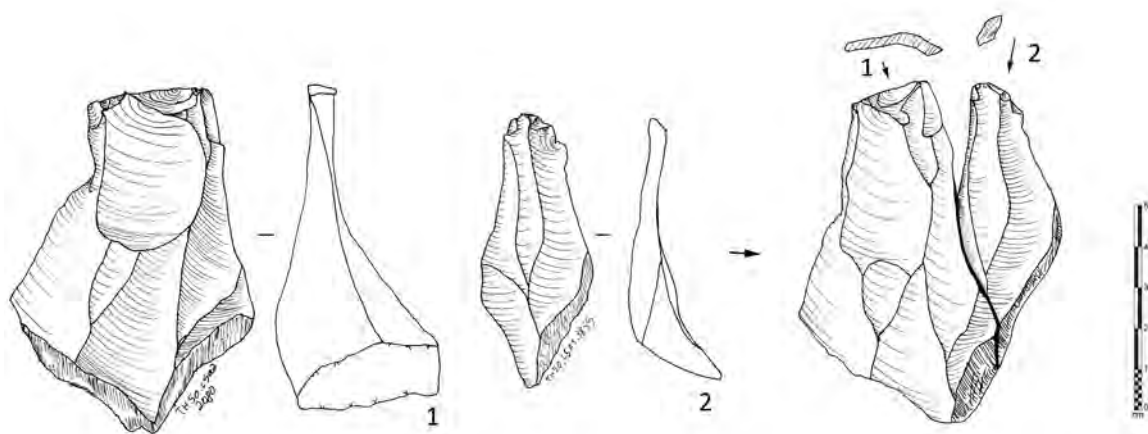


Figure 7.21 Khumseen refit #13.
(Illustrations by Y. Hilbert).

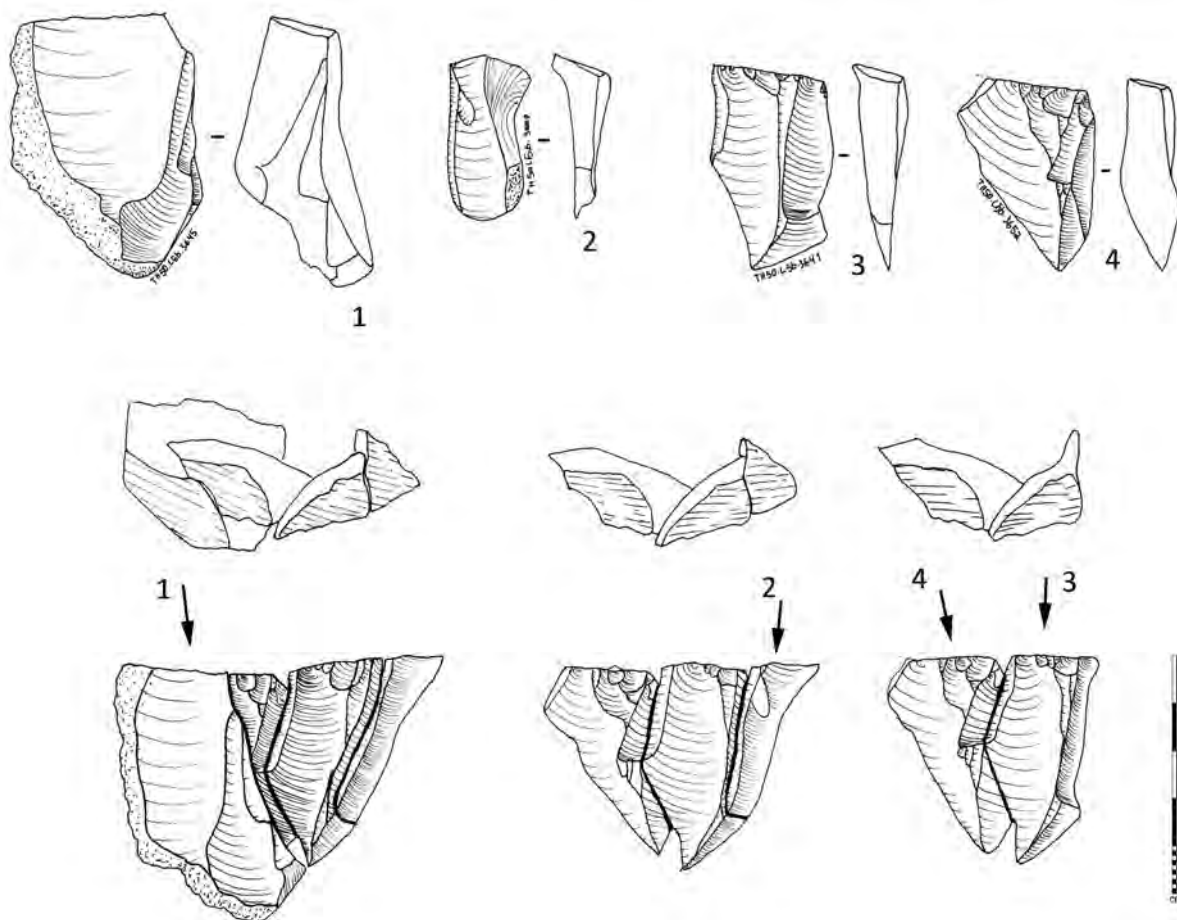


Figure 7.22 Khumseen refit #14.
(Illustrations by Y. Hilbert).

The remaining refits are subscribed to early stages of decortication and discreet phases within the continuous reduction of raw material volumes at the site. The patterns of reduction based on the analysis of the *débitage* and the cores are exemplified and enforced by the aforementioned constellations.

The discussion of the refits from Khumseen Rockshelter concludes the presentation of the data gathered from this site. A discussion of the patterns identified across the analysis of the material will follow in the discussion section that summarized the data from both buried sites chosen from the BRAVO transect.

7.2 Ghazal Rockshelter (TH.47)

Ghazal Rockshelter, although not more than an 80 cm high overhang overlooking a primary drainage system running northwards and conjoining with a network of drainages that forms one of Wadi Dawkah's southern tributaries, contains two superimposed Nejd Leptolithic archaeological levels. Found during the 2010 DAP campaign and excavated over that and the following field season, the site has yielded the largest number of refits and conjoins, thus representing a crucial milestone in understanding blade reduction strategies during the Late Palaeolithic period of Dhofar. Absolute dating methods have been applied to the excavated geological Horizon's (GH) and are used to anchor the two excavated lithic assemblages into a chronological framework that is, to a certain extent, comparable to that from Khumseen Rockshelter. Over the next pages the sites location, its eminent geological surrounding, sampling strategies, dating, stratigraphic succession and the results of the lithic attribute and refit analyses will be presented and discussed.

7.2.1 Site location

Situated in the eastern portion of the BRAVO Transect the site lies in a similar geographical position as Khumseen Rockshelter and al Hatab. Just south of the geographical frontier between the northern part of the Dhofar Escarpment and the southern border of

the Nejd Plateau, Ghazal Rockshelter is approximately 500 metres west of al Hatab and c.a. 1500 metres east of Khumseen Rockshelter. A web of small tributaries and gullies dissecting the rugged terrain marks the site's eminent surroundings. This complex and interconnected network of gullies has aided both the sediment aggregation and the preservation of the archaeological bearing layers. During phases of increased precipitation these gullies would have become active, some would have experienced flash flood stream like conditions, while others would have carried less water. The site is cut by one such gully that was not overly active during the past, thus sediment erosion was not as intense as in similar situations across the southern Nejd Plateau. To the southeast and northeast, two inselbergs tower some 50 to 70 metres above the site. The slopes of these two elevations are covered by debris that made its way into the entwined gully network below. A moderately steep rise marks the site to the east, which is dotted with outcropping raw material.

Local geology is marked, as for the greater portion of the southern Nejd, by the contact between the *Gahit* and the *Aybut members* of the *Rus Formation*. The overhang, which at some point during the Early Holocene made up the low roof of the shelter, lay collapsed on top of the site and aided the stagnation of sedimentary erosion (Figure 7.23); preserving the sediments within the site.

The site is c.a. 1,5 metres lower than the surrounding pediment and sediments have accumulated in this depression. The visible pediment is composed of the lower portion of the bioturbated calcarinitic portion of the *Gahit member*, while the geological formation below that is much softer and more vulnerable to erosion. As noted in chapter Four, this facies is composed of the chalky *Aybut member*. As the upper *Aybut member* was cut back by erosion, the lower *Gahit member* eroded away slowly, thus creating the slight overhang situation. Over the course of the Early Holocene, sediments of both colluvial and eolian origin filled the depression and the little rockshelter in its back.



Figure 7.23 Photograph of the Ghazal prior to excavation and during excavations. (Photographs by Dr. J. Rose and Y. Hilbert).

Whitish weathered artefacts were outcropping from the slightly inclined sediments talus, backing against the collapsed overhang. A six square metre test pit was dug in front of the collapsed roof of the shelter, in order to examine the site's potential; during the 2011 campaign excavation activities were resumed and additional nine square metres were excavated (Figure 7.24).

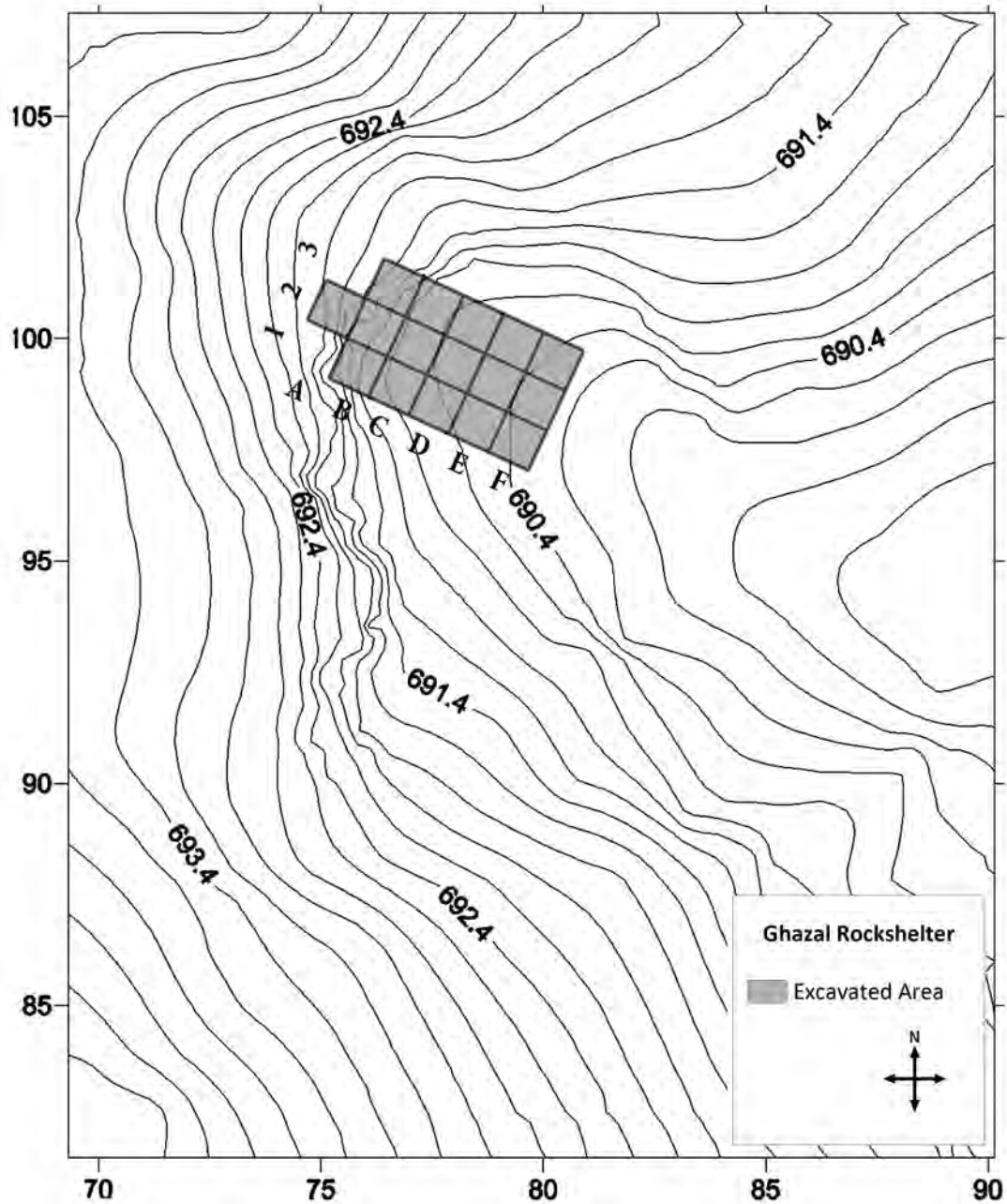


Figure 7.24 Topographic map of Ghazal.

Squares A2, B3 and parts of B2 were situated below the roof of the shelter.
(Image by Y. Hilbert).

7.2.2 Sampling Strategy

Although the excavations at Ghazal Rockshelter were relatively extensive, a total of fifteen square metres were excavated, if compared to that of Khumseen Rockshelter or al Hatab only a relatively small sample was recovered from the sediments. Granted, the maximum depth of the excavations did not exceed 60cm below surface, but artefact density within the excavated sediments was equally modest. Nonetheless, the character of the sediments and their deposition preserved two distinct archaeological levels entitled level 1 and level 2.

Excavations were confined to one square metre units and followed the identified GH. The excavated sediments were sieved and artefacts attributed to their GH of origin. Documentation of profiles and local topography followed that applied at the rockshelters of Khumseen and Al Hatab. The 3D and 2D topographic maps help to better illustrate the position of the excavated square metres and elucidate possible causes for the sediment accumulated at the site (Figure 7.25). At this point, it is important to inform the reader that the squares A and B are situated under the 80cm roof of the small shelter in the back of the site; this suggests that the material pertaining to the archaeological levels could not have slumped in from the area above or adjacent to the site.

Five GH's have been identified during the excavations and are visible in the documented profiles. Photogrammetry methods have been applied to the three profiles, the schematic profiles produced using these images is presented here (Figures 7.26, 7.27 and 7.28). The profile EAST1 was documented on the eastern side of the square metre units C1, C2 and C3. EAST2 was oriented in the same manner as EAST1, only one square metre further to the east. The SOUTH1 profile depicts the longitudinal axis of the excavated area and was documented in squares A2 and B3; two planimetric images have been stitched together, in order to illustrate how the GHs looks along that axis.

The sedimentary sequence is characterized by the interchange between sedimentary units with a larger portion of eolian material, indicating periods of aridity and

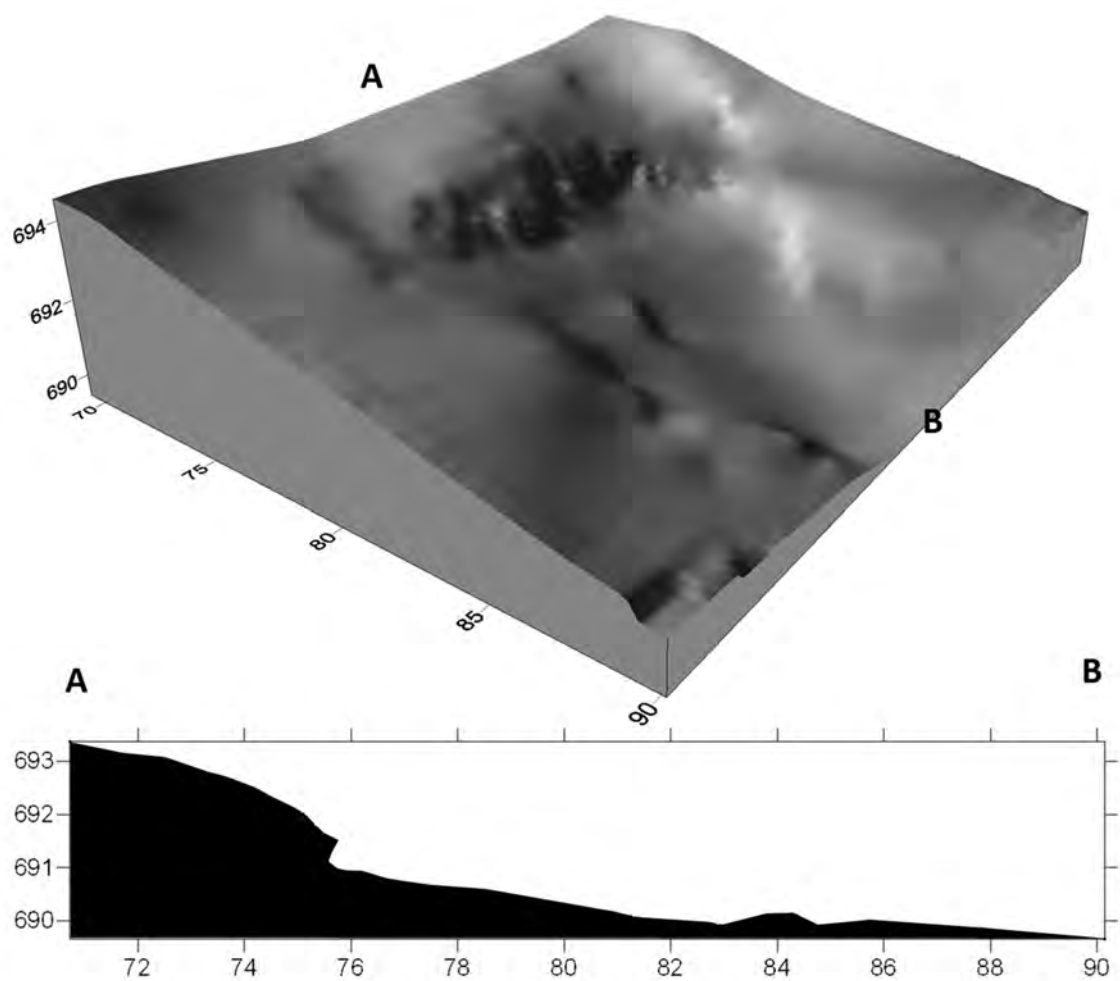


Figure 7.25 Surface plot of Ghazal.
(Image by Y. Hilbert)

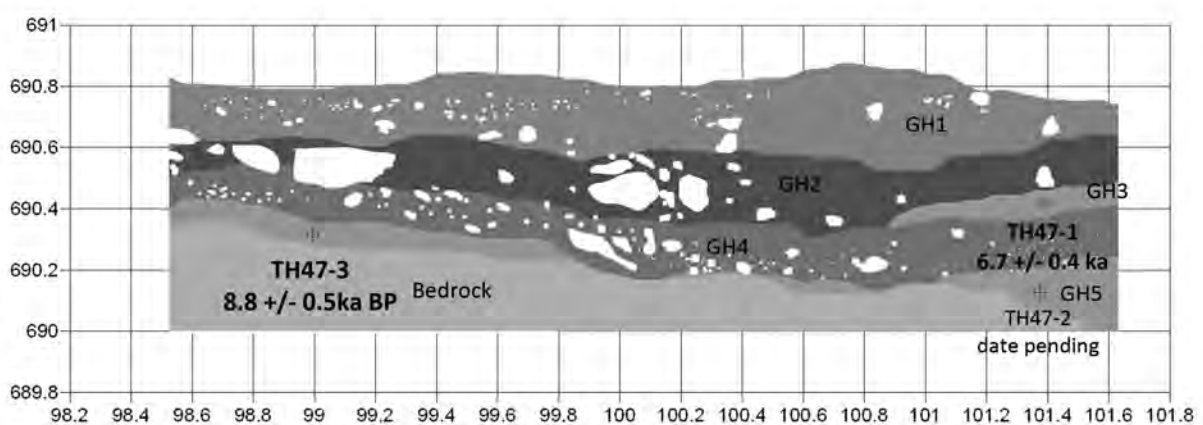


Figure 7.26 Profile EAST 1 from Ghazal.
OSL samples and respective dates are also shown in the figure.
(Image by Y. Hilbert)

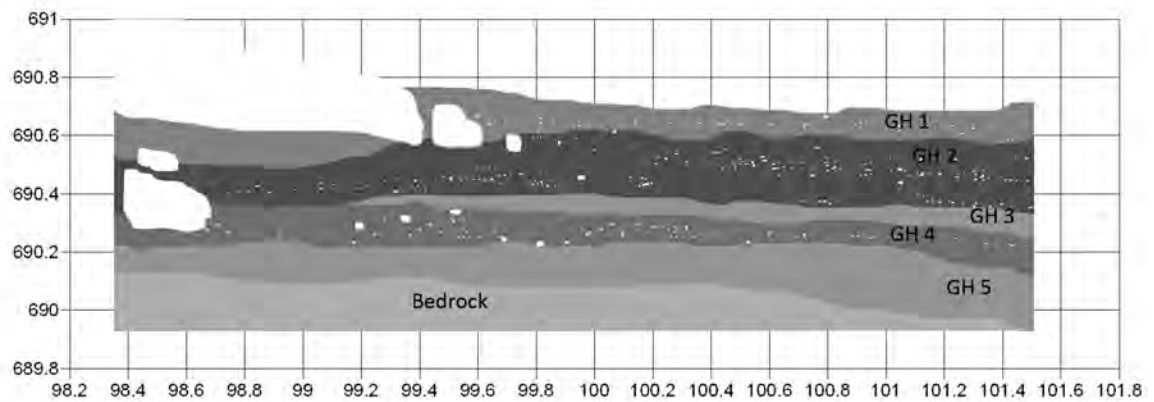


Figure 7.27 Profile EAST 2 from Ghazal.

Profile EAST 2 has been recorded one meter behind EAST ; GH 3 is better preserved and well articulated as a sterile sand layer. (Image by Y. Hilbert)

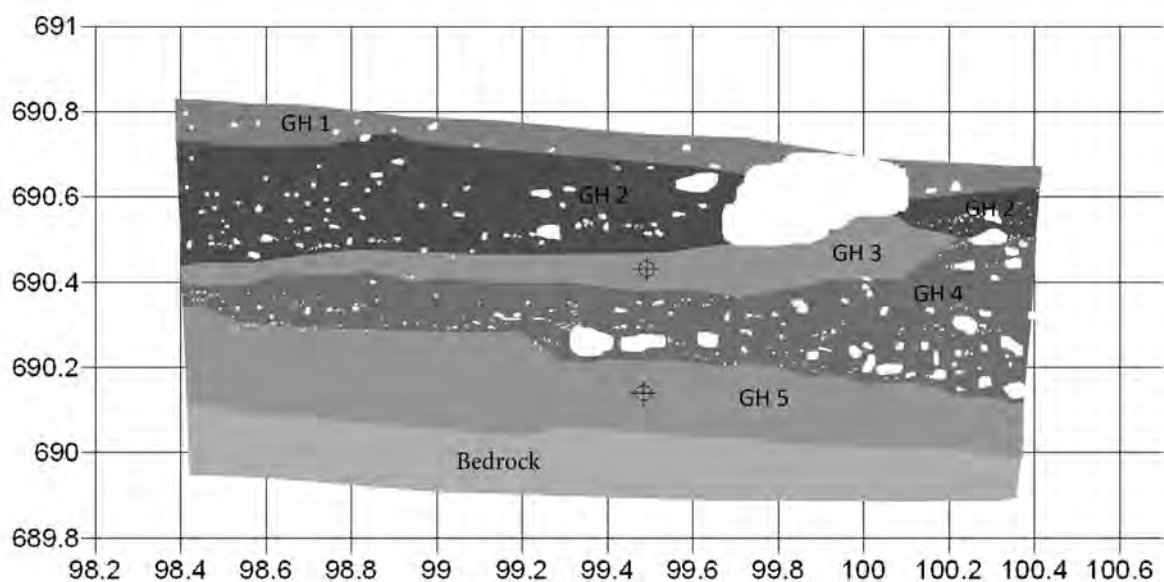


Figure 7.28 Profile SOUTH 1 from Ghazal.

Profile SOUTH 1 has been recorded perpendicular to profiles EAST 1 and 2. (Image by Y. Hilbert)

availability of eolian sediments, and coarser portions with quartz sand matrix, indicating the admixture of the eolian fractions with both archaeological and geological inclusions. GH1 is composed of poorly sorted sediment with angular limestone shatter in a sand/dust matrix. Occasionally, brown patinated chert debris was recovered from the sediments. The chert inclusions indicate that some redeposition had taken place not too long ago. GH2 consists of fairly sorted sediment, containing fine limestone shatter; the sediment was slightly more concreted than GH1. Light yellowish to brown in colour, the sediments containing the archaeological level 1 included medium to small sized flat limestone debris. The sediments composing this unit were slightly concreted.

GH3 was preserved solely under the roof collapse in the south area of the section EAST1 (Figure 7.29), and is composed of fairly homogenous light brownish yellow sand/dust sediments. In section EAST2, however, the GH3 could be observed throughout the profile, indicating that GH3 had been completely eroded away in the western area of excavation. In section SOUTH1 the inclination and subsequent petering out of this unit can be observed, indicating the erosion of the sediments.



Figure 7.29 Photograph of the roof collapse and eolian sediments below. (Image by Y. Hilbert)

The GH containing the archaeological level 2, GH4, is made up of poorly sorted, rocky, pale yellow sand/dust layer, containing larger limestone blocks and small angular limestone shatter. Some of the limestone blocks show signs of in-place deterioration. The sediments are looser than those of GH2. The contact zone between GH4 and GH5 is a clear one; most of the archaeological material excavated was lying in the contacts zone. The GH5 presented itself as a homogenous sterile sand/dust layer observed across the entire excavation unit. This sterile sand layer was resting on top of the bedrock, which consisted of dolomitic chalk. The fact that a great deal of the find bearing strata, mostly GH2, was destroyed by erosion explains the limited sample size for level 1.

Absolute dating methods were applied to GH3 and GH5; given the eolian character of these two sediment units, OSL dating methods were used. The area from which these two samples have been retrieved is shown in the profile schematics. The analysed samples returned dates of 8.800 ± 500 B.P. for sample TH47-3 taken from GH5 (47 cm below surface) and 6.700 ± 400 B.P. (TH47-1, taken 34 cm below surface) for the sample from GH3. The deposition of the sediments holding the archaeological level 2 assemblage occurred after the deposition of the lower eolian stratum, while the level 1 assemblage postdates the 6.700 ± 400 B.P. sedimentary event.

7.2.3 Spatial Distribution

Artefact density per square metre varies greatly between levels 1 and 2; while archaeological level 2 artefacts were found scattered across nearly every square metre excavated, level 1 artefacts are confined to squares A2, B1 and B2. Post-depositional erosion of the upper GH's across the western squares from the excavation area greatly affected the spatial distribution of the two occupational events. GH 3, which served as a clear hiatus between the two archaeological occupations in squares A and B, was destroyed by later erosional events in the remaining squares. GH1 and GH2 appeared to be convoluted into one horizon. The further westwards excavations proceeded, the less sediments were left

to excavate given that the bedrock was slightly more elevated in this area. In squares E and F only GH4 could be securely identified below a 10 cm mixed horizon. Within the mixed GH, artefacts that at some point were clearly embedded within GH4 have been excavated; refits of a core fragment found in GH 4 and the mixed horizon above confirm this (Figure 7.30). Nonetheless, artefacts excavated from this upper horizon have been excluded from the analysis, given the insecurity regarding their original position within the previously described sedimentary succession.

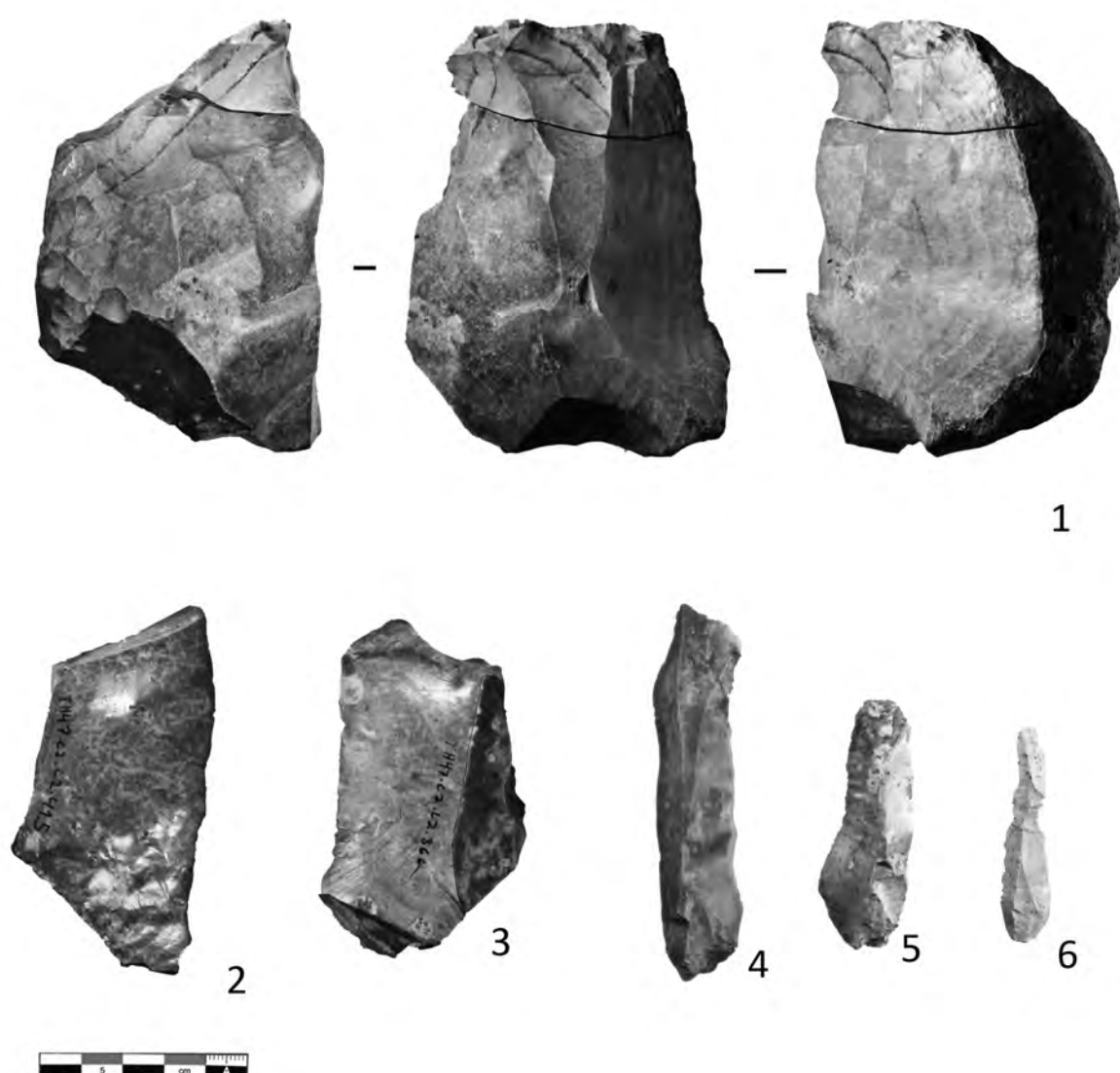


Figure 7.30 Artefacts from Ghazal.

The core depicted above has been reconstructed using a fragment from level 2 and a fragment from the surface. (Photograph by Y. Hilbert).

Distribution per square metre of level 2 artefacts show that the highest density clusters around square D2, E2 and F2; a smaller concentration is observed in the north eastern corner of the excavated area at square B1. The artefact distributions are confined to a small area and have yielded several refits (n=27), showing some degree of scattering (Figure 7.31). Archaeological level 1 is constrained to the eastern corner of the excavated area, precisely around square B2, with some dispersion into squares A2 and B1 situated below the roof of the shelter.

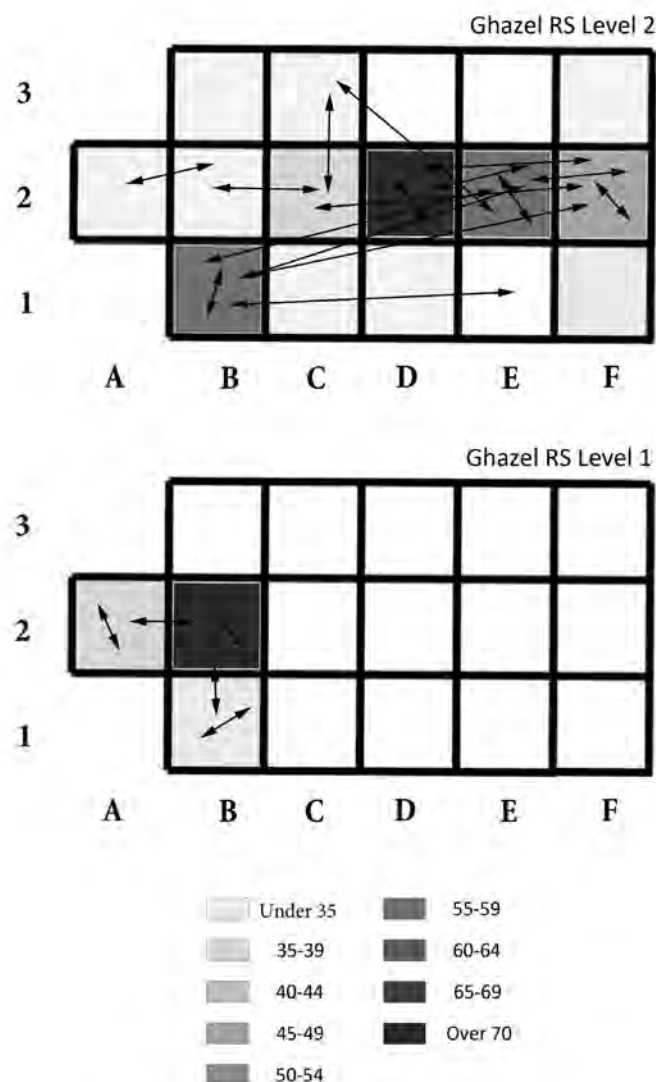


Figure 7.31 Distribution of artefacts per square meter.

The arrows between the different squares indicate the approximate position of the refitted artefacts from each level (Image by Y. Hilbert).

Given the low energy deposition of the sediment holding the artificial inclusions at Ghazal Rockshelter, a total of 34 refits have been made. Fortunately, no intra level refits have been made, attesting the site's archaeological level integrity.

7.2.4 The assemblage

The lithic assemblage from Ghazal Rockshelter is composed of 425 artefacts pertaining to two distinctive levels separated by a sterile sand layer. No raw material differences were observed between the two levels. Artefacts are made from fist sized chert nodules and larger chunks, measuring up to 20 cm in maximum diameter, that outcrop from the *Gahit member*.

Although coming from the same geological formation, chert nodules presented some variability in regard to the difference in inclusions observed within the grey silicified matrix of the raw material and varying thickness of cortex. The differences in cortex thickness and texture are attributed to taphonomic processes afflicting the nodules within their geological context. The chert used at the site is very homogenous; no *Aybut member* chert, so common within the Khumseen assemblage, has been identified. The variability observed between nodules of the same type aided the refitting analysis given that raw material groups could be established.

7.2.5 Level 2

A total of 304 artefacts were retrieved from level 2; 286 artefacts have been identified as *débitage*, also incorporated within the sample are fourteen cores and four tools (Table 7.3). The 32 chips, measuring less than 10 mm in maximum dimension, found within the assemblage, have been excluded from the formal analysis.

Table 7.3 Artefacts from Ghazal Level 2.

	TOTAL n	%
<i>Flakes</i>	82	27
<i>Blades</i>	57	19
<i>Bladelets</i>	20	7
<i>C. Flakes</i>	47	15
<i>C. Blades</i>	16	5
<i>D. Flakes</i>	8	3
<i>D. Blades</i>	18	6
<i>Chips</i>	35	10
<i>Burin Spalls</i>	3	1
<i>Cores</i>	14	4
<i>Tools</i>	4	1
TOTAL	304	100

7.2.5.1 Débitage

Leptolithic *débitage* (blades, bladelets, *débordant* blade and primary blades) make up a fair amount of the *débitage* assemblage (n=111). Also relatively high is the amount of cortical pieces (primary elements); 63 pieces have over 50% dorsal cortical cover. This suggests that raw material nodules were carried to the site in an unaltered form. The core to *débitage* ratio of c.a. 1:20 indicates a balanced amount of *débitage* and cores. Considering the limitations of dealing with subsurface archaeological remains in regard to the completeness of the sample, intra artefact type comparisons such as ratios and expected amount of created *débitage* per reduced core must remain tentative and viewed as partial. The *débordant* blade to blade ratio of c.a. 1: 3 suggests that these pieces played a consistent roll in core convexity maintenance.

Specific *débitage*, related rather to volume transformation as opposed to volume creation, have been found within the assemblage of level 2; three bladelets have been identified as burin spalls, related to the production of this specific tool type.

Artefacts have been found in nearly pristine condition, edge damage was minimal across the sample; no artefacts showing medium or heavy edge damage were observed. Artefacts consistently show a white patina, likely caused by chemical weathering within the sediments. Blank fragmentation, however, has been observed across all *débitage* types. Bladelets were highly fragmented, only eight specimens (40%) were complete. This fact is possibly related to the slender and fragile character of this blank type. Flakes, which are thicker and more robust, are far less fragmented; 71% of all flakes have been found to be complete (n=58); 5% (n=4) showed minimal fracturing and, therefore, have been deemed incomplete. Nonetheless, full measurements could be obtained deeming the variation between the complete object and the incomplete ones within the range of measurement variability between two researchers measuring the same object. Blades are slightly more fragmented than flakes; 63% (n= 36) were complete and 9% (n=5) incomplete. *Débordant* blades show the smallest amount of breakage, considering that these pieces are thicker and heavier than other non-cortical *débitage* this poses no surprise. In total 78% (n=14) pieces have been found to be complete (Figure 7.32).

Cortical *débitage*, both flakes and blades, showed a higher percentage of pieces with 76% to 100%, totalling 56% (n= 35), as opposed to pieces with 51% to 75%, which encompasses 44% (n=27). Non-cortical *débitage* was, to a greater extent, completely free of cortex.

Flakes, blades and bladelets with 0% to 10 % of cortical cover, respectively 49% (n=39), 73% (n=41) and 100% (n=20), were observed in higher percentages than pieces with 11% to 25% or 26% to 50%. In contrast, *débordant* blades show elevated values in regard to this aspect; of the twenty pieces identified, a total of twelve (67%) presented cortical value between 26% to 50%. This indicates that once the exploited core's working surface had been freed of cortex, recurrent reduction of blades, bladelets and, to a certain extent, flakes took place and was interceded by *débordant* removals from the core's working surface peripheries.

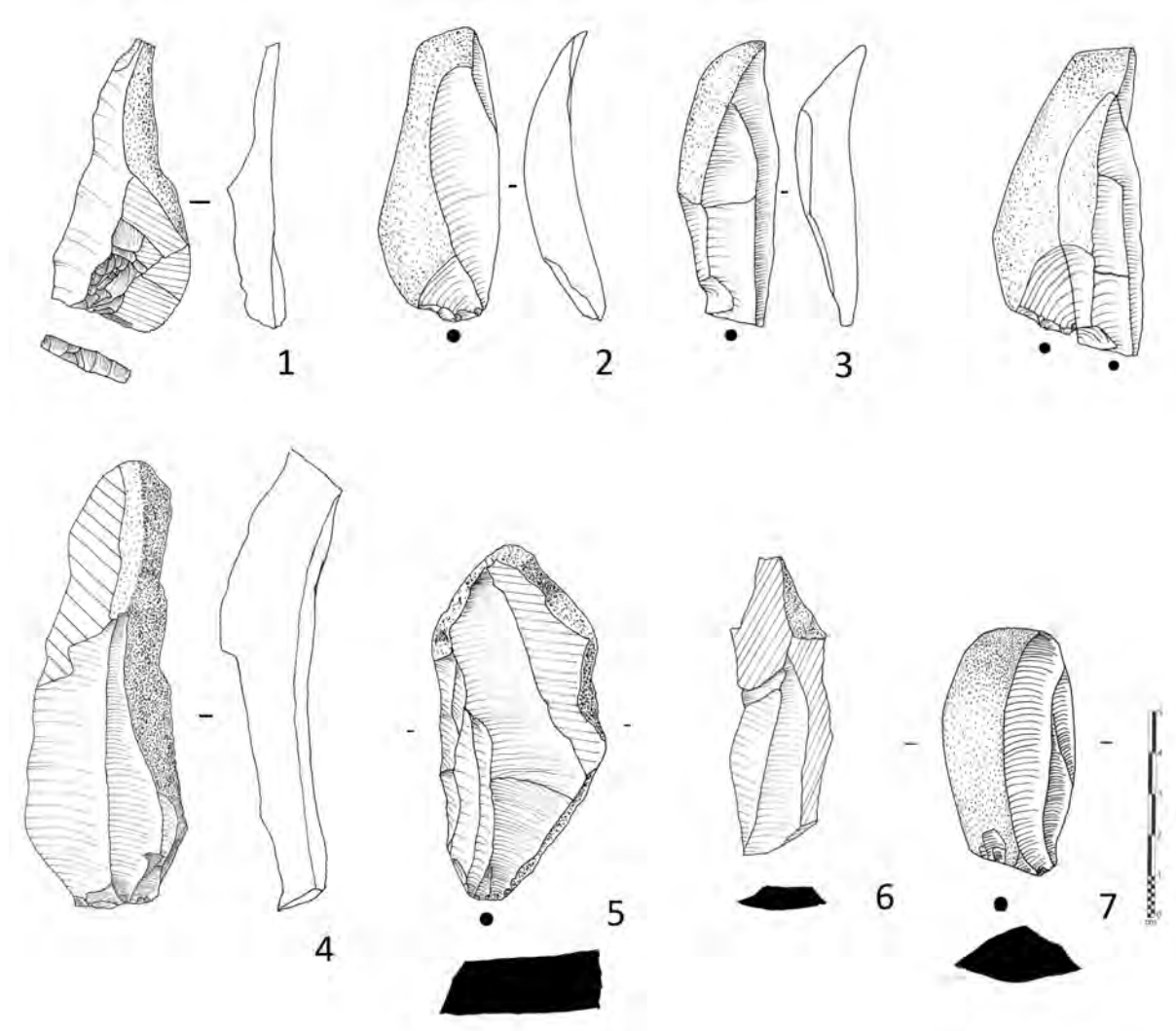


Figure 7.32 Ghazal *débordant* débitage Level 2.

1, *débordant* with unidirectional crested scar pattern; 2 and 3, refitted *débordant* blades; 4 to 5, *débordant* blades (Illustrations by Y. Hilbert).

Striking platforms on blades, flakes, *débordant* blades and bladelets showed mostly simple configurations. Plain striking platforms were observed more often than any other platform configuration: 61% (n=39) of the blades, 79% of the flakes (n=37), 73% (n=11) of the *débordant* blades and 59% (n=7) of the bladelets had this particular configuration.

Flakes have the greatest variability with 6% dihedral (n=4), 2% transverse (n=1) and 2% faceted (n=1) platforms. The occurrence of these types of striking platforms within this assemblage is not related to core striking platform curation manners, as

will be seen later. Blades show less variability than flakes; one blank with dihedral and two with transverse striking platforms have been observed. Two *débordant* blades show cortical striking platforms, indicating the early set up of a core's working surface.

While platform lipping was completely absent from the assemblage, striking platform abrasion was observed on 21% (n=38) of the available *débitage*; 5% of the *débitage* had consistent and extensive platform abrasion. This pattern was observed on six blades and two flakes.

Flake, blade and *débordant* blade midpoint cross-sections showed an expected range of variability, or lack thereof. Blades had, to a larger extent, triangular or trapezoidal cross-sections: respectively, 40% (n=23) and 46% (n=26) of the analysed specimens have such cross-sections.

Débordant blades had 22% (n=4) triangular, 28% (n=5) lateralized and 33% (n=6) trapezoidal cross-sections. Flakes showed the highest amount of variability in respect to this feature; triangular, lateralized, and trapezoidal and three vectored cross-sections have been observed in similar amounts on 85% of the specimens (in total n=68). Flat, rectangular and convex cross-sections were observed on the 15% remaining flakes (n=12). The discrepancy between the cross-sections observed on the blade and flakes indicates that either diverging core working surface usages gave rise to these blanks, or that the flakes served different intentions within the existing reduction pattern. That is to say, flakes were used to remove irregularities from the core working surfaces.

The longitudinal blank cross-sections revealed significantly diverging patterns; while 50% (n=27) of the blades and 59% (n=46) of the flakes have generally straight profiles, flakes show the tendency toward incurvate profiles; 31% of the flakes have this pattern (n=24). Blades, on the other hand, exhibit 30% of twisted profiles (n=16), indicating different reduction gestures for the manufacture of blades and flakes. *Débordant* blades are 82% incurvate in profile (n=14), indicating that their reduction took place from the core's lateral working surface situated in the raw material's peripheries parallel to the

cores technological axis. As will be demonstrated in refit #5, the exploitation of lateral supplementary working surfaces on the core served both the curation of the core and the expansion of used volume surface on the core itself.

Débordant blades showed, therefore, a high percentage of pieces with overpassed terminations, 53% (n=9); indicating that exceeding force and unsuitable core convexities dictated the removal of these pieces. Blades and flakes presented mostly feathered terminations: 82% of the blades and 63% of the flakes correspond to that pattern (n=41 and n=46). Flakes also showed 26% of hinged (n=19) and 11% of overpassed (n=8) terminations. Reduction of flakes must have therefore taken place when core's working surface convexity was suboptimal.

Blanks were, to a greater part, removed in correspondence with the technological axis observed on their dorsal scar pattern. A great portion of the blades, flakes and *débordant* blades were removed on axis; respectively, 58% (n=33), 48% (n=38) and 44% (n=8) of the three main *débitage* classes correspond to that pattern.

Blade and flake shape are marked by two diverging patterns (Figure 7.33), while blades and bladelets show to 34% and 50% parallel (n=17 and n=9) and 42% and 50% convergent (n=21 and n=9) edges. The majority of flakes have expanding edges, 27% (n=20) of the analysed specimens. Flakes have 17% of parallel (n=13), 16% of converging (n=12), 16% of ovoid (n=12), and of 23% irregular edges (n=17). *Débordant* blades are, to a greater part, lateralized in shape and have cortical backs.

Blank dorsal scar pattern analysis revealed some variability as to the flake scar patterns, while blades, *débordant* blades and bladelets exhibited relatively uniform results. Flakes have mostly simple unidirectional scar patterns. These pieces have also, unidirectional crossed, parallel and convergent scar patterns: respectively, these patterns were seen on 12%, 10% and 14% (n=10, n=8 and n=11). A small number of flakes had scar patterns inconsistent with a simple unidirectional reduction pattern; two flakes had radial, one flake opposed and another two transverse scar patterns.

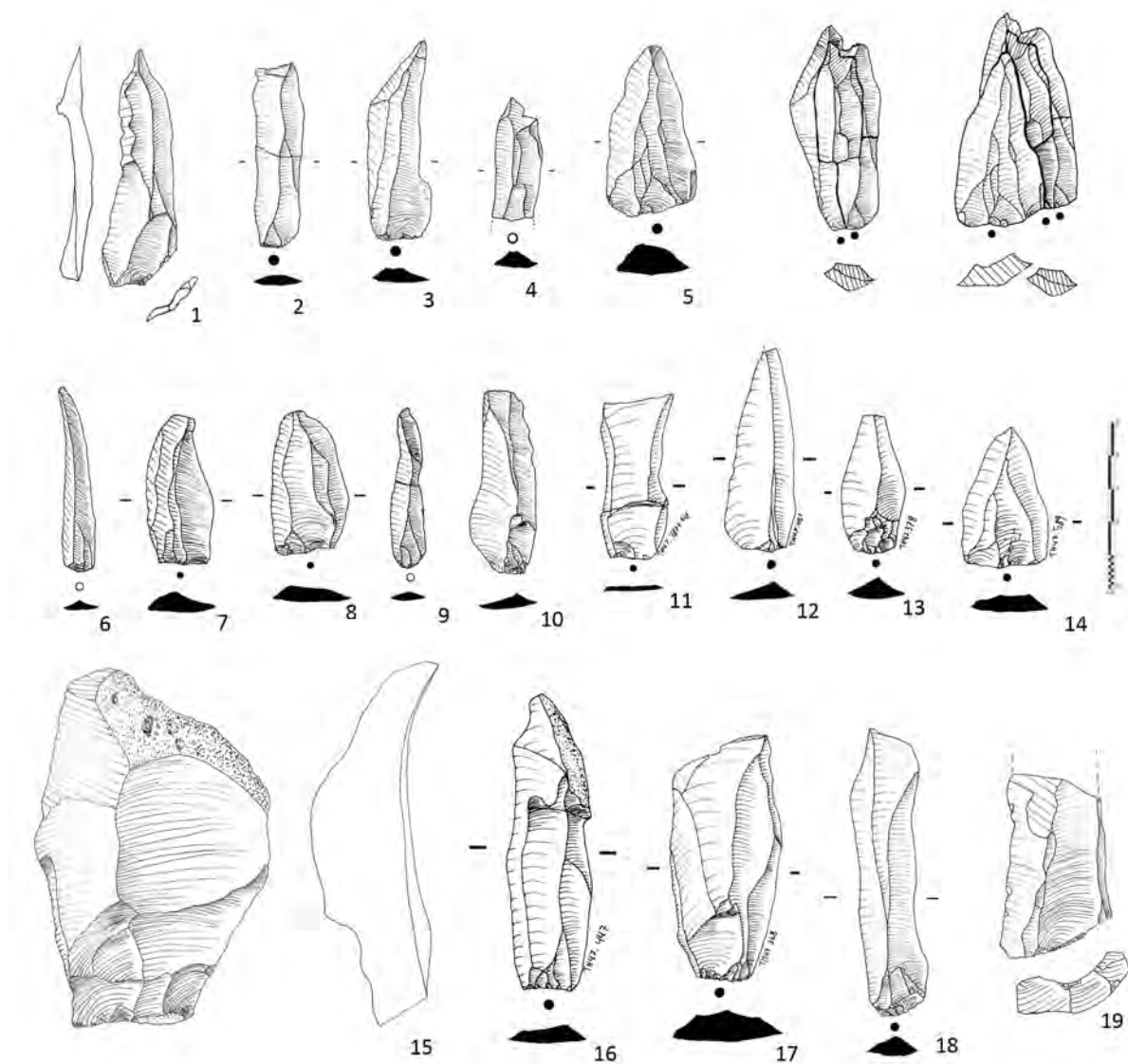


Figure 7.33 Ghazal débitage from Level 2.

1 and 19, blanks with faceted striking platform; 2 to 5 refitted blades and blade fragments; 6 and 9, bladelets; 7, 8, 10 and 11 blades with unidirectional scar pattern; 12 to 14; blades with convergent edges; 15 flake; 16 to 18, blades. (Illustrations by Y. Hilbert)

Blades and *débordant* blades exhibit 51% and 72% unidirectional (n=29 and n=13) scar patterns; to a smaller extent unidirectional crossed, with 7% and 11% (n=4 and n=2), and parallel, with 9% and 6% (n=5 and n=1), scar patterns.

Blades have 31% (n=18) with convergent scar patterns, a relatively high percent when compared to the *débordant* blades; only 11% (n=2) presented this particular pattern. One blade has bidirectional scars on its dorsal surface.

Metrical analysis of the Ghazal Rockshelter level 2 *débitage* assemblage revealed three important patterns that led to the classification of the technologies used during the Early Holocene of Dhofar. These are: (a) the manifestation of blade production by means of a unidirectional parallel reduction modality; (b) the evident metrical divergence between these very same lamellar products from the *débordant* elements with blade proportions; and, (c) the divergence between the flakes and blades beyond the simple elongation indices. Granted, the sample is not as robust as one might wish, however, variability, or the lack thereof, within the *débitage* categories are consistent and, therefore, representative for the inventory discussed here.

Débitage dimensions are dictated by two agents; first, the dimensions of the raw material used to produce both the by-products and the actual desired blanks and, second, the culturally inherited constraints to the technology used. The later is dominant over the earlier and, therefore, is comprehensible through the analysis done here.

Flakes have a wide range in length; pieces measure on average 41,41 mm but show a relatively high standard deviation (s.d. 18,82). Blades and bladelets show less variability (s.d. 14,69 and 10,54), averaging respectively 57,22mm and 32,14mm in length. *Débordant* blades are on average larger than blades (75,17mm) and show relatively high variability (s.d. 19,22). Cortical elements are, as expected, longer than non cortical *débitage*; cortical elements with blade proportions are on average 69,96 mm, while flake proportioned cortical elements have an average length of 59,66 mm. Flake widths is highly variable (s.d. 16,29), in average flakes measure 34,86 mm in midpoint widths. Blades and bladelets, artefact classes characterized by their constrained width dimensions, have proven to be less variable (s.d. 6,5 and 2,25), averaging respectively 18,77 mm and 8,42 mm. Following the pattern observed on the *débordant* blades, mean width for this category is larger than that of the blades (31,93 mm) and has proven to be more variable as well (s.d. 9,47). *Débordant* blades have the highest average thickness and the highest variability among the non-cortical *débitage* (s.d. 7,81 and avg. 14,86mm). Blades and bladelets show little

variability in that respect (respectively, s.d. 2,91 avg. 6,17 mm and s.d. 0,89 avg. 2,38 mm).

Striking platform proportions, as illustrated by the IPF, are relatively uniform for the Ghazal Rockshelter *débitage*, generally being wider than thick. If regarded in conjunction with the respective dorsal volume for each of the *débitage* categories, some variability may be seen. The RPS index for both blades and *débordant* blades, for instance, has the highest average values for the non-cortical *débitage* (respectively, avg. 18,33 and 19,45). Blades were slightly more variable than *débordant* blades (respectively, s.d. 15,09 and 14,41). These values indicate that platforms are relatively small in comparison to the dorsal surface of the blanks. Flakes have lower values (avg. 13,28) with a comparable standard deviation to those of the *débordant* blades (s.d. 14,53). That is, flakes have smaller dorsal surfaces in respect to their striking platforms.

Blank length/width proportions, illustrated by the IOE, are used to differentiate the leptolithic *débitage* from one another. Blades, although diminutive in length, are on average three times as long as they are wide (avg. 3,03), bladelets have even higher IOE values (4,35). *Débordant* blades are characterized by shorter dimensions (avg. 2,63), and low variability (s.d. 0,53). Ghazal Rockshelter level 2 flakes are, as for most assemblages described here, of truncated dimension, averaging IOE of 1,29 and low variability (s.d. 0,36).

7.2.5.2 Cores

Fourteen pieces have been identified as cores; one core preform has been excluded from the description of the analysis. Only two cortical flakes have been removed from the frontal surface of this core, these removals were parallel to each other and removed from a flat surface made up of a natural fracture. The remaining thirteen cores have been reduced using single platform unidirectional technology; three single platform convergent, seven unidirectional parallel and three two unopposed platform cores have been identified. Although small, the core assemblage is consistent with the overall pattern of the *débitage*.

In fact, eight of these thirteen cores have been partly reconstructed through refits.

The three unidirectional convergent cores share similar technological features, while their morphology shows some variability but well within the range of this core type. Striking platforms are plain; mostly natural fracture surfaces have been used as striking platforms, while one possessed a plain striking platform created by the removal of a single blow that detached a cortical flake from the top portion of a elongated chert block. All three cores were abandoned due to faulty convexities. Two had suffered overshoot removals on their working surface, while one was abandoned because the working surface had become too short for further reduction. This third piece (Figure 7.34), presented a relatively wide working surface from which bladelets had been removed; the core's working surface still retained some of its longitudinal convexity and would have possibly sustained a few additional removals. The remaining two pieces were rather elongated, one showed removals on its frontal face, while the other was removed from a convex working surface that extended from its narrow to its frontal face. This latter one exhibited a horizontally convex working surface. All three pieces presented a single plane of removal from which blanks had been detached. Unidirectional convergent cores were heavy in comparison to other core types (286g, 303g and 298g).

The seven unidirectional parallel cores have been only partially freed from cortex, showing either *51% to 75%* or *75% to 100%* of cortical cover. The main working surface, freed from cortex, was positioned either on the frontal face of a chert nodule, or, in some cases, an additional lateral portion of the raw material was exploited from the same platform as the main working surface. The platforms were straight, in some cases a natural fracture on the raw material nodule was used and in some a blow that removed the nodule's cap, creating the striking platform. While unidirectional convergent cores have wide core working surfaces, unidirectional parallel cores had elongated rectangular planes of removal. On average, these cores were 72,09 mm long, 63,37 mm wide and 42,93 mm thick, most of them being severely exploited and abandoned due to faulty longitudinal

convexities (Figure 7.35).

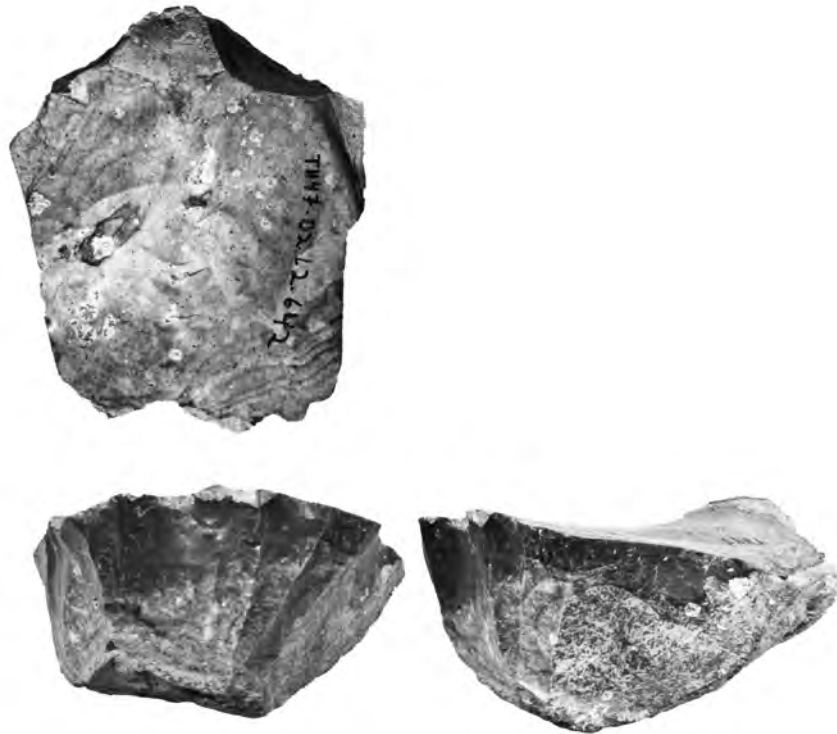


Figure 7.34 Ghazal convergent core from Level 2.
(Photograph by Y. Hilbert),

The three two unopposed platform cores had been partially freed from cortex; amounts arranged between 51% and 75%. The two non-opposing striking platforms were created by a single blow or reduction took place from an equally suitable neocortex surface on the chunk of raw material. The two non- intersecting platforms were placed perpendicular to each other on the core's frontal and lateral faces; in one case the two platforms were placed opposite to each other on the raw material blocks front and back. These working surfaces are, for the greater part, covered by hinge fractures, making any further removal, without proper maintenance, difficult. The core's planes of removal were likely reduced sequentially, each plane reduced at a time. Two unopposed platform cores varied greatly in size and shape, weighing 63g, 154g and 466g.

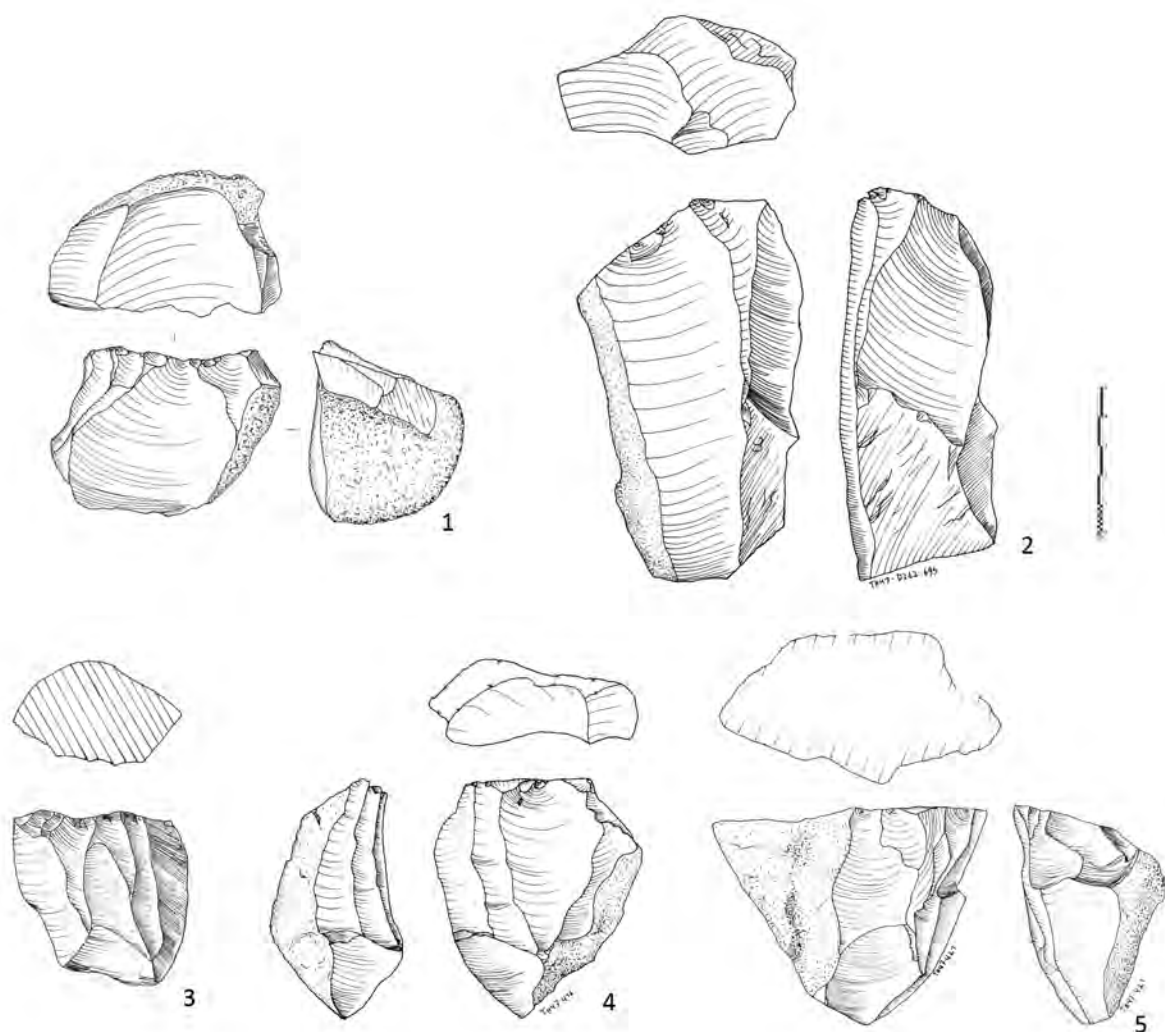


Figure 7.35 Ghazal cores from Level 2.

1 and 2 Unidirectional parallel with two unopposed work surfaces; 3 and 5 Unidirectional core with convex work surface; 4 Unidirectional parallel core with frontal and lateral work surface. (Illustrations by Y. Hilbert)

7.2.5.3 Tools

Unfortunately, the tool assemblage of Ghazal level 2 is very small; it consists of one endscraper, one piercer, one burin and a hammerstone. A 289g round chert nodule was used as a hammerstone (Figure 7.36 and 7.37); the piece had active impact scars on opposite ends. Both the endscraper and the burin had been made on lamellar products. The endscraper was retouched on its distal portion, which was covered by cortex prior to the removals; the retouch is double rowed and forms a steep working surface. The burin

was made on a blade totally freed from cortex. The burin blow was on the distal portion of the blade and administered on a snap. Additionally, three burin spalls were retrieved that indicate the active production of this tool type on site.

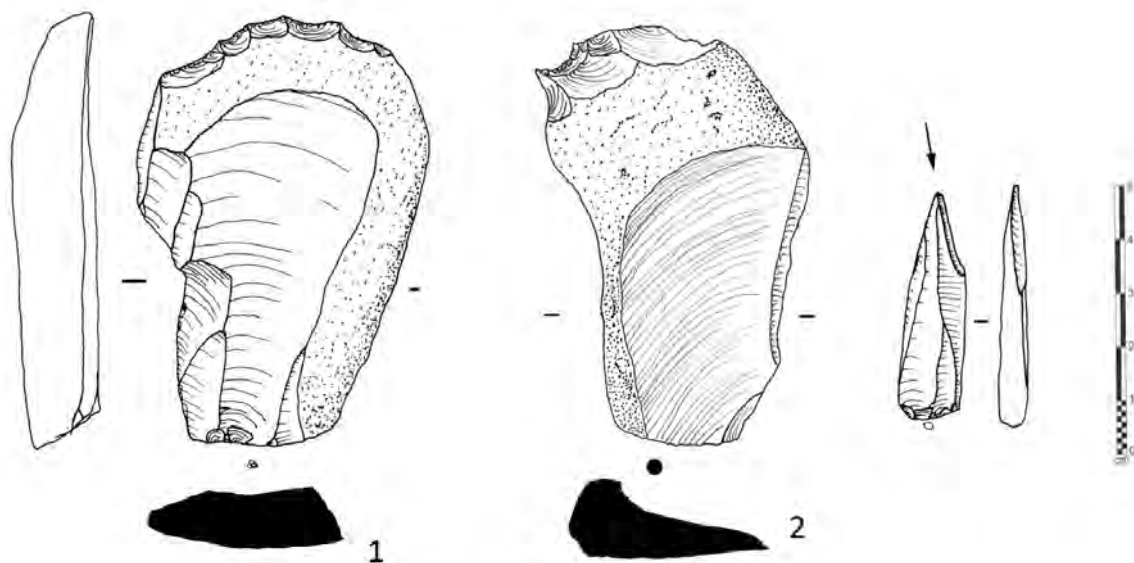


Figure 7.36 Ghazal tools from Level 2. 1, endscraper; 2, piercer; 3 burin on snap (Illustrations by Y. Hilbert).



Figure 7.37 Hammerstone from Ghazal Level 2.
(Photograph by Y. Hilbert)

7.2.5.4 Level 2 refittings

Twenty seven refits and conjoins have been made using the combined tool, core and *débitage* assemblage from Ghazal Rockshelter level 2; eight of these involving *débitage* to core refits help to clarify the rhythm behind their reduction. To describe and illustrate all these constellations would be intensively time consuming and tedious for both the writer and the reader, therefore, only the more significant and nearly complete reconstructions will be described in detail. Refits # 2, #5, #19, #20 and #25 present impartial information on the reduction modalities used at the site during the 7.800 B.P. to 6.700 B.P. occupation.

Refit #2 depicts eight blanks reattached to their respective core. The core was reduced by means of unidirectional parallel removals, first using its short face on the distal end of the nodule; subsequently, the piece was turned and reduced on its frontal face (Figures 7.38 and 7.39). That is to say, the reduction on the first plane of removal did not intend to set up this core's platform, rather a maximization of raw material use may explain the change from one working surface to the next. The core's working surface exploited first became the striking platform from which the main face of the nodule was reduced.

The reconstruction described here will deal with the removals performed on the principal dorsal core's working surface. The flintknapper used the natural ridge on raw volume to remove a cortical blade from its frontal face; subsequently, reduction shifted to a lateral plane. One cortical flake was removed from that plane. Then, reduction concentrated on the plane created by the previous cortical blade removal. The core was turned sideways and reduction restarted, using the plane created earlier as a striking platform. The scars on the blank removed after shows that change of directionality. Reduction was unsuccessful at that point and blank production shifted back to the central technological axis. Two blades were struck; the first, a *débordant* blade, created the convexity and the latter, a slender blade, exploited it. Reduction continued using the same plain. A third blade was removed followed by the reduction of a large *débordant* blade that overshoot the core's

plane of removal. Reduction halted, although the core still had sufficient convexity.

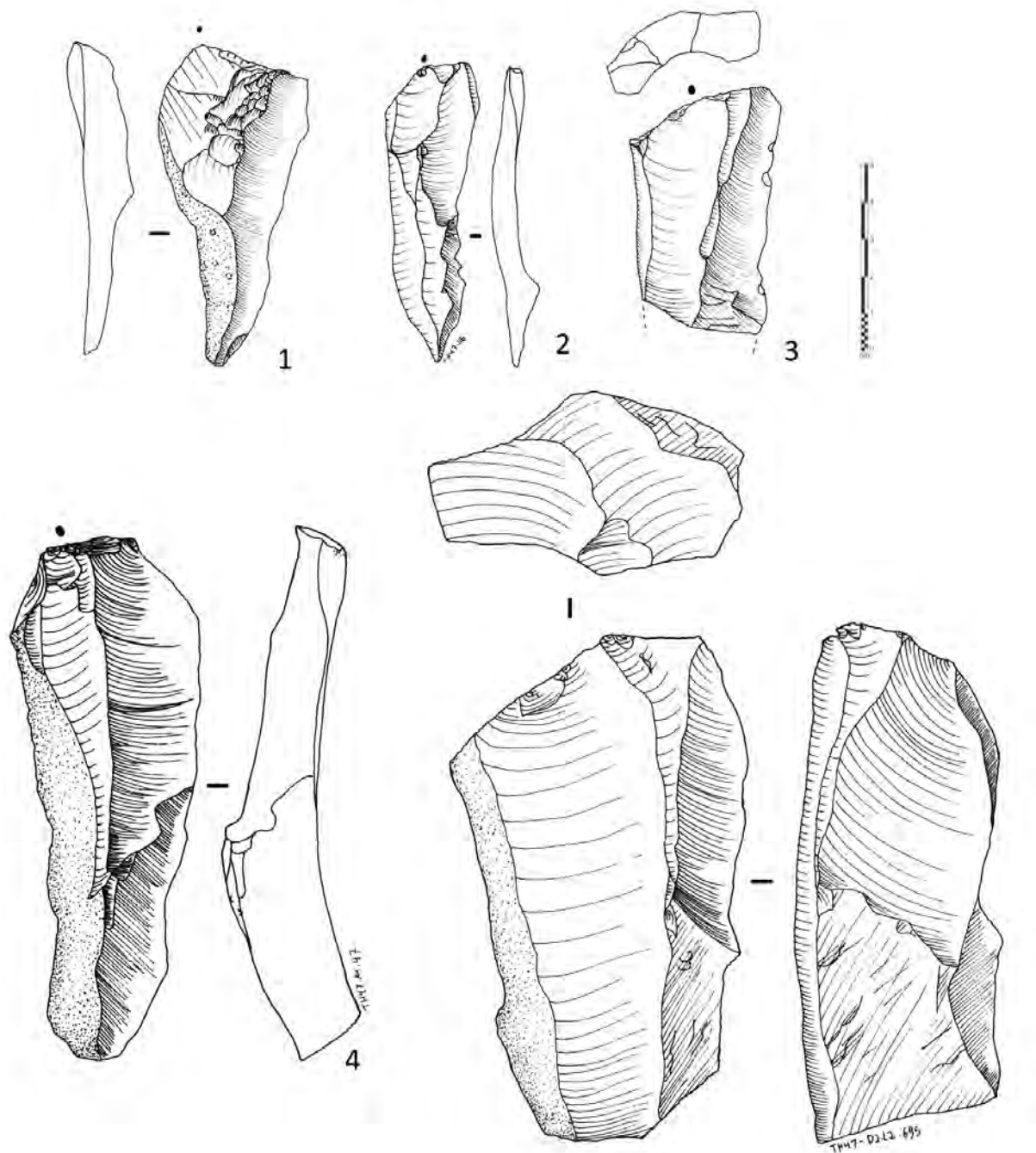


Figure 7.38 Ghazal level 2 refit #2 débitage.
(Illustrations by Y. Hilbert)

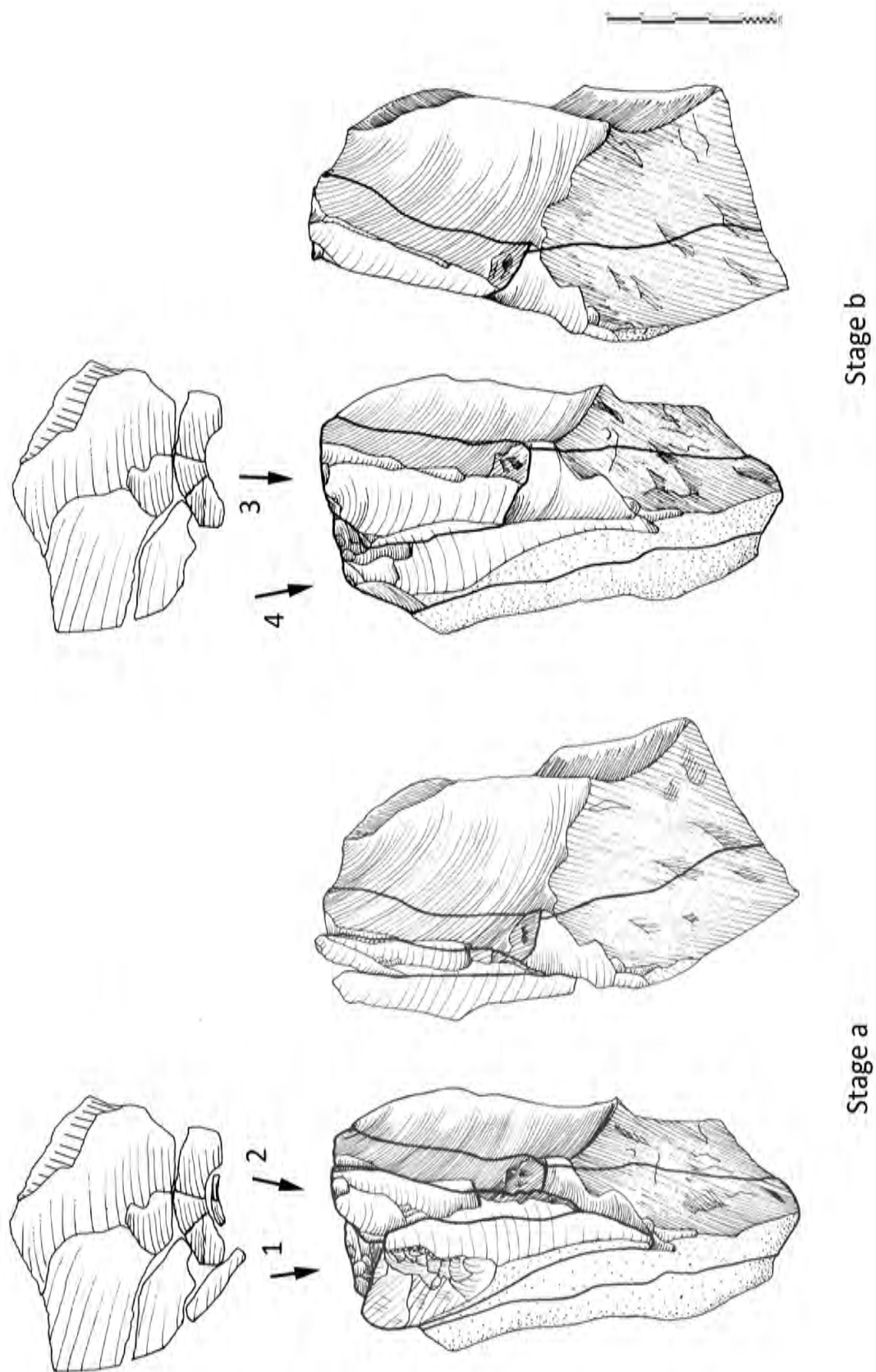


Figure 7.39 Ghazal level 2 refit #2. (Illustrations by Y. Hilbert)

Refit #5 depicts seven blanks reattached to a unidirectional parallel core with two working surfaces; one placed on the dorsal face of the core and the second, reduced from the same platform as the former, placed on the periphery of the nodule. The core's striking platform was created during an earlier stage of reduction, refits depicting this phase could not be established, however, the two negatives visible on the striking platform indicated that some effort was made in accomplishing that task. The possibility of a shift from an older plane of removal to the actual working surface reconstructed by the refit, as seen in refit #2, must also be entertained. Reduction started from the central plane and moved towards the narrow working surface, only to return to the central plane as soon as convexity was restored. The second plane of removal was used to remove three *débordant* elements of varying size; these reestablished the core's convexity on the frontal plain. Reduction shifted back to the main plane of removal from which a blade and a converging flake had been struck prior to the core abandonment (Figures 7.40 and 7.41).

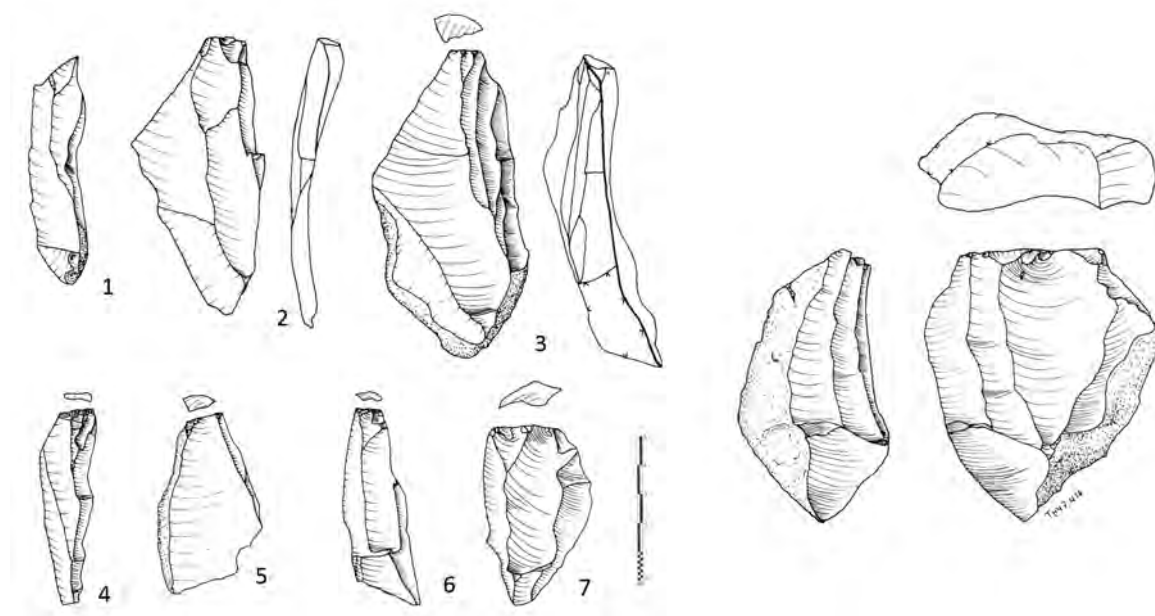


Figure 7.40 Ghazal level 2 refit #5 débitage.
(Illustrations by Y. Hilbert)

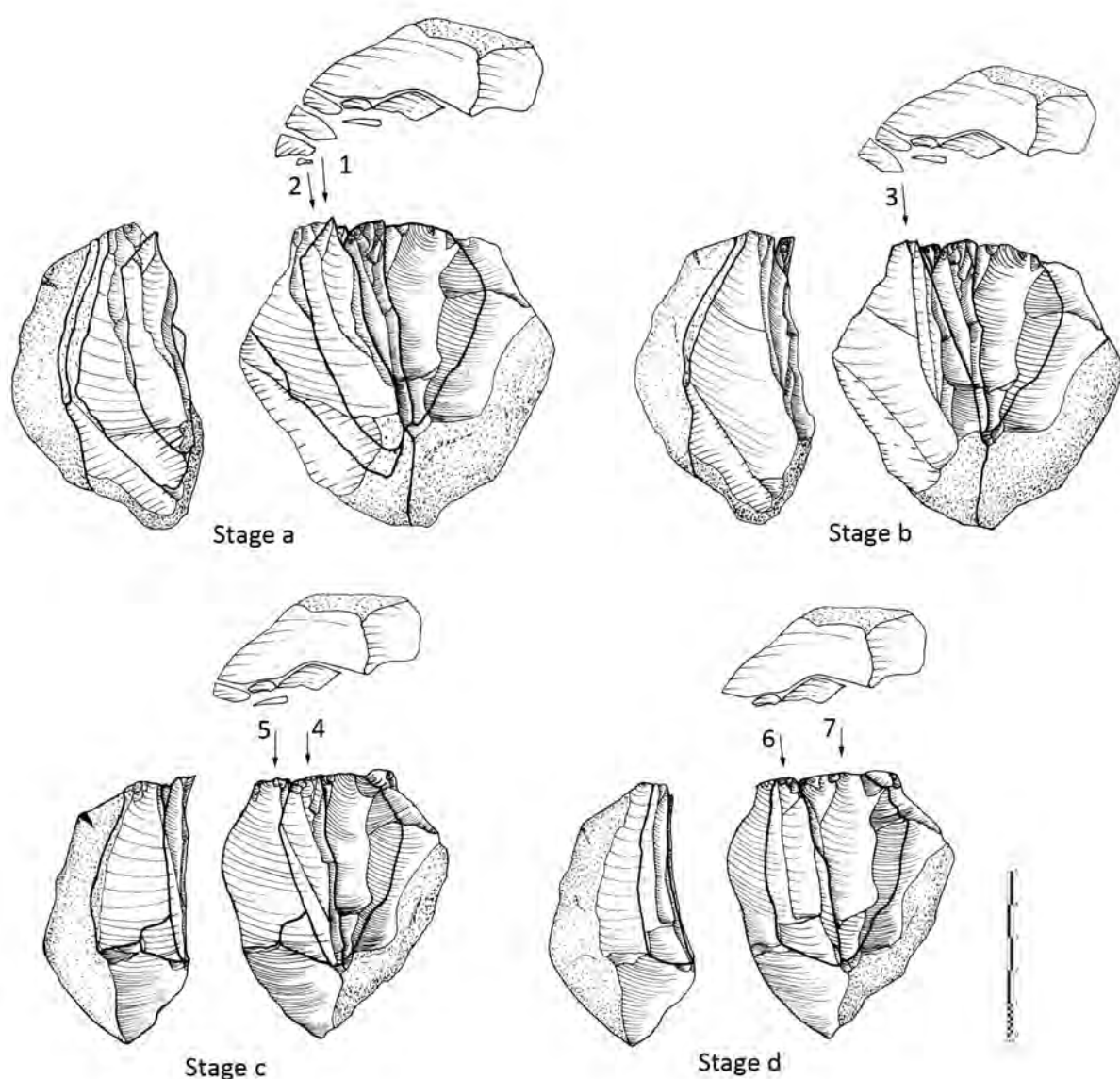


Figure 7.41 Ghazal level 2 refit #5.
(Illustrations by Y. Hilbert)

Given its completeness, refit #20 is of considerable importance to the reconstruction of the reduction modalities used at the site. Refit #20 depicts the shift from one core working surface to another (Figures 7.42 and 7.43). Three blanks were reattached to the two planes of removal on a unidirectional parallel core. During the first stage, the long and narrow portion of a core was reduced. Three consecutively struck flakes had been removed, using a plain striking platform created by a blow to the top portion of the nodule. Subsequently, reduction shifted back to the top portion of the nodule. At this point, the

elongated brick shape of the volume was being reduced from the former plane of removal, following the technological axis that created the striking platform earlier in the sequence. Three flakes were reattached, not to the core itself, but to the ventral surface of the last removal administered to the former plane of removal on the core. The combined dorsal scar pattern on these three refitted flakes, which had been removed starting from one end of the working surface and moved across to its opposite side, indicates that the core was subjected to at least two additional phases, mirroring that depicted in the illustration; one prior to the reduction displayed and one after.

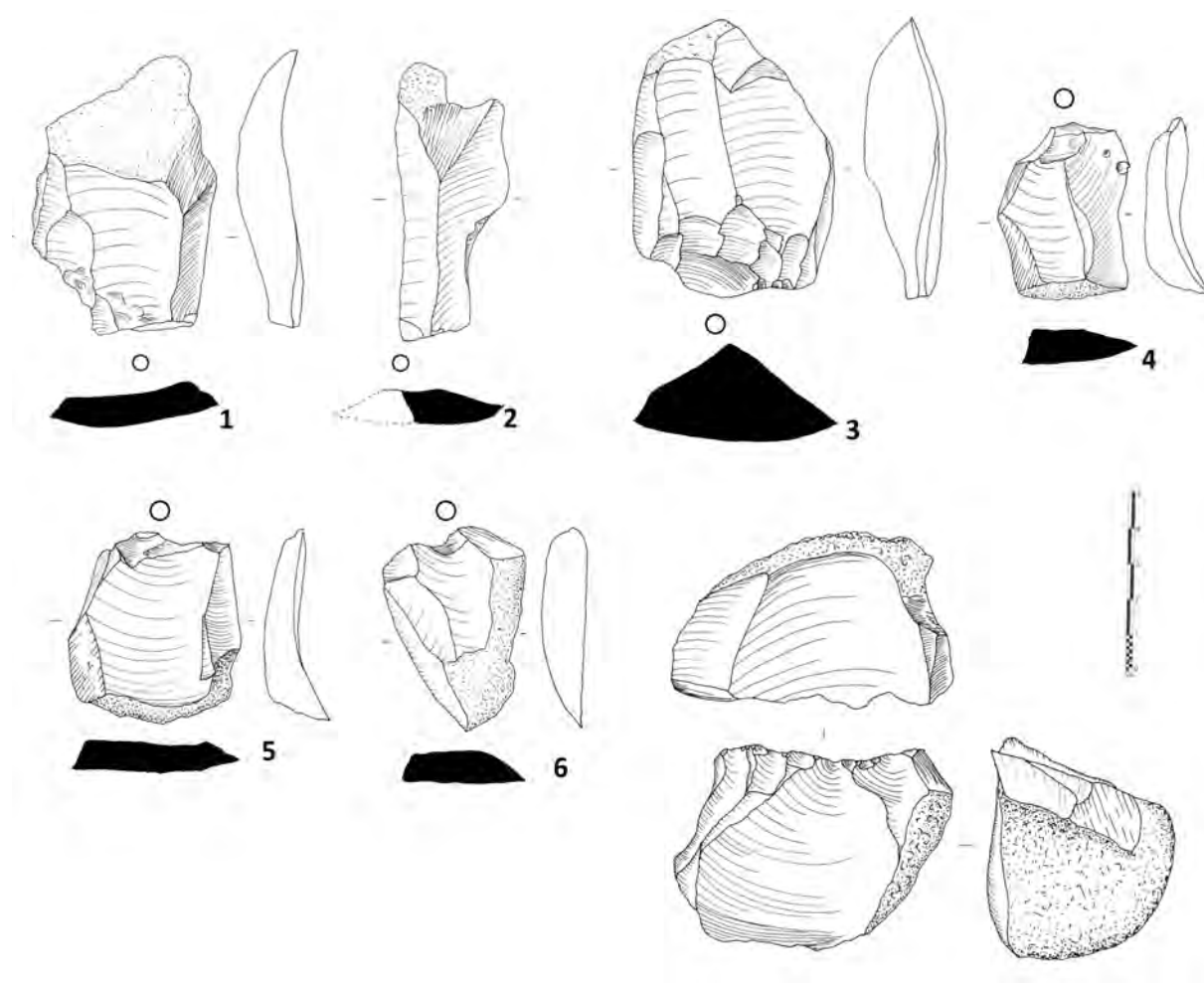


Figure 7.42 Ghazal level 2 refit #20 débitage.
(Illustrations by Y. Hilbert).

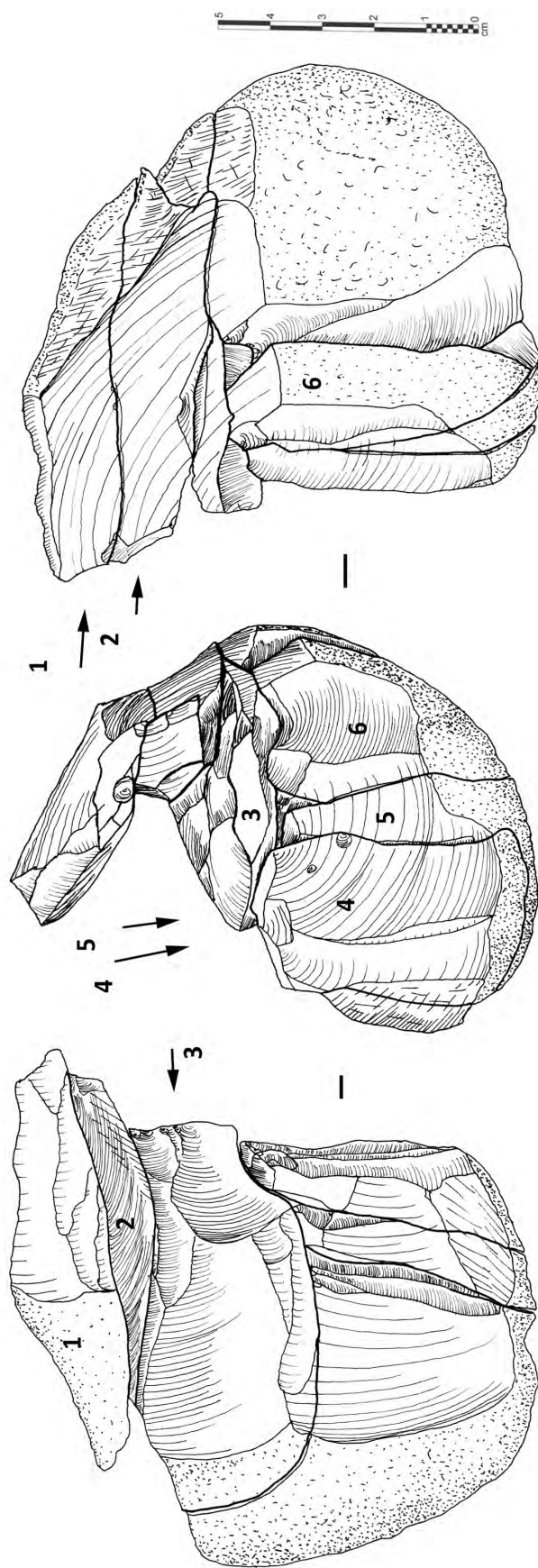


Figure 7.43 Ghazal level 2 refit #20. (Illustrations by Y. Hilbert)

Refit #25 depicts an alternative modality of blank production. A single platform unidirectional core was reduced from plain striking platform. The removals created a convex plane of removal across the core's main and supplementary working surfaces. The core's striking platform received no particular treatment; as a matter of fact, a natural fracture on the top part of the nodule served the intended purpose. A total of five blanks have been incorporated into this particular constellation (Figures 7.44 and 7.45).

Reduction commenced on the core's narrow edge from which the first large cortical removal was taken. The flintknapper attempted repeatedly to remove *débordant* blanks from the left periphery of the core; these attempts failed causing repeated hinging on that side of the core. Reduction then shifted towards the opposite side of the core, initiating a second plane of removal. Both *débordant* elements and blades were produced. The core was subsequently abandoned, given its spoiled convexity caused by overpassing and hinging.

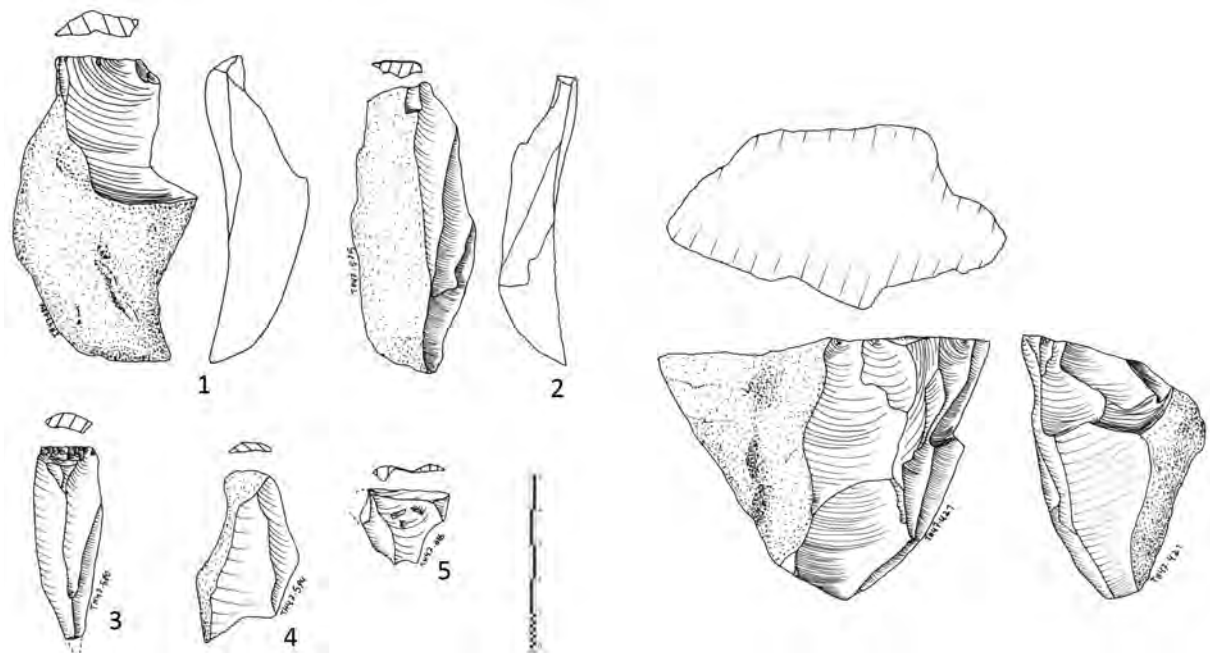


Figure 7.44 Ghazal level 2 refit #25 débitage.
(Illustrations by Y. Hilbert).

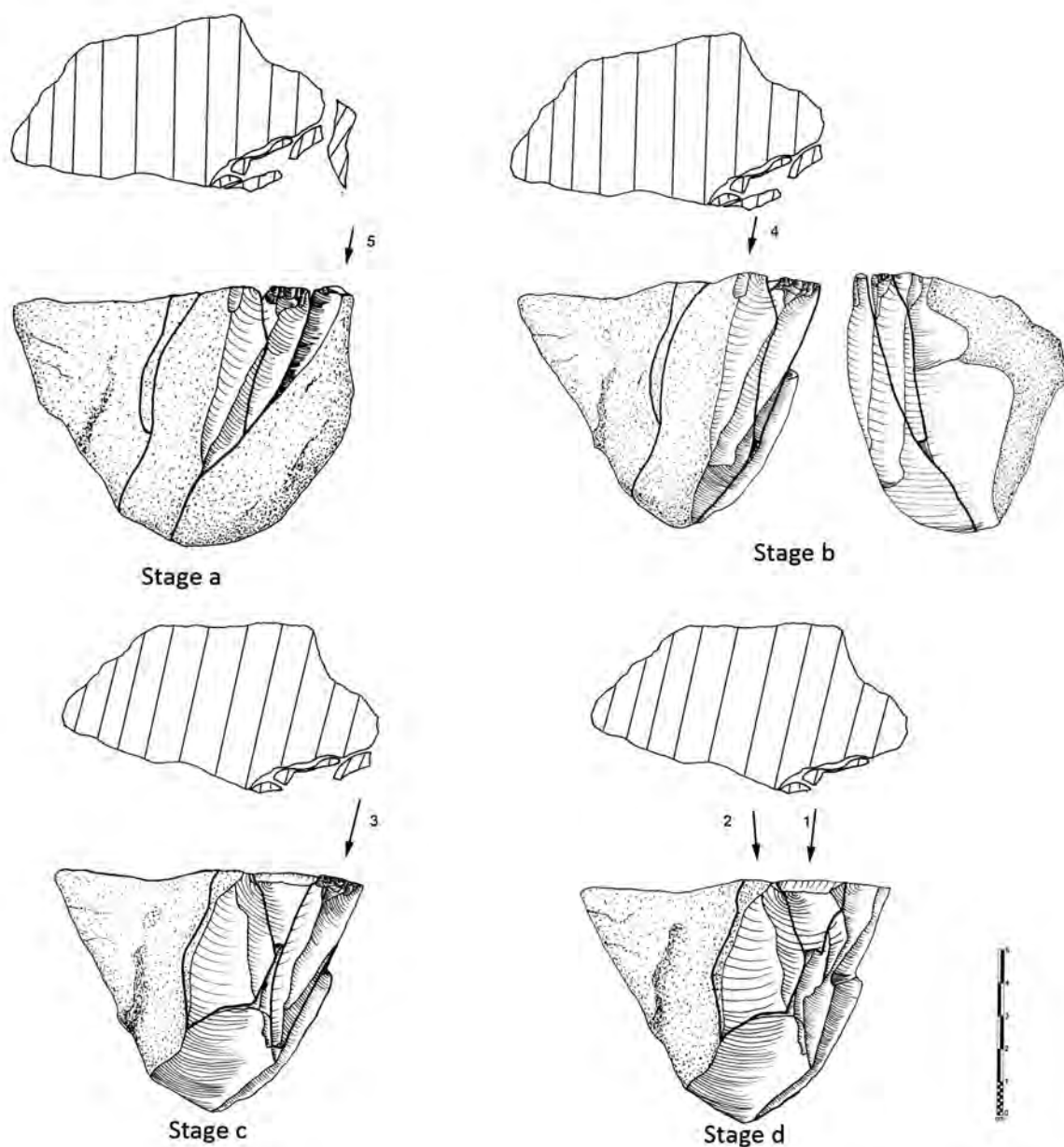


Figure 7.45 Ghazal level 2 refit #25.
(Illustrations by Y. Hilbert).

Refit #19 presents eight flakes and blades; all *débitage* incorporated into that constellation had convergent sides (Figures 7.46 and 7.47). Although the core pertaining to this constellation could not be found among the artefacts excavated from the sediments, the reduction pattern identified based on this refit gives some insights as to how the core's working surface might have looked and how it changed during its reduction.

Two diagnostic technological elements were identified based on the refit; (a) the use of overpassed *débordant* elements struck from either side of the core's working surface to produce a dihedral plane of removal; and (b) the recurrent production of elongated blanks with convergent sides, using the previously created convexity.

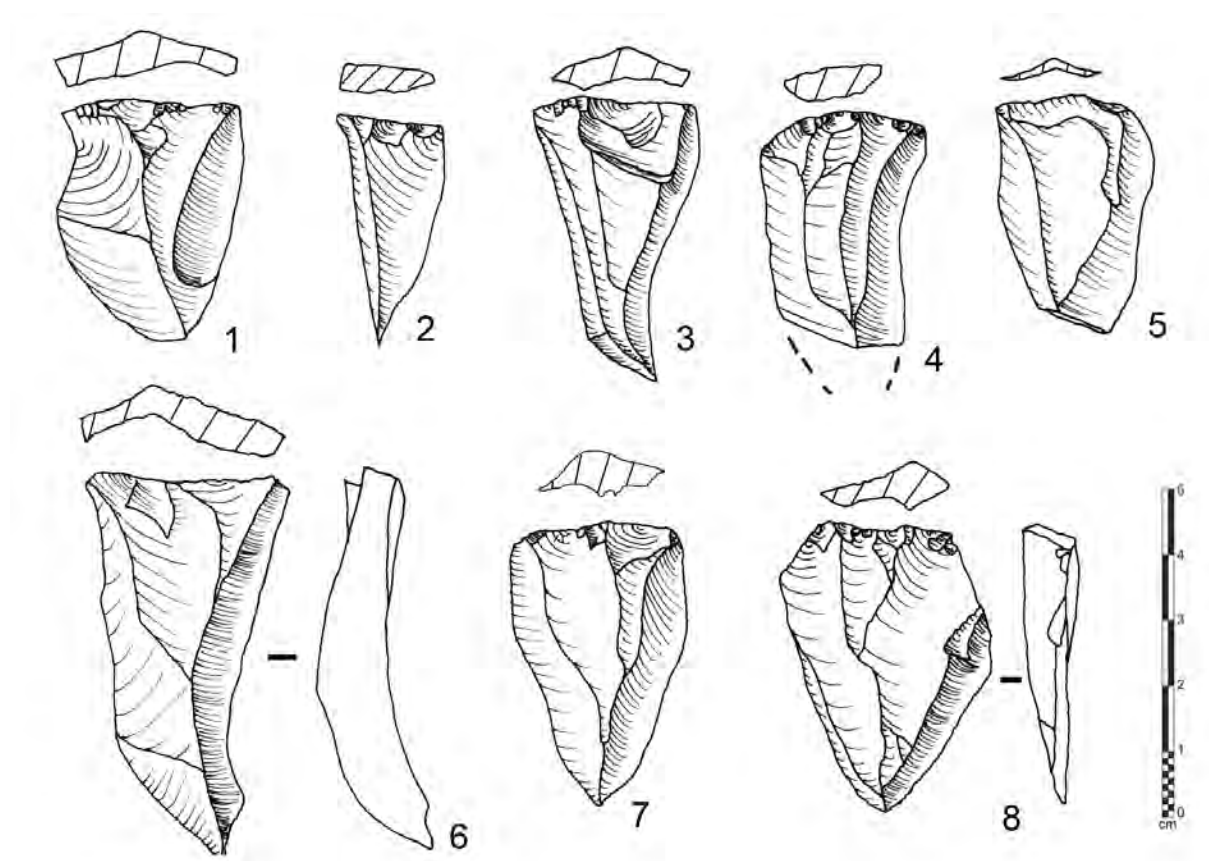


Figure 7.45 Ghazal level 2 refit #19 débitage.
(Illustrations by Y. Hilbert)

The striking platform from which the blanks were struck received no specific treatment; a natural fracture served the flintknapper's purposes without further modification. Following the creation of the horizontal and longitudinal convexities, a minimum of ten blanks was removed; six of these are shown in the illustration. After the convexity was exhausted, resetting of the core's working surface took place. This re-preparation resulted in increase in blank size and the narrowing of the blades. A consequence of this relative size growth was the reduction of the intervals between

blank production and core maintenance. The core's working surface would have changed considerably in morphology across the blank production process.

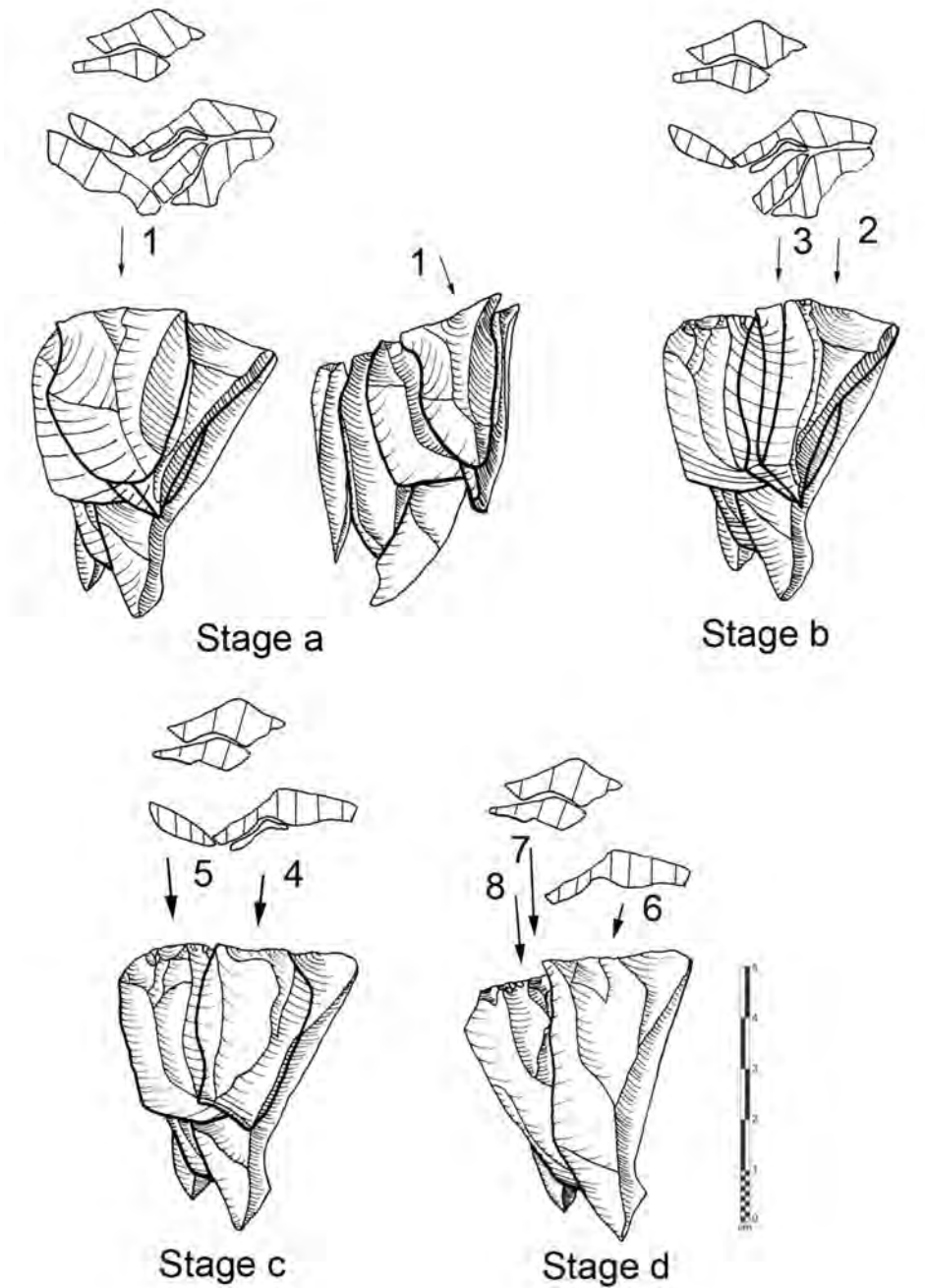


Figure 7.47 Ghazal level 2 refit #19.
(Illustrations by Y. Hilbert).

7.2.6 Level 1

A total of 121 artefacts have been retrieved from Ghazal Rockshelter level 1; seventeen have been identified as chips and will be excluded from the formal attribute analysis. Given the erosion of GH2 in the squares in front of the shelter, undisturbed level 1 material was only retrieved from the squares situated under the small shelter or behind the collapsed roof fall. Although the sample is far from robust, a total of 96 artefacts have been refitted into seven constellations (Table 7.4), four of these containing the cores from which the *débitage* was spawned. Given the completeness of the sample in that respect, core to *débitage* and cortical to non-cortical *débitage* ratios are representative for the linear production of leptolithic *débitage* for the time period postdating the 6.700 ± 400 BP sedimentary event.

Table 7.4 Artefacts from Ghazal Level 1

	TOTAL n	%
<i>Flakes</i>	23	19
<i>Blades</i>	28	23
<i>Bladelets</i>	9	8
<i>C. Flakes</i>	18	15
<i>C. Blades</i>	7	6
<i>D. Flakes</i>	5	4
<i>D. Blades</i>	9	7
<i>Crested blade</i>	1	1
<i>Cores</i>	4	3
<i>Chips</i>	17	14
<i>TOTAL</i>	121	100

The 1:25 core to *débitage* ratio is consistent with the pattern revealed by the refittings. The cortical to non-cortical ratio of 1:3 and the refittings indicate that all phases of core reduction took place at the site. The leptolithic character of the sample is expressed in the high percentage of blade-proportioned *débitage*; blades, bladelets, cortical blades and *débordant* blades make up 54% of the *débitage* (n=54). One blade, with typological characteristics that warranted its classification as a crested blade, unidirectional crested scar pattern and triangular lateralized midpoint cross-section, has been incorporated into refit #31. Although typologically correct, the technological pattern dominating the

reduction strategy is inconsistent with true volumetric blade technology.

7.2.6.1 *Débitage*

The level 1 assemblage is characterized by its pristine condition; little to no edge damage has been observed on the artefacts themselves, while blank fracturing was found to be equally low. Of the 100 pieces of *débitage*, 77 were complete, the remaining 23 pieces were broken into either proximal or distal fragments (n=11), false burin blows (n=2) or have experienced minimal breakage still enabling the recording of all metrics (incomplete n=9). Flakes, blades and bladelets show the least amount of dorsal cortical cover; 64% (n=18) of all blades, 67% (n=6) of all bladelets and 35% (n=8) of all flakes have 0% to 10% cortical cover. *Débordant* blades have a higher percentage of cortical cover; two pieces (22%) show 11% to 25%, while the remaining seven pieces (78%) show 26% to 50% cortical cover. Cortical blades and flakes presenting 76% to 100% of cortical cover encompass 80% (n=20) of the total primary blanks samples.

As was the case for the level 2 samples, striking platform treatment was minimal for the level 1 blanks. Both flakes and blades have 82% and 70% plain striking platforms (n=18 and n=14); one flake has a dihedral striking platform, adding some minimal variability to the overall simple pattern. The remaining four blades have crushed striking platforms. The remaining *débitage* mirrors the pattern identified on the blades striking platforms. Striking platform abrasion was observed on the *débitage*. Blades have 48% (n=10) partial edge grinding; four pieces have fully abraded striking platforms. Flakes and bladelets exhibit infrequent use of this feature; four bladelets and five flakes have partial abrasion of the intersection between their dorsal surfaces and the exterior edge of the striking platform. The remaining *débitage* shows no platform abrasion.

Blade midpoint cross-sections are in 32% of the cases triangular (n=9) and in 43% (n=12) trapezoidal. To a smaller extent, triangular and lateralized have also been observed. Flakes exhibit some variability in regard of their midpoint cross-sections: one

flake is flat, and two have triangular (n=2 9%) cross-sections. Additionally, 22% (n=5) of the flakes have lateralized cross-sections, while 35% (n=8) have trapezoidal (n=8 35%) and 30% (n=7) three vectored cross-sections. Counting the exception of one *débordant* blade with a rectangular cross-section, the remaining leptolithic *débitage* follows the pattern observed on the blades.

Level 1 blank longitudinal cross-sections have similar patterns to the *débitage* from level 2. While 39% of flakes have incurvate and twisted profiles (both n=9), blades are marked by the repeated occurrence of twisted longitudinal cross-sections: 54% (n=15) of all blades. Only 25% of the blades have straight (n=7 25%) profiles, while 21% (n=6) have incurvate longitudinal cross-sections. The remaining leptolithic *débitage* shows results comparable to that of the blades. In that respect, 67% (n=6) of the *débordant* blades are incurvate (n=6 67%); one piece has a twisted longitudinal cross-section.

Blanks were reduced following the technological axis of the core and the negatives on the dorsal side of the *débitage*. Among the 57 pieces on which this feature could be determined, eight were struck off axis.

Blank distal terminations are marked by a relatively high percentage of specimens with hinged terminations: of the 74 blanks on which this feature could be recorded 31% (n=23) are hinged. A total of thirty pieces have feathered terminations (41%) and twenty one (28%) have overshoot distal ends.

Blades have in 32% (n=9) of the observed cases parallel and 21% (n=6) converging edges. The remaining 18% (n=5) of the blades have lateralized and expanding edges. To a smaller extent, one ovoid piece and two pieces with irregular (n=2 7%) silhouettes were identified. Flakes have to a greater part expanding edges: 43% (n=10) of all flakes. *Débordant* blades display 45% (n=4) with lateralized edges.

Blank dorsal scars are mostly simple unidirectional. Blades and flakes show some variability in the configuration of these unidirectional reduction strategies. Blades have a predominately unidirectional convergent scar pattern expressed by 43% (n=12)

of the analysed specimens. A small number, representing 7% (n=2) of the blades, have unidirectional crossed and 11% (n=3) have unidirectional parallel scar patterns. Flakes have mostly simple unidirectional scar patterns, 52% (n=12). Flakes have also distinct variations of this feature; unidirectional crossed, 17% (n=4), convergent, 13% (n=3), parallel and unidirectional crested, both with 9% (n=2) were observed.

Blades are on average 52,13 mm long, 17,97 mm wide and 6,13 mm thick. In direct comparison, the *débitage* from level 1 is smaller than the *débitage* from level 2. Flakes are on average 40,92 mm in length, 29,5 mm in width and 8,15 mm in thickness; index of elongation values are slightly higher than that of level 2 (avg. 1,49 s.d. 0,95). Based on the metrics and the IOE, level 1 flakes are slightly smaller and more elongated. Platforms from level 1 flakes are relatively wide based on the IPF (avg. 3,31). In relation to the dorsal volume, however, the platforms are relatively small (RPF avg. 27,23 s.d. 25,96).

Blades index of elongation is comparable to that observed in level 2 (avg. 2,99), indicating that the blades from Ghazal Rockshelter are of similar dimensions. Assuming that the two occupation events at the site were making use of the same space and possibly the same raw material outcrop, interpreting the metrical divergence between these two samples is no easy task. A possible scenario envisions the group that occupied the site between 7.800 ± 500 BP and 6.700 ± 400 BP making use of the larger blocks of raw material available at the outcrop. The following occupation, postdating the 6.700 ± 400 B.P. sedimentary event, would only have found smaller chert nodules at the outcrop. It is also possible that the occupants of level 1 Ghazal rockshelter deliberately chose the smaller nodules available at the outcrop.

In respect to the platform dimensions on the blades from level 1 these have been found to be wider than the platforms on the flakes. RPS index, however, indicates that platforms are large in comparison to the volume of the blades (avg. 18,27 s.d. 12,46).

Débordant blades are larger than blades and show relatively truncated dimensions (avg. length 55,51 mm, thickness 25,96 mm and width 10,82 mm), although the elongation

index still indicates that these are rightfully included into the leptolithic category (avg. 2,15 s.d. 0,41). The remaining cortical *débitage*, cortical flakes and blades are larger and heavier than non-cortical one.

7.2.6.2 Cores

Four cores were found within the level 1 layer from Ghazal Rockshelter; two single platform convergent, one single platform parallel and one two unopposed platform core (Figure 7.48). Granted, the sample is relatively small and statements on variability in size and morphology must be regarded with some reservation. The importance of the level 1 assemblage lies in the reconstruction of these cores and how these change across their reduction sequence. Each of these cores will be described individually as to their morphological features and metrics.

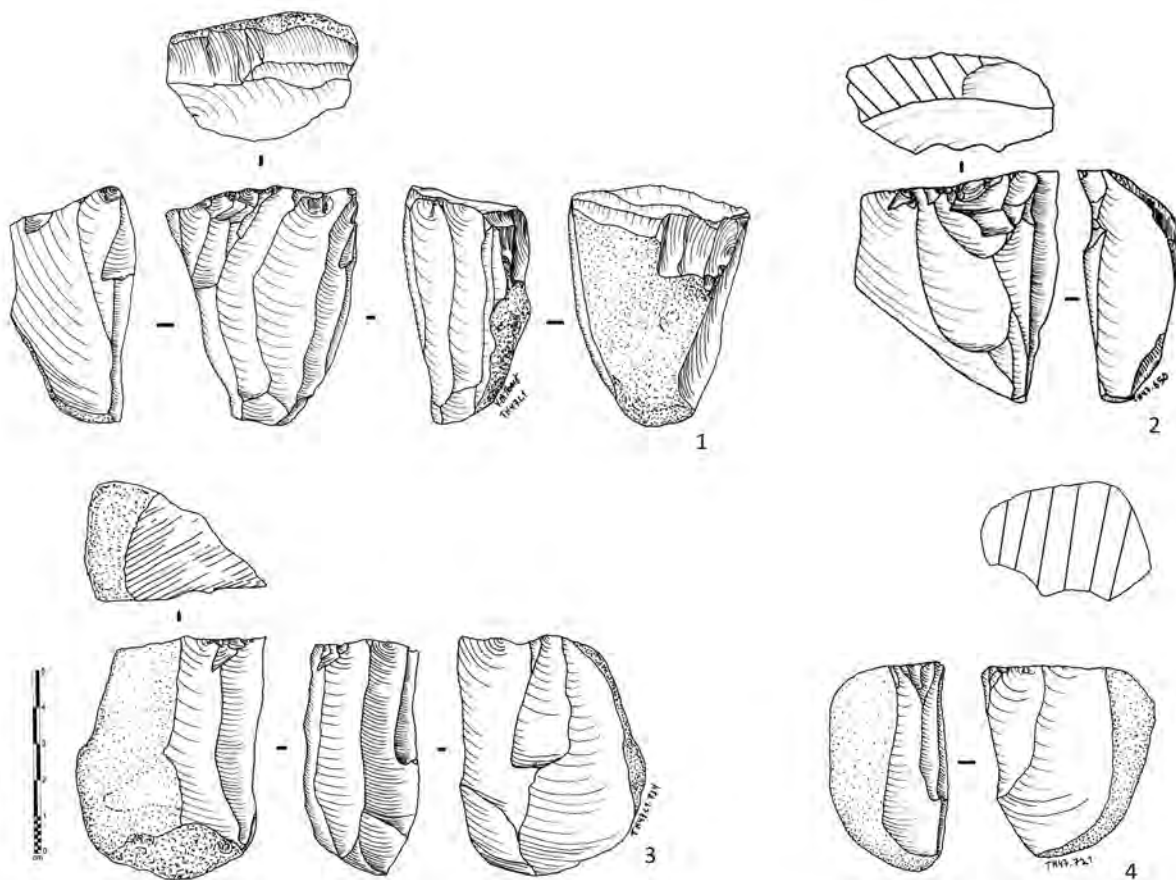


Figure 7.48. Ghazal Level 1 cores. 1, Semi pyramidal blade core; 2 to 4, unidirectional convergent cores (Illustrations by Y. Hilbert).

The two unidirectional convergent cores (TH.47.L1.721 and TH.47.L1.734) are incorporated into refits #29 and #30. The core labelled with the number 734 is 61,16 mm in length, 42,67 mm wide and 29,38 mm thick, weighing 102 g. It is also the largest core in the assemblage. The single platform core has been mostly freed from cortex (*11% to 25%*) and was exploited using a frontal plane of removal and two additional planes, one on each side of the main face. Reduction was administered from an unprepared striking platform made up of a natural fracture on the raw material. The planes of removal on the core are covered by hinge fractures, impeding further reduction. The second unidirectional convergent core (TH.47.L1.721) has been incorporated into refit # 30. The piece is of relatively small dimensions (49,61mm in length, 29,25 mm in width and 39,89 mm in thickness). Weighing 77g, it was primarily reduced from two planes of removal. The main working surface was placed on the narrow edge of a chert nodule, while the second plane of removal expanded towards the lateral, wider face of the raw volume. The striking platform is unprepared. Aside from the two working surfaces, the core has a considerable amount of cortex cover (*51% to 75%*). The core was abandoned due to hinge fractures at the intersection between the two planes of removal.

The single platform unidirectional parallel core (TH.47.L1.650) has been incorporated into refit #27. It is 55,86 mm long, 50,93 mm wide, 25,55mm thick and weighs 75g. A blow to the top of a chert nodule created the platform from which the reduction took place. One single plane of removal placed on the frontal face of the nodule served the production of blades and flakes. The core was not totally freed from cortex and exhibited a fully cortical back. Horizontal and longitudinal convexities were totally exhausted.

The two unopposed platform core was incorporated into the refit #31. Compared to the original volume of the raw material block used to produce blades and flakes, this core had been exceedingly reduced. Measuring 54,32 mm in length, 42,15 mm in width, 32,06 in thickness and weighing 86 g the core presents what seems to be a faceted striking platform. Under further inspection and thanks to the core reconstruction, it was possible

to identify this striking platform as an earlier plane of removal on the core. The plane of removal used last, in order to produce blanks of varying shape and morphology, was placed on the frontal face of the volume. Two supplementary working surfaces were identified flanking the main plain on both sides. The piece was relatively freed from cortex and although some hinge fractures covered the main plane of removal convexities, both horizontal and longitudinal, would have accommodated a few further removals. The plane of removal that was later used as striking platform exhibited a fair number of hinge fractures that would have impeded any further removal without appropriate curation.

7.2.6.3 Level 1 refittings

As mentioned earlier, all cores found within the above described levels are incorporated into the four main constellations of level 1 (Table 7.5). The morphological differences observed on the cores are clarified by the reconstructions. These four refits will be described and illustrated in order to compare blade reduction modalities across the Early and Mid Holocene occupations of the site.

Table 7.5 Refittings from Ghazal level 1

	Refit 28	Refit 29	Refit 30	Refit 31
<i>Flakes</i>	1	2		13
<i>Blades</i>	4	4	1	14
<i>Bladelets</i>	3			3
<i>Cortical pieces</i>	3	3	1	7
<i>Débordant Flakes</i>	3			2
<i>Débordant Blades</i>		1	4	
<i>Crested Blades</i>				1
<i>Chips</i>	1			6
<i>Core</i>	1	1	1	1
Total	15	10	7	47

A total of fifteen pieces were incorporated into refit #28, all stages of core reduction were reconstructed. The illustration of the refit (Figures 7.49 and 7.50) depicts the pattern of reduction following the early decortication and platform preparation. The striking platform was prepared by a single blow to the upper portion of the raw volume,

this single blow created a flat surface with an appropriate angle for blank production. After the accomplishment of this step, reduction commenced on the left side of what would later become the main core's working surface. Reduction shifted towards the opposite side of the core and a second cortical element was reduced creating a dihedral plane of removal. This plane was then exploited by the flintknapper; three blanks were removed, one of these was incorporated into the constellation while the other two were probably removed from the site for further modification. At this point the cores convexity was re-prepared by the removal of two *débordant* flakes, one from each side of the core's working surface. Having re-established the desired convexity, reduction did pick up again and additional blades and flakes were produced; four blanks were attributed to this phase. Two additional blanks were missing in order to complete the refit, these pieces were either removed from the site or are still buried in the sediments.

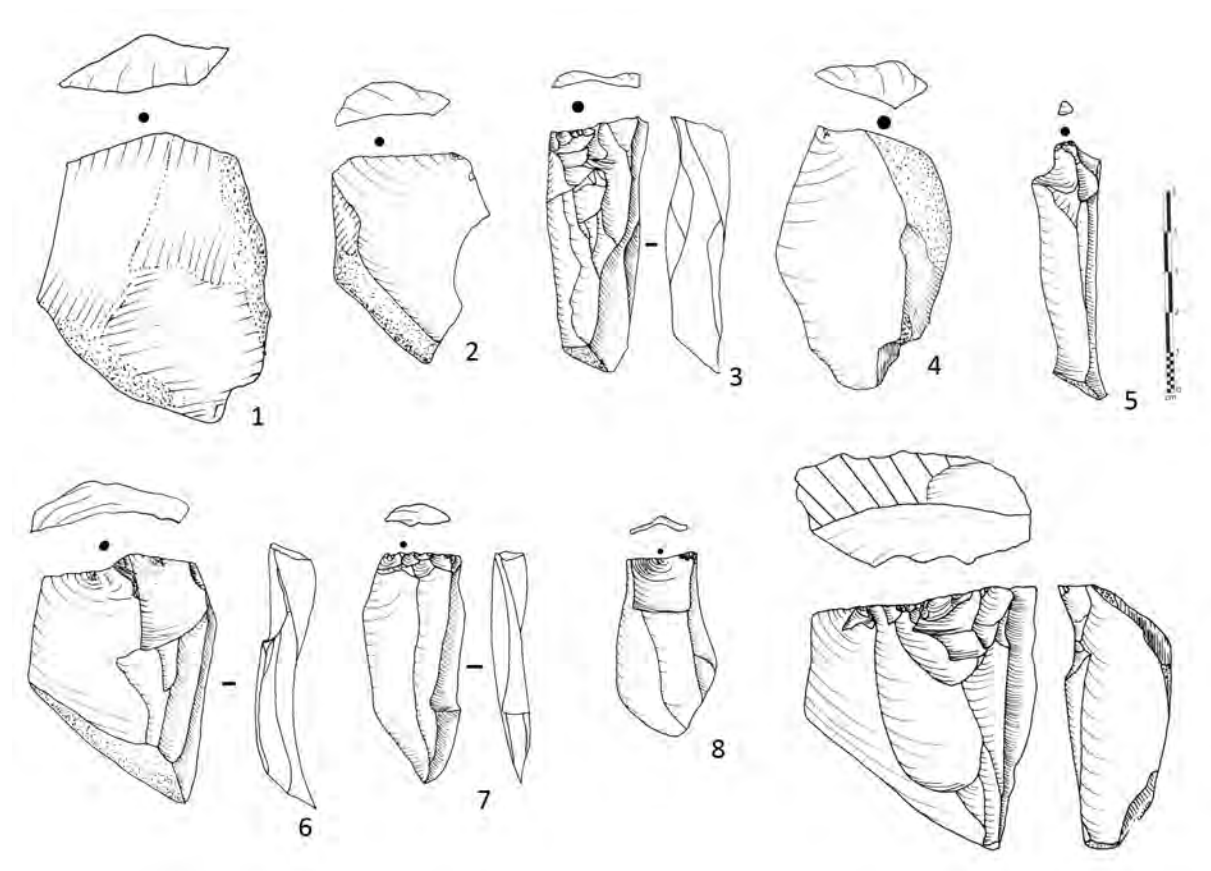


Figure 7.49 Ghazal level 1 refit #28 débitage.
(Illustrations by Y. Hilbert)

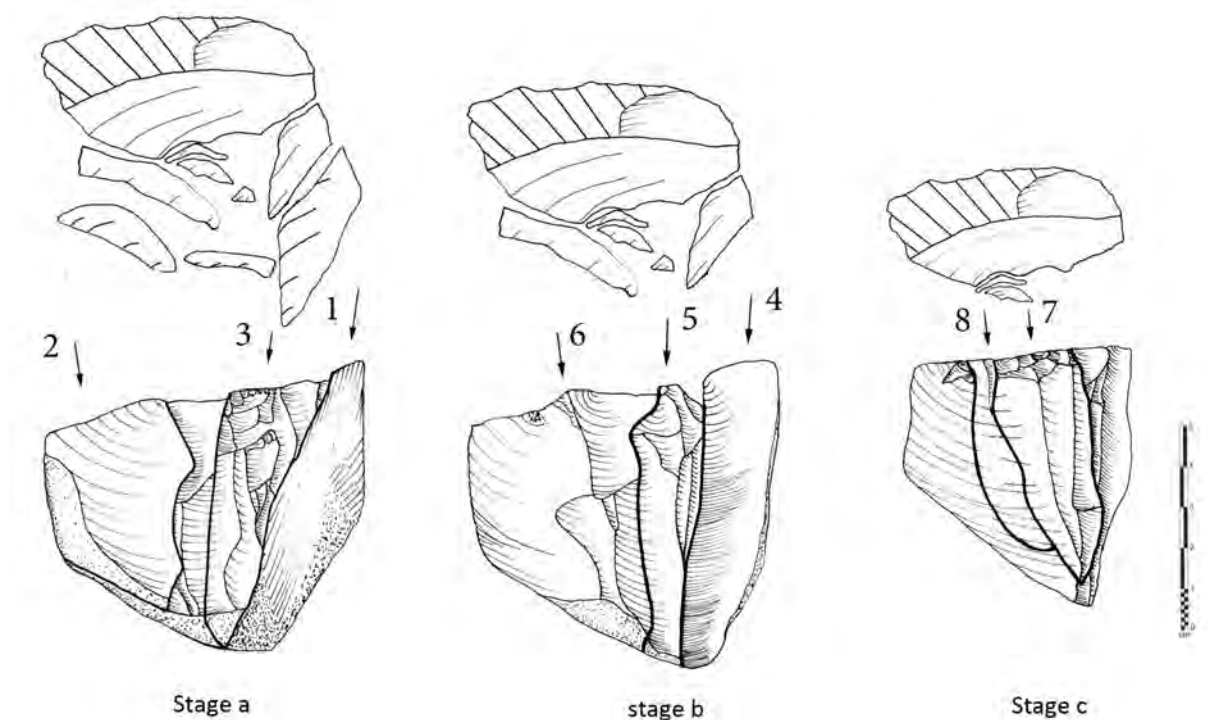


Figure 7.50 Ghazal level 1 refit #28.
(Illustrations by Y. Hilbert)

Refit #29 was fully reconstructed, which is to say all blanks produced were reattached to the core (Figure 7.51). The facts that all artefacts were found suggests that the occupation was both restricted in its distribution and suffered little post-depositional disturbance; also this refit indicates that the pieces missing from the other constellations were possible removed from the site. Giving its completeness, refit #29 offers interesting insights into raw material exploitation and the reduction modality used. Prior to its transformation the raw material volume weight c.a. 314 g, the discarded core weight 102 g; a total of 212 g of raw volume had been produced. Reduction of the volume started immediately, given that a neocortex surface on the chert nodule served as a striking platform. A large overpassed cortical flake was reduced on one of the nodules faces, a second primary removal followed. The second removal was administered ajar to the previous removal creating an acute working surface. The third blank, a flake with triangular cross-section, was removed on the intersection of these two removals.

Attempting to exploit the triangular working surface created by this last removal, a forth flake, with hinged termination, was produced. Trying to restore the core's working surface convexity, the flintknapper removed a *débordant* blade from the works surface's left periphery. The removal did not enhance the cores architecture and the following blade removal failed to produce a symmetrical blank; reduction shifted towards the opposite side of the nodule. Following the removal of a cortical flake on the right plane of removal, two irregular shaped blanks, one hinged flake and one hinged blade, were removed; the core was subsequently abandoned.

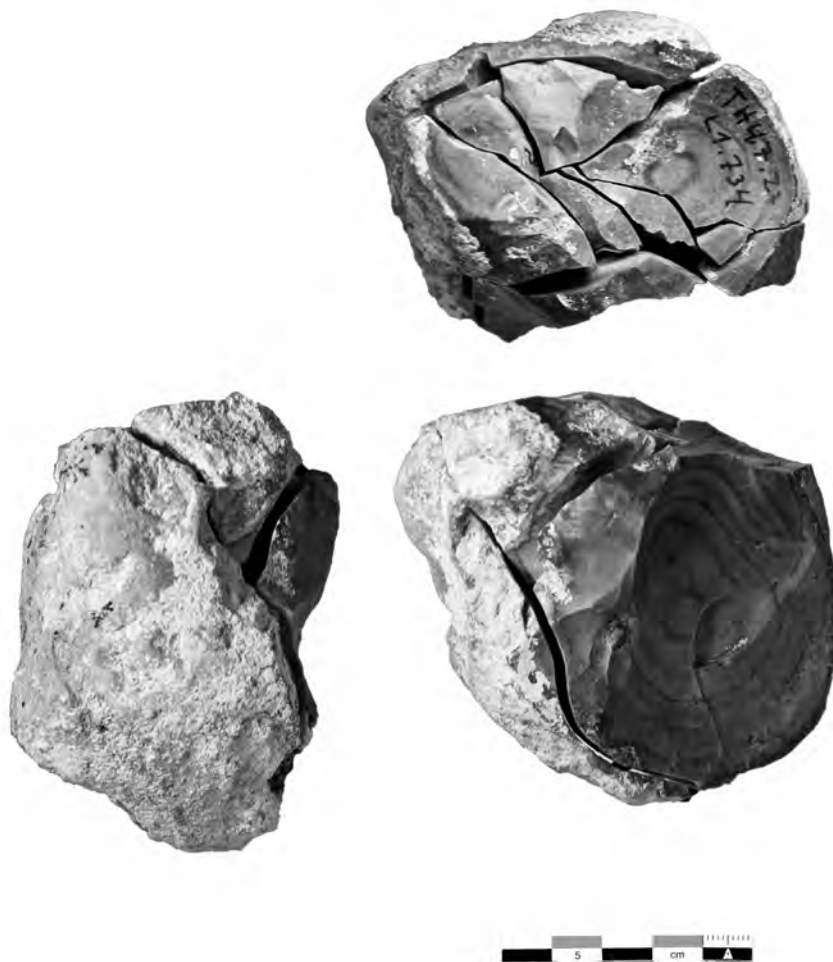


Figure 7.51 Ghazal level 1 refit #29.
(Photograph by Y. Hilbert)

Refit #30 depicts the second complete reconstruction from Ghazal level 1; six blanks were refitted to a single platform convergent core (Figure 7.52 and 7.53). Blank production took place from a flat neocortex striking surface exploiting the narrow edge of a flat chert nodule. After the removal of a primary blade from the centre of what later becomes the main plane of removal, reduction continued on the same technological axis. Two *débordant* blades, one from each side of the core's working surface were removed, ideal convexity, however, was not achieved. A third *débordant* removed from the right side of the core expanded towards the lateral side of the volume. The ridge created by this last removal was tentatively exploited, the banks was irregular and hinged. The core was not further reduced.

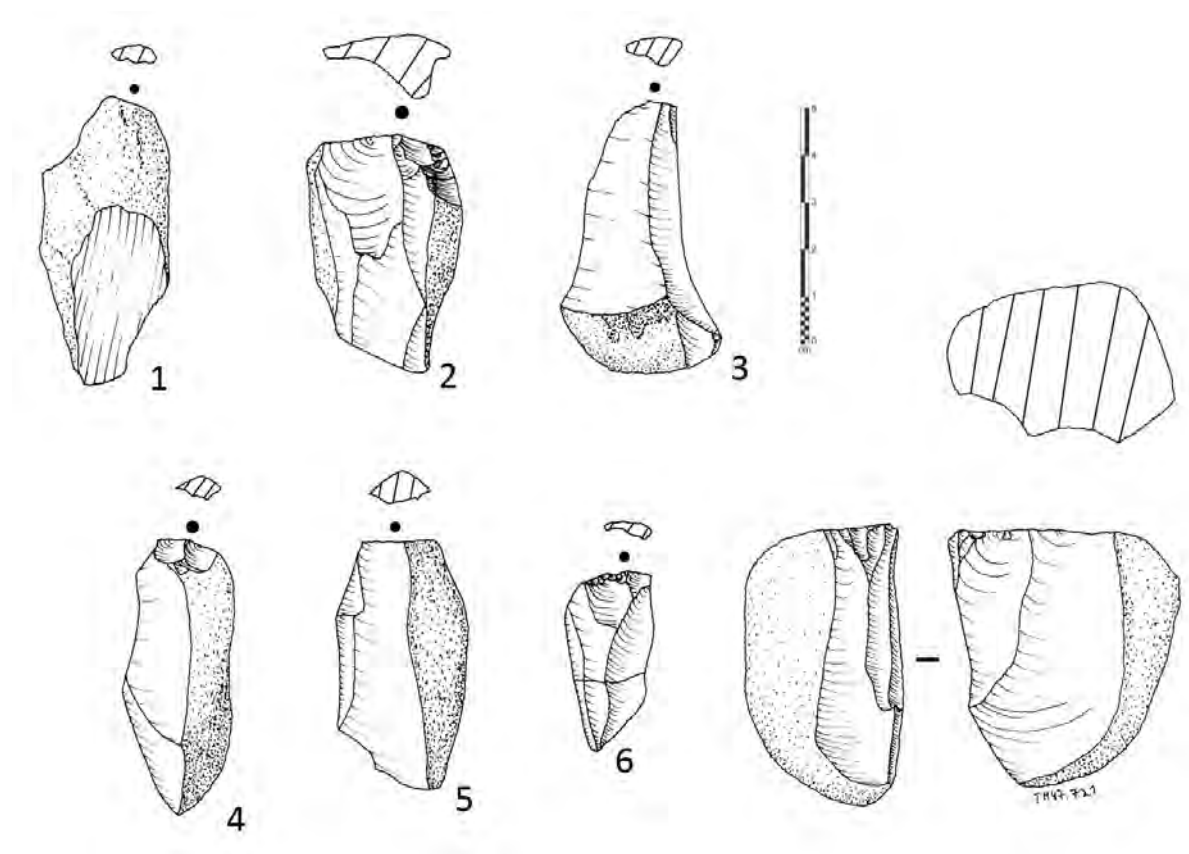


Figure 7.52 Ghazal level 1 refit #30 débitage.
(Illustrations by Y. Hilbert).

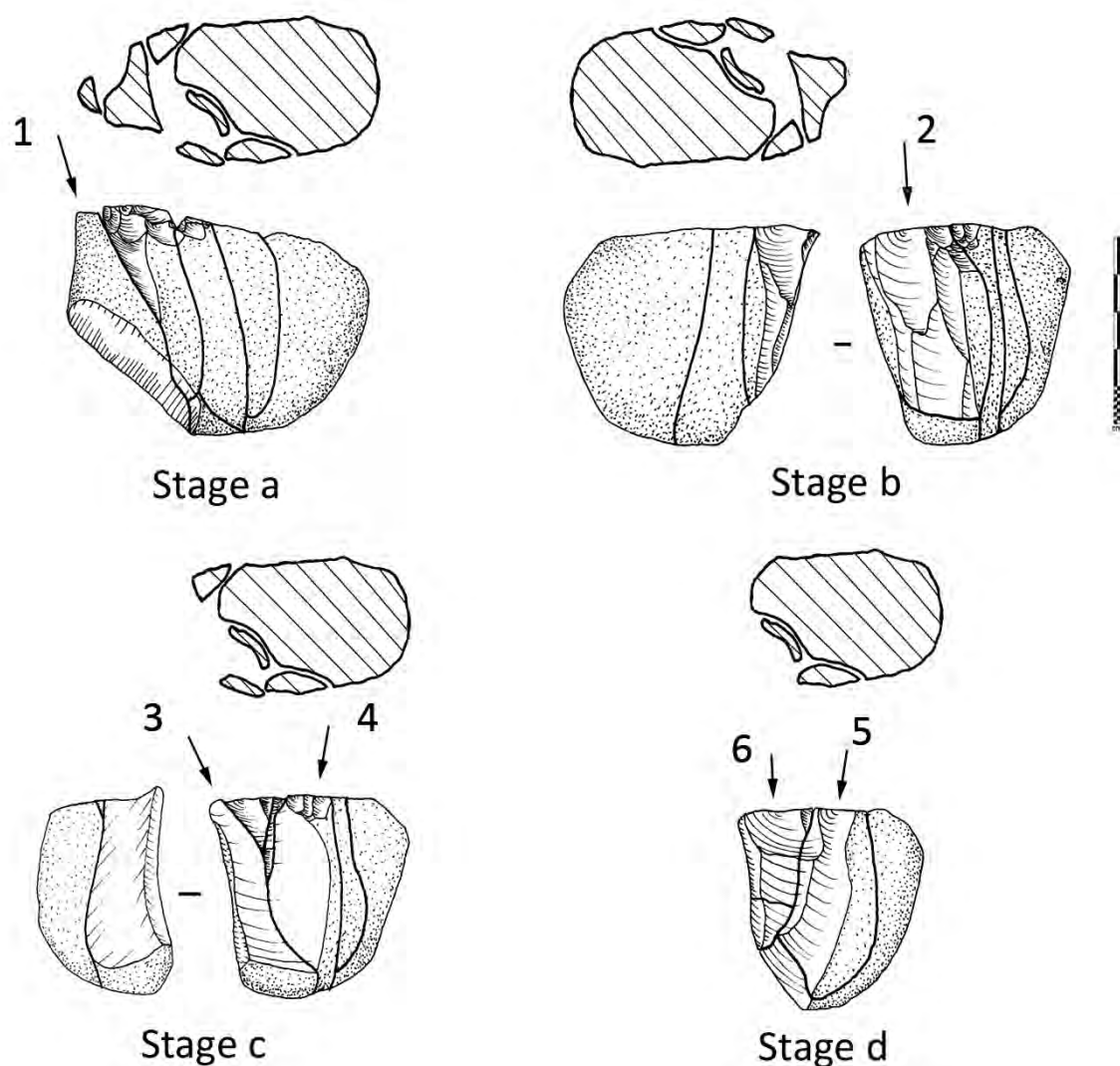


Figure 7.53 Ghazal level 1 refit #30.
(Illustrations by Y. Hilbert)

Refit #31 is a relatively complex constellation; relative given that no complex technological procedures such as crest preparation or core tablet technology have been applied. It is complex in that a great number of blanks were produced using the core at hand and that during the early stages of core reduction; different platforms and planes of removal have been created and exploited. A loaf shaped chert nodule served as a starting point for this reduction (Figure 7.54).

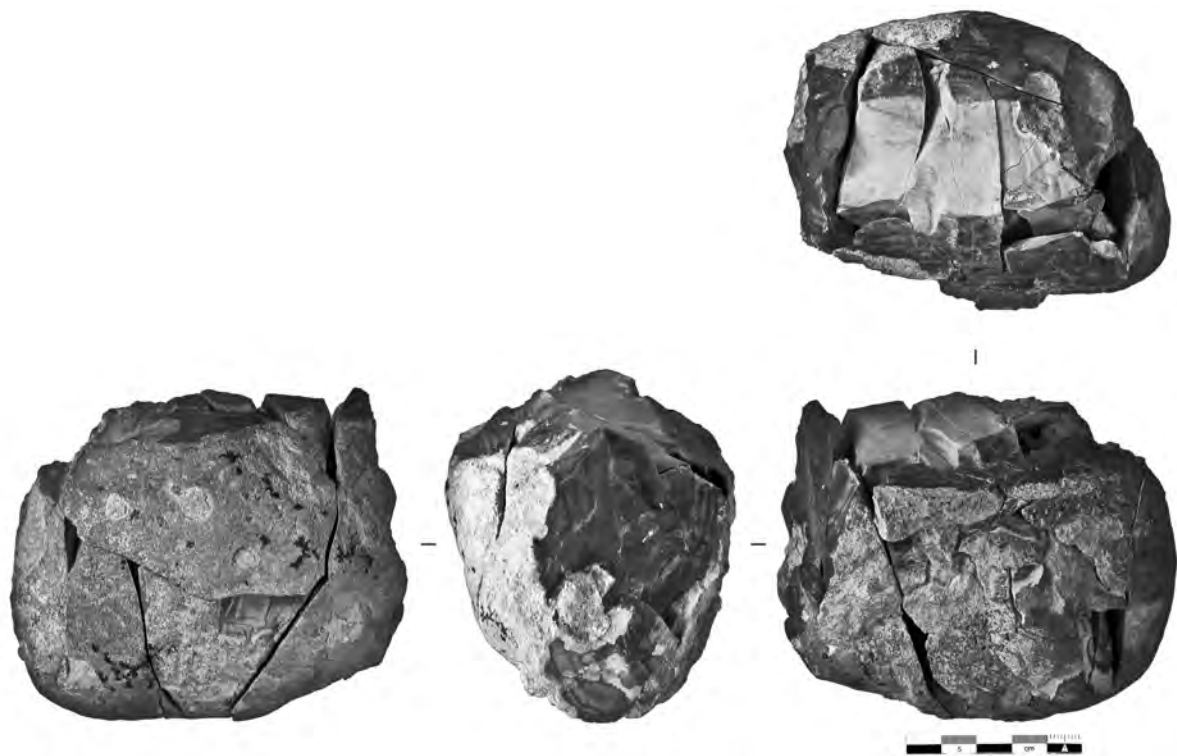


Figure 7.54 Ghazal level 1 refit #31 débitage.
Stage a (Illustrations by Y. Hilbert).

Initial reduction of the core commenced by creating a striking platform on the left side of the chert nodule; two consecutive flakes, one of them a cortical flake, were reduced creating the first used striking platform. Reduction proceeded on the narrow, long face of the nodules. Using the same striking platform a second large cortical flake was reduced from the left periphery of plane of removal (Figure 7.55).

The plane of removal was, in the second stage of reduction, converted into a striking platform from which reduction took place perpendicular to the previous removal on the last core's working surface (Figure 7.56). A set of approximately four primary flakes and blades were reduced.

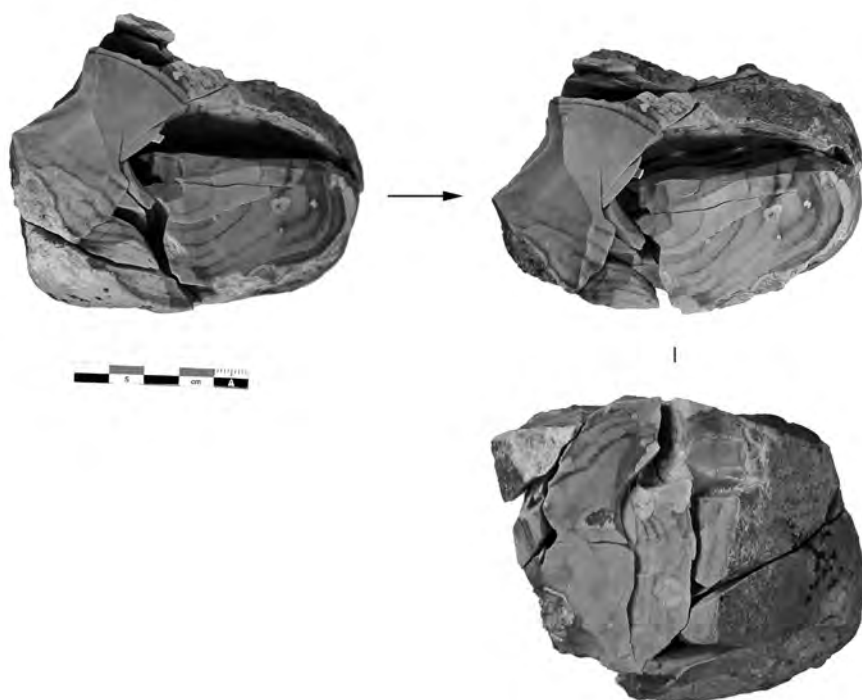


Figure 7.55 Ghazal level 1 refit #31. Stage b (Photograph by Y. Hilbert)

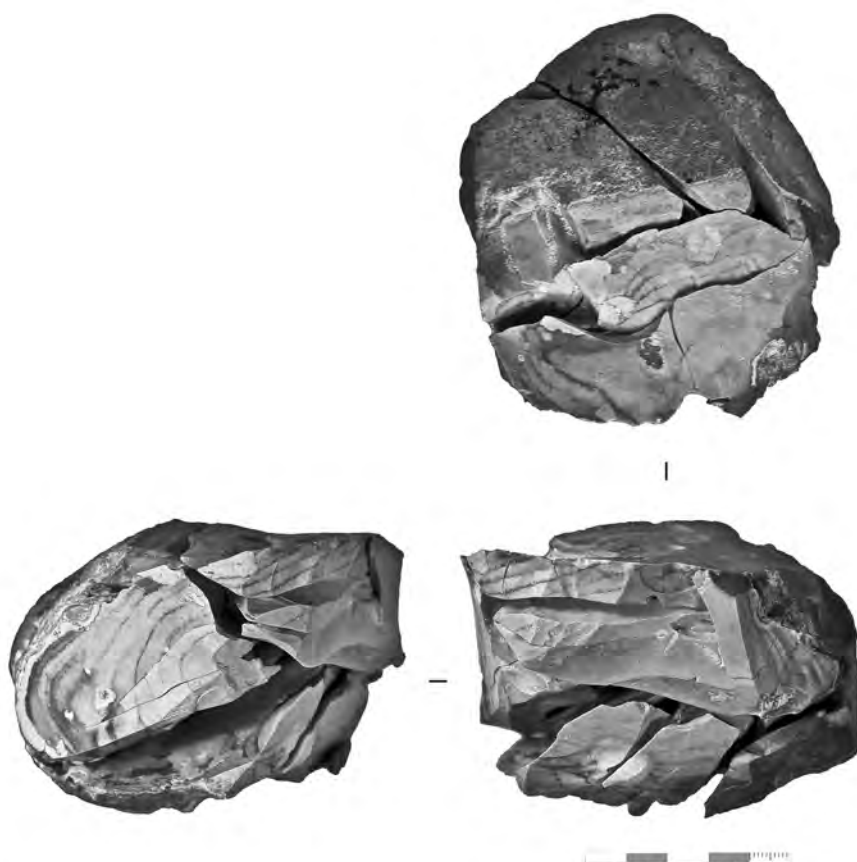


Figure 7.56 Ghazal level 1 refit #31. Stage c (Photograph by Y. Hilbert)

Reduction then shifted back to the first striking platform removing the one crested blade in the level 1 assemblage. As stated earlier, the refit shows that the creation of this typological element was by no means related to crested blade technology. The crested blade was the result of the removal from the intersection of the previously used striking platform and plane of reduction administered transversely to the previous technological axis of the core. That is to say change in reduction axis, a feature also observed in level 2 refit #20, serves the optimal usage of the volume available to the flintknapper at Ghazal Rockshelter. The further exploitation of the currently used core's working surface continued until the core was exhausted, manifested by the flat plane of removal. Attempts to expand the working surface towards the right side (viewed in technological axis) of the nodule failed due to repeated hinge fractures. At this point the last change of orientation and conversion of the plane of removal into a striking platform took place (Figure 7.57).

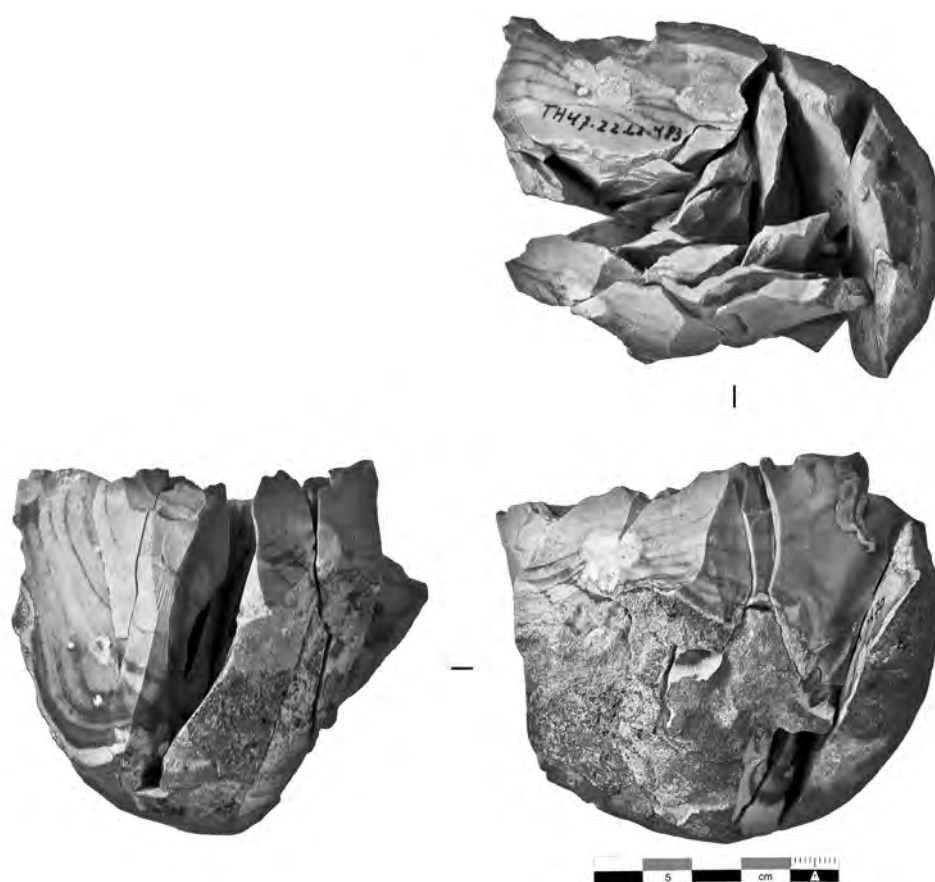


Figure 7.57 Ghazal level 1 refit #31. Stage d
(Photograph by Y. Hilbert).

From this point on reduction continued conform to the technological axis, no plane of removal curration elements, *débordant* blades or flakes, were produced and reduction proceeded in volumetric fashion until the core was abandoned (Figures 7.58 and 7.59).

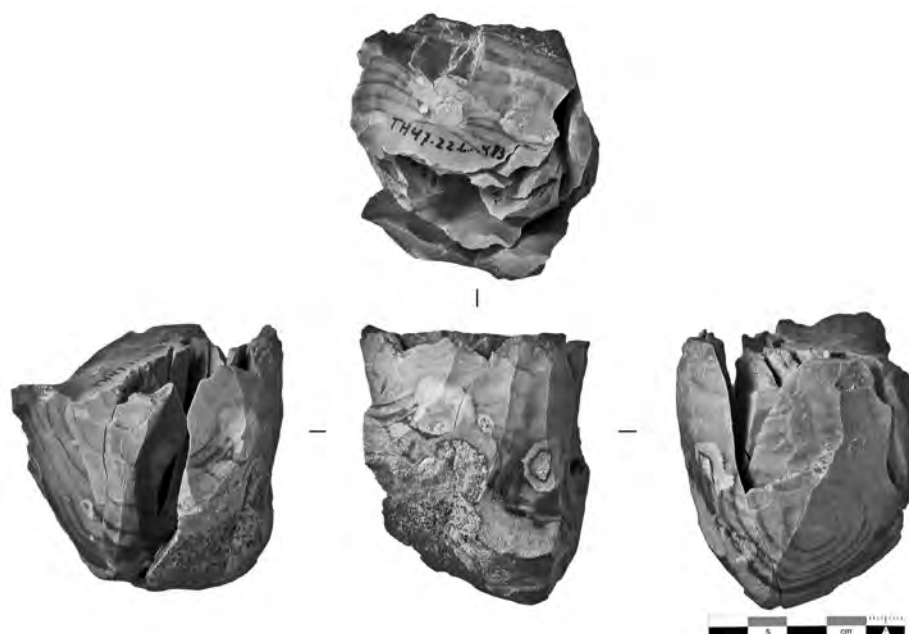


Figure 7.58 Ghazal level 1 refit #31. Stage e
(Photograph by Y. Hilbert)



Figure 7.59 Ghazal level 1 refit #31. Stage f
(Photograph by Y. Hilbert).

7.3 BRAVO Transect Comments

7.3.1 Khumseen Rockshelter

The results of the attribute analysis of the lithic assemblage from the leptolithic levels of Khumseen Rockshelter point to intensive blank production, using unidirectional parallel technology. Although post-depositional factors have skewed the sample to a certain extent, the main modalities of reduction used at the site have been crystalized. Chiefly dictated by the recurrent reduction of blades, flakes and bladelets, with discreet interconnected convex maintaining and creation phases, cores have been exploited up to the point where the sheer size of these specimens did not support the further reduction of leptolithic *débitage*. That is to say, cores and their volumes were reduced to full exhaustion or were prematurely abandoned due to botched working surfaces.

Variability identified among the three main *débitage* categories found at the site indicates some degree of specialization towards the deliberate production of blades, flakes and bladelets. While all three blank types were produced using single platform unidirectional cores, the progression of the reduction cycles of these blanks is deemed responsible for a shift from blade production to flake and bladelet production. Short bladelets with twisted and straight profiles have been struck from unidirectional convergent cores with relatively short, broad working surfaces. The exploitation of additional volume on globular multiple platform cores yielded primarily short blades and elongated flakes.

The tool spectrum, although small and unilateral considering the lack of variability includes two projectile points, which can now, based on the dates, be ascribed securely to the Early Holocene.

7.3.2 Ghazal Rockshelter

The Ghazal rockshelter assemblage is composed of two samples, both characterized

by the production of elongated blanks; the samples are separated stratigraphically by a sterile sand layer. Although no absolute dates for the actual occupations of the site could be produced (e.g. fireplaces, organic remains which would have yielded C¹⁴ dates were missing), the OSL samples retrieved from the GH bracketing the level 2 industry provide a fair chronological marker for that layer and the one above. Spatially, both industries were confined to different areas within the excavated perimeters; level 1 being constrained to the areas within and in the proximity of the small overhang, while level 2 artefacts were found mainly in front of the rockshelter.

Although limited in numbers, both assemblages revealed, based on the refits, similar patterns of blank production, but some variability in regard to core workings surface use. *Débitage* attribute analysis revealed nearly identical patterns for both levels; blades produced from simple unidirectional cores using ridges across the plane of removal as guiding element's following the technological axis of the cores. The creation and maintenance of these ridges was aided by the removal of *débordant* from the cores peripheries. Two modes of convexity exploitation have been observed; a recurrent approach, based on refit #19 from level 2 and refit #28 from level 1 and the approach visible in refit #25 and refit #30. The recurrent approach makes use of the created convexity by reducing a set of blanks, while the second approach is so designed that a single elongated, triangular shaped blanks is achieved from the core's working surface. While the recurrent approach is composed of a long sequence, starting from convexity creation to blank production and subsequent exhaustion of the plane of removal, the second approach is marked by short alternation exploitation and convexity creation phases.

Also repeatedly observed in both levels is the tendency towards shifting core architecture, in that the striking platform becomes the plane of removal and *vis a versa*; examples for this behaviour are seen in level 2 refits #2 and 20 and level 1 refit #31.

The tool sample for level 2 (level 1 is devoid of any modified blanks) is discreet but concrete; a burin, an endscraper on a thick blank and a piercer have been found.

As such, the reduction modalities and the tools identified within the stratified sites of the BRAVO transect can be found within surface sites all over the Nejd Plateau. Wadi Haluf, a particularly rich zone within the southern Nejd has produced a high density of Nejd Leptolithic sites. The perusal of the stone tools retrieved from the GULF transect, which has been laid across the Wadi Haluf valley should help to further define technological and typological plasticity within the Nejd Leptolithic technocomplex.

GOLF TRANSECT

While the data gathered from BRAVO transect allows for a chronological categorization of the lithic samples collected from the sites found along the ALPHA transect, sites found along the GULF transect are used to further grasp technological and typological plasticity within the here defined entity. This chapter will finalize the data section of this dissertation. In addition to the systematic surface collection undertaken at Wadi Haluf 1 (TH.124b), three localities identified along the GOLF survey transect are of interest to this study, given the core reconstructions these provided (Figure 8.1). The transect laid at Wadi Haluf served to assess the archaeological potential of this landscape and identify its chrono-cultural variability, based on the recognition of typological and technological diagnostics artefacts on the surface.



Figure 8.1 GULF transect and sites mentioned in text.

Wadi Haluf 1 N 17.383920° and E 53.929160°, TH.125 N 17.386570° and E 53.935750°; TH.128 N 17.390490° and E 53.940030°; TH.133 N 17.396790° and E 53.941460° (Satellite image courtesy of Google© Earth).

Of the 31 recorded sites along the 4.3 km of the GOLF transect, twenty have been attributed to the Nejd Leptolithic tradition. The GOLF transect was so placed that diverse micro-areas between Wadi Haluf and Wadi Haylah, one of wadi Haluf's tributaries to the north, could be surveyed. Starting within the wadi valley, the transect continued over the southwestern facing cuesta of Jebel Ardif up to a dissected low plateau. This heavily dissected plateau was rich in both raw material outcrops and archaeological sites. The transect ends at wadi Haylah, which joins wadi Haluf further north.

8.1 Gulf Transect Sites

8.1.1 TH.125

The TH.125 occurrence was found on the southwestern facing cuesta of the plateau adjacent to the Wadi Haluf valley (Figure 8.2). The scatter, composed of seven *débordant* blades and one single platform unidirectional core, was spatially well delimited. No raw material source was found in the proximity of the scatter. The patination observed on the artefacts is of dark brown colour. No edge damage was observed on the blanks or the core, suggesting little to no post-depositional movement or trampling of the scatter.



Figure 8.2 Photograph of TH.125 locality.

Y. Hilbert working on the core reconstruction in the field. (Photograph by Dr. J. Rose)

All artefacts could be refitted revealing a succession of core preparations and exploitations phases. No early decortication flakes or striking platform preparation *débitage* was found, suggesting that the core received some treatment prior to the deliberate blank production at the TH.125 locality. It is conceivable that decortication and striking platform preparation was undertaken at the raw material source and that the prepared core was then transported to the locality (Figure 8.3).

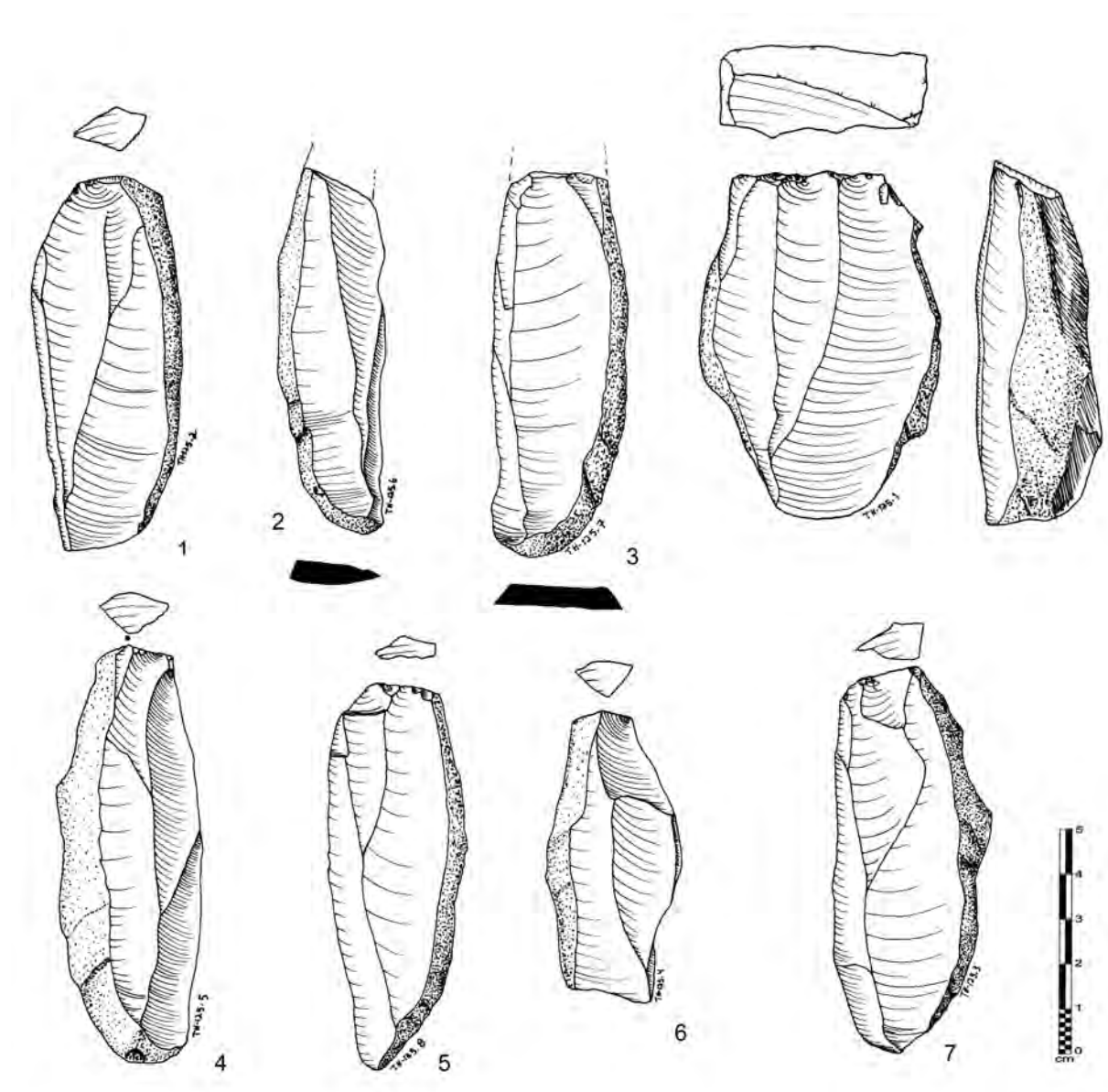


Figure 8.3 TH.125 refitting débitage.
(Illustration by Y. Hilbert)

The seven blanks exhibit very similar morphologies. Striking platforms are plain and received little treatment prior to blank detachment. Bulbs of percussion on the ventral surfaces are prominent, suggesting the use of hard hammer percussion. Two of the blanks had missing striking platforms and, given that these have been reduced just like the other *débitage*, it is conceivable that these share the same morphological features. All blanks exhibit cortical backs, these have been found to be in an approximate 90° angle to the dorsal surface, allowing the classification of these objects as *débordant* blades. Five of these were found to share the same overpassed terminations, lateralized blank shapes and trapezoidal midpoint cross-sections, as well as curved longitudinal profiles. The two other blanks with feathered terminations and parallel edges complete the *débitage*. All *débordant* blades exhibit a unidirectional convergent scar pattern.

The core exhibited a plain striking platform in concordance with the pattern observed on the blanks; the longitudinal disposition of the dorsal face is straight, while horizontal convexity is still somewhat present. The core's working surface is positioned on its frontal plane with no indications of any additional working surfaces.

As noted above, decortication and platform preparation have been undertaken elsewhere, reduction undertaken at the TH.125 occurrence was restricted to deliberate blank production and successive convexity maintenance procedures (Figure 8.4). Reduction started with the removal of *débordant* elements; this removal created a dihedral working surface on the core. A central ridge served as guiding ridge for the preferential removal of an elongated blade with convergent edges. This blank was not found at the site and had been purposefully removed for further modification elsewhere. The subsequent removal, undertaken on the opposite side of the core, re-established the dihedral morphology of the core's working surface and was followed by an additional preferential removal. The negative visible on the reconstructed core gives an idea of what the desired products created by this recurrent reduction looked like. A third *débordant* element was removed from the right edge of the core and was also followed by the removal of a triangular and

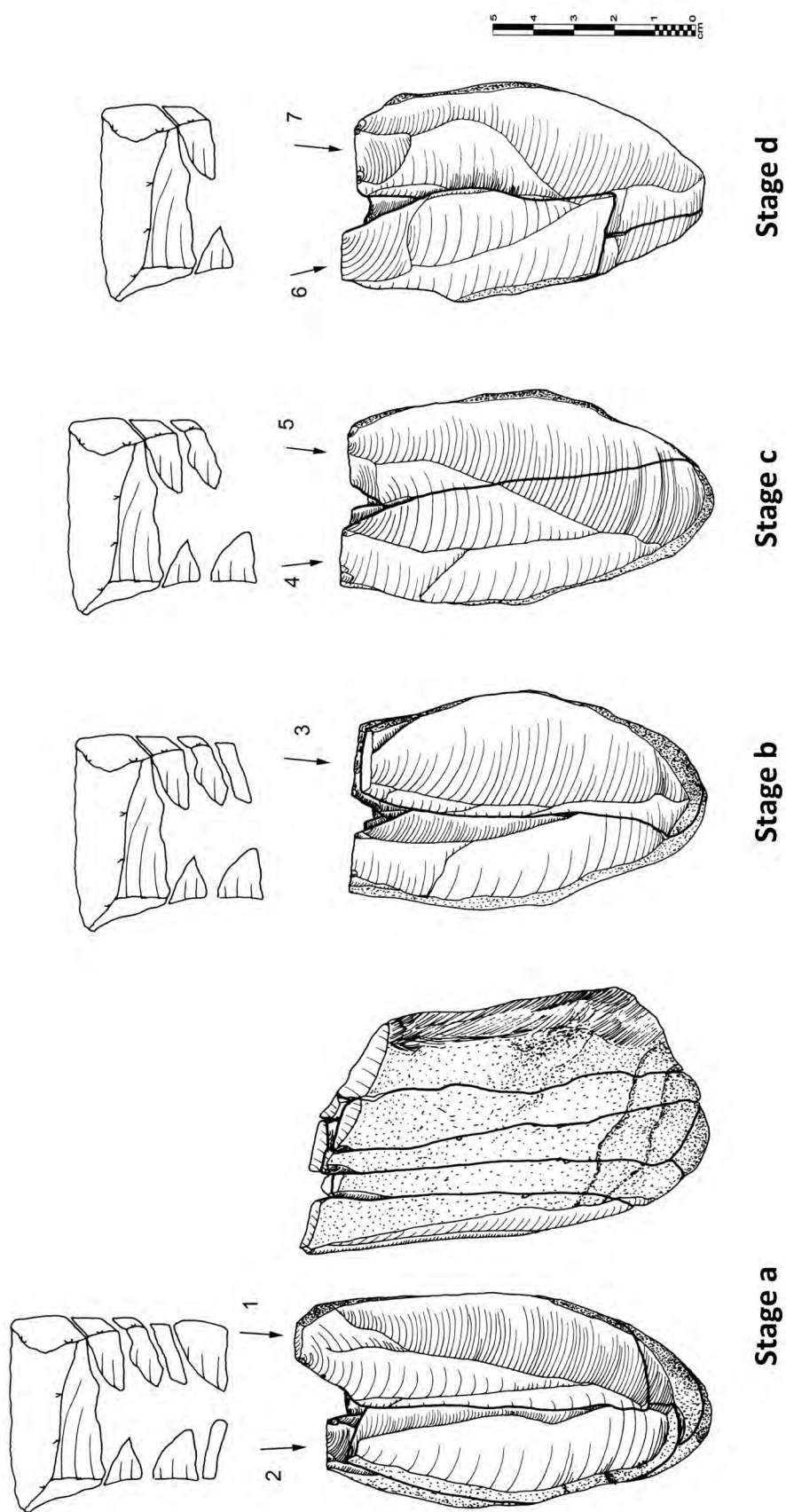


Figure 8.4 TH.125 refitting. (Illustration by Y. Hilbert)

elongate blank. After this step, the core's working surface presented two ridges converging in the bottom portion of the flaking surface. Two successive removals, one from the left and one from the right side of the core served to re-establish the dihedral working surface. The ridges created by these removals served the reduction of a cortex free elongated blank with triangular cross-section. The reduction of the core continued after re-establishing the guiding ridge. One last *débordant* element was struck, followed by the removal of an elongated triangular blade from the centre of the core. Given the cores flat working surface morphology and increased volume loss, the piece was abandoned.

8.1.2 TH.128

The TH.128 surface scatter is located on top of a low plateau upon Jebel Ardif. The plateau is dissected by several erosional gullies that cut into the limestone bedrock. A deflated surface composed of eolian material, limestone debris and both worked and unworked chert covers the plateau (Figure 8.5). Raw material is available and of high quality, nodules of medium to large size are present and were used to produce stone tools. Artefacts found at the site were manufactured exclusively on the chert cropping from the *gahit member*. The site itself is a medium to low density workshop much like Wadi Haluf 1, only less extensive. It is marked by a discontinuous flint carped that stretched over approximately 60 square metres.



Figure 8.5 Photograph of TH.128 locality. (Photograph by Y. Hilbert)

Blade manufacture was the most common form of reduction used on site. Survey activities undertaken at TH.128 have revealed the existence of a *façonnage* component, attested by the presence of a bifacial pre-form (Figure 8.6). Unlike the immediate refit from TH.125, the scatter at TH.128 was not entirely isolated, but recovered from a carpet of artefacts, geofacts and limestone shatter. Nonetheless, the combined effort of three DAP team members for over 30 minutes produced the reconstruction of a flint nodule composed of a core and nine pieces of *débitage*.



Figure 8.6 Photograph of TH.128 biface.
(Photograph by Y. Hilbert)

The refit illustrates all phases of blade production undertaken on one raw material nodule (Figures 8.7 and 8.8). Artefact patination observed on site is of dark to light brown colour; the variation spectrum and additional surface modifications observed have been found indicative of chronologically constrained knapping events.

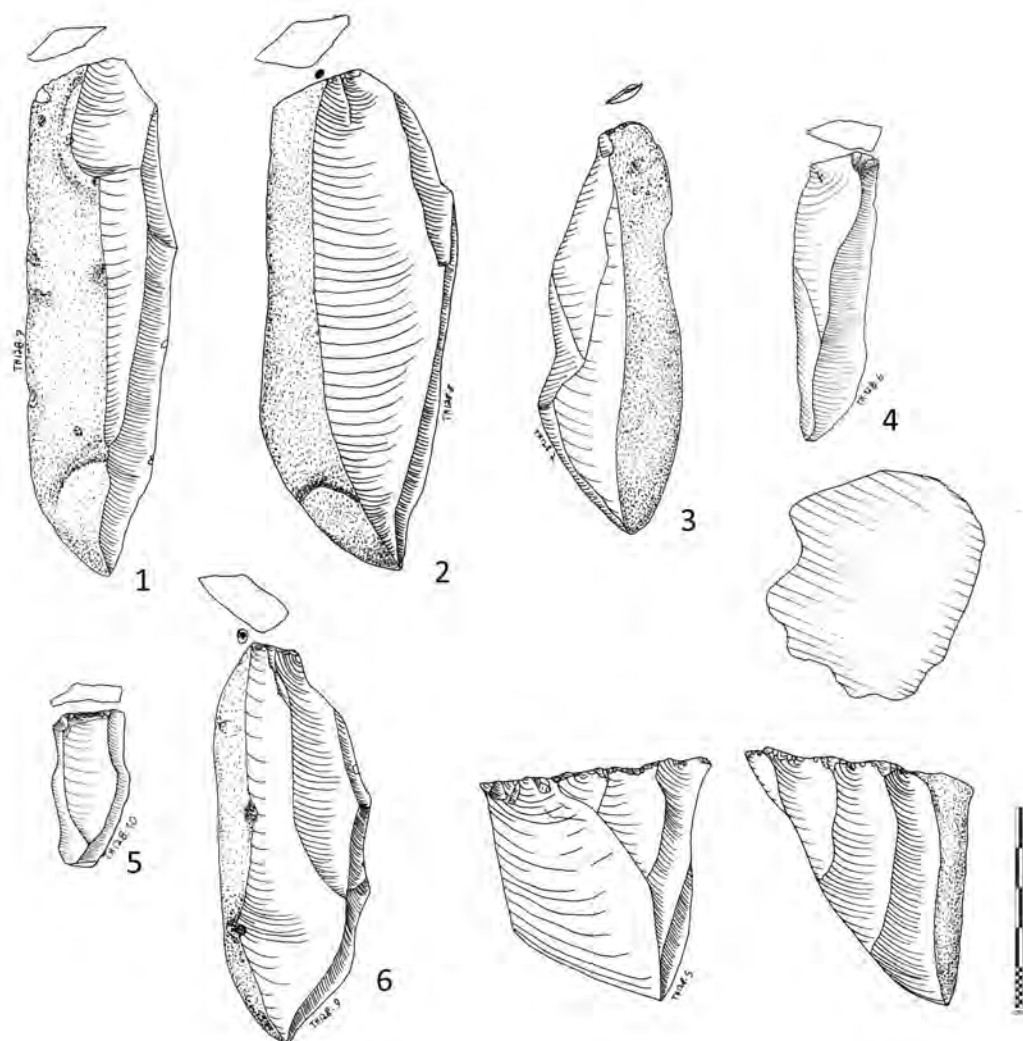


Figure 8.7 TH.128 refitting débitage.
(Illustration by Y. Hilbert).

The core recovered exhibited a main working surface extending across half its circumference. The core exhibits a cortical back, whereas the frontal working surface was formed by five unidirectional parallel to sub-parallel removals. Longitudinal convexity had been exhausted due to an overpassed removal that detached part of the core's distal portion. The *débitage* collected includes four *débordant* blades, three cortical blades and two blades. Blank size varies greatly; the largest pieces were detached after initial decortication, while two smaller blades were removed at the end of the core reduction. The core reconstruction is incomplete, possibly three to four pieces had been removed from the site.

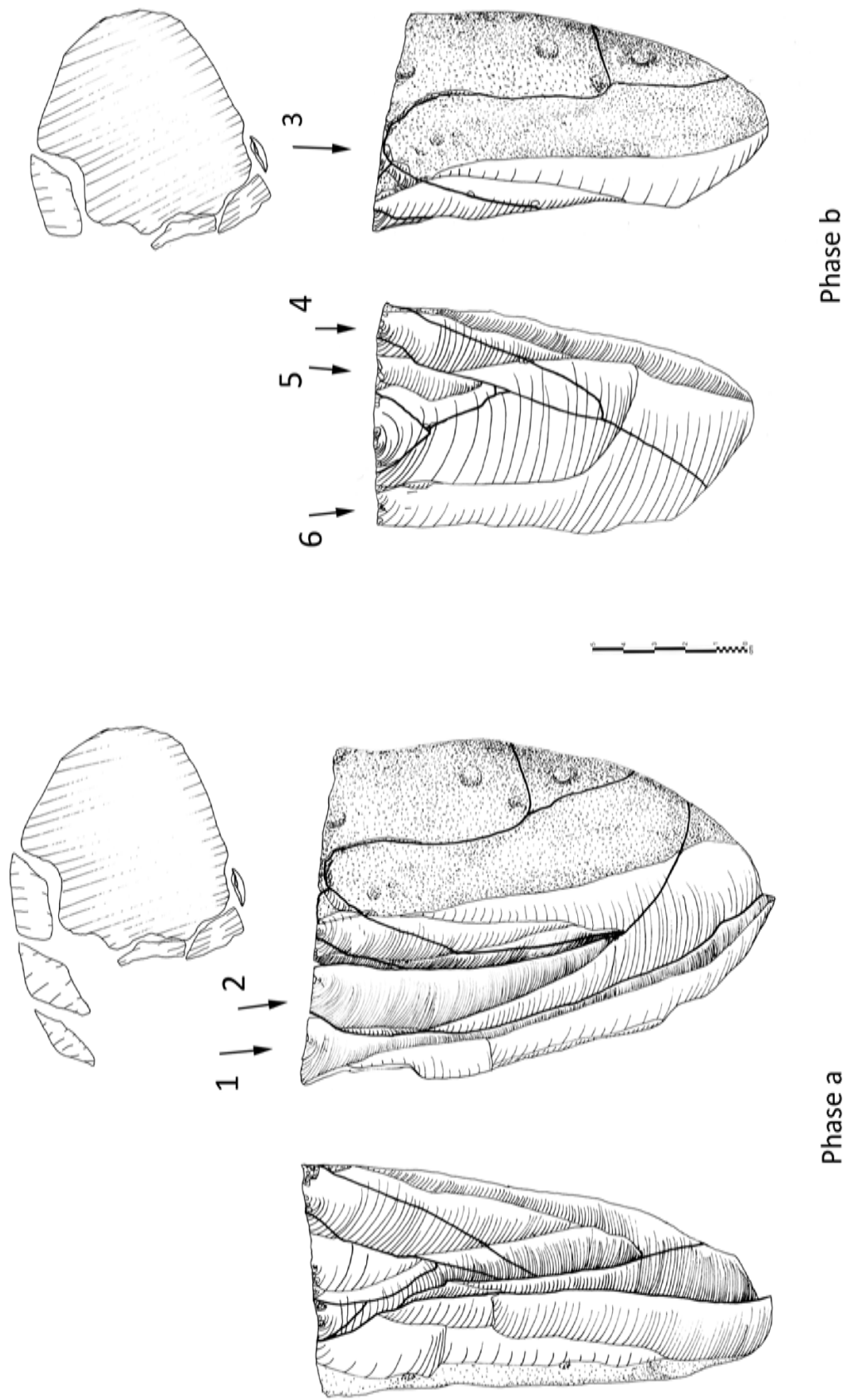


Figure 8.8 TH.128 refitting . (Illustration by Y. Hilbert).

Reduction started with the decortication of the nodule's narrow edge, no platform was set up, given that the nodule exhibited a natural fracture plane in a nearly 90° angle to the technological axis used for blank production. Subsequent to the removal of the first cortical blade, a succession of three large *débordant* elements were struck, two exhibiting overpassed terminations. The two initially reduced *débordant* blades were removed from the left side of the core's plane of removal. Subsequently reduction shifted to the right side in order to correct the core working surface symmetry. These removals left a keeled surface on the core's working surface that was subsequently exploited. The blanks removed from the central area of the core are missing from the refit. Based on the negatives visible on the reconstructed plane of removal, the blanks would have been elongated with converging edges and free of cortex. Interconnected with the production of these elongated converging blanks, surface control detachments from the core's lateral peripheries would have maintained horizontal and longitudinal convexity.

As reduction progressed and the core's working surface reached a point where reduction could not continue without producing blanks with hinged terminations, convexity restoration measures were initiated. Following the removal of an overpassed *débordant* element from the core's right edge, convexity was tentatively re-established. The following removal would have presented a symmetrical triangular cross-section and diamond shaped lateral edges. These pieces have been removed from the site. The disposition of the blanks negative is used to infer the configuration of the desired end products. The subsequently removed blank, however, exhibited an irregular shaped silhouette. It's cross-section, although trapezoidal, was equally asymmetrical. The subsequently removed blank could not be found at the site; however, the following removal was present and could be reattached to the core. The last removal gave the core its deserved "deathblow"; this elongated *débordant* removal detached the cores distal portion, spoiling the object's symmetry beyond rectification. Reduction of the nodule halted and the core was abandoned.

8.1.3 TH.133

The surface scatter TH.133 was found on a low primary terrace overlooking a minor tributary of Wadi Haylah. The slope of a secondary terrace located three metres above the primary terrace where the scatter had been identified served as raw material source for the prehistoric populations occupying the site. Conform to the local geology, large flint nodules with thin dark cortex have been found outcropping from the *gahit member*.

The locality is characterized by a moderate- to high-density artefact cover, again artefacts, geofacts and limestone shatter litter the surface of the site. Technologically distinct blank production methods have been identified at the site, apart from the ubiquitous production of elongated blanks, using a unidirectional single platform reduction, the production of flakes from a flat face of flint nodules, using a radial reduction method was observed. The undifferentiated flakes and radial cores had a lighter patination than the blade vestiges found at the site. Also, as in most of the sites located in the immediate proximity of a raw material outcrop, the technologically diverging blank production modalities were found constrained and spatially separated from each other. Given the technological divergence observed on the artefacts, TH.133 is considered to be the result of two different groups separated in time and exerting diverse reduction strategies. Considering the focus of this dissertation, collection and descriptions were limited to the Nejd Leptolithic component of the site.

Refitting activities undertaken directly at the site revealed an artefact constellation depicting the reduction of a core in its advanced stage of preparation. A total of six elongated blanks and their corresponding core were collected and will be described here, in order to help identify variability within the blade production used (Figure 8.9).

The core has a single unprepared flat striking platform, made up of a natural fracture on the raw material nodule. The piece exhibits a cortical back and five unidirectional parallel removals on its working surface, which is positioned on the narrow edge of the

raw material nodule. Horizontal and longitudinal convexities were completely exhausted. The *débitage* pertaining to the constellation encompasses five *débordant* elements and one blade. The *débordant* elements exhibit either overpassed or feathered terminations; morphologically little variation is seen among the *débitage*. The single blade reattached to the refit has parallel sides, a unidirectional scar pattern and an overpassed termination. All *débitage* exhibit plain unprepared striking platforms consistent with the striking platform observed on the core.

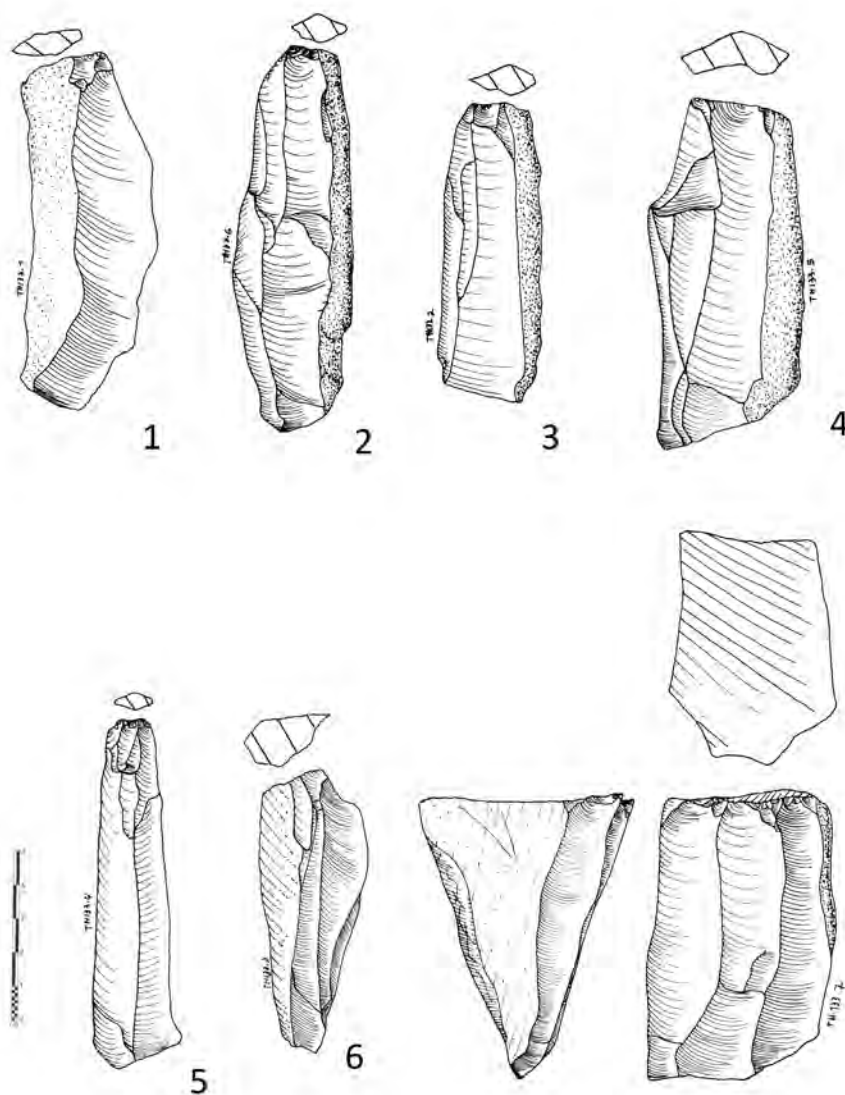


Figure 8.9 TH.133 refitting débitage.
(Illustration by Y. Hilbert).

The refit does not mirror the complete reduction procedure, but an entire cycle of reduction starting with the convexity maintenance procedures, the exploitation of the created convexity and subsequent discard of the core were recorded (Figure 8.10). Three *débordant* elements were reattached to the core, these have been removed between convexity exploitation phases, as may be seen on the converging negatives visible on the dorsal surface of the blanks reduced from the right edge. The *débordant* element struck from left edge of the core's working surface was detached earlier in the reduction process and displays a single large unidirectional negative on its dorsal surface. The blanks pertaining to the exploitation of the created ridges could not be found and were possibly transported away from the site for further manipulation.

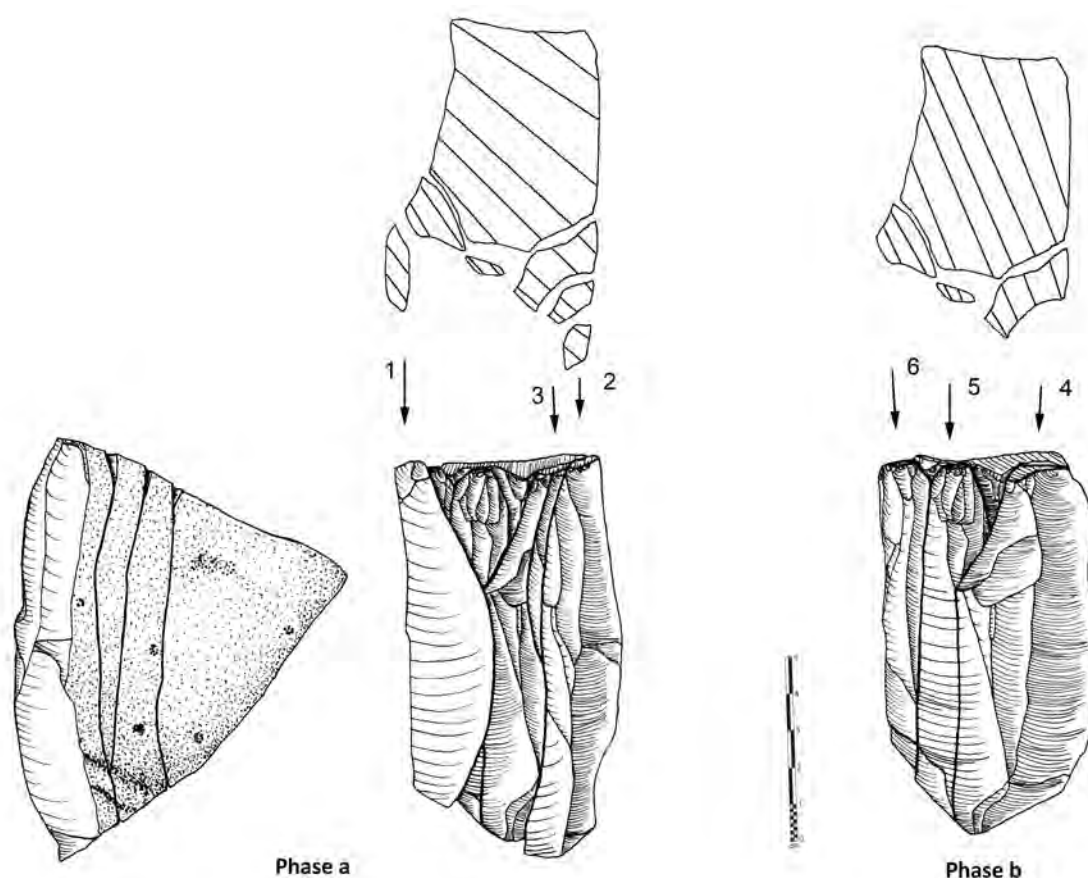


Figure 8.10 TH.133 refitting.
(Illustration by Y. Hilbert)

The reduction of the *débordant* elements from both left and right portions of the core's working surface created a keeled plain, which was then exploited. After two elongated blanks with converging sides were detached and removed from the site, a *débordant* element was removed from the right edge of the core, thus creating a centrally running ridge on the core's plane of removal. The overpassed blade reattached to the central portion of the core, overshooting the core's working surface; nonetheless, the slightly lateralized ridge created by this removal was used to produce an elongated blank with converging sides. The last removal, a *débordant* blade detached from the core's left side failed to restore convexity and the core was abandoned.

8.2 Wadi Haluf 1 (TH.124b)

8.2.1 Site Location

Found during the field season of 2011, the Wadi Haluf 1 site is located in the upper portion of the wadi that bears the same name. Wadi Haluf runs north westwards from the Dhofar Escarpment before joining Wadi Ghadun in the central region of the Nejd Plateau. Running in a southeast to northwest axis, the wadi valley extends for approximately 35 km, measuring approximately 2,5 km wide at its broadest point. On its course across the southern Nejd, Wadi Haluf dissects a rugged table landscape composed of tertiary Limestone of the *Rus Formation* of the middle part of the Hadhramaut group. The wadi course itself is currently dry, filled with fluvial detritus and partially covered by an eolian blanket. The braided fluvial pattern visible in the dry wadi bed bears witness to a gradual decrease in fluvial energy and the subsequent suffocation of the stream by fluvial detritus and larger boulders. Adjacent to the dry wadi bed, a low and undulating plain, dotted with inselbergs and dissected by small erosional gullies may be seen (Figure 8.11).



Figure 8.11 Wadi Haluf 1 photographs.
scatter situation; 2 Wadi Haluf 1 find scatter (Photograph Dr. J. Rose
and Y. Hilbert).

The site itself is situated on the eastern side of the wadi in the immediate proximity of a group of low inselberg. These low hills have been identified as remnants of the Upper Hadhramaut Group, more precisely to the *gahit member*. Colluvial detritus composed of limestone shatter and chert nodules, supported by an eolian matrix, covers the piedmont of these inselbergs. Very few artefacts have been found on the slopes; the majority of lithics were found scattered across the undulating plain composed of fairly sorted and rounded fluvial gravels of medium size (5-15 cm in diameter), covered by gypsum and blanketed by a 5 -15 cm thick eolian carpet.

Wadi Haluf 1 is a medium to high-density surface scatter, covering approximately 300 square metres. Within this large surface site, smaller concentrations have been detected. Raw material used and patination observed on the artefacts is very homogenous. Given this uniform appearance, the lithics found at the site have been tentatively attributed to a single cultural period, namely the Nejd Leptolithic (Hilbert *et al.*, 2012).

8.2.2 Sampling strategy and documentation

In order to sample the Wadi Haluf 1 site, a spatially constrained grid was placed over a concentration of artefacts. The 3 x 4 metre grid was divided into 1 square metre units; all artefacts within these units were collected and the surface eolian cover excavated for further “buried” artefacts. No artefacts were found lodged within the gypsum layer. All artefacts found were subjected to lithic attribute analysis and refitting studies.

Prior to the artefact collection, each of the square metre units was photographed in a nearly vertical angle. The twelve pictures were later arranged against one other, in order to reconstruct the collected surface. Thanks to the photographic documentation of the collected surface, the position and spatial relation between the refitted objects could be traced, providing valuable information regarding spatial patterning at the site.

8.2.3 Spatial distribution

As noted above, the Wadi Haluf 1 scatters stretch across a large area and undoubtedly has been deposited over a considerable amount of time. Unfortunately, absolute dating methods could not be applied to the site, making a secure chronological attribution of the lithic assemblage impossible; however, thanks to the spatial analysis and the refits, relative chronological affinity between some of the artefacts collected from the sampled area could be established.

The twelve square metres collected and documented for this study exhibit a large number of artefacts found on the surface and slightly below the surface, averaging 41 artefacts per square metre (Figure 8.12).

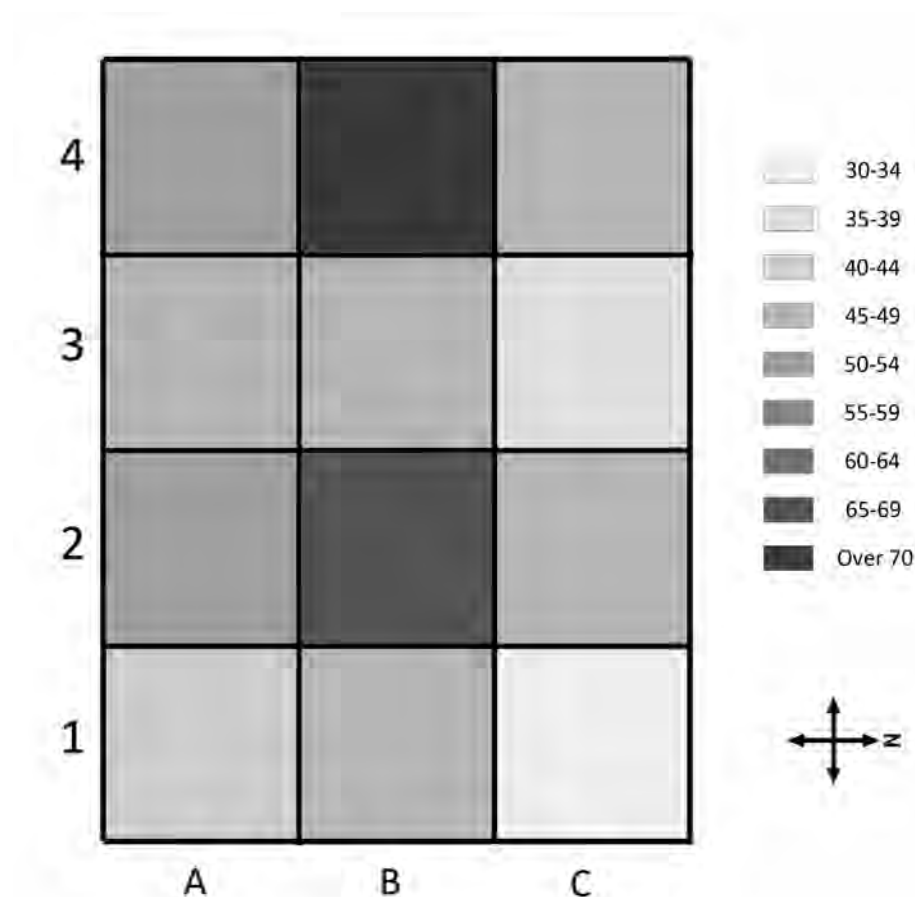


Figure 8.12 Wadi Haluf 1 artefact density.
(Image by Y. Hilbert)

Within these twelve units, fourteen refits have been made; their locations within the sampled area are illustrated in Figure 8.13. Based on these refits and the intensified distribution of artefacts within two higher concentration *loci* inside the collection grid, the following statements may be made concerning spatial distribution: (a) artefacts have suffered little post-positional displacement, (b) the different concentrations reflect knapping events. The main concentration, based on the refits and artefact distributions, was observed around squares B2 and B4. Refits have been successfully accomplished between artefacts laying in squares A3, B1, b2, C1 and C2. The refits around B4 are less numerous and possibly relate to a second concentration to the west of the collection area.

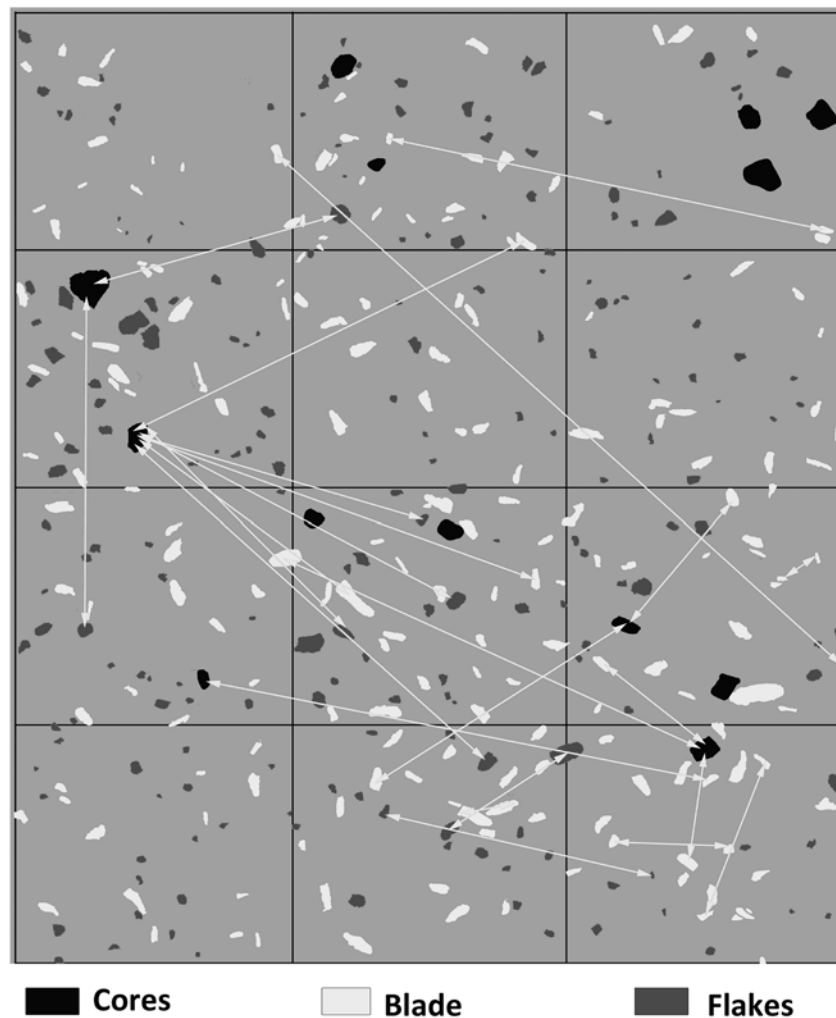


Figure 8.13 Wadi Haluf 1 spatial distribution.
(Image by Y. Hilbert).

8.2.4 The assemblage

In total, 590 artefacts were recovered, including thirteen cores, three tools, and 574 pieces of *débitage* (Table 8.1). Of these 574 pieces of *débitage*, 76 were classified as chips, leaving a total of 498 *débitage* elements on which attribute analysis have been undertaken.

Table 8. 1 Wadi Haluf 1 artefact count.

	TOTAL n	%
<i>Flakes</i>	93	16
<i>Blades</i>	164	28
<i>Bladelets</i>	13	2
<i>Cortical Flakes</i>	51	9
<i>Cortical Blades</i>	50	8
<i>Débordant Flakes</i>	18	3
<i>Débordant Blades</i>	107	18
<i>BTF</i>	2	0,5
<i>Chips</i>	76	13
<i>Cores</i>	13	2
<i>Tools</i>	3	0,5
<i>Total</i>	590	100

Blades and *débordant* blades are by far the most numerous types of *débitage* found within the assemblage. Flakes are less numerous than blades and *débordant* elements accounting for only 16% of the *débitage*. Cortical elements, as in cortical blades and flakes, are slightly more numerous than flakes and make up 17% of the blanks.

Only thirteen cores were found within the assemblage. The low core to *débitage* ratio of 1:44 is noteworthy, possible reasons for this will be discussed later. Three tools were found at the site and will also be discussed here.

Blank production using varying modalities of unidirectional parallel reduction was the main activity undertaken at the site based on the *débitage* analysis. To a minor extent, the production of trifaces is attested by two bifacial thinning flakes and a triface preform collected in the proximity of the sampled area.

Raw material and patination are very homogenous; all artefacts were made of chert nodules outcropping from the *gahit member*. Chert nodules found in the proximity

of the collection area show the same characteristics as those observed on the collected artefacts. Raw Material varies in dimension from kiwi- to watermelon-sized nodules, usually displaying an nearly ovoid cross-sections. The cortex is thin and smooth textured, displaying dark hues of colour. When found directly cropping from the limestone, the cortex exhibits lighter shades of brown and slightly courser texture. Freshly knapped pieces of this raw material exhibit a light grey colour, while the archaeological material is dark grey with shadings of dark yellow.

8.2.5 Débitage

As noted above, blank production was the most frequent activity undertaken at the site. No severe edge damage was found on the *débitage*, suggesting little post-depositional displacements by erosional forces; attesting to a fairly undisturbed sample. Although no trampling fractures have been observed on the artefacts, breakage is considered high among the *débitage*. The three most significant blank classes within the assemblage, *débordant* blades, flakes and blades, exhibit a high amount of breakage. Of the 164 blades found at the site only 70 (57%) were found to be complete. Flakes were less fractured; 63% of all flakes (n=59) were complete. *Débordant* elements were even less fractured than flakes; of the 107 *débordant* blades 73% (n=78) were complete.

The ratio of cortical elements (cortical flakes and cortical blades) to non-cortical is 1:4, indicating that on site decortication took place; 72% of the blades (n=116) have between 0% to 10% of cortical cover. Flakes show a similar pattern, a total of 60% (N=55) have between 0% to 10% of cortical cover. Both blades and flakes have generally less dorsal cortical cover. *Débordant* elements, regardless whether flake or blade proportioned, show higher amounts of dorsal cortical cover. In total, 51% of the *débordant* blades (n=54) exhibit 11% to 25% of cortical cover; the second most numerous, with 44% (n=47), are the *débordant* blades with 26% to 50% of cortical cover. As for the *débordant* flakes, of the eighteen found, eleven (61%) show between 11% and 25% and six (33%) between 26%

and 50% of cortex cover, consistent with the pattern observed on the *débordant* blades. The thirteen bladelets and two BTFs exhibit no or only very little cortex.

Débitage platform morphology is painstakingly uniform, striking platforms are predominantly plain. Cortical elements, blades and flakes show minimum variability in striking platform disposition, in that only four flakes display faceted striking platforms and two display dihedral striking platforms. Blades are less variable, only two dihedral striking platforms have been observed. Two of the 51 cortical flakes had faceted striking platforms. The *débordant* elements and the bladelets display plain striking platforms, while the two identified BTFs show either faceted or crushed striking platforms.

Striking platform dimension analysis based on IPF indicated that blank platforms are wider than they are deep. Flake striking platforms have show the highest amount of variability (s.d. 1,16 avg. 2,69). Blades and *débordant* blades exhibit identical average IPF values (avg. 2,33). *Débordant* blades exhibit greater variability based on the standard deviation values (s.d. 0,73). Cortical elements produced diverging IPF; pieces with flake proportions exhibit a higher average value (avg. 2,48) than the blade proportioned cortical elements (avg. 2,24).

Débitage mid point cross-section shows little variability. Flakes, blades and *débordant* blades possess mostly trapezoidal cross-sections, respectively, 30%, 42% and 59% (n=30, n=68 and n=63). *Débordant* blades with trapezoidal cross-sections have one cortical lateral edge; also observed among the *débordant* blades were equal amounts of triangular and triangular lateralized cross-sections (16%, both n=17). To a lesser extent, *débordant* blade's midpoint cross-sections had in 7% (n=7) of the observed cases more than three vectors. Blades presented a high percentage of pieces with triangular cross-section totalling 33% (n=54). Such cross-sections are indicative for the use of a guiding ridge left on the core's working surface by previous removals. Flakes have a wider range of midpoint cross-sections: 19% were flat (n=17), while triangular and triangular lateral steep cross-sections were observed in similar percentages (19%) in the flake sample

(n=15 for both triangular and triangular lateral steep). The thirteen bladelets found at the site display to a greater extent triangular cross-sections (n=9) and to a lesser extent trapezoidal or more than three vectors (n=3 and n=1). The bifacial thinning flakes have been found to possess either flat or more than three vector cross-sections.

Flakes and blades show similar longitudinal cross-sections: 54% and 50%, respectively presented flat profiles (n=43 and n=67). While 27% of the flakes (n=21) have curved profiles, only 19% (n=26) of the blades have such a pattern. Blades show a greater number of specimens with twisted longitudinal cross-sections (n=41). Such a pattern indicates that blades were removed from guiding ridges positioned at the lateral periphery of the core's working surfaces. *Débordant* blades have shown a contrary pattern; 42% of the *débordant* blades have curved longitudinal profiles (n=43). Flat and twisted profiles occur on 26% (n=26) and 32% (n=33) of the *débordant* blades, respectively.

The distal terminations observed on the *débordant* blades has been found to be overpassed in 38% (n=38) of the observed cases. Both the distal termination and longitudinal profile of the *débordant* elements indicate the use of these removals as core working surface convexity correction measures. A greater portion of these *débordant* blades, 53% to be exact, exhibit feathered terminations (n=52), indicating that the overshoot character observed on some of these blanks is not a desired feature but more the result of excessive force in the blank removal procedure. Additionally, a logical consequence of the overpassed termination is the reduction of the core's working surface; representing volume that can no longer be purposefully exploited. Only 9% of the *débordant* blades possess hinged terminations (n=8).

Flakes and blades have similar blank termination types, as do the *débordant* elements; feathered terminations have been found on 60% of the flakes and on 73% of the blades (n=47 and n=80). Hinged terminations were observed on 31% of the flakes and on 18% of the blades (n=24 and n=20), while overpassed terminations were recorded on fewer pieces; both 9% (respectively n=7 and n=10).

The percentage of pieces detached off axis has been found to be relatively balanced among the three main *débitage* types found at Wadi Haluf 1; 29% of the flakes and 23% blades were struck in off axis (n=18 and n=19). *Débordant* blades percentages were found to be slightly higher with 35% of the observed cases struck off axis (n=29).

Blank shape has been found to be predominantly rectangular, displaying parallel edges; nonetheless, some differences among the *débitage* classes have been observed. The three major *débitage* classes have mostly parallel edges, 38% of the flakes (n=35), 50% of the blades (n=80) and 37% of the *débordant* blades (n=40). The elongated *débitage* has a higher percentage of pieces with converging sides, 23% of the blades (n=37) and 20% of the *débordant* blades (n=21) present a triangular silhouette (Figure 8.14). Additionally, *débordant* blades exhibit in 17% of the cases a lateralized silhouette (n=18), a slightly higher percentage when compared to flakes and blades where only 6% and 7% have such a shape (respectively, n=5 and n=11). While 18% of flakes and 19% *débordant* blades (respectively, n=16 and n=20) exhibit expanding edges, this shape is seldom observed among blades; only 9% have this shape (n=15). To a lesser extent, the three main *débitage* types exhibit either ovoid or irregular lateral morphologies. *Débordant* flakes exhibit either expanding or lateralized edges, while bladelets are exclusively rectangular or triangular in shape. Of the two BTF, one exhibits lateralized shape, while the other is of irregular shape.

Flake, blade and *débordant* blade dorsal scar patterns are marked by the prevalence of the unidirectional scar pattern over the other configurations. A total of 66% of all flakes, 67% of the blades and up to 82% of the *débordant* blades have this particular scar pattern (respectively, n= 60, n= 107 and n=88). Flakes have greater variability; unidirectional crossed, parallel and convergent have been observed on 8%, 12% and 7% (n=7, n=11 and n= 6) of the flakes. A small number of flakes have bidirectional or transverse scar patterns: respectively, 2 and 7% (n=2 and n=5). Blades have a slightly higher percentage of unidirectional convergent over unidirectional parallel scar patterns; while 17% are convergent, 14% of all blades show unidirectional parallel scar patterns

(n=27 and n=22). Only 2% have unidirectional crossed patterns (n=4). *Débordant* blades have the lowest amount of variability; blanks have either unidirectional parallel (12%), convergent (5%) or bidirectional (1%) scar patterns. The few bladelets found within the sample exhibit unidirectional scar patterns. The BTF's possess bidirectional or opposed oriented scars (Figure 8.15).

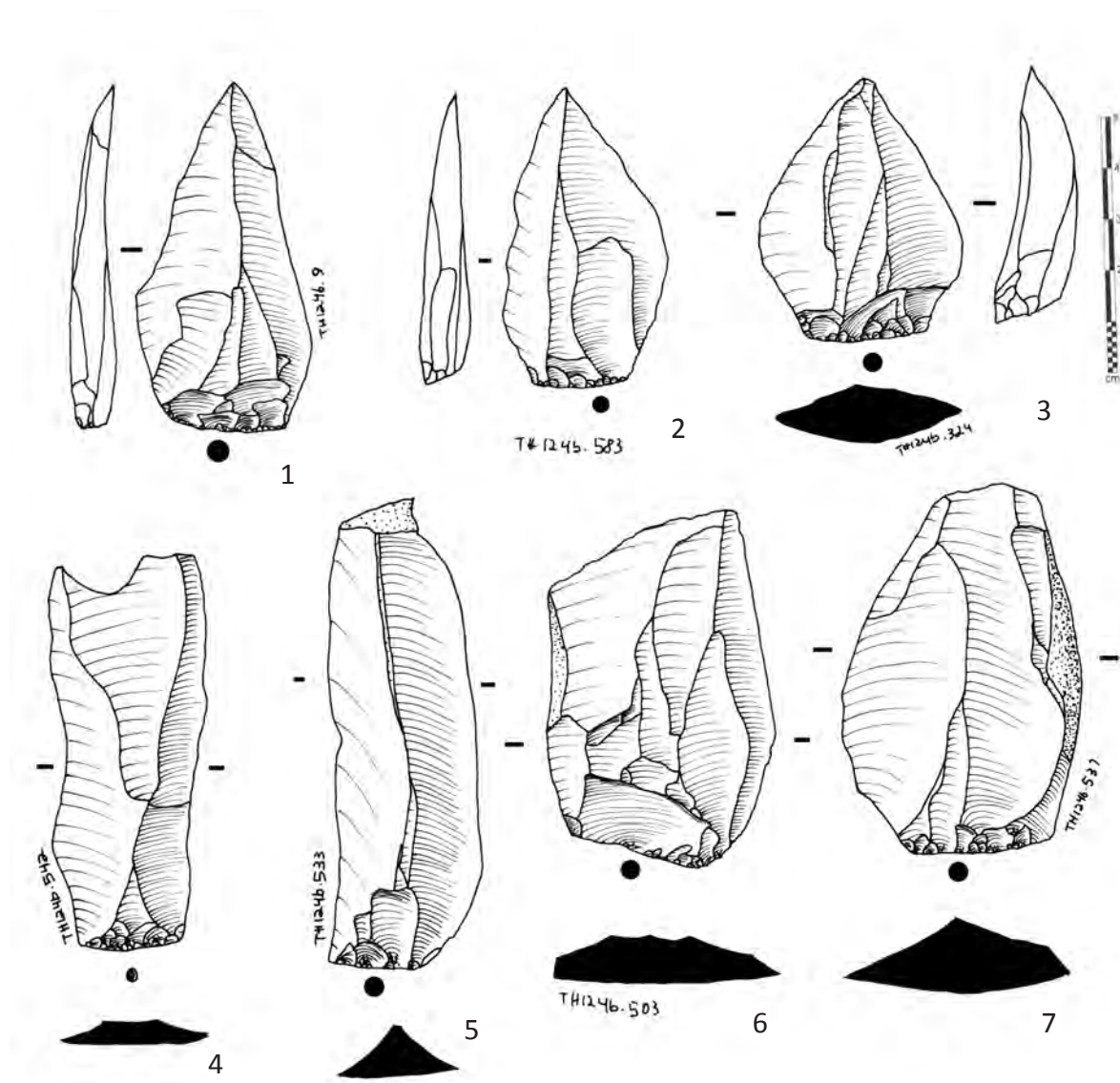


Figure 8.14 Wadi Haluf 1 débitage.

1 to 3 convergent blanks with complex cross sections and unidirectional convergent scar pattern; 4 and 5, blades with parallel sides and unidirectional scar pattern; 6 and 7, flakes removed from the central portion of the core working surface (Illustration by Y. Hilbert)

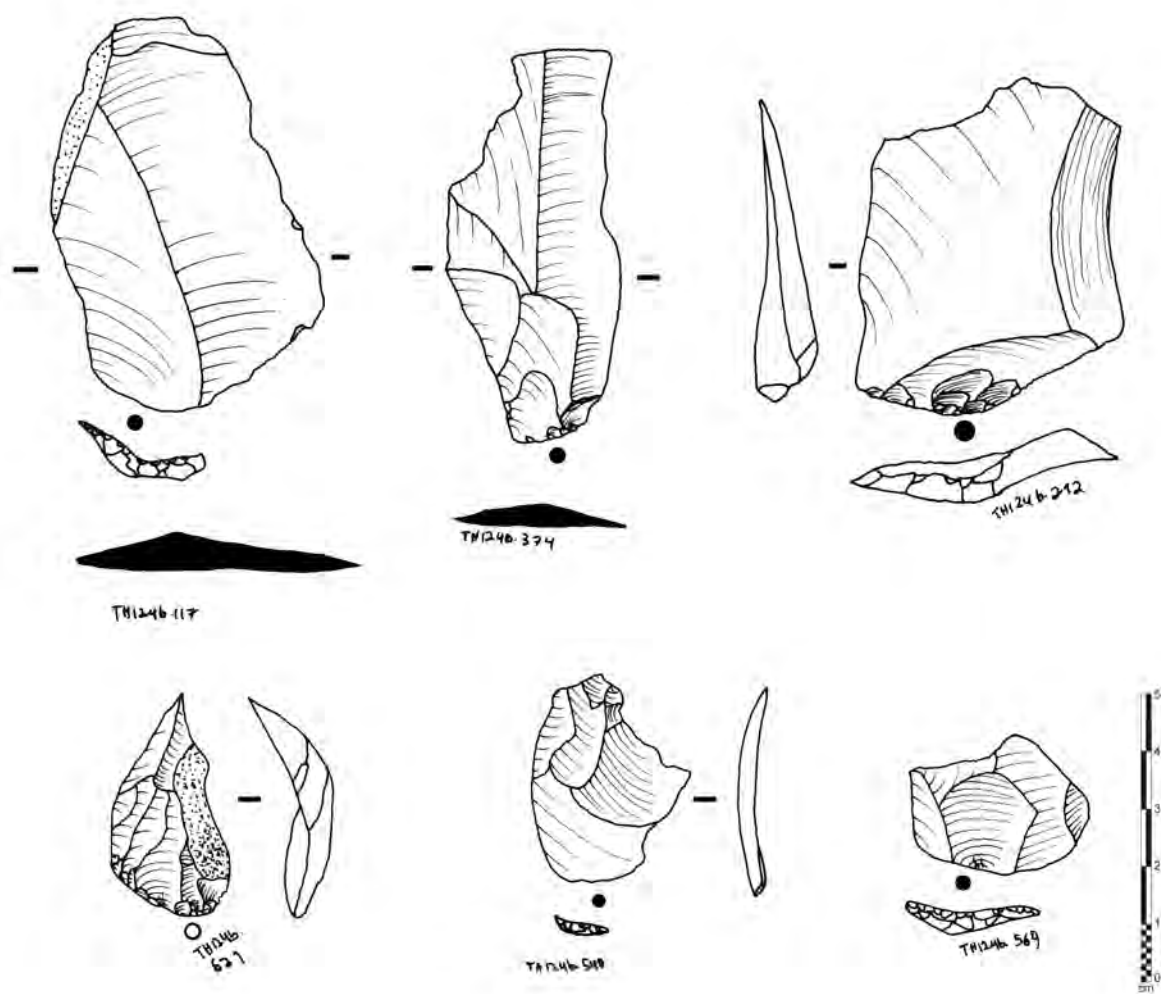


Figure 8.15 Wadi Haluf 1 BTF's .
(Illustration by Y. Hilbert)

Metrical variability expresses a clear divergence in dimensional configurations between each of the identified bank types. This is no surprise, considering that classification of blanks into the main categories (flakes, blades, chips...) rests partly on metrical observations. Average blank surface measurements indicate a tendency towards the production of elongated end products, an equally expected fact when considering that 56% of the artefacts recorded have proven to be twice as long as they are wide. Cortical elements are larger on average than the flakes, blades and *débordant* elements, while blade *débordant* are larger and thicker than blades. Interestingly, relative platform size (RPS) of *débordant* blades are higher than blade RPS (22,12 and 14,84), indicating that *débordant* blanks surface size in relation to platform size is higher than that of blades. This

feature sustains the segregation of these *débitage* elements as core surface enhancement agents, while through the removal of these pieces a large portion of the core's working surface was transformed, core platforms suffered less decrease in relative size.

8.2.6 Cores

The thirteen cores collected from the Wadi Haluf 1 sampling area mirror the configuration of the *débitage*. The majority of these artefacts (n=10) are unidirectional single platform parallel blade cores. Platform preparation was kept minimal; six of the examined cores of this class possess straight striking platforms created by a single blow. The remaining four unidirectional parallel cores have natural plain striking platforms. Core flaking surfaces were either placed on a narrow edge of a flint nodule (n=3) or on a frontal face, with an additional supplementary lateral working surface (n=4). To a lesser extent, working surfaces were set up in a convex manner across the core's frontal face to one of its lateral faces (n=2) or on a frontal plain with two additional working surfaces, one of each side of the core (n=1). All except one single platform unidirectional parallel core exhibited faulty longitudinal convexities; four cores had working surfaces ruined by overshoot removals. Three cores had flat working surfaces, showing no indication of attempts to re-establish horizontal and longitudinal convexities, two had working surfaces covered by severe hinge fractures. Cores have elongated working surfaces, conforming to blade production (Figure 8.16). On average, unidirectional parallel cores weigh 427,2 g, with cores presenting additional working surfaces, either on one or both sides, weighing less than other cores. Unidirectional parallel cores were, on average, 82,58 mm in long, 58,22 mm wide and 60,6 mm thick.

A two unopposed platform core was found among the assemblage. This specimen is a textbook example of this core type as observed among the Nejd Leptolithic tradition (Figure 8.17). Similar to the unidirectional parallel blade cores, the two unopposed platform core has been exploited after minimal preparation; two opposed natural plain

striking platforms were used. The reduction surfaces were placed on opposite faces of the core, thus creating two separate unidirectional parallel working surfaces on one nodule. Both surfaces exhibit exhausted lateral and longitudinal convexities. Metrically, the core fits well within the pattern observed for the unidirectional parallel blade cores.

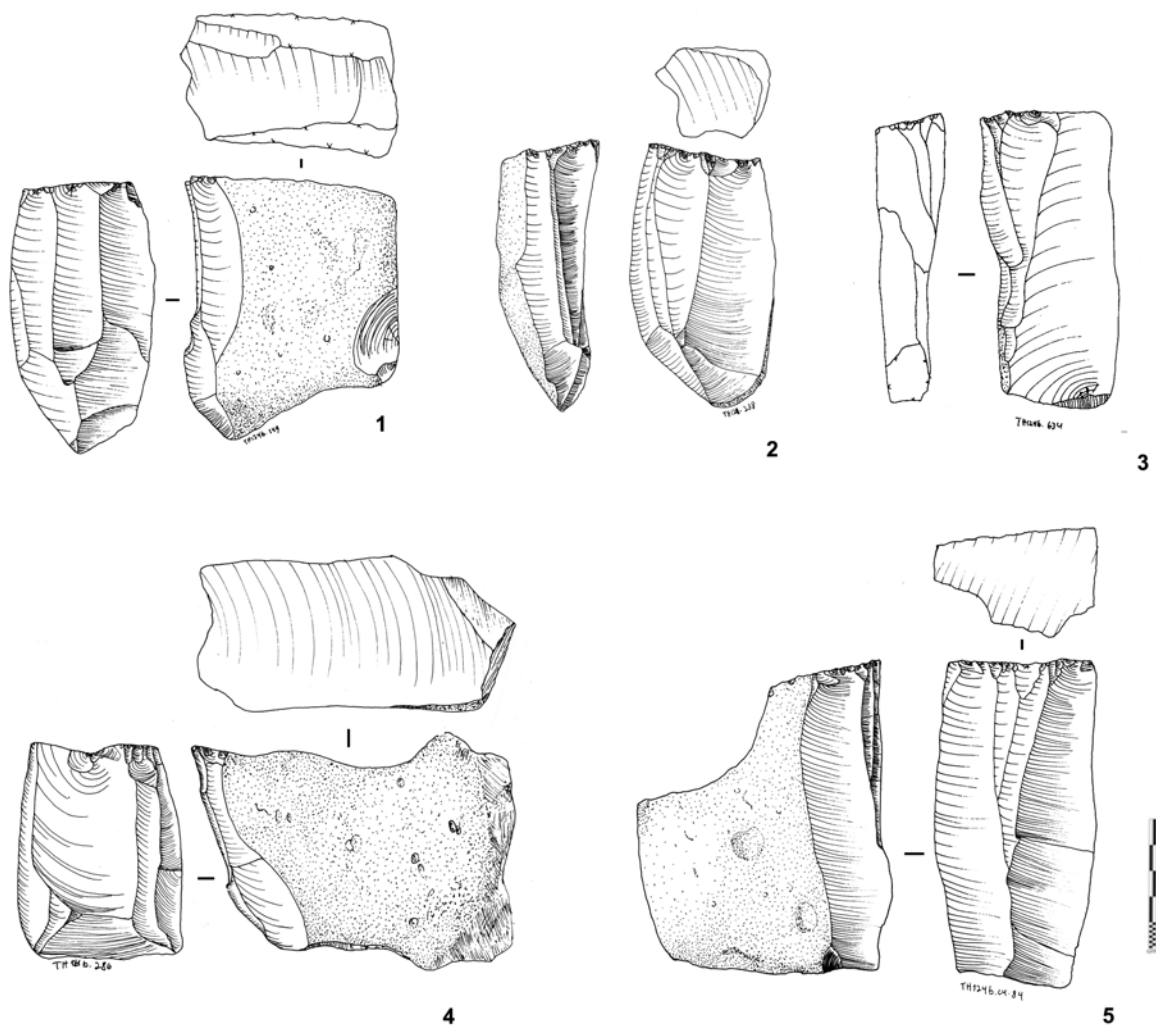


Figure 8.16 Wadi Haluf 1 cores. 1, 2, 4 and 5 unidirectional parallel cores; 3 core on blank. (Illustration by Y. Hilbert)

The two remaining cores have been deemed preforms, based on the early stage of reduction; both exhibited fewer than three negatives.

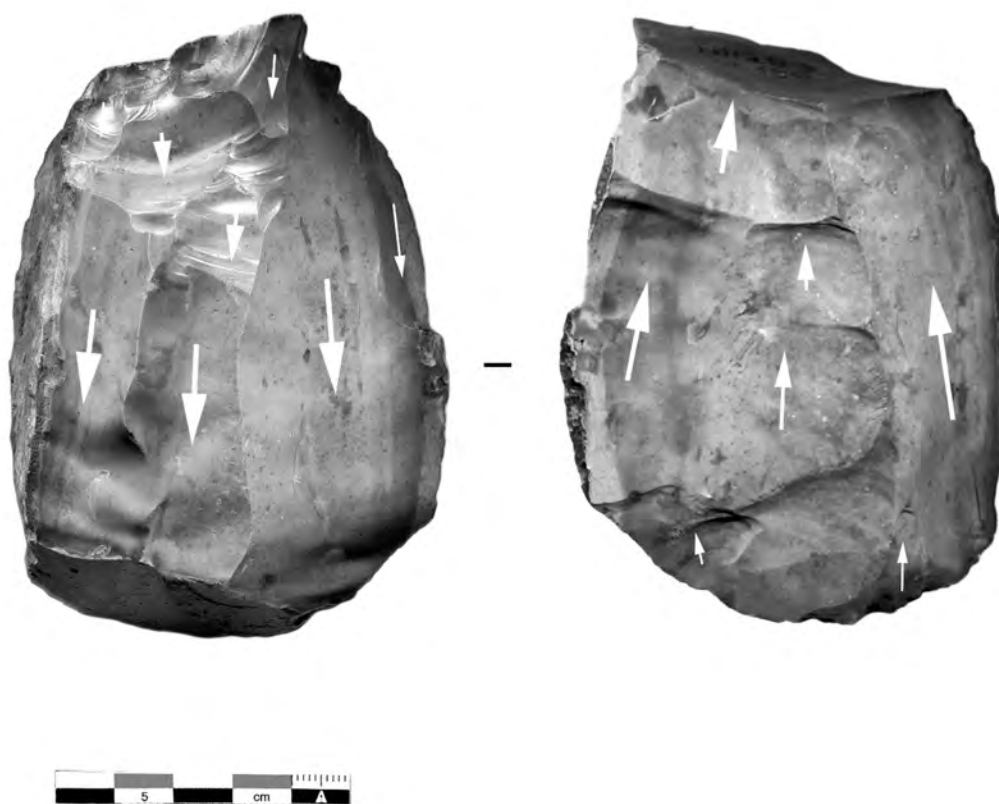


Figure 8.17 Wadi Haluf 1 two unopposed platform core.
(Photograph by Y. Hilbert)

8.2.7 Tools

Three tools were found in the collected area: two informally retouched blanks and one simple endscraper (Figure 8.18). The end scraper was made on a curved blade; unfortunately the piece is incomplete, only the distal retouched portion of the tool was found. Retouch was done by direct percussion and was steep. The two remaining retouched objects were manufactured on blades; both pieces received normal retouch across one third of the blades lateral sides. The retouched edge on one of these gave the piece a slightly concave working edge.

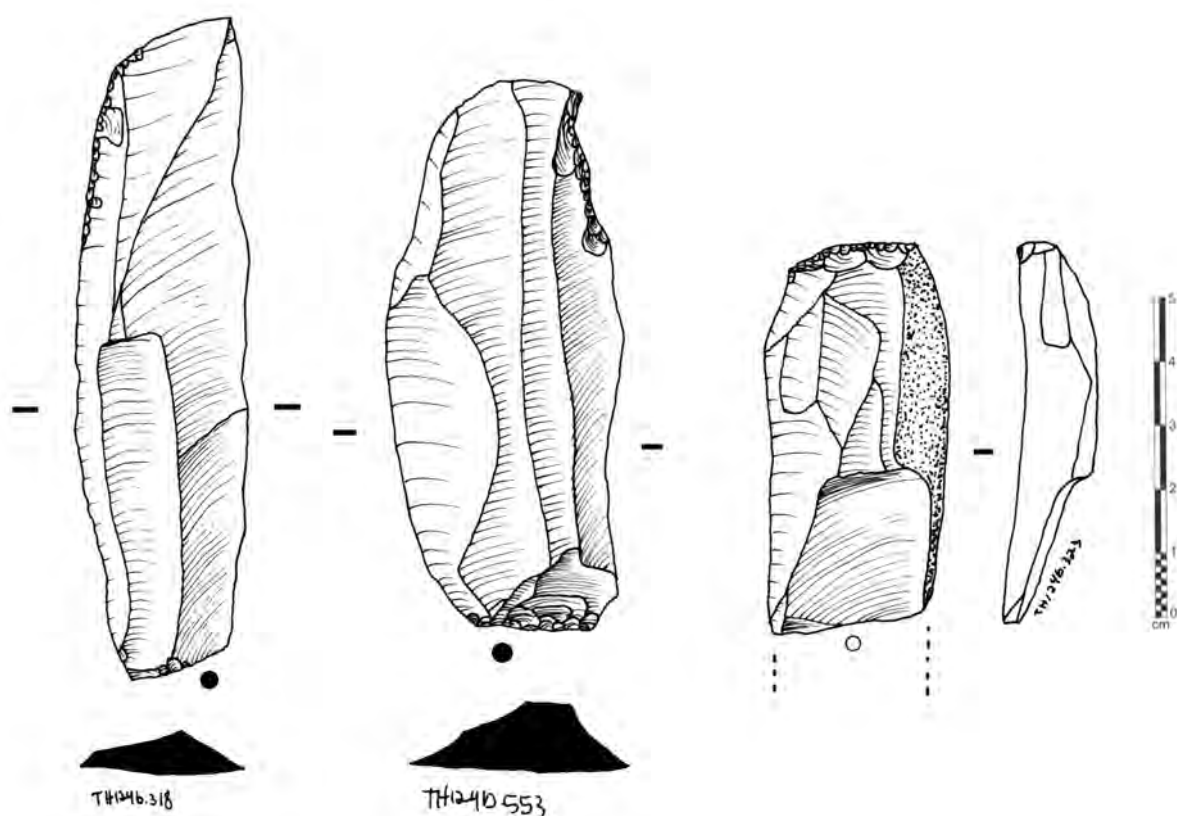


Figure 8.18 Wadi Haluf 1 tools.

1 and 2, retouched blades; 3, endscraper (Illustration by Y. Hilbert).

Two additional tools were found in the proximity of the collection area; one triface preform and a triface (Figure 8.19). Although association between these objects to the manufacturers of the blades found at the site must remain questionable, little indicates that there is any contamination of the site by either older Palaeolithic or younger Neolithic components. Supporting the triface manufacture at Wadi Haluf 1, a series of flakes presenting faceted striking platforms were found in the collection area. These pieces did not present morphologies associated with classical biface production. Most of these pieces have opposed to bidirectional scar patterns and flat longitudinal cross-sections.

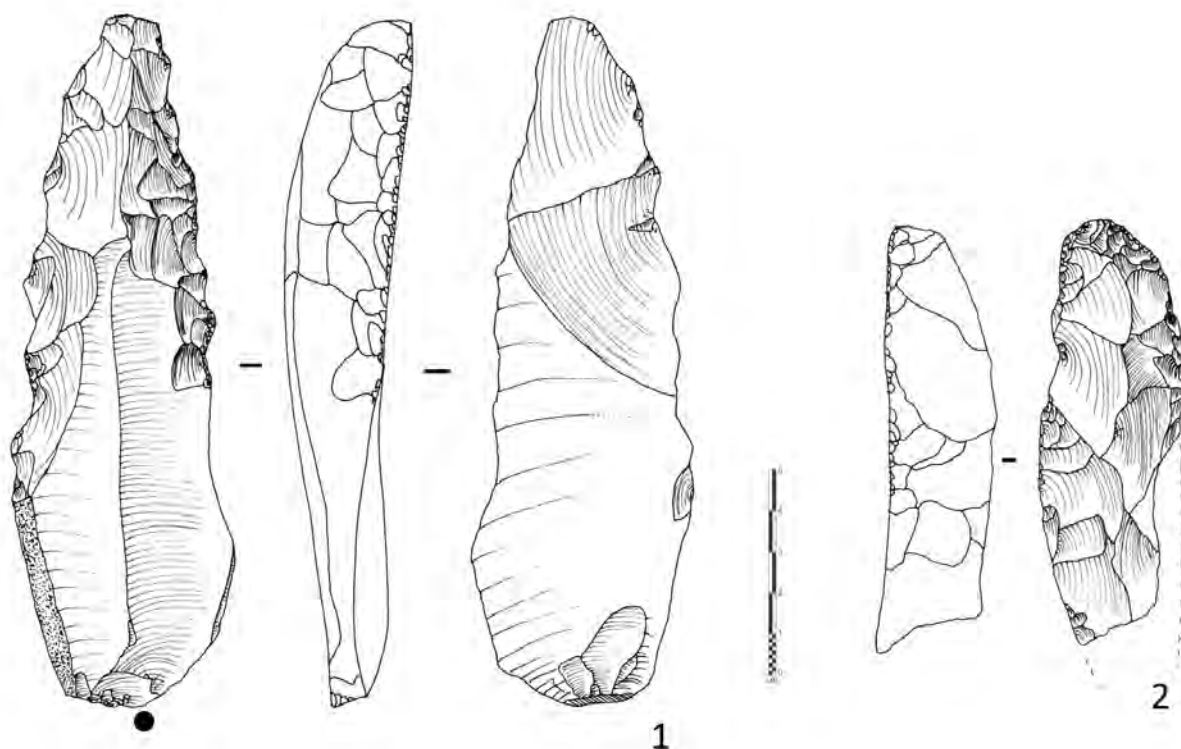


Figure 8.19 Wadi Haluf 1 trifaces.

1, triface preform made on large blade; 2 triface fragment.

(Illustration by Y. Hilbert)

8.2.8 Refits

A total of fourteen refits and conjoins have been made; of these, refit # 14 provided the greatest amount of information. Refit #14 shows seven blanks refitted to a single platform unidirectional core (Figures 8.20 and 8.21). The core's striking platform was created by the removal of a large cortical blade. Two *débordant* elements reduced from the same side of the core's central plane of removal were detached. Subsequently, one *débordant* flake was detached from the opposite side of the core's plane of removal. Afterwards, one overshoot and twisted, irregularly shaped blade was removed from the centre of the core's working surface. Then, two blanks were removed; these were not

present at the site. The negatives of the subsequent removals indicate that these were regular in shape (parallel sides) and possibly represented desired products. Further reduction along the centre of the plane of removal took place; two blades were removed of which one was present at the site, while the other not. The last blank removed from the core was a flake from the centre of the core's working surface. At this point the dorsal convexity had been exhausted and the flake had a hinged termination.

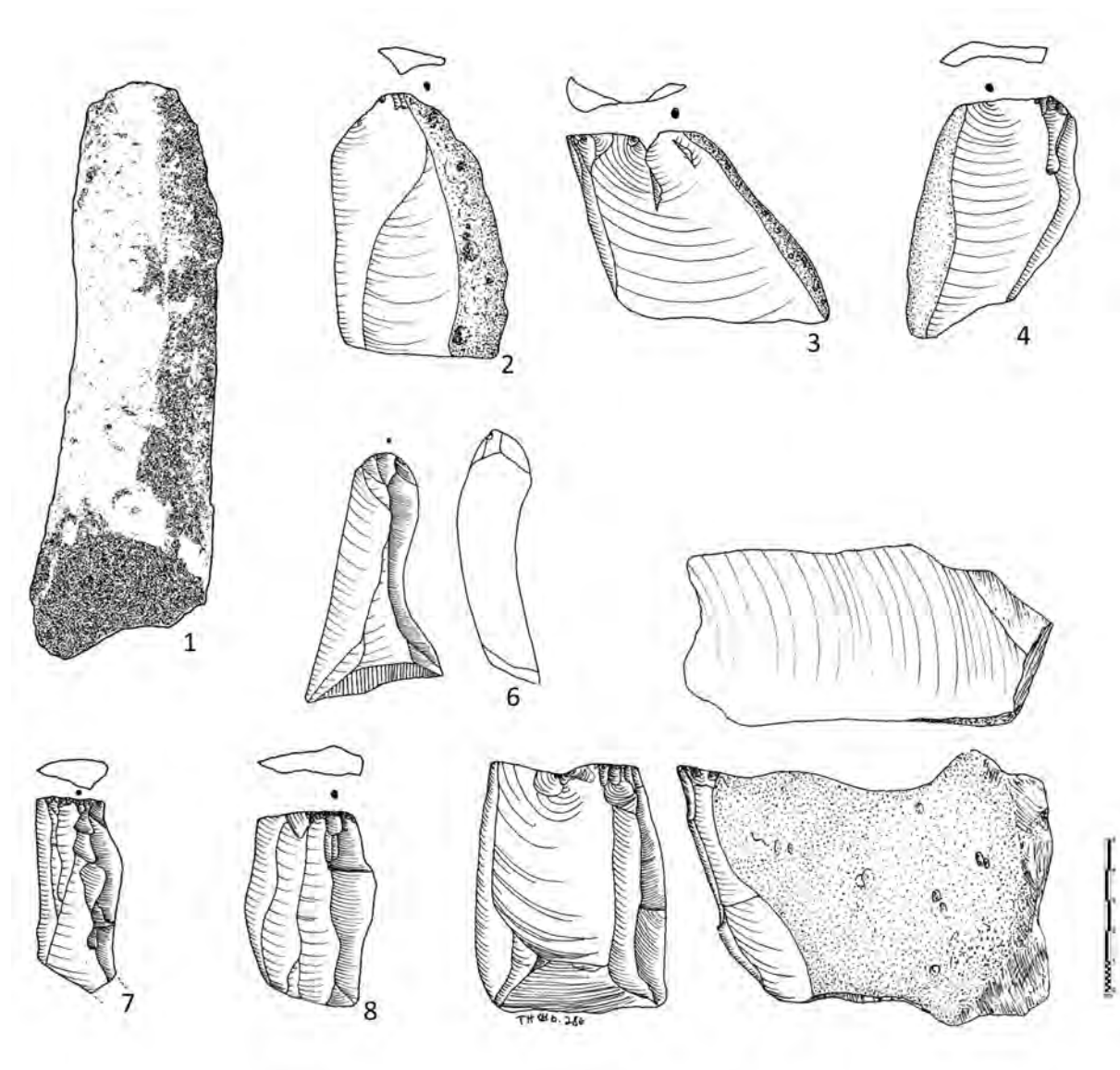


Figure 8.20 Wadi Haluf 1 refit #14 débitage.
(Illustration by Y. Hilbert)

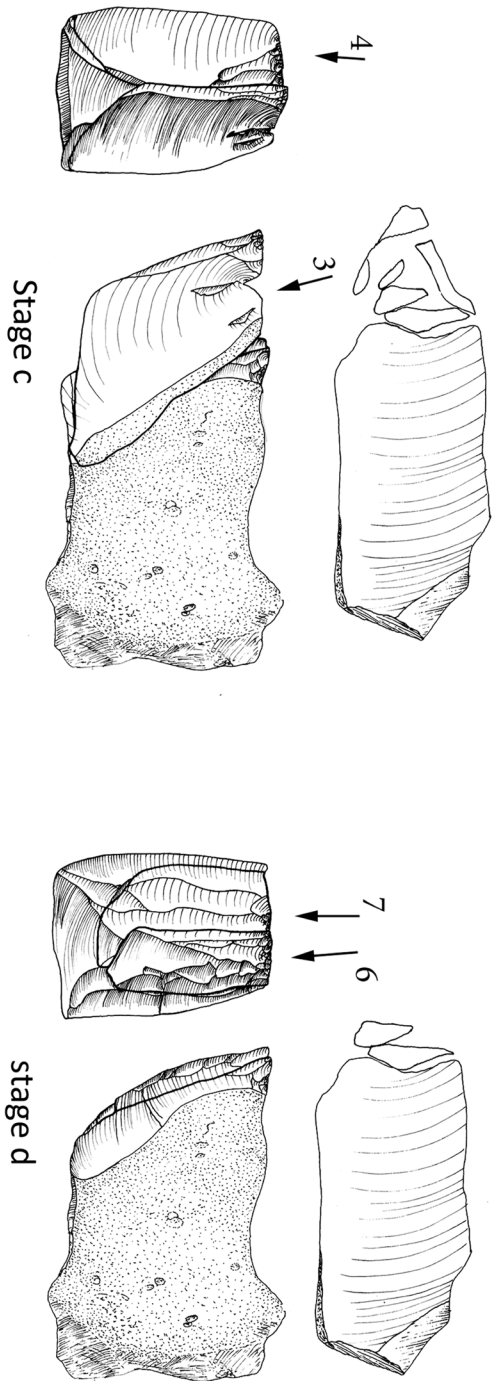
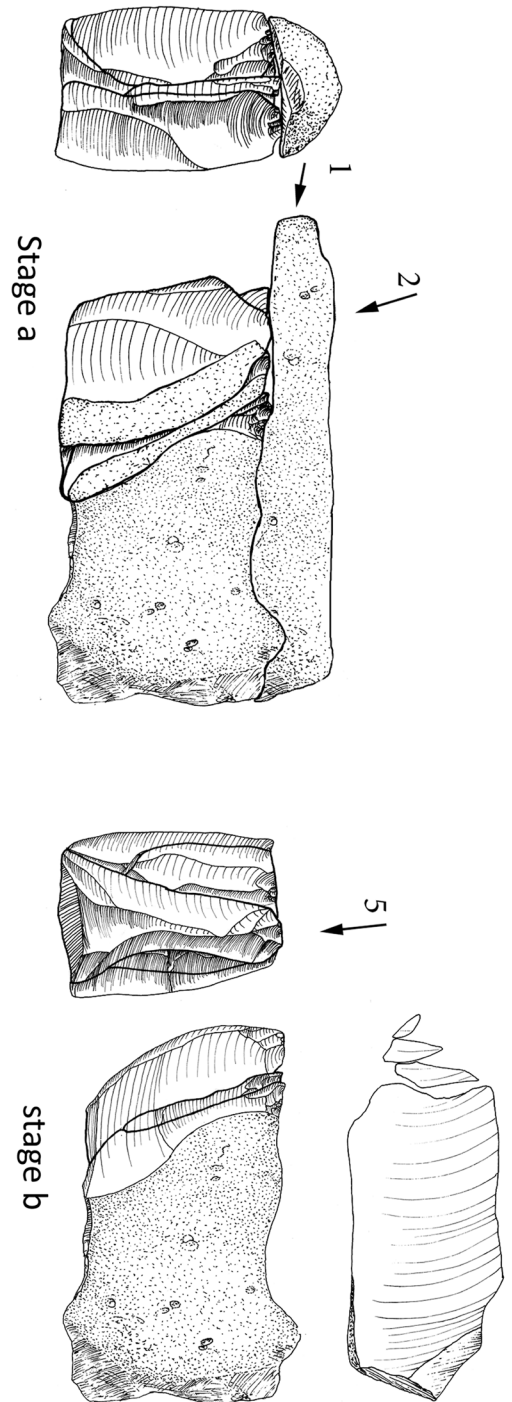


Figure 8.21 Wadi Haluf 1 refit #14.
(Illustration by Y. Hilbert)



Refit #1 and #5 depict isolated phases within the reduction of individual cores; based on these refits, interpretation regarding these particular phases are strengthened. Constellation #1 is marked by two *débordant* blanks refitted to a single platform unidirectional parallel core (Figure 8.22). The two *débordant* blades are of different size; the larger piece was reduced during an early reduction cycle, while the later blank likely represents an attempt to restore the core's convexity. The last removal did not considerably alter the core's convexity, resulting in the abandonment of the core.

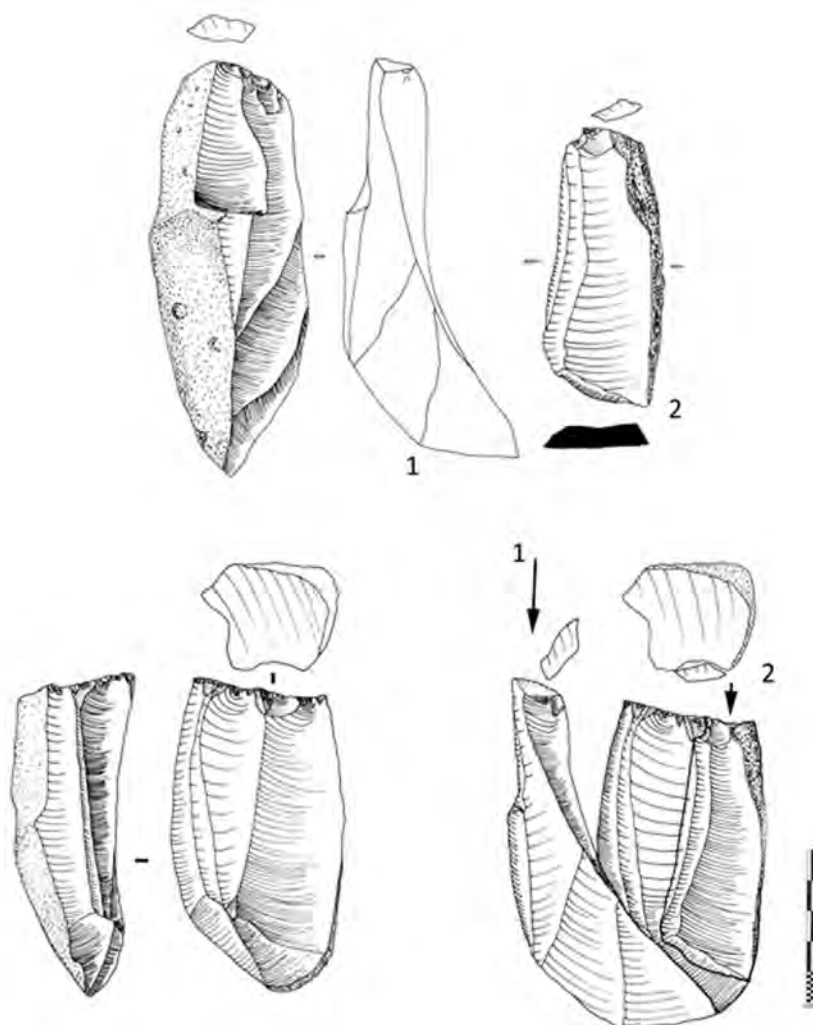


Figure 8.22 Wadi Haluf 1 refit #1.
(Illustration by Y. Hilbert)

Constellation # 5 is composed of three *débordant* blades refitted to a single platform core (Figures 8.23 and 8.24). After a cortical blade was removed (piece present), two unidirectional removals followed (pieces are missing from the site). Subsequently, a large blank was detached from the core's lateral edge (piece was also not found). The first *débordant* was removed, followed by unidirectional removals exploiting the created convexity on the core's working surface. In order to restore convexity, the last *débordant* was removed. All refitted blanks were removed from the supplementary platform located on the core's right side.

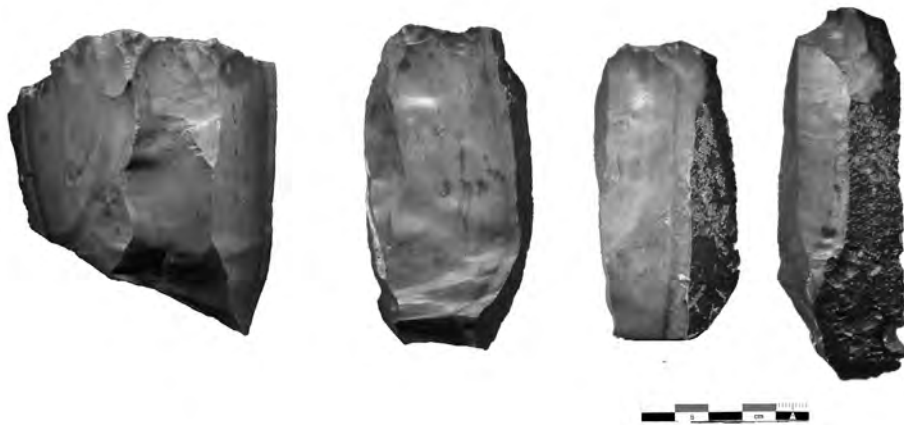


Figure 8.23 Wadi Haluf 1 refit #5 débitage. Above (Photograph by Y. Hilbert)

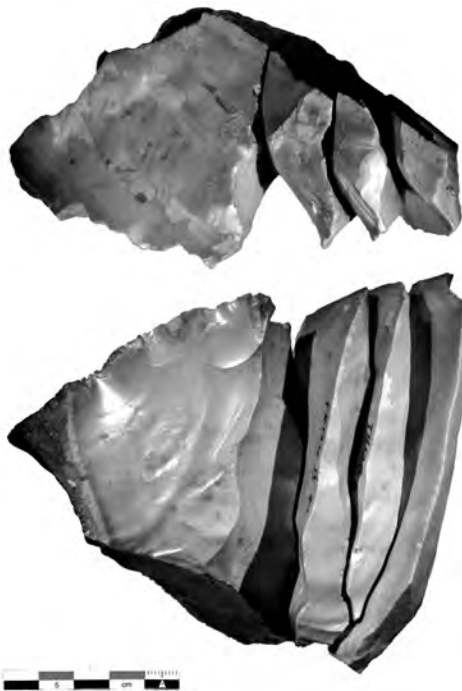


Figure 8.24 Wadi Haluf 1 refit #5. Left (Photograph by Y. Hilbert)

Refits #2, #3, #7, #8, and #9 depict phase refits where two *débordant* blades are attached one onto the other; all refitted blanks have overshoot terminations. Between these *débordant* detachments a convexity exploitation removal took place; the negatives on the lateral, non-cortical peripheries of the refitted *débordant* blades supports this notion.

Refit #4 mirrors the removal of two cortical flakes from a nodule, presenting two opposed cortical platforms. These two reattached removals were the only modification the nodule suffered.

Refit #6 shows a blank reattached to a core. A large overpassed and twisted *débordant* flake was removed from the frontal face of a unidirectional parallel core. After that removal the piece was further reduced on its narrow side and then discarded due to ruined convexity. The remaining refits (#10, #11, #12 and #13) are conjoins of fragmented *débitage*.

8.3 GOLF transect comments

8.3.1 TH.125, TH.128 and TH.133 refits

The selective sampling undertaken at TH.125, TH.128 and TH.133 sites of the GULF transect have produces valuable refits that help established variability within the unidirectional parallel reduction method of the Late Palaeolithic. These three constellations additionally allow the identification of past economic patterns. It has been shown that the creation of convexity and the exploitation of this created convexity are intertwined within a reduction continuum. The removal of *débordant* elements, in most cases, was followed by the production of an elongated converging blank. These pieces have not been found at the sites, although the reconstruction of the TH.125 refits indicates that at least five of these blanks were produced.

In regard to the raw materials exploitation and handling strategies used, varying strategies have been observed: (a) Cores were prepared and used to produce desired

blanks at a given site. Cores and blanks are transported away from this primary site; subsequently, the core is further reduced at a secondary site. Desired blanks are removed from the site for further processing. (b) Cores are prepared and exploited directly at the site and only blanks are removed from the site.

Although valuable for the reconstruction of such patterns, insecurity regarding the absolute chronological placement of these artefacts should not be underestimated. An attribution of these constellations to the Nejd Leptolithic tradition is possible thanks to the identification of identical technological patterns in stratified and dated contexts (Ghazal, Khumseen and al Hatab rockshelters).

8.3.2 Wadi Haluf 1 comments

At Wadi Haluf 1 a very simple and prolific blade production technology was identified. Both blades and flakes collected at this surface scatter come from simple unidirectional single platform cores, as indicated by the dorsal scar patterns and blank striking platform morphologies. Metrical analysis support this statement in that the average index of elongation of all complete *débitage* collected is 2,35 (n=330), indicating that these are at least twice as long as they are wide. Considering the high number of hinge terminations among the flakes, which is indicative for core convexity loss, these *débitage* elements have likely been reduced, while working surface configuration was poor.

All phases of core preparation and exploitation have been observed at the site. The large numbers of decortication blanks indicate that this process was administered on site. As seen on the refits, particularly refit #14, core convexity maintenance phases preceded the exploitation of parallel to convergent shaped, elongated blanks with triangular to trapezoidal cross-section. *Débordant* elements with small striking platform dimensions in relation to blank size fulfilled that purpose. The low core to *débitage* ratio of 1:44 mirrors the efficiency with which the cores have been reduced. Also, it is likely that “*Vollkerne*” (Hahn, 1993), prepared cores, were extracted from the sample by the flintknappers and

further reduced elsewhere.

The few tools provide little indication of the activities additionally undertaken at the site. The few *façonnage* elements, preforms and thinning flakes, are the only indications of any technologically divergent procedure undertaken at the site.

CONCLUSIONS

... an Arabian assemblage may fall into one of two different inter-regional contexts:

1. An assemblage's immediate origin is to be found in an adjacent region. This would show in clear technological and typological patterning that closely parallels patterning from a near contemporaneous industry in an adjacent region.[...] 2. An assemblage's immediate origin lies in Arabia. Its technological and typological patterning most closely parallels earlier local assemblages that show no direct, specific parallels with any industry from an adjacent region.

–Anthony E. Marks, *The Paleolithic of Arabia in an inter-regional Context*

I have learned more over these three years of research than I have written, and I have written more than I had planned. This is primarily due to the sheer number of sites mapped and sampled during the 2010-2012 DAP field seasons. A lot of rocks make for a lot of data and, consequently, a lot of written pages. This chapter aims to synthesize these data and attempts to draw some conclusions from the various threads of information presented throughout this dissertation.

This study has conducted technological and typological analyses of diverse samples from different sites generally classified as Nejd Leptolithic. Concerning the Nejd Leptolithic, Rose (2006) writes that:

These assemblages seem to represent a widespread blade industry observed at a number of findspots throughout the Nejd Plateau. The term Nejd Leptolithic is used, although in the absence of an in situ type site, this taxonomic designation should not be considered a proper industrial label. (Rose, 2006, 283)

So, at this stage the Nejd Leptolithic should be viewed as a loosely defined lithic technocomplex, *sensu latu*, encompassing multiple industries that share one or more specific technological elements over a span of time (Kleindienst, 1967; 2006). The four major sites analysed and presented in chapters Six to Eight: Ghazal and Khumseen Rockshelters, Jebel Eva and Wadi Haluf 1 surface collections, all fall within one specific

industry of the Nejd Leptolithic technocomplex or tradition. The analysis of the lithic material and the absolute dating of the associated sediments allow for the description and chronological attribution of a specific technological package shared by the assemblages collected from these sites. The data collected from the localities TH.125, TH.128, TH.133, and TH.59 will also be discussed regarding their technological variability, stone tool typology, and extrapolated economic behaviour.

Following a description of the specific elements that constitute the Late Palaeolithic assemblages presented here (e.g., technology, typology, raw material, economic behaviour, etc.), climatic fluctuation found across the landscape of Dhofar at the Pleistocene/Holocene divide is then considered. In examining intra-regional affinities over time, this study notes parallels between MIS 3 and 2 sites found in the South Arabian Highlands and the Late Palaeolithic sites presented here, hinting at Late Pleistocene demographic continuity in the South Arabian Highlands. Given the paucity of archaeological data from MIS 3 and 2, comparisons must be viewed as preliminary.

Bolstering the emerging archaeological picture of indigenous groups present in South Arabia prior to the onset of the Holocene, additional evidence in the form of genetic data are integrated into the discussion. This study considers the distribution of mtDNA haplogroup R lineages found among modern groups throughout the South Arabian Highlands and the estimated coalescence ages of these peoples. Finally, using the archaeological evidence generated in this dissertation, implications of this Late Palaeolithic industry are considered in reference to the Late Palaeolithic/Neolithic transition.

9.1 The Late Palaeolithic of Dhofar

Over the next pages, the data discussed and presented across this dissertation will be summarized in order to classify one distinct lithic industry pertaining to the Nejd Leptolithic technocomplex. The technological package composing any industry is represented by the reduction modalities anchored within a technological system, which

is used to produce a relatively standardized array of stone tool types. This is particularly significant, as it is the primary, if not only available material culture in prehistoric contexts found across Dhofar. In other words, the *débitage* and cores found at a given site are the products of a reduction system and raw material economy that is the most durable expression of culturally transmitted behaviour in prehistory.

Stone tool technology found across sites pertaining to the same industry will, therefore, be the same or show some degree of similarity. Variability between sites of the same industry does occur (e.g. blank size, core, blank, and tool type frequencies), but is often related to different raw material economies and site function, rather than cultural variability. This variability is mainly expressed in artefact type counts and slight differences in attributes. Within a given industry, however, these are but minor variations from the overall technological pattern expressed by the cores and *débitage* contained in an assemblage. Thus, on the whole, assemblages comprising a given industry will share the same essential technological features aimed at producing an overlapping range of tool types. The stone tools examined in this study provide enough insight to this aspect of the material culture to help make the industry recognizable across the archaeological landscape.

9.1.1 Reduction modalities

Blanks were almost exclusively produced by unidirectional reduction strategies. This method of core reduction is dictated by a unidirectional recurrent and facial (*sensu* Meignen, 1995; Delagnes, 2000; Hilbert *et al.*, 2012) approach to the core's volume that was accompanied, in smaller parts, by a flexible and alternating use of additional platforms and core working surfaces. For the purposes of this dissertation, the distinction between parallel and convergent cores was made based on morphological parameters (i.e., core and core working surface shape). The morphology of any given core found at a site represents only the last phase of its reduction (e.g. Inizan *et al.*, 1992; Andrefsky, 2005).

Thanks to the pristine character of both surface scatters and stratified sites, a number of refittings have been made. These refits have been illustrated and described as to the succession of removals and dynamic core morphologies through the reduction sequence. These refittings show that both unidirectional convergent and parallel cores have been produced using the same reduction strategies; unidirectional reduction method.

Consequently, the blank production sequences could be further divided into three distinct reduction modalities based on evidence from core reconstructions. These reduction modalities are defined by the refittings, which are distinct from one another; two refits may depict the same reduction pattern but express it differently. This flexibility emerges as a result of the flintknapper's fluid technological gestures marked by successive adjustments to the cores convexity, which are never absolutely reproducible but may be classified into comparable stages within the *chaîne opératoire*. These phases of adjustment are followed by phases of convexity exploitation. Thus, the differentiation of recurrent single platform unidirectional reduction methods was achieved by identifying variability within convexity maintenance measures applied to the core's working surface.

The modalities presented here are schematics, which means that the attribution of specific refits or *débitage* samples to any one scheme is inherently a generalisation. This creates potential problems with borderline cases that sometimes must be shoehorned into existing modalities, rather than creating additional modalities for every refit. Borderline cases aside, however, the 85 refits made and analysed for this studied fit comfortably into one of the three reduction modalities defined in this analysis.

Modality 1 uses a single plane of removal on a raw material nodule or block; striking platform preparation is minimal and consists of one, maximum two removals from the top of the nodule. Often, the striking platforms are flat cortical or fracture planes used without any further preparation. Subsequently, *débordant* elements are struck from the lateral edges of the core's working surface to create a keel-like plane of removal (Figure 9.1). This convexity is then exploited by three to five elongated recurrent removals; after

the production of non-cortical *débitage*, the core convexity must be prepared anew.

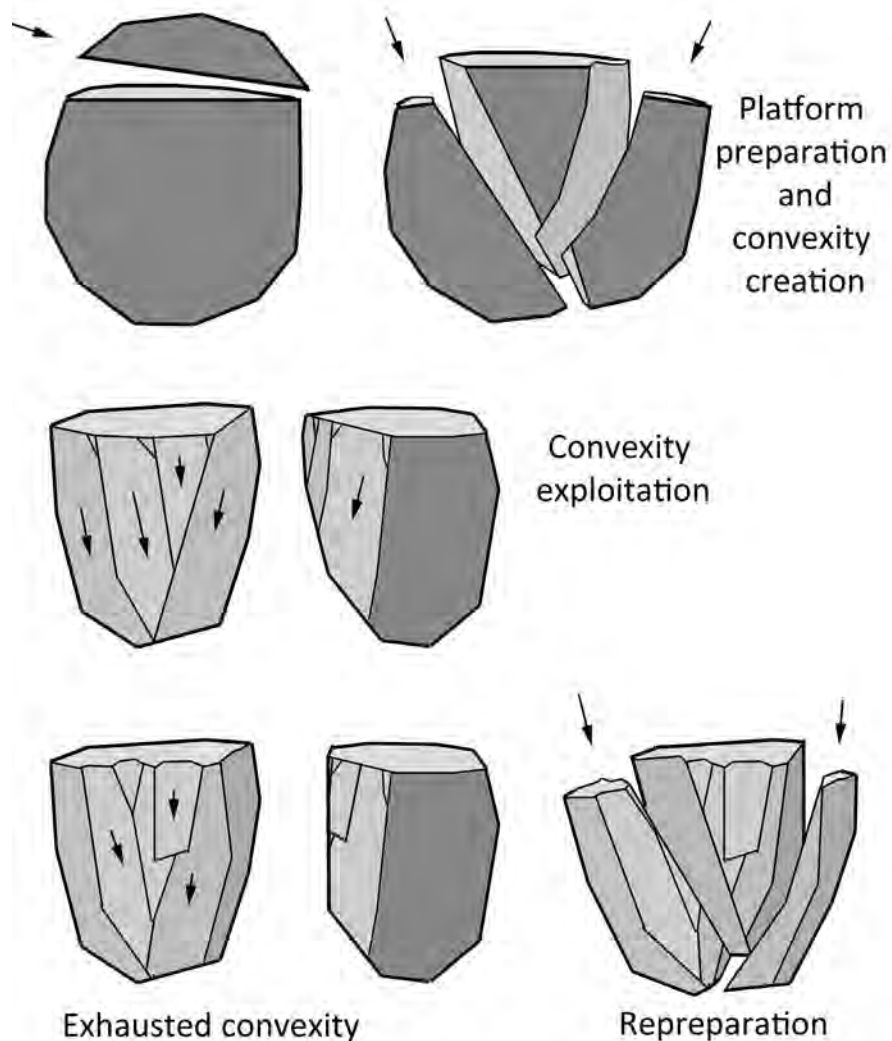


Figure 9.1 Reduction modality 1 schematic.
(Image by Y. Hilbert)

This reduction modality – the simplest of the three recognized reduction methods – has been observed more frequently than the other two (Table 9.1). Refitting #14 from Wadi Haluf 1 best depicts this specific variation; further examples were recorded for localities TH.133, TH.128, Ghazal Rockshelter level 2 refits #2 and #5 and Khumseen refit #11. Particularly at Ghazal, reduction modality 1 was used in an alternating fashion, which means that after exhaustion of one working surface, an additional surface was subsequently exploited on the same nodule. At Ghazal Rockshelter level 2 and Wadi Haluf

1, the identification of this particular reduction method allowed for the recognition of technologically diagnostic *débitage* (*sensu* Monigal, 2002). These are by-products that are indicative of a specific kind of reduction (Figure 9.2). In the case of Modality 1, the technologically diagnostic *débitage* include *débordant* elements with cortical backs, as well as triangular flakes and blades with flat profiles and complex midpoint cross-section (trapezoidal, three vectored and pitched). These latter types are not preferential products as identified with Levallois convergent technology (for examples of refits see Demidenko & Usik, 1995). These are produced when the core's working surface convexity must be restored, achieved by the removal of a blank that eliminates excessive convexity. This phase is often followed by the removal of *débordant* elements from the peripheries of the core's working surface in order to re-establish the desired convexity.

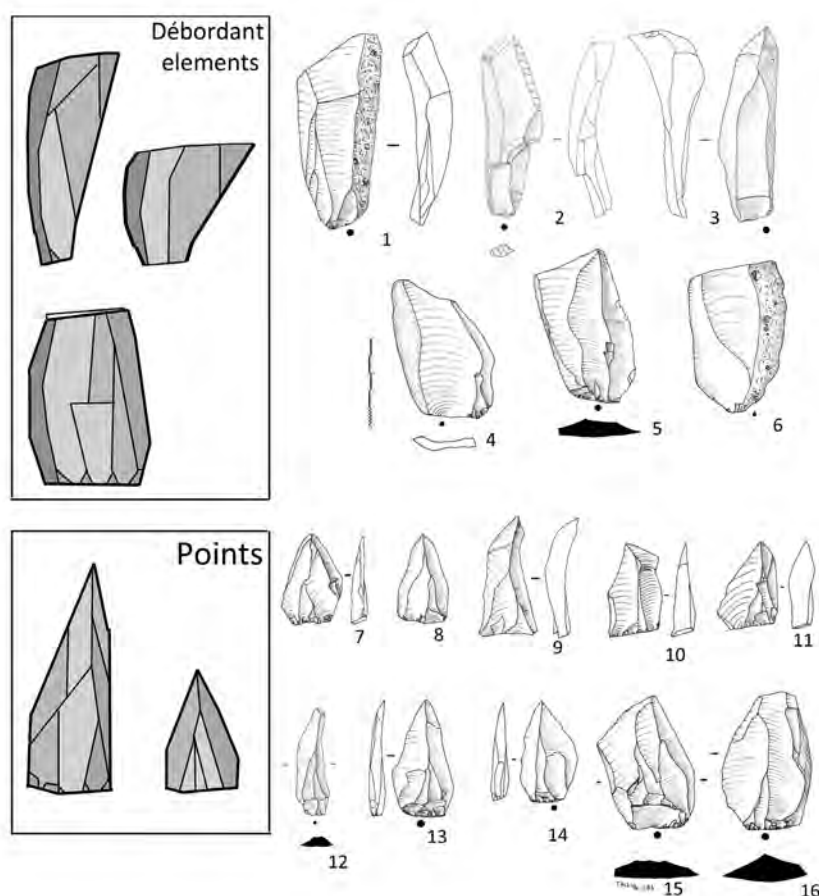


Figure 9.2 Technologically diagnostic *débitage* produced by Modality 1. 1, 4 to 6 and 13 to 16, Wadi Haluf 1 artefacts; 2, 3 and 12; Jebel Eva Artefacts; 7 to 9, Ghazal Rockshelter; 10 and 11, Khumseen Rockshelter. (Image and illustrations by Y. Hilbert)

Modality 2 is characterized by the volumetric reduction of elongated blanks across multiple working surfaces on the core; these removals are administered from a single platform (Figure 9.3). This process results in the formation of a convex and convergent plane of removal from which recurrent blade production takes place. Characterisation of this specific type of reduction is based on refittings and core attribute analysis. It is notably less common than modality 1. Ghazal Level 1 refit #31 is a classic example of this modality, as is Ghazal level 2 refit #25. Two of the convergent flat cores found at Jebel Eva also suggest the use of this reduction modality (Table 9.1).

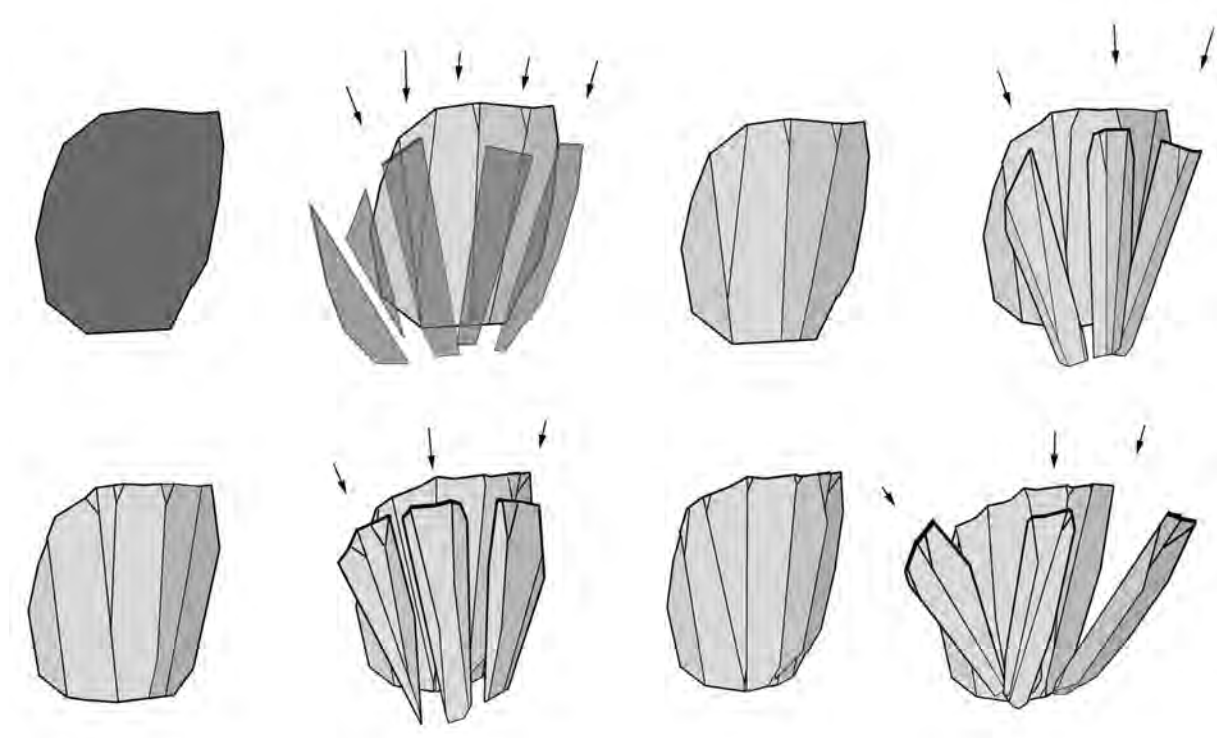


Figure 9.3 Reduction modality 2 schematic.
(Image by Y. Hilbert)

During such recurrent reduction as seen in Modality 2, there is no curation, hindering the identification of technologically diagnostic *débitage*. The recurrent character of this reduction allows the flintknapper to place each blow that creates a blank in a way that the flake negative symmetry on the core is not disturbed by either hinge or step fractures. This modality allows the flintknapper to continuously produce blanks, without

having to resort to core convexity measures. Although *débordant* blanks are sometimes created by this process, these are not nearly as numerous as within modalities 1 and 3. Artefacts morphologically analogous to core tablets and crested blades do also occur within modality 2, but are not related to either crest preparation or core striking platform rejuvenation procedures. This is best visible on the reconstructions done for Ghazal Level 1 (Figures 7.53 to 7.57).

Modality 3 is distinguished by its deliberately short cycle of core reduction, where successive *débordant* removals are used to form a convex working surface, resulting in a predetermined, elongated and diamond-shaped blank. This technique produces a single end product, so that the plane of removal must be reformed within each cycle (Figure 9.4).

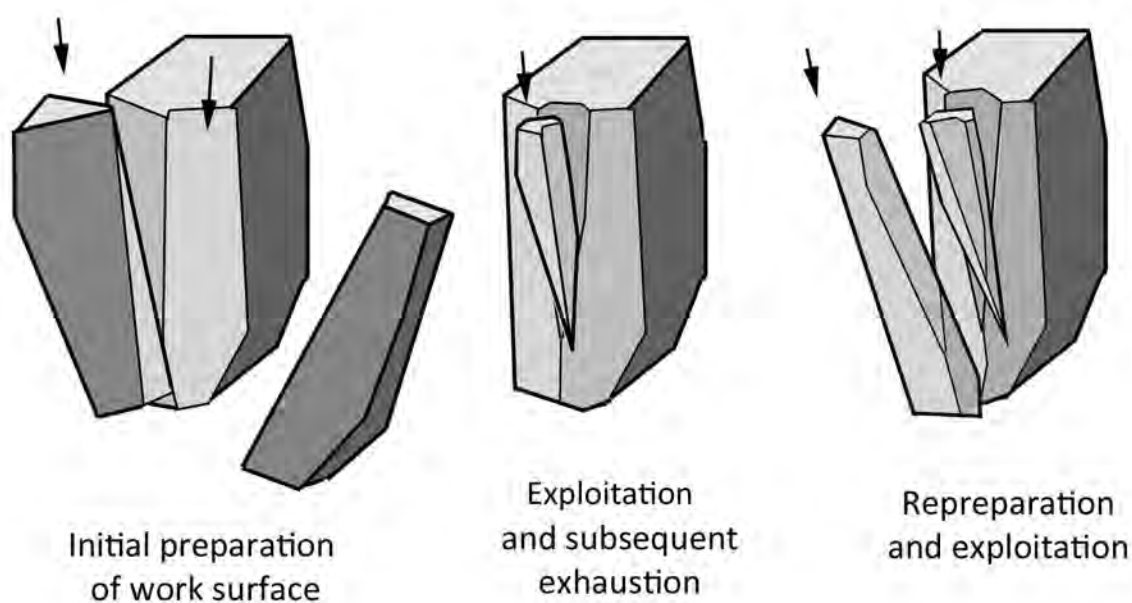


Figure 9.4 Reduction modality 3 schematic.
(Image by Y. Hilbert).

According to the short reduction and subsequent convexity preparation, a considerably larger number of *débordant* elements are created using this reduction modality. This has been observed at Jebel Eva and Wadi Haluf 1, where *débordant* blades outnumber all other blank types. This reduction modality is illustrated by refits #3 and #11 from Jebel Eva (Figures 6.15 and 6.16). Additional examples are given by the refits

from localities TH.125 and TH.59 (respectively Figures 8.3 to 8.4 and 6.5 to 6.7). Modality 3 is recorded in situ at Khumseen rockshelter GH 5 based on refit #10 (Figure 7.16) and other phase refits (see Chapter Five, section 5.1.1 for explanation on refit nomenclature).

Mirroring modality 1, this modality uses *débordant* elements to produce convexity. Often, one or two *débordant* blanks are struck to achieve the preferential diamond shaped blank. These *débordant* blanks are marked by a specific dorsal scar pattern appearing as a “λ” shaped scar pattern inclined towards the non-cortical periphery of the blank (Figure 9.5).

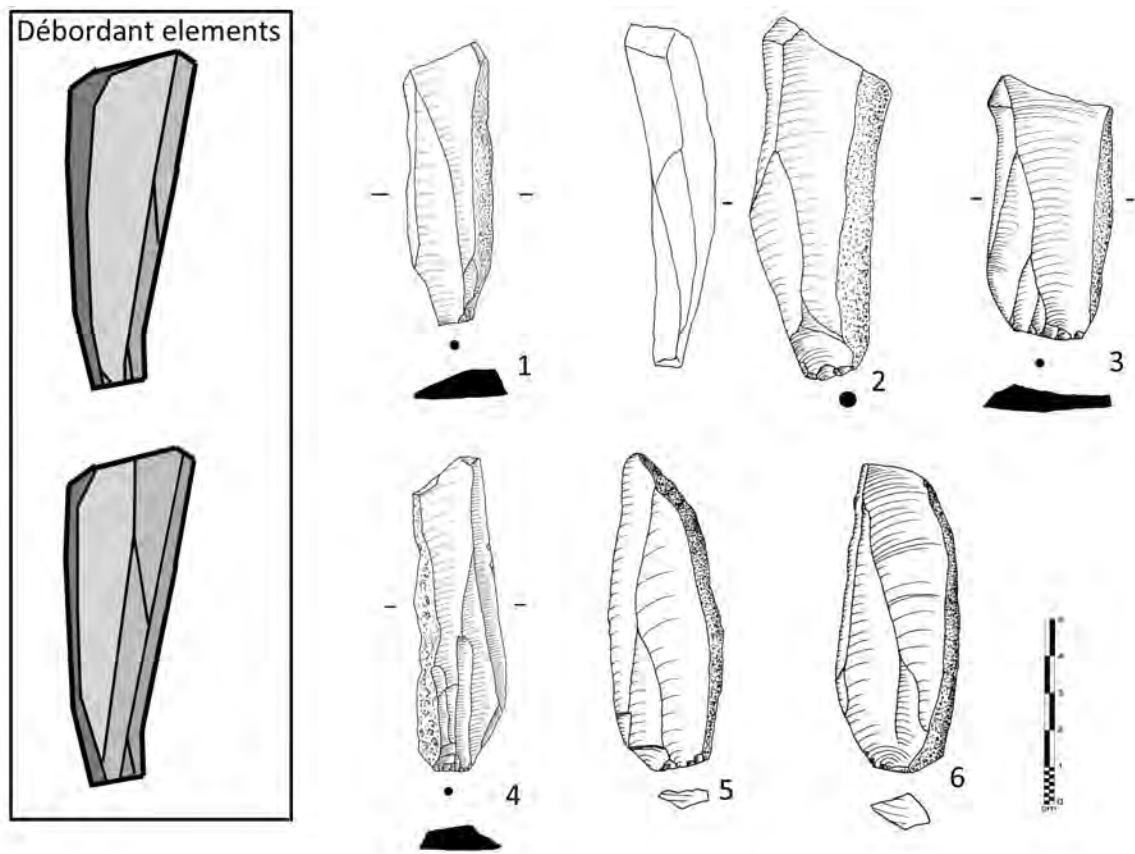


Figure 9.5 Technologically diagnostic débitage produced by Modality 3.

1 and 4 Jebel Eva; 2 and 3 Aybut al Auwal (TH.59); 5 and 6, TH.125. (Image and illustrations by Y. Hilbert).

The determination of specific reduction modalities based solely on *débitage* attribute analysis is made possible through the identification of technological diagnostic *débitage* (Table 9.1). For Ghazal, Khumseen, Jebel Eva, and Wadi Haluf 1, the presence of

débordant elements is indicative of all three reduction modalities. At Ghazal and Wadi Haluf 1, the identification of triangular blanks with complex cross-sections and flat profiles has been found indicative of modality 1, while at Jebel Eva the high amount of *débordant* blades with convergent “λ” shaped negatives is associated with modality 3. Reduction modality 2 is more difficult to detect and has primarily been identified based on refittings.

Table 9.1 Distribution of the reduction modalities across the analysed samples.

	Modality 1*	Modality 2*	Modality 3*	TDD M1**	TDD M3**
<i>Khumseen</i>	YES	NO	YES	YES	YES
<i>Ghazal Level 1</i>	YES	YES	YES	YES	YES
<i>Ghazal Level 2</i>	YES	YES	YES	YES	YES
<i>Jebel Eva</i>	YES	YES	YES	YES	YES
<i>Wadi Haluf 1</i>	YES	NO	NO	YES	YES
<i>TH.59</i>	NO	NO	YES	-	-
<i>TH.125</i>	NO	NO	YES	-	-
<i>TH.128</i>	YES	NO	NO	-	-
<i>TH.133</i>	YES	NO	NO	-	-

*Represented by core reconstructions

**Represented by TDD found within the assemblages

Because they only provide a static view of the reduction process after discard, cores have provided little information for differentiating the three identified reduction modalities. Aspects of core morphology such as striking platforms, position of working surface and longitudinal convexity have shown little to no variability. Striking platform preparation and reduction directionality have been found to be similar across the analysed samples. Primarily straight (90°) platforms have been used to produce blanks in a unidirectional fashion. Striking platforms created by more than three removals were interpreted as the result of rejuvenating the working surface on the core. That is to say, a former working surface was used as a striking platform. Additional information could be gained by analysing the location and disposition of the core’s working surfaces. Cores had either one frontal working surface placed on a narrow edge of a nodule or on its broad side. Additionally, cores with convex working surfaces and two unopposed working surfaces have been detected. Through refitting, however, it is apparent that all of these

diverse morphological stages may occur across a single core reduction episode, which in turn is anchored within a simple unidirectional recurrent reduction. Further work on the development of an appropriate analytical method that integrates core morphology and core reconstructions is needed to better understand and classify this artefact category.

9.1.2 Débitage and cores

The by-products of any knapping process, *débitage* and cores, give some indication of what modality has been applied and some indications as to the function of the site. The theoretical underpinnings to this discussion are presented in Chapter Five, section 5.2. Here, this dissertation will compare the patterns that have been recognized from the attribute analysis at Jebel Eva, Wadi Haluf 1, Ghazal and Khumseen rockshelters. This, in turn, enables the characterization of the Late Palaeolithic based on the description and frequencies of the *débitage* and cores found at these sites. Whether the three recognized reduction modalities can be detected through attribute analysis is also discussed.

From the general *débitage* and core count per site (Figure 9.6), some variability can be seen. While Ghazal Level 2 and Levels 5 at Khumseen share similar *débitage* and core distributions, the two surface sites, Jebel Eva and Wadi Haluf 1, present their own distinct patterns. This variability is expected, given that the samples from Jebel Eva and Wadi Haluf 1 have been recovered from exposed surfaces. In both cases, these are large workshop sites where a higher ratio of *débitage* to cores has been found. This is possibly caused by raw material exploitation and transport from the site, which means that preferential end products and prepared cores will be transported away from the site leaving the inevitable by-products of the employed reduction at the site. Also, *débordant* elements have been observed more frequently at surface sites as opposed to stratified sites. This pattern relates to the reduction modalities dominating the assemblage, the sample size, and the aforementioned blank selection. Which goes to show that the majority of the *débitage* found within large-scale surface sites are not desired end products, but rather represent

the inevitable by-products of the reduction modalities used. This makes it possible to identify which modality is being used based on the *débitage* found at these sites.

In respect to aspects of the attribute analysis other than blank type and core ratio, a uniform pattern has been observed throughout the here analysed samples. Scar patterns, platform types, blank shape, blank termination, and blank profile recorded at the four sites show equivalent frequencies (Figures 9.7 to 9.13). Blank mid point cross-section, however, has shown some variability (Figure 9.11). This is particularly apparent at Jebel Eva, where there is a high frequency of rectangular cross-sections. One explanation is that this is a function of raw material morphology and reduction strategy used at the site (i.e., thin chert plaquettes in combination with modalities 1 and 3). During the reduction of thin plaquettes using modalities 1 and/or 3, the entire core's working surface may be removed, producing blanks with rectangular to pitched cross-sections; usually the lateral sides of these blanks is covered by cortex.

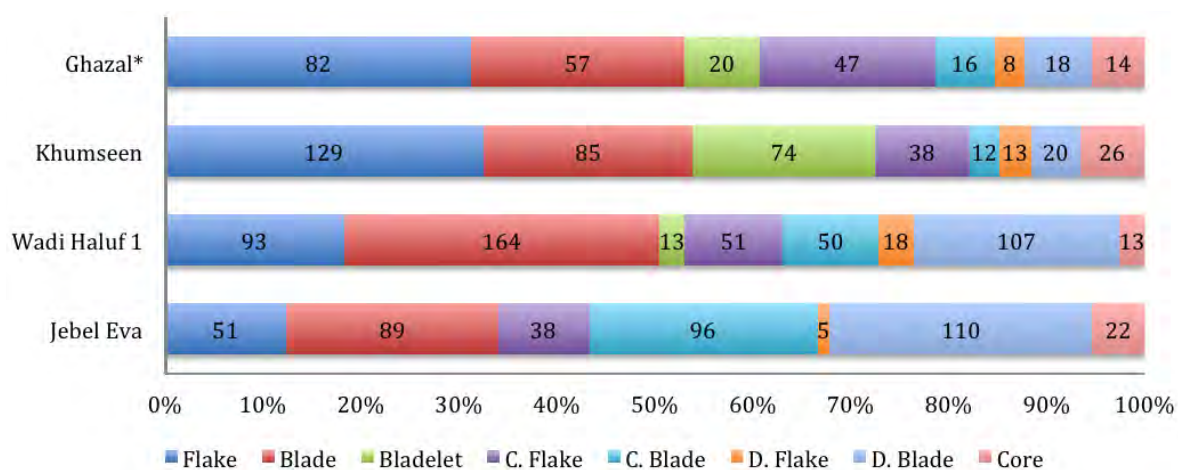


Figure 9.6 Artefact count per site.

*Numbers for Ghazal Level 2.

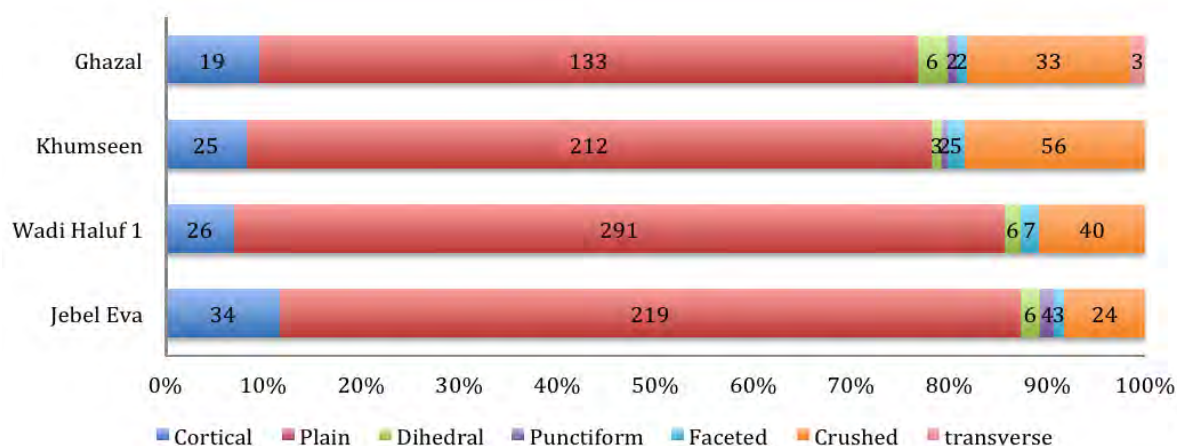


Figure 9.7 Artefact platform type.

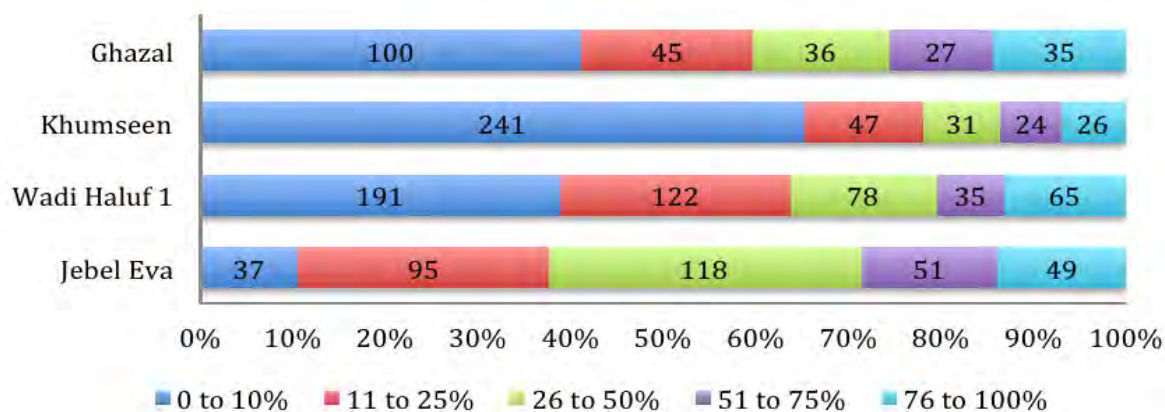


Figure 9.8 Artefact cortical cover.

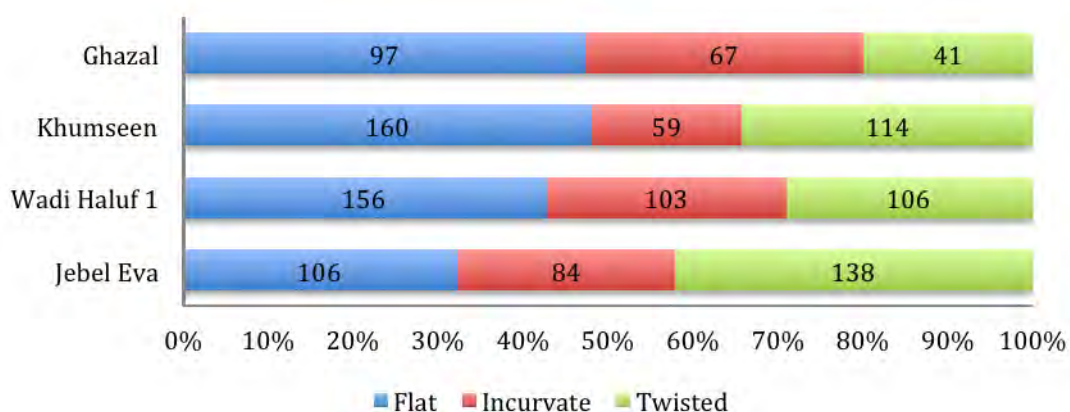


Figure 9.9 Artefact longitudinal profile.

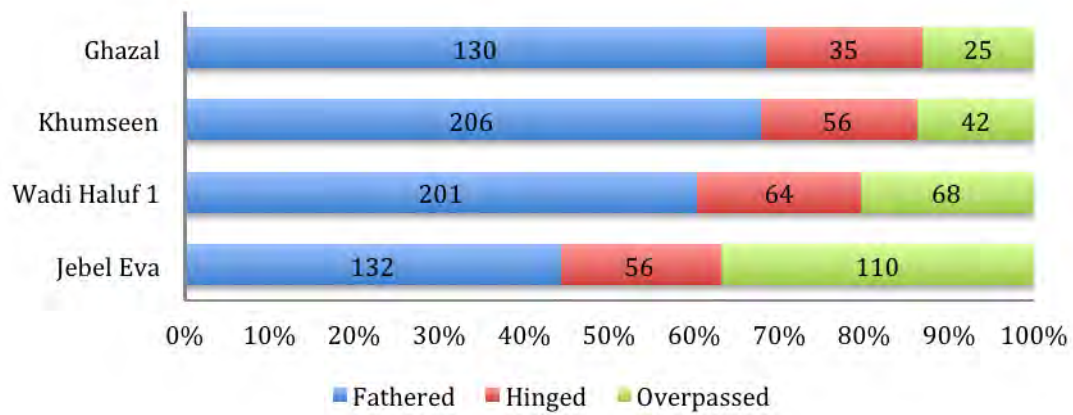


Figure 9.10 Artefact termination.

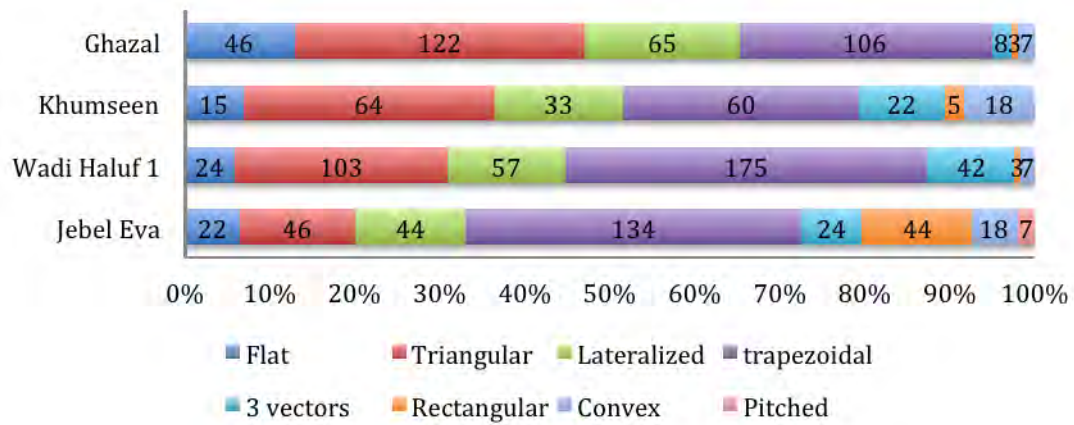


Figure 9.11 Artefact midpoint cross section.

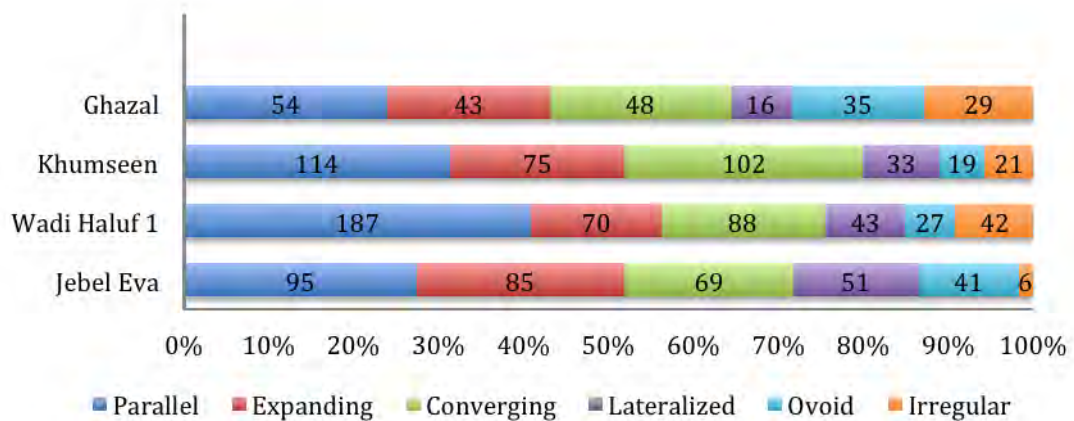


Figure 9.12 Artefact shape.

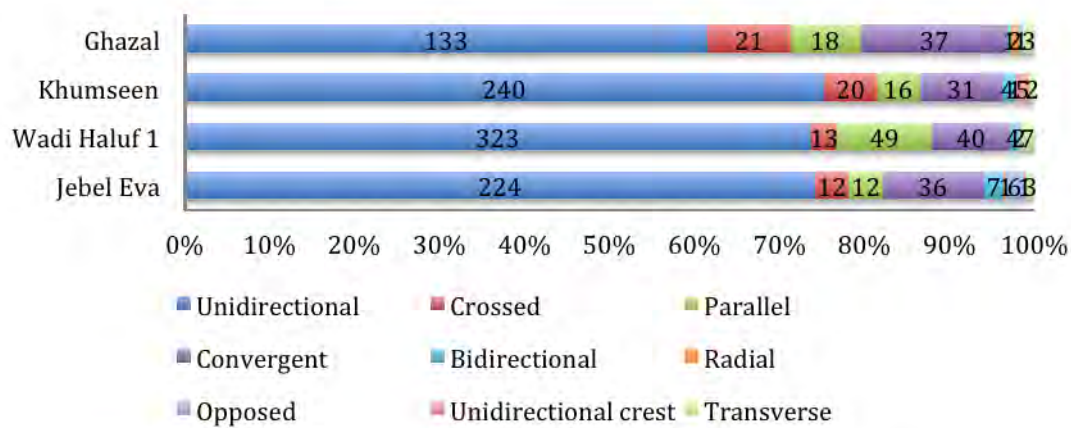


Figure 9.13 Artefact scar pattern.

The metric variability expressed by the size of the artefacts found across the samples relates primarily to raw material size at each of the localities. Thus, the sample from Wadi Haluf 1, where large raw material nodules have been found, stands out metrically with larger-than-average blank sizes. This would obscure technological similarities between samples containing large blanks and samples with smaller blanks; for example Wadi Haluf 1 and the Late Palaeolithic levels at Khumseen (see appendix B).

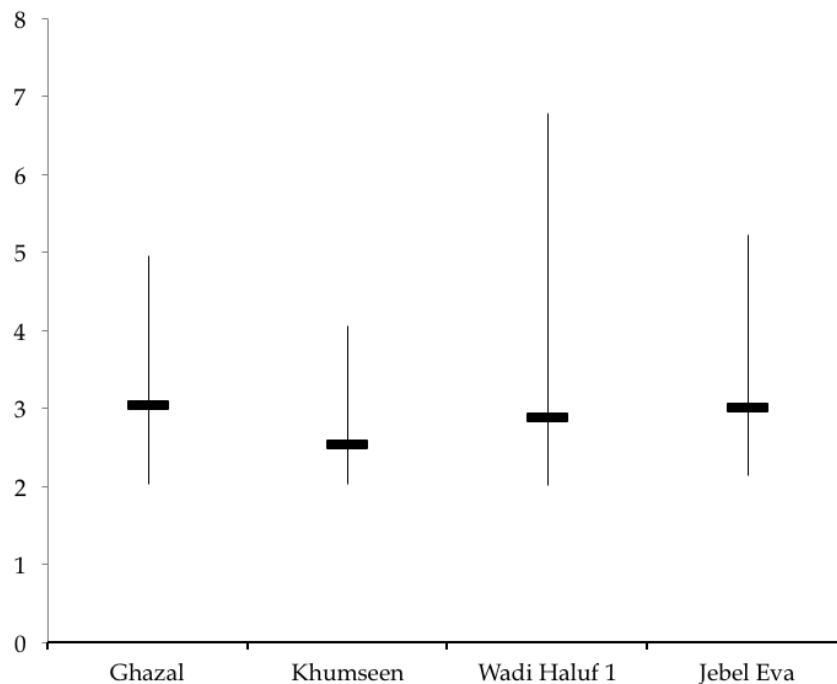


Figure 9.14 Blade index of elongation.

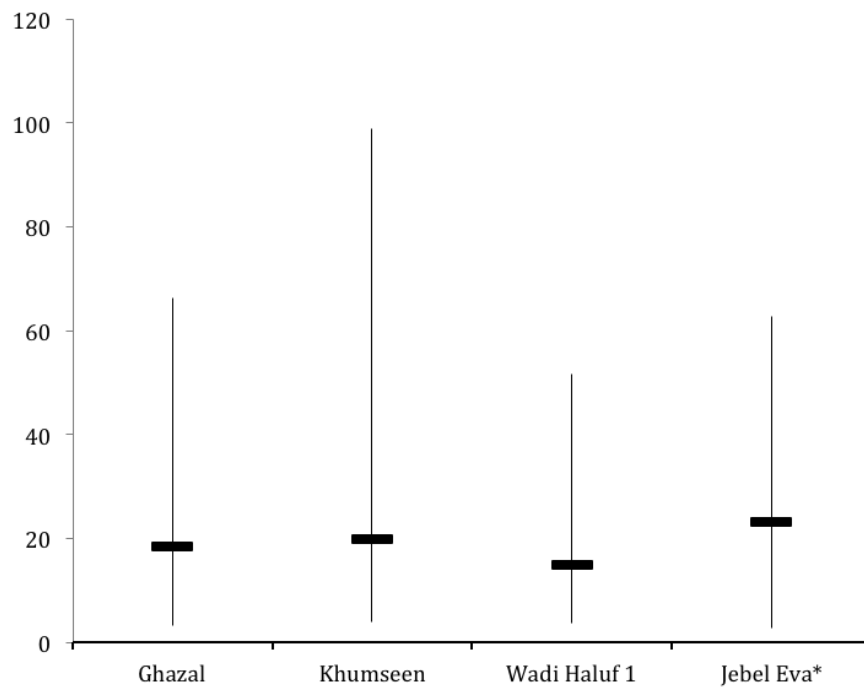


Figure 9.15 Blade relative platform size.

*One outlier removed.

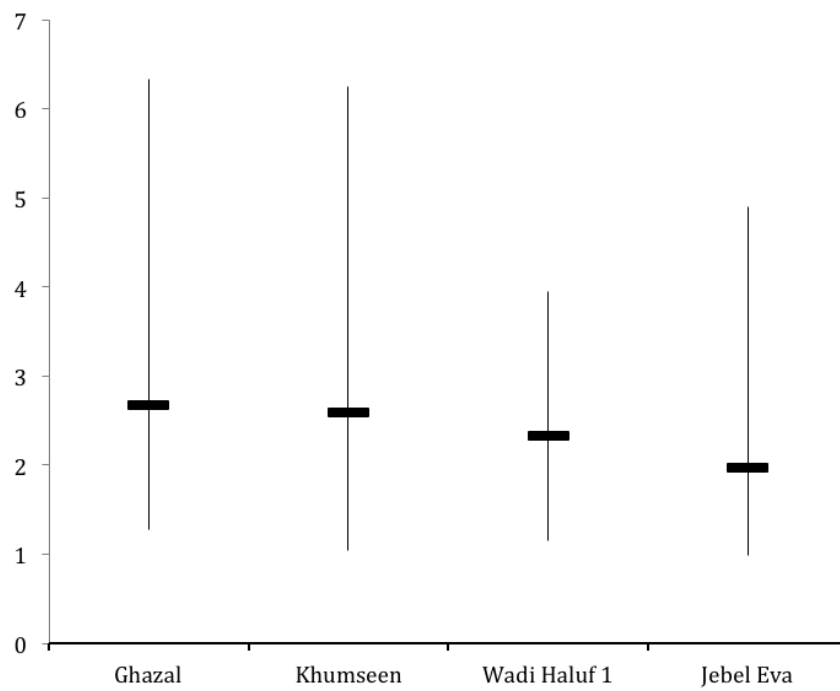


Figure 9.16 Blade index of platform flattening.

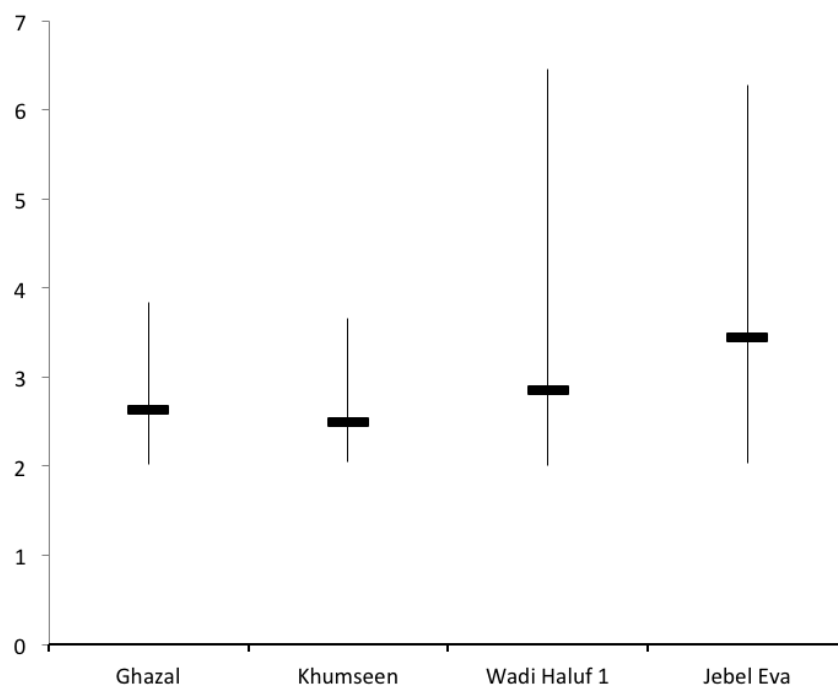


Figure 9.17 Débordant blade index of elongation.

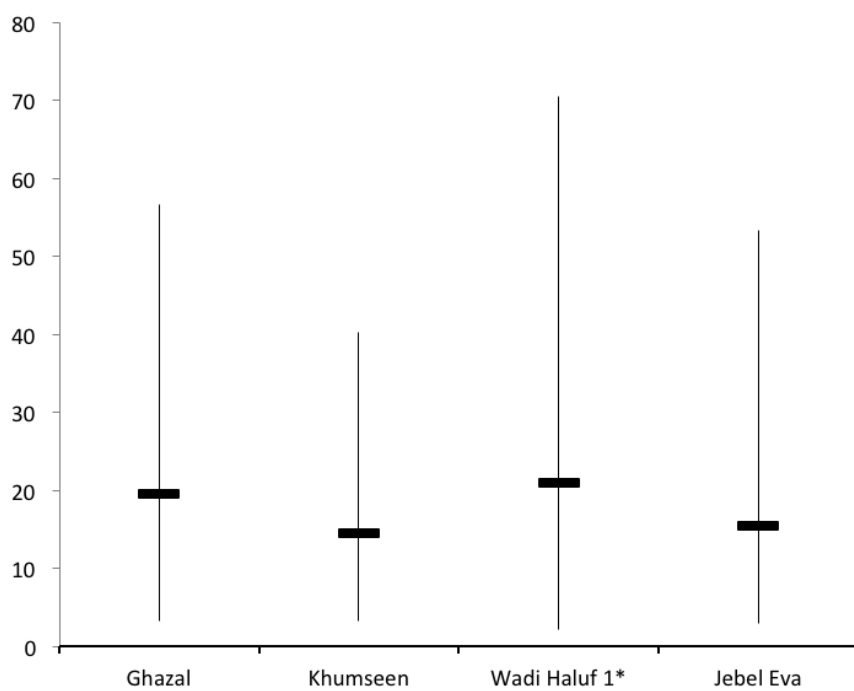


Figure 9.18 Débordant blade index if relative platform size.

*One outlier removed.

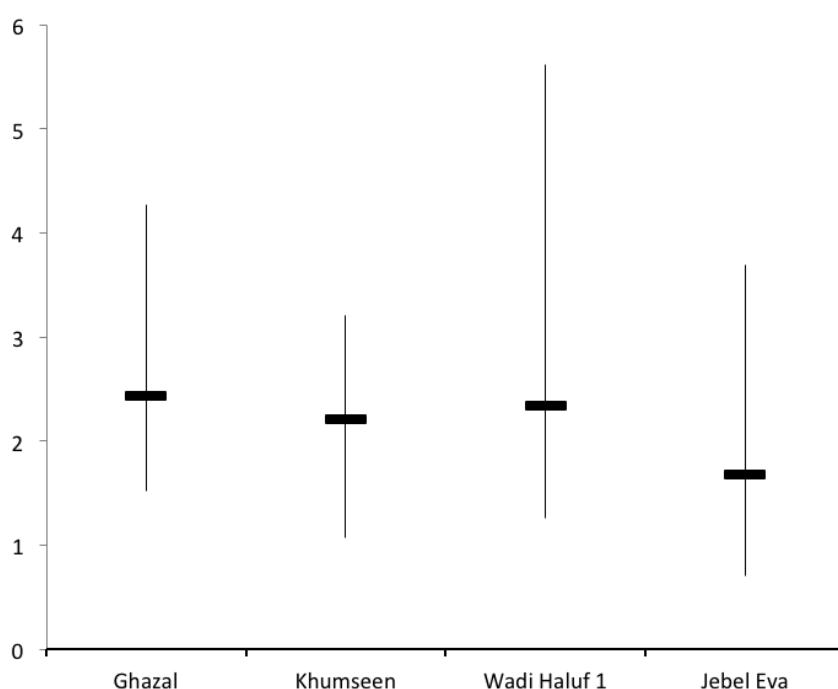


Figure 9.19 Débordant blade index of platform flattening.

Results of indices comparing blades and *débordant* blades metrics have been examined in order to show the consistency across the samples from Khumseen, Ghazal, Jebel Eva and Wadi Haluf 1. The results show comparable values across all samples. Blades have generally more slender dimensions than *débordant* blades (Figures 9.14 to 9.16), while relative platform size expressed by both blank types have shown similar mean values (Figure 9.17 to 9.19). These metrical observations attest to the homogeneity of the leptolithic *débitage* in respect to its dimensions. Clearly, metric variability is dependent on raw material size, rather than technical skill or cultural choice.

The amount of cortical pieces and the total amount of cortex found on the *débitage* at Khumseen Rockshelter stands out as being lower than that observed among other assemblages, indicating that primary decortication of nodules was less frequently carried out on site; more likely, flintknappers brought previously prepared cores there. Thus, Khumseen Rockshelter may represent a habitation site where activities beyond blank production took place. Its position on the talus slope of a large rockshelter, adjacent

to a drainage system, would suggest as much. The Khumseen Rockshelter sample has also provided the highest number of tools, supporting the notion that domestic activities were carried out at the site. On the other hand, nearby Ghazal Rockshelter has shown high cortical values, indicating that blank production and core preparation were the main activity undertaken at the site. Unlike the expansive Khumseen Rockshelter, Ghazal Rockshelter is a small (one meter in height) overhang that acted as a sediment trap. Although it is located near a source of freshwater, the shelter would hardly have served as a residential site, thus, more likely it was a workshop site or served some other specialized function. The tool sample uncovered at Ghazal is extremely meagre constraining further inferences on that matter. At Wadi Haluf 1 and Jebel Eva, blank production was by far the main activity undertaken, also warranting these localities as workshops.

9.1.3 Tools

The tool samples within the analysed assemblage are rather limited. Tool forms found across the documented sites indicate that the Late Palaeolithic tool kit is composed of a combination of both informal (*ad hoc*) and standardised equipment. The informal tool category is composed of marginally retouched blanks, in which retouch is discontinuously spread across the blanks' peripheries, and is achieved using direct hard hammer percussion that did not considerably modify the shape of the affected blank. Standardised tools, on the other hand, have received a sufficient amount of retouch to alter the shape of the blank, and are repeated within the assemblage, so that the working edge corresponds to a desired archetypal form.

Within the analysed assemblages, simple endscrapers, piercers, burins both on truncation and snap, unifacial tanged projectiles (i.e., Fasad points), trifaces, and pseudo-backed knives have been identified. Endscrapers have been created by direct percussion retouch at the distal end of the blank; retouch is commonly obverse and continuous. Such pieces have been found at Khumseen, Jebel Eva and Wadi Haluf 1. The specimen

found at Ghazal Rockshelter was manufactured on an elongated cortical flake; the retouch has partially removed the cortex. Although burins have previously been considered a characteristic feature of the Nejd Leptolithic (Rose & Usik, 2009), as they are among the most common tool types at Al Hatab Levels 1 and 2 and distinctive Nejd Leptolithic “burin factory” surface sites TH.84b and TH.267, only a single specimen was recorded in this study. The one burin, found at Ghazal Level 2, was manufactured on a blade; the burin blow was administered to a snapped surface at the distal portion of the blank. Additionally, three burin spall fragments have been found at the site, one of these had an elaborately faceted striking platform indicative of the production of burins on truncation. What evidence there is indicates the burins are part of the techno/typological package of the Late Palaeolithic. The fact that not many specimens have been found across the Khumseen, Ghazal, Jebel Eva and Wadi Haluf 1 samples may relate to site function rather than temporal differences and variability within the Late Palaeolithic Industries.

Tanged points have been found at Jebel Eva and Khumseen Rockshelter. All specimens have been manufactured on bladelets and show well articulated tangs manufactured using direct and abrupt unifacial retouch, which in every case was obverse. As these have been considered a *fossile directeur* marking the expansion of PPNB Levantine pastoralists, demographic implications of their presence within these assemblages are considered later on in this chapter. Trifaces, as defined in section 5.4.1 of chapter Five, have been identified at Wadi Haluf 1. Presumably associated with the manufacture of these implements, thinning flakes have also been identified within the sampled localities at Wadi Haluf 1. One of the trifacials collected has been manufactured on a large blade produced from a unidirectional parallel core. Although it is impossible to determine contemporaneity, consistent weathering would suggest as such. Given that no visible differences could be discerned between the patination on the blade and the retouch on the tool, it is likely that the blank was manufactured on site and further transformed into a trifacial within the same period.

Pseudo-backed knives are standardised tools found repeatedly across the Nejd, making them a useful diagnostic marker. Pseudo-backed knives are elongated cutting tools showing a clear distinction between the cutting edge and the back of the knife. The specimen found at Jebel Eva has received partial, semi-abrupt retouch to the back edge of the blade while the cutting edge displayed only nibbling retouch, possibly to straighten the lateral working edge. The clear differentiation between the retouch on the sides of these tools is found to be indicative of diverging functions: the back was used as a prehension element (*manual grasping*, see Rots, 2010), while the opposed periphery represents the working edge. Comparable specimens to the one observed at Jebel Eva have been found at SJ.51, on the eastern Nejd, and TH.200 (Figure 9.20). These have been found associated with extensive blade scatters that are technologically homologous to the ones described in this study.

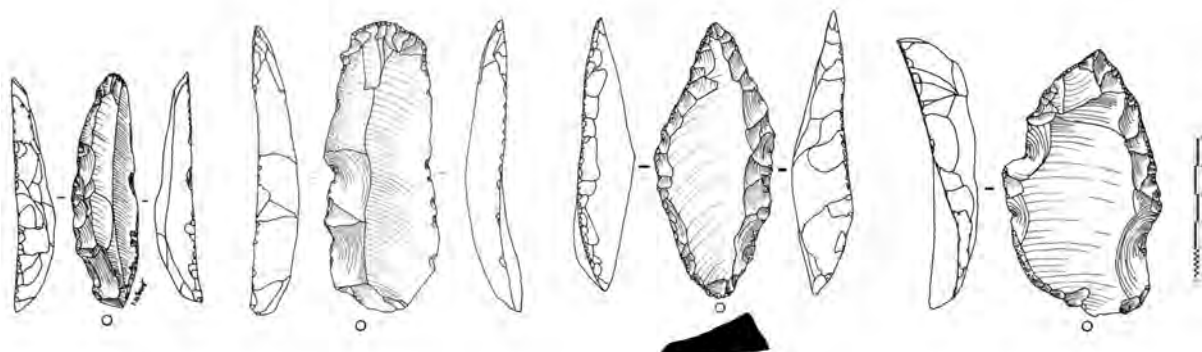


Figure 9.20 Pseudo-backed knives.

1, Jebel Eva; 2 and 4, TH.200; 3, SJ.51. (Illustration by Y. Hilbert)

Three piercers have been identified at Khumseen and Ghazal Rockshelters. Two of these specimens, one from each site, are manufactured on *débordant* blades with thick cross-sections. Modification is minimal and limited to the formation of a small bit, in both cases not wider than two millimetres and longer than one centimetre, found on the distal-lateral portion of the blank. The third specimen, found in the Late Palaeolithic levels of

Khumseen, presented comparable modifications, although the tool was made on a small flake rather than blade.

9.1.4 Raw material economy

The Nejd Plateau provided its prehistoric inhabitants with a virtually limitless supply of high quality raw material for the production of stone tools. Every chert outcrop identified by the DAP team in the field was also a prehistoric workshop site. Different types of chert have been found outcropping from the various exposed geological members, varying across the southern, central, and northern Nejd. Aside from the three main chert types found (Aybut, Gahit, and Mudayy), coarsely crystalized quartzite blocks of undetermined geological provenance have been identified as an additional resource. These were detected on lag surfaces and incorporated into desert pavements. This specific raw material seems to have only been used if no other superior resource was immediately available.

The archaeological visibility across this predominantly deflated landscape is nearly 100%, enabling the identification of prehistoric sites at a very high resolution. Where raw material outcrops were absent (e.g., the lithological formations and chert-bearing members were not exposed), Late Palaeolithic sites were almost always absent. Given the ubiquity and variety of high quality outcrops across the plateau, this was seldom the case. So, raw material availability could not have been a significant constraining factor for Late Palaeolithic populations inhabiting the Nejd. As for raw material procurement, use, and exploitation, the assemblages presented in this study indicate a flexible use of available resources. That is to say, flintknappers had the ability to execute any of the aforementioned reduction modalities to produce standardised blanks, regardless of which raw material they had at their disposal. This flexibility was coupled with a dynamic approach to volume selection and transportation to and from the studied localities, as depicted by the refit analysis presented through chapters Six to Eight.

Discrete knapping events identified at TH.59 and TH.125 offer insight into this

phenomenon. At both sites, a complete reconstruction of core reduction was achieved. In the case of TH.125, located away from any visible raw material outcrop, a core demonstrating three separate phases of production and core convexity curation was identified. The core was brought to the locality already decorticated and prepared. On the other hand, at TH.59, which is situated directly on a raw material outcrop, *débitage* resulting from Modality 3 decortication, preparation, and exploitation phases were refit. The core, however, could not be found and may have been carried away from the site for further reduction elsewhere. The products of this reduction strategy, symmetrical diamond shaped bladelets, were likely taken away from the site as well.

Based on these data, the following general observations may be drawn: (a) site location is largely a function of raw material availability; (b) a variety of resources were carried away from raw material outcrops including unmodified nodules, plaquettes, blocks, selected *débitage*, and prepared cores; (c) prepared cores have been reduced whenever blanks were needed. These aforementioned specifics have greatly influenced the configuration of open and subsurface sites in respect to their artefact type frequencies.

9.1.5 The Khashabian: a new south Arabian lithic industry

It is possible to define new lithic industry based on the technological and typological characteristics described in the previous sections. This industry is designated the “Khashabian,” after the Umm al Khashab region, where the two stratified type-sites – Ghazal and Khumseen Rockshelters – are situated.

Khashabian blank production is limited to hard hammer percussion and falls within three different core reduction modalities. While separate, these modalities are all variations of a unidirectional recurrent reduction strategy. All three modalities serve the purpose of creating expedient blade and bladelet blanks. It is noteworthy that the bladelets have been produced via the three core reduction modalities described in this study, rather than resulting from a separate technological sequence targeting the specific

production of these blanks. Based on refittings and *débitage* characteristics, Modalities 1 and 3 are the most commonly applied blade production methods within the analysed Khashabian assemblages. Less common, Modality 2 is a particular technological sequence that utilises alternating platforms to access a new working surface on a previously worked block of raw material. This particular modality is only characteristic of the Khashabian when the reduction is consistent with unidirectional recurrent production of elongated blanks. When this is not the case an attribution to the Khashabian industry is unwarranted.

Tools found within the Khashabian include endscrapers, burins, piercers, Fasad points, trifaces and pseudo-backed knives (Figure 9.21). Among these, the Fasad points, the trifaces and the pseudo-backed knives represent clear diagnostic markers of the industry – *fossile directeurs*. This was the case at Khumseen Rockshelter, where two Fasad points were found in the Khashabian Levels, as well as surface assemblages collected from Jebel Eva and Wadi Haluf 1. In every case, they were associated with the Khashabian core reduction modalities.

The stratified sites presented in this work provide some insight into the age of the Khashabian industry. At Khumseen and Ghazal Rockshelters, minimum ages for the assemblages are established by a series of OSL measurements (Table 9.2).

Table 9.2 Absolute dates for sediments holding Khashabian assemblages.

Site	Layer	Depth	Date	Laboratory Nr.
Ghazal	GH.3	34 cm	6.700 ± 400 BP*	TH47.1
<i>Ghazal</i>	GH.5	47 cm	8.800 ± 500 BP	TH47.3
Khumseen	GH.5a	140.8 cm	7.100 ± 400 BP	TH50.2
Khumseen	GH.5b	179.9 cm	9.400 ± 800 BP	TH50.1

*BP (before present) dates are uncalibrated.

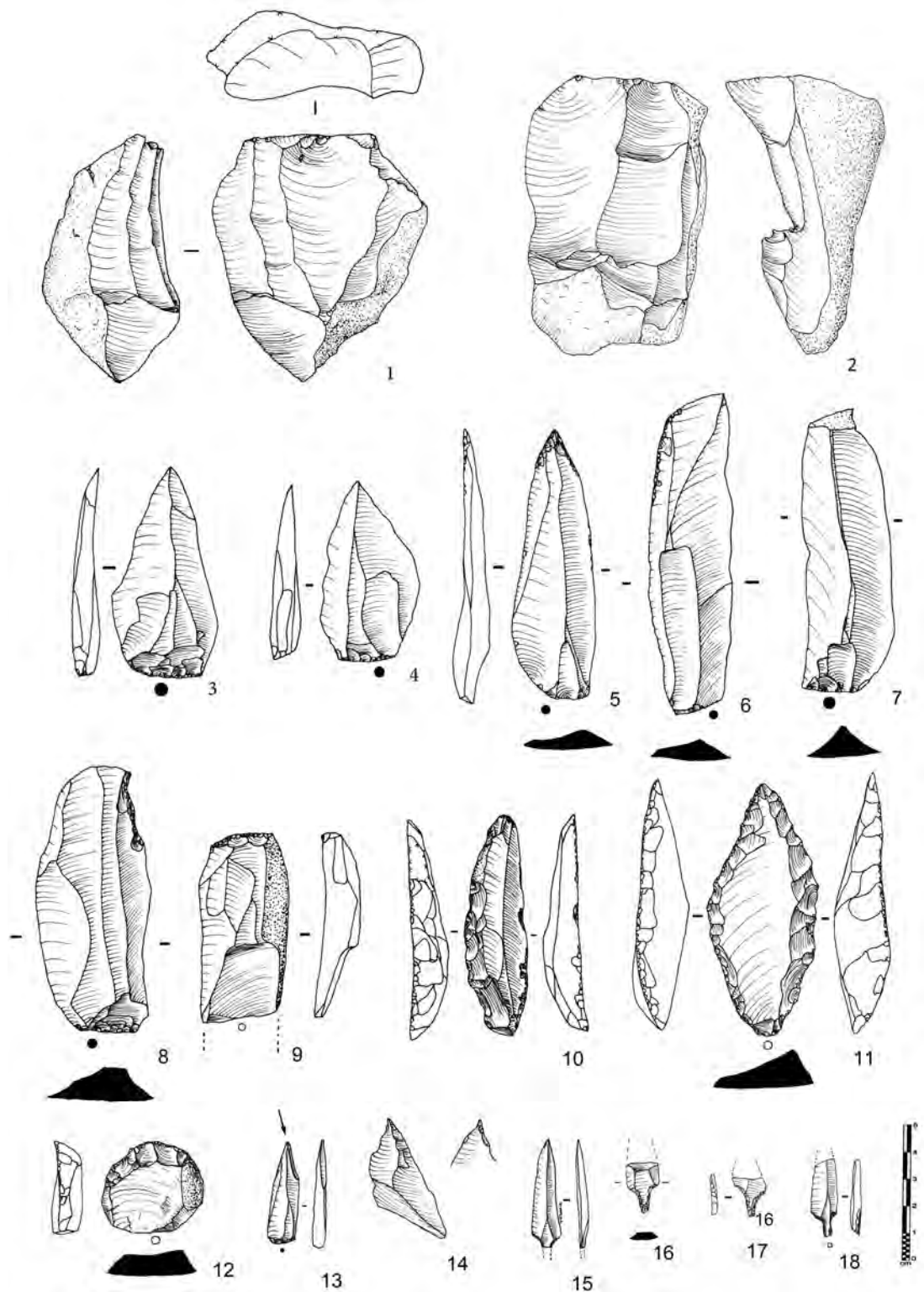


Figure 9.21 Selected Artefacts typical for the Khashabian.

1 and 2, unidirectional parallel cores from Ghazal and Khumseen; 3 to 8, convergent blanks and retouched blades from Wadi Haluf; 9 and 12 endscrapers from Wadi Haluf and TH.200; 10 and 11, pseudo-backen knives from Jebel Eva and SJ.51; 13, burin from Ghazal; 14, piercer from Khumseen; 15 to 18 Fasad points from TH.200, Khumseen and Jebel Eva. (Illustration Y. Hilbert).

The dates from Khumseen Rockshelter were retrieved from GH.5a and 5b, together these GH are over one meter in depth indicating that considerable sediment accumulation had occurred between approximately 10 and 7 ka BP. The fact that a significant number of refits have been made indicates that sediment deposition took place continuously and that little post-depositional displacement had occurred. At Ghazal Rockshelter, sediment accumulation was less intense. The two OSL dates have been retrieved from sterile eolian layers that mark periods of increased eolian activity. The lower eolian event was dated to 8.8 ± 0.5 ka BP. The sediments overlaying the sterile layer contain the Khashabian industry. This sedimentary unit accumulated during the early Holocene wet phase. The superimposed GH, also a sterile sand layer, was dated to 6.7 ± 0.4 ka BP and separates the Khashabian sample from the Ghazal Level 1 sample.

Based on these dates it is inferred that the Khashabian represents the material culture pertaining to the populations that inhabited the Dhofar between approximately 10 to 7 ka BP.

9.2 The Khashabian: landscape and climate

Based on the DAP survey results, it appears that the Khashabian population occupied the entire Nejd Plateau; stretching from the northern border of the Dhofar Mountain chain to the verge of the Rub al Khali desert. No Khashabian archaeological remains have been found by the DAP within the Dhofar mountain chain or on the coastal plain¹. Based on the overwhelming quantity of Nejd Leptolithic tradition sites found across the Plateau (n=226), these groups likely favoured the Nejd over the coast and the mountains. Since the timeframe of the Khashabian corresponds with the Early Holocene wet phase, environmental conditions across the Nejd would have supported a considerably larger biomass than at its present state.

The distribution of sites presented in this dissertation indicates the ubiquitous

¹ As will be seen in the following section (9.3) Cremaschi and Negrino (2002; 2005) report archaeological findings from the Dhofar escarpment that are analogous with the Khashabian.

presence of Khashabian findspots across a relatively diverse and varied landscape. In both the southern and central Nejd, Khashabian findspots are primarily located along raw material outcrops in proximity to drainage systems. Clearly, the availability of raw material and proximity to ancient wadi systems, which under more favourable conditions would have been active riparian environments (Berger *et al.*, 2012), are the two most significant variables patterning site distribution.

The influence of the Early Holocene wet phase were not limited to Dhofar, but affected the entire South Arabian Highlands (and beyond). West of Dhofar, in the Hadhramaut valley, heightened precipitation also fuelled local riparian systems. Fluvial sediments from the northern Hadhramaut basin, dated to the Early Holocene wet phase, indicate that a constant sediment aggregation, rather than downcutting and erosion, occurred. Such a pattern correlates with the occurrence of riparian forests and wetland grasslands within the wadi systems (Lézine *et al.*, 1998; 2007; Berger *et al.*, 2012). This observation begs the question: does the distribution of Khashabian sites extend further westward, across the continuous dissected plateau that comprises the South Arabian Highlands? Perhaps more significantly, from where did it originate?

9.3 The Khashabian in Arabia

To address whether the Khashabian extends beyond Dhofar, it is necessary to review the Early Holocene archaeological record of southern Arabia. Here, the geographical extent of the Khashabian is articulated and intra-regional variability within the Early Holocene archaeological record of southern Arabia is explored. This synthesis will concentrate on stratified assemblages and surface occurrences attributed to the Early Holocene on the basis of techno/typological analysis and absolute, and relative dating methods.

The Early Holocene occupation uncovered at Jebel Faya NE-1, in the Emirate of Sharjah, has been dated by C¹⁴ to 8,454 – 7,761 2σ Cal. BC. The lithic material is marked

by the presence of Fasad points made on blades produced from “more or less prepared cores” (Uerpmann *et al.*, 2009, 209). Fasad points have also been uncovered at the site of Nad-al Thaman situated approximately 15 km south of the Faya NE-1. Excavations have uncovered lithic artefacts buried under 50 cm of sand. Aside from the diagnostic Fasad points, various bifacial implements such as foliates and arrowheads have also been uncovered. A single C¹⁴ date of 6,997–6,444 2σ Cal. BC. provides some chronological affiliation for these finds (*Ibid*).

Fasad points have been found in surface scatters throughout the UEA, Oman and Yemen (e.g. Pullar, 1974; Charpentier, 1996; 2008; Zarins, 2001; Uerpmann *et al.*, 2009; Jagher *et al.*, 2011). Unfortunately these artefacts are seldom described in conjunction with the blank production systems found at each occurrence or any other associated artefact class. Additional assemblages containing Fasad points have been reported by Cremaschi and Negrino (2002; 2005) from rockshelters found along the southern fringes of the Jebel Qara escarpment, Dhofar. At KR213, KR108 and KR276 Fasad point made on blades and flakes, sidescrapers, notches and denticulates have been found logged within sediment date to 8750 ± 50 BP and 8720 ± 60 BP. These tools have been found associated with an undetermined blade reduction strategy.

Tanged projectile points are also known from Qatar B group sites. First detected and dated to 6970±130 BC by the Danish Mission (Kapel, 1967) and later techno/typologically described by Inizan (1980a; 1980b) the Qatar B blade industry is geographically restricted to the Qatar Peninsula. This industry is marked by the production of blades using a bidirectional reduction method with elaborate crest preparation. Following the creation of two opposed striking platform's from which crested blades are reduced from either the primary or opposed platforms, volumetric blade production takes place. Blades are further transformed into tanged projectile points. Retouch is administered to the tip of the projectiles and the tangs, which in most of the illustrated cases resemble Biblos points from the Levant (Inizan, 1980). In addition to the projectile points the tool spectrum

encompasses endscrapers, sidescrapers, piercers and retouched blades.

In recent years Crassard (2007; 2008a; 2008b) has identified a reduction method aiming at the production of standardised elongated volumes. This reduction, entitled Wa'shah method, has been recognized on the basis of artefact analysis undertaken primarily on surface scatters in the Hadhramaut region of Yemen. Technologically, this reduction method is marked by a specific preparation of the core's working surface. Two unidirectional removals struck from the peripheries of the core create a dihedral plain that subsequently spawns one preferential convergent/diamond shaped blade or bladelet, equivalent to the end product of modality 3. Crassard also identifies the "Wa'shah point", which is the intended product of this specific *chaîne opératoire*. The Wa'shah point is an armature produced by semi-abrupt to abrupt retouch restricted to the proximal portion of a symmetric elongated blank. In some cases, Crassard also notes the creation of bifacial tangs. An Early Holocene age for this reduction modality and its associated end product is partially confirmed by the presence of Wa'shah *débitage* in the lower levels of HDOR 419; a multilayer site in the Hadhramaut region of central Yemen. Although this unit (layer 6) is undated, the superimposed horizon provides a terminus post quem radiocarbon date between 7272 ± 120 BP and 6931 ± 48 BP.

At Wadi at Tayyilah 3 (WTH3), situated in the southern portion of the Asir Highlands, Fedele (2008; 2009) has identified a distinct assemblage ascribed to a pre-Neolithic industry. This industry is marked by the production of diverse tool forms and flake and blade blanks. The toolkit is primarily composed of cutting, boring and scraping tools. Burins, utilized blades and "segments" accompanied by stout unifacial points, truncated tablets and the occasional foliated piece are also reported (Fedele & Zaccarra, 2005). The excavations at the site have also yielded the oldest portable figurative "art" found in Yemen (Fedele, 1986), a small figurine made of unfired clay possibly representing a female torso. Although the pre-Neolithic occupation of WTH3 is undated, its stratigraphic position below the Neolithic strata hints at an Early Holocene to Terminal Pleistocene age

contemporary with the Khashabian.

The Arabian assemblages characterized by the presence of Fasad points and blade production (Faya NE-1, Nad-al Tammam and other surface scatters) may all belong to one broad Early Holocene technocomplex. Unfortunately, insufficient technological descriptions hinder systematic comparison with the Khashabian industry. In the case of KR108, KR213 and KR276 from Jebel Qara in Dhofar, their absolute ages and general techno/typological appearance are consistent with the Khashabian techno/typological package.

Although association between the Fasad point bearing assemblages from Dhofar and the Qatar B group have been made in the past (e.g. Zarins, 2001) the here presented techno/typological package shows minimal overlap with the Qatar material. Nor have any other assemblages with Qatar B affinities been noted across the South Arabian Highlands.

The Wa'shah surface occurrences found throughout the Hadhramaut region display strong affinities with the Khashabian industry. The Wa'shah method of blade production is technologically identical to Modality 3 of Khashabian blade production. Wa'shah points have been found in Dhofar, however a clear association with the Khashabian assemblages are at this point speculative given that the material remains unstudied. Although the Wa'shah method in Hadhramaut has been thoroughly described, there is no secure chronological attribution.

The pre-Neolithic assemblage uncovered at WTH3 is unlike any of the Fasad bearing assemblages identified across Arabia. No parallels with the Khashabian could be detected based on the review of the published data indicating that these are two different industries.

Based on this review of the South Arabian Early Holocene archaeological record, it is clear that there is need for additional research. A unified taxonomic system applicable to these assemblages would also greatly aid in intra-regional comparisons. Nonetheless, a coarse pattern emerges that warrants further discussion. Given the technological and

typological differences between the Qatar B sites and the Fasad bearing assemblages, including the Khashabian, this study sees no connection between the two entities. Further research is needed on the individual Fasad bearing assemblages lacking technological descriptions, in order to clarify whether these are part of a single technocomplex or represent unrelated regional industries. The differences between the Khashabian, the Pre-Neolithic of western Yemen and the Qatar B may indicate that diverse populations exhibiting dissimilar material cultures populated Arabia during the Early Holocene.

9.4 The Khashabian: local or exogenous?

The repeated identification of the Khashabian techno/typological package across numerous sites in Dhofar verifies the validity of this industry as a legitimate cultural unit. It is then possible to compare the Khashabian to other industries across both time and space and explore its region of origin. As noted by Marks (2009), the widely oscillating environment of Arabia is such that industries will either have a local, Arabian source or have exogenous origins. Both scenarios warrant review in light of the new evidence presented in this dissertation.

9.4.1 Exogenous

The Pleistocene/Holocene transition across southern Arabia followed a drastic climatic downturn culminating in the LGM around 18 ka. If a *tabula rasa* event were assumed to have occurred during the LGM in southern Arabia, local industries would terminate at this time. The succeeding Khashabian would then represent an industry with an exogenous source, implying that industries with comparable techno/typological packages should be found in one of Arabia's adjacent regions. Historically, researchers have looked towards the Levant when explaining the origins of Early Holocene Arabian occupation (e.g. Kapel, 1967; Inizan, 1980; Drechsler, 2009; Uerpmann *et al.*, 2009). Such Levantine assemblages are reviewed below. In addition, roughly coeval industries in the

Horn of Africa and the southern Zagros mountains are also considered, since these too border Arabia and are potential reservoirs of Early Holocene demographic input.

Assemblages dating to the Pleistocene/Holocene boundary in the Horn of Africa are marked by inventories dominated by bipolar (anvil) technology, blade and micro-bladelet core reduction. Blank production is bidirectional using two opposed platform cores, unidirectional using small conical cores or using *piece ecaillé* (e.g. Clark, 1954; Barham & Mitchell, 2008). Sites known from Ethiopia and Somalia pertaining to the “Ethiopian Blade Tool Tradition” include tools such as microliths, scrapers, burins as well as long “utilised” blades (Brandt, 1986). In southern Somalia, at the end of the Pleistocene and the early Holocene, the Eibian industry has been identified. Characteristics for the industry are elaborately made pressure flaked unifacial and bifacial points (Brandt, 1986; 1988). The majority of the assemblages known in the Horn, however, are primarily marked by blade and microlith producing industries via the bipolar technique (Brandt & Brook, 1984; Brandt, 1986; Barham & Mitchell, 2008).

Assemblages contemporary with the Khashabian industry found in the Levant belong to the Pre-Pottery Neolithic (PPN) (11,7–ca. 8,4 cal. BP). This well studied period is further divided into two phases termed PPNA and PPNB (Figure 9.22). Blank production is dominated by bidirectional naviform core technology (e.g. Nishiaki, 1993; 2000; Abbés, 2003; Barzilai, 2010). Volumetric unidirectional blade and bladelet production is also known and underlays complex technical preparations methods such as crested blade and core tablet technologies. Prominent within the PPN toolkit are sickle blades, ground stone tool stools, burins, endscrapers, truncated pieces, backed elements, and projectile points (e.g. Servello, 1976; Kozłowski, 1999; Kuijt & Goring-Morrise, 2002; Barzilai, 2010). The PPN period is marked by profound changes in subsistence economies with a shift towards food production rather than acquisition by hunting and gathering. Linked to this economic shift, the establishment of elaborate architectural features and semi-permanent settlements are found in the archaeological record. Figurative art in form of clay figurines,

elaborate burials, and storage facilities are other considerable developments found within incipient Levantine Neolithic society (e.g. Bar-Yosef, 1981; Kuijt, 1994; Kuijt & Goring-Morrise, 2002; Asouti, 2006).

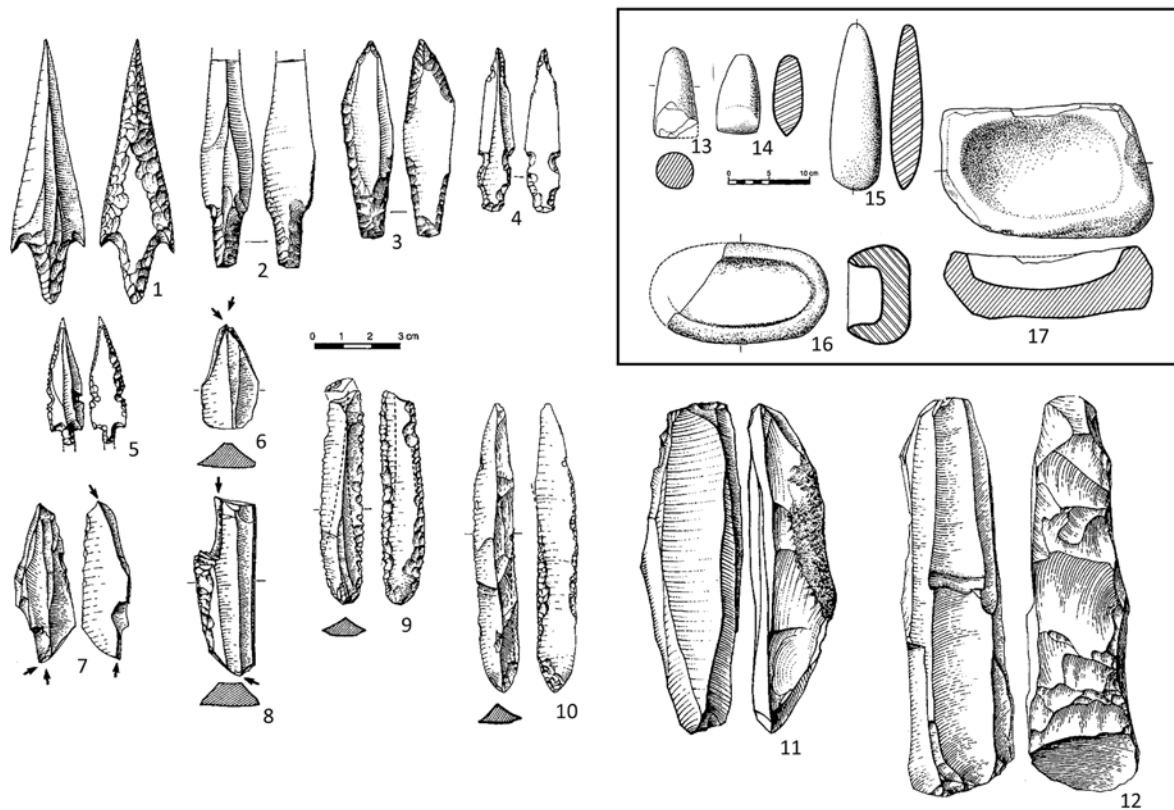


Figure 9.22 Selected Artefacts typical for the PPNB.
(Modified after Kuijt & Goring-Morrise, 2002, fig. 11 and 12)

Recent archaeological investigations of Proto-Neolithic cave sites in the Bolaghi Valley of southern Iran have recorded microlithic assemblages dating roughly between the 9 and 8 millennium BC (Tsuneki *et al.*, 2007). Standardised tool types include endscrapers, thumbnail scrapers, sidescrapers, burins, lunates and baked bladelets. Blank production is strictly laminar and oriented towards the production of micro blades and bladelets (Figure 9.23). Cores have been reduced in both uni- and bidirectional fashion; these exhibit conical silhouettes and have a partially or completely exploited striking platform circumference. Core tablets and core rejuvenation flakes are technologically diagnostic débitage that result from this reduction strategy.

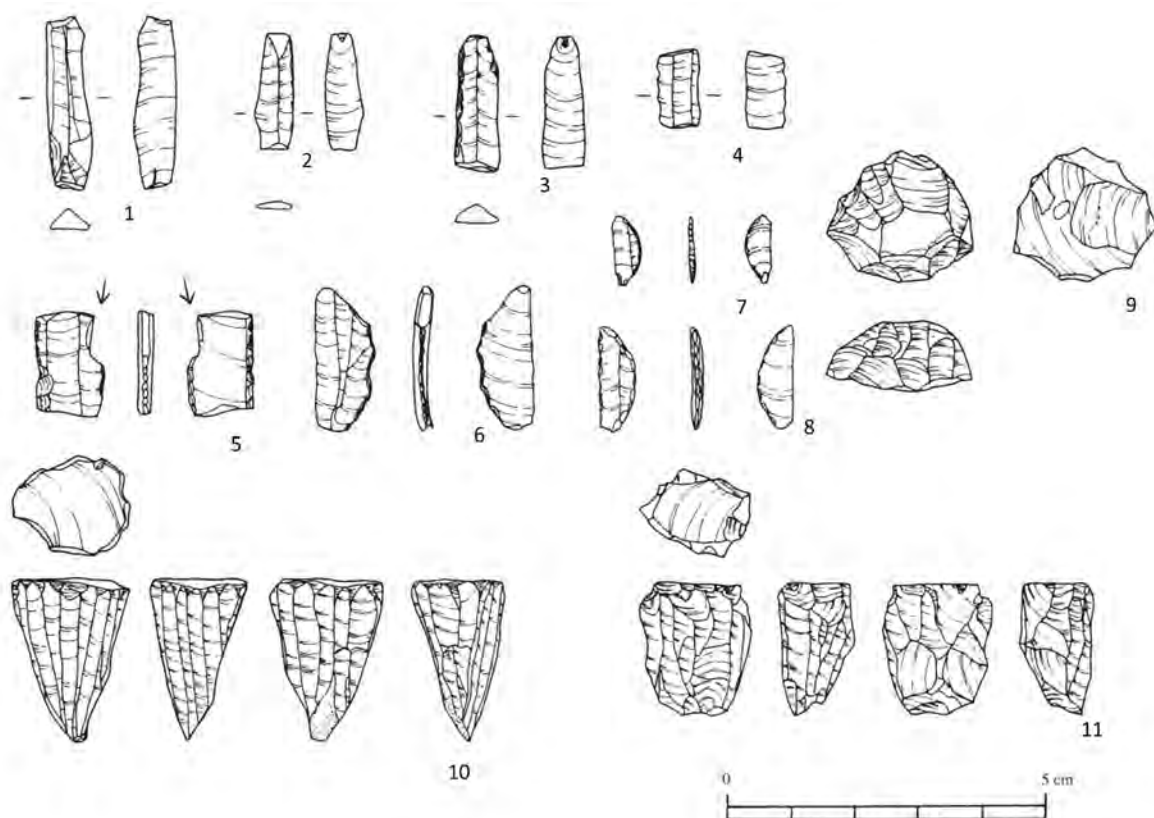


Figure 9.23 Selected Artefacts typical for the Proto-Neolithic.
(Modified after Tsuneki et al., 2007, fig. 15 and 16).

None of the technologies found in regions adjacent to the Arabian Peninsula exhibit techno/typological overlap with the Khashabian. Assemblages from the Horn of African are marked by bipolar (anvil) technique and simple unidirectional blade production. The bipolar technique is found at Iron Age site in Yemen (e.g. Crassard, 2008a; Khalidi, 2009); however, it is not known within the Khashabian technological repertoire. Additionally, no lunates, backed pieces or microliths are found within the Khashabian. The bidirectional naviform blade and bladelet cores found within PPN assemblages have not been identified in Dhofar. Although pedunculated projectile points occur in both Khashabian and the PPNA/B industries, these are morphologically different and produced by different reduction systems. The PPN points are made on blanks produced using bidirectional blade technology and are modified by direct percussion and pressure flaking.

Also missing within the Khashabian are architectural features and symbolic artefacts, making a connection between the PPN Levant and Dhofar unlikely. The microlithic lunates and trapezoidal forms found in the Proto-Neolithic sites of Iran are also absent within the Khashabian. While the blank production systems found at the sites are also laminar, they are oriented towards bladelet production, following unidirectional and bidirectional reduction strategies. This feature is inconsistent with the reduction modalities of the Khashabian. It is clear, from this cursory review, that there are no technological and/or typological resemblances between these industries and the Khashabian. Therefore, the roots of this industry are more likely to have been located within Arabia itself, derived from a lithic tradition that endured the LGM in one of the speculative refugia.

9.4.2 A local source

The statement of a local origin for the Khashabian has significant demographic implications; there was no complete *tabula rasa* and at least some part of Arabia was inhabited during MIS 2. Two recently discovered may lie along the same technological continuum and have been discussed in Chapter Two: al Hatab and Shi'bat Dihya.

At SD1 and SD2, dated between 55 – 45 ka BP (Delagnes *et al.*, 2012), blank production is anchored within a simple and highly efficient unidirectional recurrent blade producing system much like that of al Hatab and the Khashabian assemblages. Convexity maintenance is equally achieved through the removal of débordant elements from the core's working surface peripheries, while end products from SD 1 share morphological features with the TDD found within modality 1 of the Khashabian. The lack of core tablets and crested blade technology is also noteworthy given that these technological elements are absent across the Late Palaeolithic. One difference is the low frequency of recurrent Levallois-like technologies identified at SD1 and SD2, which is completely absent in the Khashabian and other Nejd Leptolithic tradition assemblages.

The dates for the Nejd Leptolithic occupation at al Hatab fall between 14 and

10 ka BP (Rose & Usik, 2009), preceding the Khashabian industry and falling into the later half of the LGM. Reduction systems observed within the Khashabian and al Hatab assemblages are virtually identical. Blank production at al Hatab is dictated by a unidirectional recurrent reduction; cores and *débitage* analysis indicate the use of the same modalities that have been detected at Khumseen and Ghazal Rockshelters (Hilbert *et al.*, 2012). Typologically, the occurrence of Fasad Points, burins on truncation and endscrapers parallel the Khashabian. On the other hand, the kombewa method, reported by Rose and Usik (2009) to be part of the earlier Nejd Leptolithic techno/typological package, is absent from Khashabian sites. However, this discrepancy may be due, in part, to different analytical schemes used by researchers. In addition, the lack of pseudo-backed knives and trifaces at al Hatab also indicates typological variability between Khashabian and al Hatab assemblages.

Clearly, the Khashabian was not brought to the Arabian Peninsula by populations from the Horn of Africa, Iran or the Levant. Therefore, it may have developed in a refugium. Given the distribution of similar Late Palaeolithic sites, this was most likely in the South Arabian and/or Yemeni Highlands, out of a population that had survived the apparently catastrophic desiccation during the Late Glacial Maximum (LGM). In terms of classification, it is suggested that the Khashabian belongs to a late phase of the Nejd Leptolithic tradition, developing from the preceding phase represented at al Hatab. The Nejd Leptolithic, in turn, may be rooted in the reduction systems found at SD1/SD2.

To verify such a scenario on the basis of archaeological data is only possible with a high resolution chronological sequence built from sites across the South Arabian Highlands in Yemen. Until fieldwork activities can be resumed in this part of Arabia, however, archaeological investigation alone will not be able to address the question. On the other hand, the field of archaeogenetics lends some insight into the origins of modern South Arabian peoples.

9.3.3 Palaeodemographics and genetics

Genetic research undertaken in Yemen adds to our understanding of prehistoric demographics across the South Arabian Highlands during the latter half of the Late Pleistocene. Based on the study of haplotype R0a variability and distribution in Yemen by Černý *et al.* (2011), a model for the past 20 ka demographics of southern Arabia has been proposed (Figure 9.24). The source of the R0a lineage was once posited to be in southern Asia (the Middle East, the Indus Valley and East Asia) where the greatest variety of this clade has been observed so far (e.g. Richards *et al.*, 2000; Metspalu *et al.*, 2004; Cabrera *et al.*, 2009). The recent discovery of R0a founder haplotypes within the Arabia Peninsula, however, indicates that this region may represent an additional center for the endemic development of this haplogroup (Černý *et al.*, 2011). Two chronologically separate demographic expansions tied to wet climatic conditions have been suggested, of which R0a took place prior to the LGM. Later expansions, related to R0a2, R0a3 and R0a1a haplogroups, succeeded after the LGM but before the Pleistocene/Holocene transition. Given that a local source for the R0a haplogroup can at this point not be ruled out, the possibility for the persistence of indigenous Arabian populations living within climatic refugia during the LGM is a legitimate possibility.

While the coalescence age estimates for the R0a haplogroup, or any genetic dating for that matter, are imprecise and increasingly contentious (see Ho & Endicott, 2008; Endicott & Ho, 2008; Endicott *et al.*, 2009), the general observation of an indigenous origins for southern Arabia populations across the Terminal Pleistocene (Černý *et al.*, 2008; 2011; Fernandes *et al.*, 2012; Al-Abri *et al.*, 2012) correspond to the archaeological data. Evidence from the Wadi Surdud site complex indicates that populations occupied the western Yemeni highlands during an arid period within MIS 3 (Delagnes *et al.*, 2012). In which case, the populations responsible for the Shi'bat Dihya 1 and 2 assemblages might represent ancestral R0 haplotypes. The observed technological continuum between the Wadi Surdud sites and Late Palaeolithic assemblages from Dhofar supports this

proposition.

If, indeed, this is the case, these MIS 3 populations must have survived the LGM in southern Arabia. Following the environmental amelioration corresponding to the Bølling-Allerød interstadial (Fleitmann *et al.*, 2007; Parker, 2009), we may speculate that indigenous groups within the Yemeni refugium expanded eastwards and (re) populated the South Arabian Highlands, possibly as far to the east as the Haushi-Huqf depression in central Oman. The subsequent climatic downturn during the Terminal Pleistocene was responsible for isolating this once larger population into smaller separated communities across South Arabian refugia. Consequently, this seclusion may have caused genetic drift between populations inhabiting the region at the Pleistocene/Holocene divide. The three haplotypes R0a1a, R0a2 and R0a3 would consequently represent the fluorescence of different lineages stemming from the ancestral R0a population.

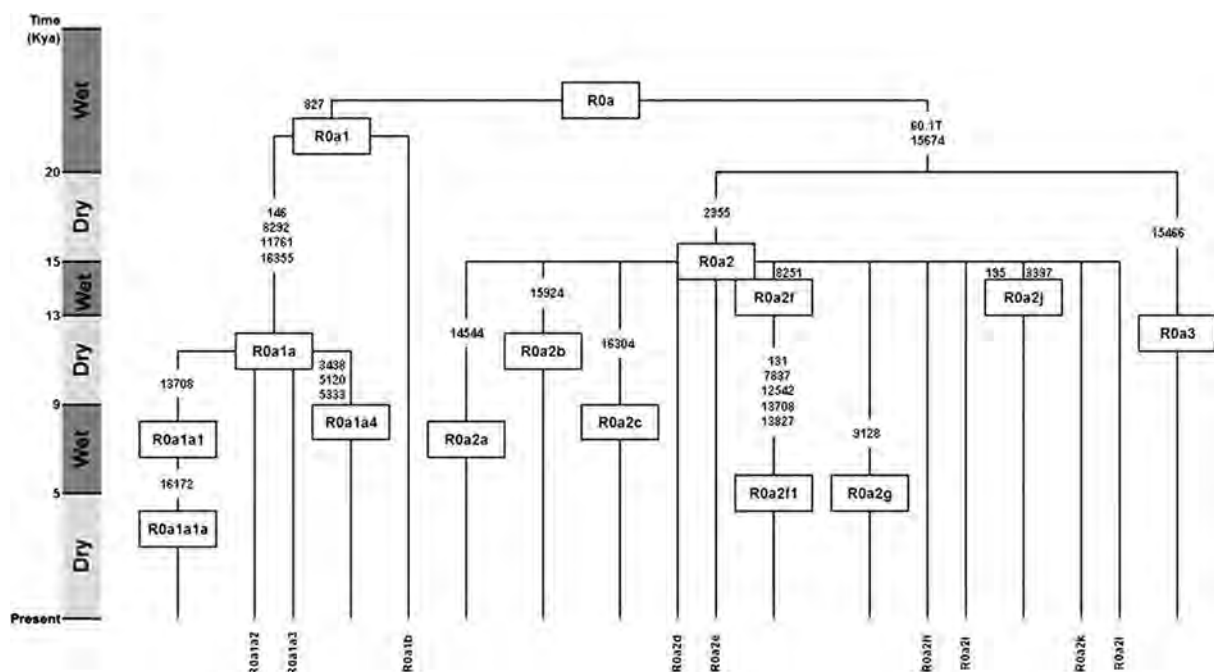


Figure 9.24 Main branches of the complete R0a mtDNA tree.
(After Černý *et al.*, 2011, fig. 3).

It must be kept in mind, however, that these genetic data are not directly equivalent to stone tool technology, that is to say, transmitted cultural behaviour. We cannot assume lithic industries are equal to genes. Regardless, the mtDNA does suggest population continuity across the Pleistocene/Holocene divide, supporting a local (Arabian) source for the Khashabian industry.

9.5 Transition to the Neolithic

Transitions are understood as the change, shift or passage from a stable state to a different equally stable state (*Oxford Dictionary*). Discussion of the local transition from the Khashabian to the Neolithic requires the clear definition of both entities. This dissertation has dealt with the definition of the Khashabian; the Neolithic period is much better described than the Late Palaeolithic and has been summarized in a number of publications (e.g. Kallweit, 1996; Zarins, 2001; Crassard *et al.*, 2006; Charpentier 2008).

The transition from the Khashabian to the Neolithic in Dhofar is here understood as a period of environmental and socio-economical change. Between 9 and 6 ka BP, hunter-pastoralist “Neolithic” groups are thought to have expanded across southern Arabia (e.g. Edens & Wilkinson, 1998; Fedele & Zaccara, 2005; Cleuziou & Tosi, 2007; Charpentier, 2008; Crassard, 2009; McCorriston *et al.*, 2012). Whether these groups evolved locally out of an indigenous Arabian population, as Fedele (2009) suggests, or stem from Levantine pastoralist populations cannot yet be addressed given the limited chronological data. What is known, however, is that the hunting and domestic equipment these Arabian “Neolithic” populations produced and utilised represent a material culture with no parallels outside of Arabia. Armatures are finely made trihedral and triangular projectiles, and winged projectiles manufactured by parallel pressure flaking are also documented. Also prevalent within the Arabian Neolithic toolkit are sidescrapers, endscrapers, burins, and diverse types of bifaces made using soft hammer *façonnage*.

Blank are primarily produced from multiple platform flake cores, and to a lesser

extent, using radial core technologies. Blade production is notably underrepresented. In cases where organic material has been preserved, these assemblages are accompanied by faunal remains that indicate the use of a hybrid subsistence strategy based on hunting and foraging, supplemented by domestic goat, sheep, and cattle husbandry (e.g. Fedele, 2008; 2009; Martin *et al.*, 2009; McCorriston & Martin, 2009).

At Khumseen Rockshelter, Neolithic horizons overlying the Khashabian levels have been identified within GH 4a and 4b. A fireplace within the lower stratum of GH 4b was dated by C¹⁴ to 6950 and 6740 Cal. BP (BETA-281554). Neolithic surface sites and stratified occurrences are fairly widespread across the Nejd. Additional assemblages comprising the Neolithic technological package, including diagnostic trihedral rods (Figure 9.25), have been recorded across the plateau by the DAP and other researchers (Zarins, 2001; Rose 2006).

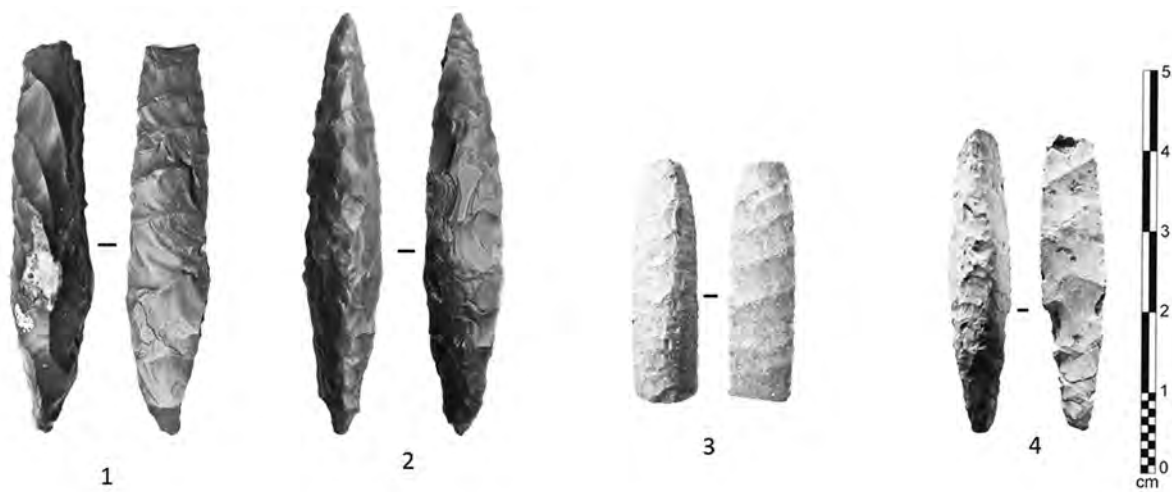


Figure 9.25 Trihedral projectile points from diverse sites across the Nejd. (Photograph by Y. Hilbert).

The relatively sudden appearance of such a profoundly different toolkit and subsistence strategy around 7 ka BP across Dhofar invokes Galton's Problem of migration versus diffusion. In other words, was it ideas or people that expanded into Dhofar at this time? An *in situ* evolution of these technological and typological elements within Dhofar, derived from the Khashabian, is unlikely given the marked differences in tool forms and

core reduction strategies.

At Ghazal Rockshelter two superimposed archaeological occupation and subsequent sedimentation phases could be identified, making it possible to distinguish two distinct archaeological horizons. The package identified at Ghazal Level 2 has been found corresponding to the Khashabian industry, whereas the sample from Level 1 was deemed too small to warrant a concrete classification as Khashabian. Notably however, the technological pattern observed at Ghazal Level 1 is consistent to that of the Khashabian. Divergences are noted in the increased use of modality 2 and the presence of striking platform grinding. The sedimentary event that buried the level 1 assemblage took place after the eolian accumulation, which sealed level 2 from the remaining sequence above. This eolian event was dated by OLS to $6,7 \pm 0.4$ ka BP, corresponding to the onset of the Middle Holocene dry phase identified across southern Arabia (e.g. Cremaschi & Negrino, 2005; Parker *et al.*, 2006a; Fleitmann *et al.*, 2007; Berger *et al.*, 2012).

This implies that a late Khashabian occupation was present as late as the Middle Holocene in Dhofar. In turn, suggesting that two distinct populations inhabited the Nejd Plateau at that time –Late Palaeolithic Khashabian hunter-gatherers and Neolithic pastoralists. This observation raises a number of interesting questions: how did these groups interact, did acculturation occur, and ultimately, what happened to the Khashabian toolmakers? The recent identification of haplogroup R2 in Dhofar, a derivative of R0, indicates that at least part of this relict South Arabian lineage still persists today (Al-Abri *et al.*, 2012).

9.6 Summary

Based on lithic analysis undertaken on both surface scatters and *in situ* assemblages collected across the Nejd Plateau, the Khashabian industry is defined in this study. Using OSL and C¹⁴ dating methods, it is bracketed within the Early Holocene (10 - 7 ka BP). The Khashabian is found to be similar to other assemblages from Yemen (Shi'bat Dihya) and

Oman (al Hatab) dating roughly between 45 and 10 ka BP.

Technologically, the Shi'bat Dihya assemblages and the Khashabian industry share a unidirectional parallel *tournant* blade production method, and use similar modalities of convexity exploitation and containment. The chronological gap between these assemblages, however, is too great to argue for demographic continuity across Southern Arabian from MIS 3 onwards.

The Khashabian appears to derive from a Terminal Pleistocene laminar industry in Dhofar, such as the one identified at al Hatab. The persistence of the Nejd Leptolithic technocomplex across the Pleistocene/Holocene boundary refutes the "Levantine hypothesis" (*sensu* Uerpmann *et al.*, 2009), at least as it pertains to demography in Dhofar. Based on a review of the Early Holocene archaeological record across South Arabia, it is argued that the region was populated by at least three different culture groups: 1) the Pre-Neolithic of the Yemeni Highlands, 2) the Late Palaeolithic blade producing tradition found throughout the South Arabian Highlands, and 3) the Qatar B type assemblages noted in eastern Arabia. It is argued that the Khashabian was not the predecessor of the Neolithic hunter-herder populations, who expanded across the South Arabian Highlands between 9 and 6 ka BP. To what extent the Khashabian survived into the Middle Holocene must still be determined.

APPENDIX A

Lithic Attribute Analysis from the DAP 2010-2012 Assemblages

Khumseen		% amount of dorsal cortical cover.					
	TOTAL	<>*	0 to 10	11 to 25	26 to 50	51 to 75	76 to 100
Flake	129	2	93	21	13		
Blade	82		73	8	1		
Bladelet	74		67	6	1		
Cortical Flake	38					16	22
Cortical Blade	12					8	4
Débordant Flake	13		2	5	6		
Débordant Blade	23		6	7	10		

Ghazal							
	TOTAL	<>	0 to 10	11 to 25	26 to 50	51 to 75	76 to 100
Flake	82	2	39	23	18		
Blade	57	1	41	13	2		
Bladelet	20		20				
Cortical Flake	47	1				19	27
Cortical Blade	16					8	8
Débordant Flake	7			3	4		
Débordant Blade	18			6	12		

Jebel Eva							
	TOTAL	<>	0 to 10	11 to 25	26 to 50	51 to 75	76 to 100
Flake	56		21	21	14		
Blade	86	1	16	37	32		
Cortical Flake	36	15				7	14
Cortical Blade	80	17			2	37	24
Débordant Flake	5			3	1	1	
Débordant Blade	109	3		34	69	3	
Natural crests	16	2				3	11

Wadi Haluf 1							
	TOTAL	<>	0 to 10	11 to 25	26 to 50	51 to 75	76 to 100
Flake	93	1	55	26	11		
Blade	164	4	116	30	14		
Bladelet	13		13				
Cortical Flake	51	2				12	37
Cortical Blade	50					22	28
Débordant Flake	18		1	11	6		
Débordant Blade	107		5	54	47	1	
BTF	2		1	1			

*Undetermined.

Blank striking platform morphology.

Khumseen

	TOTAL	<>	Cortical	Plain	Dihedral	Faceted	Crushed	Other*
Flake	129	20	8	79		3	19	
Blade	82	19	3	45	3	1	9	2
Bladelet	74	21	2	34			17	
Cortical Flake	38	6	7	20			5	
Cortical Blade	12	1	2	6		1	2	
Débordant Flake	13		2	10			1	
Débordant Blade	23	1	1	18			3	

Ghazal

	TOTAL	<>	Cortical	Plain	Dihedral	Faceted	Crushed	Other*
Flake	82	14	4	39	4	1	15	1
Blade	57	10	1	37	1		6	2
Bladelet	20	5		7			4	1
Cortical Flake	47	8	9	23		1	6	
Cortical Blade	16	1	2	11			1	1
Débordant Flake	7	1	1	5				
Débordant Blade	18	1	2	11	1		1	

Jebel Eva

	TOTAL	<>	Cortical	Plain	Dihedral	Faceted	Crushed	Other*
Flake	56	9	14	26	1		4	2
Blade	86	16	5	54			10	1
Cortical Flake	36	15	6	10	2		2	1
Cortical Blade	80	19	4	47	3	2	5	
Débordant Flake	5	1		4				
Débordant Blade	109	36	4	65		1	3	
Natural crests	16	2	1	13				

Wadi Haluf 1

	TOTAL	<>	Cortical	Plain	Dihedral	Faceted	Crushed	Other*
Flake	93	19	4	54	2	4	10	
Blade	164	56	3	88	2		15	
Bladelet	13	3		7			3	
Cortical Flake	51	12	14	17		2	6	
Cortical Blade	50	4	3	31	2		2	
Débordant Flake	18	2		16				
Débordant Blade	107	25	2	78			3	
BTF	2					1	1	

*Punctuated, Transverse faceted (see Chapter 5 for further definitions).

Khumseen

Striking platform abrasion.

	TOTAL	<>	Not Abraded	Abraded	Partial
Flake	129	39	71	3	16
Blade	82	29	34	7	12
Bladelet	74	38	27	3	6
Cortical Flake	38	11	25		2
Cortical Blade	12	4	7		1
Débordant Flake	13		12	1	
Débordant Blade	23	4	14	2	3

Ghazal

	TOTAL	<>	Not Abraded	Abraded	Partial
Flake	82	23	44	2	13
Blade	57	14	29	6	8
Bladelet	20	10	5		5
Cortical Flake	47	13	30		4
Cortical Blade	16	3	12	1	
Débordant Flake	7	1	4		2
Débordant Blade	18	2	10		6

Jebel Eva

	TOTAL	<>	Not Abraded	Abraded	Partial
Flake	56	12	39	4	1
Blade	86	25	54	6	1
Cortical Flake	36	17	19		
Cortical Blade	80	26	54		
Débordant Flake	5	1	4		
Débordant Blade	109	38	70	1	
Natural crests	16	2	14		

Wadi Haluf 1

	TOTAL	<>	Not Abraded	Abraded	Partial
Flake	93	23	57		13
Blade	164	59	69		36
Bladelet	13	3	7		3
Cortical Flake	51	21	28		2
Cortical Blade	50	13	33		4
Débordant Flake	18	2	15		1
Débordant Blade	107	24	77		6
BTF	2		1		1

Blank cross-section.

Khumseen											Blank cross-section:
TOTAL	<>	Flat	Triangular	Lateralized	Trapezoidal	3 vectors	Rectangular	Convex	Pitched		
Flake	129	8	17	32	24	41	5	1	1		
Blade	82	4	2	28	9	36	3				
Bladelet	74	1	1	34	16	22					
Cortical Flake	38		23	6	1	2		2	4		
Cortical Blade	12		2	7	1				2		
Débordant Flake	13			4	6	3					
Débordant Blade	23	1	1	11	8	2					

Ghazal										
	TOTAL	<>	Flat	Triangular	Lateralized	Trapezoidal	3 vectors	Rectangular	Convex	Pitched
Flake	82	2	10	16	17	20	15	1	1	
Blade	57			23	4	26	4			
Bladelet	20			14	1	5				
Cortical Flake	47	22	5	3	2		1	1	13	
Cortical Blade	16	6		4				2	4	
Débordant Flake	7				4	3				
Débordant Blade	18			4	5	6	2	1		

Jebel Eva

	TOTAL	<>	Flat	Triangular	Lateralized	Trapezoidal	3 vectors	Rectangular	Convex	Pitched
Flake	56		12	11	7	14	6	4		2
Blade	86			12	4	48	7	11		4
Cortical Flake	36	16	9	4	3		1	2	1	
Cortical Blade	80	18	1	15	9	11	1	19	6	
Débordant Flake	5			1		2	1	1		
Débordant Blade	109	3		13	21	59	8	4		1
Natural crests	16	2						3	11	

Wadi Haluf 1

	TOTAL	<>	Flat	Triangular	Lateralized	Trapezoidal	3 vectors	Rectangular	Convex	Pitched
Flake	93	2	17	15	15	30	11	1	2	
Blade	164	4	4	54	14	68	20			
Bladelet	13			9		3	1		3	
Cortical Flake	51	44	2	2						
Cortical Blade	50	36		5	5	1	1	1	1	
Débordant Flake	18			1	6	10	1			
Débordant Blade	107	1		17	17	63	7	1	1	

Khumseen		Longitudinal cross-section.			
	TOTAL	<>	Flat	Incurvate	Twisted
Flake	129	21	53	27	28
Blade	82	9	38	6	29
Bladelet	74	3	40	5	26
Cortical Flake	38	3	17	9	9
Cortical Blade	12	1	3	5	3
Débordant Flake	13		3	3	7
Débordant Blade	23	1	6	4	12

Ghazal					
	TOTAL	<>	Flat	Incurvate	Twisted
Flake	82	4	46	24	8
Blade	57	3	27	11	16
Bladelet	20	1	11	2	6
Cortical Flake	47	26	8	10	3
Cortical Blade	16	10	1	4	1
Débordant Flake	7		3	1	3
Débordant Blade	18		1	14	2
BTF	3			1	2

Jebel Eva					
	TOTAL	<>	Flat	Incurvate	Twisted
Flake	56	3	21	18	14
Blade	86	10	32	16	28
Cortical Flake	36	15	12	5	4
Cortical Blade	80	21	13	17	29
Débordant Flake	5		3	1	1
Débordant Blade	109	9	24	24	52
Natural Crest	16	2	1	3	10

Wadi Haluf 1

	TOTAL	<>	Flat	Incurvate	Twisted
Flake	93	14	43	21	15
Blade	164	30	67	26	41
Bladelet	13	1	5	1	6
Cortical Flake	51	46	3	2	
Cortical Blade	50	37	4	5	4
Débordant Flake	18		8	3	7
Débordant Blade	107	5	26	43	33
BTF	2			2	

Khumseen		Blank's distal morphology.			
	TOTAL	<>	Fathered	Hinged	Overpassed
Flake	129	29	63	20	17
Blade	82	20	40	16	6
Bladelet	74	12	50	11	1
Cortical Flake	38	4	25	5	4
Cortical Blade	12	1	7	1	3
Débordant Flake	13		8	1	4
Débordant Blade	23	1	13	2	7

Ghazal					
	TOTAL	<>	Fathered	Hinged	Overpassed
Flake	82	9	46	19	8
Blade	57	7	41	8	1
Bladelet	20	6	13	1	
Cortical Flake	47	25	18	2	2
Cortical Blade	16	8	4	1	3
Débordant Flake	7	1	2	2	2
Débordant Blade	18	1	6	2	9

Jebel Eva

	TOTAL	<>	Fathered	Hinged	Overpassed
Flake	56	4	30	16	6
Blade	86	18	34	16	18
Cortical Flake	36	16	10	6	4
Cortical Blade	80	22	22	5	31
Débordant Flake	5		2	1	2
Débordant Blade	109	14	34	12	49
Natural Crest	3	3			

Wadi Haluf 1

	TOTAL	<>	Fathered	Hinged	Overpassed
Flake	93	15	47	24	7
Blade	164	54	80	20	10
Bladelet	13	6	4	2	1
Cortical Flake	51	46	3	2	
Cortical Blade	50	36	7	1	6
Débordant Flake	18		6	6	6
Débordant Blade	107	8	52	9	38
BTF	2		2		

Khumseen			Blank axis.	
	TOTAL	<>	On	Off
Flake	129	56	41	32
Blade	82	30	35	17
Bladelet	74	31	35	8
Cortical Flake	38	21	10	7
Cortical Blade	12	6	6	
Débordant Flake	13	2	5	6
Débordant Blade	23	3	6	14

Ghazal				
	TOTAL	<>	On	Off
Flake	82	27	38	17
Blade	57	15	33	9
Bladelet	20	11	9	
Cortical Flake	47	32	6	9
Cortical Blade	16	11	2	3
Débordant Flake	7		3	4
Débordant Blade	18	5	8	5

Jebel Eva				
	TOTAL	<>	On	Off
Flake	56	18	25	13
Blade	86	29	38	19
Cortical Flake	36	31	2	3
Cortical Blade	80	57	5	18
Débordant Flake	5	1	1	3
Débordant Blade	109	41	16	52
Natural Crest	16	14		2

Wadi Haluf 1				
	TOTAL	<>	On	Off
Flake	93	30	45	18
Blade	164	82	63	19
Bladelet	13	7	5	1
Cortical Flake	51	48	2	1
Cortical Blade	50	41	7	2
Débordant Flake	18	2	6	10
Débordant Blade	107	25	53	29
BTF	2	2		

Khumseen Blank shape.

	TOTAL	<>	Parallel	Expanding	Converging	Lateralized	Ovoid	Irregular
Flake	129	5	31	33	26	11	13	10
Blade	82		32	16	25	5		4
Bladelet	74	1	30	8	28	6		1
Cortical Flake	38	1	8	9	8	3	6	3
Cortical Blade	12		3	2	5	1		1
Débordant Flake	13		1	4	5	2		1
Débordant Blade	23		9	3	5	5		1

Ghazal

	TOTAL	<>	Parallel	Expanding	Converging	Lateralized	Ovoid	Irregular
Flake	82	7	13	20	12	1	12	17
Blade	57	7	17	5	21	2	1	4
Bladelet	20	2	9		9			
Cortical Flake	47	4	10	9	2	1	16	5
Cortical Blade	16	1	3	5	1	2	2	2
Débordant Flake	7			3		1	2	1
Débordant Blade	18	1	2	1	3	9	2	

Jebel Eva										Blank shape.	
	TOTAL	<>	Parallel	Expanding	Converging	Lateralized	Ovoid	Irregular			
Flake	56	1	8	20	10	5	11	1			
Blade	86	1	32	22	21	6	3	1			
Cortical Flake	36	16	1	5		5	7	2			
Cortical Blade	80	18	17	13	11	8	13				
Débordant Flake	5		2	2		1					
Débordant Blade	109	3	31	21	25	25	2	2			
Natural Crest	16	2	4	2	2	1	5				

Wadi Haluf 1										Blank shape.	
	TOTAL	<>	Parallel	Expanding	Converging	Lateralized	Ovoid	Irregular			
Flake	93	2	35	16	15	5	8	12			
Blade	164	4	80	15	37	11	3	14			
Bladelet	13		7		3			3			
Cortical Flake	51	23	8	9	1		7	3			
Cortical Blade	50	12	13	3	11	2	6	3			
Débordant Flake	18		4	7		6	1				
Débordant Blade	107		40	20	21	18	2	6			
BTF	2					1		1			

Khumseen

Blank dorsal scar pattern.

	TOTAL	<>	Unidirectional	Crossed	Parallel	Convergent	Bidirectional	Opposed	Uni. crest*	Transverse
Flake	129	13	90	16	2	4		1	1	2
Blade	82	4	52		12	13	1			
Bladelet	74	2	58		2	12				
Cortical Flake	38	24	12			1			1	
Cortical Blade	12	6	6							
Débordant Flake	13	1	6	3					3	
Débordant Blade	23	2	16	1		1	3			

Ghazal

	TOTAL	<>	Unidirectional	Crossed	Parallel	Convergent	Bidirectional	Radial	Opposed	Transverse
Flake	82	2	46	10	8	11		2	1	2
Blade	57		29	4	5	18	1			
Bladelet	20		11		4	5				
Cortical Flake	47	23	20	3		1				
Cortical Blade	16	6	7	2						1
Débordant Flake	7		7							
Débordant Blade	18		13	2	1	2				

*Unidirectional crested.

Jebel Eva Blank dorsal scar pattern.

	TOTAL	<>	Unidirectional	Crossed	Parallel	Convergent	Bidirectional	Radial	Opposed	Uni. crest*	Transverse
Flake	56	2	36	9	3	1		1	1		3
Blade	86		57	2	8	14	4		1		
Cortical Flake	36	30	6								
Cortical Blade	80	37	38	1	1				3		
Débordant Flake	5		4			1					
Débordant Blade	109	4	81			20	3			1	
Natural Crest	16	13	2						1		

Wadi Haluf 1

	TOTAL	<>	Unidirectional	Crossed	Parallel	Convergent	Bidirectional	Opposed	Transverse
Flake	93	2	60	7	11	6	2		5
Blade	164	4	107	4	22	27			
Bladelet	13		11	1		1			
Cortical Flake	51	33	15	1				1	1
Cortical Blade	50	21	25		3	1			
Débordant Flake	18		17						1
Débordant Blade	107		88		13	5	1		
BTF	2						1	1	

*Unidirectional crested.

APPENDIX B

Metrical Analysis from the DAP 2010-2012 Assemblages

Length

Khumseen

	Flake	Blade	Bladelets	D Blades	D Flakes	C Flakes	C Blades
MAX	82,78	77,78	43,25	103,08	65,42	69,25	74,19
MIN	15,95	16,89	13,49	31,08	28,2	17,83	25,31
AVERAGE	32,14	44,69	25,14	57,74	41,71	38,82	53,88
STD	12,62	13,51	6,9	19,48	11,07	16,09	17,92
n	92	52	50	22	13	29	10

Width

Khumseen

	Flake	Blade	Bladelets	D Blades	D Flakes	C Flakes	C Blades
MAX	67,5	33,89	11,97	40,67	39,47	53,18	35,35
MIN	3,16	12,1	3,31	6,09	15,56	13,44	7,05
AVERAGE	23,57	17,33	8,35	22,32	26,73	27,47	21,46
STD	10,06	5,008	2,05	8,47	7,22	11,32	9,04
n	126	81	74	22	13	38	12

Thickness

Khumseen

	Flake	Blade	Bladelets	D Blades	D Flakes	C Flakes	C Blades
MAX	24,66	11,91	5,8	25,64	30,36	24,66	21,49
MIN	1,91	1,84	1,25	3,71	5,25	3,18	2,92
AVERAGE	6,71	4,79	2,73	11,72	12,86	8,17	10,18
STD	3,99	1,72	1,08	6,87	7,79	5,02	6,24
n	128	82	72	22	13	38	12

Weight

Khumseen

	Flake	Blade	Bladelets	D Blades	D Flakes	C Flakes	C Blades
MAX	100	35	4	119	73	76	51
MIN	1	1	1	3	4	1	2
AVERAGE	8,6	5,3	1,57	28,45	18,54	14,97	17,27
STD	15,23	4,96	0,79	35,58	20,73	21,69	16,69
n	121	76	23	20	13	38	11

IPF						Khumseen
	Flake	Blade	Bladelets	D Blades	D Flakes	Cort.el.*
<i>MAX</i>	4,98	6,25	4,26	3,21	4,58	4,98
<i>MIN</i>	1,01	1,04	0,76	1,07	0,92	1,05
<i>AVERAGE</i>	2,5	2,58	2,36	2,21	2,17	2,57
<i>STD</i>	0,84	1,03	0,76	1,88	1	0,94
<i>n</i>	81	50	35	19	12	33

IOE						Khumseen
	Flake	Blade	Bladelets	D Blades	D Flakes	Cort. el.*
<i>MAX</i>	1,98	4,04	7,99	3,66	1,87	5,04
<i>MIN</i>	0,68	2,01	2,04	2,04	0,94	0,61
<i>AVERAGE</i>	1,39	2,53	3,18	2,49	1,58	1,71
<i>STD</i>	0,33	0,46	0,95	1,94	0,26	0,79
<i>n</i>	88	47	49	21	13	39

RPS						Khumseen
	Flake	Blade	Bladelets	D Blades	D flakes	Cort. el.*
<i>MAX</i>	80,15	98,86	37	40,23	29,99	53,18
<i>MIN</i>	1,95	3,75	1,98	3,13	2,42	2,83
<i>AVERAGE</i>	12,85	19,84	8,68	14,5	10,93	14,71
<i>STD</i>	13,83	19,39	6,58	11,79	8,48	11,52
<i>n</i>	65	38	29	19	12	29

*Cortical elements, including blades and flakes with over 50% of dorsal cortical cover.

<i>Length</i>							Ghazal
	Flake	Blade	Bladelets	D Blades	D flakes	C Flakes	C Blades
MAX	106,13	91,55	49,21	131,87	83,56	90,88	102,15
MIN	12,38	32,18	17,78	43,53	42,73	18,3	28,73
AVERAGE	41,41	57,22	32,14	75,17	63,08	59,66	69,96
STD	18,82	14,69	10,54	19,22	13,79	18,57	22,36
n	69	44	10	16	7	43	16

<i>Width</i>							Ghazal
	Flake	Blade	Bladelets	D Blades	D flakes	C Flakes	C Blades
MAX	93,58	39,35	11,99	52,72	56,46	80,56	47,77
MIN	11,87	11,64	3,61	15,4	26,39	16,3	9,96
AVERAGE	34,86	18,77	8,42	31,93	43,9	44,25	30,75
STD	16,29	6,5	2,25	9,47	10,13	14,73	12,48
n	79	57	20	18	7	47	16

<i>Thickness</i>							Ghazal
	Flake	Blade	Bladelets	D Blades	D flakes	C Flakes	C Blades
MAX	27,81	14,76	4,07	33,08	28,57	36,65	32,23
MIN	1,35	2,24	0,86	5,84	5,08	3,94	5,24
AVERAGE	8,62	6,17	2,38	14,86	16,26	15,17	14,67
STD	6,01	2,91	0,89	7,81	8,76	8,04	8,51
n	82	57	20	18	7	47	16

<i>Weight</i>							Ghazal
	Flake	Blade	Bladelets	D Blades	D flakes	C Flakes	C Blades
MAX	157	53	3	145	130	211	155
MIN	1	1	1	5	9	3	1
AVERAGE	19,93	9,55	1,7	48,56	48,57	49,21	52,94
STD	30,53	10,81	0,82	41,77	41,78	44,28	51,78
n	80	55	10	18	7	47	16

<i>IPF</i>							Ghazal
	Flake	Blade	Bladelets	D Blades	D flakes	C Flakes	C Blades
MAX	7,67	6,34	2,89	4,27	2,75	4,61	3,77
MIN	1,47	1,28	1,46	1,51	1,69	1,23	1,63
AVERAGE	2,98	2,67	2,29	2,43	2,14	2,75	2,42
STD	1,07	1,04	0,53	0,71	0,43	2,75	0,58
n	49	40	7	13	6	28	11

<i>IOE</i>							Ghazal
	Flake	Blade	Bladelets	D Blades	D flakes	C Flakes	C Blades
MAX	1,92	4,95	5,46	3,8	1,68	1,88	3,75
MIN	0,52	2,01	3,25	2,01	1,04	0,75	2,01
AVERAGE	1,29	3,03	4,35	2,63	1,46	1,33	2,46
STD	0,36	0,75	0,77	0,53	0,22	0,31	
n	66	44	10	16	7	43	15

<i>RPS</i>							Ghazal
	Flake	Blade	Bladelets	D Blades	D flakes	C Flakes	C Blades
MAX	76, 14	66,13	46,51	59,67	31,77	109,39	56,26
MIN	3,01	3,09	2,98	3,14	3,67	4,08	5,1
AVERAGE	13,28	18,33	17,45	19,45	12,54	21,4	17,71
STD	14,53	15,09	17,9	14,41	10,79	21,9	15,48
n	47	36	5	13	6	28	11

<i>Blank Lengths</i>						Jebel Eva
	Flake	Blade	D Blades	C Flakes	C Blades	
MAX	83,96	157,96	134,87	102,58	168,07	
MIN	27,36	30,92	42,67	23,38	41,39	
AVERAGE	48,25	73,5	81,21	52,41	88,06	
STD	14,94	21,29	18,41	22,89	24,53	
n	46	73	88	21	62	

<i>Blank Widths</i>						Jebel Eva
	Flake	Blade	D Blades	C Flakes	C Blades	
MAX	82,2	41,65	43,87	74,9	45,82	
MIN	18,1	14,66	12,35	21,23	15,62	
AVERAGE	37,08	25,29	24,58	41,63	28,58	
STD	12,96	6,25	5,74	14,54	6,96	
n	56	86	105	21	64	

<i>Blank thickness</i>						Jebel Eva
	Flake	Blade	D Blades	C Flakes	C Blades	
MAX	27,66	24,68	35,09	22,43	85	
MIN	6,62	4,33	6,45	3,66	5,18	
AVERAGE	9,85	11,02	15,31	11,91	19,03	
STD	5,39	4,23	5,19	4,63	11,79	
n	56	86	105	21	64	

Blank weight

Jebel Eva

	Flake	Blade	D Blades	C Flakes	C Blades
<i>MAX</i>	89	200	443	130	392
<i>MIN</i>	3	3	9	2	6
<i>AVERAGE</i>	22,78	30,46	42,53	35,09	71,36
<i>STD</i>	20,05	27,68	45,62	28,75	77,28
<i>Total</i>	1253	2681	4509	772	4496
<i>n</i>	55	88	106	22	63

IOE

Jebel Eva

	Flake	Blade	D Blades	C Flakes	C Blades
<i>MAX</i>	1,98	5,22	6,27	1,98	5,44
<i>MIN</i>	0,45	2,12	2,03	0,67	2,09
<i>AVERAGE</i>	1,32	3,01	3,44	1,26	3,14
<i>STD</i>	0,45	0,78	0,91	0,41	0,79
<i>n</i>	46	76	89	23	62

IPF

Jebel Eva

	Flake	Blade	D Blades	C Flakes	C Blades
<i>MAX</i>	4,55	4,9	3,69	3,74	3,05
<i>MIN</i>	1,49	0,98	0,7	1,4	0,57
<i>AVERAGE</i>	2,64	1,97	1,67	2,54	1,86
<i>STD</i>	0,84	0,8	0,6	0,88	0,52
<i>n</i>	39	60	70	14	52

RPS

Jebel Eva

	Flake	Blade	D Blades	C Flakes	C Blades
<i>MAX</i>	37,7	375	53,21	46,68	33,45
<i>MIN</i>	2,41	2,67	2,84	2,35	3,75
<i>AVERAGE</i>	9,96	23	15,36	12,66	12,64
<i>STD</i>	7,52	50,87	10,37	12,41	7,3
<i>n</i>	38	55	67	14	50

Blank Lengths

Wadi Haluf 1

	Flake	Blade	D Blades	C Flakes	C Blades
MAX	99,54	121,61	133,88	115,42	186,92
MIN	20,56	29,27	36,34	23,41	46,25
AVERAGE	45,78	63,32	84,96	50,58	88,15
STD	17,35	18,88	18,43	22,82	28,85
n	68	85	81	36	37

Blank Widths

Wadi Haluf 1

	Flake	Blade	D Blades	C Flakes	C Blades
MAX	64,05	46,92	65,17	83,58	59,04
MIN	16,4	12,32	6,55	14,92	15,22
AVERAGE	32,23	22,45	30,8	36,87	31,81
STD	9,91	6,95	9,34	15,26	10,4
n	88	154	107	46	50

Blank thickness

Wadi Haluf 1

	Flake	Blade	D Blades	C Flakes	C Blades
MAX	25,53	17,18	37,79	39,09	66
MIN	2,8	2,06	3,81	4,69	5,28
AVERAGE	7,69	6,86	11,29	9,3	15,77
STD	3,78	2,75	5,31	5,39	9,99
n	92	160	107	47	50

Weight

Wadi Haluf 1

	Flake	Blade	D Blades	C Flakes	C Blades
MAX	207	58	369	261	442
MIN	1	1	5	2	5
AVERAGE	16,47	12,15	43,17	24,96	61,02
STD	26,05	11,77	45,97	42,5	82,46
n	92	160	106	51	49

IOE

Wadi Haluf 1

	Flake	Blade	D Blades	C Flakes	C Blades
MAX	1,99	6,78	6,46	2,14	4,81
MIN	0,69	2	2	0,62	1,66
AVERAGE	1,42	2,87	2,85	1,42	2,74
STD	0,35	0,73	0,89	0,42	0,82
n	65	81	82	35	38

IPF

Wadi Haluf 1

	Flake	Blade	D Blades	C flakes	C Blades
MAX	9,62	3,95	5,62	4,21	3,46
MIN	1,25	1,15	1,26	1,4	0,94
AVERAGE	2,69	2,33	2,33	2,48	2,24
STD	1,16	0,71	0,73	0,7	0,6
n	58	87	81	30	36

RPS

Wadi Haluf 1

	Flake	Blade	D Blades	C Flakes	C Blades
MAX	35,49	51,44	127,04	25,66	55,92
MIN	3,24	3,65	2,17	3,37	3,3
AVERAGE	12,1	14,84	22,12	12,87	17,94
STD	8,22	10,71	19,81	7,12	12,85
n	49	51	73	24	32

BIBLIOGRAPHY

- Abbés, F. (2003). *Les outillages néolithiques en Syrie du Nord: Méthode de débitage et gestion laminaire durant le PPNB*. British Archaeologica Report, Int. series 1150, Oxford.
- Ackermann, R. (1964). Lichens and the Patination of Chert in Alaska. *American Antiquity* 29 (3), 386-387.
- Adams, J. (2002). *Ground Stone Analysis, a Technological Approach*. Center for Desert Archaeology, The University of Utah Press, Tucson.
- Adler, D. & Conard, N. (1997). Analysis of the Lithic Artifacts from Wallertheim D. In Conard, N. & Kandel, A (Ed.), *Reports for the Second Wallertheim Workshop* (pp. 1-13). Institut für Ur- und Frühgeschichte Tübingen.
- Aitken, M. (1998). *An introduction to optical dating: the dating of Quaternary sediments by the use of photon-stimulated luminescence*. Oxford University Press, Oxford.
- Ahler, S. (1989). Mass Analysis of Flaking Debris: Studying the Forest Rather Than the Tree. Archeological Papers of the American Anthropological Association, Special Issue: Alternative Approaches to Lithic Analysis. Volume 1, 85–118.
- Al-Abri, A., Podgorna, E., Rose, J., Pereira, L., Mulligan, C., Silva, N., Bayoumi, R., Soares, P. & Černý, V. (2012). Pleistocene-Holocene Boundary in Southern Arabia From the Perspective of Human mtDNA Variation. *American Journal of Physical Anthropology*. DOI 10.1002/ajpa.22131.
- Ambrose, S. (1998). Late Pleistocene human population bottlenecks, volcanic winter, and differentiation of modern humans. *Journal of Human Evolution* 34, 623–651.
- Ambrose, S. (2003). Population Bottleneck. In Robinson, R. (Ed.), *Genetics*, Vol. 3 (pp.167-171). MacMillan Reference, New York.
- Amirkhanov, H. (1994). Research on the Palaeolithic and Neolithic of Hadhramaut and Mahra. *Arabian Archaeology and Epigraphy* 5, 217-228.
- Amirkhanov, H. (2006). *Stone Age of South Arabia*. Moscow (in Russian). Nauka.
- Andrefsky, W. (1986). A Consideration of Blade and Flake Curvature. *Lithic Technology* 15 (2), 48-54.
- Andrefsky, W. (1994). Raw Material Availability and the Organization of Technology. *American Antiquity* 59 (1), 21-34.
- Andrefsky, W. (2001). Emerging directions in débitage analysis. In Andrefsky, W. (Ed.), *Lithic Debitage. Context Form Meaning* (pp.2-14). The University of Utah Press, South Lake City.
- Andrefsky, W. (2005). *Lithics. Macroscopic approaches to analysis*. Cambridge Manuals in Archaeology. Cambridge University Press, Cambridge.
- Andrefsky, W. (2009). The Analysis of Stone Tool Procurement, Production, and Maintenance. *Journal of Archaeological Research* 17, 65 -103.

Anton D., (1984). Aspects of geomorphological evolution: Paleosols and dunes in Saudi Arabia. In Jado, A. & Zötl J. (ed.), *Quaternary period in Saudi Arabia*. Vol. 2. Sedimentological, hydrogeological, hydrochemical, geomorphological, and climatological investigations of Western Saudi Arabia. Springer, Wien.

Armitage, S., Jasim, S., Marks, A., Parker, A., Usik V. & Uerpmann, H.P. (2011). The Southern Route “Out of Africa”: Evidence for an Early Expansion of Modern Humans into Arabia. *Science* 331, 453 – 456.

Asouti, E. (2006). Beyond the Pre-Pottery Neolithic B interaction sphere. *Journal of World Prehistory* 20, 87–126.

Ballin, T. (2000). Classification and Description of Lithic Artefacts: a Discussion of the Basic Terminology. *Lithics* 21,2000,9-15

Bar-Yosef, O. (1980). Prehistory of the Levant. *Annual Review in Anthropology* 9, 101-130.

Bar-Yosef, O. (1981). The “Pre-Pottery Neolithic” period in the Southern Levant. In Cauvin, J. & Sanlaville, P. (Ed.), *Préhistoire du Levant* (pp. 551–570). CNRS, Paris.

Bar-Yosef, O. & Meignen, L. (1992). Insights Into Levantine Middle Paleolithic Cultural Variability. In Dibble, H. & Mellars, P. (Ed.), *The Middle Paleolithic: Adaptation, Behaviour and Variability* (pp. 163-182). University Museum Press, Philadelphia.

Bar- Yosef, O. & Van Peer, P. (2009). The Chaîne Opératoire Approach in Middle Paleolithic Archaeology. *Current Anthropology* 50 (1), 103 -129.

Barham, L. & Mitchell, P. (2008). *The First Africans: African Archaeology from the earliest toolmakers to most recent foragers*. Cambridge World Prehistory. Cambridge University Press, New York.

Barkai, R., Gopher, A., Shimelmitz, R., (2005). Middle Pleistocene blade production in the Levant: an Amudian assemblage from Qesem Cave, Israel. *Eurasian Prehistory* 3, 39-74.

Barzilai, O. (2010) *Social Complexity in the Southern Levantine PPNB as Reflected Through Lithic studies: the Bidirectional Blade industry*. British Archaeology Reports int. Ser. 2180, Oxford.

Beck, C., Taylor, A., Jones, G., Fadem, C., Cook, C. & Millward, S. (2002). Rocks are Heavy: Transport Costs and Paleoarchaic Quarry Behavior in the Great Basin. *Journal of Anthropological Archaeology* 21, 481-507.

Beineke, J. (2006). *Spät-Quartäre Paläogeographie der Arabischen Halbinsel*. Ph.D dissertation, Universität Paderborn.

Berger, J-F., Bravard, J-P., Purdue, L., Benoist, A., Mouton, M. & Braemer F. (2012). Rivers of the Hadramawt watershed (Yemen) during the Holocene: Clues of late functioning. *Quaternary International* 266, 142-161.

Biagi, P. (1994). An Early Paleolithic site near Saiwan (Sultanate of Oman). *Arabian Archaeology and Epigraphy* 5, 81-88.

Binford, L. (1977). Forty-seven Trips. A Case Study in the Character of Archaeological Formation Processes. In Wright, R. (Ed.), *Stone tools as cultural markers, change, evolution and complexity*, (pp. 24-36). Humanities Press, New Jersey.

Binford, L. (1979). Organization and Formation Processes: Looking at Curated Technologies. *Journal of Anthropological Research* 35, 255-272.

Blades B. (2001). *Aurignacian Lithic Economy: Ecological Perspectives from Southwestern France*. Kluwer Academic/ Plenum Publishers, New York.

Blades, B. (2005). Small bladelet cores from Aurignacian levels at la Ferrassie (Dordogne, France). In Le Brun-Ricales (Ed.), *Productions lamellaires à l'Aurignacien* (pp. 245-254). ArchéoLogiques 1, Luxembourg.

Blechs Schmidt, I., Matter, A., Preusser, F., & Rieke-Zapp, D. (2009). Monsoon triggered formation of Quaternary alluvial megafans in the interior of Oman. *Geomorphology* 110 (3-4), 128-139.

Bleed, P. (2002a). Obviously sequential, but continuous or staged? Refits and cognition in three late Paleolithic assemblages from Japan. *Journal of Anthropological Archaeology* 21, 329-343.

Bleed, P. (2002b). Cheap, regular and reliable: Implications of design variation in late Pleistocene Japanese microblade technology. In Elston, R. & Kuhn, S. (Ed.), *Thinking small: global perspective on microlithizations* (pp. 95-102). Archaeological papers of the American anthropological Association 12, Arlington.

Bradbury, A. & Carr, P. (1995). Flake typologies and alternative approaches: an experimental assessment. *Lithic Technology* 20, 100-115.

Bradbury, A. & Carr, P. (1999). Examining stage and continuum models of flake debris analysis: An experimental approach. *Journal of Archaeological Science* 26, 105-116.

Bradley, B. (1975). Lithic reduction sequence: a glossary and discussion. In Swanson, E. (Ed.), *Lithic Technology: Making and Using Stone Tools* (5-14). The Hague, Mouton.

Brandt, S. (1986). The Upper Pleistocene and early Holocene prehistory of the Horn of Africa. *African Archaeological Review* 4 (1), 41-82.

Brandt, S. (1988). Early Holocene Mortuary Practices and Hunter-Gatherer Adaptations in Southern Somalia. *World Archaeology* 20(1), 40-56.

Brandt, S. & Brook, G. (1984). Archaeological and Paleoenvironmental Research in Northern Somalia. *Current Anthropology* 25(1), 119-121.

Bräuer, G. (1992). Africa's Place in the Evolution of Homo Sapiens. In Bräuer, G. & Smith, F. (Ed.), *Continuity or replacement: Controversy in Homo Sapiens evolution* (pp. 83-98). Balkema, Rotterdam.

Breuil, H. (1909). Etudes de morphologie paléolithique. Transition du Moustérien vers l'Aurignacien à L'Abri Audi (Dordogne) et au Moustier. *Revue de l'Ecole d'Anthropologie de Paris*, XIX, 320-340.

Brew, J. O. (1946). The use and abuse of taxonomy. The archaeology of Alkali Ridge Utah. *Papers of the Peabody Museum of Archaeology and Ethnology* 21, 44–66.

Brown, A. (1997). *Alluvial Geoarchaeology: Floodplain Archaeology and Environmental Change*. Cambridge University Press, Cambridge.

Boëda, E. (1990). De la Surface au Volume: Analyse des Conceptions de Débitage Levallois et Laminaire. In Farizy C. (Ed.), *Paléolithique moyen récent et Paléolithique supérieur ancien en Europe* (pp. 63-68). Mémoires du Musée de Préhistoire, Ile-de-France.

Boëda, E. (1993). Le débitage discoïde et le débitage levallois récurrent centripède. *Bulletin de la Société Préhistorique Française* 90, 392-404.

Boëda, E. (1994). *Le Concept Levallois: Variabilité des Méthodes*. CNRS, Monograph du CRA no. 9., Paris.

Boëda, E. (1995). Levallois : A Volumetric Construction, Methods, a Technique. In Dibble, H. & Bar-Yosef, O. (Ed.), *Definition and Interpretation of Levallois Technology* (pp. 41-68). Monographs in World Archaeology 23. Prehistory Press, Madison.

Boëda, E., Genest, J.-M. & Meignen, L. (1990). Identification de chaînes opératoires lithiques du Paléolithique ancien et moyen. *Paléo* 2, 43-80.

Bonnichsen, R. (1977). Models for Deriving Informations from Stone Tools. Mercury Series, *Archaeological Survey of Canada Papers* 60, National Museum of man, Ottawa.

Bordes, F. (1961). *Typologie du paléolithique ancien et moyen*. Université de Bordeaux, Bordeaux.

Bordes, F. (1980). Le débitage Levallois et ses variants. *Bulletin de la Société Préhistorique Française* 77, 45-49.

Bordes, F. (1988). *Typologie du paleolithique ancien et moyen* (fifth edition). CNRS, Paris.

Bordes, F. & Crabtree, D. (1969). The Corbiac blade technique and other experiments. *Tebiwa* 12 (2), 1-21.

Bourlon, M. (1911). Essai de classification des burins- leurs modes d'avivage. *Revue anthropologique*, XXI, 267-278.

Bosinski, G. (1967). *Die Mittelpaläolithischen Funde im Westlichen Mitteleuropa*. Fundamenta, Böhlau Verlag, Köln and Gratz.

Bosinski, G. & Hahn, J. (1972). Der Magdalenien-Fundplatz Andernach (Martinsberg). *Beiträge zum Paläolithikum im Rheinland. Rhein. Ausgrabungen* 11, 81-257.

Burns, S., Matter, A., Frank, N. & Mangini, A. (1998). Speleothem-based paleoclimate record from northern Oman. *Geology* 26, 499 - 502.

Burns, S., Fleitmann, D., Matter, A., Neff, U. & Mangini, A. (2001). Speleothem evidence from Oman for continental pluvial events during interglacial periods. *Geology* 29, 623 - 626.

Burroni, D. Donahue, R. & Pollard, M. (2002). The Surface Alteration Features of Flint Artefacts as a Record of Environmental Processes. *Journal of Archaeological Science* 29, 1277–1287.

Cabrera, M., Abu Amero, K., Larruga, J. & González, A. (2009). The Arabian peninsula: Gate for Human Migration Out of Africa or Cul-de-sac? A Mitochondrial DNA Phylogeographic Perspective. In Petraglia, M. & Rose, J. (Ed.), *Evolution of Human Populations in Arabia: Paleoenvironments, Prehistory and Genetics* (pp. 79-87). Springer Academic Publishers, Dordrecht.

Cahen D. (1976). Das Zusammensetzen Geschlagener Steinartefakte. *Archäologisches Korrespondenzblatt* 6, 81- 93.

Caton-Thompson, G. (1954). Some Palaeoliths from South Arabia. *Proceedings of the Prehistoric Society* 29, 189-218.

Caton-Thompson, G. & Gardner, E. (1939). Climate, Irrigation, and Early Man in the Hadhramaut. *The Geographical Journal* 93 (1), 18-35.

Černý, V., Mulligan, C., Rídl, J., Zaloudkova, M., Edens, C., Hájek, M. & Pereira, L. (2008). Regional Differences in the Distribution of the Sub-Saharan, West Eurasian, and South Asian mtDNA Lineages in Yemen. *American Journal of Physical Anthropology* 136, 128-137.

Černý, V., Mulligan, C., Fernandes, V., Silva, N., Alshamali F., Non, A., Harich, N., Cherni, L., El Gaaied, A., Al-Meer, A. & Pereira, L. (2011). Internal Diversification of Mitochondrial Haplogroup R0a Reveals Post-Last Glacial Maximum Demographic Expansions in South Arabia. *Molecular Biology and Evolution* 28(1), 71-78.

Chauhan, P. (2009). Near the Gate of Tears : Examining the Paleoanthropological Records of Djibouti and Yemen. In Hovers, E. & Braun, R. (Ed.), *Interdisciplinary Approaches to the Oldowan* (pp. 49- 60). Springer Academic Publishers, Dordrecht.

Charpentier V. (1996). Entre sables du Rub'al Khali et mer d'Arabie, Préhistoire récente du Dhofar et d'Oman: Les industries à point de "fasad". *Proceedings of the Seminar of Arabian Studies* 26, 1- 14.

Charpentier, V. (2008). Hunter-gatherers of the "empty quarter of the early Holocene" to the last Neolithic societies: chronology of the late prehistory of south-eastern Arabia (8000-3100 BC). *Proceedings of the Seminar for Arabian Studies* 38, 59-82.

Clark, I. & Fontes, J-C. (1990). Palaeoclimatic Reconstruction in Northern Oman Based on Carbonates from Hyperalkaline Groundwaters. *Quaternary Research* 33, 320-336.

Clark, J. (1954). *The Prehistoric Cultures of the Horn of Africa*. Cambridge University Press, Cambridge.

Clark, J. (1993). African and Asian Perspectives on the Origin of Modern Humans. In Aitken, M., Stringer, S. & Mellars, P. (Ed.), *The Origin of Modern Humans and the Impact of Chronometric Dating*, (pp. 118-131). Princeton University Press, Princeton.

Claussen, M., Ganopolski, A. & Brovkin, V. (2003). Simulated global-scale response of the climate

system to Dansgaard/Oeschger and Heinrich events. *Climate Dynamics* 21, 361–370.

Clemens, S., W. Prell, D. Murray, G. Shimmield, & G. Weedon. (1991). Forcing Mechanisms of the Indian Ocean Monsoon. *Nature* 353, 720–725.

Cleuziou S. & Tosi, M. (2000). Ra's al-Jinz and the prehistoric coastal cultures of the Ja'alan. *Journal of Oman Studies* 11, 19–73.

Cleuziou, S. & Tosi, M. (2007). *In the Shadow of the Ancestors: The Prehistoric Foundation of the Early Arabian Civilization in Oman*. Ministry of Heritage and Culture, Sultanate of Oman. Al-Nahdha Printers, Muscat.

Conard, N., Soressi, M., Parkington, J., Wurz, S. & Yates, R. (2004). A Unified Lithic Taxonomy Based on Patterns of Core Reduction. *South African Archaeological Bulletin* 59 (179), 13–17.

Cordier, G. (1961). Le fond de cabane néolithique des Beaux au Grand-Pressigny. *Gallia préhistoire* 4, 183–192.

Cotterell, B. & Kamminga, J. (1979). The mechanics of flaking. In Hayden, B. (Ed.), *Lithic Use-Wear Analysis* (pp. 90–112). Academic Press, New York.

Crabtree, D. (1970). Flaking stone with wooden implements. *Science* 169, 146 – 153.

Crassard, R. (2007). *Apport de la Technologie Lithique à la Définition de la Préhistoire du Hadramawt, Dans le contexte du Yémen et de L'Arabie du Sud*. Ph.D thesis, l'Université Paris 1, Paris.

Crassard, R. (2008 a). *La Préhistoire du Yémen. Diffusions et diversités locales à travers l'étude d'industries lithiques du Hadramaut*. British Archaeology Reports int. Ser. S1842, Oxford.

Crassard, R. (2008 b). The “Wa'shah method”: an original laminar debitage from Hadramawt, Yemen. *Proceedings of the Seminar of Arabian Studies* 38, 3–14.

Crassard, R. (2009). Modalities and characteristics of human occupations in Yemen during the Early/Mid-Holocene. *Geoscience* 341, 713–725.

Crassard, R. & Bodu, P. (2004). Préhistoire du Hadramawt Yemen: Nouvelles Perspectives. *Proceedings of the Seminar of Arabian Studies* 34, 67–84.

Crassard, R. & Thiébaud, C. (2011). Levallois points production from eastern Yemen and some comparisons with assemblages from East-Africa, Europe and the Levant. *Etudes et Recherches Archéologiques de l'Université de Liège* 999, 1–14.

Crassard, R., McCorriston, J., Ochse, E., Bin'Aqil, A., Espagne, J. & Sinnah, M. (2006). Manayzah, early to mid-Holocene occupations in Wadi Sana (Hadramawt, Yemen). *Proceedings of the Seminar for Arabian Studies* 36, 151–173.

Cremaschi M. & Negrino F. (2002). The Frankincense of Sumhuram: palaeoenvironmental and prehistorical background. In Avanzini, A. (Ed.), *Khor Rori report 1* (pp. 325–363) . Università di Pisa, Pisa.

Cremaschi, M. & Negrino, F. (2005). Evidence for an Abrupt Climatic Change at 8700 14C yr B.P. in Rockshelters and Caves of Gebel Qara (Dhofar-Oman): Palaeoenvironmental Implications. *Geoarchaeology: An International Journal* 20(6), 559–579.

Crew, H. (1975). *An examination of the Variability of the Levallois Method: its implications for the internal and external relationships of the Levantine Mousterial*. Ph.D Dissertation, Southern Methodist University, Dallas.

Crew, H. (1976). The Mousterian site of Rosh Ein Mor. In Marks, A. (Ed.), *Prehistory and paleoenvironments of the Central Negev, Israel, volume 1: the Avdat/ Aqev area part 1* (pp. 75-111). Southern Methodist University, Dallas.

David, G. (1993). Mousterian Tool Selection, Reduction, and Discard at Ghar, Israel. *Journal of Field Archaeology* 20 (2), 205-218.

Davidson, I. & Nobel, W. (1993). Tools and Language in Human Evolution. In Gibson, K. & Ingold, T. (Ed.), *Tools, Language and Cognition in Human Evolution* (pp. 363- 388). Cambridge University Press, Cambridge.

Davies, C. (2006). Holocene paleoclimates of southern Arabia from lacustrine deposits of the Dhamar highlands, Yemen. *Quaternary Research* 66, 454–464.

De Wilde, D. & De Bie, M. (2011). On the origin and significance of microburins: an experimental approach. *Antiquity* 85, 729-741.

Debénath, A. & Dibble, H. (1994). *Handbook of Palaeolithic Typology, vol.1 : Lower and Middle Paleolithic of Europe*. University Museum, University of Pennsylvania, Philadelphia.

Delagnes, A. (2000). Blade production during the Middle Paleolithic in Northwestern Europe. *Proceedings of 1999 Beijing International Symposium on Paleoanthropology. Acta Anthropol. Sinica (Suppl. to vol. 19)*, 181-188.

Delagnes, A., Macchiarelli, R., Jaubert, J., Peigne, S., Tournepiche, J-F., Bertran, P. & Cassard, R. (2008). Middle Paleolithic settlement in Arabia: first evidence from a stratified archaeological site in western Yemen. Meeting of the Paleoanthropological Society, Van-couver, British Columbia, March 25–26.

Delagnes, A., Tribolo, C., Bertran, P., Brenet, M., Crassard, R., Jaubert, J., Khalidi, L., Mercier, N., Nomade, S., Peigné, S., Sitzia, L., Tournepiche, J-F., Al-Halibi, M., Al-Mosabi, A. & Macchiarelli, R. (2012). The Middle Paleolithic assemblage of Shi'bat Dihya 1 (Wadi Surdud site complex, Yemen). *Journal of Human Evolution*, 1-23.

Demidenko, Y. & Usik, V. (1993a). The Problem of Change in Levallois Technique During the technological Transition From the Middle to Upper Palaeolithic. *Paléorient* 19(2), 5-15.

Demidenko, Y. & Usik, V. (1993b). On the *Lame à crête* technique in the Paleolithic. *European Prehistory* 4, 33-48.

Demidenko, Y. & Usik, V. (1995). Establishing the potential evolutionary possibilities of “Point”

Levallois- Mousterian: Korolevo I site-Complex 2b in the Ukrainian Transcarpathians. In Dibble, H. & Bar-Yosef, O. (Ed.), *Definition and interpretation of Levallois technology* (pp. 439-454). *Monographs in World Archaeology* 23. Prehistory Press, Madison.

Demidenko, Y. & Usik, V. (2003). Into the mind of the maker: Refitting study and technological reconstruction. In Henry D. (Ed.), *Neanderthals in the Levant. Behaviour organization and the beginnings of human modernity* (Pp. 107 – 155). Continium, London and New York.

Derricourt, R. (2005). Getting “Out of Africa”: Sea Crossings, Land Crossings and Culture in the Hominin Migrations. *Journal of World Prehistory* 19, 119–132.

Dibble, H. (1984). Interpreting Typological Variation of Middle Paleolithic Scrapers: Function, Style, or Sequence of Reduction? *Journal of Field Archaeology* 11, 431-436.

Dibble, H. (1987). The Interpretation of Middle Paleolithic Scraper Morphology. *American Antiquity* 52 (1), 109-117.

Dibble, H. (1997). Platform variability and flake morphology: a comparison of experimental and archaeological data and implications for interpreting prehistoric lithic technological strategies. *Lithic Technology* 22, 150 - 170.

Dibble, H. & Whittaker, J. (1981). New Experimental Evidence on the Relation Between Percussion Flaking and Flake Variation. *Journal of Archaeological Science* 8, 283-296.

Dibble, H. & Rezek, Z. (2009) Introducing a new experimental design for controlled studies of flake formation: results for exterior platform angle, platform depth, angle of blow, velocity, and force. *Journal of Archaeological Science* 36, 1945 - 1954.

Dubreuil, L. (2004). Long term trend in Natufian subsistence: a use-wear analysis of ground stone tools. *Journal of Archaeological Science* 31, 1613-1629.

Dunnell, R. (1978). Style and Function: A Fundamental Dichotomy. *American Antiquity* 43, 192-202.

Dunnell, R. (1990). Artifact size and lateral displacement under tillage: comments on Odell and Cowan experiment. *American Antiquity* 55 (3), 592-594.

Edens, C. & Wilkinson, T. (1998). Southwest Arabia During the Holocene: Recent Archaeological Developments. *Journal of World Prehistory* 12 (1), 55-119.

Endicott, P. & Ho, S. (2008). A Bayesian evaluation of human mitochondrial substitution rates. *American Journal of Human Genetics* 82, 895–902

Endicott P., Ho S. Y. W., Metspalu M. & Stringer, C. (2009). Evaluating the mitochondrial time scale of human evolution. *Trends in Ecology & Evolution*, 515-521.

Eren, M., Boehm, A., Morgan, B., Anderson, R. & Andrews, B. (2011). Flaked Stone Taphonomy: a Controlled Experimental Study of the Effects of Sediment Consolidation on Flake Edge Morphology. *Journal of Taphonomy* 9 (3), 201-217.

- Ericson, J. (1984). Towards the analysis of lithic production systems. In Ericson, J. & Purdy, B. (Ed.), *Prehistoric Quarries and Lithic Production* (pp. 1-9). Cambridge University Press, Cambridge.
- Evans, J. & O'Connor, T. (1999). *Environmental Archaeology: Principles and Methods*. Sutton Publishing, Somerset.
- Fedele, F. (1986). Neolithic and Protohistoric cultures. Excavations and researches in the eastern Highlands. In de Maigret, A. (Ed.), *Archaeological activities in the Yemen Arab Republic, 1986* (pp. 396-400). East and West 36, 376-470.
- Fedele, F. (2008). Wadi at Tayyilah 3, a Neolithic and Pre-Neolithic occupation on the eastern Yemen Plateau, and its archaeofaunal information. *Proceedings of the Seminar for Arabian Studies* 38, 153-172.
- Fedele, F. (2009). Early Holocene in the Highlands: Data on the Peopling of the Eastern Yemen Plateau, with a Note on the Pleistocene Evidence. In Petraglia, M. & Rose, J. (Ed.), *Evolution of Human Populations in Arabia: paleoenvironments, prehistory and Genetics* (pp.215- 236). Springer Academic Publishers, Dordrecht.
- Fedele F, Zaccara D. (2005) .Wādī al-Tayyila 3 a mid-Holocene site on the Yemen Plateau and its lithic collection. In Sholan A., Antonini, S.& Arbach, M., (Ed.) *Sabaeen Studies* (pp. 213- 245). University of San'a' and Centre Français d'archéologie et de sciences sociales, Naples.
- Fernandes, P., Le Bourdonnec, F-X., Raynel, J-P, Popeau, G., Piboule, M. & Moncel, M-H. (2007). Origins of prehistoric flints: The neocortex memory revealed by scanning electron microscopy. *C. R. Palevol* 6, 557-568.
- Fernandes, V., Alshamali, F., Alves, M., Costa, M., Pereira, J., Silva, N., Cherni, L., Harich, N., Černý, V., Soares, P., Richards, M. & Pereira, L. (2012). The Arabian Cradle: Mitochondrial Relicts of the First Steps along the Southern Route out of Africa. *The American Journal of Human Genetics* 90 (2), 347-355.
- Field, J. & Lahr, M. (2006). Assessment of the Southern Dispersal: GIS-Based Analyses of Potential Routes at Oxygen Isotopic Stage 4. *Journal of World Prehistory* 19 (1), 1-45.
- Field, J., Petraglia, M. & Lahr, M. (2007). The southern dispersal hypothesis and the South Asian archaeological record: Examination of dispersal routes through GIS analysis. *Journal of Anthropological Archaeology* 26, 88 - 108.
- Fish, P. (1976). *Interpretative Potential of Mousterian Debitage*. Ph.D Dissertation, Arizona State University, Arizona.
- Fleitmann, D. & Matter, A. (2009). The speleothem Record of climate variability in Southern Arabian. *C.R. Geosciences* 341, 633-642.
- Fleitmann, D., Burns, S., Mudelsee, M., Neff, U., Kramers, J., Mangigi, A. & Matter, A. (2003). Holocene Forcing of the Indian Monsoon Recorded in a Stalagmite from Southern Oman. *Science* 300, 1737 - 1739.

Fleitmann, D., Matter, A., Pint, J. & Al-Shanti, M. (2004). The speleothem record of climate change in Saudi Arabia. Saudi Geological Survey, Jeddah, Kingdom of Saudi Arabia.

Fleitmann, D., Burns, S., Mangini, A., Mundelsee, M., Kramers, J., Villa, I., Neff, U., Al-Subbary, A., Beutner, A., Hippler, D. & Matter, A. (2007). Holocene ITCZ and Indian monsoon dynamics recorded in stalagmites from Oman and Yemen (Socotra). *Quaternary Science Reviews* 26, 170–188.

Fleitmann, D., Burns, S., Pekala, M., Mangini, A., Al-Subbary, A., Al-Aowah, M., Kramers, J. & Matter, A. (2011). Holocene and Pleistocene pluvial periods in Yemen, southern Arabia. *Quaternary Science Reviews* 30, 783 – 787.

Ford, J. (1952). Measurements of some prehistoric design developments in the southern States. *Anthropological papers of the American Museum of Natural History* 44, 3.

Fuch, M. & Buerkert, A. (2008). A 20 ka sediment record from the Hajar Mountain range in N-Oman, and its implication for detecting arid–humid periods on the southeastern Arabian Peninsula. *Earth and Planetary Science Letters* 265, 546–558.

Gathorne-Hardy, F. & Harcourt-Smith, W. (2003). The super-eruption of Toba, did it cause a human bottleneck? *Journal of Human Evolution* 45, 227–230.

Ghazanfar, S. (1992). Quantitative and biogeographic analysis of the flora of the Sultanate of Oman. *Global Ecology and Biogeography Letters* 2: 189-195.

Ghazanfar, S. (1999). Present flora as an example of palaeoclimate: examples from the Arabian Peninsula. In Singhvi, A. & Derbyshire, E. (Ed.), *Paleoenvironmental Reconstruction in Arid Lands* (pp. 263–275). Balkema, Rotterdam.

Ghazanfar, S. (2004). Biology of the Central Desert of Oman. *Turkish Journal of Botany* 28, 65-71.

Glennie, K. (2005). *The Desert of Southern Arabia: Environments and Sediments*. Arabian Printing and Publishing House Manama, Bahrain.

Glennie, K. & Singhvi, A. (2002). Event stratigraphy, palaeoenvironment and chronology of SE Arabian deserts. *Quaternary Science Reviews* 21, 853 – 869.

Goldberg, P. & Macphail, R. (2006). *Practical and theoretical geoarchaeology*. Blackwell Publishing company, Malden, Oxford and Carlton.

Goodwin, A. (1960). Chemical Alteration (Patination) of Stone. In Heizer R. & Cook S (Ed.), *The Application of Quantitative Methods in Archaeology* (pp.300-324). Viking Fund Publications in Anthropology 28.

Goudi, A., Collins, A., Stokes, S., Parker, A., White, K. & Al-Farraj, A. (2000). Latest Pleistocene and Holocene dune construction at the north-eastern edge of the Rub Al Khali, United Arab Emirate. *Sedimentology* 47, 1011 – 1021.

Gregg, S., Kintigh, K. & Whallon, R. (1991). Linking Ethnoarchaeological Interpretation

and Archaeological Data: The Sensitivity of Spatial Analytical Methode to Postdepositional Disturbances. In Kroll, E. & Price, D. (Ed.), *The Interpretation of Archaeological Spatial Patterning* (pp. 149-197). Plenum Press, New York and London.

Hahn, J. & Owen, L. (1985). Blade technology in the Aurignacian and Gravettian of Geissenklosterle Cave, Southwest Germany. *World Archaeology* 17(1), 61-75.

Hahn, J. (1993). *Erkennen und Bestimmen von Stein- und Knochenartefakten: Einführung in die Artefaktmorphologie*. Verlag Archaeologica Venatoria 10. Tübingen

Hays M. & Lucas G. (2001). Experimental Investigations of Aurignacian Bladelets. In Hays M. & Thacker P. (Ed.), *Questioning the Answers: Resolving Fundamental Problems of the Early Upper Paleolithic* (pp. 109-116). British Archaeological Reports, Oxford.

Hietala, H. (1983). Boker Tachtit: Intralevel and Interlevel Spatial Analyses. In Marks, A. (Ed.), *Prehistory and Paleoenvironment in the Central Negev, Israel, volume III, the Avdat/Aqev Area, Part 3* (pp. 217-281). Southern Methodist University, Dallas.

Hilbert, Y. (2011) The South Arabian Prehistory after the Last Interglacial: a Case of Population Continuity or Discontinuity? *Rosetta* 9 (5), 40-46.

Hilbert, Y. & Azzarà, V. (2012). Lithic technology and spatial distribution of artefacts at the Early Bronze Age site HD-6 (Sharqiyya Region, Sultanate of Oman). *Arabian Archaeology and Epigraphy* 23, 7-25.

Hilbert, Y., Rose, J. & Roberts, R. (2012). Late Palaeolithic core-reduction strategies in Dhofar, Oman. *Proceedings of the Seminar for Arabian Studies* 42, 1–18.

Ho, S. & Endicott, P. (2008) The crucial role of calibration in molecular date estimates for the peopling of the Americas. *American Journal of Human Genetics* 83, 142–146

Hodder, I. & Hutson, S. (2003) *Reading the Past, current approaches to interpretation in archaeology* (Third edition). Cambridge University Press, Cambridge.

Hofman, J. (1992). Putting the pieces together: an introduction to refitting. In Hofman J. & Enloe J. (Ed.), *Piecing together the past: applications of refitting studies in archaeology*, (pp. 1-21). British Archaeology Reports Int. Ser. 578, Oxford.

Holm, D., (1960). Desert Geomorphology in the Arabian Peninsula. *Science* 132, 1369-1379.

Hoorn, C., & Cremaschi, M. (2004). Late Holocene Palaeoenvironmental History of Khawr Rawri and Khawr Al Balid (Dhofar, Sultanate of Oman). *Palaeogeography, Palaeoclimatology, Palaeoecology* 213, 1–36.

Hublin, J-J. (1993). Recent Human evolution in North West Africa. In Aitken, M., Stringer, C. & Mellars, P. (Ed.), *The Origin of Modern Humans and the Impact of Chronometric Dating* (pp. 118-131). Princeton University Press, Princeton.

Hulse, F. (1971). *The Human Species: An introduction to Physical Anthropology* (Second edition). Random House, New York.

- Hunt, C. (1954). Desert Varnish. *Science* 120 (3109) 183-184.
- Hurst, V. & Kelly, A. (1961). Patination of Cultural Flints. *Science* 134 (3474) 251-256.
- Immensauser, A., Dublyansky, Y., Verwer, K., Fleitmann, D. & Pashenko, S. (2007). Textural, Elemental, and Isotopic character of the Pleistocene Phreatic Cave deposits (Jabal Madar, Oman). *Journal of Sedimentary Research* 77, 68–88.
- Ingold, T. (1993). Technology, Language, Intelligence: A reconsideration of basic concepts. In Gibson, K. & Ingold, T. (Ed.), *Tools, Language and Cognition in Human Evolution* (pp. 449- 472). Cambridge University Press, Cambridge.
- Inizan, M-L (1978). Première mission archéologique Française a Qatar. *Paléorient* 4, 347- 351.
- Inizan, M-L. (1980a). Premiers resultats des fouilles prehistoriques de la region de Khor. In Tixier J. (Ed.), *Mission Archéologique Française a Qatar* (pp. 51-97). Dar al-Uloom.
- Inizan, M-L. (1980b). Sur les industrie a lames de Qatar. *Paleoorient* 6, 233-236.
- Inizan, M-L., Roche, H. & Tixier, J. (1992). *Thechnology of Knapped Stone*. Prehistoire de la Pierre Taillee. EX Libris, Meudon Crep.
- Ivanochko, T. (2004). *Sub-Orbital Scale variations in the Intensity of the Arabian Sea Monsoon*. Ph.D dissertation, University of Edinburgh, Edinburgh.
- Ivanova, E., Schieble, R., Singh, A., Schmiedl, G., Niebler, H-S. & Hemleben, C. (2003). Primary production in the Arabian Sea during the last 135 000 years. *Palaeogeography, Palaeoclimatology, Palaeoecology* 197, 61-82.
- Jagher, R. (2009). Recent research in southern Arabia and reflection on the prehistoric evidence. In Petraglia, M. & Rose, J. (Ed.), *Evolution of Human Populations in Arabia: paleoenvironments, prehistory and Genetics* (pp.139-150). Springer Academic Publishers, Dordrecht.
- Jagher, R. & Pümpin, C. (2010). A New Approach to Central Omani Prehistory. *Proceedings of the Seminar of Arabian Studies* 40, 145-160.
- Jagher, R., Pümpin, C., Wegmüller, F. & Winet, I. (2011) Central Oman palaeolithic survey, report of the 2007 season. *The Journal of Oman Studies*, 17. S. 15-50.
- Jelinek, J. (1976). Form, function and style lithic analysis. In *Cultural Change and Continuity, Essays in honor of James Bennett Griffin* (pp. 19-33). Academic Press, New York, San Francisco, London.
- Johnson, P. (1998). Tectonic map of Saudi Arabia and adjacent areas (Technical Report USGS-TR-98-3 IR-948). Deputy Ministry for Mineral Resources, Jeddah.
- Juyal, N., Chamyal, L., Bhandari, S., Bhuschan, R. & Singhvi, A. (2006). Continental record of the southwest monsoon during the last 130 ka: evidence from the southern margin of the Thar Desert, India. *Quaternary Science Reviews* 25, 2632–2650.
- Kallweit, H. (1996). *Neolithische und Bronzezeitliche besidlung in Wadi Dhahr, Republik Jemen*.

Eine Untersuchung auf der Basis von Geländebegehungen und Sondagen. Ph.D Dissertation, Albert-Ludwigs-Universität zu Freiburg.

Kapel, H. (1967). *Atlas of the Stone-age Cultures of Qatar*. Aartus University Press, Denmark.

Keeley, L. (1974). Technique and Methodology in Microwear Studies. *World Archaeology* 5, 323-36.

Keeley, L. (1980) *Experimental Determination of Stone Tool Uses: A Microwear Analysis*. University of Chicago Press, Chicago.

Kelly, R. (2003). Colonization of new land by hunter-gatherers: expectations and implications based on ethnographic data. In Rockman, M. & Steel, J. (Ed.), *Colonization of unfamiliar landscapes: the archaeology of adaptation* (pp. 44-58). Routledge, London and New York.

Kerkhof, F. & Müller-Beck, H-J. (1969). Zur bruchmechanischen Deutung der Schlagmarken and Steingeräten. *Zeitschrift für Glaskunde* 42, 439-448.

Khalidi, L. (2009). Holocene Obsidian Exchange in the Red Sea Region. In Petraglia, M. & Rose, J. (Ed.), *Evolution of Human Populations in Arabia: paleoenvironments, prehistory and Genetics* (pp.279-291). Springer Academic Publishers, Dordrecht.

Kleindienst, M. (1967). Questions of terminology in regard to the study of Stone Age industries in eastern Africa: "Cultural stratigraphic units". In Bishop, W. & Clark, J. (Ed.), *Background to Evolution in Africa* (pp. 821-859). University of Chicago Press, Chicago.

Kleindienst, M. (2006). On Naming Things: Behavioral Changes in the Later Middle to Earlier Late Pleistocene, Viewed From the Eastern Sahara. In Hovers, E. & Kuhn, S. (Ed.), *Transotion before the Transition: Evolution and Stability in the Middle Paleolithic and Middle Stone Age* (pp. 13-28). Springer, New York.

Knight, J. (1993). Technological Analysis of the Anvil (Bipolar) Technique. *Newsletter of the Lithic Studies Society* 2-4, 56 – 87.

Kooyman, B. (2000). *Understanding Stone Tools and Archaeological Sites*. University of New Mexico Press, Albuquerque.

Kozlowski, S. (1999). *The eastern wing of the fertile crescent: Late prehistory of greater Mesopotamian lithic industries*. British Archaeology Reports Int. Series 760, Archaeopress, Oxford.

Kuhn, S. (1995). *Mousterian Lithic Technology: an ecological perspective*. Princeton University Press, Princeton.

Kuhn, S. (2002). Pioneers of Microlithization: The "Proto- Aurignacian" of Southern Europe. Archeological Papers of the American Anthropological Association Special Issue: Thinking Small: Global Perspective on Microlithization 12, 83-93.

Kuijt, I. (1994). Pre-Pottery Neolithic A period settlement systems of the southern Levant: New data, archaeological visibility, and regional site hierarchies. *Journal of Mediterranean*

Archaeology 7(2), 165–192.

Kuijt, I. & Goring-Morris, N. (2002). Foraging, Farming, and Social Complexity in the Pre-Pottery Neolithic of the Southern Levant: A Review and Synthesis. *Journal of World Prehistory* 16 (4), 361-440.

Lahr, M. & Foley, R. (1994). Multiple dispersals and modern human origins. *Evolutionary Anthropology* 3, 48-60.

Lambeck, K. (1996). Shoreline reconstructions for the Persian Gulf since the last glacial maximum. *Earth and Planetary Science Letters* 142, 43-57.

Le Brun-Ricalens, F. (2005). Reconnaissance d'un concept technoculturel de l'Aurignacien Ancien? Modalités, unités et variabilités des productions lamellaires du site D'Hui (Beauville, Lot-et-Garonne, France): Significations et implications. In Le Brun-Ricalens (Ed.), *Productions lamellaires à l'Aurignacien* (pp. 157-190). ArchéoLogiques 1, Luxembourg.

Leroi-Gourhan, A. & Brézillon M. (1966). L'habitation magdalénienne no. 1 de Pincevent près Montereau (Seine-et-Marne). *Gallia Préhistoire* IX 2, 263-385.

Leuschner, D. & Sirocko, F. (2000). The low-latitude monsoon climate during Dansgaard/Oeschger cycles and Heinrich Events. *Quaternary Science Reviews* 19, 243 – 254.

Leuschner, D. & Sirocko, F. (2003). Orbital insolation forcing of the Indian Monsoon a motor for global climate changes? *Palaeogeography, Palaeoclimatology, Palaeoecology* 197, 83 – 95.

Lézine, A., Saliège, J-F, Robert, C., Wertz, F. & Inizan, M. (1998). Holocene Lakes from Ramlat as-Sab'atayn (Yemen) Illustrate the Impact of Monsoon Activity in Southern Arabia. *Quaternary Research* 50, 290–299.

Lézine, A., Tiercelin, J., Robert, C., Saliège, F., Cleuziou, S., Inizan, M. & Braemer, F. (2007). Centennial to millennial-scale variability of the Indian monsoon during the Early Holocene from asediment, pollen and isotope record from the desert of Yemen, *Palaeogeography, Palaeoclimatology, Palaeoecology*. 243, 235–249.

Lyman, R. (1994). *Vertebrate Taphonomy*. Cambridge Manual In archaeology. Cambridge University Press, Cambridge.

Macchiarelli, R. (2009). From Africa to Asia through Arabia: models, predictions, and witnesses of first phases of human settlement. In Suleimenov, O. & Iwamoto, W. (Ed.), *First Great Migrations of Peoples* (pp. 19-25). UNESCO, Paris.

Macumber, P. (2011) A geomorphological and hydrological underpinning for archaeological research in northern Qatar. *Proceedings of the Seminar for Arabian Studies* 41, 1–14.

Marks, A. (1976). Glossary. In Marks, A. (Ed.), *Prehistory and paleoenvironments of the Central Negev, Israel, volume 1: the Avdat/Aqev area part 1* (pp. 371-383). Southern Methodist University, Dallas

Marks, A. (1983a). Introduction, The Central Negev Project: 1969 – 1983. In Marks, A. (Ed.), *Prehistory and paleoenvironments of the Central Negev, Israel, volume 3: the Avdat/Aqev area*

part 3 (pp. ix -xv). Southern Methodist University, Dallas.

Marks, A. (1983b). The sites of Boker and Boker Tachtit: a brief introduction. In Marks, A. (Ed.), *Prehistory and paleoenvironments of the Central Negev, Israel, volume 3: the Avdat/ Aqev area part 3* (pp. 15 - 38). Southern Methodist University, Dallas.

Marks, A. (1987). Terminal Pleistocene and Holocene hunters and gatherers in the eastern Sudan. *African Archaeological Review* 5, 79 - 98.

Marks, A. (2008). Into Arabia, perhaps, but if so, from where? *Proceedings of the Seminar of Arabian Studies* 38, 15-24.

Marks, A. (2009). The Paleolithic of Arabia in an intra-regional context. In Petraglia, M. & Rose, J. (Ed.), *Evolution of Human Populations in Arabia: Paleoenvironments, Prehistory and Genetics* (pp.293-309). Springer Academic Publishers, Dordrecht.

Marks, A. (2011). The first early Modern Humans leaving Africa: Who, which way and when? In Conard, N., Drechsler, P. & Morales, A. (Ed.), *Between Sand and Sea The Archaeology and Human Ecology of Southwestern Asia Festschrift in honor of Hans-Peter Uerpmann* (21- 32). Kerns Verlag, Tübingen.

Marks, A., Hitala, H. & Williams, J. (2001). Tool Standardization in the Middle and Upper Palaeolithic: a Closer Look. *Cambridge Archaeological Journal* 11 (1), 17–44.

Marks, A. & Conard, N., (2006). Technology vs. Typology: The case for and against a transition from the MSA to the LSA at Mumba Cave, Tanzania. In Aubry ,T., Almeida, F., Araújo A. C. & Tiffagom, M. (Ed.), *Space and Time: Which Diachronies, which Synchronies, which Scales? Typology vs. Technology* (pp. 123-131). Proceedings of the XV UISPP World Congress in Lisbon September 4-9. British Archaeology Reports S1831, Oxford.

Martin, L., McCorriston, J. & Crassard, R. (2009). Early Arabian pastoralism at Manayzah in Wādī Sanā, Hadramawt. *Proceedings of the Seminar for Arabian Studies* 39, 271–282.

McBrearty, S., Bishop, L., Plummer, T., Dewar, R. & Conard, N. (1998). Tools Underfoot: Human Trampling as Agent of Lithic Artifacts Edge Modification. *American Antiquity* 63 (1), 108 – 129.

McBrearty, S. & Brookes, A. (2000). The revolution that wasn't: a new interpretation of the origin of modern human behavior. *Journal of Human Evolution* 39(5), 453-563.

McLaren, S., Al-Juaidi, F., Bateman, M. & Millington, A. (2009). First evidence for episodic flooding events in the arid interior of central Saudi Arabia over the last 60 ka. *Journal of Quaternary Science* 24, 198-207.

McClure, H. (1976). Radiocarbon chronology of Late Quaternary lakes in the Arabian Desert. *Nature* 263, 755 – 756.

McClure, H. (1978) Ar Rub al Khali. In Al-Sayari, S. & Zötl, J. (Ed.), *Quaternary Period in Saudi Arabia. Vol. 1: sedimentological, hydrogeological, hydrochemical, geomorphological, and climatological investigations in central and eastern Saudi Arabia*. Springer-Verlag, Wien.

McClure, H. (1984). *Late Quaternary Paleoenvironments of the Rub' al Khali*. Ph.D. Dissertation,

University of London, London.

McClure, H. (1988). Late Quaternary paleogeography and landscape evolution of the Rub al Khali. In Potts, D. (Ed.) *Araby the Blest*.

McCorriston, J., Oches, E., Walter, D. & Cole, K. (2002). Holocene Paleoecology and Prehistory in Highland Southern Arabia. *Paléorient* 28 (1), 61-88.

McCorriston, J. & Martin, L. (2009). Southern Arabia's Early Pastoral Population History: Some Recent Evidence. In Petraglia, M. & Rose, J. (Ed.), *Evolution of Human Populations in Arabia: Paleoenvironments, Prehistory and Genetics* (pp. 237- 278). Springer Academic Publishers, Dordrecht.

McCorriston, J., Harrower, M., Martin, L. & Oches, E. (2012). Cattle Cults of the Arabian Neolithic and Early Territorial Societies Issue. *American Anthropologist* 114 (1), 45-63.

Meignen, L. (1995). Levallois lithic production systems in the Middle Palaeolithic of the Near East: the case of the unidirectional method. In Dibble H. & Bar-Yosef O. (Ed.), *The Definition and Interpretation of Levallois Technology* (pp. 361-380, Monographs in World Archaeology 23, Prehistory Press, Madison.

Meignen, L. & Bar-Yosef, O. (1988). Variabilité technologique au Proche-Orient: l'exemple de Kebara. In Otte, M. (Ed.), *L'Homme de Néandertal, Vol. 4, La Technique* (pp.81-95). Euraul 31, Liège.

Mellars, P. (2006). Archeology and the Dispersal of Modern Humans in Europe: Deconstructing the "Aurignacian". *Evolutionary Anthropology* 15, 167-182.

Metspalu, M., Kivisild, T., Metspalu, E., Parik, J., Hudjashov, G., Kaldma, K., Serk, P., Karmin, M., Behar, D., Gilbert, M., Endicott, P., Mastana, S., Papiha, S., Skorecki, K., Torroni, A. & Villems, R. (2004). Most of the extant mtDNA boundaries in South and Southwest Asia were likely shaped during the initial settlement of Eurasia by anatomically modern humans. *BMC Genetic* 5, 26-27.

Monigal, K. (2002). *The Levantine Leptolithic: Blade Technology from the Lower Palaeolithic to the Dawn of the Upper Palaeolithic*. Ph.D. Dissertation, Southern Methodist University, Dallas.

Moreau, L. (2009). *Geisenklösterle, das Gravettien der Schwäbischen Alb im Europäischen Kontext*. Kern Verlag, Tübingen.

Munday, F. (1976). *The mousterien of the Negev: a Description and Explication of Site Variability*. Ph.D Dissertation, Southern Methodist University, Dallas.

Neff, U. (2001). *Massenspektrometrische Th/U-Datierung von Höhlensintern aus dem Oman: Klima Archive des Asiatischen Monsuns*. Ph.D. Dissertation, Ruprecht-Karls-Universität, Heidelberg.

Neff, U., Burns, S., Mangini, A., Mudelsee, M., Fleitmann, D. & Matter, A. (2001). Strong coherence between solar variability and the monsoon in Oman between 9 and 6 kyr ago. *Nature* 411, 290 – 293.

Newman, J. (1994). The Effects of Distance on Lithic Material Reduction Technology. *Journal of*

Field Archaeology 21 (4), 491-501.

Nishiaki, Y. (1993). Lithic Analysis and Cultural Change in the Late Pre-Pottery Neolithic of North Syria. *Journal of the Anthropological Society of Nippon* 101 (1), 91- 110.

Nishiaki, Y. (2000). *Lithic technology of Neolithic Syria*. British Archaeological Report Int. Ser. 840, Oxford.

Odell, G. (1981). The Mechanics of Use- Breakage of Stone Tools: Some Testable Hypotheses. *Journal of Field Archaeology* 8, 197-209.

Odell, G. (2004) *Lithic Analysis. Manuals in Archaeological Method Theory and Techniques*. Kluwer Academic/ Plenum publisher, New York.

Odell, G. & Cowan, F. (1986). Experiments with Spears and Arrows on Animal Targets. *Journal of Field Archaeology* 13 (2), 195-212.

Oppenheimer, S. (2002). Limited global change due to the largest known Quaternary eruption, Toba E4 kyr BP? *Quaternary Science Reviews* 21, 1593–1609.

Oppenheimer, S. (2008). The great arc of dispersal of modern humans: Africa to Australia. *Quaternary International* 202, 2–13.

Orembelli, O., Maggi, V. & Delmonte, B. (2010), Quaternary stratigraphy and ice cores. *Quaternary International* 219, 55–65.

Orton, C. (2000). *Sampling in Archaeology. Cambridge Manuals in Archaeology*. Cambridge university Press, Cambridge.

Owen, L. (1988). *Blade and microblade technology. Selected assemblages from the North American Arctic and the Upper Paleolithic of Southwest Germany*. British Archaeology Reports Int .Ser.441, Oxford.

Parker, A. (2009). Pleistocene Climate Change in Arabia- developing a Framework for Hominid Dispersal over the Last 350 KYR. In Petraglia, M. & Rose, J. (Ed.), *Evolution of Human Populations in Arabia: Paleoenvironments, Prehistory and Genetics* (pp. 1-25), Springer Academic Publishers, Dordrecht.

Parker, A., Eckersley, I., Smith, M., Goudie, A., Stokes, S., Ward, S., White, K., & Hodson M. (2004). Holocene vegetation dynamics in the northeastern Rub al-'Khali, Arabian Peninsula, a phytolith, pollen, and carbon isotope study. *Journal of Quaternary Science* 19(7), 665-676.

Parker, A., Goudie, A., Stokes, S., White, K., Hodson, M., Manning, M., & Kennet, D., (2006a). A record of Holocene climate change from lake geochemical analyses in southeastern Arabia. *Quaternary Research*. 66, 465–476.

Parker, A., Preston, G., Walkington, H., & Hudson, M. (2006b). Developing a framework of Holocene climatic change and landscape archaeology for the lower Gulf region, southeastern Arabia. *Arabian Archaeology and Epigraphy* 17, 125 – 130.

Parker, A. & Rose, J. (2008). Climate change and human origins in southern Arabia. *Proceedings of the Seminar for Arabian Studies* 38, 25–42.

Parton, A., Parker, A., Farrant, A., Leng, M., Uerpmann, H-P., Schwenninger, J-L., Galletti, C. & Wells J. (2010). An early MIS3 wet phase at palaeolake Aqabah: preliminary interpretation of the multi-proxy record. *Proceedings of the Seminar for Arabian Studies* 40, 267–276.

Parton, A., Farrant, A., Leng, M., Schwenninger, J-L., Rose, J., Uerpmann, H-P. & Parker, A. (2012). An early MIS3 pluvial phase within southeast Arabia: climatic and archaeological implications. *Quaternary International*.

Pelegrin, J. (2006). Long blade technology in the Old World: an experimental approach and some archaeological results. In Apel, J. & Knutsson (Ed.), *Skilled Production and Social Reproduction* (pp. 37–68). Societas Archaeologica Upsaliensis, Uppsala.

Perlès, C. (1987). *Les Industries Lithique Taillées de Franchthi, Argolides: Présentation Générale et industries Paléolithiques*. Indiana University Press, Terre Haute.

Pettersson, L. (1990). Characteristics of Bifacial-Reduction Flake-Size Distribution. *American Antiquity* 55 (3), 550-558.

Petit, J., Jouzel, J., Raynaud, D., Barkov, N., Barnola, J-M., Basile, I., Bender, M., Chappellaz, J., Davis, M., Delaygue, G., Delmotte, M., Kotlyakov, V., Legrand, M., Lipenkov, V., Lorius, C., Pépin, L., Ritz, C., Saltzman, E. & Stievenard, M. (1999). Climate and atmospheric history of the past 420,000 years from the Vostok ice core, Antarctica. *Nature* 399, 429 -436.

Petruglia M. (2003). The lower Paleolithic of the Arabian peninsula: occupations, adaptations, and dispersals. *Journal of World Prehistory* 17, 79-141.

Petruglia, M. (2011). Trailblazers across Arabia. *Nature* 470, 50-51.

Petruglia, M. & Alsharekh, A. (2003). The Middle Palaeolithic of Arabia: implications for modern human origins, behavior and dispersal. *Antiquity* 77 (298), 671-684.

Petruglia, M., Korisettar, R., Boivin, N., Clarkson, C., Ditchfield, P., Jones, S., Koshy, J., Lahr, M., Oppenheimer, C., Pyle, D., Roberts, R., Schwenninger, J-L., Arnold, L. & White, K. (2007). Middle Paleolithic Assemblages from the Indian Subcontinent Before and After the Toba Super-Eruption. *Science* 317, 114- 116.

Petruglia, M., Drake, N. & Alsharekh, A. (2009). Acheulean Landscapes and Large Cutting Tool Assemblages in the Arabian Peninsula. In Petruglia, M. & Rose, J. (Ed.), *Evolution of Human Populations in Arabia: Paleoenvironments, Prehistory and Genetics* (pp. 103- 116). Netherlands, CT: Springer Academic Publishers.

Petruglia, P., Alsharekh, A., Crassard, R., Drake, N., Groucutt, H., Parker, A. & Roberts, R. (2011). Middle Paleolithic occupation on a Marine Isotope Stage 5 lakeshore in the Nefud Desert, Saudi Arabia. *Quaternary Science Reviews* 30 (13-14), 1555–1559.

Picin, A., Peresani, M. & Vaquero, M. (2011). Application of a new typological approach to classifying denticulate and notched tools: the study of two Mousterian lithic assemblages. *Journal of Archaeological Science* 38, 711-722.

Platel, J., Roger, J., Petters, T., Mercolli, I., Kramers, J. & Le-Métour, J. (1992). *Geological map of Salalah, explanatory notes*. Sultanat of Oman: Ministry of Petroleum and Minerals.

- Plisson, H. & Geneste, J.-M. (1989). Analyse technologique des pointes à cran solutréennes du card (Charente), du Fourneau du Diable, du Pech de la Boissiere et de Combe Saunière (Dordogne). *Paleo* 1, 65-106.
- Preusser, F., Radies, D. & Matter, A. (2002). A 160,000-Year Record of Dune Development and Atmospheric Circulation Southern Arabia. *Science* 296, 2018-2020.
- Preusser, F., (2009). Chronology of the impact of Quaternary climate change on continental environments in the Arabian Peninsula. *C. R. Geoscience* 341 (8), 621-632.
- Pullar, J. (1974). Harvard archaeological survey in Oman, 1973: flint sites in Oman. *Arabian Seminar* 4, 33-48.
- Purdy, B. & Clark, D. (1979). Electron Microprobe Analysis of Weathered Florida Chert. *American Antiquity* 44 (3), 517-524.
- Purdy, B. & Clark, D. (1987). Weathering of Inorganic Materials: Dating and Other Applications. *Advances in Archaeological Method and Theory* 11, 211-253.
- Rezek, Z., Kin, S., Iovita, R. & Dibble, H. (2011). The relative effect of core surface morphology on flake shape and other attributed. *Journal of Archaeological Sciences* 38, 1346-1358.
- Radies, D., Preusser, F., Matter, A. & Mange, M. (2004). Eustatic and climatic controls on the development of the Wahiba Sand Sea, Sultanate of Oman. *Sedimentology* 51, 1359-1385.
- Richards, M., Macaulay, V., Hickey, E., Vega, E., Sykes, B., Guida, V., Rengo, C., Sellitto, D., Cruciani, F., Kivisild, T., Villems, R., Thomas, M., Rychkov, S., Rychkov, O., Rychkov, Y., Gölge, M., Dimitrov, D., Hill, E., Bradley, D., Romano, V., Cali, F., Vona, G., Demaine, A., Papiha, S., Triantaphyllidis, C., Stefanescu, G., Hatina, J., Belledi, M., Di Rienzo, A., Novelletto, A., Oppenheim, A., Norby, S., Al-Zaheri, N., Santachiara-Benerecetti, S., Scozari, R., Torroni, A. & Bandelt, H. (2000). Tracing European founder lineages in the Near Eastern mtDNA pool. *American Journal of Human Genetics* 67, 1251-1276.
- Ridl, J., Edens, C. M. & Cerny, V. (2009). Mitochondrial DNA Structure of Yemeni Populations: Regional Difference and the Implications of Different Migratory Contributions. In Petraglia, M. & Rose, J. (Ed.), *Evolution of Human Populations in Arabia: Paleoenvironments, Prehistory and Genetics* (pp. 69-78). Springer Academic Publishers, Dordrecht.
- Riquet, R. & Cordier, G. (1957). L'ossuaire néolithique du Bec-des-Deux-Eaux, commune de Ports, I.-et-L. *l'Anthropologie*, LXI, 28-44.
- Rixen, T., Haake, B. & Ittenkkot, V. (2000). Sedimentation in the western Arabian Sea the role of coastal and open-ocean upwelling. *Deep-Sea Research II* 47, 2155 - 2178.
- Rose, J. (2000). *A Reconstruction of Pleistocene Arabia: the state of research and avenues for further inquiry*. M.A. Thesis, Boston University, Boston.
- Rose, J. (2002). Survey of prehistoric sites in Mahra, Eastern Yemen. *Adumatu* 6, 7-20.
- Rose, J. (2004). The question of Upper Pleistocene connections between East Africa and South

Arabia. *Current Anthropology* 45 (4), 551-555.

Rose, J. (2006). *Among Arabian Sands: Defining the Palaeolithic of Southern Arabia*. Ph.D dissertation, Southern Methodist University, Dallas.

Rose, J. (2007). The Arabian Corridor migration model: archaeological evidence for hominin dispersals into Oman during the Middle and Upper Pleistocene. *Proceedings of the Seminar for Arabian Studies* 37, 219–237.

Rose, J. (2010). New light on human prehistory in the Arabo-Persian Gulf oasis. *Current Anthropology* 51(6), 849-883.

Rose, J. & Parker, A. (2008). Climate change and human origins in southern Arabia. *Proceedings of the Seminar for Arabian Studies* 38, 25–42.

Rose, J. & Bailey, J. (2008). Defining the Palaeolithic of Arabia? Notes on the Roundtable Discussion. *Proceedings of the Seminar for Arabian Studies* 38, 65–70.

Rose, J. & Usik, V. (2009). The “Upper Paleolithic” of South Arabia. In Petraglia, M. & Rose, J. (Ed.), *Evolution of Human Populations in Arabia: Paleoenvironments, Prehistory and Genetics* (pp. 169-185). Springer Academic Publishers, Dodrecht.

Rose, J., Usik, V., Marks, A., Hilbert, Y., Galletti, C., Parton, A., Geiling, J., Cerny, V., Morley, M., & Roberts, R. (2011a). The Nubian Complex of Dhofar, Oman: An African Middle Stone Age Industry in Southern Arabia. *PLoS ONE* 6 (11).

Rose, J., Usik, V., Angelucci, D. & Al-Mahrooqi, A. (2011b). A Stratified Early/Middle Holocene Site inside the Qārat al-Kibrīt Dome. *Journal of Oman Studies* 17, 51-71.

Rosenberg, T., Preusser, F., Blechschmidt, I., Fleitmann, D., Jagher, R. & Matter, A. (2012). Late Pleistocene palaeolake in the interior of Oman: A potential key-area for the dispersal of anatomically modern humans out-of-Africa? *Journal of Quaternary Science* 27 (1), 13-16.

Roth, B. & Dibble, H. (1998). Production and Transport of Blanks and Tools at the French Middle Paleolithic Site of Combe-Capelle Bas. *American Antiquity* 63 (1), 47-62.

Rots, V. (2004). Prehensile Wear on Flint Tools. *Lithic Technology* 29 (1), 7-32.

Rots, V. (2005). Wear Traces and the Interpretation of Stone Tools. *Journal of Field Archaeology* 30 (1), 61-73.

Rots, V. (2010). *Prehension and Hafting Traces on Flint Tools: a Methodology*. Leuven University Press, Leuven.

Rots, V. & Williamson, B. (2004). Microwear and residue analyses in perspective: the contribution of ethnoarchaeological evidence. *Journal of Archaeological Science* 31, 1287–1299.

Rottländer, R. (1975). The formation of patina on flint. *Archaeometry* 17(1), 106-110.

- Rottländer, R. (1978). Schwierigkeiten bei der Datierung von Silices. Mineralische Rohstoffe als kulturhistorische Informationsquelle (pp.190-99). Kennicke, Hagen.
- Sackett, J. (1982). Approache to Style in Lithic Archaeology. *Journal of Anthropological Archaeology* 1, 59 – 112.
- Sackett, J. (1989). Statistics, Attributes, and the Dynamics of Burin Typology. *Archeological Papers of the American Anthropological Association* 1(1), 51–82.
- Saher, M., Peeters, F. & Kroon, D. (2007). Sea surface temperatures during the SW and NE monsoon seasons in the western Arabian Sea over the past 20,000 years. *Palaeogeography, Palaeoclimatology, Palaeoecology* 249, 216-228.
- Schiffer, M. (1983). Toward the Identification of Formation Processes. *American Antiquity* 48 (4) 675-706.
- Schimelmitz, R., Barkai, R. & Gopher, A. (2011). Systematic blade production at late Lower Paleolithic (400—200 kyr) Qesem Cave, Israel. *Journal of Human Evolution* 61,458-479.
- Schulz, H., van Rad., U. & Erlenkeuser, H. (1998). Correlation between Arabian Sea and Greenland climate oscillations of the past 110,000 years. *Nature* 393, 54 – 57.
- Schulz, H., van Rad, U. & Rolf, C. (2002a). The Toba Volcanic Event and Interstadial/Stadial Climates at the Marine Isotopic Stage 5 to 4 Transition in the Northern Indian Ocean. *Quaternary Research* 57, 22–31.
- Schulz, H., van Rad, U. & Ittenkkot, V. (2002b). Planktic Foraminifera, particle flux and oceanic productivity off Pakistan, NE Arabian Sea: modern analogues and implications to the palaeoclimatic record. In Clift, P., Kroon, D., Gaedicke, C. & Craig, J. (Ed.), *The tectonic and climatic evolution of the Arabian Sea Region* (pp. 499-516). Geographucal Society, Special Publications 195, London.
- Schultz, D. (2005). *The ecozones of the world: the ecological divisions of the geosphere*. Springer-Verlag, Stuttgart.
- Schulz, E. & Whitney, J. (1986). Upper Pleistocene and Holocene lakes in the An Nafud, Saudi Arabia. *Hydrobiologia* 143, 175-190.
- Schwarcz, H. P. (1994). Chronology of modern humans in the Levant. In Bar-Yosef O. & Kra R. S. (Ed.), *Late Quaternary Chronology and Paleoclimate of the Eastern Mediterranean* (pp. 21-31). Tucson, CT: Radiocarbon.
- Scott-Jackson, J., Scott-Jackson, W. & Rose, J. (2009). Paleolithic Stone Tool Assemblages from Sharjah and Ras al Khaimah in the United Arab Emirates. In Petraglia, M. & Rose, J. (Ed.), *Evolution of Human Populations in Arabia: Paleoenvironments, Prehistory and Genetics* (pp. 125-138). Springer Academic Publishers, Dodrecht.
- Sellet, F. (1993). Chaîne Operatoire: the concept and its applications. *Lithic Technology* 18, 106-112.
- Semenov, S. (1964). *Prehistoric Technology: an experimental study of the oldesttools and artefacts*

from traces of manufacture and wear. Cory, Adams and Mackay, London.

Servello, F. (1976). Nahal Divshon: a Pre-Pottery Neolithic B Hunting Camp. In Marks, T. (Ed.), *Prehistory and paleoenvironments of the Central Negev, Israel, volume 1: the Avdat/ Aqev area part 1* (pp. 349-370). Southern Methodist University, Dallas.

Shelley, P. (1990). Variation in Lithic Assemblages: An Experiment. *Journal of Field Archaeology* 17(2), 187-193.

Shott, J. (1994). Size and Form in the Analysis of Flake Debris: Review and Recent Approaches. *Journal of Archaeological Method and Theory* 1 (1), 69- 110.

Shott, J. (2003). Chaîne Opératoire and Reduction Sequence. *Lithic Technology* 28, 95- 105.

Shott, J & Weedman, K. (2007). Measuring reduction in stone tools: an ethnoarchaeological study of Gamo hidescrapers from Ethiopia. *Journal of Archaeological Science* 34, 1016-1035.

Singer, R. & Wymer, J. (1982). *The Middle Stone Age at Klasies River Mouth in South Africa*. University of Chicago Press, Chicago.

Sonneville-Bordes, D. & Perrot, J. (1956). Lexique typologique du Paléolithique supérieur: Outillage lithique IV Burins. *Bulletin de la Société Préhistorique Française* 53(7), 408 - 412

Stafford, B. (1977). Burin Manufacture and Utilization: An Experimental Study. *Journal of Field Archaeology* 4, 235-246.

Stafford, C. & Stafford, B. (1983). The Functional Hypothesis: A Formal Approach to Use-Wear Experiments and Settlement-Subsistence. *Journal of Anthropological Research* 3 (4), 351-375.

Steward, J. & Stringer, C. (2012). Human Evolution Out of Africa: The Role of Refugia and Climate Change. *Science* 335, 1317 – 1321.

Stokes, S. & Bray, H. (2005). Late Pleistocene eolian history of the Liwa region, Arabian Peninsula. *GSA Bulletin* 117, 1466 – 1480.

Stout, D. (2002). Skill and Cognition in Stone Tool Production: An Ethnographic Case Study from Irian Jaya. *Current Anthropology* 43 (5), 693- 722.

Stringer, C. (2000) Coasting out of Africa. *Nature* 405, 24-27.

Stringer, C. (2003) Out of Ethiopia. *Nature* 423, 692-695.

Sullivan, A. & Rozen K. (1985). Debitage analysis and archaeological interpretation. *American Antiquity* 50, 755-779.

Taller, A. & Floss, H., (2011). Die Lithische Technologie der Gravettien-Fundstelle Azé-Camping de Rizerolles (Dép. Saône-et-Loire). *Archäologisches Korrespondenzblatt* 41 (2), 155- 171.

Tchernov, E. (1992). Eurasian-African biotic exchanges through the Levantine corridor during the Neogene and Quaternary. *Courier Forsch.-Institute Senckenberg* 153, 103-123.

Teyssandier, N. (2003). *Les Débuts de l'Aurignacien en Europe: Discussion à partir des sites de Geissenklösterle, Willendorf II, Krems-Hundssteig et Bacho Kiro*. Ph.D thesis, Université de Paris X-Nanterre, Paris.

Teller, J., Clennie, K., Lancaster, N. & Singhvi, A. (2000). Calcareous dunes of the United Arab Emirates and Noah's Flood: the postglacial reflooding of the Persian (Arabian) Gulf. *Quaternary International* 68 -71, 297-308.

Thesiger, W. (1959). *Arabian Sands*. E.P. Dutton and Company, Inc, New York.

Thiébout, C. (2007). Le Moustérien à denticulés des années cinquante à nos jours: définitions et caractérisation. *Bulletin de la Société Préhistorique Française* 104(3), 461-481.

Tixier, J. (1963). *Typologie de l'épipaléolithique du Maghreb. Mémoires du centre de recherches anthropologiques, préhistoriques et ethnographiques, II (Algeria)*. Arts et Métiers Graphiques, Paris.

Tixier, J. (1978). *Méthode pour l'étude des outillages lithiques*. Ph.D Thesis. Université de Paris X, Paris.

Tixier, J. (1984). Lames. In Tixier J. (Ed.), *Préhistoire de la pierre taillée*. Volume 2: économie du débitage laminaire: technologie et experimentation (pp. 13-21). CERP, Paris.

Tixier, J., Inizan, M. & Roche, H. (1980). *Préhistoire de la Pierre Taillée 1: Terminologie et technologie*. Recherches e d'Etudes Préhistoriques, Valbonne.

Tixier, J. & Turq A. (1999) Kombewa et al. *Paleo* 11, 135-143.

Thompson, A. (2000). *Origins of Arabia*. Stacey International, London.

Tosi, M. (1986). The emerging picture of prehistoric Arabia. *Annual Review of Anthropology* 15, 461-490.

Tostevin, G. (2007). Levels of theory and social practice in the Reduction Sequence and Chaîne Opératoire methods of lithic analysis. In Tostevin, G. (Ed.), *Reduction Sequence, Chaîne opératoire, and other methods: The epistemologies of different approaches to lithic analysis*. Monograph of the electronic symposium at the 71 annual Meeting of the society for American Archaeology San Juan, Puerto Rico.

Tsuneki, A., Zeidini, M. & Ohnuma, K. (2007). Proto-Neolithic caves in the Bolaghi Valley, South Iran. *Journal of Persian Studies* 45, 1-22.

Uerpmann, H-P. (1989) Problems of Archaeo-Zoological Research in Eastern Arabia. In Costal, P. & Tosi, M. (Ed.), *Oman Studies, Papers on the Archaeology and History of Oman* (pp. 163-168). Instituto Italiano per il Medio ed Estremo Oriente, Roma.

Uerpmann, M. (1992). Structuring the Late Stone Age of Southwestern Arabia. *Arabian Archaeology and Epigraphy* 3, 65-109.

Uerpmann, H-P, Potts, D. & Uerpmann, M. (2009). Holocene (RE-) Occupation of Eastern Arabia. In Petraglia, M. & Rose, J. (Ed.), *Evolution of Human Populations in Arabia: Palaeoenvironments, Prehistory and Genetics* (pp. 205-214). Springer Academic Publishers, Dordrecht.

Urban, B. & Buerkert, A. (2008). Palaeoecological analysis of a Late Quaternary sediment profile in northern Oman. *Journal of Arid Environments* 73, 296–305.

Usik, V. (1989). Korolevo – transition from Lower to Upper Paleolithic according to reconstruction data. *Anthropologia (Brno)* XXVII (2-3), 179-212.

Usik, V. (2004). Problems of Kombewa Methode and some Features of Non-Levallois Reduction Strategies of the Middle Palaeolithic Complex 2 of Korolevo Site (Transcarpathian Region): Refitting and Technological Data. XIVth UISPP Congress, University of Liege, Belgium. British Archaeological Report, Int. Ser. 1239, Oxford.

Usik, V. (2006). The problem of Levallois Methode in Level II/8 of Kabazi II. In: Chabai, V., Richter, J. & Uthmeier, T. (Ed.), *Kabazi II: the 70000 years since the last interglacial* (pp. 143-168). Simferpol, Köln.

Usik, V., Rose, J., Hilbert, Y., Van Peer, P. & Marks, A. (2012). Nubian Complex reduction strategies in Dhofar, southern Oman. *Quaternary International*.

Valladas, H., Reyss, I. L., Joron, J. L., Valladas, G., Bar-Yosef, O. & Vandermeersch, P. (1988). Thermoluminescence Dating of Mousterian “Proto-Cro-Magnon” remains from Israel and the origin of modern man. *Nature* 331, 614-616.

Van Beek, G. (1958). Frankincense and myrrh in ancient South Arabia. *Journal of the American Oriental Society* 78 (3), 141–152.

Van Peer, P. (1992). *The Levallois Reduction Strategy*. Monographs in World Prehistory 13. Prehistory Press, Madison.

Van Peer, P., Fullagar, R., Stokes, S., Bailey, R., Moeyersons, J., Steenhoudt, F., Greet, A., Vanderbeken, T., De Dapper, M. & Geus, F. (2003). The Early To Middle Stone Age Transition and the Emergence of Modern Human Behavior at Site 8-B-11, Sai Island, Sudan. *Journal of Human Evolution* 45, 187-193.

Van Peer, P. & Vermeersch, P. (2007). The place of Northeast Africa in the Early History of Modern Humans: New Data and Interpretation on the Middle Stone Age. In Mellars, P., Boyle, K., Bar-Yosef, O. & Stringer (Ed.), *Rethinking the Human Revolution* (pp.187-198). Cambridge, CT: McDonald Institute for Archaeological Research.

Van Peer, P., Vermeersch, P. & Paulissen, E. (2010). *Chert Quarrying, Lithic Technology and a Modern Human Burial at the Palaeolithic Site of Taramsa 1, Upper Egypt*. Leuven University Press, Leuven.

Van Rad, U., Schulz, H., Reich, V., den Dulk, M., Berner, U. & Sirocko, F. (1999). Multiple-monsoon-controlled breakdown of oxygen-minimum conditions during the past 30000 years documented in laminated sediments off Pakistan. *Palaeogeography, Palaeoclimatology, Palaeoecology* 152, 129–61.

- Volkman, P. (1983). Boker Tachtit: core reconstruction. In Marks, A. (Ed.), *Prehistory and paleoenvironments of the Central Negev, Israel, volume 3: the Avdat/ Aqev area part 3* (Pp. 127-190). Southern Methodist University, Dallas.
- Volkman, P. (1989). *Boker Tachtit: the technological shift from the Middle to the Upper Paleolithic in the Central Negev, Israel*. Ph.D. dissertation, Southern Methodist University, Dallas.
- Waerlbroeck, C., Frank, N., Jouzel, J., Parrenin, F., Masson-Delmotte, V. & Genty, D. (2008). Transferring radiometric dating of the last interglacial sea level high stand to marine and ice core records. *Earth and Planetary Science Letters* 265, 183–194.
- Warren, A. & Alison, D. (1998). The palaeoenvironmental significance of dune size hierarchies. *Palaeogeography, Palaeoclimatology, Palaeoecology* 137, 289-303.
- Webb, T. & Bartlein, P. (1992). Global Change during the last 3 million Years: Climatic controls and biotic responses. *Annual Review of Ecology and Systematics* 23, 141 – 173.
- Wilkinson, T. (2009). Environment and Long-Term Population Trends in Southwest Arabia. In Petraglia, M. & Rose, J. (Ed.), *Evolution of Human Populations in Arabia: Paleoenvironments, Prehistory and Genetics* (pp. 51 - 66). Springer Academic Publishers, Dordrecht.
- Whalen, N., Zoboroski, M. & Schibert, K. (2002). The Lower palaeolithic in southwestern Oman. *Adumatu* 5, 27-34.
- Whalen, N. & Schatte, K. (1997). Pleistocene sites in southern Yemen. *Arabian Archaeology and Epigraphy* 8, 1–10.
- Whittaker, J. (1994). *Flintknapping: Making and understanding Stone Tools*. University of Texas Press, Austin.
- Wood, W., Sanford, W. & Al Habschi, A. (2002). The source of solutes in the coastal sabkha of Abu Dhabi. *Bulletin of the Geological Society of America* 114 (3), 259–268.
- Zarins, J. (1998). View from the South: the greater Arabian Peninsula. In Henry, D. (Ed.) *Prehistoric Archaeology of Jordan* (pp. 179-194). British Archaeology Reports International Series 705, Oxford.
- Zarins, J. (2001). *The Land of Incense: Archaeological work in the Governorate of Dhofar, Sultanate of Oman, 1990-1995*. Sultan Qaboos University Publications, Muscat